Precise Tools for Site-Directed RNA Editing and Induction of NO Signaling

Dissertation

der Mathematisch-Naturwissenschaftlichen Fakultät
der Eberhard Karls Universität Tübingen
zur Erlangung des Grades eines
Doktors der Naturwissenschaften
(Dr. rer. nat.)

vorgelegt von
Anna Sofia Imrich geb. Stroppel
aus Darmstadt

Tübingen
2023

Gedruckt mit Genehmigung der Mathematisch-Naturwissenschaftlichen Fakultät der Eberhard Karls Universität Tübingen.

Tag der mündlichen Qualifikation:	16. 11. 2023
Dekan:	Prof. Dr. Thilo Stehle
1. Berichterstatter:	Prof. Dr. Thorsten Stafforst
2. Berichterstatter:	Prof. Dr. Dirk Schwarzer

Mein aufrichtiger Dank

Ich danke Prof. Dr. Thorsten Stafforst für die Betreuung meiner Doktorarbeit. Neben den guten wissenschaftlichen Gesprächen möchte ich mich explizit für die Möglichkeit bedanken, seiner Arbeitsgruppe als ursprünglich reine Chemikerin beizutreten und meinem Interesse an der Biochemie nachzugehen.

Prof. Dr. Thomas Ziegler gilt ebenfalls mein Dank für die Unterstützung bei der Verknüpfung meiner Interessen im chemischen und biochemischen Bereich, unter anderem durch die Kooperation in der Betreuung meiner Masterarbeit, sowie für die Zweitbetreuung der vorliegenden Doktorarbeit.

Mein herzlicher Dank gilt auch Prof. Dr. Dirk Schwarzer für die Tätigkeit als Berichterstatter, sowie die Möglichkeit zur Messung von LC-MS Spektren.

Den ehemaligen und aktuellen Mitgliedern der Arbeitsgruppe Stafforst danke ich für den angenehmen Austausch, Beratungen und die Weitergabe von Fachwissen. Besonders herzlich möchte ich mich bei Alfred Hanswillemenke, Oliver Hess, Ngadhnjim Latifi und Paul Vogel für die tolle Büroatmosphäre, zahlreiche hilfreiche Besprechungen und die gute Zusammenarbeit bedanken.

Mein weiterer Dank gilt den Mitgliedern der Arbeitsgruppen Maček und Amann für die nette Zellkultur-Nachbarschaft, sowie der Arbeitsgruppe Schwarzer für die Mitwirkung an den LC-MS Messungen.

Großer Dank gilt nicht zuletzt auch meinem Partner, meiner Familie und meinen Freunden für die anhaltende Unterstützung in jedweder Form.

Contents

Abstract

RNA editing represents an important class of posttranscriptional alterations with various physiological and pathophysiological effects. ADARs catalyze deaminations of adenosines in double stranded RNA to inosines (A-to-I), APOBECs deaminations of cytidines to uridines (C-to-U). The SNAP-ADAR system provides a tool for site-directed A-to-I RNA editing by fusion of a catalytically active ADAR deaminase domain to the self-labeling SNAP-tag. SNAP-tag reacts covalently with short guideRNAs carrying an O^6-benzylguanine modification, thus allowing for targeted recruitment of SNAP-ADAR to a specific adenosine by Watson Crick base pairing.

In the dissertation at hand, the SNAP-ADAR platform has now been expanded by HALO-ADAR as second editase with orthogonal recruitment mechanism. While SNAP-ADAR is steered with O^6-benzylguanine modified guideRNAs, chloroalkyl modifications were applied for HALO-ADAR. This permitted the independent, parallel steering of SNAP-ADAR2 and HALO-ADAR1 in mammalian cells, which yielded optimal editing for an extended substrate scope. Moreover, the combination of HALO-ADAR1 with APOBEC1-SNAP enabled targeted, concurrent and orthogonal A-to-I and C-to-U editing, which may be exploited for the investigation of the interplay between A-to-I and C-to-U editing events in the future.

Furthermore, SNAP-ADAR editing was put under control of small molecule induction. Design of separate SNAP-GID1A and $GAI_{1\text{-}92}$-ADAR1 fusions rendered the recruitment of editing activity dependent on chemically induced dimerization of GID1A and $GAI_{1\text{-}92}$ with gibberellic acid (GA_3). As a result, tightly controlled GA_3 inducible A-to-I editing was achieved. The extent of editing was tunable by GA_3 dosage control, which is particularly beneficial for sites requiring careful adjustment to exclude potential detrimental effects.

Additionally, a tool for photoinduced activation of the NO-cGMP signaling pathway has been developed. Nitric oxide (NO) represents a versatile secondary messenger. Among others, it induces cGMP production and consequently the cGMP signaling cascade with various implications in smooth muscle tone regulation as well as neuronal processes. The highly reactive NO can be supplied by NO releasing drugs, including diazeniumdiolates, in physiological settings.

In the work at hand, the *N*-bound diazeniumdiolate of pyrrolidine, PYRRO/NO, which releases NO within seconds under physiological conditions, has been photoprotected as MeNPOM-PYRRO/NO in order to stabilize the compound in the absence of light. Application of MeNPOM-PYRRO/NO in primary vascular smooth muscle cells allowed for generation of well-defined cGMP signals upon illumination with long-wavelength UV light. The excellent spatiotemporal control provided by photoactivation should enable spatial control at subcellular level, which may prove valuable for the prospective elucidation of cGMP compartmentalization.

Zusammenfassung

RNA Editierungen stellen eine wichtige Kategorie der posttranskriptionalen Veränderungen dar, welche in zahlreiche physiologische und pathophysiologische Vorgänge involviert ist. ADARs katalysieren Desaminierungen von Adenosinen in doppelsträngiger RNA zu Inosinen (A-nach-I), APOBECs Desaminierungen von Cytidinen zu Uridinen (C-nach-U). Im SNAP-ADAR System wird ein Fusionsprotein aus einer katalytisch aktiven ADAR Desaminasedomäne mit einem SNAP-tag zur zielgerichteten A-nach-I RNA Editierung eingesetzt. Der SNAP-tag geht eine kovalente Bindung zu guideRNAs mit einer O^6-Benzylguanin-Modifikation ein, wodurch SNAP-ADAR über Watson Crick Basenpaarung gezielt an ein definiertes Adenosin rekrutiert werden kann.

In der vorliegenden Dissertation wurde die SNAP-ADAR Plattform nun um HALO-ADAR als zweite Editase mit orthogonalem Rekrutierungsmechanismus erweitert. Während SNAP-ADAR mittels guideRNAs mit O^6-Benzylguanin-Modifikationen dirigiert werden kann, kamen für HALO-ADAR Chloralkan-Modifikationen zum Einsatz. Dies ermöglichte die unabhängige parallele Steuerung von SNAP-ADAR2 und HALO-ADAR1 in Humanzellen, wodurch sich eine erweiterte Bandbreite an optimal editierbaren Substraten ergab. Des Weiteren gestattete die Kombination von HALO-ADAR1 mit APOBEC1-SNAP die zeitgleiche, zielgerichtete und orthogonale A-nach-I und C-nach-U Editierung. Dies könnte künftig für Untersuchungen bezüglich des Zusammenspiels von A-nach-I und C-nach-U Editierungen genutzt werden.

Darüber hinaus wurde ein System zur Kontrolle der Editierung mit SNAP-ADAR mittels Stimulation mit einer niedermolekularen Verbindung erarbeitet. Durch die Bildung separater SNAP-GID1A und $GAI_{1\text{-}92}$-ADAR Fusionsproteine war die Rekrutierung der Editierungsaktivität auf chemisch induzierte Dimerisierung von GID1A und $GAI_{1\text{-}92}$ mit Gibberellinsäure (GA_3) angewiesen. Als Folge der benötigten Induktion mit GA_3 wurde hochgradige Kontrolle über die A-nach-I Editierung erlangt. Der Editierungsgrad konnte dabei über Steuerung der GA_3-Dosierung eingestellt werden. Dies ist vor allem für Editierungsstellen von Vorteil, die sorgfältige Justierung erfordern, um potentielle schädliche Effekte auszuschließen.

Zudem wurde ein Verfahren zur photoinduzierten Aktivierung des NO-cGMP Signalweges entwickelt. Stickstoffmonoxid (NO) stellt einen vielseitigen Sekundärbotenstoff dar. Es induziert unter anderem die Herstellung von cGMP und in Folge die cGMP Signalkaskade mit diversen Auswirkungen auf die Regulierung des vaskulären Muskeltonus' sowie neuronale Vorgänge. Das hochreaktive NO kann durch verschiedene Pharmaka, darunter Diazeniumdiolate, in physiologischen Umgebungen bereitgestellt werden.

In der vorliegenden Arbeit wurde das *N*-gebundene Diazeniumdiolat von Pyrrolidin, PYRRO/NO, welches unter physiologischen Bedingungen innerhalb von Sekunden NO freisetzt, zur Stabilisierung in der Abwesenheit von Licht als MeNPOM-PYRRO/NO photogeschützt. In primären vaskulären glatten Muskelzellen konnten mittels MeNPOM-PYRRO/NO unter Bestrahlung mit langwelligem UV-Licht klar definierte cGMP-Signale erzeugt werden. Die Photoaktivierung bietet hervorragende räumliche und zeitliche Kontrollmöglichkeiten und sollte auf subzellulärer Ebene räumlich kontrollierte Freisetzung von NO ermöglichen. Dies könnte sich als wertvoll für die zukünftige Aufklärung der Kompartmentalisierung von cGMP erweisen.

List of Publications

Publication 1 (published):

Harnessing self-labeling enzymes for selective and concurrent A-to-I and C-to-U RNA base editing

Anna S. Stroppel, Ngadhnjim Latifi, Alfred Hanswillemenke, Rafail Nikolaos Tasakis, F. Nina Papavasiliou, Thorsten Stafforst, *Nucleic Acids Res.* **2021**, *49*, e95.

Personal contributions: Chemical synthesis of clip, halo, halo-snap, $(halo)_2$, TMR-chloroalkane and TMR-BG. Generation of guideRNAs, with exception of snap-UAG, snap-UAU, snap-CAG_2, snap-CAU and $(snap)_2$-ACC. Cloning of duo constructs and preparation of Flp-In T-REx cell lines. Performance of staining and Western Blotting experiments. Design, execution and analysis of editing experiments, with exception of the experiments for benchmarking with RESCUE. Preparation of RNA samples for whole transcriptome sequencing. Interpretation and discussion of data, together with all authors. Preparation of all Figures, Schemes and Tables, production of Supporting Information, discussion and contribution to manuscript preparation.

Publication 2 (published)

Controlling Site-Directed RNA Editing by Chemically Induced Dimerization

Anna S. Stroppel, Ruth Lappalainen, Thorsten Stafforst, *Chem. – Eur. J.* **2021**, *27*, 12 300 – 12 304.

Personal contributions: Design of duo constructs. Planning, supervision and analysis of experiments conducted by RL, i.e. cloning of duo constructs, preparation of Flp-In T-REx cell lines and snap-GAPDH guideRNA, part of Western Blotting and editing experiments in Figure 3 a, c and partly d. Execution of editing experiments in Figure 3 b, e and partly d and part of Western Blotting experiments. Interpretation and discussion of all data, together with TS. Preparation of all Figures, Tables and of Supporting Information. Contribution to writing of the manuscript and extension of the initial manuscript as requested by reviewers, i.e. primarily addition of experiment for repair of MECP2 R106Q in main text, Figure 3 e and Supporting Information, as well as response to further reviewer inquiries.

Publication 3 (published)

Npom-Protected NONOate Enables Light-Triggered NO/cGMP Signalling in Primary Vascular Smooth Muscle Cells

Anna S. Stroppel, Michael Paolillo, Thomas Ziegler, Robert Feil, Thorsten Stafforst, *ChemBioChem* **2018**, *19*, 1312 – 1318.

Personal contributions: Chemical synthesis and characterization of PYRRO/NO and MeNPOM-PYRRO/NO. Performance and analysis of experiments for investigation of photolytic decay, including determination of deprotection kinetics and Griess assay. Design, execution and interpretation of real-time cGMP imaging experiments and VASP phosphorylation assay, together with MP and TS. Performance and analysis of examination regarding potential cytotoxicity of MeNPOM-PYRRO/NO. Interpretation and discussion of data, together with all authors. Preparation of Schemes and Figures, contribution to writing of the manuscript and production of Supporting Information.

Publication 4 (submitted)

Light-controlled RNA-Targeting with Two Self-Labeling Enzymes

Alfred Hanswillemenke, Tim Stefan Berneiser, Marius Blackholm, Johann Kaiser, Anna S. Stroppel, Karthika D. Kiran Kumar, Thorsten Stafforst.

Personal contributions: Synthesis and characterization of BC-NH_2 and BC-OH (clip). Scientific discussion and chemical advice. Contribution to preparation of Supporting Information (synthesis of BC-OH). Proofreading and discussion of the manuscript and Supporting Information.

Within the framework of the dissertation at hand, the bachelor thesis of Ruth Lappalainen has been supervised scientifically and experimentally. Accordingly, partial results of the work at hand have also been included in said thesis.

1 Introduction

1.1 Labeling and steering of proteins via protein tags

The main aspiration of biochemical research is the understanding and manipulation of chemical processes within living organisms. In order to achieve this, tools for visualization and control of proteins are fundamental. Multiple techniques exist for such purposes, among which labeling of the protein of interest (POI) as a fusion protein with a small protein tag is one of the most broadly applied.[1] Since their genetic encoding guarantees absolute specificity, autofluorescent proteins, such as the green fluorescent protein (GFP), are well suited for specific tagging and visualization of a POI, for instance via fluorescence microscopy.[2]

However, the spectral and biochemical properties of autofluorescent protein tags can only be modified to a limited extent and with considerable effort via laborious protein engineering.[3, 4, 5] Therefore, self-labeling protein tags became established as an even more powerful tool. In this chemical labeling approach, the genetically encoded protein tag fused to the POI reacts with its substrate, which carries an interchangeable label.[6] This allows for labeling with a multiplicity of different organic fluorescent dyes with the desired characteristics, superior fluorescence quantum yield and photostability, and facilely adjustable properties.[7] For example, self-labeling protein tags can also be exploited for the examination of subcellular microenvironments with labels sensitive to signaling molecules[8, 9] or ion concentrations.[10, 11] Additionally, a variety of labels can be attached to the same fusion proteins, thus enabling applications like pulse-chase analyses by successive treatment with substrates carrying different labels.[12, 13] Moreover, entirely different types of labels beyond fluorescent dyes can be transferred to such protein tags, as it was applied in the dissertation at hand with guideRNAs and the three self-labeling protein tags SNAP-tag,[6] CLIP-tag[14] and HALO-tag.[15]

1.1.1 SNAP-tag

While non-covalent chemical labeling strategies such as the tetracysteine tag which complexes with biarsenical compounds[16] had already been applied for fluorescent labeling before, the SNAP-tag was the first covalent self-labeling protein tag described in 2003 by the Johnsson laboratory.[6] It is based on human O^6-alkylguanine-DNA alkyltransferase (hAGT), which plays a major role in the repair of carcinogenic O^6-alkylated guanine in DNA, e.g. introduced by methylating agents.[17] Via its helix-turn-helix motif (HTH), hAGT binds within the minor groove of O^6-alkylguanine-DNA, thereby promoting nucleotide flipping and placement of the alkylated guanine inside hAGT's active site. Transfer of the alkyl group from the guanine to hAGT then takes place via nucleophilic attack of a cysteine residue (Figure 1).[18]

Its unusual stoichiometric and irreversible, covalent mechanism makes hAGT an excellent candidate for development of self-labeling protein tags. Importantly, hAGT also accepts O^6-benzylguanines (BGs) with substituted benzyl rings as substrates and the rate of reaction exhibits little dependency on the substituent. Therefore the SNAP-tag developed

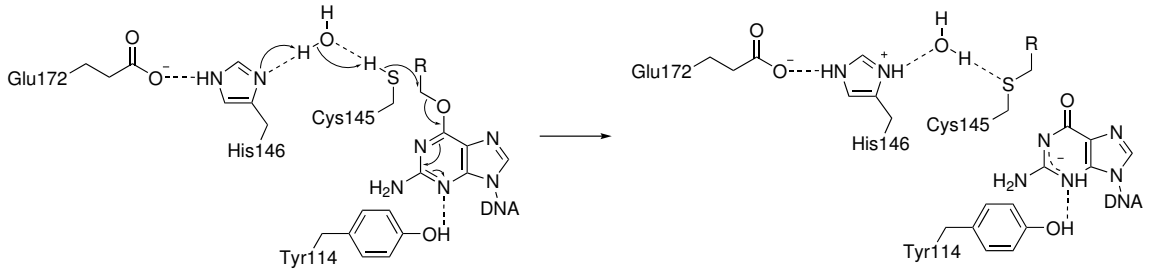

Figure 1. Extrahelical repair of O^6-alkylguanine-DNA by hAGT. Nucleophilicity of the thiol of Cys145 is enhanced by the sequence of hydrogen bonds between Glu172, His146 and an H_2O molecule. The guanine's alkyl substituent is transferred to Cys145 in a S_N2 reaction. The resulting negative charge on the guanine may be stabilized by a neighbouring Tyr114 hydrogen bond donor. Adapted from [18].

from hAGT can mediate labeling of a fused POI with a variety of different labels via BGs derivatized with said labels (Figure 2).[6] Development of the SNAP-tag was conducted via several rounds of directed evolution for optimization of labeling efficiency,[19, 20] resistance to oxidizing environments by substitution of nonessential cysteine residues,[20, 21] suppression of affinity towards alkylated DNA[20, 21] and reduction in size by truncation after residue 182.[21] The resulting SNAP-tag and its variant with faster reaction kinetics, the $SNAP_f$-tag,[22] show labeling rate constants in the range of $10^4 - 10^6\,\mathrm{M}^{-1}s^{-1}$.[23] In the dissertation at hand, all work was carried out with $SNAP_f$-tag, which is referred to as SNAP(-tag) for short in the following.

Figure 2. Labeling of SNAP-tag fusions with BG derivatives. The reactive cysteine residue attacks the BG derivative carrying the desired label. Consequently, the benzyl ring with the attached label is transferred to the SNAP-POI fusion under release of dealkylated guanine.

Notably, BG is cell permeable and derivatives can easily be generated by peptide coupling of a free benzylic amine at BG with activated esters, which are commercially available for a wide variety of organic dyes and other chemical labels. Furthermore, the SNAP-tag can be attached both N- and C-terminally[6, 24] and has been successfully applied for various purposes, including, but not limited to, super-resolution imaging, in vivo imaging, determination of protein dynamics and conformation, protein-protein interaction studies and photocontrolled chemically induced dimerization (see also 1.4).[7, 25]

1.1.2 CLIP-tag

Striving for selective labeling of two proteins at the same time, the Johnsson laboratory developed a second self-labeling protein tag starting from the SNAP-tag, dubbed CLIP-tag. The CLIP-tag reacts with O^6-benzylcytosines (BCs) instead of BGs (Figure 3), which was achieved by mutation of several of the key residues in binding of the guanine via directed evolution and selection for preference of BC over BG.[14] Analogous to the SNAP-tag, a fast variant dubbed $CLIP_f$-tag[22] was developed, which was applied for all experiments in the dissertation at hand.

The CLIP-tag exhibits labeling rate constants in the range of $10^3 - 10^5\,\mathrm{M}^{-1}s^{-1}$, about one

order of magnitude lower than SNAP-tag. The selectivity of the two tags for their respective substrates has been reported as high, though not reaching absolute specificity (Table 1).[23]

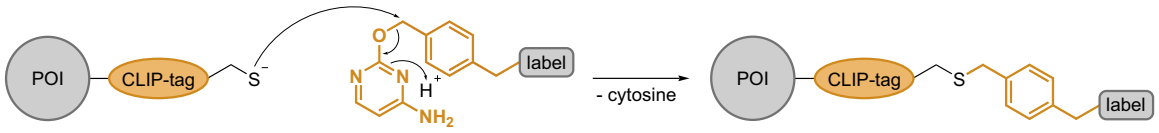

Figure 3. Labeling of CLIP-tag fusions with BC derivatives. Analogous to the SNAP-tag, the reactive cysteine residue attacks the BC derivative and the attached label is transferred to the CLIP-POI fusion under release of dealkylated cytosine.

The CLIP-tag is mainly employed in combination with the SNAP-tag for the originally intended purpose of labeling two proteins concurrently.[26] Applications include dual pulse chase experiments,[27] Förster resonance energy transfer (FRET) sensors for neurotransmitters, so-called Snifits,[28] and selective cross-linking to determine protein interactions (S-CROSS).[29]

Table 1. Selectivity of SNAP- and CLIP-tag. Shown are the labeling rate constants in $\mathrm{M}^{-1}s^{-1}$ of both tags with BG-TMR and BC-TMR.[23]

	BG-TMR	BC-TMR	selectivity
SNAP-tag	10^5	10^2	1000×
CLIP-tag	10^2	10^4	100×

1.1.3 HALO-tag

Independently from SNAP- and CLIP-tag, the HALO-tag was developed from *Rhodococcus* haloalkane dehalogenase (DhaA) by *Promega*.[15] Haloalkane dehalogenases belong to the α/β hydrolase superfamily and catalyze the hydrolysis of various haloalkanes in some prokaryotes' metabolisms. The haloalkanes enter the hydrophobic active site cavity through an access channel and are converted to their respective alcohols via an ester intermediate formed with an aspartate residue (Figure 4[1]).[30]

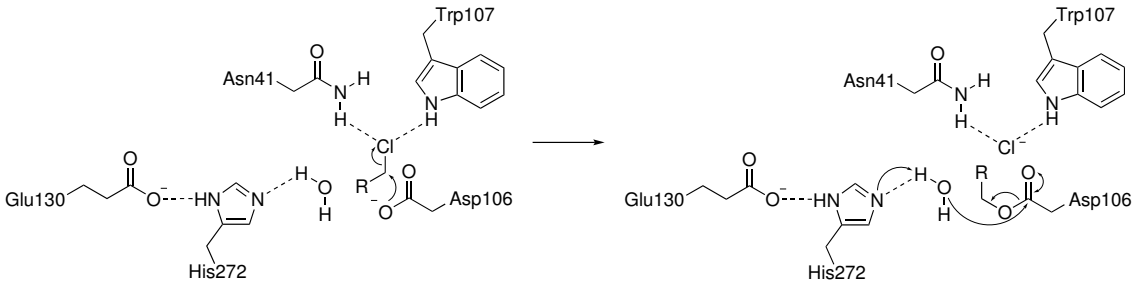

Figure 4. Catalytic hydrolysis of a chloroalkane by DhaA. The alkyl moiety is transferred to Asp106 in an S_N2 reaction and the substituted halide stabilized by Asn41 and Trp107. Nucleophilic Asp106 is subsequently regenerated by base-catalyzed saponification of the resulting ester with His272, assisted by a hydrogen bond from adjacent Glu130. Adjusted from [15].

[1]Note that in [30] amino acid positions are shifted by +11 due to the N-terminal introduction of a His-tag.

In contrast to hAGT, DhaA exhibits a classic catalytic mechanism. Therefore, in order to attain a self-labeling protein tag with stable covalent attachment of the alkyl moiety to the dehalogenase, the histidine residue responsible for ester hydrolysis was mutated. Additionally, engineering towards fast labeling kinetics and optimized expression both as N- and as C-terminal tag was performed via site saturation and random mutagenesis.[31] This yielded the final variant HALO-tag7, generally referred to as HALO-tag for short, with which all work in the dissertation at hand was conducted. As substrates, primary 6-chlorohexyl-PEG_2 moieties attached to the desired label are employed (Figure 5), which can be obtained via straightforward synthesis and are commercially available in a wide variety.[15, 32] In comparison to SNAP- and CLIP-tag, the nature of the attached label has a stronger influence on HALO-tag mediated labeling, with labeling rate constants varying from $10^4 - 10^9\,\mathrm{M}^{-1}s^{-1}$ for different fluorophores and particularly outstanding performance with rhodamine derivatives.[23, 33] Owing to their lower hydrophilicity and smaller size, HALO-tag substrates tend to show higher cell permeability than their respective BG and BC analogues.[23] The HALO-tag (297 aa) itself is of larger size than the SNAP- and CLIP-tag (182 aa), which on the one hand leads to a higher risk of perturbation of the POI's structure and function, but on the other hand, in combination with its net negative charge at physiological pH, enhances the solubility of HALO-tag fusion proteins.[7]

Figure 5. Labeling of HALO-tag fusions with chlorohexane derivatives. The reactive aspartate residue attacks the chlorohexane derivative carrying a PEG_2 linker (omitted for clarity) followed by the desired label. Consequently, the alkyl moiety with the attached label is transferred to the HALO-POI fusion under release of a chloride ion.

Apart from imaging, the HALO-tag has numerous applications, including determination of protein-protein interactions,[7] photocontrolled chemically induced dimerization,[34, 35, 36] redox signaling studies[37] and selective protein degradation with proteolysis targeting chimeras (HaloPROTAC, see also 1.4.2).[38]

1.2 Epitranscriptomics

In analogy to the epigenome, the epitranscriptome comprises co- or posttranscriptionally introduced biochemical variations of ribonucleic acid (RNA). The research area has gained a lot of momentum with the rise of advanced high-throughput sequencing methods over the past decade. Starting with the exploration of modifications in highly expressed non-coding RNAs (ncRNAs), primarily ribosomal RNA (rRNA) and transfer RNA (tRNA), the study of messenger RNA (mRNA) modifications has also been advanced in recent years.[39]

Historically, epitranscriptomic alterations have been grouped into RNA modifications and RNA editing. This classification is not used uniformly and further definitions in the field are also often ambiguous and context-dependent. Keeping this in mind, the division into modifications and editing will be applied in the following for the sake of clear arrangement.

1.2.1 RNA Modifications

RNA modifications include all changes in nucleotides that do not alter the RNA sequence. Almost all classes of RNA are subject to modification to varying extents[40] and to date, more than 170 types of RNA modifications have been reported,[39] a selection of which is depicted in Figure 6. The reported functions of such modifications are manifold and span all aspects of transcriptome processing and turnover, such as regulation of stability and folding, splicing, nuclear export, translation rate, and also stress response and cell differentiation.[39, 40]

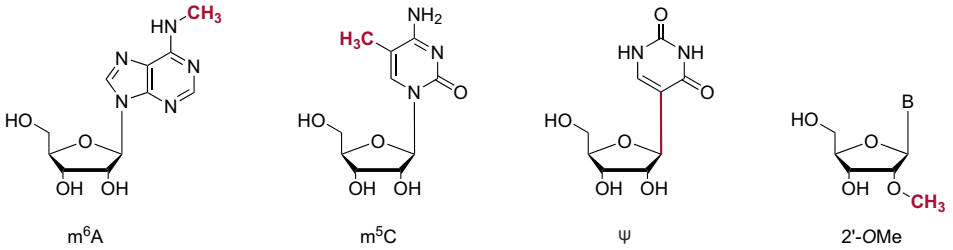

Figure 6. Selection of epitranscriptomic RNA modifications: N^6-methyladenosine (m^6A), 5-methylcytosine (m^5C), pseudouridine (Ψ) and 2'-*O*-methylation (2'-*O*Me).

The modification that was first mapped on mRNA[41, 42] was N^6-methyladenosine (m^6A), which is currently by far the best characterized. It is highly abundant in mammalian mRNA with $0.2 - 0.6\%$ of all adenosines (As) being methylated, predominantly in vicinity of stop codons and 3'-untranslated regions (UTRs).[41, 42] The methylation is carried out by several methyltransferase-like (METTL) enzymes, the writers of this epitranscriptomic mark. The diverse effects of methylation are context-dependently mediated by a variety of different readers.[40] For example, the m^6A binding protein YTH N^6-methyladenosine RNA binding protein 2 (YTHDF2) effectuates the targeted decay of m^6A-modified mRNA.[43] The implementation of m^6A is dynamically regulated and demethylation can be performed by erasers, such as the dioxygenases fatt mass and obesity-associated protein (FTO) and AlkB homolog 5 (AlkBh5).[40] While specific erasers are known to reverse m^6A methylation, it is not yet settled whether RNA modifications are generally actively removed by erasers or if their dynamic nature is rather given by the RNAs' relatively short half-lives.[39]

There is significantly less knowledge on the N^1 isomer of methylated adenosine (m^1A). While its abundance in rRNA and tRNA is well documented, it has been suggested that in mammalian mRNA there are only few m^1A sites, which are modified at ultra-low levels.[44] However, there are still many uncertainties and the frequencies, as well as the regulation and functions of m^1A, remain subject of debate. A plethora of further methylated modifications, such as 5-methylcytosine (m^5C), are being investigated, many of which are poorly characterized so far.[39]

Pseudouridine (Ψ), the C^5-glycoside isomer of uridine (U), is another modification with high abundance in mammalian mRNA. Comparable to m^6A, $0.2 - 0.6\%$ of Us are pseudouridylated.[45] Pseudouridylation is performed by either pseudouridine synthases (PUSs) or by H/ACA box small nucleolar ribonucleoprotein particles (snoRNPs).[40] To date, no readers and erasers have been identified and the mechanisms and functions are not well understood.

Beyond modified bases, nucleosides are susceptible to modifications at the carbohydrate moiety. For example, ribose can be 2'-*O*-methylated (2'-*O*Me), a modification which is introduced by C/D box small nucleolar RNAs (snoRNAs) and mostly found in ncRNA but

also suggested to be present in mRNA in small amounts.[46]

An overarching difficulty is the specific detection and precise mapping of the different RNA modifications. While detection via liquid chromatography-mass spectrometry (LC-MS) provides specificity to the modification in question, it can be challenging to obtain site-specific information. In contrast, high-throughput sequencing allows resolution at single nucleotide level, as well as relative quantification. However, a specific detection method, such as implementation of mismatches, deletions or truncation at modified sites during reverse transcription, has to be established for every single modification. Oftentimes a prior enrichment is carried out, whereby the applied antibodies' cross-reactivity with similar modifications is frequently an issue. Altogether, these hurdles have repeatedly lead to revocation of supposed findings and the research area remains rife with uncertainty.[39]

1.2.2 RNA editing

RNA editing results in a nucleotide sequence which differs from the genetically encoded one. This can either occur through alteration at the base, eliciting the interchange of a nucleotide or, in some cases, through insertion or deletion.[40] By far the most common forms of RNA editing are the deaminations of adenosine (A) and cytidine (C).

Adenosine-to-Inosine editing

Adenosine deamination leads to substitution with inosine (I), a reaction called A-to-I editing, which occurs in double stranded RNA (dsRNA) and is catalyzed by the family of adenosine deaminases acting on RNA (ADARs). ADARs can be found in all metazoa and all types of ADARs contain one or multiple N-terminal double stranded RNA binding domains (dsRBDs) and a C-terminal catalytic domain.[47] In humans, three different ADARs, hADAR1, 2 and 3, exist (Figure 7 a).[47] hADAR1 occurs in two isoforms.[48] The short isoform p110 is constitutively expressed and consists of three dsRBDs and its catalytically active deaminase domain (DD). Furthermore, it contains a bipartite nuclear localization signal (NLS) clasping the third dsRBD and a Z-DNA binding domain (Zβ), which helps targeting nascent RNA substrates that are actively being transcribed.[49] The long isoform p150 is expressed from an alternative, interferon (IFN) inducible promoter and is extended N-terminally by a second Z-DNA binding domain (Zα) and a nuclear export signal (NES), which, in combination with the NLS, leads to shuttling between nucleus and cytoplasm.[50] hADAR2 is composed of a NLS,[51] two dsRBDs and its deaminase domain, hADAR3 additionally carries an N-terminal arginine-rich domain (R) which has been proposed to add single stranded RNA (ssRNA) binding capability[52] as well as act as a NLS.[53] hADAR3 lacks editing activity, and while it is known to be involved in the regulation of the editing active ADARs and affect hippocampal functions,[54] its precise implications remain elusive.[47]

The adenosine deamination reaction catalyzed by ADARs takes place by hydrolysis upon activation of H_2O for nucleophilic attack by a Zn^{2+} ion in the active site (Figure 7 b, c).[56] Substrate selection is determined mainly sequence-independently by structure recognition of dsRNA,[47] conveyed by interactions of the dsRBDs, as well as the RNA binding loop in the deaminase domain, with backbone phosphates and 2'-OHs over a range of approximately 20 nucleotides (Figure 7 d).[55] A crystal structure of hADAR2 DD in complex with a dsRNA mimicking the hemiaminal intermediate identified the interactions between hADAR2's RNA binding loop (aa 454 − 477) and the dsRNA.[55] Although no high resolution crystal structure

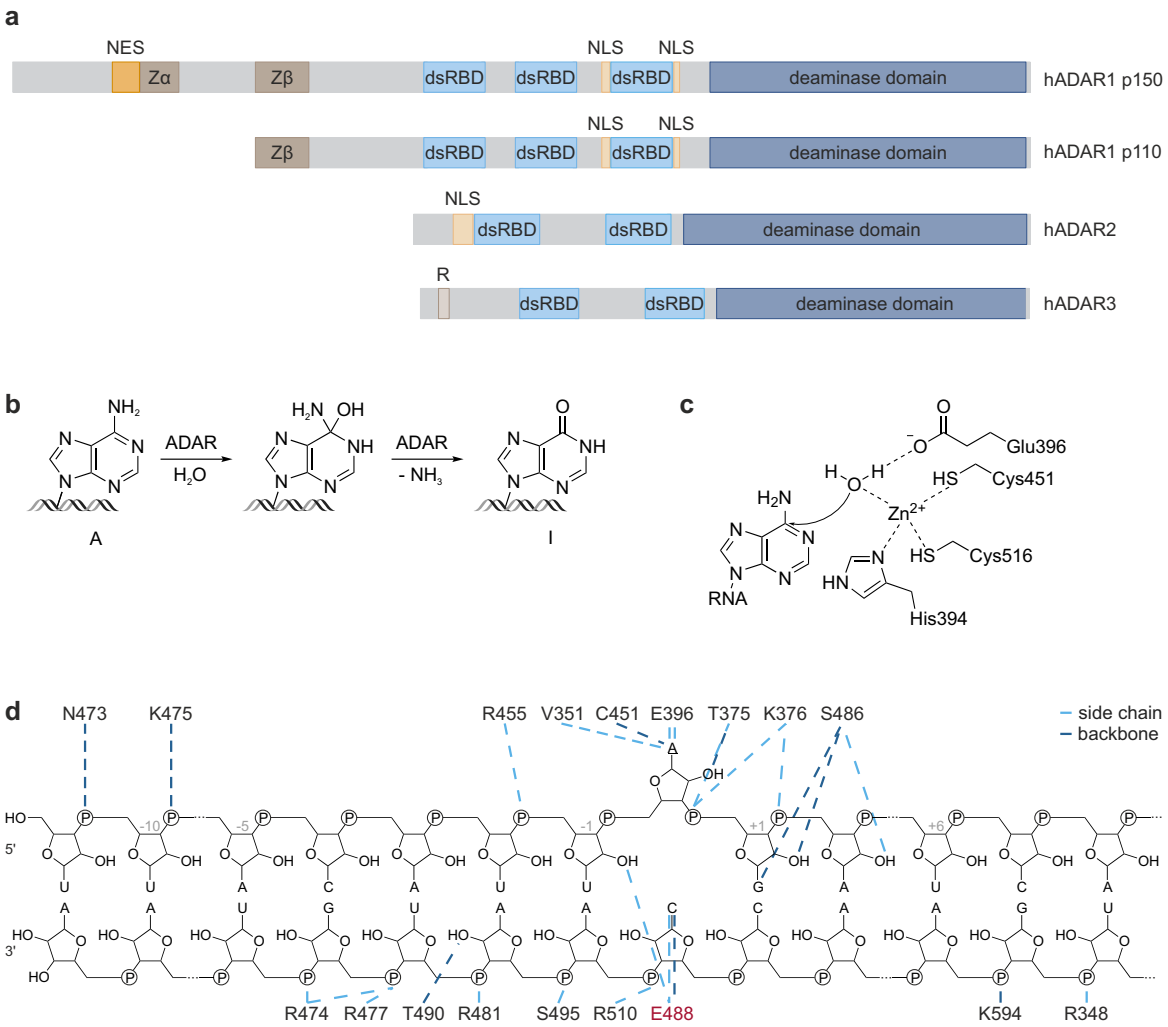

Figure 7. Domain structures of human ADARs and deamination reaction catalyzed by ADARs. **a** Each human adenosine deaminase acting on RNA (hADAR) features a C-terminal deaminase domain, two to three N-terminal double stranded RNA binding domains (dsRBDs) and some form of nuclear localization signal (NLS). The long hADAR1 p150 isoform additionally includes two Z-DNA binding domains (Zα, Zβ) and a nuclear export signal (NES), the short p110 isoform only one Z-DNA binding domain. hADAR3 furthermore contains an arginine-rich domain (R). Domain orders and sizes taken from the National Center for Biotechnology Information (NCBI)[2] and scaled accordingly. **b** ADARs hydrolyze adenosines in dsRNA to inosines via a tetrahedral hemiaminal intermediate. **c** H_2O is activated for nucleophilic attack by a zinc ion coordinated in the active site, as shown here for ADAR2.[55] **d** Interactions between hADAR2 DD and a dsRNA with a covalent hydrate mimicking the hemiaminal intermediate at the edited site (A), as obtained by crystallography.[55] Interactions of the target site, orphaned base in the opposite strand and dsRNA backbone with the indicated amino acids' side chains (light blue) and backbones (dark blue) stimulate base flipping, stabilize the RNA's distorted conformation and induce deamination. The glutamic acid residue in the base flipping loop is highlighted in red, nucleotide positions relative to target sites indicated in grey.

of hADAR1 has been obtained to date, a distinct RNA binding loop has been located.[57, 58] These differences in their RNA binding loops may explain the fact that the endogenous target scope differs for hADAR1 and hADAR2.[58] Furthermore, it has been shown that homodimerization may be crucial for efficient targeting and editing of some substrates.[59] However, the extent and fraction of affected sites for which this is the case remain to be elucidated.

[2] hADAR1 p150: NM_001111, hADAR1 p110: NM_001025107, hADAR2: NM_015833, hADAR3: NM_018702

In nature, ADARs can deaminate adenosines both promiscuously as well as highly selective, depending on the substrate.[47] Typically, RNAs with a long perfectly double-stranded region (> 50 bp) are edited to a high extent, with up to half of all As being deaminated, while in shorter double-stranded segments As are deaminated more selectively.[60] As a result, disruptions in the double-stranded region which frequently occur in endogenous substrates, such as mismatches, bulges and loops, play a major role in site selectivity.

In order to access the target A, ADARs flip the respective base out of the dsRNA helix. In this base flipping mechanism, a glutamic acid residue penetrates the helix, leading to an A accessible for editing and hydrogen bonding of said glutamic acid residue to the thereby orphaned base in the complementary strand (Figure 7 d).[55] Both for hADAR1 and hADAR2, a hyperactive E/Q mutant, E1008Q[61] and E488Q[62] respectively, has been identified. As evident from hADAR2's crystal structure, this corresponds to the residue penetrating the helix and the boosted activity may be attributed to the fact that glutamine is fully protonated at physiological conditions and therefore supports the role as hydrogen bond donor to the orphan base. Since this hydrogen bond is sterically hindered with purines, ADARs favor an AC mismatch or AU base pair at the target site over an AA or AG mismatch.[55]

Moreover, ADARs exhibit preferences for the target A's adjacent bases, specifically its 5' and 3' nearest neighbors (Table 2). These preferences are similar, but distinct for hADAR1 and hADAR2 and mainly determined by the deaminase domain, with minor contributions of the dsRBDs.[63] Altogether, the factors contributing to editing site selectivity are manifold and influenced by both the deaminase as well as the RNA substrate.

Table 2. 5' and 3' nearest neighbor preferences of the deaminase domains of hADAR1 and hADAR2.[63]

	5'	3'
hADAR1 DD	U > A > C > G	G > C > A > U
hADAR2 DD	U > A > C > G	C ∼ G ∼ A > U

Millions of A-to-I sites can be found in metazoan transcriptomes and the effects and functions of ADAR editing activity are manifold. I is translated as G, therefore editing in coding regions of mRNAs can lead to nonsynonymous substitutions, thereby creating altered proteins with different structure or function, and thus contributing to a greatly diversified proteome. Specifically, A-to-I editing can incorporate missense mutations to exchange a variety of amino acids, as well as nonstop mutations. Many of these recoding events occur in mRNAs involved in the nervous system, such as neurotransmitter receptors[64] and ion channels,[65] deriving particular benefit from their dynamic regulation that allows for fine tuning of protein function and adapted response to external stimuli. For example, the first essential A-to-I site characterized in mammals leads to a Q/R mutation in ionotropic glutamate receptor B (GluR-B) and is almost quantitvatively deaminated by ADAR2.[66] Additionally, silent mutations can also influence mRNA fate via the induced structural changes.

The majority of A-to-I editing events in mammals, however, occurs in non-coding regions.[47] A-to-I editing can elicit alternative splicing by creating novel splice donor (GU) or acceptor (AG) sites, and destructing splice acceptor sites and branch point As. Given that splicing and editing transpire contemporaneously, interdependence of the processes has been suggested, for example hADAR2 self-regulates its activity via splice isoforms.[67] Furthermore, editing can impact gene expression by altering microRNA (miRNA) binding sites

in 3'-UTRs, thereby regulating miRNA-mediated silencing. Aside from that, biogenesis of miRNAs themselves can be influenced by editing of the double stranded pri-miRNA precursors.[68] ADARs can also mark RNA for degradation by endonucleases cleaving I containing RNA[69] and excert influence on RNA localization, for instance by retaining dsRNA in the nucleus, thereby impeding undesired translation.[70] ADAR1 p150 plays a crucial role in the regulation of immune responses by marking endogenous dsRNAs to distinguish them from viral dsRNA and consequently averting erroneous activation of the innate immune system by endogenous dsRNA.[47] Generally, ADARs can lead to up- as well as downregulation of genes and control processes not only via their editing activity, but also via their RNA binding capability, for example by competing with other interaction partners, and at times it is challenging to unravel the individual contributions.[47]

Cytidine-to-Uridine editing

Cytidine to uridine deamination (C-to-U editing) occurs in single stranded DNA (ssDNA) as well as RNA and is catalyzed by the activation-induced cytidine deaminase (AID)/apolipoprotein B mRNA editing enzyme, catalytic polypeptide-like (APOBEC) family, comprising AID and APOBECs 1−4 (Figure 8 a). In humans, there are seven APOBEC3 paralogs, namely hAPOBEC3A−H.[71] While all APOBECs except APOBEC2 and 4 exhibit ssDNA editing capability,[72] RNA editing activity has only been found for hAPOBEC1,[73] 3A[74] and 3G.[75] Hundreds of RNA editing sites have been identified, mostly in 3'-UTRs, but also in coding sequences (CDSs).[76] As the ADARs, APOBECs belong to the zinc-dependent deaminase superfamily and all APOBECs share a conserved zinc-dependent deaminase domain (ZDD) (Figure 8 b). While hAPOBEC1 and hAPOBEC3A contain one ZDD, hAPOBEC3G contains two, however, the N-terminal ZDD does exhibit nucleic acid binding ability but no deamination activity.[71] Hydrolytic deamination again takes place via H_2O activation for nucleophilic attack at the target (d)C by a Lewis acidic Zn^{2+} ion that is coordinated through histidine and cysteine residues. Also completely analogous to ADARs, a proximal glutamic acid mediates the required proton shuttling (Figure 7 c).[72]

Due to the potential for aberrant mutational activity by editing of endogenous ssDNA, the expression and subcellular localization of APOBECs need to be tightly regulated, which is performed by different mechanisms depending on the specific APOBEC.[71] hAPOBEC1 contains a NES and a NLS, which allows for shuttling between cytoplasm and nucleus, where editing actively takes place (Figure 8 b).[77] hAPOBEC3A and G are mainly cytoplasmic,[71] for hAPOBEC3G a strong cytoplasmic retention signal (CRS) has been identified, strictly precluding passage to the nucleus.[78]

APOBECs recognize their nucleic acid substrates via ionic interactions between surface areas with positively charged residues and the negatively charged phosphate backbone and additional aromatic stacking interactions of aromatic residues with the nucleic acid bases.[71, 79] APOBEC1 editing of some, but not all, of its targets is cofactor-dependent and while APOBEC1 by itself is little selective for specific RNA sequences, selectivity is gained by such RNA-binding cofactors. To date, two cofactors have been identified for APOBEC1, APOBEC1 complementation factor (A1CF)[80] and RNA-binding protein 47 (RBM47),[81] which target different sets of transcripts[82] but whose precise interdependence is yet to be unraveled. Early on, a mooring sequence 3' of the targeted C consisting of 11 nucleotides has been found to recruit A1CF to RNA substrates,[83] and a preference for AU rich regions has been proposed.[84] A recent crystal structure for hAPOBEC1 in combination with structure-guided mutagenesis suggests Trp121 may contribute to APOBEC1's substrate recognition of

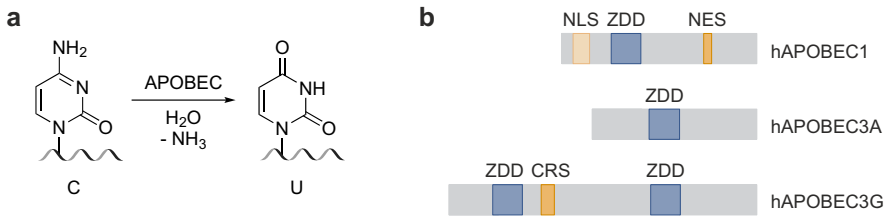

Figure 8. Deamination reaction catalyzed by APOBECs and domain structures of human APOBECs capable of RNA editing. **a** APOBECs hydrolyze cytidines in ssDNA and RNA to uridines. **b** hAPOBEC1 and hAPOBEC3A contain one catalytically active zinc-dependent deaminase domain (ZDD), hAPOBEC3G two ZDDs, of which only the C-terminal possesses catalytic activity. hAPOBEC1 contains an N-terminal NLS as well as a C-terminal NES and shuttles between nucleus and cytoplasm, hAPOBEC3G is strictly retained in the cytoplasm by a cytoplasmic retention signal (CRS). Domain sizes taken from National Center for Biotechnology Information (NCBI)[3] and scaled accordingly.

RNA over DNA by hydrogen bonding with 2'-OH.[76] Concerning APOBEC3s, it remains to be determined whether cofactors also play a role in substrate selection. APOBEC3A and G exhibit a preference for RNA deamination of Cs in the loop region of hairpins with stable stem structures,[85] with rather lax nearest neighbor preferences.[71]

APOBECs form a variety of homo- and heterooligomers, mediated either directly via protein-protein interactions or indirectly via additional nucleic acid interactions or zinc ions.[71] Oligomerization may have multiple functions, for example regulation of subcellular localization and catalytic activity. The crystal structure of hAPOBEC1 shows that the unique APOBEC1 C-terminal hydrophobic domain (A1HD) folds back onto its deaminase domain, which allows for both internal hydrophobic packaging as well as mediates homodimerization.[76] While A1HD is essential for RNA editing activity, dimerization is not and might instead prevent aggregation.[76] In general, owing to the multitude of APOBEC enzymes and their differing mechanisms for steering of the various aspects of editing activity, many details remain unclear and are yet to be explored.

The functions of APOBECs are not yet fully investigated, but it is clear that C-to-U RNA editing affects mRNA localization, stability and translation. APOBEC1 activity was first discovered for editing of *apolipoprotein B* (*ApoB*) mRNA.[73] *ApoB* is edited in small intestine, resulting in a Q/X mutation and therefore expression of truncated ApoB 48 protein, whereas full length ApoB 100 is expressed in liver. Due to apolipoproteins' role in the formation of plasma-lipoproteins for transport of water-insoluble lipids and cholesterol, APOBEC1 consequently is important for a functioning lipoprotein metabolism. *ApoB* editing is cofactor-dependent and, contrary to APOBEC1 itself, *A1CF*[86] and *RBM47*[81] are essential genes, indicating further implications of said RNA-binding proteins. The key function of APOBEC3s lays in the innate immune response to retroviruses and endogenous retroelements by hypermutation of the viral genome.[79] Beyond that, little is known of the implications of APOBEC3 editing. Comprehension of correlations is complicated by the interplay of ssDNA and RNA editing activity. For example, it has been suggested that RNA-binding may competitively inhibit ssDNA editing.[87] Furthermore, as for ADARs, APOBECs can also act via their nucleic acid binding capability independently from their editing activity, for instance by increasing mRNA stability by binding to their AU rich 3'-UTRs.[88] Overall, APOBECs are far from being exhaustively explored and further studies are needed.

[3] hAPOBEC1: NM_001304566, hAPOBEC3A: NM_145699, hAPOBEC3G: NM_001349436

RNA editing in human pathology

Numerous associations between RNA modifications and disease have been identified. Dysregulation of epitranscriptomic marks, like methylation, pseudouridylation and RNA base editing, is linked to various kinds of cancers.[89] These dysregulations may be represented by altered expression, catalytic activity or mutations of epitranscriptomic writers, readers or erasers and oftentimes it is not yet settled whether they are driving forces or downstream consequences of oncogenesis. In regard to RNA base deamination, hyper- or hypoediting has been recorded in a wide variety of cancers and altered expression and activity levels of ADARs and APOBECs are tied to tumorigenesis. In accordance with the different ways of function, editing can influence tumorigenesis in several possible manners. Recoding editing events may lead to activation of oncogenes, inactivation of tumor suppressor genes or even expression of new proteins with oncogenic characteristics. Furthermore, tumor-specific protein isoforms can emerge from editing induced alternative splicing and changes in miRNA binding sites or miRNA biogenesis can give rise to anomalously altered expression of oncogenes.[47, 90] Especially for APOBEC3s, dysregulated localization further contributes to tumorigenesis as a consequence of their intrinsic mutagenic activity on genomic DNA. Beyond that, downregulation and mutations in APOBEC1's cofactor RBM47 are also affiliated with cancer.[91]

Besides, RNA editing is dysregulated in several maladies of the central nervous system (CNS). Hypoediting at the aforementioned essential Q/R site of *GluR-B* by ADAR2 increases Ca^{2+} influx and results in epilepsy and, depending on the extent of reduced editing, early postnatal death.[92] Furthermore, it has been proposed to lead to progressive degeneration of motor neurons in amyotrophic lateral sclerosis (ALS).[93] Notably, APOBEC1 editing of cerebral *glycine receptor* (*GlyR*) is linked to epilepsy as well.[94] Multiple psychiatric disorders, such as anxiety, depression and schizophrenia are associated with dysregulated editing of *2C subtype of serotonin receptor* (*5-$HT_{2C}R$*). In suicidal patients, excessive A-to-I editing of *5-$HT_{2C}R$*[93] and C-to-U editing of *tryptophane hydroxylase 2* (*TPH2*)[95] have been found to interfere with serotonin signaling. Furthermore, hyperediting of *5-$HT_{2C}R$* also contributes to Prader-Willi syndrome (PWS), a condition characterized by hyperphagia and diabetes.[96] Additionally, the dysregulation of the ratio between full length ApoB 100 and truncated ApoB 48 is linked to obesity and diabetes, as well as atherosclerosis.[90]

Consistent with ADAR1's function in innate immunity, aberrant editing activity and mutations in ADAR1 itself are involved in several autoimmune disorders. For example, hypoediting is observed in psoriasis patients,[97] while hyperediting, particularly in *Alu* elements, is reported in systemic lupus erythematosus (SLE), a multisystemic autoimmune disease.[98] Moreover, dyschromatosis symmetrica hereditaria (DSH), a skin condition with pigmentation defects, is caused by a multitude of mutations in *ADAR1*[47] and in the inflammatory neurodevelopmental Aicardi-Goutières syndrome (AGS) several genes, including *ADAR1*, carry mutations.[99] While less is known about APOBECs, IFN stimulated APOBEC3s also seem to be involved in autoimmune pathologies, as has been suggested by increased expression and editing activity in SLE patients.[98]

1.2.3 Therapeutic potential of RNA-based technologies

The application of RNA oligonucleotides to cure or alleviate maladies is an attractive approach. Watson Crick base pairing allows for rational design of antisense oligonucleotides

(ASOs) that base pair very specifically to a desired target RNA. In contrast to gene therapy targeting DNA, no permanent off-target mutations arise when operating on the RNA level, thereby significantly reducing the risk of permanent unwanted side effects. In addition to its transient nature, RNA targeting is also tunable, if needed, and RNA is accessible more easily than the tightly packed DNA.

ASOs can be administered systemically, e.g. by intravenous or subcutaneous injection, as well as locally, e.g. by intramuscular or intravitreal injection or by inhalation.[100] Subsequently, ASOs need to be delivered to their site of action, which can be performed by multiple technologies. Importantly, in the process RNase-mediated degradation of the ASOs needs to be averted and endosomal release promoted. In lipid nanoparticles (LNPs), the negatively charged oligonucleotides are encapsulated in cationic or ionizable lipids, a method that improves cellular uptake and has recently received attention for the use in mRNA vaccines.[101] The uptake in hepatocytes is particularly favored with ionizable LNPs, since they bind to apolipoprotein E (ApoE) and are consequently integrated via the ApoE receptor at the hepatocytic cell membrane.[102] An alternative delivery method to hepatocytes exploits their asialoglycoprotein receptor (ASGPR), which is able to internalize oligonucleotides carrying *N*-acetylgalactosamine (GalNAc) residues.[103] Moreover, encodable ASOs can be delivered by viral vectors, such as adeno-associated viruses (AAVs).[104]

ASOs are often chemically modified at the ribophosphate backbone to improve their characteristics for therapeutic application. For example, target affinity can be augmented by 2'-*O*Me, 2'-*O*-methoxyethyl (2'-MOE), 2'-F, locked nucleic acids (LNAs) and peptide nucleic acids (PNAs). Furthermore, most of these modifications (2'-*O*Me, 2'-MOE, LNA, PNA) additionally enhance RNA stability, as do phosphorothioates (PTOs), which also facilitate cellular uptake. Immunogenicity can also be reduced by implementation of modifications such as 2'-*O*Me, 2'-MOE, PTO and PNA.[100, 105]

Several types of RNA oligonucleotides have been approved by the FDA for therapeutic use.[100] Firstly, small interfering RNAs (siRNAs) can be applied to silence gene expression by base pairing to a target mRNA and thereupon recruiting RNA-induced silencing complex (RISC) and initiating RNA interference (RNAi).[106, 107] Secondly, gapmers can elicit degradation of a target mRNA by RNase H.[108] Gapmers are chimeric ASOs, whose ribonuclear basic structure is interrupted by four deoxyribonucleotides in the center. RNase H1 is fetched by RNA-DNA duplexes and consequently cleaves the target mRNA. Thirdly, ASOs can also be employed to sterically block splicing in order to correct splicing defects by binding at intron-exon junctions.[109]

Beyond these modes of action, the targeting of RNA modifications that are introduced via RNA-steered mechanisms is a promising approach to tackle treatments on a single nucleotide level. This is particularly attractive since almost 60 % of the approximately 55 000 mutations known to cause diseases are point mutations.[110] On the one hand, this includes RNA modifications mediated by snoRNAs, namely Ψ and 2'-*O*-methyl (2'-*O*Me), on the other hand A-to-I and C-to-U RNA editing. snoRNAs guide the site-selective introduction of a modification by binding their target RNA via an antisense moiety ($10 - 20$ nt) and assembly of at least four core proteins to form a snoRNP, which then implements the modification. Pseudouridylation is conveyed by H/ACA box snoRNAs, which are composed of a hairpin structure, followed by a single stranded hinge containing the H box motif, another hairpin and a single stranded tail containing the ACA box motif. Each of the hairpins contains a pseudouridylation pocket, i.e. a loop with complementary sequence to the target RNA that determines the pseudouridylation site.[111] Since pseudouridylation of the inital U of premature stop codons (PTCs) results in readthrough during translation and averts

nonsense-mediated decay, this could be exploited for treatment of diseases caused by nonsense mutations.[112] 2'-*O*-methylation is mediated by C/D box snoRNAs, in which two single stranded regions that are complementary to the target RNA are framed by the C and less conserved D' box motives or D and less conserved C' box motives, respectively.[113] Targeted 2'-*O*-methylation could be utilized to block pathogenic splicing by masking the branch point 2'-OH imperative for the initial lariat formation during splicing.[114]

Site-directed RNA editing (SDRE) represents an even more powerful tool. More than half of the disease-causing point mutations are G-to-A or T-to-C substitutions and are thus susceptible to restoration by A-to-I or C-to-U editing.[110] The first SDRE was reported in 1995, where it was applied for repair of a UAG PTC in *dystrophin* mRNA, which is associated with muscular dystrophy, *in vitro* and in one-cell stage *Xenopus* embryos.[115] In the past decade, SDRE has evolved into a very active and dynamic field of research. Multiple new methods and substantial developments of established systems emerged recently during the course of the dissertation at hand. To provide an overview of the current state of affairs, the most prominent techniques are briefly presented in the following.

Site-directed A-to-I RNA editing

Among the systems for A-to-I RNA editing reviewed below, all apply a C as counter base to the target A, consistent with ADAR's preference for an AC mismatch at the target site. Several biotechnology companies have emerged from these systems, contributing to the preclinical and clinical development of medical applications of site-directed A-to-I RNA editing.

Recruitment of engineered ADARs

In order to intercept the natural substrate selection of ADARs and render the editing activity site-specific in a targetable way, several engineered ADAR deaminases have been developed (Figure 9).

SNAP-ADAR The first SDRE approach following the initial report in 1995 was the SNAP-ADAR system, which was developed by the Stafforst group in 2012 (Figure 9 a).[116] Here, ADAR's natural dsRBDs are substituted with the SNAP-tag, resulting in a C-terminal fusion of the ADAR deaminase domain ($ADAR_{DD}$) to the SNAP-tag. The SNAP-tag reacts covalently with BGs carrying a 5'-coupled 22 nucleotide (nt) ASO as substituent. These so-called snap-guideRNAs (gRNAs) assemble the required double stranded secondary structure as well as recruit the deaminase domain to the desired target site. In the original publication, the deaminase domain of hADAR1 was employed,[116] and in the following, the system was readily adopted and extensively characterized with application of ADAR2,[121] ADAR1Q and ADAR2Q.[122, 123] While the snap-guideRNAs are not genetically encodable, their shortness allows for efficient transfection with well established technologies. Chemical modification of the guideRNAs in an antagomir[124]-inspired pattern significantly enhances their stability against nucleases, cellular uptake and target selectivity. Specifically, all ribonucleotides except the three nucleotides around the target counter base are 2'-*O*-methylated (2'-*O*Me) and termini are stabilized by phosphorothiolation (PTO, 2 at 5'-terminus and 4 at 3'-terminus).[121] Bystander editing in the gRNA/mRNA duplex,[121] and even at the nearest neighbors of the target A,[123] can be impeded by sequence optimization[125] and chemical modification of the guideRNAs.[121, 123] Single copy genomic integration of SNAP-ADARs has been achieved by application of the Flp-In T-REx system and leads to controlled, tetracycline inducible, homogeneous expression at lower, thus closer to endogenous, expres-

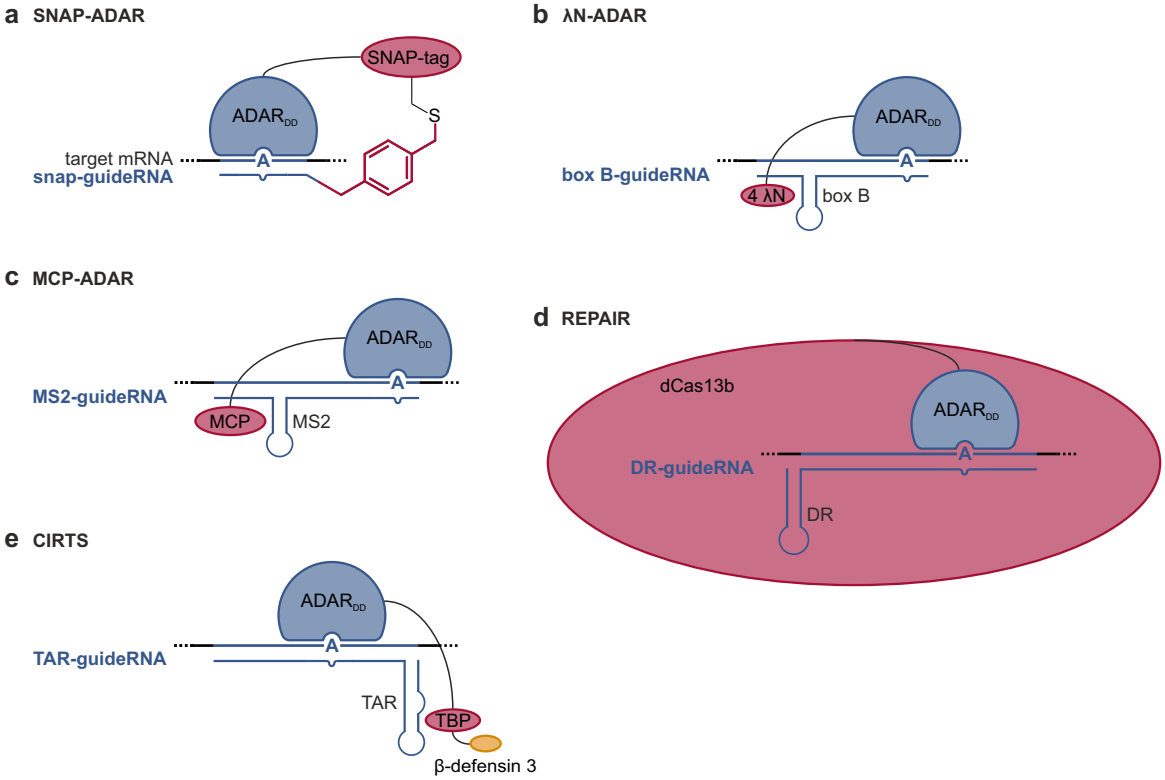

Figure 9. Systems for site-directed A-to-I RNA editing via recruitment of engineered ADARs. In all systems, guideRNAs form an AC mismatch at the target site. **a** The SNAP-ADAR platform utilizes the reaction of the SNAP-tag (182 aa) with O^6-benzylguanines (BGs). The 22 nt long, chemically modified snap-guideRNAs carry a BG at the 5' end and thus covalently bind to the SNAP-tag, thereby directing the editing to the target site.[116] **b** In the λN-ADAR system, editing is directed by interaction of one to four λN peptides (22 aa each) with guideRNAs containing one or two box B hairpins. In the depicted version with one box B motif, the hairpin is positioned 19 nt 5' of the target A and the total length of the guideRNA is ∼55 nt.[117] **c** Analogous to the λN system, the interaction between MCP (129 aa) and MS2 RNA hairpins (six applied, only one depicted for clarity) can also be utilized to direct editing.[118] **d** REPAIR steers editing activity via a catalytically inactive Cas13 (1135 aa), which binds to guideRNAs containing a DR region. The length of the antisense region ranges from 30 to 84 nt, the total length of a guideRNA with the mainly applied 50 nt antisense region is ∼85 nt.[119] **e** The CIRTS system exploits the interaction between TBP (100 aa) and guideRNAs carrying one or two TAR hairpins for recruitment of deaminase activity. The guideRNA's antisense region is furthermore stabilized by the ssRNA binding β-defensin 3 and the total length of the 1 TAR guideRNA is ∼75 nt.[120] Relative sizes of protein domains and guideRNAs to scale, respectively.

sion levels of the enzyme compared to transient transfection.[122, 123] Efficient editing is still achieved at these expression levels with the covalent guideRNA-SNAP-ADAR conjugates. Genomic integration as well as the short length of the applied guideRNAs result in moderate transcriptome-wide off-target editing, which mainly arises guideRNA-independently from the expression of the engineered ADAR.[123]

The SNAP-ADAR system has been implemented in mammalian cell culture,[121] as well as in one cell zygotes of the marine annelid *Platynereis dumerilii*.[126] It has been applied for editing of endogenous signaling transcripts *Kirsten rat sarcoma virus* (*KRAS*) and *signal transducer and activator of transcription 1* (*STAT1*) with medium to high editing yields (50 % – 75 %),[123] as well as for the N- and C-terminal integration of localization signals by editing of start and stop codons.[122] This allowed not only subcellular protein translocation from cyto- to nucleoplasm, but also the more challenging cotranslational isoform switch from cytoplasmic to outer membrane localization. Furthermore, a photoprotected BG derivative can be readily coupled to a fully synthesized guideRNA, which has been exploited for on-

switch of RNA editing upon irradiation with UV-light (see also 1.3.1).[126]

λN-ADAR Shortly after the first publication of the SNAP-ADAR system, the Rosenthal group reported a similar approach for site-directed A-to-I editing with an engineered ADAR in 2013 (Figure 9 b).[117] In this system, the deaminase domain of hADAR2 is fused to the small λN peptide, i.e. the RNA-binding domain of λ bacteriophage antiterminator protein N. The λN peptide selectively binds to the box B motif, a 19 nt RNA hairpin,[127] and guideRNAs consisting of a box B and an antisense moiety are able to recruit the deaminase domain to a target adenosine. Editing efficiencies were later on improved by fusion of four λN peptides, application of ADAR2Q, and inclusion of a second box B motif in the guideRNA.[128] The system elicits considerable bystander and transcriptome-wide off-target editing, which can be reduced to a certain extent by nuclear localization of the editase.[129] Since all components are genetically encodable, they can be delivered by transient plasmid transfection[117, 128, 129] as well as AAV transduction.[130, 131] Quite recently, the λN-ADAR platform has been employed for repair of a mutation in *methyl CpG binding protein 2* (*MECP2*) implicated with Rett syndrome *in vivo* in murine neural cells, achieving roughly 50 % editing yield and restored protein function.[131]

MCP-ADAR Similarly, the interaction of MS2 bacteriophage coat protein (MCP) with a 21 nt MS2 RNA hairpin motif has also been exploited for SDRE (Figure 9 c). In the original publication from 2017, the deaminase domain of ADAR1 was fused to MCP and recruited by a guideRNA containing an antisense moiety and six MS2 hairpins for repair of a PTC in *eGFP* mRNA with 5 % editing yield.[118] The system was recently extended to ADAR2 and characterized in regard to optimal length of the antisense region, implementation of MS2 hairpins on both sides of the antisense moiety, hyperactive ADAR E/Q variants and localization.[132] While this resulted in moderate editing yields on endogenous mRNAs, comparably high transcriptome-wide off-target editing was observed, likely due to unspecific binding of MCP to various RNA structures.[133] In the same study, MCP-ADAR1Q was applied *in vivo* in the *mdx* mouse model for Duchenne muscular dystrophy, which yielded ∼3 % repair of a PTC in *dystrophin* mRNA and small amounts of restored protein.[132]

REPAIR Another system dubbed RNA Editing for Programmable A to I Replacement (REPAIR) was developed by the Zhang group in 2017[119] and exploits the RNA-binding ability of CRISPR-associated protein (Cas) 13 (Figure 9 d). Specifically, a catalytically inactive mutant of Cas13b from *Prevotella spp.*, dCas13b, is fused to the deaminase domain of ADAR2Q. Recruitment of deaminase activity occurs by guideRNAs containing a direct repeat (DR) stem-loop forming region for Cas binding and an antisense region, ranging from 30 to 84 nt. The system was applied to endogenous targets and transiently expressed disease-relevant transcripts, yielding moderately high editing efficiencies. The considerable bystander and off-target editing events could be vastly reduced in REPAIRv2 by implementation of a T375G mutation in the deaminase domain, however, at the expense of reduction in on-target editing as well.[119] Due to the large size of dCas13b, delivery for therapeutic application might be challenging, for example, the REPAIR construct can not be packaged into AAV without preceding size reduction.[119]

CIRTS The CRISPR-Cas-Inspired RNA Targeting System (CIRTS) developed by the Dickinson group in 2019 encompasses multiple platforms with modular composition for the steering of different RNA effector proteins by guideRNAs (Figure 9 e).[120] All CIRTS com-

prise a positively charged protein for non-specific ssRNA binding, a RNA hairpin binding protein and an effector protein mediating the desired effect on the target RNA. Recruitment to the target RNA is carried out by a guideRNA containing the cognate RNA hairpin (16 – 31 nt) and an antisense region (20 – 40 nt), which is stabilized by weak interaction with the ssRNA binding domain. In the original publication, CIRTS-7 and -8, comprising the hADAR2 or hADAR2Q deaminase domain as effector domain, respectively, were applied for A-to-I editing in a dual-luciferase assay.[120] The positively charged β-defensin 3 serves as ssRNA binding domain and a TAR-binding protein (TBP), engineered to bind the HIV trans-activation response element (TAR) hairpin (31 nt) as guideRNA interacting domain. Some CIRTS are entirely of human origin, which minimizes immunogenic potential, but also bears the risk of interference with endogenous targets. In a very recent extension, the CIRTS system was put under the control of chemically induced dimerization (CID) upon induction with abscisic acid (ABA, see also 1.4).[134] After the implementation of a guideRNA carrying two trans-activation response element (TAR) hairpins, low editing levels on endogenous targets were obtained and the system subsequently applied for editing of a luciferase reporter *in vivo* in mice.

Recruitment of wild-type ADARs

While engineered ADARs have grand strengths concerning high efficiency, variability and optimization potential, thus providing excellent tools for basic research, global off-target editing elicited by ectopic expression of a deaminase poses a challenge. For clinical application, it is thus desirable to also work towards guideRNAs that enable harnessing of wild-type (wt), and eventually endogenous ADARs. Besides restraining off-target sites, this might also reduce the immunogenic potential, as well as facilitate delivery, e.g. via viral vectors, since only the small guideRNAs need to be introduced.

R/G motif-guideRNAs In 2017, the Stafforst group achieved SDRE by recruitment of full-length wild-type hADAR2 for the first time (Figure 10 a).[135] The guideRNA design is modeled on a well-known natural ADAR2 target site in *glutamate receptor B* (*GluR-B*), dubbed R/G site, since A-to-I editing results in a R/G mutation.[139] At the R/G site, a cis-located intron folds back on the preceding complementary exon, generating an imperfect hairpin structure called R/G motif. ADAR2 is then recruited to the formed double-stranded secondary structure via its dsRBDs and consequently selectively deaminates the adenosine at the R/G site.[140] This modality was now exploited for the site-directed recruitment of wt hADAR2 by imitating the R/G site's secondary structure by trans-acting guideRNAs containing the 45 nt R/G stem-loop structure motif and a 16 nt antisense region complementary to a given target mRNA.[135] GuideRNA design was optimized regarding the position of the target site inside the double-stranded structure,[135] substitution of A/U base pairs in the R/G motif with G/C base pairs[141] and inclusion of a box B motif at the 3'-terminus for stabilization.[135] R/G motif-guideRNAs have been applied for repair of a mutation in *PTEN-induced kinase 1* (*PINK1*) that disturbs mitochondria turnover and is linked to hereditary early onset Parkinson's disease, and achieved restored protein function and rescued mitophagy. Due to their genetic encodability, R/G motif-guideRNAs can be delivered by plasmid transfection, as well as AAV transduction. This enables straightforward transfer to *in vivo* application, as demonstrated by repair of a splice donor site mutation in *ornithine transcarbamylase* (*OTC*) pre-mRNA in the spf^{ash} mouse model for OTC deficiency with ∼ 5 % editing efficiency and partial protein restoration.[132]

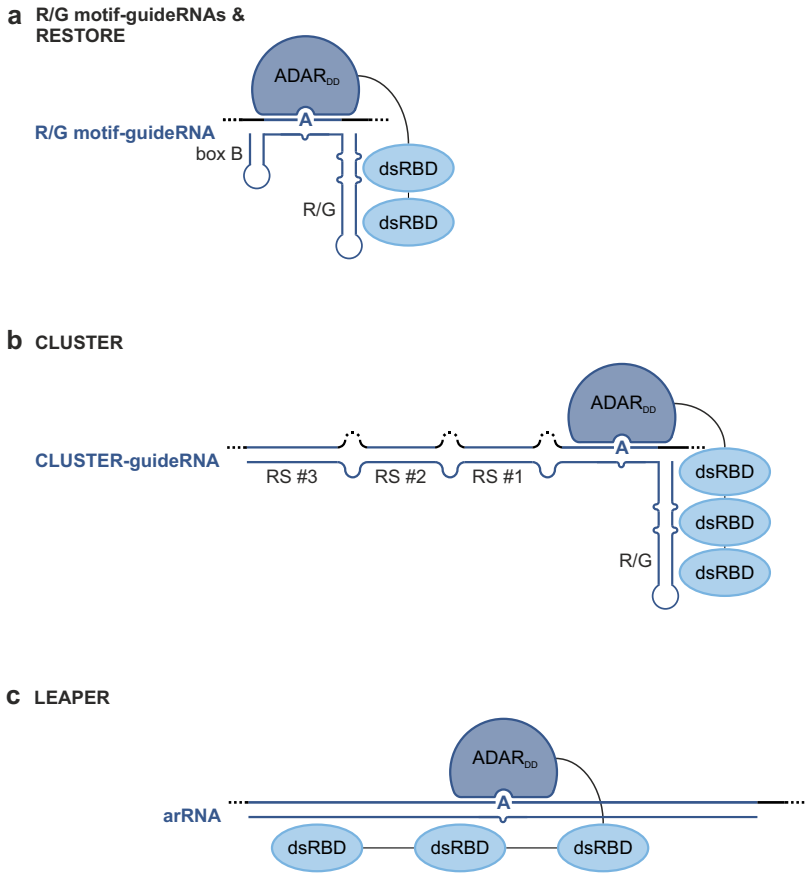

Figure 10. Systems for site-directed A-to-I RNA editing via recruitment of wt ADARs. In all systems, guideRNAs form an AC mismatch at the target site. **a** Wt ADAR2 can be recruited via its natural dsRBDs (∼200 aa each) with R/G motif-guideRNAs. The depicted guideRNA consists of the 45 nt R/G motif as ADAR recruiting domain, a 16 nt antisense specificity domain and an optional box B motif for stabilization, amounting to ∼60 – 85 nt guideRNA length.[135] In the related RESTORE system, endogenous ADAR1 p150 is recruited with chemically modified guideRNAs of analogous structure.[136] **b** Genetically encodable CLUSTER-guideRNAs carry an additional cluster of recruitment sequences (RSs) and enable efficient recruitment of endogenous ADAR1 p110. Typical CLUSTER-guideRNAs contain three RSs with 20, 15, 15 nt, respectively, and a 20 nt specificity domain, amounting to a total guideRNA length of ∼135 nt. Short (15 – 62 nt) and long (375 – 460 nt) distances between the target mRNA's RS binding sites are accepted.[137] **c** In the LEAPER system, arRNAs, consisting of a plain antisense oligonucleotide, form a long double-stranded structure around the target A, thereby harnessing endogenous ADAR1. The arRNAs' length typically varies between 111 nt (depicted here) and 151 nt.[138] Relative sizes of protein domains and guideRNAs to scale, respectively.

RESTORE A further development of the R/G motif-guideRNAs, published by the Stafforst group in 2019 and dubbed RESTORE (Recruiting endogenous ADAR to specific transcripts for oligonucleotide-mediated RNA editing), even allows for the recruitment of endogenous hADAR1 (Figure 10 a).[136] Based on the observation that R/G motif-guideRNAs are also capable of harnessing ADAR1 to some extent,[141] the R/G motif was engineered toward recruitment of ADAR1. As before, the resulting ASOs consist of an invariant ADAR recruiting domain, deduced from the R/G motif, and an antisense region called specificity domain.[136] In contrast to the R/G motif-guideRNAs before, RESTORE ASOs are chemically stabilized with 2'-*O*Me and PTO modifications, employing the same modification pattern for the specificity domain as for snap-guideRNAs in the SNAP-ADAR system. Further chemical modification, as well as lengthening of the specificity domain, allow for enhancement of target affinity. Since no ectopic expression of any deaminase is required, the system attains

excellent specificity, as reinforced by the virtual absence of transcriptome-wide off-target sites. Recruitment of endogenous ADAR1 with RESTORE has been achieved in a variety of immortalized human cancer cell lines, as well as human primary cells from different tissues. Editing is mainly performed by the IFN inducible ADAR1 p150 isoform and thus editing efficiencies can be boosted by simple IFNα treatment. RESTORE has been applied for editing *STAT1* mRNA in primary fibroblast, reaching ∼ 20 % editing yield without and ∼ 30 % with IFNα induction. Furthermore, repair of the E342K PiZZ mutation in *serpin family A member 1* (*SERPINA1*) mRNA, which causes α_1-antitrypsin (A1AT) deficiency, was achieved with up to 20 % yield in HeLa cells.[136]

CLUSTER-guideRNAs Very recently, efficient harnessing of endogenous ADAR with genetically encodable CLUSTER-guideRNAs was reported, again by the Stafforst group (Figure 10 b).[137] In addition to the previously established R/G motif as ADAR recruiting domain and an antisense region as specificity domain, CLUSTER-guideRNAs contain a 3' cluster of single stranded recruitment sequences (RSs) complementary to binding sequences with flexible distribution over the target mRNA, which significantly enhance binding affinity. Positioning of the RS is optimized *in silico* with the custom developed recruitment cluster finder tool for minimization of bystander editing as well as inhibitory secondary structure of the guideRNA. The system was meticulously investigated by means of a dual-luciferase assay, which brought forth a design with three RSs with a length of 20, 15 and 15 nt respectively, with considerable flexibility in terms of positioning, and a 20 nt specificity domain. Excellent specificity with very little bystander and transcriptome-wide off-target editing is achieved. Unlike RESTORE-guideRNAs, CLUSTER-guideRNAs mainly recruit the constitutively expressed ADAR1 p110 isoform. Furthermore, their genetic encodability allows for viral delivery, as demonstrated by editing upon adenoviral transduction in mutliple difficult-to-transfect cell lines. CLUSTER-guideRNAs have also been applied for repair of a PTC in *α-L-iduronidase* (*IDUA*) in patient fibroblasts, which is linked to Hurler syndrome, the most severe form of Mucopolysaccharidosis type I (MPS I), caused by IDUA deficiency. 24 % editing yield and enzyme activity at the level of the significantly milder Scheie syndrome were achieved with CLUSTER-guideRNAs in the form of chemically synthesized ASOs. Moreover, plasmid-borne CLUSTER-guideRNAs have been employed *in vivo* in wt mice for editing of a dual-luciferase reporter upon hydrodynamic tail vein injection with ∼ 10 % editing yield.[137]

LEAPER The LEAPER (Leveraging endogenous ADAR for programmable editing of RNA) system, published in 2019 by the Wei group, exploits the formation of long double-stranded guideRNA/mRNA duplexes for recruitment of endogenous ADAR1 (Figure 10 c).[138] The guideRNAs, dubbed ADAR recruiting RNAs (arRNAs), consist of one plain antisense moiety of typically 111 nt or 151 nt length, with a single AC mismatch in the center defining the target site. While very minor transcriptome-wide off-target editing occurs, substantial bystander off-target editing within the long double-stranded region has been observed. To an extent, bystander sites can be suppressed by implementation of AG mismatches, however, at times, at the expense of significant reduction in on-target efficiency.[138] In comparison to CLUSTER-guideRNAs, similar on-target efficiencies were achieved with LEAPER, though with considerably more bystander editing.[137] On the one hand, genetically encoded arRNAs have been delivered to human embryonic kidney 293 cells (HEK 293) by lentiviral transduction, on the other hand editing in primary T cells was achieved upon electroporative delivery of chemically synthesized LEAPER-ASOs. Furthermore, editing of the above mentioned PTC in *IDUA* pre-mRNA with such ASOs in Hurler patient fibroblasts yielded

$\sim$30 % editing and restoration of IDUA activity above Scheie level.[138]

Site-directed C-to-U RNA editing

The field of C-to-U RNA editing is considerably less advanced as compared to A-to-I editing so far. Some platforms for recruitment of different engineered cytidine deaminases emerged in recent years, however they remain significantly less powerful than their adenosine counterparts.

RESCUE The first platform for site-directed C-to-U RNA editing was published in 2019 by the Zhang group (Figure 11 a).[142] RESCUE (RNA Editing for Specific C-to-U-Exchange) is derived from REPAIR, again combining a catalytically inactive mutant of Cas13b, from *Riemerella anatipestifer* in this case, with a deaminase domain. To enable C-to-U editing steered by guideRNAs, ADAR2Q's substrate selectivity was relaxed to accept cytidines by introduction of 16 mutations via rational mutagenesis and several rounds of directed evolution. Consistent with the ADAR2 deaminase domain's 5' nearest neighbor preferences, RESCUE is primarily practicable for 5'-U<u>C</u>N and 5'-A<u>C</u>N codons. GuideRNAs consist of a DR stem-loop and a 30 nt antisense moiety with either a CC or CU mismatch at the target site. The exact mismatch position, as well as preferred counter base, are recommended to be optimized for each target. Due to RESCUE's persisting adenosine deamination activity, the transcriptome-wide off-target profile is basically composed of REPAIR's A-to-I off-target landscape and additional C-to-U off-target sites. RESCUE-S, containing an additional S375A mutation, shows strong reduction of off-target effects, however, at the cost of on-target efficiency.[142] RESCUE has been applied for editing of a phosphorylation site in the *β-catenin* (*CTNNB1*) transcript, which resulted in activation of the Wnt/β-catenin signaling pathway as well as increased cell growth. Furthermore, Cas13's intrinsic processing activity allows for concurrent editing of two sites by addition of a pre-CRISPR RNA (pre-crRNA) containing two distinct guideRNAs. First efforts to shrink the large Cas13 construct for facilitated delivery indicate that C-terminal truncation of dRanCas13b up to 200 amino acids might be accepted.[142]

MCP-APOBEC In 2020, the Tsukahara group transferred their MCP-ADAR system to C-to-U editing (Figure 11 b).[143] For this, they fused the ZDD of hAPOBEC1 ($APO1_{ZDD}$) to MCP, which enables redirection of APOBEC deaminase activity with guideRNAs carrying six MS2 hairpins and a 21 nt antisense moiety which forms a CA mismatch at the target site. The method was applied for editing of a point mutation in a *blue fluorescent protein* (*BFP*), which results in restoration of *GFP*. 20 % on-target editing were achieved, accompanied by significant global off-target editing.[143] Beyond this, MCP-APOBEC has not been tested or investigated in detail.

CURE CURE (C-to-U RNA Editor), developed by the Chi group in 2020, utilizes the catalytically inactive dPspCas13b for steering of APOBEC3A Y132D (Figure 11 c).[144] CURE exclusively allows deamination of 5'-U<u>C</u>N targets which are positioned in the loop region of hairpin structures, mimicking natural APOBEC3A (A3A) substrates. Consequently, apart from the DR stem-loop for Cas13 recruitment, the guideRNAs contain a 32 nt antisense moiety that induces a loop in the target mRNA. Significant global C-to-U RNA, as well as some DNA, off-target editing occurs, whereat Us in DNA are repaired via base excision repair (BER), thus preventing elicitation of C-to-T DNA mutations.[144] CURE has been

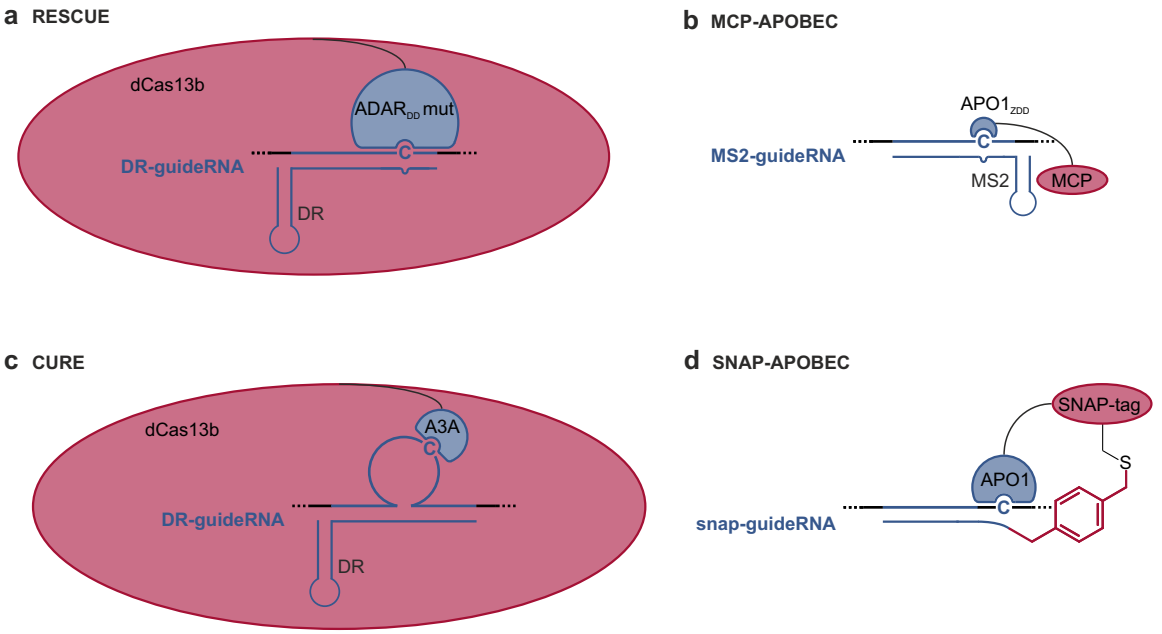

Figure 11. Systems for site-directed C-to-U RNA editing via recruitment of engineered cytidine deaminases. **a** RESCUE comprises a catalytically inactive Cas13 (1095 aa) fused to a mutated ADAR deaminase domain with loosened substrate requirements that also accepts cytidines for deamination. Recruitment is mediated by guideRNAs of ∼65 nt length, containing a DR region and a 30 nt antisense moiety, with a CC or a CU mismatch, usually between position 18 and 28, defining the target C.[142] **b** hAPOBEC1's ZDD can be recruited via interaction of a fused MCP (129 aa) with a guideRNA carrying six MS2 hairpins (only one shown for clarity). The antisense moiety is 21 nt long and builds a CA mismatch at position 7.[143] **c** In the CURE system, APOBEC3A is recruited via a catalytically inactive Cas13 (1135 aa). The DR-guideRNAs induce a 14 nt loop with a UAUC motif containing the target C in the center and bind across 32 complementary nucleotides, amounting to a total length of ∼65 nt.[144] **d** The covalent binding of the SNAP-tag (182 aa) to snap-guideRNAs can be utilized for steering of APOBEC1. The chemically modified snap-guideRNAs are 22 nt long and bind 4 – 6 nt upstream of the target C.[145] Relative sizes of protein domains and guideRNAs to scale, respectively.

applied for editing of endogenous targets in cell culture, including nuclear long non-coding RNAs (lncRNAs) with a nucleoplasmic localization variant.[144]

SNAP-APOBEC Interconnected with the dissertation at hand, the steering of mAPOBEC1 via the SNAP-tag was explored by another group member (Figure 11 d).[145] Without pre-empting too much, in short, mAPOBEC1-SNAP can be recruited by snap-guideRNAs with a 21 nt antisense moiety binding 4 nt upstream of the target C. More detailed results will be discussed in section 3.1 and in Publication 1.[145]

1.3 Photocontrolled protecting groups

Steering chemoselectivity by masking functional groups with a suitable protecting group is a commonly employed method in organic synthesis. A variety of protecting groups exists to block all kinds of functional groups, such as carboxylic acids, ketones, alcohols and amines from reacting. As for implementation of the protection, there are different strategies for cleavage and restoration of the original functional group.[146] For example, deprotection may be executed by acidic or basic conditions or by reduction. A further possibility is the use of illumination. In this case, the functional group concerned is protected with a photocleavable protecting group (PPG), which contains a moiety that undergoes a photochemical reaction

upon absorption of light in the UV/Vis range.[147] Illumination with photons of the energy hν corresponding to the energy difference of an electronic transition from a bonding or non-bonding to an antibonding orbital (typically a ππ* transition) results in absorption and conversion to an electronically excited state. From this higher energy state a photoreaction then takes place, yielding in the cleavage of the protecting group.

Generally, a good PPG is characterized by strong absorption and high quantum yield in a clean photoreaction.[147] Furthermore, solubility and stability in the respective solvent are required. The photoreaction's byproducts should be inert as to not evoke side reactions. Depending on the application, special focus is placed on further factors. PPGs have proven valuable tools for the defined release of biologically active compounds. For such applications, it is of special importance that the excitation wavelength is as long as possible, at best well above 300 nm, to avoid absorption and damage of the biological surroundings, as well as provide good tissue penetration. Additionally, low irradiation intensities reduce phototoxicity and short illumination pulses, combined with fast release of the active compound, enable the tracking of rapid biological responses. Moreover, the protected compounds might need to pass cell membranes and need to exhibit low background activity, which includes the requirement to be stable in the biological environment and not to be cleaved by endogenous enzymes, such as esterases for example.[147, 148, 149] Photoswitchable protecting groups even allow for multiple rounds of optical switching between two isoforms with different properties, for example biological activity.[148] In the so-called azoextension, an azobenzene derivative is attached to a molecule of interest. The azobenzene can be switched between its *trans* and *cis* configuration with irradiation triggers at two distinct wavelengths between 300 nm and 500 nm.[150, 151, 152] Another class of photoswitchable protecting groups are the donor–acceptor Stenhouse adducts (DASAs), which can be switched from an open to a cyclic form by illumination with wavelengths above 500 nm and switch back to the open form passively via thermal relaxation.[153]

As for other layers of control, such as protein tags (see 1.1) and chemically induced dimerization (see 1.4), utilization of orthogonal PPGs may allow for sequential deprotection of multiple compounds at different wavelengths, thereby allowing for analysis of more complex processes. In this case, potential overlaps of the respective absorption and emission spectra have to be taken into consideration to choose a suitable combination and illumination sequence of PPGs.[148] Naturally, the choice of PPG depends on the functional group to be protected as well as the above-mentioned factors. The two most commonly applied classes of PPGs, namely nitroaryl and coumarinyl groups, will be presented in the following.

1.3.1 Nitroaryl protecting groups

The basic frameworks of nitroaryl protecting groups are the *ortho*-nitrobenzyl (*o*NB) and the 1-(2-nitrophenyl)ethyl (NPE) structure. Figure 12 a shows the mechanism of release of alcohols from *o*NB protection.[154] Upon absorption of a photon, the nitroaryl compound **1** is transfered into a singlet excited state (**2**). From this excited state, [1,5]-hydrogen transfer from the benzylic methylene group to the *o*-nitro group takes place, yielding the ground state (*Z*)-*aci*-nitro compound **3**. Cyclization to 1,3-dihydrobenz[*c*]isoxazol-1-ol **4** and subsequent ring opening results in hemiacetal **5**, which is then cleaved to release the free alcohol (**7**) and byproduct *o*-nitrosobenzaldehyde (**6**). The nitroso byproduct is the main disadvantage of nitrobenzyl protection groups, due to its toxicity and its absorption properties which elicit an internal light filtering effect. As for many types of PPGs, the mechanism as well as the rate determining step may vary depending on the nature of the leaving group, additional substituents and on the type and pH of the medium.[147]

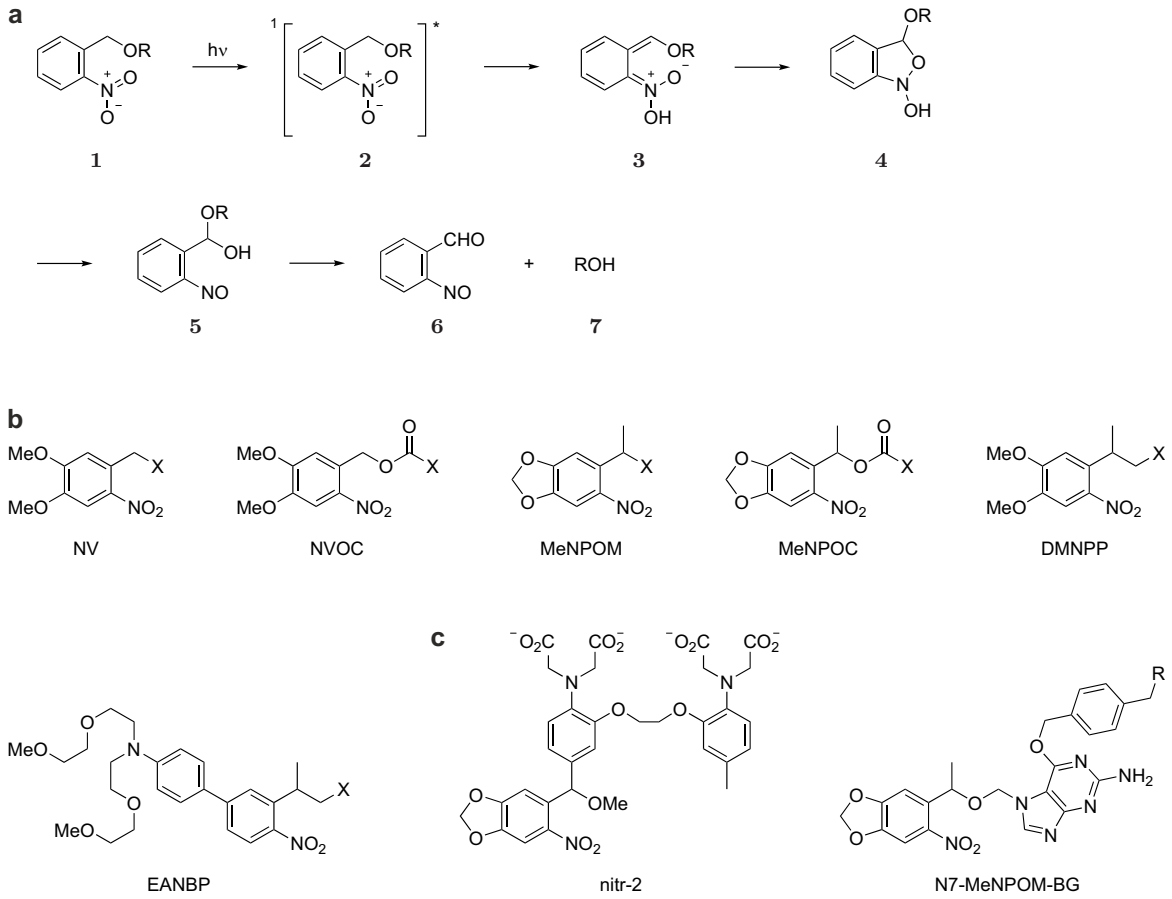

Figure 12. Nitroaryl protecting groups. **a** Mechanism of release of alcohols from *o*NB protection. **b** Selection of nitroaryl PPGs: *o*NB-based 6-nitroveratryl (NV), 6-nitroveratryloxycarbonyl (NVOC), α-methyl-(6-nitropiperonyloxymethyl) (MeNPOM) and 3,4-(methylenedioxy)-6-nitrophenylethoxycarbonyl (MeNPOC) and NPE-based 2-(4,5-dimethoxy-2-nitrophenyl)-propyl (DMNPP) and 2-(4'-(bis((2-methoxyethoxy)ethyl)-amino)-4-nitro-[1,1'-biphenyl]-3-yl)propan-1-ol (EANBP). **c** Exemplary applications of *o*NB-based PPGs for controlled provision of metal ions and photoactivatable SNAP-ADAR editing. The nitr-2 ligand chelates Ca^{2+} via its amine, carboxylate and phenol ether groups. Upon irradiation the attached NPOM moiety is cleaved, releasing methanol, and yielding a ligand with vastly diminished Ca^{2+} affinity. In N7-MePOM-BG, the SNAP-tag substrate is caged with a MeNPOM group via an oxymethylene linker. Assembly of the editase from N7-MeNPOM-snap-guideRNAs with SNAP-ADARs is triggered by illumination.

A multitude of functional groups can be protected with *o*NB-based groups. While good leaving groups like thiols, carboxylic acids or phosphates are typically carried directly at the benzylic site, alcohols and amines are often fused as carbonic acid derivatives.[147] This generates a superior leaving group and deprotection under cleavage of an equivalent of CO_2 releases the free compound.[155, 156] Moreover, an oxymethylene linker is sometimes inserted, deprotection is then accompanied by release of formaldehyde.[157, 158]

Various modifications of the nitrobenzyl backbone have been utilized to improve and tune properties of *o*NB-based protecting groups (Figure 12 b). Excitation wavelength can be regulated by adjusting the energy levels of the orbitals involved in the excitation through suitable implementation of substituents. Most importantly, addition of *meta* and *para* methoxy substituents (NV, NVOC, Figure 12 b) or a methylenedioxy bridge (NPOM, NPOC) results in significant bathochromic shifts and strong absorbance above 350 nm.[147] Extension of the aromatic core, for instance in 2-nitronaphtalene derivatives, also creates a bathochromic shift.[159] Quantum yield is significantly boosted by addition of a benzylic methyl substituent,[160] as for example in MeNPOM and MeNPOC (Figure 12 b). This

has the additional advantage that a less toxic *o*-nitrosoacetophenone byproduct is generated instead of the *o*-nitrosobenzaldehyde. For benzylic substituents, however, it should be borne in mind that a chiral center is created, which may influence the protection of chiral molecules. In order to enhance water solubility for protections in aqueous environments, additional carboxylic acid groups can be implemented.[161]

Some nitroaryl-based PPGs, such as EANBP (Figure 12 b),[162] also allow for deprotection upon two-photon excitation (2PE) with visible red or near-infrared (NIR) light. Here, two photons are simultaneously absorbed, which enables the relatively energy-intensive excitation of electrons with longer wavelength photons. This brings the great advantage of irradiation in the phototherapeutic window between 650 nm and 950 nm, in which tissue is most transparent. 2PE requires high intensity irradiation, that is most commonly delivered by a pulsed Ti:sapphire laser. Decisive for the eligibility of a PPG for 2PE is its two-photon absorption cross section δ at the irradiation wavelength, which should reach minimum $\delta = 10^{-50}$ cm^{4}s per photon and molecule, can be increased by extension of the conjugated π system and may be improved by employment of triplet sensitizers with high δ.[147]

Owing to the mild deprotection conditions and the excellent orthogonality to other common protection groups, nitroaryl-based PPGs are helpful in chemical synthesis, particularly of complex molecules, such as natural product synthesis[163, 164] or automated oligonucleotide synthesis.[157] The first application of a nitroaryl-based PPG to biology was the protection of 3'-5'-cyclic adenosine monophosphate (cAMP) with simple *o*NB in 1977.[165] 3'-5'-Cyclic nucleotides (cNMPs), particulary cAMP and cGMP, are important secondary messengers with multiple functions in signal transduction (see also 1.5.1). Among others, they activate cAMP-dependent protein kinase (PKA) and cGMP-dependent protein kinase (cGK), respectively, which leads to phosphorylation of various cellular proteins and diverse resulting effects, including regulation of transcription, smooth muscle relaxation and ion channels.[166, 167] Cyclic nucleotide-gated (CNG) ion channels, which allow diverse cations to pass upon cAMP/cGMP activation, play important roles in olfactory receptors as well as retinal photoreceptors.[168, 169] A further application of *o*NB-derivatives is the controlled release of metal ions with secondary messenger functions, such as Ca^{2+}.[170, 171, 172] For instance, in nitr-2, Ca^{2+} is chelated with a ligand carrying a NPOM moiety which loses Ca^{2+} affinity upon irradiation (Figure 12 c).[173] *o*NB-based PPGs have also been utilized for control of further small molecules, for example in photoactivatable and -cleavable inducers of dimerization (see also 1.4). Furthermore, a NVOC protected BG-rhodamine 110 derivative has been applied for super resolution microscopy.[174]

Another branch of optochemical biology constitutes the control of peptides. In this regard, photocaged unnatural amino acids (UAAs), such as caged Lys, Tyr, Cys and Ser, play a major role.[175] After genetic code expansion with the implementation of an orthogonal tRNA synthetase and cognate tRNAs, a caged UAA can be installed at a site crucial for protein structure or function. For instance, MeNPOC-Lys may be utilized for caging conserved lysine residues in the active site of a variety of kinases.[156, 176] Moreover, drug delivery can be facilitated with the help of photocleavable linkers. Fusing small molecules and proteins to hydrogels via a photocleavable linker allows for precisely controlled release.[177] ASOs have also been delivered by attaching cell-penetrating peptides (CPPs) to a nucleobase via a photocleavable moiety.[178]

There are also multiple strategies that enable photocontrol of the hybridization of oligonucleotides and thus regulation of biological processes involving oligonucleotides. Hybridization can be both activated and deactivated. Photoactivation can be implemented by attaching a hairpin forming inhibitory strand or by circularization of an ASO via a photocleavable linker.

Furthermore, the nucleotides themselves can be caged at the nucleobase, their phosphate backbone or, for RNA, the ribose's 2'-OH. Photodeactivation can be achieved by inserting a photocleavable linker within the antisense strand itself or attachement of a hairpin forming inhibitory strand containing caged nucleotides. These methods have been applied for the optical regulation of siRNAs for RNAi,[179, 180, 181, 182] antagomirs[183, 184, 185] and morpholinos[186, 187, 188] for translation inhibition, transcription factors,[189, 190, 191] molecular beacons,[192, 193] aptamers,[194, 195] and many more, via nitroaryl PPGs. Importantly, the MeNPOM group was also employed for photoactivatable A-to-I RNA editing with SNAP-ADAR (see 1.2.3), where it was attached to the SNAP-tag substrate BG at N7 via an oxymethylene linker (Figure 12 c).[126] Lastly, *o*NB-based PPGs have been applied for transcriptome sequencing on a single cell level with the TIVA (transcriptome *in vivo* analysis)-tag, allowing for spatiotemporally controlled investigation of single cells within their live microenvironment.[196]

1.3.2 Coumarinyl protecting groups

Another frequently used class of PPGs are coumarin-4-yl-methyl (CM) derivatives. They exhibit high absorption at wavelengths above 300 nm and fast release rates on a scale of nanoseconds.[197] Furthermore, the intrinsic fluorescence of CM provides a handy method for tracking of the reaction. Figure 13 a shows the mechanism of optically triggered deprotection of a (7-methoxycoumarin-4-yl)methyl (7-MCM) caged organophosphate (**8**). Irradiation creates a singlet excited state (**9**), which in this case can either relax to the ground state nonproductively via nonradiative decay or via fluorescence emission, or can react via heterolytic bond cleavage to create carbocation **10** and organophosphate **11**. Upon solvent separation and reaction of the carbocation with a nucleophile, e.g. a solvent molecule such as H_2O, 7-MCM derivative **12** is formed and free organophosphate **11** released. In accordance with the mechanism, the rate of reaction is enhanced by highly polar solvents and a leaving group with low pKa of the corresponding acid.[197] Consequently, CM derivatives provide excellent PPGs for phosphates, sulfonates and carboxylic acids. Inferior leaving groups, such as thiols, alcohols and amines, are caged as their respective carbonic acid derivative and deprotected under release of CO_2.[147]

Several substituents have been applied to enhance the performance, i.e. absorption and fluorescence properties, quantum yields and hydrophilicity, of CM-based PPGs (Figure 13 b). This includes methoxy, amino, bromine and carboxylic acid groups, particularly at C6 and C7 position.[147] First generation CM PPGs carry 7-alkoxy substitutents, in the second generation 7-amino substitutents make for bathochromic shift of the absorption and increased quantum yields. Furthermore, polyaromatic analogues, such as 5,6- and 7,8-benzocoumarines, have been developed.[198, 199] Simple CM-based groups are typically more accessible for 2PE than simple NPE-based groups (e.g. DMNPP, Figure 12 b).[147] For example, DEACM and BHCM (Figure 13 b) have been applied for 2PE deprotection.[200, 201, 202]

CM-based PPGs also have numerous fields of application, similar to *o*NB-based groups. CM groups have been employed for optically controlled release of several cNMP derivatives,[203, 204] including the release of 8-nitro-cGMP from DMACM protection in the Stafforst group.[205] Furthermore, CM-based PPGs can be applied for photocontrol of CID (see also 1.4). Photoprotected conjugate bases of strong acids, such as phosphates or sulfates, can serve as caged proton sources, which enable the triggering of prompt drops in pH and thus serve as useful tools in the examination of proton regulated signaling processes. This has been implemented with both *o*NB- and CM-based PPGs.[206, 207] In comparison to pro-

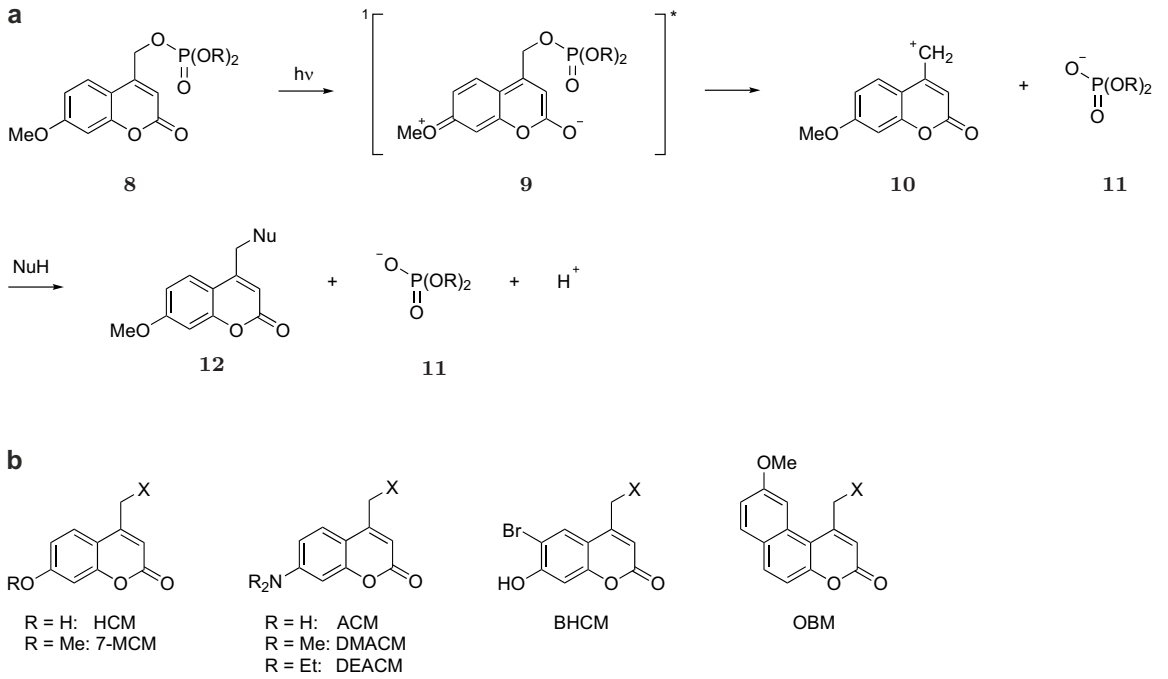

Figure 13. Coumarinyl protecting groups. **a** Mechanism of release of organophosphates from 7-MCM protection. **b** Selection of coumarinyl PPGs: (7-hydroxycoumarin-4-yl)methyl (HCM), (7-methoxycoumarin-4-yl)methyl (7-MCM), (7-aminocoumarin-4-yl)methyl (ACM), [7-(dimethylamino)coumarin-4-yl]methyl (DMACM), [7-(diethylamino)coumarin-4-yl]methyl (DEACM), (6-bromo-7-hydroxycoumarin-4-yl)methyl (BHCM) and 5,6-benzocoumarin 9-methoxy-1-methylene-3-oxo-3*H*-benzo[*f*]benzopyran (OBM).

tection with a simple *o*NB-based group, DMACM deprotection enabled faster proton release rates and irradiation at longer wavelengths, since simple CM groups have absorption maxima at higher wavelengths than simple *o*NB groups.[207]

Moreover, CM groups have also been applied in genetic code expansion. For example, HCM-Lys enables deprotection in the visible range, as opposed to the above mentioned MeNPOC-Lys, which requires UV light. Caging with BHCM even allows for 2PE.[208] A further benefit of the different absorption properties of CM and *o*NB groups is the facilitated orthogonal application, as for instance in the orthogonal release of small molecules and proteins from hydrogels.[177] Orthogonal CM- and *o*NB-based PPGs have also been exploited to control the hybridization of oligonucleotides with the orthogonal two-photon release of DNA strands from DEACM and 2-(4'-(dimethyl)amino)-4-nitro-[1,1'-biphenyl]-3-yl)propan-1-ol (ANBP) protection,[200] as well as sequential gene silencing with cyclic morpholinos.[209] Furthermore, CM controlled aptamers have been developed.[210, 211]

1.4 Induced proximity

In order to cooperate in forming living organisms, the wide plethora of biological processes requires careful regulation. In this regard, the distance between molecules, such as proteins, is an essential and ubiquitous regulatory mechanism. Physical proximity initiates and controls various events, including protein structure, transcription and cellular signaling. Hence, systems that are capable of inducing proximity in a defined manner provide valuable tools. Since many natural processes are controlled by dynamic protein interactions spanning a vast temporal scale, an optimal inducer of proximity would not only elicit an immediate effect,

but also allow for precise spatiotemporal control, as well as reversible switching between proximity and distance.[212, 213]

Proximity between proteins may be introduced directly via complementary surface areas or mediated by a peptide, nucleic acid or small molecule.[212] In research tools, chemically induced dimerization (CID) is most commonly used. In CID, two POIs are brought into proximity via fused proteins that dimerize upon treatment with a small molecule (Figure 14 a).[212] This allows for timed intervention at a site of choice in a pathway and examination of resulting effects. The first chemical dimerizers were developed by the Crabtree group in 1993 and are based on the immunosuppressive drug FK506 (Figure 14 b).[214] FK506 binds to the abundant immunophilins FK506 binding protein (FKBP). The FKBP-FK506 complex then binds to calcineurin (calcium-dependent serine-threonine phosphatase), inactivating it and thereby impeding T cell receptor (TCR) signaling. In FK1012s, two FK506 moieties are bridged via a linker, replacing FK506's allyl group that is important for calcineurin binding (Figure 14 c). Consequently, FK1012s loose FK506's calcineurin binding ability and the resulting immunosuppressive activity, and instead induce FKBP12 homodimerization. FK1012-A was applied for CID of a myristylated cytoplasmic domain of TCR's ζ chain fused to three tandem copies of FKBP12 and successfully induced receptor mediated transmembrane signaling.[214] A major strength of CID is the dosage control of the chemical dimerizer, enabling dose-dependent fine tuning of activity levels over several orders of magnitude. Furthermore, CID may be reversed by displacing the dimerizing agent with a competitive inhibitor, as in the case for FK1012s by simple addition of a FK506 derivative, FK506-M (Figure 14 b).[214]

A variety of further CID systems with different properties have been developed. Dimerization is induced within seconds to minutes, allowing for precise examination of correlations,[149, 213, 215] which may be additionally aided by theoretical models.[212, 215] Furthermore, systems have been optimized for high specifitiy, binding affinity, bioorthogonality, reversibility and cell permeability of the dimerizers.

Dimerization can also be induced by light, either in optogenetic dimerization or in chemo-optogenetic dimerization. For optogenetic dimerization, the dimerizing proteins are based on photoreceptors, such as light-, oxygen-, or voltage-sensitive proteins (LOVs) or cryptochromes (CRYs) that undergo conformational change upon stimulation with light, resulting in induced protein dimerization.[149] Reversion can either occur passively in the dark or upon illumination at a different wavelength, with on/off kinetics ranging from seconds to days. Proteins for dimerization at various wavelengths over the range of the optic spectrum, as well as for two photon excitation, have been developed.[149] However, tuning of excitation wavelengths is much more straightforward for organic dyes, a major advantage of chemo-optogenetic dimerization. Here, CID is extended by a further layer of control by implementation of photoactivatable or photocleavable small-molecule dimerizers (Figure 15 a, b). This allows for superb spatiotemporal resolution, not only enabling subcellular spatial control, but also eliminating the influence of the dimerizer's diffusion rate into the cell from kinetics.[149] On the other hand, small molecule dimerizers are capable of penetrating deeper tissues that are inaccessible to light.

In the following, a selection of systems for chemically induced dimerization will be presented. The multitude of methods with diverse characteristics allows to choose the most suitable for a given application.

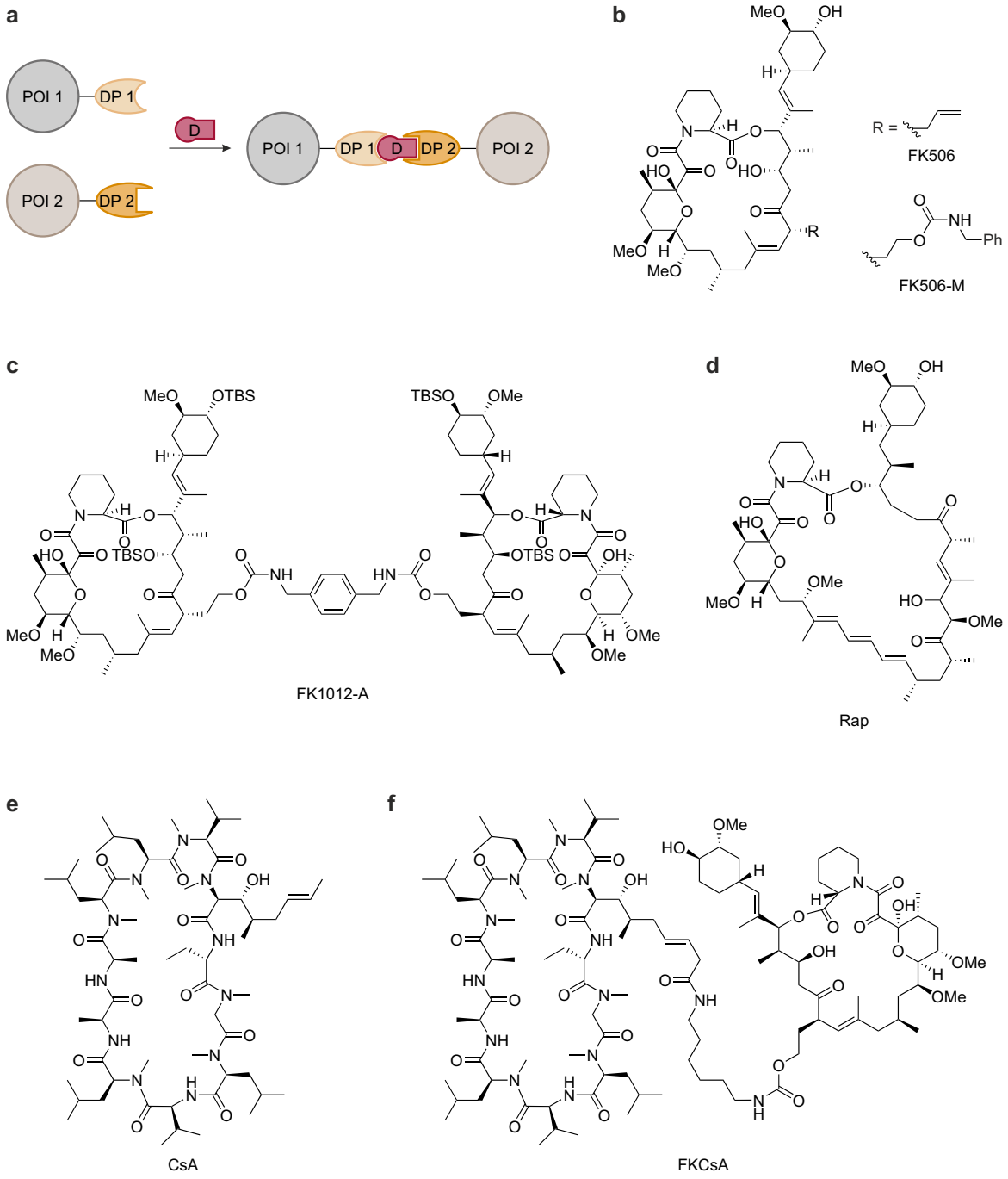

Figure 14. Principle of chemically induced dimerization (CID) and selection of chemical dimerizers for immunophilin-based systems. **a** Dimerization of two proteins of interest (POI 1, 2) can be mediated via fused dimerizing proteins (DP 1, 2) by addition of a small molecule dimerizer (D). **b** Immunosuppressive FK506 binds FKBP and calcineurin, its derivative FK506-M does not bind calcineurin. **c** FK1012-A induces homodimerization of FKBP12 (12 kDa). **d** Rapamycin (Rap) induces heterodimerization of FKBP12 (12 kDa) and FRB (11 kDa). **e** Immunosuppressive cyclosporine A (CsA) binds CyP and calcineurin. **f** FKCsA induces heterodimerization of CyP (18 kDa) and FKBP12 (12 kDa).

1.4.1 Systems for chemically induced dimerization

Immunophilin-based systems

Beyond FKBP12 homodimerization with FK1012s, immunophilin-based systems for induced heterodimerization exist. Like FK506, rapamycin (Rap, Figure 14 d) binds to FKBP, followed by formation of a ternary complex with the FKBP-rapamycin binding domain (FRB) of mechanistic target of rapamycin (mTOR) with high binding affinity (K_D in nM range).[216] A variety of rapamycin derivatives, dubbed rapalogs, has been developed.[212, 215] Most importantly, immunosuppression caused by mTOR inhibition can be overridden by utilization of rapalogs that bind to artifically designed FRB mutants instead of wild-type FRB, a concept which has also been applied for other immunophilin-based systems.[217]

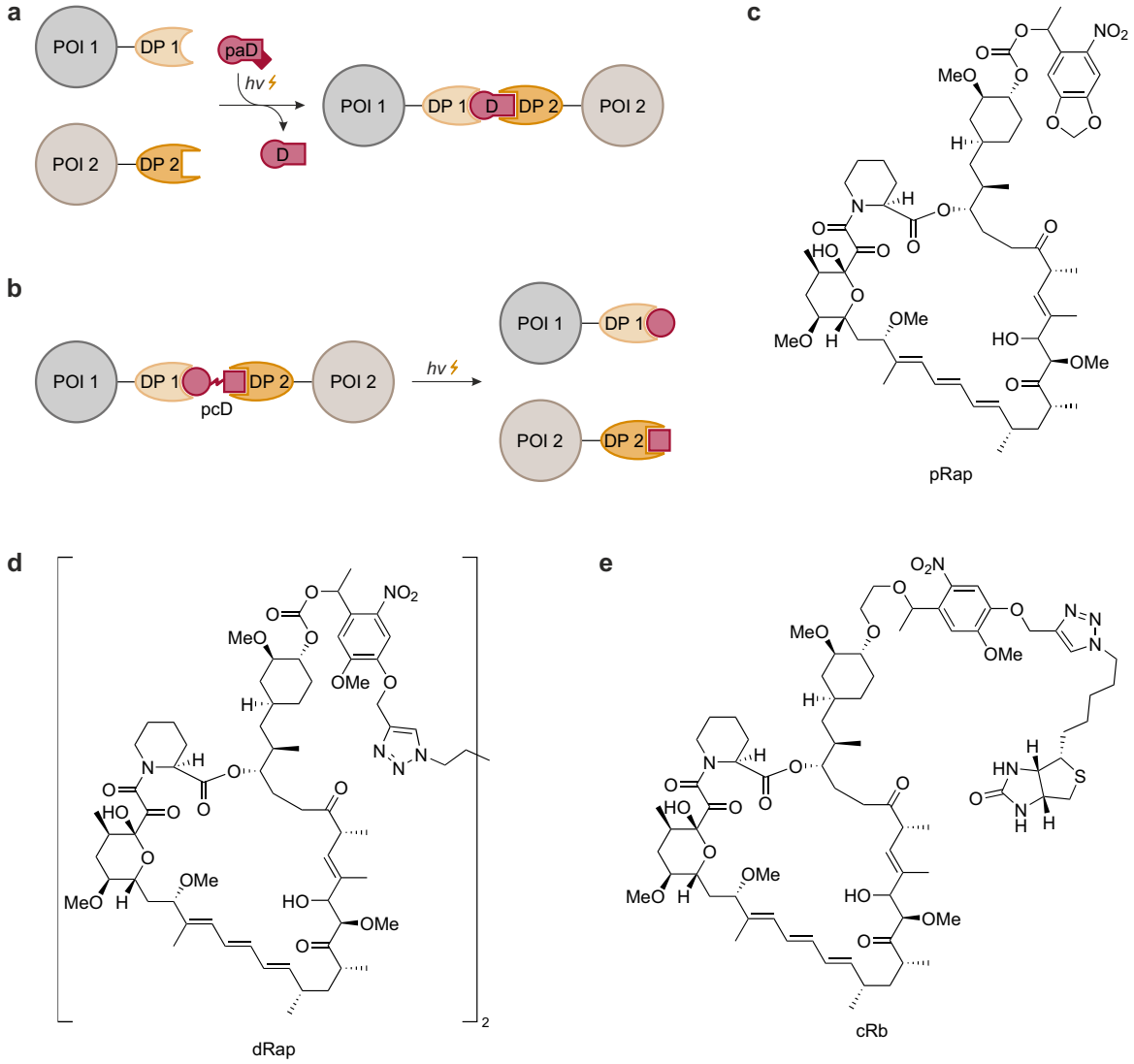

Figure 15. Principle of chemo-optogenetic dimerizations and selection of photoactivatable rapalogs. **a** Photoactivatable dimerizers (paD) carry a photoprotection group and induce dimerization only after deprotection by illumination. **b** Photocleavable dimerizers (pcD) induce dimerization in the dark, but contain a photocleavable linker which allows for induced dedimerization upon illumination. **c** pRap carries MeNPOC at C40 and is photoactivatable by illumination at 365 nm. **d** In dimeric dRap, two Rap monomers are linked via a MeNVOC linker, active Rap is released upon illumination at 365 nm. **e** cRb consists of Rap coupled to biotin via a MeNVOC linker.

Due to its high binding affinity and slow dissociation, the classical Rap CID system is practically irreversible, and thus less suitable for the examination of reversible signal transduction.[213] Several photoactivatable rapalogs have been designed for chemo-optogenetic dimerization (Figure 15 c – e).[149] pRap employs MeNPOC photoprotection,[218] dRap photocleavable MeNVOC linking two Rap units.[219] In cRb, Rap is photocleavably linked to a biotin moiety. Since cellular uptake occurs only after photocleavage of the ensuing large Rap-avidin conjugate, cRb exhibits excellently low background activity.[220]

Cyclosporine binding cyclophilins (CyP), the second family of immunophilins besides FKBPs have also been exploited for CID (Figure 14 e, f). Cyclosporine A (CsA) is an immunosuppressive calcineurin inhibitor that binds CyP and calcineurin. The combination of CsA with FK506 yields FKCsA, which induces heterodimerization of CyP and FKBP.[221]

Abscisic acid

Several CID systems have been derived from plant hormones (Figure 16). Their forte is the minimized disturbance due to endogenous binding partners in mammalian cells, however, at the cost of a higher risk of immunogenicity. Abscisic acid (ABA) regulates signaling in response to environmental stress (Figure 16 a). It can be exploited for CID since it binds to the pyrabactin resistance-like regulatory component of ABA receptors (PYL), inducing dimerization with the protein phosphatase 2C (PP2C) catalytic domain of abscisic acid insensitive 1 (ABI1).[222] In contrast to Rap induced dimerization, abscisic acid (ABA) induced dimerization is reversible without the need for a competitive binder by simple washout of the dimerizer and exhibits a more graduated response to changes in dimerizer concentration, thus facilitating dosage control.[222] ABA derivatives with NV and DEACM photoprotection have been developed for photoactivatable CID (Figure 16 a).[223]

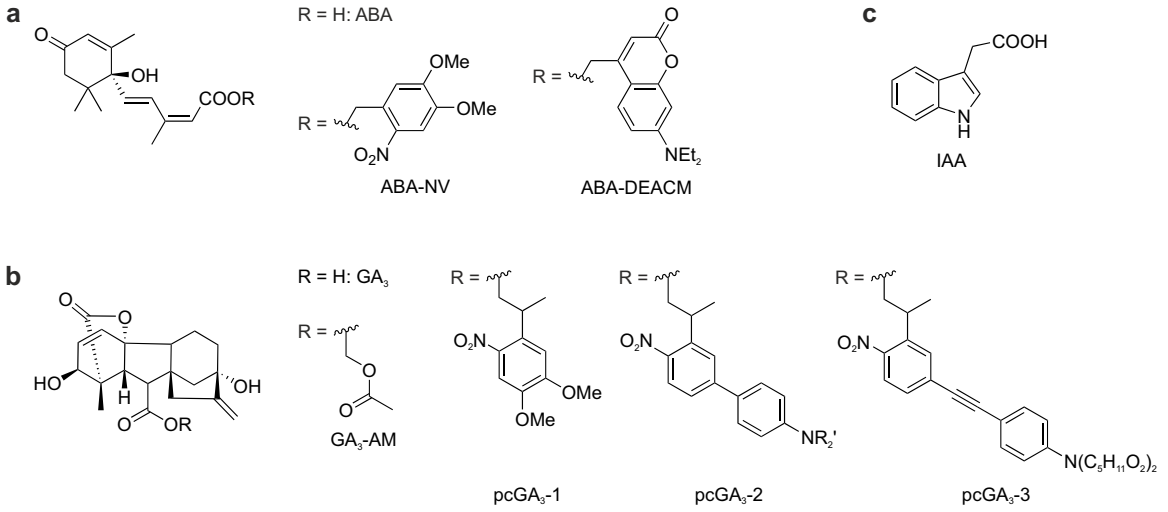

Figure 16. Chemical dimerizers for CID systems based on plant hormones. **a** Abscisic acid (ABA) induces dimerization of PYL (19 kDa) and the PP2C catalytic domain of ABI1 (33 kDa). Photoprotection of the carboxylic acid moiety with NV yields ABA-NV, which is cleaved upon illumination at 365 nm, ABA-DEACM is photoactivatable by illumination at 405 nm. **b** Gibberellic acid (GA_3), delivered via its cell permeable ester derivative GA_3-AM, can be applied for dimerization of GID1A (38 kDa) and $GAI_{1\text{-}92}$ (10 kDa). Photoprotected $pcGA_3$-1 carries a 2-(4,5-dimethoxy-2-nitrophenyl)-propyl (DMNPP) group, $pcGA_3$-2 a 2-(4'-(bis((2-methoxyethoxy)ethyl)amino)-4-nitro-[1,1'-biphenyl]-3-yl)propan-1-ol (EANBP) group and $pcGA_3$-3 contains an additional ethinyl bridge. All three $pcGA_3$ derivatives undergo photolysis upon irradiation at 412 nm, $pcGA_3$-2 and -3 are additionally susceptible to two-photon photolysis at 800 nm. **c** The auxin indole-3-acetic acid (IAA) induces dimerization of TIR1 (63 kDa) and $IAA17_{71\text{-}114}$ (5 kDa).

Gibberellic acid

The plant hormone gibberellic acid (GA_3) promotes germination as well as stem and root growth.[215] It binds to gibberellin insensitive dwarf 1A (GID1A), eliciting a conformational change which then triggers dimerization with gibberellic acid insensitive (GAI). For utilization as CID system, C-terminally truncated $GAI_{1\text{-}92}$ is applied and GA_3 is delivered as its cell permeable acetoxymethyl ester (GA_3-AM), which is cleaved to active GA_3 by endogenous esterases (Figure 16 b).[224] Moreover, GA_3 derivatives that are photoactivatable by one- as well as two-photon-absorption have been developed, namely pcGA_3-1, -2, -3 (Figure 16 b).[225] While photoactivatable CID with the ABA system requires illumination pulses of 60 s and dimerizes on a timescale of minutes, illumination times of 3 s suffice with the GA_3 system and dimerization occurs within 20 s.[223, 225] On the downside, dimerization with GA_3 lacks reversibility.[149]

Auxins

Auxins play a role in plant gene expression control.[226] The natural auxin indole-3-acetic acid (IAA) binds to transport inhibitor response 1 (TIR1) and thereby induces interaction of SCF-TIR1 E3 ubiquitin ligase with the transcription repressor auxin-responsive protein IAA17 (Figure 16 c).[226] A truncated version of IAA17 fused to a POI can therefore be exploited as auxin-inducible degron (AID*).[227] Recently, the system has been extended to CID applications with biological effects other than degradation.[228] Dimerization is reversible by removal of IAA.[226]

Covalent CID

Enhanced spatial resolution can be achieved by implementation of covalent protein dimerizers. Covalently anchoring one of the POIs to a selected subcellular compartment via a localized self-labeling protein tag eliminates blurring in resolution which otherwise arises due to diffusion. This has been put into practice with a dimerizing agent consisting of a HALO-tag substrate (halo) linked to trimethoprim (TMP), which binds to bacterial dihydrofolate reductase (DHFR).[229] Photoprotection of TMP allows for prelocalization of the dimerizer, followed by prompt dimerization within 1 s upon illumination (Figure 17 a). Moreover, dimerization is rapidly reversible by simple displacement of the dimerizer with TMP.[230]

Similar systems have been developed for photocleavable CID (Figure 15 b, Figure 17 b). TMP-NVOC-halo induces dimerization of DHFR and HALO in the dark, while dedimerization can be precisely triggered by illumination.[34] Analogously, the completely covalent dimerizer BG-MeNVOC-halo also allows for dedimerization within seconds upon illumination.[36] Combination of photoactivatable as well as -cleavable moieties even creates photoswitchable dimerizers that induce dimerization and dedimerization at different wavelengths. As such, coumarinyl protected TMP-NVOC-halo allows the dose- and wavelength-dependent fine tuning of the degree of dimerization.[35]

1.4.2 Applications of chemically induced dimerization

The fields of application of CID are manifold. Firstly, CID serves as a research tool for the exploration of protein roles in health and disease. Thanks to the targeted control, protein functions, as well as the regulation and dynamics can be dissected and elucidated

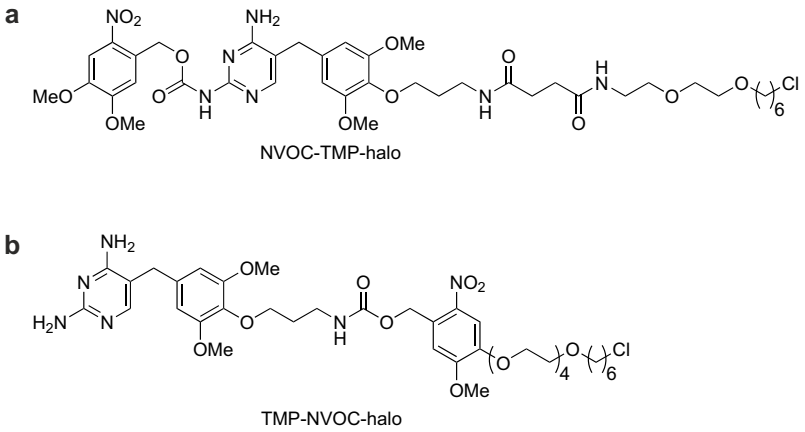

Figure 17. Covalent dimerizers enable anchored CID at a defined subcellular localization. **a** NVOC-TMP-halo induces dimerization of DHFR (18 kDa) and anchored HALO-tag (33 kDa) upon illumination at 405 nm. **b** Dimerization induced by the photocleavable dimerizer TMP-NVOC-halo can be abrogated by illumination.

individually, and with less interference by indirect effects than with other methods.[212] For investigation of more complex processes, multiple orthogonal CID systems, as for example the Rap and GA_3 system, can be combined.[231] Moreover, combination of multiple photoactivatable and/or -cleavable CID systems opens up even further possibilities.[149, 232]

CID has been applied for study of numerous biological processes in a variety of biological systems, ranging from yeasts to mammalian cells to animal models.[213] Oftentimes, proteins are translocalized between cellular compartments, such as the cytoplasm,[233] nucleus,[234] endoplasmatic reticulum,[235] Golgi apparatus,[236] or the plasma membrane.[230] With the help of CID, it could be shown that dimerization is important for activation of a variety of proteins with a role in signal transduction pathways.[212] Reversible CID systems are particularly useful for the elucidation of signaling cascades.[149] Split proteins that can be reconstituted by CID are another helpful approach.[213] Beyond signal transduction, induced proximity has been applied to initiate transcription, manipulate protein folding, regulate chromatin dynamics as well as stimulate trans-splicing.[149, 212, 215] Furthermore, CID can be applied to evoke or control proteasomal degradation by creating fusion proteins which are unstable in the absence of a chemically induced ternary complex or by harnessing of an E3 ligase, such as with the initial auxin system.[212, 215]

Beyond research tools, the use of CID systems for therapeutic applications is promising as well. For example, conditionally replication-competent vectors under the control of a rapalog dimerizer can represent an efficient and safe delivery route in gene therapies.[237] An evolution of the general idea of proteasomal degradation has been the development of proteolysis targeting chimeras (PROTACs), bivalent small molecules consisting of a ligand for the POI linked to a ligand for an E3 ligase, which induce specific ubiquitylation and consequent degradation of the target protein by the ubiquitin-proteasome system.[238] Different E3 ligases can be recruited with different ligand motifs. Immunomodulatory imide drug (IMiD) motifs based on thalidomide (brand name contergan) which bind to cereblon (CRBN), the receptor of an E3 ubiquitin ligase complex, are most commonly used.[239] Other ligands include motifs for the recruitment of von Hippel-Lindau (VHL) and cellular inhibitor of apoptosis protein 1 (cIAP1) E3 ligases.[240] To date, over 20 PROTACs have entered phase I clinical trials, mainly for various types of cancer, but also for immune-related and neurodegenerative diseases.[239, 240] Two PROTACs are currently being investigated in phase II clinical trials, ARV-110 for the treatment of prostate cancer by degradation of an-

drogen receptors, and ARV-471 for treatment of estrogen-receptor positive breast cancer by degradation of estrogen receptors.[240]

CID can also be utilized to harness large steric hindrances with only a small molecule needing to be delivered. For instance, β-Amyloid (Aβ) aggregation, which is elemental in pathogenesis of Alzheimer's disease, can be inhibited by CID with FKBP.[241] Further therapeutic applications lay in the protection against possibly occurring adverse events in cellular therapies.[242, 243] This includes a safety switch that allows to avert graft-versus-host disease (GVHD), which may arise in response to leukemia treatment with hematopoietic stem cells. T cells expressing a caspase 9 construct which can be activated to induce apoptosis by dimerization with an FK1012 analog in the event of GVHD show promising results in phase I clinical trials.[244, 245]

1.5 Nitric oxide as secondary messenger

Nitric oxide is an important secondary messenger with a multitude of biological functions and implications in human health and disease. The highly reactive radical has a short half-life and can rapidly diffuse in surrounding tissue due to its small, uncharged structure.[246] Several differential NO signaling pathways exist and precise regulation is crucial, as dysregulation results in various pathologies.

Nitric oxide is generated by nitric oxide synthases (NOSs) via oxidation of L-arginine's guanidine group (Figure 18).[247] Several isoforms of NOS exist, all of which are active in a homodimeric form.[166] Neuronal NOS (nNOS) and endothelial NOS (eNOS) are both constitutively expressed and require Ca^{2+}-dependent formation of a calmodulin complex for activity. nNOS is abundantly expressed in many brain areas, as well as in some cell types of the CNS and peripheral nervous system (PNS), eNOS is expressed in endothelial cells in the brain and PNS, among others.[248] Besides, Ca^{2+}-independent inducible NOS (iNOS) is only lowly expressed in the CNS, but induced upon triggers such as viral infection, brain injury or inflammation, yielding drastic increase in NO formation.[166, 248, 249] NOS require various cofactors, including stoichiometric amounts of NADPH as oxidizing agent, FAD, flavin mononucleotide (FMN) and tetrahydrobiopterin (BH_4), and NOS regulation is intertwined with Ca^{2+} signaling in several ways.[247, 248]

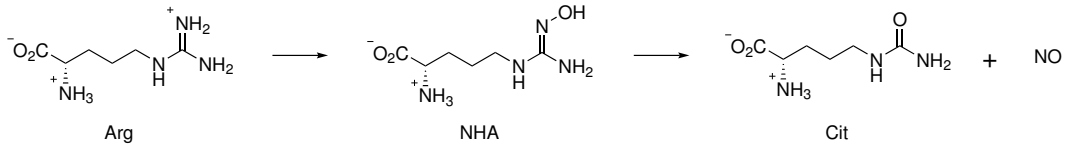

Figure 18. Generation of nitric oxide by NOS. The guanidine group of arginine (Arg) is oxidized in two steps, via intermediate N^{ω}-hydroxy-arginine (NHA) and subsequently to NO, under formation of citrulline (Cit).

1.5.1 NO-cGMP signaling

Generation of cGMP

In 1987, NO was first determined to be the signaling molecule mediating vascular smooth muscle relaxation, which had previously been known as endothelium-derived relaxing factor (EDRF).[250] The NO trigger activates a NO-cGMP signaling cascade with a variety of

downstream effects by stimulating soluble guanylate cyclase (sGC) activity, which in turn generates 3'-5'-cyclic guanosine monophosphate (cGMP) from GTP (Figure 19).[251] NO coordinates to Fe^{2+} in the heme moiety of sGC with picomolar affinity. As a consequence, at continual low levels of NO, stable low levels of cGMP are produced.[252, 253] A rise in NO concentration enables a second NO to be bound to sGC at a non-heme site with nanomolar affinity. This fully activates sGC[252, 253] and results in an increase in cGMP within milliseconds.[254] With subsidence of the NO trigger signal, the second NO dissociates and sGC returns to the low activity state.[252] To a much lesser extent, sGC can also be activated by CO.[166, 167]

Excess exposure to NO results in desensitization of sGC toward NO via *S*-nitrosylation of relevant cysteine residues. Furthermore, oxidative stress can lead to oxidation of the heme Fe^{2+} to Fe^{3+}, which can result in loss of heme and degradation of the resulting heme-free sGC.[252] Diminished sGC activity is linked to several pathologies, including cardiopulmonary and neurodegenerative diseases.[252] Activity may be therapeutically boosted with NO-releasing drugs (see 1.5.3), or sGC stimulators and activators. While stimulators activate sGC with a single heme-bound NO, activators even induce activity of heme-free sGC.[252] Notably, sGC stimulators have been approved for clinical application. Riociguat is approved for treatment of pulmonary arterial hypertension (PAH) and chronic thromboembolic pulmonary hypertension (CTEPH)[255] and its structural analogon vericiguat for treatment of heart failure with reduced ejection fraction (HFrEF).[256]

Besides the NO initiated pathway, cGMP can also be generated by particulate guanylate cyclase (pGC). As opposed to sGC, pGC is activated by polypeptides that are secreted by the heart and vascular system, the natriuretic peptides (NPs).[166]

Functions of cGMP

cGMP operates via three classes of effectors, namely cGMP-dependent protein kinases (cGKs), cyclic nucleotide phosphodiesterases (PDEs) and the aforementioned CNG ion channels (Figure 19).[166, 167] cGKs are activated upon cGMP binding and phosphorylate serine and threonine side chains in various substrates. Two main isoforms of cGK exist. cGKI prevails in the cardiovascular system and is highly expressed in vascular smooth muscle and endothelial cells, among others. cGKII is primarily expressed in kidney, brain and intestine.[166]

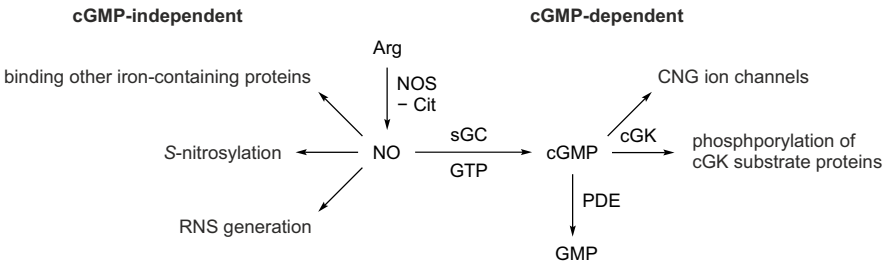

Figure 19. NO as secondary messenger. The overview summarizes NO generation and cGMP-dependent (right) and -independent (left) effects.

NO-cGMP signaling is essential for the regulation of smooth muscle tone. Smooth muscle contracts via myosin-actin interactions that are induced by phosphorylation of the myosin light chain (MLC) by Ca^{2+}-calmodulin-dependent MLC kinase. Different stimuli can trigger an increase in free intracellular Ca^{2+} concentration by intracellular release from

the sarcoplasmatic reticulum and inflow through ion channels, which then activates MLC kinase.[257] Vice versa, relaxation occurs upon decrease of intracellular Ca^{2+} concentrations. This is impacted by the phosphorylation status of different cGK substrates, which regulates intracellular Ca^{2+} concentration as well as calcium sensitivity and thin filament interaction. For example, vasodilator stimulated phosphoprotein (VASP) is phosphorylated by cGKI in vascular smooth muscle cells (VSMCs) and as a result exhibits weaker binding to actin filaments. Consequently, aberrant NO-cGMP signaling is involved in systemic and pulmonary hypertension.[166]

Furthermore, NO-cGMP signaling affects proliferation and differentiation of VSMCs.[258, 259] VSMCs show remarkable phenotypic plasticity. Upon vascular injury or *in vitro* culturing, VSMCs can dedifferentiate from their contractile to a secretory phenotype. Such a phenotypic switch may be promoted by cGMP and is linked to the development of atherosclerosis, restenosis and pathogenic angiogenesis, as is common in many ischemic and inflammatory pathologies and cancer.[258, 259]

NO and its regulation are also important for proper functioning of neuronal processes. While NO conveys neuroprotective effects at physiological amounts, it becomes neurotoxic at high concentrations.[248] NO-cGMP signaling is involved in neurosecretion and neurotransmission, including the regulation of further neurotransmitters such as γ-aminobutyric acid (GABA). In the CNS, NO-cGMP signaling affects synaptic plasticity, in the PNS, gastrointestinal and urogenital functions are regulated in a NO-cGMP-dependent fashion via smooth muscle relaxation.[248]

Degradation of cGMP

cGMP is catabolized to GMP by PDEs (Figure 19).[166] Eleven main PDE isoforms with differing selectivities for cGMP and cAMP and different expression levels depending on the tissue exist. Major cross-regulation complexly interconnects cGMP and cAMP signaling pathways.[166, 167]

PDE3, for instance, holds functions in regulating vascular smooth muscle tone and VSMC phenotypic plasticity. It is able to degrade both cAMP and cGMP, but mainly catabolizes cAMP and is competitively inhibited by cGMP.[166] PDE5, on the other hand, is activated by cGMP and selective for cGMP degradation. PDE5A is highly expressed in the lung and corpus cavernosum and several PDE5A inhibitors have been approved for clinical use. Sildenafil and Tadalafil are approved drugs for treatment of erectile dysfunction, PAH and benign prostate syndrome, vardenafil as well, with the exception of PAH.[167] Furthermore, PDE1 inhibitor ITI-214 is currently undergoing phase II clinical trials for treatment of Parkinson's disease[260] and multiple PDE3 inhibitors have been approved for treatment of heart failure (HF).[261]

1.5.2 cGMP-independent effects

Beyond cGMP signaling, NO can exert control on multiple further processes (Figure 19). Apart from sGC, it can bind to other enzymes from the haemoprotein family and as a consequence influence stress responses.[247, 248] NO can also react with nonheme iron ions, such as in Fe-S clusters, and thus alter the functionality of iron-sulfur proteins. Specifically, this includes iron regulatory protein (IRP), endowing NO with an important role in iron homeostasis.[249]

Moreover, NO *S*-nitrosylates various proteins, which contributes to regulation of signaling

pathways and can have both neuroprotective or neurotoxic effects.[248] NO can also elicit significant nitrosative stress, which can be beneficial in immune function, but also contribute to pathologies. High spikes in NO concentration following iNOS induction combat bacterial and viral pathogens by DNA damaging and degradation of Fe-S centers.[247, 249] However, many neurodegenerative disorders also involve aberrantly high NO production and generation of reactive nitrogen species (RNS), i.e. mainly peroxynitrite and dinitrogen trioxide, from NO under oxidizing conditions is linked to development of Alzheimer's, Huntington's and Parkinson's disease.[248]

1.5.3 Nitric oxide releasing substrates

Direct inhalation of gaseous nitric oxide can be applied for acute treatment of pulmonary hypertension.[262] For many applications, however, nitric oxide itself is not suitable due to its instability. Therefore, a variety of compounds that are more stable, but able to release nitric oxide spontaneously or upon triggering have been developed for clinical and research purposes.

Nitrites and nitrates

Organic and inorganic nitrites and nitrates can be enzymatically reduced to NO and embody the classical nitrovasodilator therapy. Amyl nitrite has been clinically applied for treatment of angina pectoris as early as 1867.[263] To date, organic nitrite and nitrate esters represent the drugs of choice for treatment of coronary heart disease (CHD). Nitroglycerin (NG) and isosorbide nitrates (ISMN, ISDN, Figure 20) are approved standard treatments for angina pectoris and secondary options for HF.[261] They exist in short-acting and long-acting formulations, for acute and chronic application, respectively.[261, 262] The utility of nitrates is limited by the possible development of tolerance due to inhibition of the metabolism to bioactive NO.[261, 264] The risk of tolerance can be reduced by intermittent dosing.[262] Moreover, nicorandil, a nicotinamide nitrate ester approved for treatment of angina pectoris, shows promising indications regarding absence of tolerance development (Figure 20).[261]

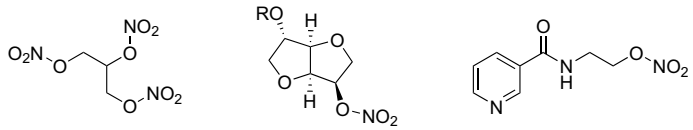

Figure 20. Selection of NO releasing nitrates: nitroglycerin (NG), isosorbide mononitrate (ISMN), isosorbide dinitrate (ISDN) and nicorandil.

Furthermore, several inorganic nitrates are currently under clinical investigation. Sodium and potassium nitrate, dietary nitrate, as well as sodium nitrite, are currently undergoing phase II clinical trials for treatment of HF, heart failure with preserved ejection fraction (HFpEF) or angina pectoris, among others.[261]

Metal nitrosyl complexes

NO can also be released from nitrosyl complexes, where NO is coordinated to a transition metal (Figure 21). The most prominent representative of this category is sodium

nitroprusside (SNP), $Na_2[Fe(CN)_5NO]$, which is approved for treatment of HF and hypertensive crisis.[261] NO release from SNP can occur via several mechanisms. For mammalian tissue, it has been suggested that SNP reacts with available thiol compounds to form *S*-nitrosothiols (SNOs), such as *S*-nitroso-glutathione (GSNO),[265] which serve as endogenous NO carriers. Furthermore, aqueous SNP photochemically releases NO under formation of $[Fe(CN)_5OH_2]^{2-}$.[266] On the one hand, this might be applied for photocontrolled release with UV/Vis irradiation. On the other hand, sensitivity to ambient light hampers all research experiments and has led to misinterpreted results in the past.[267, 268] As concomitant release of cyanide may occur, potential cyanide toxicity represents a grave side effect.[267, 269] Further limitations of SNP application include the unfeasibility of enteral administration and possible development of tolerance.[262, 268]

Esters of Roussin's red salt (RSE, $Fe_2(\gamma\text{-}SR)_2(NO)_4$) are able to release up to four equivalents of NO upon photoactivation. A derivative carrying protoporphyrin IX (PPIX) moieties as light-harvesting antennas even allows for 2PE in the near-IR range.[270]

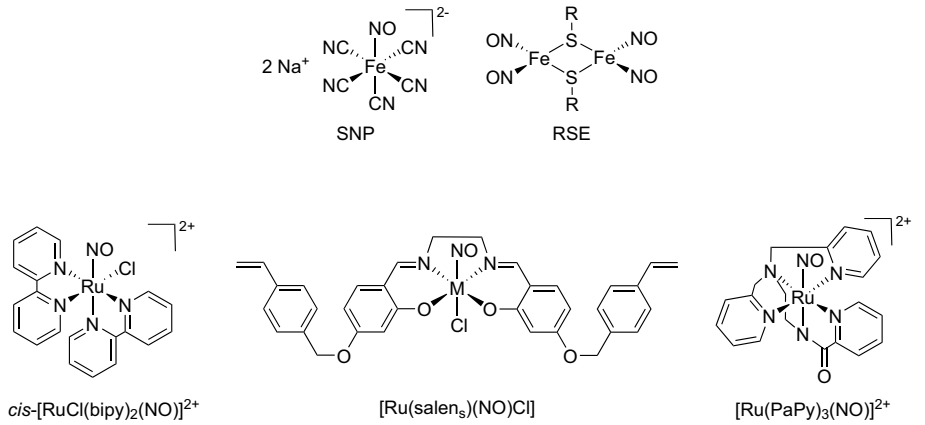

Figure 21. Selection of NO releasing metal nitrosyl complexes: sodium nitroprusside (SNP), Roussin's red ester (RSE), *cis*-$[RuCl(bipy)_2(NO)]^{2+}$, $[Ru(salen_s)(NO)(Cl)]$, $[Ru(PaPy)_3(NO)]^{2+}$.

Furthermore, ruthenium nitrosyls provide versatile, photoactivatable NO precursors (Figure 21). Simple $K_2RuCl_5(NO)$ and *cis*-$[RuCl(bipy)_2(NO)](PF_6)_2$ release NO upon irradiation with UV light.[271, 272] The styrene-bearing Ru-salen complex $[Ru(salen_s)(NO)(Cl)]$ has been covalently immobilized in a methacrylate polymer, enabling light triggered release of NO from the porous material.[273] This strategy holds promise for application in antimicrobial coatings of medicinal products or bandage materials, since only the small, uncharged NO is able to escape the material, while potentially toxic coproducts remain inside the polymer.[268, 274] Moreover, it allows for tuning of the release rate by adjusting pore size. Analogously, several further porous materials containing metal nitrosyls have been developed, as for example with ruthenium and manganese nitrosyl complexes carrying the pentadentate $PaPy_3$ ligand.[275, 276] The manganese analogue is excitable with visible light[277] and its absorption can even be redshifted to the near-IR range by appropriate substitution at the ligands.[278, 279]

A further possibility to increase absorption at longer wavelengths is the attachment of a fluorophoric light harvesting antenna, either directly as coordinating ligand or as substituent of an existing ligand.[280, 281] This entails the advantage that it additionally enables tracking of the NO precursor. A variant of this strategy can be utilized for quantification of NO release and super-resolution imaging. Here, fluorescence is activated only upon illumination at an activating wavelength and consequently occurs concurrently with NO release.[281]

Diazeniumdiolates

N-bound diazen-1-ium-1,2-diolates (NONOates) spontaneously release up to two equivalents NO at physiological conditions (Figure 22 a).[282] The release rate greatly varies with the nature of the amine and can therefore be selected to suit a given application (Figure 22 b). Pyrrolidin-1-yl-NONOate (PYRRO/NO) releases NO with a half-life of 3 s at physiological conditions,[283] diethylamino-NONOate (DEA/NO) has a half-life of 2 min[284] and spermine-N^2-NONOate (SPER/NO) of 40 min.[282] The first clinical study of a NONOate successfully applied aerosolized diethylenetriamine-N^2-NONOate (DETA/NO) for selective pulmonary vasodilation in acute respiratory distress syndrome (ARDS).[285] DETA/NO has a half-life of 20 h and has also been shown to exhibit anticancer effects.[286]

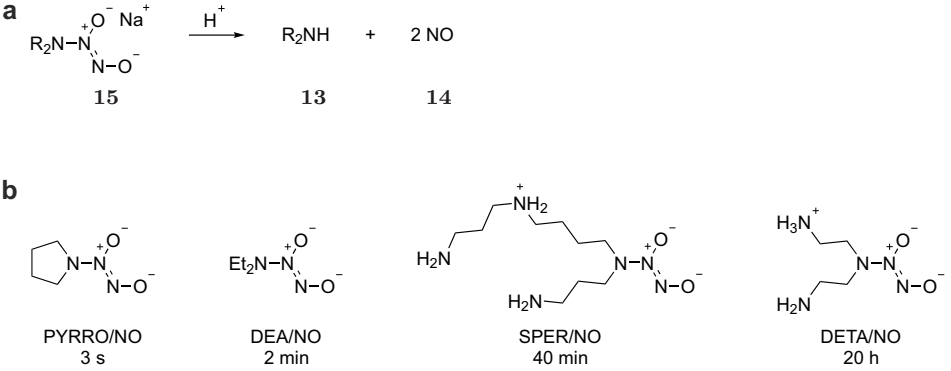

Figure 22. Spontaneous release of NO from *N*-bound NONOates. **a** At physiological conditions, simple *N*-bound NONOates **15** spontaneously decompose to two equivalents NO (**14**) and the fused amine **13**. **b** Structures and half-lives $t_{\frac{1}{2}}$ of basic NONOates at 37 °C, pH 7.4.

In addition, the rate of NO release is strongly dependent on pH. While it proceeds very slowly at basic pH values, it is very rapid at acidic conditions.[282] NONOates are usually employed in form of their stable sodium salts and reaction conditions during synthesis are kept alkaline.[282, 287] Although no metal toxicity has to be considered for NONOates, toxic byproducts of NO release, such as potentially carcinogenic nitrosamines, may occur.[284] Analogous to polymers containing metal nitrosyl compounds, solid matrices containing NONOates allow for release of NO, but retention of byproducts inside the matrix.[288, 289]

In order to enable target specifically induced release of NO while avoiding undesired systemic side effects, O^2-protection can be applied to abrogate spontaneous decomposition (Figure 23 a). Notably, this allows for design of compounds that preferentially target cancerous tissue by attaching groups that are selectively cleaved in tumor cells.[287] For example, O^2-2,4-(dinitrophenyl) (dNP) caged PABA-DMA/NO is preferentially deprotected by glutathione *S*-transferase π (GST-π), which is overexpressed in a variety of tumor cells.[290] Furthermore, several O^2-(*p*-substituted benzyl) protected NONOates have been developed. Depending on the *para*-substituent, different kinds of deprotection mechanisms can activate release of the corresponding NONOate via 1,6-elimination.[287] NONOates carrying an indole-1,4-quinone, e.g. INDQ-DEA/NO, are activated by quinone reductase 1 (QR1), which is again overexpressed in various cancer cells.[291] Moreover, several glycosides with PYRRO/NO have been developed for prompt NO release upon enzymatic cleavage of the glycosidic bond. β-D-Gal-PYRRO/NO is hydrolyzed by β-galactosidase,[292] sialated α-NANA-PYRRO/NO carrying *N*-acetylneuraminic acid (NANA) by neuraminidase.[293] Since influenza viruses, among others, bear neuraminidases in their viral envelope, sialated NONOates hold promise for potential antiviral application.

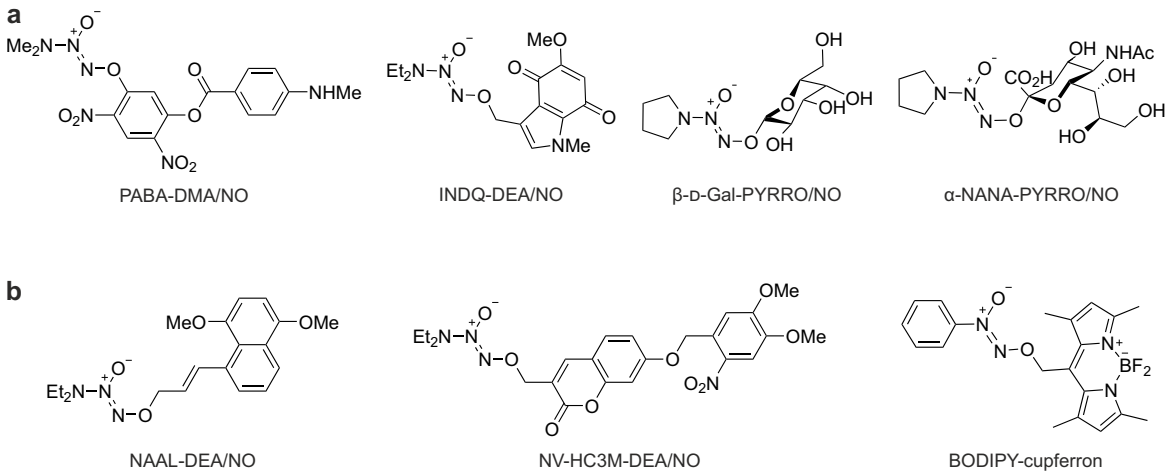

Figure 23. Induced release of NO from protected NONOates. **a** Selection of O^2-protected NONOates. **b** Selection of photoprotected NONOates.

Activation by light is also a possibility with NONOates. The first photoprotected NONOates were *o*NB-protected DEA/NO.[294] Cell membrane permeability was adjustable with appropriate substitution at the phenyl ring and thrombin-stimulated platelet aggregation could be inhibited in a light-dependent manner. Generally, two competing pathways exist for the photoreaction of alkylated NONOates. Heterolytic cleavage of the C-O bond leads to desired release of anionic NONOate under generation of the corresponding carbocation of the PPG, whereas homolytic cleavage of the N=N bond does not yield the free NONOate, but instead a potentially carcinogenic nitrosamine. While deprotection from simple *o*NB is strongly dominated by homolytic cleavage and thus generates only minor amounts of NO, heterolytic cleavage can be promoted via the *meta* effect by attaching electron donating *meta*-substituents.[269, 295] Apart from the competing nonefficient homolytic cleavage, simple *o*NB protection is complicated by operation at short-wavelength UV excitation, which might elicit secondary photolysis of the free NONOate, and potential influence of pH on the deprotection mechanism (see 1.3.1). In this regard, protection with napthylallyl derivatives, such as in NAAL-DEA/NO, is more advantageous (Figure 23 b).[296] Alternatively, a linker separating the PPG and the NONOate can also preclude homolytic C-O cleavage, while allowing for a diversified selection of PPGs. This has been exploited in NV-HC3M-DEA/NO (Figure 23 b), where deprotection of 6-nitroveratryl (NV) is followed by spontaneous 1,8-elimination from the (coumarin-3-yl)methyl alkoxide anion and DEA/NO release. As with the activated fluorescence mentioned above, fluorescence of concurrently generated 7-hydroxy-3-hydroxymethyl coumarin (HC3M) arises only after irradiation, allowing for visualization of NO release. Additionally, the fused coumarinyl enables NO release upon 2PE.[295] Lastly, *C*-bound NONOates may also be employed as light-activated NO donors, as represented by O^2-BODIPY-protected cupferron, which releases NO upon illumination with visible light with comparably high quantum efficiency (Figure 23 b).[297]

Bifunctional drugs

Beyond compounds with the main purpose of providing NO, NO-releasing moieties have been exploited in bifunctional drugs, adding beneficial characteristics onto a given drug (Figure 24). For example, gastrointestinal complaints that occur as side effect of non-steroidal anti-inflammatory drugs (NSAIDs) can be mitigated, without reducing the anti-inflammatory effect. This has been utilized by addition of a nitrate function to an as-

pirin derivative, yielding NCX-4016.[166, 262, 268] PYRRO/NO and dimethylamino-NONOate (DMA/NO) have also been attached to NSAIDs, including aspirin, ibuprofen and indomethacin.[298] Moreover, SNO moieties have been applied, for example in SNO-diclofenac and ACE inhibitor SNO-captopril.[262, 268]

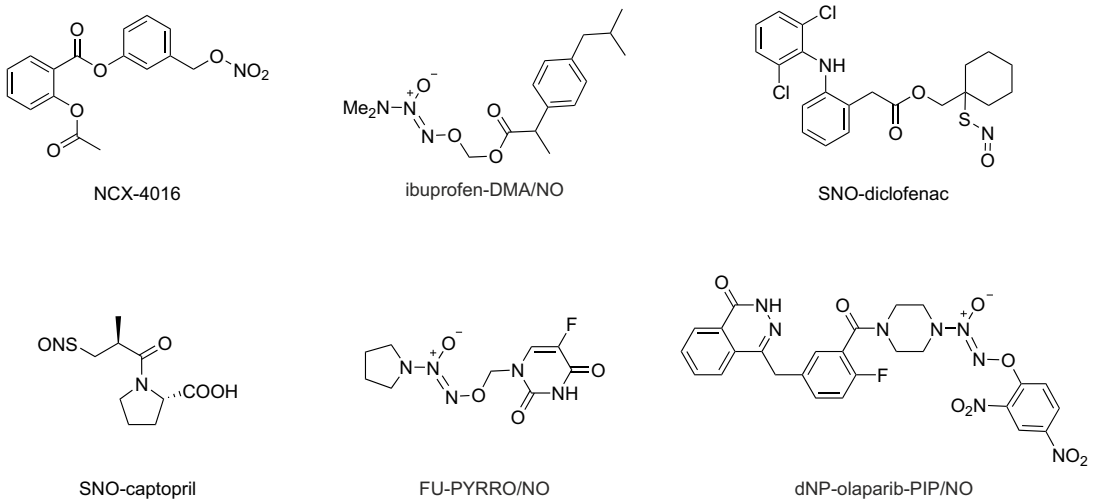

Figure 24. Selection of bifunctional NO releasing drugs.

NO donors can also be fused to anticancer drugs for improved selectivity or potency or reduced toxicity against healthy cells. For instance, FU-PYRRO/NO exhibits increased cytotoxicity against cancerous cells as compared to 5-fluorouracil (FU) alone.[299] Combination with O^2-protection is also feasible, as for example in GST-π activated dNP-olaparib-piperazino-NONOate (PIP/NO).[300] Importantly, for all bifunctional drugs, NO dosage control is required in order to release effective NO concentrations at a given effective range of the combined drug. This is of particular significance for anticancer drugs, since high concentrations of NO elicit tumor inhibition, while low concentrations may exhibit tumor promoting effects.[269, 287]

2 Aims & Motivation

Three main objectives were pursued within the dissertation at hand, with the overarching theme of developing tools with high levels of control on different layers. Precision of the different methods ought to be achieved by employment of orthogonal protein tags, small molecule induction or photocontrol, respectively.

Firstly, an orthogonal RNA editing platform ought to be devised, allowing for independent, selective editing at two distinct sites in parallel. This would be instrumental in studying effects of base mutations in greater depth, for instance by enabling investigation of the interplay between editing sites. Aiming towards this goal, as first step a new editase with a steering mechanism orthogonal to the well-established SNAP-ADAR system was to be developed. Regarding this, fusions of ADAR1 deaminase domains with self-labeling CLIP- and HALO-tag and corresponding clip- and halo-guideRNAs should be engineered and characterized. In the next step, the new editase ought to be combined with a deaminase steered by the SNAP-tag for orthogonal, concurrent editing. Additionally, options for photocontrol of the new editase might also be explored.

Secondly, a further layer of control ought to be implemented in RNA editing with the SNAP-ADAR system by combination with chemically induced dimerization. This would provide a tool which allowed to evoke editing by a small molecule, thus enabling facile tuning of editing levels by dosage control. In this regard, SNAP-tag and ADAR1 deaminase domain were to be separated and fused to gibberellin insensitive dwarf 1A (GID1A) and gibberellic acid insensitive (GAI). This way, editing activity should be triggered upon recruitment of the deaminase domain to the guideRNA-SNAP-tag conjugate by chemically induced dimerization with gibberellic acid.

Lastly, a photoactivatable NO donor ought to be designed for light-triggered NO-cGMP signaling. Since light provides excellent spatial control, this might become a useful tool for unraveling the compartmentalization of NO-cGMP signaling at a subcellular level, which has been suggested to contribute to the organization of the manifold functions and effects of NO. To this end, a MeNPOM-protected NONOate should be synthesized and evaluated in vascular smooth muscle cells.

3 Results & Discussion

In accordance with the aims of the dissertation at hand, findings will be presented and discussed sorted by the three main projects in the following. The four publications resulting from the doctoral study are included in the appendix (see A.2). The three first author publications 1 to 3 correspond to the three main projects, respectively, and important findings will be reported in the following. Results of publication 4 will not be elaborated in detail here, the personal contributions are stated in the List of Publications above.

3.1 Orthogonal RNA editing

An orthogonal RNA editing system would enable the independent recruitment of two different editing enzymes for concurrent base editing at two distinct sites. This ought to be achieved by combination of two editases consisting of two different deaminases fused to orthogonal self-labeling protein tags for independent steering, as depicted in Figure 1 a in Publication 1 (Figure 1 a $_{P1}$). For this purpose, the combination of established SNAP-ADAR (SA) with CLIP- and HALO-deaminases was tested.

3.1.1 Development of new editase

Design and trial of CLIP- and HALO-ADAR

Firstly, fusions of the different self-labeling protein tags to an ADAR deaminase domain and corresponding guideRNAs needed to be generated. CLIP-ADAR1 (CA1) and HALO-ADAR1 (HA1) were cloned and clip- and halo-guideRNAs were prepared by attachment of a BC or 6-chlorohexyl-PEG_2 instead of the BG in snap-guideRNAs, respectively. Subsequent testing of snap-, clip- and halo-guideRNAs in recruiting editing activity of SA1(Q), CA1(Q) or HA1(Q) revealed that all three guideRNAs elicit good A-to-I editing yields in combination with their corresponding editase (Figures S10 $_{P1}$ – S12 $_{P1}$). However, the clip-guideRNA in particular also gave rise to significant editing with SA1(Q). This imperfect orthogonality is not fundamentally unexpected per se, keeping in mind that the CLIP-tag is originally derived from the SNAP-tag. It also seems reasonable that the combination of clip-guideRNA with the SNAP-tag yields more editing than vice versa, due to the lower space requirement of BC as opposed to BG and the known fact that SNAP-tag also accepts smaller substrates, as for example benzyl-2-chloro-6-aminopyrimidines (BCPs), which have been exploited for their improved cell permeability.[9, 301] Slight cross-reactivity of SNAP- and CLIP-tag substrates has been reported before and may be unproblematic in certain cases. For applications in which the entirety of the protein tags reacts with a labeled substrate, imperfect orthogonality can be bypassed by labeling both protein tags simultaneously or pre-labeling of the SNAP-tag. In these cases, cross-reactivity becomes negligible and combination of SNAP- and CLIP-tag is feasible, as represented by various studies. In regard to the editing application however, the practicability of the combination of SNAP- and CLIP-tag is limited by their cross-reactivity. Imperfect orthogonality might be particularly challenging here since a majority

of SA1(Q) is not conjugated to a snap-guideRNA at concentrations present in typical editing conditions, thus remaining accessible in excess to clip-guideRNA (Figure 1 e $_{P1}$).

In addition, clip-guideRNAs were unstable upon long-term storage (Figure S12 $_{P1}$). Editing yields decreased over time, for instance for the experiment shown in Figure S12 $_{P1}$, the first editing of CA1Q with clip-guideRNA yielded 74 %, a replicate after one month exhibited 66 % editing yield and after another month the editing yield dropped to 48 %. This hurdle could not be circumvented by storage of the clip-guideRNA at −80 °C instead of the usual −20 °C (data not shown). As a consequence of both orthogonality and stability limitations concerning the CLIP-tag, the development of an orthogonal RNA editing platform was henceforth pursued with the combination of SNAP- and HALO-tag.

Selectivity in editing with SNAP- and HALO-ADAR1Q

In order to obtain reliable results under conditions similar to the endogenous environment, Flp-In T-REx 293 cells with single copy genomic integration of the respective editase were applied. Both the SA1Q and the HA1Q cell line showed doxycycline-dependent expression of the respective editase with predominantly cytoplasmic localization (Figure 1 b, c $_{P1}$). Snap- or halo-guideRNAs targeting different sites in the ORF of endogenous *GAPDH* recruited SA1Q or HA1Q, respectively, with excellent selectivity, eliciting high editing yields with the corresponding matching editase while no editing above background level was observed with the mismatching combinations (Figure 1 d $_{P1}$). Concurrent transfection of one snap- and one halo-guideRNA for different target sites was also possible with retained selectivity.

Generally, editing yields with HA1Q were slightly below those attained with SA1Q. Several plausible causations come to mind. Since HA1Q expression is higher than SA1Q expression (Figure 1 c $_{P1}$), lesser protein amounts can be excluded as potential cause. Beyond expression levels of the editases, kinetics and efficiency of guideRNA conjugation may play a role. It has been shown before that HALO-tag mediated labeling is influenced substantially more by the nature of the label than SNAP-tag labeling (see also 1.1). While screening processes in the development of SNAP- and CLIP-tag involved multiple different substrates,[19, 20, 21] the HALO-tag has been optimized for labeling with rhodamine derivatives[15, 31] and as a result exhibits inferior performance with certain other labels. Furthermore, the SNAP-tag is derived from the naturally DNA-binding hAGT, whereas the HALO-tag carries a net negative charge, with an accumulation of negative charges at the substrate entry channel.[302, 303] Consequently, the HALO-tag might be less beneficial for labeling with negatively charged substrates. Interestingly, a variant of the HALO-tag with optimized binding interface for oligonucleotide labels has been developed. In the halo-based oligonucleotide binder (HOB), the negative patch at the entry channel is exchanged for positively charged residues, resulting in improved reaction with DNA labels.[303]

Moreover, specifically with a large label like the guideRNA, the length of the linker between chlorohexyl moiety and label might have considerable impact on the labeling efficiency. It has been observed in immobilization studies that the standard PEG_2 linker can be too short depending on the application, and longer linkers have proven beneficial.[15, 304] In regards to oligonucleotides, longer linkers have been applied for labeling with DNA-like oligodeoxyfluorosides (5mers).[32] On the other hand, DNA-PAINT (DNA points accumulation in nanoscale topography) with DNA oligomers (11mers) has been realized with the standard PEG_2 linker.[305, 306]

To check for potential shortcomings regarding the conjugation of halo-guideRNAs to HA1Q in comparison to the SNAP-ADAR system, a conjugation assay under typical editing conditions was performed (Figure 1 e $_{P1}$). Both SA1Q and HA1Q similarly reacted with their

matching guideRNA, respectively, to form a guideRNA-deaminase conjugate, suggesting sufficient conjugation efficiency with the HALO-tag. It might still be conceivable that HALO-tag's negative charge hampers assembly with the target mRNA by electrostatic repulsion or that conjugated guideRNA is not fully accessible due to steric demands, however.

Since editing efficiencies with HA1Q were good, even though slightly lower than with SA1Q, and the two systems exhibited the desired selectivity, concurrent orthogonal editing with SNAP- and HALO-tag fused to different deaminases was pursued with the now established HA1Q. Nevertheless, implementation of HOB[303] and halo-guideRNAs containing a longer linker, such as T1, which carries an additional carbamate-PEG_2-carbamate spacer,[15, 304] might be worth a try for boosting editing yields in future studies.

3.1.2 A-to-I editing platform with HA1Q and SA2Q

Duo cell lines expressing HA1Q and SA2Q

To put the orthogonal platform into effect for concurrent editing in one common cell, duo Flp-In T-REx 293 cell lines expressing both HA1Q and SA2Q from a single cassette were generated. SA1Q and SA2Q had previously been characterized in regards to their substrate scope, revealing differing preferences for different 5'-NAN codons.[123] For some codons, namely 5'-CAU, 5'-CAG and 5'-GAU, ADAR1 performed significantly better than ADAR2 or vice versa. Thus, such an orthogonal HA1Q + SA2Q system would provide an extended substrate scope. In future studies, this tool would widen the possibilities for successive selective editing of multiple sites. This may prove valuable for the elucidation of the individual effects of naturally edited sites in transcripts of a common pathway on the output of said pathway.

In an effort to inquire the suitability of different construct options for the generation of duo Flp-In T-REx cell lines, five different duo constructs were designed and the resulting cell lines characterized (Figure 2 $_{P1}$). Upon doxycycline induction, all five cell lines expressed both HA1Q and SA2Q uniformly, colocalized and predominantly cytoplasmic (Figure 2 b $_{P1}$). Expression levels of HA1Q and SA2Q differed between the constructs (Figure 2 c $_{P1}$). Cell lines **1** $_{P1}$ and **2** $_{P1}$ (Figure 2 a $_{P1}$) with constructs containing two consecutive CMV promoters yielded stronger expression of the first transgene. Expression from a single CMV promoter as P2A[307] construct in cell line **3** $_{P1}$ gave more balanced expression with only slightly higher expression of the first transgene. Equal expression of the transgenes could be achieved in cell lines **4** $_{P1}$ and **5** $_{P1}$ with constructs with bidirectional CMV and EF1α promoters. Since HA1Q expression seemed to be the most limiting factor (Table S3 $_{P1}$), focus was placed on cell line **2** $_{P1}$ with the highest HA1Q expression in further experiments.

Expanded substrate scope by orthogonal editing with HA1Q and SA2Q

As shown before,[123] 5'-CAU was preferentially edited by SA1Q, whereas 5'-CAG was preferentially edited by SA2Q (Figure 3 a $_{P1}$). The novel orthogonal editing platform should now allow to recruit the preferred ADAR deaminase domain to each codon via labeling with halo- or snap-guideRNA. Specifically, targeting the 5'-CAU codon with halo-guideRNA and the 5'-CAG codon with snap-guideRNA results in the matching preferred combination (Figure 3 b $_{P1}$). This was realized for the editing of a 5'-CAU in the ORF of endogenous *GAPDH* and 5'-CAG in the ORF of *ACTB* in cell lines **2** $_{P1}$ and **5** $_{P1}$ (Figures 3 c $_{P1}$, S13 a $_{P1}$). Transfection of guideRNAs in the matching combination yielded good editing yields at both sites,

i.e. in cell line $\mathbf{2}_{P1}$ 25 % at the 5'-C<u>A</u>U and 30 % at the 5'-C<u>A</u>G codon. Conversely, the mismatching combination elicited no editing at the 5'-C<u>A</u>U and reduced editing at the 5'-C<u>A</u>G codon by factor 1.5. Again, co-transfection of two guideRNAs was also feasible. The two editases of the orthogonal platform were steerable independently and concurrently.

Moreover, bisfunctional halo-snap-guideRNAs carrying both BG and chlorohexyl moieties enabled joint recruitment of both editases, thus ensuring the presence of the preferred ADAR deaminase domain and optimal editing yields for any codon (Figure $3\,c, d_{P1}$). Analogously, bis-guideRNAs carrying two of the same moieties, i.e. $(halo)_2$- and $(snap)_2$-guideRNAs, have been explored. This may allow for recruitment of two HA1Q or SA2Q per guideRNA, respectively, and lead to an increase in editing yields to 46 % at both codons in cell line $\mathbf{2}_{P1}$ (Figure $3\,e_{P1}$). Additionally, the bis-guideRNAs allowed for 10 × reduction in guideRNA amounts (from 5.0 pmol to 0.5 pmol), further increasing selectivity without substantial loss in editing efficiencies (Figure $3\,f_{P1}$). A series of experiments with different guideRNA amounts attested that the less guideRNA, the higher selectivity (Figure $3\,g_{P1}$). For applications with an extraordinary demand for selectivity, guideRNA amounts as little as 0.1 pmol might be suitable (Figure S13 c_{P1}). The excellent selectivity exhibited here might be profitable, even though it comes at the cost of a reduction in editing yields. For example, low, controlled editing yields in the majority of cells are often more advantageous for treatment of pathologies resulting from loss-of-function point mutations than high editing yields in a minority of cells.[135]

Global off-target editing in HA1Q + SA2Q duo cell line

Finally, global off-target editing behavior of the novel orthogonal editing platform was assessed by whole transcriptome sequencing. Specifically, cell line $\mathbf{2}_{P1}$ was examined for significantly differently edited sites in comparison to a Flp-In T-REx 293 cell line without transgene, with and without preceding transfection of a $(snap)_2$- and $(halo)_2$-guideRNA. The total number of significantly differently edited sites in cell line $\mathbf{2}_{P1}$ with guideRNAs roughly corresponded to the sum of total off-targets in SA1Q and SA2Q single cell lines (Table 1_{P1}).[123] The majority of those sites occurred in UTRs or noncoding regions and were differently edited below 25 %. About 25 % of the sites lead to nonsynonymous substitutions, and about 25 % of sites exhibited differences in editing above 25 % (Figure $4\,a_{P1}$).

Interestingly, it has recently been shown that the editing activity of wild-type ADAR2 can be boosted to a certain extent by inserting the unnatural pyrimidine analogon dZ[308, 309] as counter base to the target A.[310] dZ allows for the formation of a hydrogen bond with E488 independent of protonation status, consequently its application as counter base might enable the achievement of high editing yields without requiring the use of hyperactive E/Q mutants. Since SA1 and SA2 with wild-type deaminase domain exhibit drastically less transcriptome-wide off-target editing than SA1Q and SA2Q,[123] this might be a promising approach to further minimize off-target editing elicited by the engineered editases.

Comparison of significantly differently edited sites with and without guideRNAs disclosed which off-target sites were elicited by the expression of HA1Q and SA2Q alone and which sites were caused by guideRNA mis-guiding (Table 1_{P1}, Figure $4\,b_{P1}$). Only a minor fraction of total off-target sites were guideRNA-dependent. Out of the guideRNA-dependent off-target sites, only about 5 % exhibited editing differences above 25 %, most of which were logically explainable by binding of one of the guideRNAs due to sequence similarity (Figures S17 $_{P1}$ – 19 $_{P1}$). Consequently, rational sequence optimization of guideRNAs might be feasible for such sites, if required. Additionally, the whole transcriptome sequencing data was

exploited for analysis of low frequency bystander editing sites in the *GAPDH* and *ACTB* transcripts (Tables S8 P1, S9 P1).

Overall, expression of HA1Q and SA2Q via single copy genomic integration results in moderate transcriptome-wide A-to-I off-target editing, and the presence of guideRNAs contributes a small fraction of additional events.

3.1.3 A-to-I and C-to-U editing platform with HA1Q and APO1S

Duo cell lines expressing HA1Q and APO1S

An orthogonal RNA editing platform allowing for both targeted A-to-I and C-to-U editing would provide an even more powerful tool. Not only can the two nucleotide interchanges evoke different sets of amino acid substitutions and exclusively resolve or generate stop codons, respectively. It has also been suggested that influences between A-to-I and C-to-U editing may exist and especially C-to-U editing functions are not well elucidated to date. For example, even though ADAR and APOBEC display different substrate selectivities in regards to secondary RNA structure, some transcripts are naturally edited by both ADAR and APOBEC. An orthogonal platform combining A-to-I and C-to-U editing may provide a useful tool to examine the dependency of such sites on one another, if a specific order of the editing events is required, as well as their individual effects.

Prerequisite for the realization of such a platform is a tool for targetable C-to-U editing. This had been developed in parallel to the work at hand by another member of the Stafforst group, Ngadhnjim Latifi. Briefly, a C-terminal fusion of the SNAP-tag to mAPOBEC1 allowed for recruitment of cytidine deamination activity with snap-guideRNAs. As opposed to ADAR, APOBEC is only recruited by the pairing of the guideRNA with the target mRNA, but acts outside of the RNA duplex. Preliminary studies revealed that positioning of the guideRNA $4-6$ nt upstream of the target A gave optimal editing efficiency.[311] Furthermore, cytosolic localization proved beneficial, and an additional NES signal was attached at the C-terminus. The resulting mAPOBEC1-SNAP-NES construct (APO1S) was applied for all experiments in the dissertation at hand.

APO1S was subsequently combined with the previously established HA1Q in four different duo constructs and genomically integrated into Flp-In T-REx 293 cells. Analogous to before, expression from two consecutive CMV promoters and from bidirectional CMV and EF1α promoters was explored (Figure 5 a P1). The tendencies of expression levels corresponded to those observed for the HA1Q + SA2Q duo cell lines (Figure 5 b P1). This highlights the value of careful initial examination of different constructs, since it may lead to the identification of transferable patterns, thus allowing to predict which arrangement might be suited best for a given future application.

Concurrent A-to-I and C-to-U editing with HA1Q and APO1S

The HA1Q + APO1S cell lines were applied for editing of an *eGFP* reporter transcript. The same guideRNA sequence allowed for A-to-I editing of a 5'-U<u>A</u>G codon within the RNA duplex and C-to-U editing of a proximal 5'-A<u>C</u>G codon 5 nt downstream of the RNA duplex (Figure 5 c P1). HA1Q or APO1S or both were recruited with halo-, snap- or halo-snap-guideRNA, respectively, and concurrent editing of both sites with halo-snap-guideRNA retained the high editing yields at both sites (Figures 5 d P1, S14 P1). Specifically, in cell line **9** P1, bidirectionally expressing HA1Q from the CMV and APO1S from the EF1α promoter, 68 % editing yield at the 5'-U<u>A</u>G and 47 % at the 5'-A<u>C</u>G codon were attained with

halo-snap-guideRNA. Orthogonal recruitment of A-to-I and C-to-U editing activity to different endogenous transcripts, namely a 5'-U<u>A</u>U in the ORF of *ACTB* and a 5'-A<u>C</u>C in the ORF of *GAPDH*, was also possible (Figure 5 e $_{P1}$). Editing was highly selective and gave good A-to-I and moderate C-to-U yields (Figures 5 f $_{P1}$, S13 e $_{P1}$), i.e. in cell line **9** $_{P1}$ 65 % at the 5'-U<u>A</u>U and 18 % at the 5'-A<u>C</u>C codon. Again, co-transfection of both guideRNAs was also feasible.

Furthermore, the editing efficencies of APO1S at the *eGFP* and the *GAPDH* site were compared to editing yields achievable with the C-to-U editor RESCUE (Figure S15 $_{P1}$). For both sites, significantly higher on-target editing was obtained with APO1S than with RESCUE. Moreover, editing with RESCUE produced additional A-to-I off-target sites, since the incorporated mutated ADAR deaminase domain retained A-to-I editing capability after evolution towards relaxed substrate selectivity to accept cytidines. Interestingly, this characteristic has been suggested to enable so-called multiplexed A-to-I and C-to-U editing with the RESCUE system.[142] The contained Cas13b steering moiety was able to process a common pre-crRNA (about 130 nt) into two separate guideRNAs, one targeting an A and one targeting a C in the *CTNNB1* transcript. This resulted in editing at both the A-to-I and the C-to-U site, however, with significantly reduced editing yields in comparison to single editing of each site. In contrast, the platform developed here retains editing yields upon concurrent editing of the A-to-I and the C-to-U site, both in the *eGFP* as in the *ACTB* and *GAPDH* transcripts.

Thus, the novel approach, exploiting self-labeling protein tags for the steering of independent RNA editors, allows for orthogonal and concurrent A-to-I and C-to-U editing. Currently, the variety of feasible C-to-U editing sites is still limited, due to hurdles in regards to programmability and target scope of APO1S (data of Ngadhnjim Latifi, not shown). APOBEC1 is believed to have strong preference for specific secondary structures. A possible optimization route might be to devise a SNAP-tag steered C-to-U editor carrying the ZDD of APOBEC1 only instead of the full-length protein, i.e. an APO1$_{ZDD}$-SNAP-NES construct. This might eliminate substrate selectivities whose mechanisms of action are not understood, as well as further reduce the size of the editase. Another conceivable approach under ongoing investigation bases on the replacement of Cas13b in the RESCUE system with a self-labeling protein tag for enhanced steerability, and has just been published by Ngadhnjim Latifi *et al.*[311]

Global off-target editing in HA1Q + APO1S duo cell line

Cell line **9** $_{P1}$ was also examined for transcriptome-wide off-target A-to-I and C-to-U editing, again with and without preceding transfection of a $(snap)_2$- and $(halo)_2$-guideRNA (Table 2 $_{P1}$). As expected for a cell line expressing one instead of two A-to-I editors, the total number of significantly differently A-to-I edited sites in cell line **9** $_{P1}$ was below that in cell line **2** $_{P1}$. The majority of sites occurred in the 3'-UTR and approximately 30 % of the sites lead to nonsynonymous substitutions. Again, about 25 % of the sites showed differences in editing above 25 % (Table S10 $_{P1}$). Characterization of the guideRNA-dependent fraction of significantly differently edited sites revealed that roughly 5 % of guideRNA-dependent sites exhibited editing differences above 25 % (Tables 2 $_{P1}$, S10 $_{P1}$).

For the examination of global C-to-U off-target sites, the cutoff for significantly differently edited sites was set lower than for A-to-I sites to account for the generally lower C-to-U editing levels, i.e. 5 % instead of 10 % difference in editing. C-to-U off-target sites were even more strongly accumulated in the 3'-UTR than A-to-I sites and only about 0.5 % of the

sites lead to nonsynonymous substitutions (Table 2 $_{P1}$). Approximately a third of the total sites exhibited editing differences above 10 %, only about 5 % were differently edited above 25 % (Table S11 $_{P1}$). A small fraction of the total sites were guideRNA-dependent off-targets and out of the guideRNA-dependent sites roughly 2 % exhibited differences in editing above 25 %. Analogous to cell line **2** $_{P1}$, low frequency bystander A-to-I editing sites in *ACTB* and C-to-U editing sites in *GAPDH* were also determined (Tables S12 $_{P1}$, S13 $_{P1}$).

3.1.4 Exploration of photocontrol of the new HALO-deaminase

With the development of an orthogonal editing platform having been successful, the potential for implementation of photocontrol in editing with the newly established HALO-deaminase was explored. SNAP-ADAR editing has been rendered photoactivatable before by application of photoprotected N7-MeNPOM-snap-guideRNAs (Figure 12).[122, 126] Current studies headed by another member of the Stafforst group, Alfred Hanswillemenke, additionally enabled photodeactivatable SNAP-ADAR editing with snap-^{UV}X-guideRNAs containing a photocleavable NPOM linker between the BG moiety and the guideRNA (Figures 1 $_{P4}$, 2 a $_{P4}$). Combination of a photoactivatable N7-MeNPOM-snap-guideRNA with a photocleavable snap-^{UV}X-guideRNA even allowed to photoswap between two distinct editing sites in *STAT1* with opposing effects on phosphorylation status, and consequently activity (Figure 2 c, d $_{P4}$).

In regards to the HALO-tag, substrates containing photocleavable linkers have been developed and applied in photocleavable dimerizers (see 1.4.1, Figure 15 b, Figure 17 b).[34, 35, 36] A photoactivatable HALO-tag substrate has not been realized to date, however, as far as we are aware. The length of HALO-tag's access tunnel has been determined to approximately 15 Å by computational modeling.[31] Consistently with this tunnel length, the standard 6-chlorohexyl-PEG_2 HALO-tag substrates are about 17 Å long.[31] Consequently, a PPG within this moiety would be expected to efficiently block HALO-tag labeling prior to illumination. Since the standard 6-chlorohexyl-PEG_2 lacks a functional group allowing for suitable photoprotection, an alternative potential HALO-tag substrate was designed. Replacement of the first ether oxygen by a nitrogen would generate a secondary amine at which a PPG could be installed (Figure 25). Provided that the HALO-tag accepts the unprotected N-halo as substrate, this should enable photoactivatable editing with HALO-deaminases.

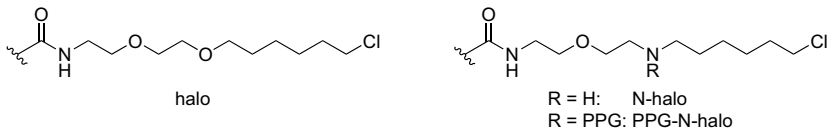

Figure 25. Design of an alternative potential HALO-tag substrate that enables implementation of photoactivation. Integration of a nitrogen generates the photoprotectable N-halo. The substrate could be coupled to a guideRNA via peptidic linkage at the terminal amine as usual.

For investigation of HALO-tag's acceptance of N-halo as substrate, a vector containing HALO-His for expression in *E. coli* and subsequent protein isolation was generated (see also A.3.1). A N-halo substrate carrying a fluorophore as label (fl-N-halo) could then be applied in *in vitro* staining of isolated HALO protein and the conjugation efficiency evaluated in comparison to a standard chlorohexyl-PEG_2 HALO-tag substrate carrying the same fluorophoric label.

Synthesis route for N-halo via reductive amination

The pursued synthesis routes for fl-N-halo and PPG-N-halo involved the reductive amination between amine **18** and aldehyde **19** as key step for the implementation of the desired secondary amine (Figure 26).[4]

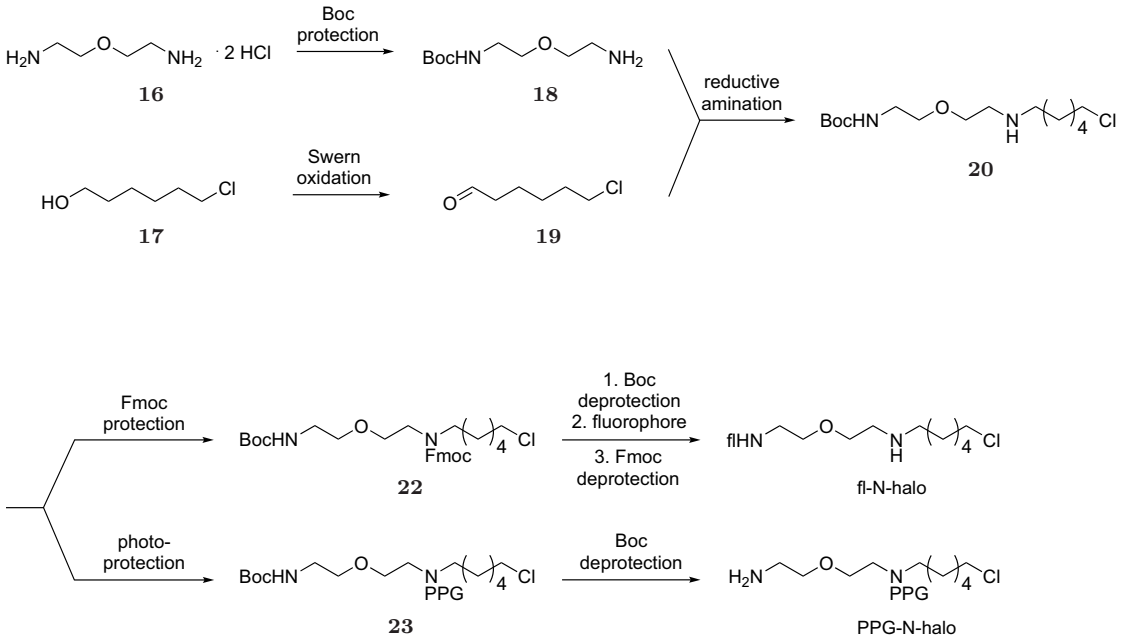

Figure 26. Planned synthesis route for the generation of N-halo via reductive amination.[4] Labeled N-halo and PPG-N-halo substrates could be synthesized from the resulting key intermediate **20** by appropriate orthogonal (de)protection steps.

Compounds **18** and **19** were synthesized from **16** and **17** via Boc protection and Swern oxidation, respectively, in high yields (Figure 27). For reductive amination of aldehyde **19** with amine **18**, three different procedures, including sodium cyanoborohydride, triacetoxyborohydride and borohydride as reducing agents, were tested (see A.3.2). Careful optimization of reaction conditions was required in order to minimize doubly alkylated byproduct **21**, a known hurdle in alkylations of amines. The best effort was achieved with imine formation in methanol and molecular sieve as dehydrating agent, followed by reduction with sodium borohydride (Figure 28, procedure 3 in A.3.2). Moderate amounts of **20** with small impurities were obtained after purification.

Next, the protection of the terminal primary amine and the secondary amine needed to be orthogonally swapped in order to allow chemoselective labeling of the N-halo substrate via the terminal amine (Figure 26). Different labels, including a fluorophore for staining of HALO protein or guideRNAs for editing, could then be attached. Column purification of **20** was complicated by strong retention on the column, hampering elution, and reducing the yield. As a consequence, Fmoc protection was tested directly with crude **20**. However, this gave a mixture of a variety of products and Fmoc-protected **22** could not be isolated. Given the obstacles earlier in the synthesis route resulting from the fact that the reductive amination was very prone to double alkylation, efforts were shifted to an alternative approach.

[4]Note that halo-guideRNAs contain a peptidic linker between the 6-chlorohexyl-PEG_2 substrate and the guideRNA (see Supporting Information of Publication 1). In the synthetic context here, the term halo refers to the 6-chlorohexyl-PEG_2 substrate only, for the sake of clarity.

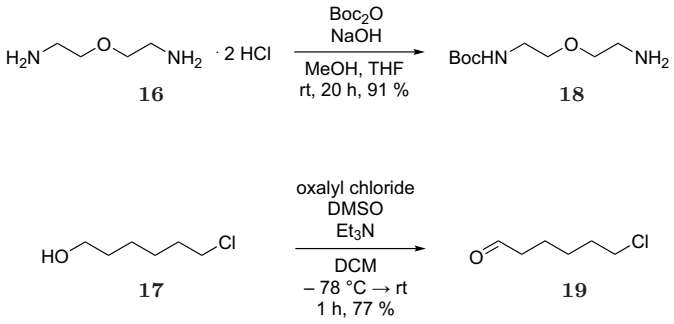

Figure 27. Synthesis of **18** by Boc protection and **19** by Swern oxidation.

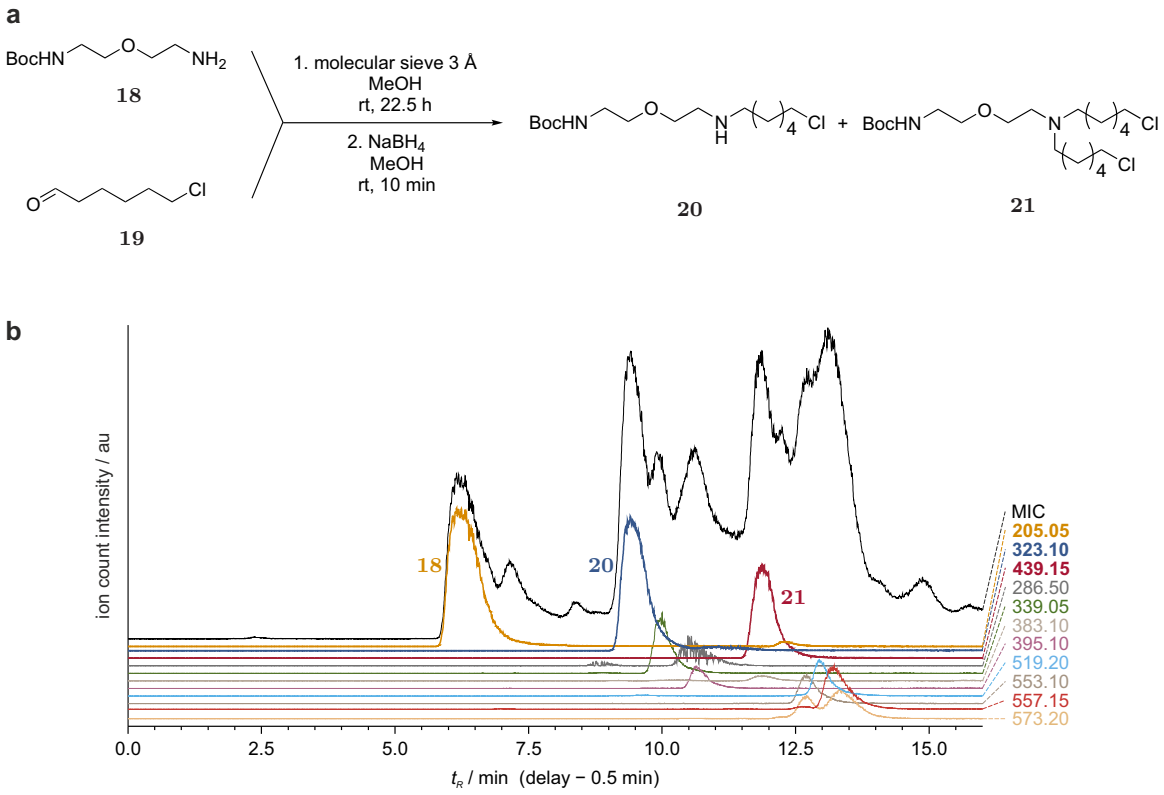

Figure 28. Reductive amination of **19** with **18** yields secondary amine **20**, but is hampered by double alkylation to side product **21** and purification complications. **a** Reaction scheme of reductive amination via procedure 3. **b** LC-MS spectrum of crude product generated via procedure 3 shows excess reactant **18** at $t_R = 5.7\,\text{min}$, product **20** at $t_R = 9.1\,\text{min}$, and doubly alkylated side product **21** at $t_R = 11.7\,\text{min}$.

Synthesis route for N-halo via amide

Since amide formation followed by reduction is an established general method to circumvent double alkylation of amines, synthesis of the secondary amine **20** was pursued via the intermediate amide **25** (Figure 29). Compound **25** was generated by peptide bond formation between amine **18** and chlorohexanoic acid (**24**) in excellent yield.

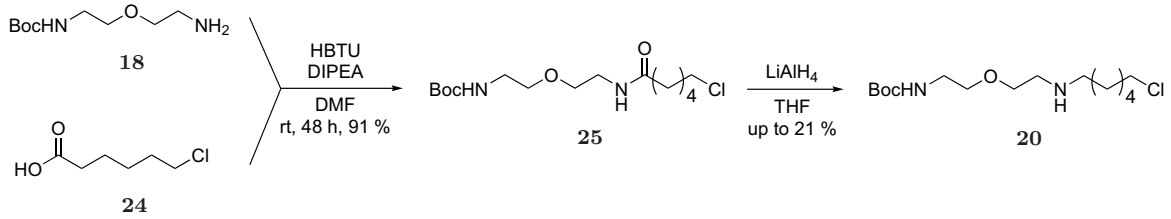

Figure 29. Alternative synthesis route for **20** via amide intermediate **25**. Amide **25** is synthesized by peptide bond formation with HBTU and subsequently reduced to **20** with $LiAlH_4$.

Reduction to **20** was performed with lithium aluminium hydride in tetrahydrofuran (Figure 29). However, amide **25** reacted only incompletely and several side products were generated, which limited product yield and rendered purification challenging. Neither repurification of the reactant nor application of freshly dried tetrahydrofuran instead of stored dry tetrahydrofuran solved these issues. Several different procedures were tested in order to achieve the best balance between sufficient reduction of the reactant and as little occurrence of side products as possible. The most promising approach was based on a short reaction time, counterbalanced by more equivalents of lithium aluminium hydride and potentially slightly elevated reaction temperature (see A.3.3, procedures 2, 3, Figure 39). Additionally, an extended aqueous workup might ensure that all reactive species get quenched prior to potential accumulation during removal of the solvents under reduced pressure (procedure 3, Figure 39 c). For future experiments, reaction under these conditions might be feasible, if conducted at larger scale and unreacted **25** is reisolated. However, this would be a suboptimal solution since overall, the limitation of incomplete reaction persists.

In conclusion, the generation of a photoactivatable HALO-tag substrate is not straightforward and, though it might be achievable upon further optimization, would require further extensive efforts. Alternatively, one could imagine applications in which the combination of photoactivatable SNAP-ADAR editing with photodeactivatable HALO-ADAR editing might prove beneficial. For this purpose, 6-chlorohexyl substrates fused to guideRNAs via a photocleavable linker, for example similar to the one in TMP-NVOC-halo (Figure 17 b), might be applicable. Notably, in Publication 4, a bisfunctional N7-MeNPOM-snap–clip-^{UV}X-poly(U)-guideRNA provided the possibility to switch from recruitment of a CLIP-tagged protein to stress granules prior to illumination to recruitment of a distinct SNAP-tagged protein after irradiation (Figure 3_{P4}). Given that the imperfect orthogonality between SNAP- and CLIP-tag has been found to be insufficient for precise editing applications, along with the instability of clip-guideRNAs (see 3.1.1), the combination of N7-MeNPOM-snap with a photocleavable halo might exhibit superior performance.

3.2 Chemically induced RNA editing

The second main project of the dissertation at hand consisted of the development of a tool for site-directed RNA editing under control of a small molecule dimerizer. This further layer of control would then allow for precise tuning of editing degrees in a dose-dependent manner at defined time points. For this purpose, SNAP-ADAR's recruiting moiety and catalytically active deaminating moiety were separated from one another and each fused to one protein component of a CID system.

3.2.1 Design and expression of constructs

Design of fusions for chemically induced dimerization of SNAP-ADAR1

The GA_3 system, with its fast induction of dimerization of GID1A with $GAI_{1\text{-}92}$ in combination with a well graduated dose response, presented an eligible CID system for application for chemically induced RNA editing. Therefore, the recruiting moiety, i.e. the SNAP-tag, and the catalytically active moiety, i.e. the deaminase domain of ADAR1, ought to be fused to one of said proteins, respectively. Analogous to the established SNAP-ADAR, the ADAR1 deaminase domain was kept at C-terminal position to avoid potential disturbance of catalytic efficiency, and fused to the natively N-terminal $GAI_{1\text{-}92}$. Since C-terminal GID1A had been proven functional in fusion with a protein tag, i.e. as eGFP-GID1A, before,[224, 225] the SNAP-tag was N-terminally fused. Consequently, editing activity should be inducible by dimerization of resulting SNAP-GID1A with $GAI_{1\text{-}92}$-ADAR1 upon addition of GA_3 (Figure 1_{P2}).

Duo constructs expressing $GAI_{1\text{-}92}$-ADAR1 and SNAP-GID1A

Next, vectors for the expression of $GAI_{1\text{-}92}$-ADAR1 and SNAP-GID1A from a single cassette were generated. Beyond practicability for defined expression in Flp-In T-REx 293 cell lines, this additionally minimizes transfection bias and assimilates expression levels upon transient expression. Construct **I** comprised two separate consecutive CMV promoters, whereas construct **II** was based on the P2A method (Figure $2\,a_{P2}$). Putting the findings from the previous investigation of duo constructs (see 3.1.2) to use, the catalytically active $GAI_{1\text{-}92}$-ADAR1 was inserted as first transgene for maximal expression. In addition, analogous constructs **III** and **IV** with the hyperactive ADAR1Q were generated.

Transient transfection of plasmids containing constructs **I** to **IV** in wild-type 293T cells yielded equally strong expression of SNAP-GID1A from all constructs (Figure $2\,c_{P2}$), whereas expression of $GAI_{1\text{-}92}$-ADAR1 was higher from P2A constructs than from the respective constructs with two consecutive CMV promoters (Figure $2\,b_{P2}$). As expected, genomic integration of constructs **I** to **IV** to generate Flp-In T-REx 293 cell lines $\mathbf{1}_{P2}$ to $\mathbf{4}_{P2}$, respectively, resulted in doxycyline-dependent expression at lower levels than under transient expression. However, expression levels of both $GAI_{1\text{-}92}$-ADAR1Q and SNAP-GID1A were substantially lower than for SA1Q from Flp-In T-REx 293 cells (Figure $2\,b, c_{P2}$).

In order to examine possible causes for this, influences of proteasome inhibitor MG-132 and GA_3-AM on expression levels were investigated (Figure 30).[5] Addition of MG-132 resulted in slightly elevated expression levels of both $GAI_{1\text{-}92}$-ADAR1Q and SNAP-GID1A in the

[5] Performed as described in Supporting Information of Publication 2 for Western Blotting of Flp-In T-REx cell lines $\mathbf{3}_{P2}$ and $\mathbf{4}_{P2}$. Samples were incubated with 10 µM MG-132 for 6 h or 10 µM GA_3-AM for 24 h prior to harvesting as indicated.

examined cell lines $\mathbf{3}_{P2}$ and $\mathbf{4}_{P2}$. The presence of GA_3 had little influence on the expression level of $GAI_{1\text{-}92}$-ADAR1Q, but exerted a drastic effect on SNAP-GID1A expression. SNAP-GID1A expression was strongly increased, and even significantly surmounted SA1Q expression.

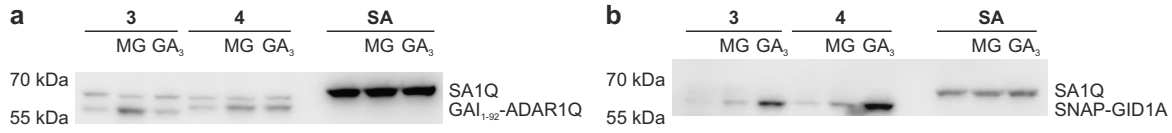

Figure 30. Influence of proteasome inhibition with MG-132 (MG) and presence of GA_3 on expression levels of **a** $GAI_{1\text{-}92}$-ADAR1Q and **b** SNAP-GID1A in cell lines $\mathbf{3}_{P2}$ and $\mathbf{4}_{P2}$. Expression of SA1Q in respective single Flp-In T-REx cell line shown for comparison.

These findings indicate that instability and degradation seem to be a major hurdle for both fusion proteins and SNAP-GID1A is tremendously stabilized by binding of GA_3. Consequently, increase in expression levels might be feasible by optimization of the fusion protein constructs in the future. For instance, replacement of the SNAP-tag with the HALO-tag or HOB[303] (see 3.1.1) might yield a more stable HOB-GID1A fusion. Furthermore, attachment of superfolder proteins such as superfolder GFP[312] may contribute to stabilization and the combination and order of the SNAP-ADAR and the CID components, as well as contained linkers, may be amenable to optimization. In principle, stable integration of a transgene at multiple sites could also provide a way to boost expression. For instance, the XLone system would allow for stable integration of a P2A construct such as **IV** at multiple sites of a HeLa cell line by PiggyBac transposase, combined with doxycycline-dependence by the Tet-On 3G system.[313] However, this would not overcome stability limitations and guideRNAs would remain irreversibly and exhaustively bound to unstable protein.

3.2.2 GA_3 induced editing

Even at the given low expression levels, editing of a 5'-U<u>A</u>G codon in the 3'-UTR of endogenous *GAPDH* yielded moderate editing efficiencies in the presence of GA_3 in cell lines $\mathbf{3}_{P2}$ and $\mathbf{4}_{P2}$ (Figure 3 a $_{P2}$). Importantly, editing strictly depended on small molecule induction with GA_3, contrary to editing with SA1Q. Editing yields were tunable by the system's graduated response to differing GA_3 doses with an $EC_{50} = 290\,nM$ GA_3-AM (Figure 3 b $_{P2}$).

The novel system for chemically induced RNA editing was also applied for GA_3-dependent editing of a 5'-U<u>A</u>U codon in the ORF of endogenous *STAT1*. Editing of this site evokes a Y701C mutation, which eliminates the Tyr701 phosphorylation site for activation of STAT1.[314] Up to 20 % editing yield were achieved in cell line $\mathbf{4}_{P2}$ with application of $(snap)_2$-guideRNA and 100 µM GA_3-AM (Figure 3 c $_{P2}$). Interestingly, higher expression levels of $GAI_{1\text{-}92}$-ADAR1(Q) and SNAP-GID1A under transient conditions had only a minor effect on maximum editing efficiencies. This highlights the superiority of homogeneous expression in stable transgenic cell lines, particularly for the targeting of endogenous transcripts (Figure 3 d $_{P2}$). Editing with high, transient expression was more tolerant towards reduction in guideRNA amount and application of wild-type ADAR1 deaminase domain instead of ADAR1Q, however (data not shown).

Finally, the system was applied for repair of the disease-causing R106Q mutation in MECP2, that results in decreased protein levels and heterochromatin binding.[130] Since deviations from healthy MECP2 levels for a given cell type in either direction, i.e. increase as well

as decrease, has pathophysiological consequences,[130, 315, 316] precise tuning of the editing extent is particularly crucial for this target. *MECP2 R106Q* was transiently transfected and the corresponding 5'-C<u>A</u>A codon GA_3-dependently edited up to 42 % with transiently expressed construct **IV** in 293T cells. Contrary to editing with SA1Q, no bystander editing above background level was detected within the sequenced area with chemically induced RNA editing. In the SA1Q cell line, multiple bystander sites occured, for example, the A one nucleotide downstream of the target site was edited 15 % with $(snap)_2$-guideRNA. The A 134 nucleotides upstream of the target A was even edited with NH_2- in addition to $(snap)_2$-guideRNA (both approximately 15 %, data not shown). While these bystander sites may be avertable by appropriate chemical modification of the guideRNA sequence, this demonstrates effectively the tight control of the chemically inducible platform, the more so as reduction in on-target editing yield in comparison to editing with SA1Q is less pronounced than for endogenous *GAPDH* and *STAT1* (Figure 3 e $_{P2}$). Notably, the obtained on-target editing level corresponds to the extent recently shown to elicit significant restoration of heterochromatin binding, i.e. $37 - 52$ %, with the λN-ADAR system (see 1.2.3).[131]

Shortly prior to Publication 2, a CIRTS system under control of CID has been reported (see 1.2.3).[134] Specifically, β-defensin 3-TBP-ABI1 and PYL-ADAR2Q dimerized upon induction with ABA. With this system, the same *MECP2 R106Q* site was edited about 15 % in the presence of 100 µM ABA, versus about 3 % in the absence of ABA.[134] In comparison, under similar conditions, the GA_3 induced SNAP-ADAR system achieved 42 % editing in the presence of 100 µM GA_3-AM, 40 % in the presence of 10 µM GA_3-AM and about 4 % in the absence of GA_3 (Figure 3 e $_{P2}$). In regards to selectivity and bystander editing, data from the two systems does not allow for direct comparison. As stated above, no significant bystander editing was observed in the vicinity of the target A on the *MECP2* transcript with the GA_3 induced SNAP-ADAR system. For the ABA induced CIRTS system, no data on potential bystander sites on *MECP2* is available. Bystander sites were investigated on a *luciferase* reporter transcript, however, which yielded five bystander sites with editing levels above 5 % in the presence of ABA, as well as 9 % on-target editing in the absence of ABA.[134] Furthermore, the tunability of editing extent appears superior for the GA_3 induced SNAP-ADAR system, which allowed for reproducible adjustment to different editing levels in a dose-dependent way (Figure 3 b $_{P2}$). This ranged from 5 % editing of the *GAPDH* target with 10 nM to 29 % with 100 µM GA_3-AM, whereas for the ABA induced CIRTS system, no significant differences in editing levels of a *luciferase* reporter transcript were reported with variation of inducer concentrations from 1 nM to 100 µM ABA.[134]

Overall, the development of a system for chemically induced RNA editing was successful, and would be amenable to further optimization in regards to expression levels of the components. In addition, the newly developed tool could gain even more precise spatiotemporal control by implementation of chemo-optogenetic dimerization. This would entail the advantage that photoactivity and guideRNA would be decoupled, as opposed to photoactivatable SNAP-ADAR editing with N7-MeNPOM-snap-guideRNAs.[126] Consequently, issues with background activity in the dark may be overcome. A membrane permeable photoprotected GA_3 derivative could simply be added to media and concentrations could be increased independent of amounts of potentially disturbing guideRNAs. Even partial release of free GA_3 upon illumination could then elicit efficient dimerization and subsequent editing activity. For example, for the *GAPDH* target, 10 µM GA_3-AM sufficed for induction of maximum editing yields and 75 % of the maximum editing yield could be attained with 1.8 µM GA_3-AM (Figure 3 b $_{P2}$). As photoprotected GA_3 derivative, pcGA_3-1 would be a suitable candi-

date, since its membrane permeability and stability towards endogenous esterases have been already established, it promptly induces dimerization upon short irradiation pulses and exhibits high quantum yield of 50 % at irradiation with 350 nm light (see 1.4.1, Figure 16 b).[225] Furthermore, pcGA$_3$-3 could even be exploited for *in vivo* applications with 2PE.

3.3 Photocontrolled NO-cGMP signaling

The third main project of the dissertation at hand also revolved around the development of a tightly controlled tool for defined manipulation of biochemical processes. Contrary to the other two main projects, however, it deviated from the theme of epitranscriptomics, in that the tool ought to be for controlled release of the second messenger NO. For this purpose, a photoactivatable NO donor was devised, which should enable the triggering of the NO-cGMP signaling cascade upon illumination with tight spatiotemporal control.

3.3.1 Generation and characterization of MeNPOM-PYRRO/NO

PYRRO/NO was chosen as NO releasing moiety based on its prompt decay under release of NO once it is liberated from photoprotection. Consequently, it should provide precise temporal as well as spatial control, since free PYRRO/NO does not spread by diffusion prior to NO release. PYRRO/NO was rendered photoactivatable by protection with MeNPOM, whereby fusion via an oxymethylene linker and appropriate substitution of the *o*NB group should result in productive heterolytic cleavage under efficient release of NO upon irradiation with long-wavelength UV light. MeNPOM-PYRRO/NO (**1**$_{P3}$) was synthesized in high yield from PYRRO/NO (**2**$_{P3}$) and MeNPOM chloride (**3**$_{P3}$, Scheme 1$_{P3}$).

The stability of MeNPOM-PYRRO/NO in the dark was confirmed and the decay upon irradiation with 365 nm UV light under physiological conditions investigated by HPLC (Figure 1 a$_{P3}$). As expected, MeNPOM-PYRRO/NO decomposed under generation of nitroso acetophenone **4**$_{P3}$ (Scheme 1$_{P3}$). Kinetic analysis revealed a first-order exponential decay with a half-life of MeNPOM-PYRRO/NO of 0.39 ± 0.02 min and high quantum yield of 66 % (Figure 1 b$_{P3}$). Additionally, the formation of NO was confirmed by Griess assay (Figure 1 c$_{P3}$).

3.3.2 Photoactivatable cGMP signaling in VSMCs

With the *in vitro* photorelease of NO from MeNPOM-PYRRO/NO being established, the compound was examined in regard to triggering NO-cGMP signaling in primary VSMCs. VSMCs were retrieved from aortae of transgenic mice expressing the FRET-based cGMP sensor cGi500.[317] cGi500 consists of a CFP-cGKI-YFP construct, which allows for real time determination of changes in cGMP concentrations in live cells upon different treatments in a superfusion chamber by fluorescence imaging (Scheme 2$_{P3}$). In the absence of cGMP, cyan fluorescent protein (CFP) and yellow fluorescent protein (YFP) are closely adjacent, consequently efficient FRET to YFP takes place upon excitation of CFP. Upon NO release and following sGC induction, cGMP is generated and binds to to the sensor's cGKI. This evokes a conformational change and results in greater distance and ultimately less FRET between CFP and YFP. Thus, NO-triggered cGMP generation can be monitored as increased ratio of CFP to YFP fluorescence.

While superfusion with MeNPOM-PYRRO/NO in the dark did not elicit a cGMP signal, a prompt increase was observed upon irradiation with long-wavelength UV light (Figure 2$_{P3}$).

As intended by the application of PYRRO/NO, cGMP signals occurred in sharp bursts, indicating the direct release of NO after deprotection, as well as return to baseline in under a minute. On the contrary, superfusion with simple, unprotected DEA/NO yielded broad cGMP signals over the course of multiple minutes, consistent with DEA/NO's half-life of 2 min versus 3 s for free PYRRO/NO. cGMP signals were reproducible and constant over a certain range of MeNPOM-PYRRO/NO concentration and irradiation time, as shown in multiple series of experimental conditions with varying concentrations from 0.1 – 100 µM (Figure 2 a, b $_{P3}$) and irradiation times from 5 – 30 s (Figure 2 c $_{P3}$).

Finally, the effect of the novel photoactivatable NO donor on the phosphorylation status of cGKI substrate VASP was investigated in order to confirm activation of the NO-cGMP signaling cascade in wild-type VSMCs (Scheme 2 a $_{P3}$). Western Blot analysis with an antibody specific for phosphorylated p-VASP revealed a strong light-dependent increase in p-VASP in the presence of MeNPOM-PYRRO/NO (Figure 2 d $_{P3}$). Additionally, slight indication of an increase by irradiation alone was observed. In accordance, occasional minuscule cGMP signals following irradiation in the absence of a NO donor compound had also been detectable in experiments with the cGi500 sensor.

In conclusion, MeNPOM-PYRRO/NO provides a tool for photoactivated NO release and consequential generation of cGMP in sharp bursts under tight control. In contrast to other photoprotected NONOates, such as NV-HC3M-DEA/NO[295] (Figure 23 b), NO release was promptly triggered by short irradiation pulses. These characteristics may result from application of a PPG with favorable properties in combination with short-lived PYRRO/NO, as opposed to DEA/NO in previous photoactivatable NONOates (Figure 23 b). The well-defined NO induced cGMP-generation may be exploited for deeper investigations concerning the regulation of the various proteins involved in the NO-cGMP signaling pathway. Controlled release of the desired amount of NO is particularly important, since sGC becomes significantly desensitized to NO upon exposure.[254] Moreover, the high spatial resolution provided by the implementation of light as a trigger may prove beneficial for studies on the compartmentalization of cGMP signaling in the future. It has previously been established that, interconnected with the various protein isoforms involved, distinct subcellular cGMP pools exist. For instance, cGMP generated by pGC upon NP induction exerts different functions than cGMP from NO stimulated sGC.[318, 319] A more detailed understanding of this compartmentalization might form the foundation for the development of strategies for precise intervention at pathophysiologically relevant targets.

4 Conclusions & Outlook

In summary, several novel and highly controllable tools were developed within the framework of the dissertation at hand. Firstly, a platform for orthogonal RNA editing was designed. The combination of SNAP- and HALO-tag as steering moieties for different base editors enabled the programmable concurrent and independent harnessing of deaminase activity to two distinct target sites. The newly introduced HALO-ADAR1Q was utilized with previously established SNAP-ADAR2Q for orthogonal A-to-I editing with extended substrate scope. In the process, constructs for optimal expression of both editases from a common cassette were developed, and principle expression patterns from such constructs were demonstrated to be transferable later on. Furthermore, concurrent orthogonal A-to-I and C-to-U editing was possible by combining HALO-ADAR1Q with mAPOBEC1-SNAP-NES. Owed to the single genomic integration of the constructs into Flp-In T-REx 293 cells, among others, both orthogonal RNA editing platforms exhibited a moderately pronounced global off-target editing profile. Implementation of photoactivation to HALO-ADAR editing was not straightforward and would require further optimization. Alternatively, the combination of photoactivatable snap-guideRNAs with photocleavable halo-guideRNAs might be more promising in regards to feasibility and potential applications.

The orthogonal RNA editing platform may be optimized further in the future. For instance, replacement of the HALO-tag with halo-based oligonucleotide binder (HOB) and introduction of longer linkers into halo-guideRNAs might improve editing efficiency. Furthermore, HALO-ADAR may be combined with a C-to-U editase exhibiting higher performance and improved programmability, such as SNAP-tag guided zinc-dependent deaminase domain of APOBEC1 or the RESCUE system's mutated ADAR2Q deaminase domain accepting cytidine as deamination substrate.

Moreover, the novel orthogonal editing platform may be exploited for investigations relating to the effects resulting from specific editing events. The combination of A-to-I and C-to-U editing may prove particularly valuable for the elucidation of potential interdependence in certain transcripts in which both A-to-I and C-to-U editing occurs naturally. Additionally, it has previously been proposed that formation of heterodimers may lead to inhibition of editing activity at naturally edited sites and consequently play a role in multiple pathologies.[92, 320] Recently, it has also been suggested that ADAR3 might inhibit catalytic activity of ADAR1 and ADAR2 by formation of heterodimers.[59] Bisfunctional halo-snap-guideRNAs may be applied for the assembly of various heterodimers, allowing to study resulting effects and unravel the requirement of homodimerization for some A-to-I sites on the one hand versus inhibition by heterodimerization on the other hand. Similar investigations in regards to the effects of various di- and oligomerizations of different APOBECs are also conceivable.

Besides RNA base editing, the principle of the orthogonal platform may also be transferred to concurrent, but independent recruitment of proteins implicated with other epitranscriptomic marks. For instance, fusion of different m^6A writers and erasers to SNAP- and HALO-tag may allow for simultaneous orthogonal introduction or removal of two distinct m^6A modifications, or for switching between introduction and removal of one site, with snap- and

halo-guideRNAs. This would provide a valuable tool for elucidation of biological effects of individual modification sites, as well as the role of active demethylation by erasers versus passive demethylation by RNA turnover. Approaches for steering of a single m^6A effector by dCas9 fusion have recently been reported.[321, 322] An orthogonal m^6A modification platform analogous to the orthogonal RNA editing system developed within the dissertation at hand would greatly expand the possibilities, along with entailing the intrinsic strengths, such as covalent binding of the guideRNA to the effector protein. Moreover, the same principle may be applicable for the even less explored N^1-methyladenosine (m^1A) modification.

Secondly, a method enabling RNA editing under control of small molecule induction was developed. To this end, SNAP-tag and ADAR1Q deaminase domain were separated and each fused to one of the protein components allowing for chemically induced dimerization with gibberellic acid. Expression levels of the resulting SNAP-GID1A and $GAI_{1\text{-}92}$-ADAR1Q fusions from different duo constructs were low, but sufficed to evoke moderate editing levels on endogenous targets. Editing activity stringently depended on the presence of small molecule dimerizer and was tunable in a dose-dependent manner. Furthermore, the system allowed for tightly controlled repair of the pathologic R106Q mutation in MECP2 to an extent that has been suggested to significantly alleviate severity of disease.

Investigation of potential causes for the low expression levels of SNAP-GID1A and $GAI_{1\text{-}92}$-ADAR1Q indicated stability of the fusion proteins as major limiting factor. Accordingly, expression levels may be amenable to future optimization by stabilization of the fusion proteins, for instance by replacement of the SNAP-tag with the aforementioned HOB, addition of superfolder proteins or variation of the combination and order of the individual components, as well as linkers. Given that the P2A duo construct, exhibiting higher expression of $GAI_{1\text{-}92}$-ADAR1Q, consistently performed superior in comparison to a construct with lower expression level, optimization towards increased expression levels appears promising for attainment of enhanced editing yields. Moreover, an additional layer of control may be implemented to the novel chemically inducible editing system by applying photoactivatable gibberellic acid derivatives.

Lastly, a tool for photoinduced, well-defined activation of the NO-cGMP signaling pathway was introduced. Photoprotected diazeniumdiolate MeNPOM-PYRRO/NO was synthesized and characterized with respect to its photolytic properties. MeNPOM-PYRRO/NO irradiation-dependently decayed with first-order kinetics, exhibiting a half-life of 0.39 ± 0.02 min and quantum yield of 66 % at 365 nm, whereupon NO was released. Subsequently, MeNPOM-PYRRO/NO was applied to primary live vascular smooth muscle cells expressing a cGMP sensor based on Förster resonance energy transfer. cGMP generation was activated by NO promptly upon illumination with long-wavelength UV light with irradiation times in the range of seconds and MeNPOM-PYRRO/NO concentrations in the micromolar range. The novel photoactivatable NO donor yielded sharp cGMP signals, clearly displaying higher precision and temporal control than other diazeniumdiolates. Additionally, triggering of VASP phosphorylation, a downstream effect of the NO-cGMP cascade, by irradiation in the presence of MeNPOM-PYRRO/NO in wild-type vascular smooth muscle cells was demonstrated.

The spatiotemporal control attained by employment of light as trigger makes MeNPOM-PYRRO/NO a suitable candidate for future investigations of NO-cGMP signaling with the need for well-defined cGMP production. This may prove particularly valuable for the pending elucidation of various aspects of the compartmentalization of distinct subcellular cGMP pools and their biologic effects in the future.

Bibliography

[1] N. Johnsson, K. Johnsson, A Fusion of Disciplines: Chemical Approaches to Exploit Fusion Proteins for Functional Genomics, *ChemBioChem* **2003**, *4*, 803–810.

[2] M. Zimmer, Green Fluorescent Protein (GFP): Applications, Structure, and Related Photophysical Behavior, *Chem. Rev.* **2002**, *102*, 759–781.

[3] R. Heim, R. Y. Tsien, Engineering green fluorescent protein for improved brightness, longer wavelengths and fluorescence resonance energy transfer, *Curr. Biol.* **1996**, *6*, 178–182.

[4] N. C. Shaner, R. E. Campbell, P. A. Steinbach, B. N. G. Giepmans, A. E. Palmer, *et al.*, Improved monomeric red, orange and yellow fluorescent proteins derived from *Discosoma* sp. red fluorescent protein, *Nat. Biotechnol.* **2004**, *22*, 1567–1572.

[5] D. S. Bindels, L. Haarbosch, L. Van Weeren, M. Postma, K. E. Wiese, *et al.*, mScarlet: a bright monomeric red fluorescent protein for cellular imaging, *Nat. Methods* **2017**, *14*, 53–56.

[6] A. Keppler, S. Gendreizig, T. Gronemeyer, H. Pick, H. Vogel, *et al.*, A general method for the covalent labeling of fusion proteins with small molecules *in vivo*, *Nat. Biotechnol.* **2003**, *21*, 86–89.

[7] C. A. Hoelzel, X. Zhang, Visualizing and Manipulating Biological Processes by Using HaloTag and SNAP-Tag Technologies, *ChemBioChem* **2020**, *21*, 1935–1946.

[8] C. Wang, X. Song, Z. Han, X. Li, Y. Xu, *et al.*, Monitoring nitric oxide in subcellular compartments by hybrid probe based on rhodamine spirolactam and SNAP-tag, *ACS Chem. Biol.* **2016**, *11*, 2033–2040.

[9] D. Srikun, A. E. Albers, C. I. Nam, A. T. Iavarone, C. J. Chang, Organelle-Targetable Fluorescent Probes for Imaging Hydrogen Peroxide in Living Cells via SNAP-Tag Protein Labeling, *J. Am. Chem. Soc.* **2010**, *132*, 4455–4465.

[10] E. Tomat, E. M. Nolan, J. Jaworski, S. J. Lippard, Organelle-Specific Zinc Detection Using Zinpyr-Labeled Fusion Proteins in Live Cells, *J. Am. Chem. Soc.* **2008**, *130*, 15 776–15 777.

[11] A. A. Ruggiu, M. Bannwarth, K. Johnsson, Fura-2FF-based calcium indicator for protein labeling, *Org. Biomol. Chem.* **2010**, *8*, 3398–3401.

[12] L. E. Jansen, B. E. Black, D. R. Foltz, D. W. Cleveland, Propagation of centromeric chromatin requires exit from mitosis, *J. Cell Biol.* **2007**, *176*, 795–805.

[13] M. A. McMurray, J. Thorner, Septin Stability and Recycling during Dynamic Structural Transitions in Cell Division and Development, *Curr. Biol.* **2008**, *18*, 1203–1208.

[14] A. Gautier, A. Juillerat, C. Heinis, J. Ivan Reis Corrêa, M. Kindermann, *et al.*, An Engineered Protein Tag for Multiprotein Labeling in Living Cells, *Chem. Biol.* **2008**, *15*, 128–136.

[15] G. V. Los, L. P. Encell, M. G. McDougall, D. D. Hartzell, N. Karassina, *et al.*, HaloTag: A Novel Protein Labeling Technology for Cell Imaging and Protein Analysis, *ACS Chem. Biol.* **2008**, *3*, 373–382.

[16] B. A. Griffin, S. R. Adams, R. Y. Tsien, Specific Covalent Labeling of Recombinant Protein Molecules Inside Live Cells, *Science* **1998**, *281*, 269–272.

[17] A. E. Pegg, Repair of O^6-alkylguanine by alkyltransferases, *Mutat. Res., Rev. Mutat. Res.* **2000**, *462*, 83–100.

[18] D. S. Daniels, T. T. Woo, K. X. Luu, D. M. Noll, N. D. Clarke, *et al.*, DNA binding and nucleotide flipping by the human DNA repair protein AGT, *Nat. Struct. Mol. Biol.* **2004**, *11*, 714–720.

[19] A. Juillerat, T. Gronemeyer, A. Keppler, S. Gendreizig, H. Pick, *et al.*, Directed Evolution of O^6-Alkylguanine-DNA Alkyltransferase for Efficient Labeling of Fusion Proteins with Small Molecules In Vivo, *Chem. Biol.* **2003**, *10*, 313–317.

[20] T. Gronemeyer, C. Chidley, A. Juillerat, C. Heinis, K. Johnsson, Directed evolution of O^6-alkylguanine-DNA alkyltransferase for applications in protein labeling, *Protein Eng., Des. Sel.* **2006**, *19*, 309–316.

[21] A. Juillerat, C. Heinis, I. Sielaff, J. Barnikow, H. Jaccard, *et al.*, Engineering Substrate Specificity of O^6-Alkylguanine-DNA Alkyltransferase for Specific Protein Labeling in Living Cells, *ChemBioChem* **2005**, *6*, 1263–1269.

[22] X. Sun, A. Zhang, B. Baker, L. Sun, A. Howard, *et al.*, Development of SNAP-Tag Fluorogenic Probes for Wash-Free Fluorescence Imaging, *ChemBioChem* **2011**, *12*, 2217–2226.

[23] J. Wilhelm, S. Kühn, M. Tarnawski, G. Gotthard, J. Tuennermann, *et al.*, Kinetic and Structural Characterization of the Self-Labeling Protein Tags HaloTag7, SNAP-tag and CLIP-tag, *Biochemistry* **2021**, *60*, 2560–2575.

[24] A. Keppler, M. Kindermann, S. Gendreizig, H. Pick, H. Vogel, *et al.*, Labeling of fusion proteins of O^6-alkylguanine-DNA alkyltransferase with small molecules in vivo and in vitro, *Methods* **2004**, *32*, 437–444.

[25] K. Kolberg, C. Puettmann, A. Pardo, J. Fitting, S. Barth, SNAP-Tag Technology: A General Introduction, *Curr. Pharm. Des.* **2013**, *19*, 5406–5413.

[26] L. Reymond, G. Lukinavičius, K. Umezawa, D. Maurel, M. A. Brun, *et al.*, Visualizing Biochemical Activities in Living Cells through Chemistry, *Chimia* **2011**, *65*, 868–871.

[27] G. A. Farr, M. Hull, E. H. Stoops, R. Bateson, M. J. Caplan, Dual pulse-chase microscopy reveals early divergence in the biosynthetic trafficking of the Na,K-ATPase and E-cadherin, *Mol. Biol. Cell* **2015**, *26*, 4401–4411.

[28] M. A. Brun, K.-T. Tan, E. Nakata, M. J. Hinner, K. Johnsson, Semisynthetic Fluorescent Sensor Proteins Based on Self-Labeling Protein Tags, *J. Am. Chem. Soc.* **2009**, *131*, 5873–5884.

[29] A. Gautier, E. Nakata, G. Lukinavičius, K.-T. Tan, K. Johnsson, Selective Cross-Linking of Interacting Proteins Using Self-Labeling Tags, *J. Am. Chem. Soc.* **2009**, *131*, 17 954–17 962.

[30] J. Newman, T. S. Peat, R. Richard, L. Kan, P. E. Swanson, *et al.*, Haloalkane Dehalogenases: Structure of a *Rhodococcus* Enzyme, *Biochemistry* **1999**, *38*, 16 105–16 114.

[31] L. P. Encell, R. F. Ohana, K. Zimmerman, P. Otto, G. Vidugiris, *et al.*, Development of a Dehalogenase-Based Protein Fusion Tag Capable of Rapid, Selective and Covalent Attachment to Customizable Ligands, *Curr. Chem. Genomics* **2012**, *6*, 55–71.

[32] V. Singh, S. Wang, E. T. Kool, Genetically Encoded Multispectral Labeling of Proteins with Polyfluorophores on a DNA Backbone, *J. Am. Chem. Soc.* **2013**, *135*, 6184–6191.

[33] R. S. Erdmann, S. W. Baguley, J. H. Richens, R. F. Wissner, Z. Xi, *et al.*, Labeling

Strategies Matter for Super-Resolution Microscopy: A Comparison between HaloTags and SNAP-tags, *Cell Chem. Biol.* **2019**, *26*, 584–592.e6.

[34] H. Zhang, C. Aonbangkhen, E. V. Tarasovetc, E. R. Ballister, D. M. Chenoweth, *et al.*, Optogenetic control of kinetochore function, *Nat. Chem. Biol.* **2017**, *13*, 1096–1101.

[35] X. Chen, Y.-W. Wu, Tunable and Photoswitchable Chemically Induced Dimerization for Chemo-optogenetic Control of Protein and Organelle Positioning, *Angew. Chem. Int. Ed.* **2018**, *57*, 6796–6799.

[36] M. Zimmermann, R. Cal, E. Janett, V. Hoffmann, C. G. Bochet, *et al.*, Cell-Permeant and Photocleavable Chemical Inducer of Dimerization, *Angew. Chem. Int. Ed.* **2014**, *53*, 4717–4720.

[37] S. Parvez, Y. Fu, J. Li, M. J. Long, H.-Y. Lin, *et al.*, Substoichiometric Hydroxynonenylation of a Single Protein Recapitulates Whole-Cell-Stimulated Antioxidant Response, *J. Am. Chem. Soc.* **2015**, *137*, 10–13.

[38] D. L. Buckley, K. Raina, N. Darricarrere, J. Hines, J. L. Gustafson, *et al.*, HaloPROTACS: Use of Small Molecule PROTACs to Induce Degradation of HaloTag Fusion Proteins, *ACS Chem. Biol.* **2015**, *10*, 1831–1837.

[39] D. Wiener, S. Schwartz, The epitranscriptome beyond m^6A, *Nat. Rev. Genet.* **2021**, *22*, 119–131.

[40] T. P. Hoernes, M. D. Erlacher, Translating the epitranscriptome, *Wiley Interdiscip. Rev.: RNA* **2017**, *8*, e1375.

[41] D. Dominissini, S. Moshitch-Moshkovitz, S. Schwartz, M. Salmon-Divon, L. Ungar, *et al.*, Topology of the human and mouse m^6A RNA methylomes revealed by m^6A-seq, *Nature* **2012**, *485*, 201–206.

[42] K. Meyer, Y. Saletore, P. Zumbo, O. Elemento, C. Mason, *et al.*, Comprehensive Analysis of mRNA Methylation Reveals Enrichment in 3' UTRs and near Stop Codons, *Cell* **2012**, *149*, 1635–1646.

[43] X. Wang, Z. Lu, A. Gomez, G. C. Hon, Y. Yue, *et al.*, N^6-methyladenosine-dependent regulation of messenger RNA stability, *Nature* **2014**, *505*, 117–120.

[44] M. Safra, A. Sas-Chen, R. Nir, R. Winkler, A. Nachshon, *et al.*, The m^1A landscape on cytosolic and mitochondrial mRNA at single-base resolution, *Nature* **2017**, *551*, 251–255.

[45] X. Li, P. Zhu, S. Ma, J. Song, J. Bai, *et al.*, Chemical pulldown reveals dynamic pseudouridylation of the mammalian transcriptome, *Nat. Chem. Biol.* **2015**, *11*, 592–597.

[46] Q. Dai, S. Moshitch-Moshkovitz, D. Han, N. Kol, N. Amariglio, *et al.*, N_m-seq maps 2'-*O*-methylation sites in human mRNA with base precision, *Nat. Methods* **2017**, *14*, 695–698.

[47] E. A. Erdmann, A. Mahapatra, P. Mukherjee, B. Yang, H. A. Hundley, To protect and modify double-stranded RNA – the critical roles of ADARs in development, immunity and oncogenesis, *Crit. Rev. Biochem. Mol. Biol.* **2020**, *56*, 54–87.

[48] C. X. George, C. E. Samuel, Human RNA-specific adenosine deaminase ADAR1 transcripts possess alternative exon 1 structures that initiate from different promoters, one constitutively active and the other interferon inducible, *Proc. Natl. Acad. Sci. U. S. A.* **1999**, *96*, 4621–4626.

[49] A. Herbert, J. Alfken, Y.-G. Kim, I. S. Mian, K. Nishikura, *et al.*, A Z-DNA binding domain present in the human editing enzyme, double-stranded RNA adenosine

deaminase, *Proc. Natl. Acad. Sci. U. S. A.* **1997**, *94*, 8421–8426.

[50] A. Strehblow, M. Hallegger, M. F. Jantsch, Nucleocytoplasmic Distribution of Human RNA-editing Enzyme ADAR1 Is Modulated by Double-stranded RNA-binding Domains, a Leucine-rich Export Signal, and a Putative Dimerization Domain, *Mol. Biol. Cell* **2002**, *13*, 3822–3835.

[51] M. Behm, H. Wahlstedt, A. Widmark, M. Eriksson, M. Öhman, Accumulation of nuclear ADAR2 regulates adenosine-to-inosine RNA editing during neuronal development, *J. Cell Sci.* **2017**, *130*, 745–753.

[52] C.-X. Chen, D.-S. C. Cho, Q. Wang, F. Lai, K. C. Carter, *et al.*, A third member of the RNA-specific adenosine deaminase gene family, ADAR3, contains both single- and double-stranded RNA binding domains, *RNA* **2000**, *6*, 755–767.

[53] S. Maas, W. M. Gommans, Identification of a selective nuclear import signal in adenosine deaminases acting on RNA, *Nucleic Acids Res.* **2009**, *37*, 5822–5829.

[54] D. Mladenova, G. Barry, L. M. Konen, S. S. Pineda, B. Guennewig, *et al.*, Adar3 Is Involved in Learning and Memory in Mice, *Front. Neurosci.* **2018**, *12*, 243.

[55] M. M. Matthews, J. M. Thomas, Y. Zheng, K. Tran, K. J. Phelps, *et al.*, Structures of human ADAR2 bound to dsRNA reveal base-flipping mechanism and basis for site selectivity, *Nat. Struct. Mol. Biol.* **2016**, *23*, 426–433.

[56] M. R. Macbeth, H. L. Schubert, A. P. VanDemark, A. T. Lingam, C. P. Hill, *et al.*, Inositol Hexakisphosphate Is Bound in the ADAR2 Core and Required for RNA Editing, *Science* **2005**, *309*, 1534–1539.

[57] Y. Wang, S. Park, P. A. Beal, Selective recognition of RNA substrates by ADAR deaminase domains, *Biochemistry* **2018**, *57*, 1640–1651.

[58] S. Park, E. E. Doherty, Y. Xie, A. K. Padyana, F. Fang, *et al.*, High-throughput mutagenesis reveals unique structural features of human ADAR1, *Nat. Commun.* **2020**, *11*, 5130.

[59] A. S. Thuy-Boun, J. M. Thomas, H. L. Grajo, C. M. Palumbo, S. Park, *et al.*, Asymmetric dimerization of adenosine deaminase acting on RNA facilitates substrate recognition, *Nucleic Acids Res.* **2020**, *48*, 7958–7972.

[60] K. Nishikura, C. Yoo, U. Kim, J. Murray, P. Estes, *et al.*, Substrate specificity of the dsRNA unwinding/modifying activity., *EMBO J.* **1991**, *10*, 3523–3532.

[61] Y. Wang, J. Havel, P. A. Beal, A phenotypic screen for functional mutants of human adenosine deaminase acting on RNA 1, *ACS Chem. Biol.* **2015**, *10*, 2512–2519.

[62] A. Kuttan, B. L. Bass, Mechanistic insights into editing-site specificity of ADARs, *Proc. Natl. Acad. Sci. U. S. A.* **2012**, *109*, E3295–E3304.

[63] J. M. Eggington, T. Greene, B. L. Bass, Predicting sites of ADAR editing in double-stranded RNA, *Nat. Commun.* **2011**, *2*, 319.

[64] C. M. Burns, H. Chu, S. M. Rueter, L. K. Hutchinson, H. Canton, *et al.*, Regulation of serotonin-2C receptor G-protein coupling by RNA editing, *Nature* **1997**, *387*, 303–308.

[65] T. Bhalla, J. J. Rosenthal, M. Holmgren, R. Reenan, Control of human potassium channel inactivation by editing of a small mRNA hairpin, *Nat. Struct. Mol. Biol.* **2004**, *11*, 950–956.

[66] M. Higuchi, S. Maas, F. N. Single, J. Hartner, A. Rozov, *et al.*, Point mutation in an AMPA receptor gene rescues lethality in mice deficient in the RNA-editing enzyme ADAR2, *Nature* **2000**, *406*, 78–81.

[67] S. M. Rueter, T. R. Dawson, R. B. Emeson, Regulation of alternative splicing by RNA editing, *Nature* **1999**, *399*, 75–80.

[68] W. Yang, T. P. Chendrimada, Q. Wang, M. Higuchi, P. H. Seeburg, *et al.*, Modulation of microRNA processing and expression through RNA editing by ADAR deaminases, *Nat. Struct. Mol. Biol.* **2006**, *13*, 13–21.

[69] A. D. J. Scadden, M. A. O'Connell, Cleavage of dsRNAs hyper-edited by ADARs occurs at preferred editing sites, *Nucleic Acids Res.* **2005**, *33*, 5954–5964.

[70] K. V. Prasanth, S. G. Prasanth, Z. Xuan, S. Hearn, S. M. Freier, *et al.*, Regulating Gene Expression through RNA Nuclear Retention, *Cell* **2005**, *123*, 249–263.

[71] J. D. Salter, R. P. Bennett, H. C. Smith, The APOBEC Protein Family: United by Structure, Divergent in Function, *Trends Biochem. Sci.* **2016**, *41*, 578–594.

[72] H. C. Smith, RNA binding to APOBEC deaminases; Not simply a substrate for C to U editing, *RNA Biol.* **2017**, *14*, 1153–1165.

[73] B. Teng, C. F. Burant, N. O. Davidson, Molecular Cloning of an Apolipoprotein B Messenger RNA Editing Protein, *Science* **1993**, *260*, 1816–1819.

[74] S. Sharma, S. K. Patnaik, R. T. Taggart, E. D. Kannisto, S. M. Enriquez, *et al.*, APOBEC3A cytidine deaminase induces RNA editing in monocytes and macrophages, *Nat. Commun.* **2015**, *6*, 6881.

[75] S. Sharma, S. K. Patnaik, R. T. Taggart, B. E. Baysal, The double-domain cytidine deaminase APOBEC3G is a cellular site-specific RNA editing enzyme, *Sci. Rep.* **2016**, *6*, 39 100.

[76] A. D. Wolfe, S. Li, C. Goedderz, X. S. Chen, The structure of APOBEC1 and insights into its RNA and DNA substrate selectivity, *NAR Cancer* **2020**, *2*, zcaa027.

[77] A. Chester, A. Somasekaram, M. Tzimina, A. Jarmuz, J. Gisbourne, *et al.*, The apolipoprotein B mRNA editing complex performs a multifunctional cycle and suppresses nonsense-mediated decay, *EMBO J.* **2003**, *22*, 3971–3982.

[78] R. P. Bennett, V. Presnyak, J. E. Wedekind, H. C. Smith, Nuclear Exclusion of the HIV-1 Host Defense Factor APOBEC3G Requires a Novel Cytoplasmic Retention Signal and Is Not Dependent on RNA Binding, *J. Biol. Chem.* **2008**, *283*, 7320–7327.

[79] H. Aydin, M. Taylor, J. Lee, Structure-Guided Analysis of the Human APOBEC3-HIV Restrictome, *Structure* **2014**, *22*, 668–684.

[80] A. Mehta, M. T. Kinter, N. E. Sherman, D. M. Driscoll, Molecular Cloning of Apobec-1 Complementation Factor, a Novel RNA-Binding Protein Involved in the Editing of Apolipoprotein B mRNA, *Mol. Cell. Biol.* **2000**, *20*, 1846–1854.

[81] N. Fossat, K. Tourle, T. Radziewic, K. Barratt, D. Liebhold, *et al.*, C to U RNA editing mediated by APOBEC1 requires RNA-binding protein RBM47, *EMBO Rep.* **2014**, *15*, 903–910.

[82] V. Blanc, Y. Xie, S. Kennedy, J. D. Riordan, D. C. Rubin, *et al.*, Apobec1 complementation factor (A1CF) and RBM47 interact in tissue-specific regulation of C to U RNA editing in mouse intestine and liver, *RNA* **2019**, *25*, 70–81.

[83] R. Shah, T. Knott, J. Legros, N. Navaratnam, J. Greeve, *et al.*, Sequence requirements for the editing of apolipoprotein B mRNA., *J. Biol. Chem.* **1991**, *266*, 16 301–16 304.

[84] J. W. Backus, H. C. Smith, Three distinct RNA sequence elements are required for efficient apolipoprotein B (apoB) RNA editing *in vitro*, *Nucleic Acids Res.* **1992**, *20*, 6007–6014.

[85] S. Sharma, B. E. Baysal, Stem-loop structure preference for site-specific RNA editing by APOBEC3A and APOBEC3G, *PeerJ* **2017**, *5*, e4136.

[86] V. Blanc, J. O. Henderson, E. P. Newberry, S. Kennedy, J. Luo, *et al.*, Targeted Deletion of the Murine apobec-1 Complementation Factor (*acf*) Gene Results in Embryonic Lethality, *Mol. Cell. Biol.* **2005**, *25*, 7260–7269.

[87] B. Polevoda, W. M. McDougall, B. N. Tun, M. Cheung, J. D. Salter, *et al.*, RNA binding to APOBEC3G induces the disassembly of functional deaminase complexes by displacing single-stranded DNA substrates, *Nucleic Acids Res.* **2015**, *43*, 9434–9445.

[88] V. Blanc, J. O. Henderson, R. D. Newberry, Y. Xie, S.-J. Cho, *et al.*, Deletion of the AU-rich RNA binding protein Apobec-1 reduces intestinal tumor burden in Apc^{min} mice, *Cancer Res.* **2007**, *67*, 8565–8573.

[89] I. Barbieri, T. Kouzarides, Role of RNA modifications in cancer, *Nat. Rev. Cancer* **2020**, *20*, 303–322.

[90] C.-P. Kung, L. B. Maggi, J. D. Weber, The Role of RNA Editing in Cancer Development and Metabolic Disorders, *Front. Endocrinol.* **2018**, *9*, 762.

[91] P. K. M. Shivalingappa, V. Sharma, A. Shiras, S. A. Bapat, RNA binding motif 47 (RBM47): emerging roles in vertebrate development, RNA editing and cancer, *Mol. Cell. Biochem.* **2021**, *476*, 4493–4505.

[92] S. Maas, Y. Kawahara, K. M. Tamburro, K. Nishikura, A-to-I RNA Editing and Human Disease, *RNA Biol.* **2006**, *3*, 1–9.

[93] W. Slotkin, K. Nishikura, Adenosine-to-inosine RNA editing and human disease, *Genome Med.* **2013**, *5*, 105.

[94] T. Lerner, F. N. Papavasiliou, R. Pecori, RNA Editors, Cofactors, and mRNA Targets: An Overview of the C-to-U RNA Editing Machinery and Its Implication in Human Disease, *Genes* **2019**, *10*, 13.

[95] M. Grohmann, P. Hammer, M. Walther, N. Paulmann, A. Büttner, *et al.*, Alternative Splicing and Extensive RNA Editing of Human TPH2 Transcripts, *PLoS ONE* **2010**, *5*, e8956.

[96] M. V. Morabito, A. I. Abbas, J. L. Hood, R. A. Kesterson, M. M. Jacobs, *et al.*, Mice with altered serotonin 2C receptor RNA editing display characteristics of Prader–Willi syndrome, *Neurobiol. Dis.* **2010**, *39*, 169–180.

[97] L. Shallev, E. Kopel, A. Feiglin, G. S. Leichner, D. Avni, *et al.*, Decreased A-to-I RNA editing as a source of keratinocytes' dsRNA in psoriasis, *RNA* **2018**, *24*, 828–840.

[98] S. H. Roth, M. Danan-Gotthold, M. Ben-Izhak, G. Rechavi, C. J. Cohen, *et al.*, Increased RNA Editing May Provide a Source for Autoantigens in Systemic Lupus Erythematosus, *Cell Rep.* **2018**, *23*, 50–57.

[99] J. Livingston, Y. Crow, Neurologic Phenotypes Associated with Mutations in *TREX1*, *RNASEH2A*, *RNASEH2B*, *RNASEH2C*, *SAMHD1*, *ADAR1*, and *IFIH1*: Aicardi–Goutières Syndrome and Beyond, *Neuropediatrics* **2016**, *47*, 355–360.

[100] H. Adachi, M. Hengesbach, Y.-T. Yu, P. Morais, From Antisense RNA to RNA Modification: Therapeutic Potential of RNA-Based Technologies, *Biomedicines* **2021**, *9*, 550.

[101] L. Schoenmaker, D. Witzigmann, J. A. Kulkarni, R. Verbeke, G. Kersten, *et al.*, mRNA-lipid nanoparticle COVID-19 vaccines: Structure and stability, *Int. J. Pharm.* **2021**, *601*, 120 586.

[102] A. Akinc, W. Querbes, S. De, J. Qin, M. Frank-Kamenetsky, *et al.*, Targeted Delivery of RNAi Therapeutics With Endogenous and Exogenous Ligand-Based Mechanisms, *Mol. Ther.* **2010**, *18*, 1357–1364.

[103] T. P. Prakash, M. J. Graham, J. Yu, R. Carty, A. Low, *et al.*, Targeted delivery of antisense oligonucleotides to hepatocytes using triantennary *N*-acetyl galactosamine improves potency 10-fold in mice, *Nucleic Acids Res.* **2014**, *42*, 8796–8807.

[104] M. Imbert, G. Dias-Florencio, A. Goyenvalle, Viral Vector-Mediated Antisense Therapy for Genetic Diseases, *Genes* **2017**, *8*, 51.

[105] K. Dhuri, C. Bechtold, E. Quijano, H. Pham, A. Gupta, *et al.*, Antisense Oligonucleotides: An Emerging Area in Drug Discovery and Development, *J. Clin. Med.* **2020**, *9*, 2004.

[106] S. M. Elbashir, J. Harborth, W. Lendeckel, A. Yalcin, K. Weber, *et al.*, Duplexes of 21-nucleotide RNAs mediate RNA interference in cultured mammalian cells, *Nature* **2001**, *411*, 494–498.

[107] D. Adams, A. Gonzalez-Duarte, W. D. O'Riordan, C.-C. Yang, M. Ueda, *et al.*, Patisiran, an RNAi Therapeutic, for Hereditary Transthyretin Amyloidosis, *N. Engl. J. Med.* **2018**, *379*, 11–21.

[108] L. Chan, T. Yokota, Development and Clinical Applications of Antisense Oligonucleotide Gapmers, in T. Yokota, R. Maruyama (eds.), Gapmers, *Methods in Molecular Biology*, vol. 2176, 21–47, Springer US **2020**.

[109] K. R. Q. Lim, T. Yokota, Invention and Early History of Exon Skipping and Splice Modulation, in T. Yokota, R. Maruyama (eds.), Exon Skipping and Inclusion Therapies, *Methods in Molecular Biology*, vol. 1828, 3–30, Springer US **2018**.

[110] H. A. Rees, D. R. Liu, Base editing: precision chemistry on the genome and transcriptome of living cells, *Nat. Rev. Genet.* **2018**, *19*, 770–788.

[111] M.-L. Bortolin, P. Ganot, T. Kiss, Elements essential for accumulation and function of small nucleolar RNAs directing site-specific pseudouridylation of ribosomal RNAs, *EMBO J.* **1999**, *18*, 457–469.

[112] J. Karijolich, Y.-T. Yu, Converting nonsense codons into sense codons by targeted pseudouridylation, *Nature* **2011**, *474*, 395–398.

[113] Z. Kiss-László, Y. Henry, J.-P. Bachellerie, M. Caizergues-Ferrer, T. Kiss, Site-Specific Ribose Methylation of Preribosomal RNA: A Novel Function for Small Nucleolar RNAs, *Cell* **1996**, *85*, 1077–1088.

[114] X. Zhao, Y.-T. Yu, Targeted pre-mRNA modification for gene silencing and regulation, *Nat. Methods* **2008**, *5*, 95–100.

[115] T. M. Woolf, J. M. Chase, D. T. Stinchcomb, Toward the therapeutic editing of mutated RNA sequences., *Proc. Natl. Acad. Sci. U. S. A.* **1995**, *92*, 8298–8302.

[116] T. Stafforst, M. F. Schneider, An RNA–Deaminase Conjugate Selectively Repairs Point Mutations, *Angew. Chem. Int. Ed.* **2012**, *51*, 11 166–11 169.

[117] M. F. Montiel-Gonzalez, I. Vallecillo-Viejo, G. A. Yudowski, J. J. C. Rosenthal, Correction of mutations within the cystic fibrosis transmembrane conductance regulator by site-directed RNA editing, *Proc. Natl. Acad. Sci. U. S. A.* **2013**, *110*, 18 285–18 290.

[118] M. T. A. Azad, S. Bhakta, T. Tsukahara, Site-directed RNA editing by adenosine deaminase acting on RNA for correction of the genetic code in gene therapy, *Gene Ther.* **2017**, *24*, 779–786.

[119] D. B. T. Cox, J. S. Gootenberg, O. O. Abudayyeh, B. Franklin, M. J. Kellner, *et al.*,

RNA editing with CRISPR-Cas13, *Science* **2017**, *358*, 1019–1027.

[120] S. Rauch, E. He, M. Srienc, H. Zhou, Z. Zhang, *et al.*, Programmable RNA-Guided RNA Effector Proteins Built from Human Parts, *Cell* **2019**, *178*, 122–134.

[121] P. Vogel, M. F. Schneider, J. Wettengel, T. Stafforst, Improving Site-Directed RNA Editing In Vitro and in Cell Culture by Chemical Modification of the GuideRNA, *Angew. Chem. Int. Ed.* **2014**, *53*, 6267–6271.

[122] P. Vogel, A. Hanswillemenke, T. Stafforst, Switching Protein Localization by Site-Directed RNA Editing under Control of Light, *ACS Synth. Biol.* **2017**, *6*, 1642–1649.

[123] P. Vogel, M. Moschref, Q. Li, T. Merkle, K. D. Selvasaravanan, *et al.*, Efficient and precise editing of endogenous transcripts with SNAP-tagged ADARs, *Nat. Methods* **2018**, *15*, 535–538.

[124] J. Krützfeldt, N. Rajewsky, R. Braich, K. G. Rajeev, T. Tuschl, *et al.*, Silencing of microRNAs in vivo with 'antagomirs', *Nature* **2005**, *438*, 685–689.

[125] M. F. Schneider, J. Wettengel, P. C. Hoffmann, T. Stafforst, Optimal guideRNAs for re-directing deaminase activity of hADAR1 and hADAR2 in *trans*, *Nucleic Acids Res.* **2014**, *42*, e87.

[126] A. Hanswillemenke, T. Kuzdere, P. Vogel, G. Jékely, T. Stafforst, Site-Directed RNA Editing in Vivo Can Be Triggered by the Light-Driven Assembly of an Artificial Riboprotein, *J. Am. Chem. Soc.* **2015**, *137*, 15 875–15 881.

[127] J. Baron-Benhamou, N. H. Gehring, A. E. Kulozik, M. W. Hentze, Using the λN Peptide to Tether Proteins to RNAs, in D. R. Schoenberg (ed.), mRNA Processing and Metabolism, *Methods in Molecular Biology*, vol. 257, 135–153, Springer US **2004**.

[128] M. F. Montiel-González, I. C. Vallecillo-Viejo, J. Rosenthal, An efficient system for selectively altering genetic information within mRNAs, *Nucleic Acids Res.* **2016**, *44*, e157.

[129] I. C. Vallecillo-Viejo, N. Liscovitch-Brauer, M. F. Montiel-Gonzalez, E. Eisenberg, J. J. C. Rosenthal, Abundant off-target edits from site-directed RNA editing can be reduced by nuclear localization of the editing enzyme, *RNA Biol.* **2018**, *15*, 104–114.

[130] J. R. Sinnamon, S. Y. Kim, G. M. Corson, Z. Song, H. Nakai, *et al.*, Site-directed RNA repair of endogenous Mecp2 RNA in neurons, *Proc. Natl. Acad. Sci. U. S. A.* **2017**, *114*, E9395–E9402.

[131] J. R. Sinnamon, S. Y. Kim, J. R. Fisk, Z. Song, H. Nakai, *et al.*, *In Vivo* Repair of a Protein Underlying a Neurological Disorder by Programmable RNA Editing, *Cell Rep.* **2020**, *32*, 107 878.

[132] D. Katrekar, G. Chen, D. Meluzzi, A. Ganesh, A. Worlikar, *et al.*, In vivo RNA editing of point mutations via RNA-guided adenosine deaminases, *Nat. Methods* **2019**, *16*, 239–242.

[133] C. Helgstrand, E. Grahn, T. Moss, N. J. Stonehouse, K. Tars, *et al.*, Investigating the structural basis of purine specificity in the structures of MS2 coat protein RNA translational operator hairpins, *Nucleic Acids Res.* **2002**, *30*, 2678–2685.

[134] S. Rauch, K. A. Jones, B. Dickinson, Small Molecule-Inducible RNA-Targeting Systems for Temporal Control of RNA Regulation, *ACS Cent. Sci.* **2020**, *6*, 1987–1996.

[135] J. Wettengel, P. Reautschnig, S. Geisler, P. J. Kahle, T. Stafforst, Harnessing human ADAR2 for RNA repair – Recoding a PINK1 mutation rescues mitophagy, *Nucleic Acids Res.* **2017**, *45*, 2797–2808.

[136] T. Merkle, S. Merz, P. Reautschnig, A. Blaha, Q. Li, *et al.*, Precise RNA editing by

recruiting endogenous ADARs with antisense oligonucleotides, *Nat. Biotechnol.* **2019**, *37*, 133–138.

[137] P. Reautschnig, N. Wahn, J. Wettengel, A. E. Schulz, N. Latifi, *et al.*, CLUSTER guide RNAs enable precise and efficient RNA editing with endogenous ADAR enzymes in vivo, *Nat. Biotechnol.* **2022**, *40*, 759–768.

[138] L. Qu, Z. Yi, S. Zhu, C. Wang, Z. Cao, *et al.*, Programmable RNA editing by recruiting endogenous ADAR using engineered RNAs, *Nat. Biotechnol.* **2019**, *37*, 1059–1071.

[139] H. Lomeli, J. Mosbacher, T. Melcher, T. Höger, J. R. P. Geiger, *et al.*, Control of Kinetic Properties of AMPA Receptor Channels by Nuclear RNA Editing, *Science* **1994**, *266*, 1709–1713.

[140] R. Stefl, F. C. Oberstrass, J. L. Hood, M. Jourdan, M. Zimmermann, *et al.*, The Solution Structure of the ADAR2 dsRBM-RNA Complex Reveals a Sequence-Specific Readout of the Minor Groove, *Cell* **2010**, *143*, 225–237.

[141] M. Heep, P. Mach, P. Reautschnig, J. Wettengel, T. Stafforst, Applying Human ADAR1p110 and ADAR1p150 for Site-Directed RNA Editing—G/C Substitution Stabilizes GuideRNAs against Editing, *Genes* **2017**, *8*, 34.

[142] O. O. Abudayyeh, J. S. Gootenberg, B. Franklin, J. Koob, M. J. Kellner, *et al.*, A cytosine deaminase for programmable single-base RNA editing, *Science* **2019**, *365*, 382–386.

[143] S. Bhakta, M. Sakari, T. Tsukahara, RNA editing of BFP, a point mutant of GFP, using artificial APOBEC1 deaminase to restore the genetic code, *Sci. Rep.* **2020**, *10*, 17 304.

[144] X. Huang, J. Lv, Y. Li, S. Mao, Z. Li, *et al.*, Programmable C-to-U RNA editing using the human APOBEC3A deaminase, *EMBO J.* **2020**, *39*, e104 741.

[145] A. S. Stroppel, N. Latifi, A. Hanswillemenke, R. Tasakis, F. Papavasiliou, *et al.*, Harnessing self-labeling enzymes for selective and concurrent A-to-I and C-to-U RNA base editing, *Nucleic Acids Res.* **2021**, *49*, e95.

[146] K. Jarowicki, P. Kocienski, Protecting groups, *J. Chem. Soc., Perkin Trans. 1* **2001**, 2109–2135.

[147] P. Klán, T. Šolomek, C. G. Bochet, A. Blanc, R. Givens, *et al.*, Photoremovable Protecting Groups in Chemistry and Biology: Reaction Mechanisms and Efficacy, *Chem. Rev.* **2013**, *113*, 119–191.

[148] N. Ankenbruck, T. Courtney, Y. Naro, A. Deiters, Optochemical Control of Biological Processes in Cells and Animals, *Angew. Chem. Int. Ed.* **2018**, *57*, 2768–2798.

[149] L. Klewer, Y.-W. Wu, Light-Induced Dimerization Approaches to Control Cellular Processes, *Chem. – Eur. J.* **2019**, *25*, 12 452–12 463.

[150] Y. Kim, J. A. Phillips, H. Liu, H. Kang, W. Tan, Using photons to manipulate enzyme inhibition by an azobenzene-modified nucleic acid probe, *Proc. Natl. Acad. Sci. U. S. A.* **2009**, *106*, 6489–6494.

[151] T. Stafforst, D. Hilvert, Modulating PNA/DNA Hybridization by Light, *Angew. Chem. Int. Ed.* **2010**, *49*, 9998–10 001.

[152] J. A. Frank, D. A. Yushchenko, D. J. Hodson, N. Lipstein, J. Nagpal, *et al.*, Photoswitchable diacylglycerols enable optical control of protein kinase C, *Nat. Chem. Biol.* **2016**, *12*, 755–762.

[153] M. M. Lerch, M. J. Hansen, W. A. Velema, W. Szymanski, B. L. Feringa, Orthogonal photoswitching in a multifunctional molecular system, *Nat. Commun.* **2016**, *7*, 12 054.

[154] Y. V. Il'ichev, M. A. Schwörer, J. Wirz, Photochemical Reaction Mechanisms of 2-Nitrobenzyl Compounds: Methyl Ethers and Caged ATP, *J. Am. Chem. Soc.* **2004**, *126*, 4581–4595.

[155] A. Patchornik, B. Amit, R. B. Woodward, Photosensitive protecting groups, *J. Am. Chem. Soc.* **1970**, *92*, 6333–6335.

[156] A. Gautier, D. P. Nguyen, H. Lusic, W. An, A. Deiters, *et al.*, Genetically Encoded Photocontrol of Protein Localization in Mammalian Cells, *J. Am. Chem. Soc.* **2010**, *132*, 4086–4088.

[157] A. Stutz, S. Pitsch, Automated RNA-Synthesis with Photocleavable Sugar and Nucleobase Protecting Groups, *Synlett* **1999**, *1999*, 930–934.

[158] H. Lusic, A. Deiters, A New Photocaging Group for Aromatic *N*-Heterocycles, *Synthesis* **2006**, *13*, 2147–2150.

[159] A. K. Singh, P. K. Khade, 3-Nitro-2-naphthalenemethanol: a photocleavable protecting group for carboxylic acids, *Tetrahedron* **2005**, *61*, 10 007–10 012.

[160] E. Reichmanis, B. C. Smith, R. Gooden, *O*-nitrobenzyl photochemistry: Solution vs. solid-state behavior, *J. Polym. Sci. Polym. Chem. Ed.* **1985**, *23*, 1–8.

[161] K. Schaper, S. A. M. Mobarekeh, C. Grewer, Synthesis and Photophysical Characterization of a New, Highly Hydrophilic Caging Group, *Eur. J. Org. Chem.* **2002**, *2002*, 1037–1046.

[162] L. Donato, A. Mourot, C. M. Davenport, C. Herbivo, D. Warther, *et al.*, Water-Soluble, Donor-Acceptor Biphenyl Derivatives in the 2-(*o*-Nitrophenyl)propyl Series: Highly Efficient Two-Photon Uncaging of the Neurotransmitter γ-Aminobutyric Acid at λ=800 nm, *Angew. Chem. Int. Ed.* **2012**, *51*, 1840–1843.

[163] K. C. Nicolaou, C. W. Hummel, M. Nakada, K. Shibayama, E. N. Pitsinos, *et al.*, Total synthesis of calicheamicin γ_1^I. 3. The final stages, *J. Am. Chem. Soc.* **1993**, *115*, 7625–7635.

[164] Y. Gareau, R. Zamboni, A. W. Wong, Total synthesis of *N*-methyl LTC4: a novel methodology for the monomethylation of amines, *J. Org. Chem.* **1993**, *58*, 1582–1585.

[165] J. Engels, E. J. Schlaeger, Synthesis, Structure, and Reactivity of Adenosine Cyclic 3',5'-Phosphate-Benzyltriesters, *J. Med. Chem.* **1977**, *20*, 907–911.

[166] E. J. Tsai, D. A. Kass, Cyclic GMP signaling in cardiovascular pathophysiology and therapeutics, *Pharmacol. Ther.* **2009**, *122*, 216–238.

[167] F. Hofmann, The cGMP system: components and function, *Biol. Chem.* **2020**, *401*, 447–469.

[168] T. Nakamura, G. H. Gold, A cyclic nucleotide-gated conductance in olfactory receptor cilia, *Nature* **1987**, *325*, 442–444.

[169] U. B. Kaupp, K. W. Koch, Role of cGMP and Ca^{2+} in Vertebrate Photoreceptor Excitation and Adaptation, *Annu. Rev. Physiol.* **1992**, *54*, 153–176.

[170] J. H. Kaplan, G. C. Ellis-Davies, Photolabile chelators for the rapid photorelease of divalent cations., *Proc. Natl. Acad. Sci. U. S. A.* **1988**, *85*, 6571–6575.

[171] G. C. Ellis-Davies, R. J. Barsotti, Tuning caged calcium: Photolabile analogues of EGTA with improved optical and chelation properties, *Cell Calcium* **2006**, *39*, 75–83.

[172] H. K. Agarwal, R. Janicek, S.-H. Chi, J. W. Perry, E. Niggli, *et al.*, Calcium Uncaging with Visible Light, *J. Am. Chem. Soc.* **2016**, *138*, 3687–3693.

[173] R. Tsien, R. Zucker, Control of cytoplasmic calcium with photolabile tetracarboxylate 2-nitrobenzhydrol chelators, *Biophys. J.* **1986**, *50*, 843–853.

[174] S. Banala, D. Maurel, S. Manley, K. Johnsson, A Caged, Localizable Rhodamine Derivative for Superresolution Microscopy, *ACS Chem. Biol.* **2012**, *7*, 289–293.

[175] A. S. Baker, A. Deiters, Optical Control of Protein Function through Unnatural Amino Acid Mutagenesis and Other Optogenetic Approaches, *ACS Chem. Biol.* **2014**, *9*, 1398–1407.

[176] A. Gautier, A. Deiters, J. W. Chin, Light-Activated Kinases Enable Temporal Dissection of Signaling Networks in Living Cells, *J. Am. Chem. Soc.* **2011**, *133*, 2124–2127.

[177] M. A. Azagarsamy, K. S. Anseth, Wavelength-Controlled Photocleavage for the Orthogonal and Sequential Release of Multiple Proteins, *Angew. Chem. Int. Ed.* **2013**, *52*, 13 803–13 807.

[178] J. M. Govan, R. Uprety, M. Thomas, H. Lusic, M. O. Lively, *et al.*, Cellular Delivery and Photochemical Activation of Antisense Agents through a Nucleobase Caging Strategy, *ACS Chem. Biol.* **2013**, *8*, 2272–2282.

[179] S. Shah, S. Rangarajan, S. H. Friedman, Light-Activated RNA Interference, *Angew. Chem. Int. Ed.* **2005**, *44*, 1328–1332.

[180] V. Mikat, A. Heckel, Light-dependent RNA interference with nucleobase-caged siRNAs, *RNA* **2007**, *13*, 2341–2347.

[181] P. K. Jain, S. Shah, S. H. Friedman, Patterning of Gene Expression Using New Photolabile Groups Applied to Light Activated RNAi, *J. Am. Chem. Soc.* **2011**, *133*, 440–446.

[182] Y. Ji, J. Yang, L. Wu, L. Yu, X. Tang, Photochemical Regulation of Gene Expression Using Caged siRNAs with Single Terminal Vitamin E Modification, *Angew. Chem. Int. Ed.* **2016**, *55*, 2152–2156.

[183] G. Zheng, L. Cochella, J. Liu, O. Hobert, W.-H. Li, Temporal and Spatial Regulation of MicroRNA Activity with Photoactivatable Cantimirs, *ACS Chem. Biol.* **2011**, *6*, 1332–1338.

[184] J. C. Griepenburg, B. K. Ruble, I. J. Dmochowski, Caged oligonucleotides for bidirectional photomodulation of *let-7* miRNA in zebrafish embryos, *Bioorg. Med. Chem.* **2013**, *21*, 6198–6204.

[185] C. M. Connelly, R. Uprety, J. Hemphill, A. Deiters, Spatiotemporal control of microRNA function using light-activated antagomirs, *Mol. BioSyst.* **2012**, *8*, 2987.

[186] I. A. Shestopalov, S. Sinha, J. K. Chen, Light-controlled gene silencing in zebrafish embryos, *Nat. Chem. Biol.* **2007**, *3*, 650–651.

[187] X. Ouyang, I. A. Shestopalov, S. Sinha, G. Zheng, C. L. W. Pitt, *et al.*, Versatile Synthesis and Rational Design of Caged Morpholinos, *J. Am. Chem. Soc.* **2009**, *131*, 13 255–13 269.

[188] S. Yamazoe, I. A. Shestopalov, E. Provost, S. D. Leach, J. K. Chen, Cyclic Caged Morpholinos: Conformationally Gated Probes of Embryonic Gene Function, *Angew. Chem. Int. Ed.* **2012**, *51*, 6908–6911.

[189] J. M. Govan, M. O. Lively, A. Deiters, Photochemical Control of DNA Decoy Function Enables Precise Regulation of Nuclear Factor κB Activity, *J. Am. Chem. Soc.* **2011**, *133*, 13 176–13 182.

[190] J. M. Govan, R. Uprety, J. Hemphill, M. O. Lively, A. Deiters, Regulation of Transcription through Light-Activation and Light-Deactivation of Triplex-Forming Oligonucleotides in Mammalian Cells, *ACS Chem. Biol.* **2012**, *7*, 1247–1256.

[191] J. Hemphill, J. Govan, R. Uprety, M. Tsang, A. Deiters, Site-Specific Promoter Caging

Enables Optochemical Gene Activation in Cells and Animals, *J. Am. Chem. Soc.* **2014**, *136*, 7152–7158.

[192] C. Wang, Z. Zhu, Y. Song, H. Lin, C. J. Yang, *et al.*, Caged molecular beacons: controlling nucleic acid hybridization with light, *Chem. Commun.* **2011**, *47*, 5708–5710.

[193] K. B. Joshi, A. Vlachos, V. Mikat, T. Deller, A. Heckel, Light-activatable molecular beacons with a caged loop sequence, *Chem. Commun.* **2012**, *48*, 2746–2748.

[194] A. Heckel, G. Mayer, Light Regulation of Aptamer Activity: An Anti-Thrombin Aptamer with Caged Thymidine Nucleobases, *J. Am. Chem. Soc.* **2005**, *127*, 822–823.

[195] Z. Tan, T. A. Feagin, J. M. Heemstra, Temporal Control of Aptamer Biosensors Using Covalent Self-Caging To Shift Equilibrium, *J. Am. Chem. Soc.* **2016**, *138*, 6328–6331.

[196] D. Lovatt, B. K. Ruble, J. Lee, H. Dueck, T. K. Kim, *et al.*, Transcriptome *in vivo* analysis (TIVA) of spatially defined single cells in live tissue, *Nat. Methods* **2014**, *11*, 190–196.

[197] B. Schade, V. Hagen, R. Schmidt, R. Herbrich, E. Krause, *et al.*, Deactivation Behavior and Excited-State Properties of (Coumarin-4-yl)methyl Derivatives. 1. Photocleavage of (7-Methoxycoumarin-4-yl)methyl-Caged Acids with Fluorescence Enhancement, *J. Org. Chem.* **1999**, *64*, 9109–9117.

[198] A. M. Piloto, D. Rovira, S. P. Costa, M. S. T. Gonçalves, Oxobenzo[*f*]benzopyrans as new fluorescent photolabile protecting groups for the carboxylic function, *Tetrahedron* **2006**, *62*, 11 955–11 962.

[199] A. M. S. Soares, S. P. G. Costa, M. S. T. Gonçalves, 2-Oxo-2*H*-benzo[*h*]benzopyran as a new light sensitive protecting group for neurotransmitter amino acids, *Amino Acids* **2010**, *39*, 121–133.

[200] M. A. H. Fichte, X. M. M. Weyel, S. Junek, F. Schäfer, C. Herbivo, *et al.*, Three-Dimensional Control of DNA Hybridization by Orthogonal Two-Color Two-Photon Uncaging, *Angew. Chem. Int. Ed.* **2016**, *55*, 8948–8952.

[201] T. Furuta, S. S.-H. Wang, J. L. Dantzker, T. M. Dore, W. J. Bybee, *et al.*, Brominated 7-hydroxycoumarin-4-ylmethyls: Photolabile protecting groups with biologically useful cross-sections for two photon photolysis, *Proc. Natl. Acad. Sci. U. S. A.* **1999**, *96*, 1193–1200.

[202] T. Furuta, H. Takeuchi, M. Isozaki, Y. Takahashi, M. Kanehara, *et al.*, Bhc-cNMPs as either Water-Soluble or Membrane-Permeant Photoreleasable Cyclic Nucleotides for both One- and Two-Photon Excitation, *ChemBioChem* **2004**, *5*, 1119–1128.

[203] V. Hagen, J. Bendig, S. Frings, T. Eckardt, S. Helm, *et al.*, Highly Efficient and Ultrafast Phototriggers for cAMP and cGMP by Using Long-Wavelength UV/Vis-Activation, *Angew. Chem. Int. Ed.* **2001**, *40*, 1045–1048.

[204] V. Hagen, S. Frings, B. Wiesner, S. Helm, U. B. Kaupp, *et al.*, [7-(Dialkylamino)coumarin-4-yl]methyl-Caged Compounds as Ultrafast and Effective Long-Wavelength Phototriggers of 8-Bromo-Substituted Cyclic Nucleotides, *ChemBioChem* **2003**, *4*, 434–442.

[205] A. Samanta, M. Thunemann, R. Feil, T. Stafforst, Upon the photostability of 8-nitro-cGMP and its caging as a 7-dimethylaminocoumarinyl ester, *Chem. Commun.* **2014**, *50*, 7120–7123.

[206] S. Khan, F. Castellano, J. Spudich, J. McCray, R. Goody, *et al.*, Excitatory signaling in bacterial probed by caged chemoeffectors, *Biophys. J.* **1993**, *65*, 2368–2382.

[207] D. Geißler, Y. N. Antonenko, R. Schmidt, S. Keller, O. O. Krylova, *et al.*, (Coumarin-4-yl)methyl Esters as Highly Efficient, Ultrafast Phototriggers for Protons and Their Application to Acidifying Membrane Surfaces, *Angew. Chem. Int. Ed.* **2005**, *44*, 1195–1198.

[208] J. Luo, R. Uprety, Y. Naro, C. Chou, D. P. Nguyen, *et al.*, Genetically Encoded Optochemical Probes for Simultaneous Fluorescence Reporting and Light Activation of Protein Function with Two-Photon Excitation, *J. Am. Chem. Soc.* **2014**, *136*, 15 551–15 558.

[209] S. Yamazoe, Q. Liu, L. E. McQuade, A. Deiters, J. K. Chen, Sequential Gene Silencing Using Wavelength-Selective Caged Morpholino Oligonucleotides, *Angew. Chem. Int. Ed.* **2014**, *53*, 10 114–10 118.

[210] Y. Li, J. Shi, Z. Luo, H. Jiang, X. Chen, *et al.*, Photoregulation of thrombin aptamer activity using Bhc caging strategy, *Bioorg. Med. Chem. Lett.* **2009**, *19*, 5368–5371.

[211] P. Seyfried, L. Eiden, N. Grebenovsky, G. Mayer, A. Heckel, Photo-Tethers for the (Multi-)Cyclic, Conformational Caging of Long Oligonucleotides, *Angew. Chem. Int. Ed.* **2017**, *56*, 359–363.

[212] A. Fegan, B. White, J. C. T. Carlson, C. R. Wagner, Chemically Controlled Protein Assembly: Techniques and Applications, *Chem. Rev.* **2010**, *110*, 3315–3336.

[213] S. Voß, L. Klewer, Y.-W. Wu, Chemically induced dimerization: reversible and spatiotemporal control of protein function in cells, *Curr. Opin. Chem. Biol.* **2015**, *28*, 194–201.

[214] D. M. Spencer, T. J. Wandless, S. L. Schreiber, G. R. Crabtree, Controlling Signal Transduction with Synthetic Ligands, *Science* **1993**, *262*, 1019–1024.

[215] B. Z. Stanton, E. J. Chory, G. R. Crabtree, Chemically induced proximity in biology and medicine, *Science* **2018**, *359*, eaao5902.

[216] L. A. Banaszynski, C. W. Liu, T. J. Wandless, Characterization of the FKBP·Rapamycin·FRB Ternary Complex, *J. Am. Chem. Soc.* **2005**, *127*, 4715–4721.

[217] S. D. Liberles, S. T. Diver, D. J. Austin, S. L. Schreiber, Inducible gene expression and protein translocation using nontoxic ligands identified by a mammalian three-hybrid screen, *Proc. Natl. Acad. Sci. U. S. A.* **1997**, *94*, 7825–7830.

[218] A. V. Karginov, Y. Zou, D. Shirvanyants, P. Kota, N. V. Dokholyan, *et al.*, Light Regulation of Protein Dimerization and Kinase Activity in Living Cells Using Photocaged Rapamycin and Engineered FKBP, *J. Am. Chem. Soc.* **2011**, *133*, 420–423.

[219] K. A. Brown, Y. Zou, D. Shirvanyants, J. Zhang, S. Samanta, *et al.*, Light-cleavable rapamycin dimer as an optical trigger for protein dimerization, *Chem. Commun.* **2015**, *51*, 5702–5705.

[220] N. Umeda, T. Ueno, C. Pohlmeyer, T. Nagano, T. Inoue, A Photocleavable Rapamycin Conjugate for Spatiotemporal Control of Small GTPase Activity, *J. Am. Chem. Soc.* **2011**, *133*, 12–14.

[221] P. J. Belshaw, S. N. Ho, G. R. Crabtree, S. L. Schreiber, Controlling protein association and subcellular localization with a synthetic ligand that induces heterodimerization of proteins., *Proc. Natl. Acad. Sci. U. S. A.* **1996**, *93*, 4604–4607.

[222] F.-S. Liang, W. Q. Ho, G. R. Crabtree, Engineering the ABA Plant Stress Pathway for Regulation of Induced Proximity, *Sci. Signaling* **2011**, *4*, rs2.

[223] C. W. Wright, Z.-F. Guo, F.-S. Liang, Light Control of Cellular Processes by Using Photocaged Abscisic Acid, *ChemBioChem* **2015**, *16*, 254–261.

[224] T. Miyamoto, R. DeRose, A. Suarez, T. Ueno, M. Chen, *et al.*, Rapid and orthogonal logic gating with a gibberellin-induced dimerization system, *Nat. Chem. Biol.* **2012**, *8*, 465–470.

[225] K. M. Schelkle, T. Griesbaum, D. Ollech, S. Becht, T. Buckup, *et al.*, Light-Induced Protein Dimerization by One- and Two-Photon Activation of Gibberellic Acid Derivatives in Living Cells, *Angew. Chem. Int. Ed.* **2015**, *54*, 2825–2829.

[226] K. Nishimura, T. Fukagawa, H. Takisawa, T. Kakimoto, M. Kanemaki, An auxin-based degron system for the rapid depletion of proteins in nonplant cells, *Nat. Methods* **2009**, *6*, 917–922.

[227] M. Morawska, H. D. Ulrich, An expanded tool kit for the auxin-inducible degron system in budding yeast, *Yeast* **2013**, *30*, 341–351.

[228] W. Zhao, H. Nguyen, G. Zeng, D. Gao, H. Yan, *et al.*, A chemically induced proximity system engineered from the plant auxin signaling pathway, *Chem. Sci.* **2018**, *9*, 5822–5827.

[229] E. R. Ballister, C. Aonbangkhen, A. M. Mayo, M. A. Lampson, D. M. Chenoweth, Localized light-induced protein dimerization in living cells using a photocaged dimerizer, *Nat. Commun.* **2014**, *5*, 5475.

[230] X. Chen, M. Venkatachalapathy, D. Kamps, S. Weigel, R. Kumar, *et al.*, "Molecular Activity Painting": Switch-like, Light-Controlled Perturbations inside Living Cells, *Angew. Chem. Int. Ed.* **2017**, *56*, 5916–5920.

[231] Y.-C. Lin, Y. Nihongaki, T.-Y. Liu, S. Razavi, M. Sato, *et al.*, Rapidly Reversible Manipulation of Molecular Activity with Dual Chemical Dimerizers, *Angew. Chem. Int. Ed.* **2013**, *52*, 6450–6454.

[232] X. Chen, M. Venkatachalapathy, L. Dehmelt, Y.-W. Wu, Multidirectional Activity Control of Cellular Processes Enabled by a Versatile Chemo-optogenetic Approach, *Angew. Chem. Int. Ed.* **2018**, *57*, 11 993–11 997.

[233] H. Haruki, J. Nishikawa, U. K. Laemmli, The Anchor-Away Technique: Rapid, Conditional Establishment of Yeast Mutant Phenotypes, *Mol. Cell* **2008**, *31*, 925–932.

[234] J. H. Bayle, J. S. Grimley, K. Stankunas, J. E. Gestwicki, T. J. Wandless, *et al.*, Rapamycin Analogs with Differential Binding Specificity Permit Orthogonal Control of Protein Activity, *Chem. Biol.* **2006**, *13*, 99–107.

[235] V. M. Rivera, X. Wang, S. Wardwell, N. L. Courage, A. Volchuk, *et al.*, Regulation of Protein Secretion Through Controlled Aggregation in the Endoplasmic Reticulum, *Science* **2000**, *287*, 826–830.

[236] J. L. Czlapinski, M. W. Schelle, L. W. Miller, S. T. Laughlin, J. J. Kohler, *et al.*, Conditional Glycosylation in Eukaryotic Cells Using a Biocompatible Chemical Inducer of Dimerization, *J. Am. Chem. Soc.* **2008**, *130*, 13 186–13 187.

[237] H. Chong, A. Ruchatz, T. Clackson, V. M. Rivera, R. G. Vile, A System for Small-Molecule Control of Conditionally Replication-Competent Adenoviral Vectors, *Mol. Ther.* **2002**, *5*, 195–203.

[238] K. M. Sakamoto, K. B. Kim, A. Kumagai, F. Mercurio, C. M. Crews, *et al.*, Protacs: Chimeric molecules that target proteins to the Skp1–Cullin–F box complex for ubiquitination and degradation, *Proc. Natl. Acad. Sci. U. S. A.* **2001**, *98*, 8554–8559.

[239] M. Békés, D. R. Langley, C. M. Crews, PROTAC targeted protein degraders: the past is prologue, *Nat. Rev. Drug Discovery* **2022**, *21*, 181–200.

[240] Z. Liu, M. Hu, Y. Yang, C. Du, H. Zhou, *et al.*, An overview of PROTACs: a promising

drug discovery paradigm, *Mol. Biomed.* **2022**, *3*, 46.

[241] J. E. Gestwicki, G. R. Crabtree, I. A. Graef, Harnessing Chaperones to Generate Small-Molecule Inhibitors of Amyloid β Aggregation, *Science* **2004**, *306*, 865–869.

[242] C. R. Y. Cruz, K. P. Micklethwaite, B. Savoldo, C. A. Ramos, S. Lam, *et al.*, Infusion of donor-derived CD19-redirected virus-specific T cells for B-cell malignancies relapsed after allogeneic stem cell transplant: a phase 1 study, *Blood* **2013**, *122*, 2965–2973.

[243] A. D. Stasi, S.-K. Tey, G. Dotti, Y. Fujita, A. Kennedy-Nasser, *et al.*, Inducible Apoptosis as a Safety Switch for Adoptive Cell Therapy, *N. Engl. J. Med.* **2011**, *365*, 1673–1683.

[244] X. Zhou, A. D. Stasi, S.-K. Tey, R. A. Krance, C. Martinez, *et al.*, Long-term outcome after haploidentical stem cell transplant and infusion of T cells expressing the inducible caspase 9 safety transgene, *Blood* **2014**, *123*, 3895–3905.

[245] X. Zhou, G. Dotti, R. A. Krance, C. A. Martinez, S. Naik, *et al.*, Inducible caspase-9 suicide gene controls adverse effects from alloreplete T cells after haploidentical stem cell transplantation, *Blood* **2015**, *125*, 4103–4113.

[246] E. M. Hetrick, M. H. Schoenfisch, Analytical Chemistry of Nitric Oxide, *Annu. Rev. Anal. Chem.* **2009**, *2*, 409–433.

[247] D. S. Bredt, S. H. Snyder, Nitric Oxide: A Physiologic Messenger Molecule, *Annu. Rev. Biochem.* **1994**, *63*, 175–195.

[248] V. Calabrese, C. Mancuso, M. Calvani, E. Rizzarelli, D. A. Butterfield, *et al.*, Nitric oxide in the central nervous system: neuroprotection versus neurotoxicity, *Nat. Rev. Neurosci.* **2007**, *8*, 766–775.

[249] C. Liu, M. C. Liang, T. W. Soong, Nitric Oxide, Iron and Neurodegeneration, *Front. Neurosci.* **2019**, *13*, 114.

[250] R. M. J. Palmer, A. G. Ferrige, S. Moncada, Nitric oxide release accounts for the biological activity of endothelium-derived relaxing factor, *Nature* **1987**, *327*, 524–526.

[251] W. P. Arnold, C. K. Mittal, S. Katsuki, F. Murad, Nitric oxide activates guanylate cyclase and increases guanosine 3':5'-cyclic monophosphate levels in various tissue preparations, *Proc. Natl. Acad. Sci. U. S. A.* **1977**, *74*, 3203–3207.

[252] B. G. Horst, M. A. Marletta, Physiological activation and deactivation of soluble guanylate cyclase, *Nitric Oxide* **2018**, *77*, 65–74.

[253] Y. Kang, R. Liu, J.-X. Wu, L. Chen, Structural insights into the mechanism of human soluble guanylate cyclase, *Nature* **2019**, *574*, 206–210.

[254] E. R. Derbyshire, M. A. Marletta, Structure and Regulation of Soluble Guanylate Cyclase, *Annu. Rev. Biochem.* **2012**, *81*, 533–559.

[255] D. Conole, L. J. Scott, Riociguat: First Global Approval, *Drugs* **2013**, *73*, 1967–1975.

[256] A. Markham, S. Duggan, Vericiguat: First Approval, *Drugs* **2021**, *81*, 721–726.

[257] R. C. Webb, Smooth muscle contraction and relaxation, *Adv. Physiol. Educ.* **2003**, *27*, 201–206.

[258] R. Feil, S. Feil, F. Hofmann, A heretical view on the role of NO and cGMP in vascular proliferative diseases, *Trends Mol. Med.* **2005**, *11*, 71–75.

[259] M. Lehners, H. Dobrowinski, S. Feil, R. Feil, cGMP Signaling and Vascular Smooth Muscle Cell Plasticity, *J. Cardiovasc. Dev. Dis.* **2018**, *5*, 20.

[260] E. A. Ataabadi, K. Golshiri, A. Jüttner, G. Krenning, A. J. Danser, *et al.*, Nitric Oxide-cGMP Signaling in Hypertension, *Hypertension* **2020**, *76*, 1055–1068.

[261] A. Petraina, C. Nogales, T. Krahn, H. Mucke, T. F. Lüscher, *et al.*, Cyclic GMP modulating drugs in cardiovascular diseases: mechanism-based network pharmacology, *Cardiovasc. Res.* **2022**, *118*, 2085–2102.

[262] C. Napoli, L. J. Ignarro, Nitric Oxide–Releasing Drugs, *Annu. Rev. Pharmacol. Toxicol.* **2003**, *43*, 97–123.

[263] T. L. Brunton, On the use of nitrite of amyl in angina pectoris., *Lancet* **1867**, *90*, 97–98.

[264] Z. Chen, J. Zhang, J. S. Stamler, Identification of the enzymatic mechanism of nitroglycerin bioactivation, *Proc. Natl. Acad. Sci. U. S. A.* **2002**, *99*, 8306–8311.

[265] L. Grossi, S. D'Angelo, Sodium Nitroprusside: Mechanism of NO Release Mediated by Sulfhydryl-Containing Molecules, *J. Med. Chem.* **2005**, *48*, 2622–2626.

[266] S. K. Wolfe, J. H. Swinehart, Photochemistry of Pentacyanonitrosylferrate(2-), Nitroprusside, *Inorg. Chem.* **1975**, *14*, 1049–1053.

[267] A. R. Butler, I. L. Megson, Non-Heme Iron Nitrosyls in Biology, *Chem. Rev.* **2002**, *102*, 1155–1166.

[268] M. R. Miller, I. L. Megson, Recent developments in nitric oxide donor drugs, *Br. J. Pharmacol.* **2007**, *151*, 305–321.

[269] C. M. Pavlos, H. Xu, J. P. Toscano, Photosensitive Precursors to Nitric Oxide, *Curr. Top. Med. Chem.* **2005**, *5*, 637–647.

[270] S. Wecksler, A. Mikhailovsky, P. C. Ford, Photochemical Production of Nitric Oxide via Two-Photon Excitation with NIR Light, *J. Am. Chem. Soc.* **2004**, *126*, 13 566–13 567.

[271] N. Bettache, T. Carter, J. E. Corrie, D. Ogden, D. R. Trentham, Photolabile donors of nitric oxide: Ruthenium nitrosyl chlorides as caged nitric oxide, in Nitric Oxide Part A: Sources and Detection of NO; NO Synthase, *Methods in Enzymology*, vol. 268, 266–281, Academic Press **1996**.

[272] V. Togniolo, R. S. da Silva, A. C. Tedesco, Photo-induced nitric oxide release from chlorobis(2,2'-bipyridine)nitrosylruthenium(II) in aqueous solution, *Inorg. Chim. Acta* **2001**, *316*, 7–12.

[273] J. T. Mitchell-Koch, T. M. Reed, A. S. Borovik, Light-Activated Transfer of Nitric Oxide from a Porous Material, *Angew. Chem. Int. Ed.* **2004**, *43*, 2806–2809.

[274] U. Schatzschneider, Photoactivated Biological Activity of Transition-Metal Complexes, *Eur. J. Inorg. Chem.* **2010**, *2010*, 1451–1467.

[275] G. M. Halpenny, M. M. Olmstead, P. K. Mascharak, Incorporation of a Designed Ruthenium Nitrosyl in PolyHEMA Hydrogel and Light-Activated Delivery of NO to Myoglobin, *Inorg. Chem.* **2007**, *46*, 6601–6606.

[276] G. M. Halpenny, B. Heilman, P. K. Mascharak, Nitric Oxide (NO)-Induced Death of Gram-Negative Bacteria from a Light-Controlled NO-Releasing Platform, *Chem. Biodiversity* **2012**, *9*, 1829–1839.

[277] K. Ghosh, A. A. Eroy-Reveles, B. Avila, T. R. Holman, M. M. Olmstead, *et al.*, Reactions of NO with Mn(II) and Mn(III) Centers Coordinated to Carboxamido Nitrogen: Synthesis of a Manganese Nitrosyl with Photolabile NO, *Inorg. Chem.* **2004**, *43*, 2988–2997.

[278] A. A. Eroy-Reveles, Y. Leung, C. M. Beavers, M. M. Olmstead, P. K. Mascharak, Near-Infrared Light Activated Release of Nitric Oxide from Designed Photoactive

Manganese Nitrosyls: Strategy, Design, and Potential as NO Donors, *J. Am. Chem. Soc.* **2008**, *130*, 4447–4458.

[279] C. G. Hoffman-Luca, A. A. Eroy-Reveles, J. Alvarenga, P. K. Mascharak, Syntheses, Structures, and Photochemistry of Manganese Nitrosyls Derived from Designed Schiff Base Ligands: Potential NO Donors That Can Be Activated by Near-Infrared Light, *Inorg. Chem.* **2009**, *48*, 9104–9111.

[280] K. L. Ciesienski, K. J. Franz, Keys for Unlocking Photolabile Metal-Containing Cages, *Angew. Chem. Int. Ed.* **2011**, *50*, 814–824.

[281] A. Fraix, S. Sortino, Photoactivable Platforms for Nitric Oxide Delivery with Fluorescence Imaging, *Chem. – Asian J.* **2015**, *10*, 1116–1125.

[282] J. Konter, G. E. A. A. H. Abuo-Rahma, A. El-Emam, J. Lehmann, The NOtizer—A Device for the Convenient Preparation of Diazen-1-ium-1,2-diolates, in Nitric Oxide, Part E, *Methods in Enzymology*, vol. 396, 17–26, Academic Press **2005**.

[283] J. E. Saavedra, T. R. Billiar, D. L. Williams, Y.-M. Kim, S. C. Watkins, *et al.*, Targeting Nitric Oxide (NO) Delivery *in Vivo*. Design of a Liver-Selective NO Donor Prodrug That Blocks Tumor Necrosis Factor-α-Induced Apoptosis and Toxicity in the Liver, *J. Med. Chem.* **1997**, *40*, 1947–1954.

[284] C. M. Maragos, D. Morley, D. A. Wink, T. M. Dunams, J. E. Saavedra, *et al.*, Complexes of ·NO with nucleophiles as agents for the controlled biological release of nitric oxide. Vasorelaxant effects, *J. Med. Chem.* **1991**, *34*, 3242–3247.

[285] C. F. Lam, P. V. V. Heerden, S. Sviri, B. L. Roberts, K. F. Ilett, The Effects of Inhalation of a Novel Nitric Oxide Donor, DETA/NO, in a Patient with Severe Hypoxaemia Due to Acute Respiratory Distress Syndrome, *Anaesth. Intensive Care* **2002**, *30*, 472–476.

[286] B. Bonavida, S. Baritaki, Dual role of NO donors in the reversal of tumor cell resistance and EMT: Downregulation of the NF-κB/Snail/YY1/RKIP circuitry, *Nitric Oxide* **2011**, *24*, 1–7.

[287] Z. Huang, J. Fu, Y. Zhang, Nitric Oxide Donor-Based Cancer Therapy: Advances and Prospects, *J. Med. Chem.* **2017**, *60*, 7617–7635.

[288] J. E. Saavedra, G. J. Southan, K. M. Davies, A. Lundell, C. Markou, *et al.*, Localizing Antithrombotic and Vasodilatory Activity with a Novel, Ultrafast Nitric Oxide Donor, *J. Med. Chem.* **1996**, *39*, 4361–4365.

[289] K. A. Mowery, M. H. Schoenfisch, J. E. Saavedra, L. K. Keefer, M. E. Meyerhoff, Preparation and characterization of hydrophobic polymeric films that are thromboresistant via nitric oxide release, *Biomaterials* **2000**, *21*, 9–21.

[290] J. E. Saavedra, A. Srinivasan, G. S. Buzard, K. M. Davies, D. J. Waterhouse, *et al.*, PABA/NO as an Anticancer Lead: Analogue Synthesis, Structure Revision, Solution Chemistry, Reactivity toward Glutathione, and in Vitro Activity, *J. Med. Chem.* **2006**, *49*, 1157–1164.

[291] K. Sharma, A. Iyer, K. Sengupta, H. Chakrapani, INDQ/NO, a Bioreductively Activated Nitric Oxide Prodrug, *Org. Lett.* **2013**, *15*, 2636–2639.

[292] X. Wu, X. Tang, M. Xian, P. G. Wang, Glycosylated diazeniumdiolates: a novel class of enzyme-activated nitric oxide donors, *Tetrahedron Lett.* **2001**, *42*, 3779–3782.

[293] T. B. Cai, D. Lu, M. Landerholm, P. G. Wang, Sialated Diazeniumdiolate: A New Sialidase-Activated Nitric Oxide Donor, *Org. Lett.* **2004**, *6*, 4203–4205.

[294] L. R. Makings, R. Y. Tsien, Caged Nitric Oxide. Stable Organic Molecules from which

Nitric Oxide can be Photoreleased., *J. Biol. Chem.* **1994**, *269*, 6282–6285.

[295] K. K. Behara, Y. Rajesh, Y. Venkatesh, B. R. Pinninti, M. Mandal, *et al.*, Cascade photocaging of diazeniumdiolate: a novel strategy for one and two photon triggered uncaging with real time reporting, *Chem. Commun.* **2017**, *53*, 9470–9473.

[296] K. M. Bushan, H. Xu, P. H. Ruane, R. A. D'Sa, C. M. Pavlos, *et al.*, Controlled Photochemical Release of Nitric Oxide from O^2-Naphthylmethyl- and O^2-Naphthylallyl-Substituted Diazeniumdiolates, *J. Am. Chem. Soc.* **2002**, *124*, 12 640–12 641.

[297] M. Blangetti, A. Fraix, L. Lazzarato, E. Marini, B. Rolando, *et al.*, A Nonmetal-Containing Nitric Oxide Donor Activated with Single-Photon Green Light, *Chem. – Eur. J.* **2017**, *23*, 9026–9029.

[298] C. Velázquez, P. N. P. Rao, E. E. Knaus, Novel Nonsteroidal Antiinflammatory Drugs Possessing a Nitric Oxide Donor Diazen-1-ium-1,2-diolate Moiety: Design, Synthesis, Biological Evaluation, and Nitric Oxide Release Studies, *J. Med. Chem.* **2005**, *48*, 4061–4067.

[299] T. B. Cai, X. Tang, J. Nagorski, P. G. Brauschweiger, P. G. Wang, Synthesis and cytotoxicity of 5-fluorouracil/diazeniumdiolate conjugates, *Bioorg. Med. Chem.* **2003**, *11*, 4971–4975.

[300] A. E. Maciag, R. J. Holland, Y. Kim, V. Kumari, C. E. Luthers, *et al.*, Nitric Oxide (NO) Releasing Poly ADP-ribose Polymerase 1 (PARP-1) Inhibitors Targeted to Glutathione S-Transferase P1-Overexpressing Cancer Cells, *J. Med. Chem.* **2014**, *57*, 2292–2302.

[301] I. R Correa, B. Baker, A. Zhang, L. Sun, C. R Provost, *et al.*, Substrates for Improved Live-Cell Fluorescence Labeling of SNAP-tag, *Curr. Pharm. Des.* **2013**, *19*, 5414–5420.

[302] R. F. Ohana, L. P. Encell, K. Zhao, D. Simpson, M. R. Slater, *et al.*, HaloTag7: A genetically engineered tag that enhances bacterial expression of soluble proteins and improves protein purification, *Protein Expression Purif.* **2009**, *68*, 110–120.

[303] K. J. Koßmann, C. Ziegler, A. Angelin, R. Meyer, M. Skoupi, *et al.*, A Rationally Designed Connector for Assembly of Protein-Functionalized DNA Nanostructures, *ChemBioChem* **2016**, *17*, 1102–1106.

[304] R. F. Ohana, T. A. Kirkland, C. C. Woodroofe, S. Levin, H. T. Uyeda, *et al.*, Deciphering the Cellular Targets of Bioactive Compounds Usinga Chloroalkane Capture Tag, *ACS Chem. Biol.* **2015**, *10*, 2316–2324.

[305] T. Schlichthaerle, M. T. Strauss, F. Schueder, A. Auer, B. Nijmeijer, *et al.*, Direct Visualization of Single Nuclear Pore Complex Proteins Using Genetically-Encoded Probes for DNA-PAINT, *Angew. Chem. Int. Ed.* **2019**, *58*, 13 004–13 008.

[306] D. J. Nieves, G. Hilzenrat, J. Tran, Z. Yang, H. H. MacRae, *et al.*, tagPAINT: covalent labelling of genetically encoded protein tags for DNA-PAINT imaging, *R. Soc. Open Sci.* **2019**, *6*, 191 268.

[307] J. H. Kim, S.-R. Lee, L.-H. Li, H.-J. Park, J.-H. Park, *et al.*, High Cleavage Efficiency of a 2A Peptide Derived from Porcine Teschovirus-1 in Human Cell Lines, Zebrafish and Mice, *PLoS One* **2011**, *6*, e18 556.

[308] D. Hutter, S. A. Benner, Expanding the Genetic Alphabet: Non-Epimerizing Nucleoside with the *py*DDA Hydrogen-Bonding Pattern, *J. Org. Chem.* **2003**, *68*, 9839–9842.

[309] Z. Yang, D. Hutter, P. Sheng, A. M. Sismour, S. A. Benner, Artificially expanded genetic information system: a new base pair with an alternative hydrogen bonding pattern, *Nucleic Acids Res.* **2006**, *34*, 6095–6101.

[310] E. E. Doherty, X. E. Wilcox, L. van Sint Fiet, C. Kemmel, J. J. Turunen, *et al.*, Rational Design of RNA Editing Guide Strands: Cytidine Analogs at the Orphan Position, *J. Am. Chem. Soc.* **2021**, *143*, 6865–6876.

[311] N. Latifi, A. M. Mack, I. Tellioglu, S. D. Giorgio, T. Stafforst, Precise and efficient C-to-U RNA base editing with SNAP-CDAR-S, *Nucleic Acids Res.* **2023**, *51*, e84.

[312] J.-D. Pédelacq, S. Cabantous, T. Tran, T. C. Terwilliger, G. S. Waldo, Engineering and characterization of a superfolder green fluorescent protein, *Nat. Biotechnol.* **2006**, *24*, 79–88.

[313] L. N. Randolph, X. Bao, C. Zhou, X. Lian, An all-in-one, Tet-On 3G inducible PiggyBac system for human pluripotent stem cells and derivatives, *Sci. Rep.* **2017**, *7*, 1549.

[314] J. Darnell, I. Kerr, G. Stark, Jak-STAT Pathways and Transcriptional Activation in Response to IFNs and Other Extracellular Signaling Proteins, *Science* **1994**, *264*, 1415–1421.

[315] M. D. Shahbazian, B. Antalffy, D. L. Armstrong, H. Y. Zoghbi, Insight into Rett syndrome: MeCP2 levels display tissue- and cell-specific differences and correlate with neuronal maturation, *Hum. Mol. Genet.* **2002**, *11*, 115–124.

[316] H. Van Esch, M. Bauters, J. Ignatius, M. Jansen, M. Raynaud, *et al.*, Duplication of the MECP2 Region Is a Frequent Cause of Severe Mental Retardation and Progressive Neurological Symptoms in Males, *Am. J. Hum. Genet.* **2005**, *77*, 442–453.

[317] M. Thunemann, L. Wen, M. Hillenbrand, A. Vachaviolos, S. Feil, *et al.*, Transgenic Mice for cGMP Imaging, *Circ. Res.* **2013**, *113*, 365–371.

[318] L. A. Piggott, K. A. Hassell, Z. Berkova, A. P. Morris, M. Silberbach, *et al.*, Natriuretic Peptides and Nitric Oxide Stimulate cGMP Synthesis in Different Cellular Compartments, *J. Gen. Physiol.* **2006**, *128*, 3–14.

[319] E. Takimoto, D. Belardi, C. G. Tocchetti, S. Vahebi, G. Cormaci, *et al.*, Compartmentalization of Cardiac β-Adrenergic Inotropy Modulation by Phosphodiesterase Type 5, *Circulation* **2007**, *115*, 2159–2167.

[320] C. Cenci, R. Barzotti, F. Galeano, S. Corbelli, R. Rota, *et al.*, Down-regulation of RNA Editing in Pediatric Astrocytomas, *J. Biol. Chem.* **2008**, *283*, 7251–7260.

[321] X.-M. Liu, J. Zhou, Y. Mao, Q. Ji, S.-B. Qian, Programmable RNA N^6-methyladenosine editing by CRISPR-Cas9 conjugates, *Nat. Chem. Biol.* **2019**, *15*, 865–871.

[322] K. Rau, L. Rösner, A. Rentmeister, Sequence-specific m^6A demethylation in RNA by FTO fused to RCas9, *RNA* **2019**, *25*, 1311–1323.

[323] N. Anitha, B. S. Reddy, N. M. Sekhar, K. V. Reddy, E. R. R. Chandrasekhar, Alternative Approach to Synthesis of 3-(4-chloro butyl)-1*H*-indole-5-carbonitrile: A Key Intermediate of Vilazodone Hydrochloride, an Antidepressant Drug, *Synth. Commun.* **2014**, *44*, 3563–3571.

A Appendix

A.1 Conference contributions

A.1.1 Short poster talk

Orthogonal protein tags – Expanding the RNA editing platform

Anna S. Stroppel, Alfred Hanswillemenke, Thorsten Stafforst, *9th German nucleic acids meeting*, 19 – 20 September **2019**, *Saarbrücken*, Germany.

A.1.2 Poster presentations

Simultaneous Site-directed A-to-I and C-to-U Editing

Ngadhnjim Latifi,* Anna S. Stroppel,* Aline M. Mack, Thorsten Stafforst, *10th German nucleic acids meeting*, 15 – 17 September **2021**, *Bad Herrenalb*. *equal contribution

Implementing photocontrol and orthogonal targeting in the SNAP-ADAR editing approach

Anna S. Stroppel,* Alfred Hanswillemenke,* Marius Blackholm, Thorsten Stafforst, *Advances in Chemical Biology*, 26 – 27 January **2021**, *Virtual Conference*. *equal contribution

Honoured with Poster Award from *ChemBioChem*.

Orthogonal protein tags – Expanding the RNA editing platform

Anna S. Stroppel, Alfred Hanswillemenke, Thorsten Stafforst, *9th German nucleic acids meeting*, 19 – 20 September **2019**, *Saarbrücken*, Germany.

Orthogonal protein tags – Expanding the RNA editing platform

Anna S. Stroppel, Thorsten Stafforst, *4th Annual PhD/Post-Doc Retreat, Interfaculty Institute of Biochemistry*, 9 – 10 May **2019**, *Freudenstadt*, Germany.

Honoured with Best Poster Award.

Orthogonal protein tags – Expanding the RNA editing platform

Anna S. Stroppel, Ngadhnjim Latifi, Alfred Hanswillemenke, Cindy Odenwald, Aline M. Mack, Thorsten Stafforst, *SPP1784 2nd Kick off meeting*, 10 – 12 December **2018**, *Mainz*, Germany.

Exploring protein tags to provide an orthogonal site-directed RNA editing system

Anna S. Stroppel, Alfred Hanswillemenke, Paul Vogel, Thorsten Stafforst, *3rd Annual PhD/ Post-doc Retreat, Interfaculty Institute for Biochemistry*, 26 – 27 July **2018**, *Hechingen*, Germany.

A.2 Publications

A.2.1 Publication 1 (published)

Harnessing self-labeling enzymes for selective and concurrent A-to-I and C-to-U RNA base editing

Anna S. Stroppel, Ngadhnjim Latifi, Alfred Hanswillemenke, Rafail Nikolaos Tasakis, F. Nina Papavasiliou, Thorsten Stafforst, *Nucleic Acids Res.* **2021**, *49*, e95.

Published online 1 July 2021

Nucleic Acids Research, 2021, Vol. 49, No. 16 e95
https://doi.org/10.1093/nar/gkab541

Harnessing self-labeling enzymes for selective and concurrent A-to-I and C-to-U RNA base editing

Anna S. Stroppel[1], Ngadhnjim Latifi[1], Alfred Hanswillemenke[1], Rafail Nikolaos Tasakis[2,3], F. Nina Papavasiliou[2,3] and Thorsten Stafforst[1,*]

[1]Interfaculty Institute of Biochemistry, University of Tübingen, Auf der Morgenstelle 15, 72076 Tübingen, Germany, [2]Division of Immune Diversity (D150), German Cancer Research Center (DKFZ), 69120 Heidelberg, Germany and [3]Faculty of Biosciences, University of Heidelberg, 69120 Heidelberg, Germany

Received November 03, 2020; Revised May 05, 2021; Editorial Decision June 07, 2021; Accepted June 18, 2021

ABSTRACT

The SNAP-ADAR tool enables precise and efficient A-to-I RNA editing in a guideRNA-dependent manner by applying the self-labeling SNAP-tag enzyme to generate RNA-guided editases in cell culture. Here, we extend this platform by combining the SNAP-tagged tool with further effectors steered by the orthogonal HALO-tag. Due to their small size (ca. 2 kb), both effectors are readily integrated into one genomic locus. We demonstrate selective and concurrent recruitment of ADAR1 and ADAR2 deaminase activity for optimal editing with extended substrate scope and moderate global off-target effects. Furthermore, we combine the recruitment of ADAR1 and APOBEC1 deaminase activity to achieve selective and concurrent A-to-I and C-to-U RNA base editing of endogenous transcripts inside living cells, again with moderate global off-target effects. The platform should be readily transferable to further epitranscriptomic writers and erasers to manipulate epitranscriptomic marks in a programmable way with high molecular precision.

INTRODUCTION

After transcription, most RNA species get processed (e.g. capped, spliced, trimmed, polyadenylated) and enzymatically modified (1). Particularly wide-spread modifications include methylation (e.g. m^6A, 2′-*O*-methylation), isomerization (pseudouridine) and deamination (e.g. A-to-I and C-to-U editing). Due to recent progress in deep sequencing technologies, the fundamental role of such epitranscriptomic modifications in human pathophysiology became apparent (2,3), including the biology of learning (4), development (5) and cancer (6,7). A detailed mechanistic understanding of the plethora of epitranscriptomic modifications is currently hampered by a lack of methods to manipulate transcripts in a programmable way with molecular precision (8). Fortunately, RNA transcripts are precisely addressable via Watson-Crick base pairing. Thus, a guideRNA can be applied to recruit a protein effector to a specific transcript in a site-specific manner. During the last years, various attempts focused on the engineering of RNA-guided RNA base editing effectors, specifically on A-to-I and C-to-U editing (8). As inosine is biochemically interpreted as guanosine, site-directed RNA editing enables the reprogramming of genetic information, e.g. substitution of amino acids, formation and removal of premature termination codons, which open novel avenues for drug discovery, promising to bypass technical and ethical issues related to genome editing (8). In this regard, our group developed an RNA-targeting platform based on fusion proteins of the self-labeling SNAP-tag (Figure 1A). To engineer a programmable A-to-I RNA base editor, we fused the SNAP-tag with the catalytic domain of the RNA editing enzyme ADAR (9,10), more specifically, we have used a hyperactive mutant (11), carrying a single glutamate (E) to glutamine (Q) mutation, indicated by the letter Q. In these fusions, the SNAP-tag (12) exploits its self-labeling activity to covalently attach to a guideRNA in a defined 1:1 stoichiometry by recognizing a benzylguanine (BG) moiety at the guideRNA (13). The guideRNA then addresses the editing of one specific adenosine residue in a selected transcript with high efficiency, broad codon scope, and very good precision (9). Competing RNA-targeting platforms, e.g. based on Cas proteins (14,15) or tethering approaches, have been developed for similar applications (8,10,16,17). Each approach has different strengths and weaknesses (8,10). A clear advantage of the SNAP-tag approach is its human origin, the small size, the ease of stable expression, the ease of transfecting one or multiple chemically stabilized guideRNA(s), which allows for concurrent editing (9), and the ready inclusion of photo control (18,19). Here, we extend the self-labeling RNA-targeting platform with HALO-tag fusions and characterize their abilities to recruit two different editing effectors in an orthogonal fash-

*To whom correspondence should be addressed. Tel: +49 7071 29 75376; Email: thorsten.stafforst@uni-tuebingen.de

e95 Nucleic Acids Research, 2021, Vol. 49, No. 16

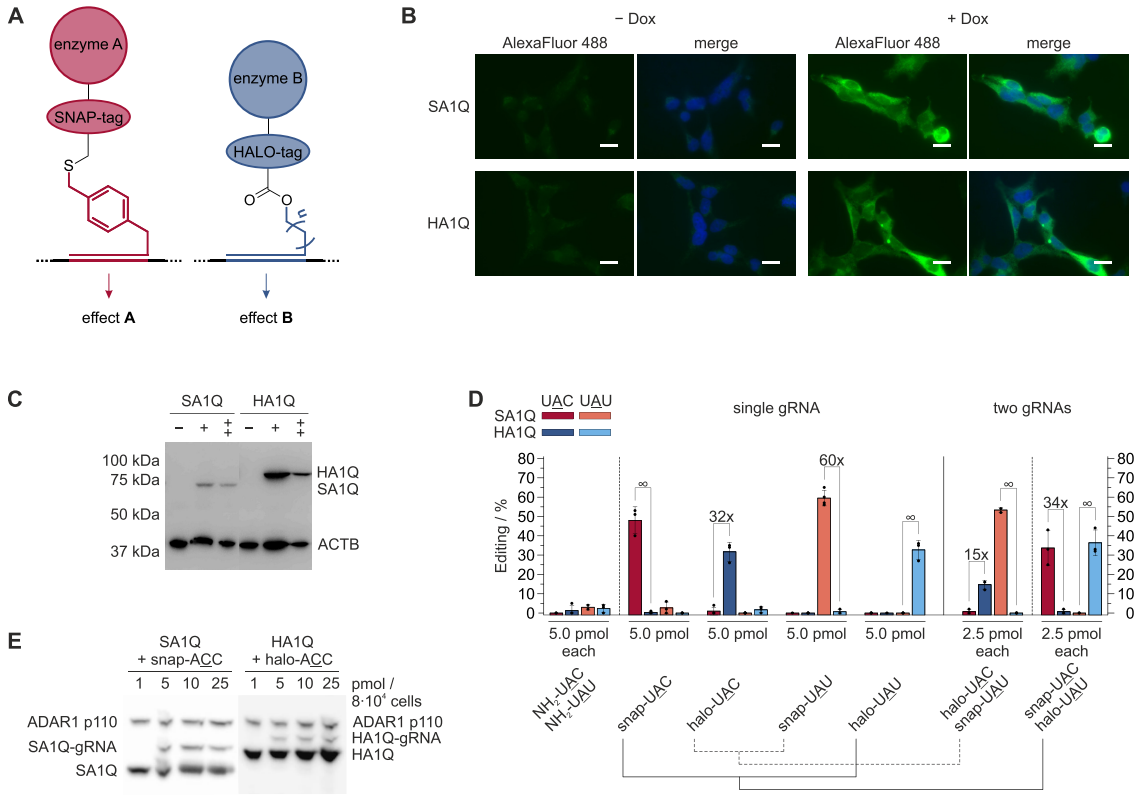

Figure 1. Recruitment of the ADAR1 deaminase domain in fusion with two different self-labeling enzymes. (**A**) Independent self-labeling enzymes, e.g. SNAP- and HALO-tag, enable for the orthogonal recruitment of various effectors, e.g. enzymes A and B. (**B**) Characterization of 293 Flp-In T-REx cell lines expressing either the Myc-tagged SA1Q or HA1Q transgene in a doxycycline-dependent fashion as visualized by immunostaining with α-Myc (green channel) and DNA staining with Hoechst 33342 (blue channel). Scale bars correspond to 15 μm. (**C**) Western blot (α-Myc) to compare SA1Q and HA1Q expression. + means 24 h, ++ means 48 h doxycycline induction. (**D**) Editing efficiency and orthogonality of four different guideRNAs (snap-UAC, halo-UAC, snap-UAU, halo-UAU) targeting either a 5′-UAC or 5′-UAU codon in the ORF of endogenous GAPDH. Either single guideRNAs (left panel) or the indicated combination of two guideRNAs (right panel) were transfected into the SA1Q or HA1Q cell line, as indicated in the legend respectively. NH_2-guideRNAs are control guideRNAs with same sequence but lacking a self-labeling moiety. Data are shown as the mean ± SD of $N = 3$ independent experiments. (**E**) Dose-dependent formation of SA1Q- and HA1Q-guideRNA conjugates (SA1Q-gRNA and HA1Q-gRNA) after transfection of 1.0, 5.0, 10 or 25 pmol snap- or halo-guideRNA per 8×10^4 cells respectively, visualized via Western blot (α-ADAR1). Endogenous ADAR1 p110 is equally expressed independent of guideRNA addition.

ion (Figure 1A). This broadens the otherwise limited codon scope of single editing enzymes, and enables site-selective, concurrent A-to-I and C-to-U editing within the same cell.

MATERIALS AND METHODS

Reagents and biological resources

Detailed information on reagents, enzymes, antibodies and kits as well as cell lines used in this study are presented in the Supporting Information.

Chemical synthesis

The self-labeling moieties that were attached to the guideRNAs, i.e. snap, clip, halo, halo-snap, $(snap)_2$ and $(halo)_2$ were synthesized via solid phase peptide synthesis as described in the Supporting Information (Supplementary Schemes S1–S3, Supplementary Figures S1–S5).

Generation of guideRNAs

As guideRNAs, 22 nt long RNAs with a 5′-C6-aminolinker (NH_2-guideRNAs) that were chemically stabilized in an antagomir-like fashion as described before (20) were applied. Additional details as well as sequences and extinction coefficients at 260 nm of all used guideRNAs can be found in the Supporting Information (Supplementary Table S1).

snap-, clip- and halo-guideRNAs were produced analogous to the previously reported protocol for Npom-guideRNAs (18). Instead of N^7-Npom-BG-Linker-COOH, 8 μl (60 mM in DMSO, 480 nmol, ∼35 eq) of either snap, clip or halo were used. snap- and clip-guideRNAs were purified via precipitation as described before (18). For halo-guideRNAs, samples were lyophilized after aqueous extrac-

tion from the urea PAGE and subsequently purified with C18 Reversed Phase Cartridges (WATERS, #020515) according to manufacturer's manual.

halo-snap-, $(snap)_2$- and $(halo)_2$-guideRNAs were produced analogous to the previously reported improved protocol with DIC activation (21), using 4 μl (60 mM in DMSO, 240 nmol, ∼17.5 eq) of either halo-snap, $(snap)_2$ or $(halo)_2$. $(snap)_2$-guideRNAs were purified via precipitation as described before (21), halo-snap- and $(halo)_2$-guideRNAs were again purified with C18 Reversed Phase Cartridges (WATERS, #020515) according to manufacturer's manual.

Generation of stable cell lines

In general, cells were cultivated in Dulbecco's modified Eagle's medium (DMEM, LIFE TECHNOLOGIES) supplemented with 10% fetal bovine serum (FBS, LIFE TECHNOLOGIES) at 37 °C with 5% CO_2 in a water saturated steam atmosphere. For generating stable, inducible cell lines, the Flp-In™ T-REx™ system by LIFE TECHNOLOGIES was used. 4×10^6 293 Flp-In T-REx cells were seeded in 10 ml DMEM/10% FBS/100 μg/ml zeocin/15 μg/ml blasticidin (DMEM/FBS/Z/B) in a 10 cm dish. After 23 h, medium was replaced with DMEM/10 % FBS (DMEM/FBS) and 1 h later 9 μg pOG 44 and 1 μg of the respective construct in a pcDNA 5 vector were forward transfected with 30 μl Lipofectamine 2000 (THERMO FISHER SCIENTIFIC). After 24 h, medium was replaced with 15 ml DMEM/10% FBS/15 μg/ml blasticidin/100 μg/ml hygromycin (DMEM/FBS/B/H), followed by selection for approximately two weeks. Then, the stable cell lines were transferred to a 75 cm^2 cell culture flask and subsequently cultivated in DMEM/FBS/B/H. Sequences of the constructs for all cell lines used in this study can be found in the Supporting Information.

Immunostaining of single cell lines

Briefly, 1.2×10^5 SA1Q or HA1Q 293 Flp-In T-REx cells were seeded on coverslips coated with poly-D-lysine in DMEM/FBS/B/H for –Dox samples or DMEM/FBS/B/H/10 ng/ml doxycycline (DMEM/FBS/B/H/10 D) for +Dox samples respectively. After 24 h, cells were fixed with 3.7% formaldehyde in PBS, permeabilized with 1% Triton X-100 in PBS and blocked with 10% FBS in PBS. Cells were then incubated with mouse α-Myc (1:1000 in 10% FBS in PBS, SIGMA ALDRICH M4439), followed by goat α-mouse Alexa Fluor 488 (1:1000 in 10% FBS in PBS, THERMO FISHER SCIENTIFIC A11001). Nuclei were stained with NucBlue™ Live ReadyProbes™ Reagent Hoechst33342 (1:100 in PBS, THERMO FISHER SCIENTIFIC R37605) and coverslips were mounted to object slides with Fluorescence Mounting Medium by DAKO. Microscopy was performed with a ZEISS AXIO Observer.Z1 with a Colibri.2 light source under 63× magnification. For further procedural details, excitation and emission wavelengths, see Supporting Information (Supplementary Table S2).

FITC-BG & TMR-chloroalkane staining of duo cell lines

5×10^4 293 Flp-In T-REx cells from cell lines **1**–**5** were seeded on coverslips coated with poly-D-lysine in DMEM/FBS/B/H for –Dox samples or DMEM/FBS/B/H/10 D for +Dox samples respectively. After 24 h, cells were stained with 2 μM FITC-BG, 5 μM TMR-chloroalkane and NucBlue™ Live ReadyProbes™ Reagent Hoechst33342 (1:100, THERMO FISHER SCIENTIFIC R37605). Cells were then fixed with 3.7% formaldehyde in PBS, permeabilized with 0.1% Triton X-100 in PBS and coverslips were mounted to object slides with Fluorescence Mounting Medium by DAKO. Microscopy was performed with a ZEISS AXIO Observer.Z1 with a Colibri.2 light source under 63× magnification. For experimental data of –Dox samples, further procedural details, excitation and emission wavelengths, see Supporting Information (Supplementary Figure S6, Table S2).

Western blotting of protein expression in single cell lines

Briefly, 1×10^5 SA1Q or HA1Q 293 Flp-In T-REx cells respectively were seeded and treated with doxycycline for 24 h (+) or 48 h (++) or left uninduced (–). After 48 h, cells were harvested and lysed in urea lysis buffer (8 M urea, 100 mM NaH_2PO_4, 10 mM Tris, pH 8.0) via shear force. Protein lysates were separated via SDS-PAGE and transferred onto a PVDF membrane (BIO-RAD LABORATORIES). After blocking in 5% dry milk in TBST containing 50 μg/ml avidin, the blot was incubated with mouse α-Myc (1:5000, SIGMA ALDRICH M4439) and mouse α-ACTB (1:40 000, SIGMA-Aldrich A5441) in 5% dry milk-TBST as primary antibodies. As secondary antibody, goat α-mouse HRP (1:10 000, JACKSON IMMUNORESEARCH 115-035-003) with added Precision Protein StrepTactin HRP conjugate (for visualisation of the Precision Plus Western C Standard, 1:25 000, BIO-RAD) in 5% dry milk-TBST was applied. Chemiluminescence was measured with a FUSION FX by VILBER. For full Western Blot and further experimental details, see Supporting Information (Supplementary Figure S7).

Western blotting of guideRNA–protein conjugation

2×10^6 SA1Q or HA1Q 293 Flp-In T-REx cells were seeded in DMEM/FBS/B/H/10 D. After 24 h, 4×10^5 cells were reverse transfected with the respective amount of snap- or halo-ACC with 2.5 μl Lipofectamine 2000. Doxycycline concentration was kept at 10 ng/ml and after further 24 h cells were lysed in 1× Laemmli (67 mM SDS, 10 mM Tris pH 6.8, 1.1 M glycerol, 0.10 M dithiothreitol, 0.15 mM bromophenol blue) in RIPA Lysis and Extraction Buffer (1% NP-40, 150 mM NaCl, 25 mM Tris·HCl pH 7.6, 1% sodium deoxycholate, 0.1% SDS, THERMO FISHER SCIENTIFIC; supplemented with 1 tablet cOmplete™ Mini EDTA-free Protease Inhibitor Cocktail by ROCHE per 10 ml). Protein lysates were separated via SDS-PAGE and transferred onto a PVDF membrane (BIO-RAD LABORATORIES). After blocking in 5% dry milk in TBST, the blot was incubated with rabbit α-ADAR1 (1:1000, BETHYL LABORATORIES A303-884) and rabbit α-GAPDH (1:1000, CELL SIGNALING #5174) in 5% dry milk-TBST as primary antibodies. As

secondary antibody, goat α-rabbit HRP (1:10 000, JACKSON IMMUNORESEARCH 111-035-003) in 5% dry milk-TBST was applied. Chemiluminescence was measured with an Odyssey Fc Imaging System (LI-COR). For additional experimental data as well as further procedural details, see Supporting Information (Supplementary Figure S8).

TMR-staining & western blotting of protein expression in duo cell lines

2×10^5 293 Flp-In T-REx cells from the respective duo cell line were seeded in DMEM/FBS/B/H for –Dox samples or DMEM/FBS/B/H/10 D for +Dox samples respectively. After 24 h, cells were harvested and lysed in NP40 lysis buffer (1% NP-40, 150 mM NaCl, 50 mM Tris pH 8.0; 1 tablet cOmplete™ Mini EDTA-free Protease Inhibitor Cocktail by ROCHE per 10 ml). For co-staining with TMR-BG and TMR-chloroalkane, protein lysate was incubated with 5 μM TMR-BG and TMR-chloroalkane each in NP40 lysis buffer for 30 min at 37°C and 600 rpm. Protein lysates were then separated via SDS-PAGE and TMR-staining was visualized on a FLA 5100 by FUJIFILM with excitation at 532 nm and emmission at 557 nm (Cy3 filter set). Subsequently, proteins were transferred onto a PVDF membrane (BIO-RAD LABORATORIES), and the blot was blocked in 5% dry milk in TBST containing 50 μg/ml avidin, followed by incubation with mouse α-ACTB (1:40 000, SIGMA-Aldrich A5441), rabbit α-SNAP-tag (1:1000, NEW ENGLAND BIOLABS P9310S) and rabbit α-HaloTag (1:1000, PROMEGA G9281) in 5% dry milk-TBST as primary antibodies. As secondary antibodies, goat α-mouse HRP (1:5000, JACKSON IMMUNORESEARCH 115-035-003) with added Precision Protein StrepTactin HRP conjugate (for visualisation of the Precision Plus Western C Standard, 1:25 000, BIO-RAD) and goat α-rabbit HRP (1:5000, JACKSON IMMUNORESEARCH 111-035-003) were applied. Chemiluminescence was measured with a FUSION FX by VILBER. For additional experimental data as well as further procedural details, see Supporting Information (Supplementary Figure S9).

Editing of endogenous targets

For the editing experiments, 4×10^5 of the respective 293 Flp-In T-REx cells were seeded in DMEM/FBS/B/H/10 D. After 24 h, 8×10^4 cells were reverse transfected with the respective amount of the guideRNA to be examined with 0.5 μl Lipofectamine 2000. Doxycycline concentration was kept at 10 ng/ml and after further 24 h (or 48 h for cell lines expressing APO1S) cells were harvested. RNA isolation was performed with the Monarch® RNA cleanup kit from NEW ENGLAND BIOLABS, followed by DNase I digestion. Samples containing $(snap)_2$-ACC were treated with a DNA oligonucleotide of complementary sequence (anti-$(snap)_2$-ACC, 1 μM) at 95°C for 3 min to trap the guideRNA. Purified RNA was then reverse transcribed to cDNA, which was amplified via Taq PCR and subsequently analyzed with Sanger sequencing (either EUROFINS GENOMICS or MICROSYNTH). A-to-I editing yields were determined by dividing the peak height for guanosine by the sum of the peak heights for both adenosine and guanosine. Additional experimental data and further procedural details are given in the Supporting Information (Supplementary Figures S12 and S13, Supplementary Table S3).

Editing of transfected reporter transcript

For editing of the reporter transcript, cells were forward transfected 24 h after seeding with 300 ng pcDNA 3.1 containing the coding sequence for eGFP-W58X with 1.2 μl Lipofectamine 2000. 24 h thereafter, 8×10^4 cells were reverse transfected with the respective amount of the guideRNA to be examined with 0.5 μl Lipofectamine 2000. Cells were harvested after further 48 h and proceeded as for editing of endogenous targets. For additional experimental data and procedural details, see Supporting Information (Supplementary Figure S14).

Next generation sequencing

For cell line **2** and **9**, four samples each were prepared for NGS, i.e. a duplicate of an empty transfection and a duplicate of a guideRNA transfection (0.5 pmol $(snap)_2$-CAG and $(halo)_2$-CAU for cell line **2**, 2.5 pmol $(halo)_2$-UAU and $(snap)_2$-ACC for cell line **9**), all under doxycycline induction. RNA was isolated, DNase I digested and purified via RNeasy MinElute Cleanup Kit from QIAGEN. mRNA next generation sequencing was then performed by CEGAT. The library was prepared with the library preparation kit TruSeq Stranded mRNA by ILLUMINA starting from 100 ng RNA. Samples were then sequenced on a NovaSeq 6000 by ILLUMINA with 50 million reads and 2×100 bp paired end. RNA-seq raw data from different lanes that belong to the same sample were pulled together. After adapter trimming with Trim Galore (v. 0.6.4; http://www.bioinformatics.babraham.ac.uk/projects/trim_galore/), the trimmed reads were aligned using STAR (v. 2.7.3a) (22) to a genome index inferred by the human reference genome (hg19) sequence, along with the RefSeq annotation, both publicly available at the genome browser at UCSC (23). For the alignments we considered reads that were uniquely mapped (STAR option: –outFilterMultimapNmax 1) to avoid multimapping between highly similar regions. Aligned data (bam files) were deduplicated, sorted and indexed with SAMtools (v. 1.9; http://samtools.sourceforge.net) (24). SNVs in our samples were called with REDItools (v2; https://github.com/tflati/reditools2.0) (25,26), considering the developers' recommendations for data preparation prior to this step. Sticking to our previously published approach (9), we considered only high-quality sites (min. MeanQ > 30 in REDItools2), and we called editing in well-covered sites (min. 50 reads in aggregate of the two replicates per sample) that showed ≥10% (for A-to-I) or ≥ 5% (for C-to-U) editing frequency when compared to the control. Additionally, fisher's exact tests were performed for all the sites that fulfilled the aforementioned criteria and significantly differentially edited sites were considered those that showed adjusted *P*-value <0.01. Sites that were reported in the first 6 sites of a read, or in homopolymeric regions, or reported in the dbSNP (v. 142; excluding cDNA-based reported SNPs: http://www.ncbi.nlm.nih.gov/SNP/), were ex-

cluded throughout our output lists. All genomic coordinates were annotated with Oncotator (v1.9.9.0) (27) and Repeat Mask for Alu-SINE elements of UCSC Genome Browser (23) both for hg19. Additional data, including scatter plots of total off-targets in all editing experiments, elaborate analysis of significantly differently edited sites with editing difference ≥25%, analysis of bystander editing sites and scatter plots of all called editing sites in the two respective replicates, as well as details on the experimental procedure can be found in the Supporting Information (Supplementary Figures S16–S23, Supplementary Tables S6–S12).

RESULTS AND DISCUSSION

The HALO-tag outperforms the CLIP-tag to complement the RNA targeting platform

Two self-labeling enzymes are to be considered to complement the SNAP-tag for RNA targeting, the HALO-tag (28) and the CLIP-tag (29). The HALO-tag covalently attaches to halo-guideRNAs, carrying a 1-chloroalkane moiety (28), the CLIP-tag to clip-guideRNAs, carrying a benzylcytosine moiety for covalent conjugation (29), both in 1:1 stoichiometry. In a preliminary experiment, we identified the HALO-tag as the preferred tag for two reasons. First, a clip-guideRNA gave notable editing also with SNAP-ADAR, indicating insufficient orthogonality (29) between SNAP- and CLIP-tag in the editing application (Supplementary Figures S10–S12). Second, the clip-guideRNA showed loss of activity upon long-term storage (Supplementary Figure S12). We thus continued to compare HALO-ADAR1 (HA1Q) with SNAP-ADAR1 (SA1Q), our best RNA editor from our previous study (9). Both fusions carried the hyperactive Q mutation in the deaminase domain. Plasmid overexpression of editing enzymes typically results in enormous variability of expression levels, massive off-target editing, and low and unsteady editing efficiency at endogenous targets (10). To avoid such artefacts, we generated cell lines stably expressing either HA1Q or SA1Q from a defined, single genomic site, under control of doxycycline, by applying the 293 Flp-In T-REx system (9,19). Both cell lines expressed the respective fusion protein in a homogenous and doxycycline-inducible manner (Figure 1B). Both fusions were localized in nucleoplasm and cytoplasm, favoring the latter. The expression level of HA1Q was slightly higher compared to SA1Q (Figure 1C).

Snap- and halo-guideRNAs recruit SNAP- and HALO-fusions with high selectivity

To examine editing efficiency and orthogonality, we generated four guideRNAs and transfected them separately either into the HA1Q or SA1Q cell line. Two guideRNAs were designed to target a 5′-UAC codon in the ORF of GAPDH and were only differing in the self-labeling moiety, being either benzylguanine (12) (snap-UAC) for SNAP-tag or chloroalkane (28) (halo-UAC) for HALO-tag conjugation. Another pair of guideRNAs was equally designed to target a 5′-UAU codon in GAPDH. We observed very selective and orthogonal editing, both snap-guideRNAs elicited editing only in the SA1Q cell line as both halo-guideRNAs did in the HA1Q cell line (Figure 1D, left panel). Furthermore, editing was reliably programmable and editing in the non-targeted codon was not observed. Even though slightly higher expressed, HA1Q was less active than SA1Q on both targets. We checked the in situ assembly of each fusion protein with its respective guideRNA by Western blot (Figure 1E). Both couples gave a similar dose-dependent formation of the protein–guideRNA conjugate not exhausting the protein component at guideRNA amounts typically applied in editing reactions. Thus, neither expression level nor conjugation efficiency explains the slightly reduced editing efficiency of HA1Q. Co-transfection of two guideRNAs, one halo- and one snap-guideRNA, gave decent editing with high selectivity for the matching enzyme in each respective cell line (Figure 1D, right panel), highlighting that the co-transfection of a guideRNA with mismatching self-labeling moiety is possible and does not interfere with the selectivity of the matching guideRNA.

Cell lines co-expressing SNAP- and HALO-tagged effectors are easily generated

Next, we explored the selective and concurrent recruitment of two different effectors based on the orthogonal self-labeling reactions mediated by SNAP- and HALO-tag within one cell (Figure 1A). As effectors, we first combined two different A-to-I RNA editing enzymes, and later one A-to-I with one C-to-U RNA editase.

ADAR1 and ADAR2 have partly complementing substrate preferences (9,30). Hence, their orthogonal recruitment inside a cell is highly desired and we decided to co-express the newly characterized HA1Q (Figure 1) with the formerly characterized (9) SA2Q. In contrast to competing RNA targeting platforms, e.g. based on Cas proteins, self-labeling proteins are of small size with only 2.2 kb for HA1Q and 1.8 kb for SA2Q. This enabled us to generate small co-expression cassettes in the pcDNA 5 backbone which allow for their targeted integration into the FRT recombination site of 293 Flp-In T-REx cells (9,19). The strong expression of two transgenes within close proximity often leads to their mutual transcriptional interference (31). Thus, we constructed five different cassettes (Figure 2A), varying the relative positioning of the two transgenes, their promotors (CMV or Ef1α), and their direction of transcription. We also tested a P2A (32) fusion construct that drives both transgenes from one promotor. All five constructs were integrated into the 293 Flp-In T-REx parent cell line by simple plasmid transfection to generate duo cell lines that express both transgenes homogenously among the cell population under doxycycline control (Figure 2B, Supplementary Figure S6). Importantly, ready-to-use duo cell lines were obtained after two weeks of antibiotic selection with no need for cumbersome clonal selection. To better characterize the relative transgene expression in duo cell lines **1**–**5**, we stained both HA1Q and SA2Q in a defined 1:1 stoichiometry with tetramethylrhodamine (TMR) by adding TMR-benzylguanine and TMR-chloroalkane to full cell lysate and analyzed the stained proteins after SDS-PAGE separation (Figure 2C, Supplementary Figure S9). In a preliminary editing experiment, we tested for the editing activity of both transgenes in all five duo cell lines and found

e95 Nucleic Acids Research, 2021, Vol. 49, No. 16

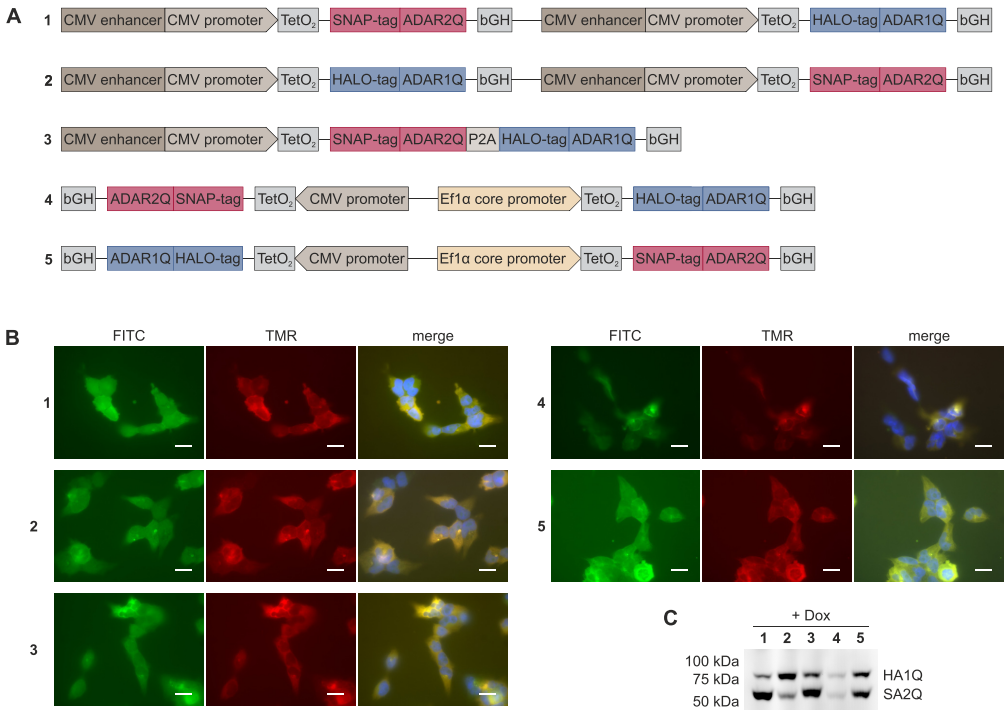

Figure 2. Generation of duo cell lines 1–5 for homogenous co-expression of two transgenes. (**A**) Constructs (**1**–**5**) were designed to co-express both transgenes (HA1Q and SA2Q) from one cassette under doxycycline control. $TetO_2$: tet operator, leads to repression of expression in the absence of a tetracycline (33); bGH: bovine growth hormone terminator; P2A: porcine teschovirus-1 self-cleaving 2A peptide (32). (**B**) All duo cell lines have been characterized for the transgene co-expression by staining with FITC-BG (green channel) and TMR-chloroalkane (red channel). Cell nuclei are stained with Hoechst 33342 (blue channel). Scale bars correspond to 15 μm. (**C**) Characterization of relative transgene expression via SDS-PAGE after co-staining with TMR-BG and TMR-chloroalkane in raw cell lysate.

HA1Q expression to be the major limiting factor (Supplementary Table S3). We continued the study largely based on duo cell line **2**, which expressed HA1Q to the highest level and SA2Q to a level sufficient to obtain good editing yields.

Selective recruitment of ADAR1 and ADAR2 activity extends the codon scope

ADAR1 and ADAR2 partly prefer different codons (34,35). We have comprehensively characterized the codon preferences of SA1Q and SA2Q before (9) and found, for example, that the 5′-CAG codon was preferentially edited by SA2Q, with a 3.3-fold higher editing yield compared to SA1Q, while the 5′-CAU codon was preferentially edited by SA1Q, with a 6.3-fold higher editing yield (Figure 3A). Thus, a cell line expressing only one of the two RNA base editors will not permit optimal editing yields in any case. In contrast, we predict that the selective recruitment of HA1Q and SA2Q with halo- and snap-guideRNAs, will enable to recruit the preferred enzyme to any substrate (matching combination, Figure 3B). Accordingly, we can predict the existence of a mismatching combination of guideRNAs that will lead to inferior editing results on both targets.

Initially, we tested this by transfection of single guideRNAs into duo cell line **2** (Figure 3C, left panel). GuideRNAs were either targeting a 5′-CAG codon in the ORF of ACTB or a 5′-CAU codon in the ORF of GAPDH. Furthermore, guideRNAs were either equipped with a BG moiety (snap-guideRNA) or with a chloroalkane moiety (halo-guideRNA) to selectively recruit SA2Q or HA1Q, respectively. Indeed, recruitment of SA2Q with the snap-CAG guideRNA always gave better editing yields for the 5′-CAG codon in ACTB than recruitment of HA1Q with the halo-CAG guideRNA. As expected, the effect was reverse for the editing of the 5′-CAU codon in GAPDH. Notably, only the halo-CAU guideRNA, selective for HA1Q, was able to induce detectable editing at all. A strength of the SNAP-ADAR platform is the ease by which the short (ca. 20 nt), chemically modified guideRNAs can be transfected into cells. In the past, we demonstrated co-transfection of up to four different guideRNAs enabling multiplexed, concurrent editing of four different substrates without loss in editing efficiency (9). Now, we co-transfected two guideRNAs, one snap- and one halo-guideRNA, either in matching or mismatching combination into cell line **2**. Clearly, the matching combination gave better editing yields for both substrates (CAG, CAU) compared to the mismatching combination. Again,

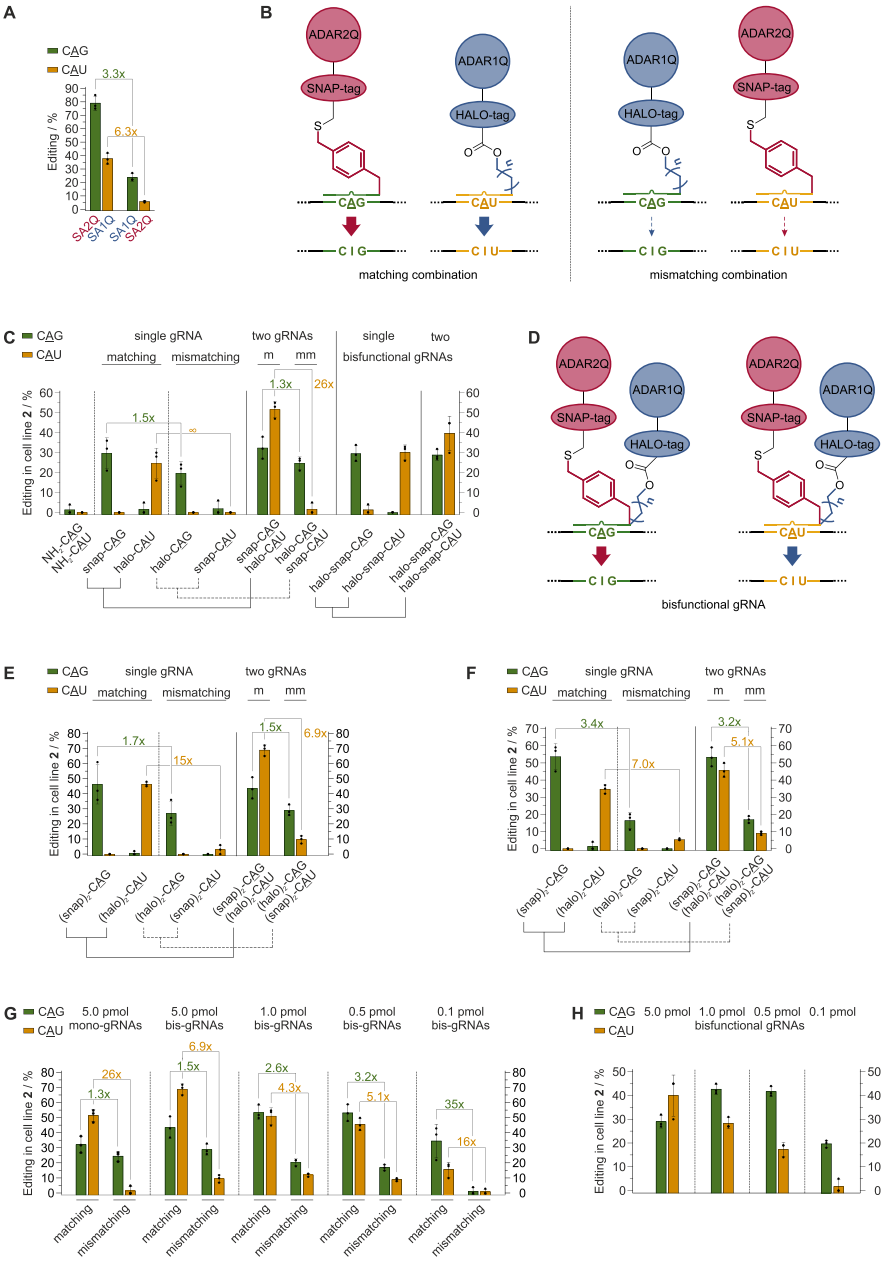

Figure 3. Editing in duo cell lines expressing HA1Q and SA2Q. (**A**) SA1Q and SA2Q have different preferences for 5′-CAG and 5′-CAU codons in the ORF of GAPDH, as described before (9). (**B**) Due to the two different self-labeling moieties (BG and chloroalkane) the SNAP-tagged ADAR2 and the HALO-tagged ADAR1 deaminase domains can be recruited either to their preferred substrates (matching combination) or to their least preferred substrates (mismatching combination). (**C**) Editing yield and selectivity after transfection of a single (5.0 pmol), matching or mismatching snap- or halo-guideRNA into duo cell line **2** compared to the co-transfection of two guideRNAs (one snap- and one halo-guideRNA, each 5.0 pmol) either in matching (m) or in mismatching (mm) combination (left panel). The right panel shows the activity of bisfunctional guideRNAs capable to recruit both editing enzymes with one guideRNA. (**D**) Bisfunctional halo-snap-guideRNAs, carrying both a chloroalkane and a BG moiety, are able to recruit both HA1Q and SA2Q, leading to maximum editing yields at any codon. (**E**) Editing yield and selectivity in duo cell line **2** after transfection of a single or co-transfection of two guideRNAs, one $(snap)_2$- and one $(halo)_2$-guideRNA, either in matching (m) or in mismatching (mm) combination (5.0 pmol each). (**F**) Same as E) but with 0.5 pmol each. (**G**) Concentration dependency of editing efficiency and selectivity in cell line **2** under co-transfection of $(snap)_2$- and $(halo)_2$-guideRNAs (bis-guideRNAs) in matching versus mismatching combination. For comparison, editing with the respective mono-guideRNAs (snap- and halo-guideRNAs) is shown. (**H**) Concentration dependency of editing yields in duo cell line **2** after co-transfection of two bisfunctional halo-snap-guideRNAs. Data in a), c), e)-h) are shown as the mean ± SD of $N = 3$ independent experiments.

choosing the matching combination was required to see editing with the CAU substrate at all. The same pattern was observed for a second duo cell line, cell line **5** (Supplementary Figure S13a). This demonstrates that the platform is able to target two editing enzymes independently from each other to their respective preferred target inside one cell line.

One could also conceive a bisfunctional guideRNA capable of recruiting both editases, HA1Q and SA2Q, simultaneously (Figure 3D). Such a halo-snap-guideRNA may enable maximum editing with any codon and substrate. To accomplish that, we synthesized halo-snap-guideRNAs carrying both, the BG and the chloroalkane moiety, targeting either the CAG or CAU substrate and tested them in duo cell line **2**. As expected, both halo-snap-guideRNAs gave good editing yields for both codons, 5′-CAU and 5′-CAG, always resembling the editing result of the formerly preferred snap- or halo-guideRNA, respectively (Figure 3C, right panel). This clearly indicates that both enzymes have been active on the substrates.

As controls, we had also synthesized $(snap)_2$- and $(halo)_2$-guideRNAs carrying either two benzylguanine or two chloroalkane moieties, respectively. Notably, editing yields have been higher with such controls (Figure 3E, F) compared to the respective guideRNAs carrying only one self-labeling moiety. This boost might be due to the recruitment of two instead of one editing enzyme per guideRNA. Similar effects have been described in the context of other RNA editing systems before (36). Interestingly, not only the yield but also the selectivity (e.g. CAG codon) was better than before (Figure 3F). One can expect that the selectivity increases further if one reduces the concentration of the guideRNA-enzyme conjugate inside the cell. Thus, we varied the amount of the two transfected guideRNAs (one $(snap)_2$- and one $(halo)_2$-guideRNA, either matching or mismatching) between 5 pmol and 0.1 pmol in four steps (Figure 3G, Supplementary Figure S13b, c). Indeed, stepwise reduction of the guideRNA amount improved the selectivity progressively. At 0.1 pmol guideRNA, excellent selectivity was obtained with virtually no residual editing on both targets (CAG and CAU) in the mismatching combination. Notably, the editing yields were satisfying also at low amounts of guideRNA. A similar trend, but with lower editing yields, was seen for the bisfunctional halo-snap-guideRNAs (Figure 3H, Supplementary Figure S13d) indicating that the recruitment of two copies of the preferred editing enzyme gives better editing yield than the co-recruitment of one preferred and one non-preferred enzyme.

Genomic co-expression of two editing enzymes elicits moderate global off-target editing

Overexpression of engineered, highly active editing enzymes leads to significant off-target editing throughout the whole transcriptome (8,10). Various strategies have been tried to minimize this (8,10). In this regard, we demonstrated that the controlled expression of SA1Q and SA2Q from single genomic loci reduces global off-target editing tremendously (9). We now determined the total off-target editing in duo cell line **2** after co-transfection with 0.5 pmol $(snap)_2$-CAG and 0.5 pmol $(halo)_2$-CAU guideRNA, by determining significantly differently edited sites in comparison with a negative control expressing no artificial editing enzyme. As the pipeline was more sensitive than the one used before (9), we re-analyzed the raw data of the total off-target editing for mono cell lines expressing SA1Q or SA2Q, in presence of an ACTB-targeting snap-guideRNA (9), with the new pipeline to allow for direct side-by-side comparison with duo cell line **2**. With 8391 sites, the amount of total off-target editing in duo cell line **2** roughly comprised the aggregate of sites found in mono cell lines SA1Q and SA2Q (Table 1, Figure 4A, Supplementary Figure S16). However, the vast majority of editing sites (ca. 75%) showed changes in editing levels below 25% (Supplementary Table S6, Figure 4A). The total off-targets comprise guideRNA-dependent and -independent editing events. To determine the guideRNA-dependent fraction we compared the off-target editing for cell line **2** with versus without co-transfection of the two guideRNAs. Our sensitive pipeline detected 653 sites that were significantly differently edited depending on the presence of the guideRNAs (Figure 4B, Table 1). Again, only a small number of sites (Supplementary Table S6) showed editing sites with levels elevated above 25%. Among these 37 sites, only five sites were missense mutations. After careful analysis, almost all 37 sites could be assigned to either binding of the GAPDH or ACTB guideRNA, respectively (Supplementary Figures S17–S19). Notably, only one missense mutation (ACTA2, 47%) achieved editing levels similar to the on-targets GAPDH (41%) and ACTB (52%), see Supplementary Table S7. This was due to the high sequence homology between ACTA2 and ACTB. In order to spot even minute guideRNA-dependent bystander editings, we manually analyzed the regions around the two on-target sites (± 500 bp) without applying the usual cutoff for editing difference. This yielded 4 bystander sites in GAPDH (editing difference ≤ 1%) and 10 sites in ACTB, with the three highest sites exhibiting editing differences between 16.0% and 7.7%, likely due to high similarity with the on-target site (Supplementary Tables S8 and S9, Supplementary Figure S20). Overall, NGS analysis demonstrated again (9,10) that total off-target effects are dominated by guideRNA-

Table 1. Number of significantly differently edited sites found in editing experiments in mono cell lines SA1Q, SA2Q, and in duo cell line **2** (HA1Q + SA2Q) in comparison to a negative control cell line (293 Flp-In T-REx) not expressing any editing enzyme (Total off-targets). The last column shows the guideRNA-dependent fraction of the total off-targets for duo cell line **2**

	Total off-targets			gRNA-dependent
	SA1Q	SA2Q	HA1Q + SA2Q	HA1Q + SA2Q
Total number	3406	4795	8391	653
incl. Alu sites	400	1190	1281	136
5′UTR	124	168	286	19
Missense mutation	769	1080	2150	166
Nonstop mutation	51	46	108	5
Start codon SNP	1	1	2	0
Silent	470	515	1079	74
3′UTR	1427	2009	3422	267
Noncoding	564	976	1343	122

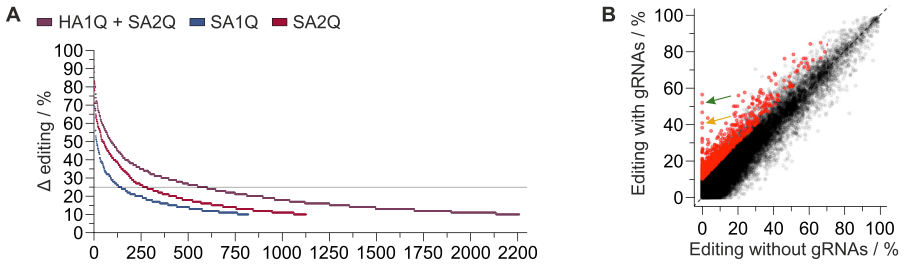

Figure 4. Off-target analysis of duo cell line **2**. (**A**) Total off-target editing of duo cell line **2** (HA1Q + SA2Q) in comparison with mono cell lines SA1Q and SA2Q. Shown are significantly differently edited sites (≥ 10% editing difference, Fisher's exact test, two-sided, adjusted $P < 0.01$, $n = 2$ experiments) that led to nonsynonymous substitutions, sorted by editing difference. (**B**) Scatter plot depicting the guideRNA-dependent off-target effects in duo cell line **2**. Significantly differently edited sites are marked in red. The two on-target sites (in ACTB and GAPDH) are marked by a green and yellow arrow respectively.

independent off-target effects rather than by mis-guiding through the guideRNAs.

Selective site-directed C-to-U and A-to-I editing can be combined within one cell

C-to-U and A-to-I RNA base editing complement one another. While A-to-I editing can remove premature STOP codons, C-to-U editing can write them and furthermore affect different amino acid substitutions, including key residues like serine and proline. APOBEC1-mediated C-to-U RNA editing plays a key role for human physiology by inducing an isoform switch in ApoB48/100 (37). In preliminary experiments, we found that a simple fusion of the SNAP-tag to the C-terminus of murine APOBEC1 generates an effector protein dubbed APO1S that can induce C-to-U editing in an RNA-guided manner. Fully analog to the duo cell lines above, we generated four duo cell lines (**6**–**9**, Figure 5A) that co-express the HA1Q and APO1S transgenes under control of doxycycline. Via western blot/SDS PAGE we characterized the relative transgene expression (Figure 5B), which suggested cell line **6** and **9** to express sufficient levels of both effectors. Notably, the inserts of cell lines **6** and **9** are constructed analog to those in cell lines **2** and **5**, indicating that these two designs might be generally applicable for the co-expression of two RNA-guided effector proteins.

A first set of editing experiments targeted a 5′-UAG codon for HA1Q-mediated A-to-I editing and a proximal 5′-ACG codon for APO1S-mediated C-to-U editing in an eGFP reporter transcript in duo cell line **9**. The target sites are close enough to design one guideRNA that can mediate both, adenosine or cytidine deamination, depending on the self-labeling moiety attached, since HA1Q requires an RNA duplex as substrate (9) whereas APO1S prefers its positioning 4–6 nt upstream of the target site (Figure 5C). As expected, the halo-eGFP guideRNA elicited A-to-I editing, the snap-eGFP guideRNA elicited C-to-U editing and a bisfunctional halo-snap-eGFP guideRNA induced both A-to-I and C-to-U editing (Figure 5D). Similar results have been obtained in the cell lines **6** and **7** (Supplementary Figure S14). Notably, the snap-eGFP guideRNA also induced some A-to-I editing. However, highly selective C-to-U editing was achieved when a snap-eGFP guideRNA was applied that was fully chemically modified (*mod*-snap-eGFP, Figure 5C, Supplementary Table S1) and that did not contain the modification gap (38) around the adenosine required for ADAR1 action (Figure 5D). This highlights another strength of the RNA targeting platform. Bystander off-target editing can be easily controlled by chemical modification of the guideRNA (9), a frequent problem (8,10) with RNA base editing approaches that apply genetically encoded guideRNAs.

In a second set of editing experiments, we applied two different guideRNAs to selectively recruit APO1S and HA1Q to two different endogenous transcripts in duo cell line **9**. The $(halo)_2$-UAU guideRNA steers HA1Q to edit the adenosine in a 5′-UAU codon in the ORF of ACTB, the $(snap)_2$-ACC guideRNA steers APO1S to edit the cytosine in a 5′-ACC codon in the ORF of GAPDH (Figure 5E). In contrast to the editing of the eGFP reporter, editing on endogenous ORF targets was very selective. The $(halo)_2$-UAU guideRNA induced site-specific A-to-I editing with excellent yields (ca. 65%) in the ACTB transcript with no detectable C-to-U editing, whereas the $(snap)_2$-ACC guideRNA induced site-specific C-to-U editing with moderate yield (ca. 20%) in the GAPDH transcript, again with no detectable A-to-I RNA editing (Figure 5F). Notably, co-transfection of both guideRNAs induced selective A-to-I and C-to-U editing in the ACTB and GAPDH transcript, respectively, without any loss of editing efficiency compared to the single guideRNA transfections. Similar results have been obtained in the cell lines **6** and **7** (Supplementary Figure S13e). Thus, concurrent C-to-U and A-to-I editing can be done within one cell under programmable target selection.

We then benchmarked the C-to-U editing efficiency achieved with APO1S in duo cell line **9** at both targets (eGFP and GAPDH) with the recently published (39) Cas13-based RESCUE approach (Supplementary Figure S15). Specifically, we tested the most active variant, RESCUEr16, and tried four different C-flip guideRNAs for each target (Supplementary Table S4). The APO1S enzyme outcompeted RESCUEr16 on both targets with respect to on-target editing yield. While we found C-to-U bystander editing for both approaches, only the RESCUE approach induced A-to-I bystander editing (Supplementary Table S5).

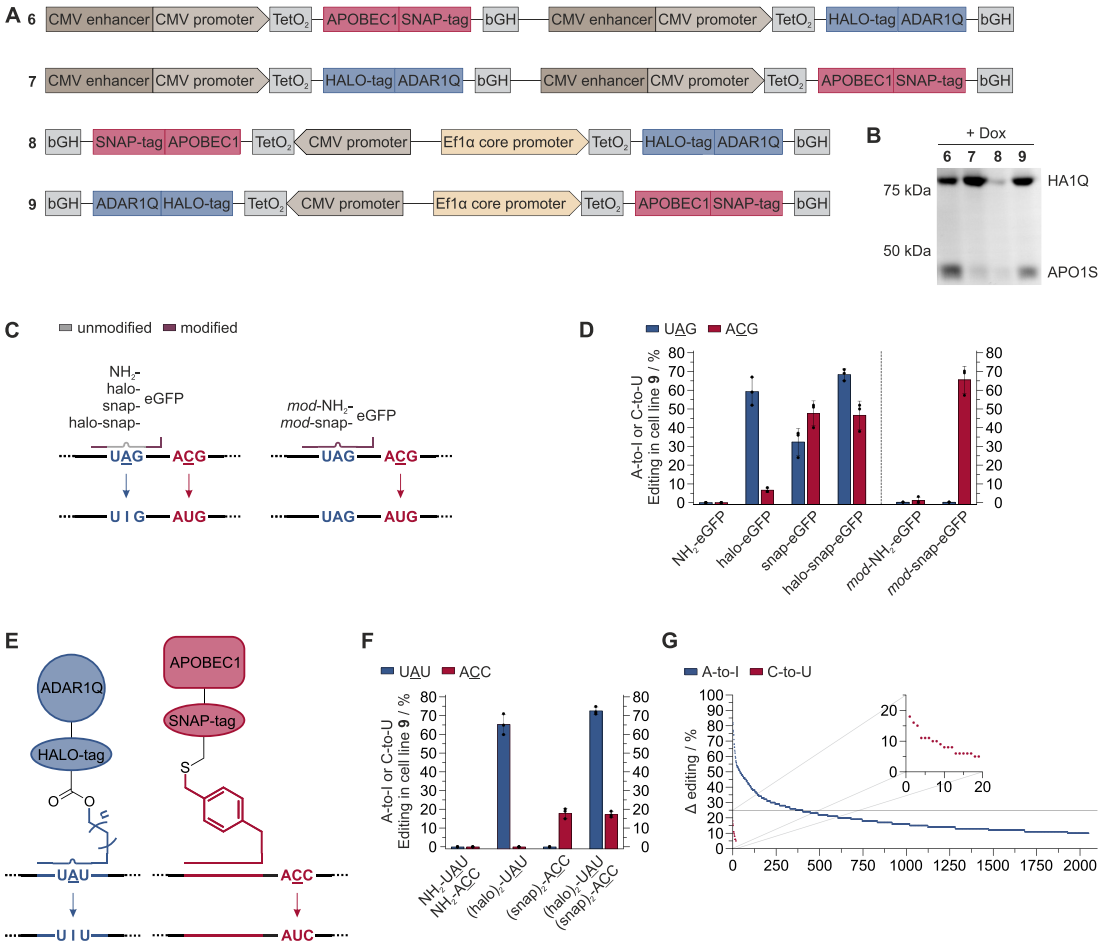

Figure 5. Selective and concurrent A-to-I and C-to-U editing. (**A**) Constructs (**6**-**9**) were designed to co-express both transgenes (APO1S and HA1Q) from one cassette under doxycycline control. $TetO_2$: tet operator, leads to repression of expression in the absence of a tetracycline (33); bGH: bovine growth hormone terminator; P2A: porcine teschovirus-1 self-cleaving 2A peptide (32). (**B**) Characterization of relative transgene expression via SDS-PAGE after co-staining with TMR-BG and TMR-chloroalkane in raw cell lysate. (**C**) GuideRNA design to enable or block concurrent A-to-I and C-to-U editing in an eGFP reporter with a single guideRNA. The modified guideRNA (*mod*-snap-eGFP) contained chemical modifications (Supplementary Table S1) that block A-to-I editing. (**D**) Editing yield in cell line **9** from concurrent A-to-I and C-to-U editing in an eGFP reporter transcript after transfection of a halo-, snap- or halo-snap-guideRNA (5.0 pmol). (**E**) GuideRNA design and recruiting strategy for concurrent and selective A-to-I and C-to-U editing at two different endogenous transcripts. (**F**) Editing yield in cell line **9** for selective and concurrent editing as depicted in E) after transfection of a single or co-transfection of two guideRNAs, one $(halo)_2$-guideRNA for A-to-I editing in ACTB and one $(snap)_2$-guideRNA for C-to-U editing in GAPDH (5.0 pmol each). Data in D) and F) are shown as the mean ± SD of $N = 3$ independent experiments. (**G**) Total off-target A-to-I and C-to-U editing of duo cell line **9**. Shown are significantly differently edited sites (for A-to-I ≥ 10% editing difference, for C-to-U ≥ 5% editing difference, Fisher's exact test, two-sided, adjusted $P < 0.01$, $n = 2$ experiments) that led to nonsynonymous substitutions, sorted by editing difference. A-to-I (in ACTB) and C-to-U (in GAPDH) on-target sites are no. 40 and no. 18, respectively.

To assess transcriptome-wide global A-to-I and C-to-U off-target editing, we applied next generation RNA sequencing to detect significantly differently edited sites in duo cell line **9** after co-transfection of 2.5 pmol $(halo)_2$-UAU and 2.5 pmol $(snap)_2$-ACC guideRNA in comparison to a cell line lacking expression of any artificial editing enzyme (Table 2, Figure 5g, Supplementary Figure S22). Expressing only one A-to-I editing enzyme (HA1Q), the total number of A-to-I off-target sites (6767) was below that of duo cell line **2**, which expresses two A-to-I editing enzymes. Again, the majority of sites exhibited differences in editing below 25% (Supplementary Table S10). A slightly higher fraction of the off-target sites was guideRNA-dependent compared to cell line **2**, which might be due to the higher guideRNA amounts applied in cell line **9**. However, in particular off-target sites with high editing differences, e.g. ≥ 25%, were typically guideRNA-independent (Supplementary Table S10). Taking the generally lower C-to-U editing yields into account, we adapted the pipeline and set the cutoff for editing differences to 5%. With this highly sen-

Table 2. Number of significantly differently edited A-to-I and C-to-U sites found in editing experiments in duo cell line **9** (HA1Q + APO1S) in comparison to a negative control cell line (293 Flp-In T-REx) not expressing any editing enzyme (Total off-targets). The guideRNA-dependent fractions of the total off-targets are shown in the right column, respectively

	A-to-I ($\Delta \geq 10\%$)		C-to-U ($\Delta \geq 5\%$)	
	Total off-targets	gRNA-dependent	Total off-targets	gRNA-dependent
Total number	6767	2148	2976	153
incl. Alu sites	729	85	17	1
5′UTR	262	92	44	3
Missense mutation	1944	704	16	1
Nonsense mutation	0	0	2	0
Nonstop mutation	104	30	0	0
Start codon SNP	2	0	0	0
Silent	979	352	17	2
3′UTR	2560	731	2593	131
Noncoding	916	239	304	16

sitive pipeline, we were able to find 2976 significantly differently edited sites (Table 2). However, the vast number of sites showed editing differences below 10%, and only 129 sites had editing differences above 25% (Supplementary Table S11). Notably, almost all off-target sites were located in the 3′-UTR, and only 18 of 2976 total sites were inducing missense or nonsense mutations. Also the number of guideRNA-dependent off-targets sites was comparably low (153 of 2976), with basically all in the 3′-UTR (Table 2, Supplementary Table S11). Again, we manually analyzed the regions (± 500 bp) around the on-target site to detect low-level bystander A-to-I editing in ACTB (Supplementary Table S13) and C-to-U bystander editing in GAPDH (Supplementary Table S12). We found one bystander site in ACTB (editing difference $\leq 1\%$) and a larger number (22) of bystander sites in GAPDH, but only one of the 22 sites had an editing difference $\geq 1\%$. Overall, our approach for concurrent A-to-I and C-to-U RNA editing, based on co-expression of two different editing enzymes gave moderate, mainly guideRNA-independent off-target effects for both effectors.

CONCLUSIONS

Here, we show for the first time that one can combine two self-labeling enzymes to create a powerful RNA targeting platform to manipulate RNA inside living cells in a yet unprecedented way. The orthogonality of HALO- and SNAP-tag sets the ground for the selective and programmable steering of two different RNA effectors. Furthermore, the approach benefits from the small size of the fusion proteins, which enable their facile genomic co-integration, and the ease by which the short (20 nt), chemically stabilized guideRNAs can be co-transfected and optimized to reduce bystander editing, if required. Recent attempts to combine two base editing activities in one protein either to target DNA (40) or RNA (39) illustrate the manifold problems of controlling two enzyme functions independently, which we could solve here for RNA base editing. We successfully demonstrate the functioning of our approach for the orthogonal and concurrent recruitment of two pairs of editing effectors. The selective recruitment of ADAR1 and ADAR2 deamination activity enables site-directed A-to-I RNA base editing with improved editing efficiency. The selective recruitment of ADAR1 and APOBEC1 deamination activity allows for target-selective, concurrent A-to-I and C-to-U editing. Notably, orthogonality is particularly effective with guideRNAs that can recruit two copies of an editase. Again, we demonstrate that genetic integration of the editing enzymes helps to control global off-target A-to-I and C-to-U editing induced by unengaged editing enzymes (9,10,16,41). Notably, even the concurrent transfection of two guideRNAs leads to only a very small number of off-target editing events caused by misguiding through the guideRNAs, and might be amenable for further sequence optimization, if required.

Furthermore, our platform benefits from the high flexibility in the linker chemistry. This makes it possible to control the composition and stoichiometry of two fusion proteins at a target with one guideRNA. We exemplify this with the generation of bisfunctional guideRNAs that are capable of co-recruiting either ADAR1/ADAR2 or ADAR1/APOBEC1 to one target with one guideRNA. The possibility of including photochemistry to the linker may add another level of spatio-temporal control in the future (18,19). The general concept we present here may be readily transferred to recruit further pairs of writers and erasers of epitranscriptomic marks with ease and unprecedented control (2,42,43).

DATA AVAILABILITY

NGS raw data for duo cell lines **2** and **9** can be found on NCBI GEO under GSE160945**.** The online Supplementary Information contains an excel sheet with all editing yields, an excel sheet with the NGS analysis, SnapGene files for all transgenic constructs, and a PDF file giving detailed information on syntheses, protocols, and additional experimental data.

SUPPLEMENTARY DATA

Supplementary Data are available at NAR Online.

FUNDING

Deutsche Forschungsgemeinschaft (DFG, German Research Foundation) [430214260, STA1053/7-1 to T.S.]; DFG priority program SPP 1784 [404867268 to F.N.P., T.S.]; European Research Council (ERC) under the European Union's Horizon 2020 research and innovation program [649019 to F.N.P., 647328 to T.S.]. Funding for open access charge: ERC; DFG.

Conflict of interest statement. T.S. holds patents on site-directed RNA editing.

REFERENCES

1. Corbett,A.H. (2018) Post-transcriptional regulation of gene expression and human disease. *Curr. Opin. Cell Biol.*, **52**, 96–104.
2. Kadumuri,R.V. and Janga,S.C. (2018) Epitranscriptomic code and its alterations in human disease. *Trends Mol. Med.*, **24**, 886–903.
3. Gagnidze,K., Rayon-Estrada,V., Harroch,S., Bulloch,K. and Papavasiliou,F.N. (2018) A new chapter in genetic medicine: RNA

editing and its role in disease pathogenesis. *Trends Mol. Med.*, **24**, 294–303.
4. Shi,H., Zhang,X., Weng,Y.-L., Lu,Z., Liu,Y., Lu,Z., Li,J., Hao,P., Zhang,Y., Zhang,F. *et al.* (2018) m^{6}A facilitates hippocampus-dependent learning and memory through YTHDF1. *Nature*, **563**, 249–253.
5. Frye,M., Harada,B.T., Behm,M. and He,C. (2018) RNA modifications modulate gene expression during development. *Science*, **361**, 1346–1349.
6. Liu,J., Eckert,M.A., Harada,B.T., Liu,S.-M., Lu,Z., Yu,K., Tienda,S.M., Chryplewicz,A., Zhu,A.C., Yang,Y. *et al.* (2018) m^{6}A mRNA methylation regulates AKT activity to promote the proliferation and tumorigenicity of endometrial cancer. *Nat. Cell Biol.*, **20**, 2085–1083.
7. Ishizuka,J.J., Manguso,R.T., Cheruiyot,C.K., Bi,K., Panda,A., Iracheta-Vellve,A., Miller,B.C., Du,P.P., Yates,K.B., Dubrot,J. *et al.* (2019) Loss of ADAR1 in tumours overcomes resistance to immune checkpoint blockade. *Nature*, **565**, 43–48.
8. Rees,H.A. and Liu,D.R. (2018) Base editing: precision chemistry on the genome and transcriptome of living cells. *Nat. Rev. Genet.*, **19**, 770–788.
9. Vogel,P., Moschref,M., Li,Q., Merkle,T., Selvasaravanan,K.D., Li,J.B. and Stafforst,T. (2018) Efficient and precise editing of endogenous transcripts with SNAP-tagged ADARs. *Nat. Methods*, **15**, 535–538.
10. Vogel,P. and Stafforst,T. (2019) Critical review on engineering deaminases for site-directed RNA editing. *Curr. Opin. Biotechnol.*, **55**, 74–80.
11. Kuttan,A. and Bass,B.L. (2012) Mechanistic insights into editing-site specificity of ADARs. *Proc. Natl. Acad. Sci. U.S.A.*, **109**, E3295–E3304.
12. Keppler,A., Gendreizig,S., Gronemeyer,T., Pick,H., Vogel,H. and Johnsson,K. (2003) A general method for the covalent labeling of fusion proteins with small molecules *in vivo*. *Nat. Biotechnol.*, **21**, 86–89.
13. Stafforst,T. and Schneider,M.F. (2012) An RNA–Deaminase conjugate selectively repairs point mutations. *Angew. Chem.*, **124**, 11329–11332.
14. Abudayyeh,O.O., Gootenberg,J.S., Konermann,S., Joung,J., Slaymaker,I.M., Cox,D.B.T., Shmakov,S., Makarova,K.S., Semenova,E., Minakhin,L. *et al.* (2016) C2c2 is a single-component programmable RNA-guided RNA-targeting CRISPR effector. *Science*, **353**, 5573.
15. Abudayyeh,O.O., Gootenberg,J.S., Essletzbichler,P., Han,S., Joung,J., Belanto,J.J., Verdine,V., Cox,D.B.T., Kellner,M.J., Regev,A. *et al.* (2017) RNA targeting with CRISPR–Cas13. *Nature*, **550**, 280–284.
16. Cox,D.B.T., Gootenberg,J.S., Abudayyeh,O.O., Franklin,B., Kellner,M.J., Joung,J. and Zhang,F. (2017) RNA editing with CRISPR-Cas13. *Science*, **358**, 1019–1027.
17. Montiel-Gonzalez,M.F., Vallecillo-Viejo,I., Yudowski,G.A. and Rosenthal,J.J.C. (2013) Correction of mutations within the cystic fibrosis transmembrane conductance regulator by site-directed RNA editing. *Proc. Natl. Acad. Sci. U.S.A.*, **110**, 18285–18290.
18. Hanswillemenke,A., Kuzdere,T., Vogel,P., Jékely,G. and Stafforst,T. (2015) Site-directed RNA editing in vivo can be triggered by the light-driven assembly of an artificial riboprotein. *J. Am. Chem. Soc.*, **137**, 15875–15881.
19. Vogel,P., Hanswillemenke,A. and Stafforst,T. (2017) Switching protein localization by site-directed RNA editing under control of light. *ACS Synth. Biol.*, **6**, 1642–1649.
20. Vogel,P. and Stafforst,T. (2014) Site-directed RNA editing with antagomir deaminases — a tool to study protein and RNA function. *ChemMedChem*, **9**, 2021–2025.
21. Hanswillemenke,A. and Stafforst,T. (2019) Protocols for the generation of caged guideRNAs for light-triggered RNA-targeting with SNAP-ADARs. *Methods Enzymol.*, **624**, 47–68.
22. Dobin,A., Davis,C.A., Schlesinger,F., Drenkow,J., Zaleski,C., Jha,S., Batut,P., Chaisson,M. and Gingeras,T.R. (2013) STAR: ultrafast universal RNA-seq aligner. *Bioinformatics*, **29**, 15–21.
23. Kent,W.J., Sugnet,C.W., Furey,T.S., Roskin,K.M., Pringle,T.H., Zahler,A.M. and Haussler,D. (2002) The human genome browser at UCSC. *Genome Res.*, **12**, 996–1006.
24. Li,H., Handsaker,B., Wysoker,A., Fennell,T., Ruan,J., Homer,N., Marth,G., Abecasis,G. and Durbin,R. (2009) The sequence alignment/map format and SAMtools. *Bioinformatics*, **25**, 2078–2079.
25. Lo Giudice,C., Tangaro,M.A., Pesole,G. and Picardi,E. (2020) Investigating RNA editing in deep transcriptome datasets with REDItools and REDIportal. *Nat. Protoc.*, **15**, 1098–1131.
26. Picardi,E. and Pesole,G. (2013) REDItools: high-throughput RNA editing detection made easy. *Bioinformatics*, **29**, 1813–1814.
27. Ramos,A.H., Lichtenstein,L., Gupta,M., Lawrence,M.S., Pugh,T.J., Saksena,G., Meyerson,M. and Getz,G. (2015) Oncotator: cancer variant annotation tool. *Hum. Mutat.*, **36**, E2423–E2429.
28. Los,G.V., Encell,L.P., McDougall,M.G., Hartzell,D.D., Karassina,N., Zimprich,C., Wood,M.G., Learish,R., Ohana,R.F., Urh,M. *et al.* (2008) HaloTag: a novel protein labeling technology for cell imaging and protein analysis. *ACS Chem. Biol.*, **3**, 373–382.
29. Gautier,A., Juillerat,A., Heinis,C., Corrêa,I.R. Jr, Kindermann,M., Beaufils,F. and Johnsson,K. (2008) An engineered protein tag for multiprotein labeling in living cells. *Chem. Biol.*, **15**, 128–136.
30. Eggington,J.M., Greene,T. and Bass,B.L. (2011) Predicting sites of ADAR editing in double-stranded RNA. *Nat. Commun.*, **2**, 319–319.
31. Palmer,A.C., Egan,J.B. and Shearwin,K.E. (2011) Transcriptional interference by RNA polymerase pausing and dislodgement of transcription factors. *Transcription*, **2**, 9–14.
32. Kim,J.H., Lee,S.-R., Li,L.-H., Park,H.-J., Park,J.-H., Lee,K.Y., Kim,M.-K., Shin,B.A. and Choi,S.-Y. (2011) High cleavage efficiency of a 2A peptide derived from porcine Teschovirus-1 in human cell lines, Zebrafish and Mice. *PLoS One*, **6**, e18556.
33. Yao,F., Svensjö,T., Winkler,T., Lu,M., Eriksson,C. and Eriksson,E. (1998) Tetracycline repressor, tetR, rather than the tetR–mammalian cell transcription factor fusion derivatives, regulates inducible gene expression in mammalian cells. *Hum. Gene Ther.*, **9**, 1939–1950.
34. Nishikura,K. (2010) Functions and regulation of RNA editing by ADAR deaminases. *Annu. Rev. Biochem.*, **79**, 321–349.
35. Tan,M.H., Li,Q., Shanmugam,R., Piskol,R., Kohler,J., Young,A.N., Liu,K.I., Zhang,R., Ramaswami,G., Ariyoshi,K. *et al.* (2017) Dynamic landscape and regulation of RNA editing in mammals. *Nature*, **550**, 249–254.
36. Montiel-González,M.F., Vallecillo-Viejo,I.C. and Rosenthal,Joshua J.C. (2016) An efficient system for selectively altering genetic information within mRNAs. *Nucleic Acids Res.*, **44**, e157.
37. Gott,J.M. and Emeson,R.B. (2000) Functions and mechanisms of RNA editing. *Annu. Rev. Genet.*, **34**, 499–531.
38. Vogel,P., Schneider,M.F., Wettengel,J. and Stafforst,T. (2014) Improving site-directed RNA editing in vitro and in cell culture by chemical modification of the GuideRNA. *Angew. Chem.*, **126**, 6382–6386.
39. Abudayyeh,O.O., Gootenberg,J.S., Franklin,B., Koob,J., Kellner,M.J., Ladha,A., Joung,J., Kirchgatterer,P., Cox,D.B.T. and Zhang,F. (2019) A cytosine deaminase for programmable single-base RNA editing. *Science*, **365**, 382–386.
40. Sakata,R.C., Ishiguro,S., Mori,H., Tanaka,M., Tatsuno,K., Ueda,H., Yamamoto,S., Seki,M., Masuyama,N., Nishida,K. *et al.* (2020) Base editors for simultaneous introduction of C-to-T and A-to-G mutations. *Nat. Biotechnol.*, **38**, 865–869.
41. Vallecillo-Viejo,I.C., Liscovitch-Brauer,N., Montiel-Gonzalez,M.F., Eisenberg,E. and Rosenthal,J.J.C. (2018) Abundant off-target edits from site-directed RNA editing can be reduced by nuclear localization of the editing enzyme. *RNA Biol.*, **15**, 104–114.
42. Rau,K., Rösner,L. and Rentmeister,A. (2019) Sequence-specific m^{6}A demethylation in RNA by FTO fused to RCas9. *RNA*, **25**, 1311–1323.
43. Liu,X.-M., Zhou,J., Mao,Y., Ji,Q. and Qian,S.-B. (2019) Programmable RNA N^6-methyladenosine editing by CRISPR-Cas9 conjugates. *Nat. Chem. Biol.*, **15**, 865–871.

Supporting Information

Harnessing Self-Labeling Enzymes for Selective and Concurrent A-to-I and C-to-U RNA Base Editing

Anna S. Stroppel[1], Ngadhnjim Latifi[1], Alfred Hanswillemenke[1], Rafail Nikolaos Tasakis[2,3], F. Nina Papavasiliou[2,3] and Thorsten Stafforst[1*]

[1]Interfaculty Institute of Biochemistry, University of Tübingen, Auf der Morgenstelle 15, 72076 Tübingen, Germany

[2]Division of Immune Diversity (D150), German Cancer Research Center (DKFZ), Heidelberg, Germany.

[3]Faculty of Biosciences, University of Heidelberg, Heidelberg, Germany

[*]correspondence to thorsten.stafforst@uni-tuebingen.de

Contents

List of Schemes

List of Figures

List of Tables

Chemical synthesis

General

All chemicals were purchased from standard chemical providers and used without further purification unless stated otherwise. Reactions that are sensible towards air or water were carried out with anhydrous solvents and under a nitrogen atmosphere using Schlenk technique.

For TLC, silica gel F_{254} foils from MERCK were used, which were visualized either under UV light at 254 nm or with 0.5 % aqueous solution of $KMnO_4$ or with 0.1 % aqueous solution of ninhydrin supplemented with 10 % ethanol. Purification by column chromatography was performed with self-packed columns of silica gel (0.04 – 0.063 mm/230 – 240 mesh), applying slight overpressure.

Analytical as well as preparative HPLC was conducted with a system by SHIMADZU consisting of a SCL-10A VP system controller, two LC-20AT prominence liquid chromatographs for buffers A and B and a SPD-20AV prominence UV/VIS detector. Buffer A consisted of H_2O:TFA, 100:0.1, buffer B of MeCN:H_2O:TFA, 90:10:0.1. For analytic measurements, a linear gradient from 5 % B to 95 % B in 25 min was applied. As analytical column, an EC 125/4 nucleodur 100-5 C18 ec column by MACHEREY-NAGEL was used, as preparative a VP 250/10 nucleodur 100-5 C18 ec column by MACHEREY-NAGEL. Spectra were analyzed with SHIMADZU CLASS-VP.

NMR spectra were measured on a BRUKER Avance III HD 300 spectrometer at 300.13 MHz or a BRUKER Avance III HDX 400 spectrometer at 400.16 MHz for ^{1}H spectra or 100.62 MHz for ^{13}C spectra respectively. Chemical shifts in ppm were calibrated to the signal of the deuterated solvent. Melting points were determined with a Melting Point M-560 from BÜCHI. UV spectra were measured with a Cary 300 Scan UV/Visible spectrophotometer from Agilent.

LC/MS spectra were recorded on a SHIMADZU LCMS-2020 with kinetex C18 column. Buffer A consisted of H_2O:HCO_2H, 100:0.1, buffer B of MeCN:H_2O:HCO_2H, 80:20:0.1. A linear gradient from 5 % B to 95 % B in 10 min was applied. For high resolution HR-ESI-TOF mass spectra, a BRUKER Daltonics maxis 4G mass spectrometer was used. Elemental analysis was performed with the elemental analyser Euro EA 3000 from HEKATECH.

BG-linker-OH (snap)

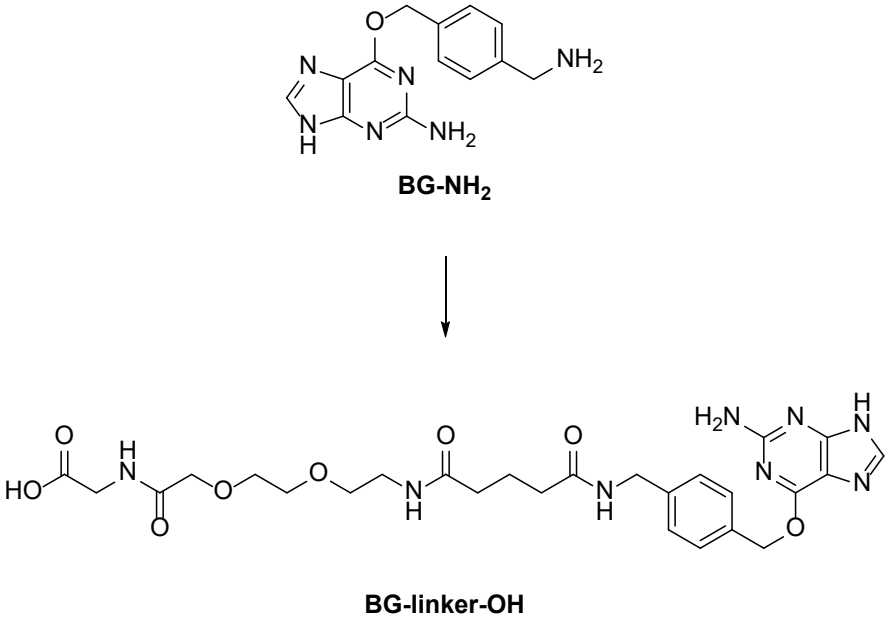

Scheme S1. Structures of BG-NH2 and BG-linker-OH (snap).

Literature known O^6-(4-aminomethyl-benzyl)guanine (BG-NH_2)[1] and BG-linker-OH (snap)[2] were synthesized starting from commercially available 6-chloro-guanine according to previously reported protocols.

BC-linker-OH (clip)

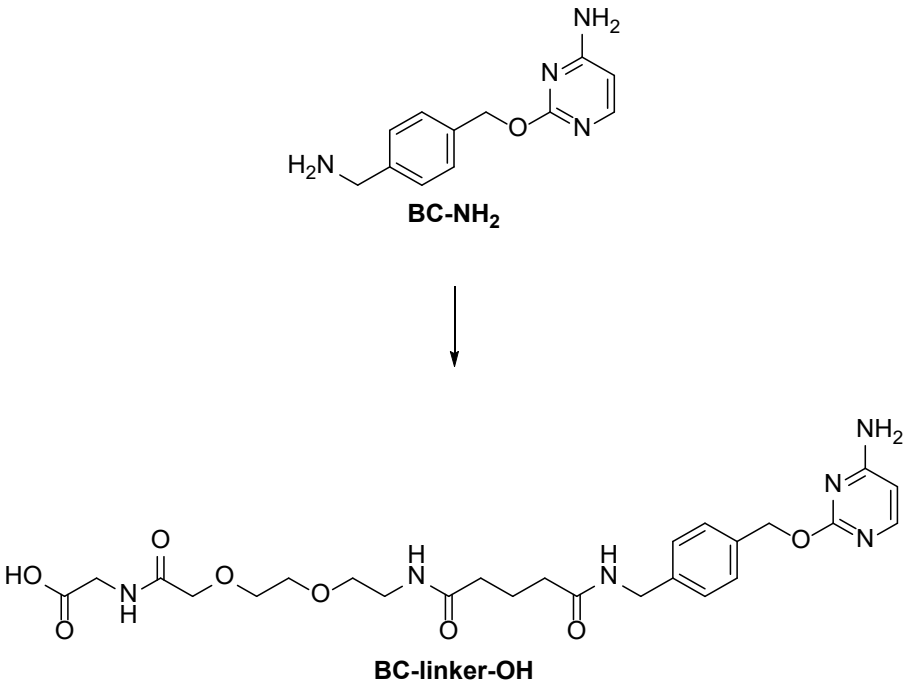

Scheme S2. Structures of BC-NH_2 and BC-linker-OH (clip).

2-(4-(Aminomethyl)-benzyloxy)-4-aminopyrimidine (BC-NH_2) was prepared from commercially available methyl-4-(aminomethyl)benzoate hydrochloride according to literature.[3-5] BC-linker-OH (clip) was obtained via the solid phase peptide synthesis protocol described for BG-linker-OH[2] starting from 413 mg (260 µmol, 1.00 eq) H-Gly-2-chlorotrityl resin by using 20 mg (87.0 µmol, 0.33 eq) BC-NH_2 in step 7. The resulting crude product was dissolved in 20 % buffer B, filtered and purified via preparative HPLC (5 % B to 40 % B in 40 min), which yielded 31 mg (58.8 µmol, 65 %) BC-linker-OH as a colorless powder after lyophilization.

mp = 111.4 °C (H_2O/MeCN); UV spectrum (MeOH): λ_{max} = 270 nm, $\varepsilon_{260\,nm}$ = 4.24 $mM^{-1}cm^{-1}$; t_R = 6.8 min; *m/z* calculated for $[C_{25}H_{34}N_6O_8+H]^+$: 547.25109, found: 547.25159.

Chloroalkane-linker-OH (halo)

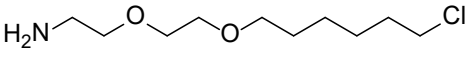

chloroalkane-NH_2

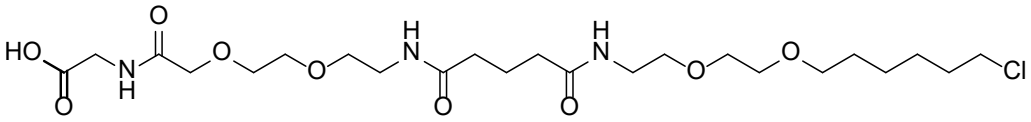

chloroalkane-linker-OH

Scheme S3. Structures of chloroalkane-NH_2 and chloroalkane-linker-OH (halo).

2-(2-((6-Chlorohexyl)oxy)ethoxy)ethanamine (chloroalkane-NH_2) was synthesized from commercially available 2-(2-aminoethoxy)ethanol according to literature.[6] Chloroalkane-linker-OH (halo) was obtained via the protocol described for BG-linker-OH[2] starting from 413 mg (260 µmol, 1.00 eq) H-Gly-2-chlorotrityl resin by using 19 mg (85.8 µmol, 0.33 eq) chloroalkane-NH_2 in step 7. The resulting crude product was dissolved in 10 % buffer B, filtered and purified via preparative HPLC (15 % B to 70 % B in 40 min), which yielded 12 mg (22.0 µmol, 26 %) chloroalkane-linker-OH as a colorless powder after lyophilization.

mp = 67.2 °C (H_2O/MeCN); t_R = 11.7 min; *m/z* calculated for $[C_{23}H_{42}ClN_3O_9+Na]^+$: 562.25018, found: 562.25036. Elemental analysis: calculated: C: 51.15 %, H: 7.84 %, N: 7.78 %, found: C: 51.11 %, H: 7.95 %, N: 7.87 %.

Chloroalkane-BG-linker-OH (halo-snap)

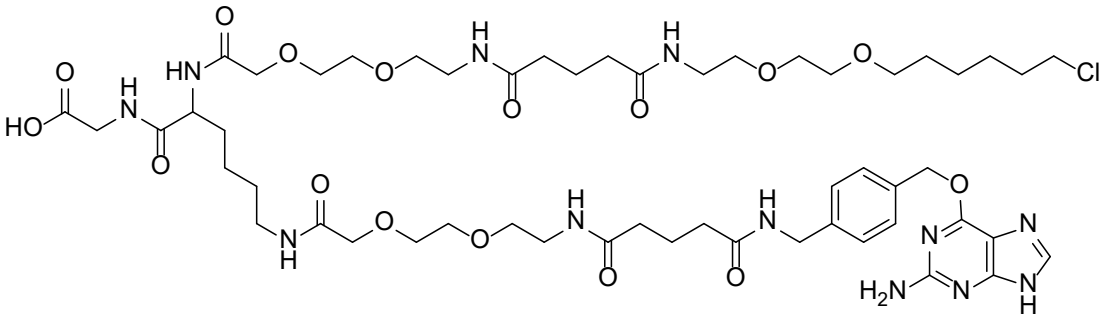

chloroalkane-BG-linker-OH

Figure S1. Structure of chloroalkane-BG-linker-OH (halo-snap).

All reaction steps were performed at room temperature on a peptide shaker at 1000 rpm. Unless indicated otherwise, washing refers to washing 3 × each with 5 ml NMP/DCM (1:1), then DCM, then NMP.

In a 10 ml syringe with a polyethylene frit, 75 mg (40.6 µmol, 1.00 eq) H-Gly-2-chlorotrityl resin were swelled in NMP for 1 h. 92 mg (203 µmol, 5.00 eq) FmocLys(Alloc)-OH, 69 mg (183 µmol, 4.50 eq) HBTU, 27 mg (203 µmol, 5.00 eq) HOBt and 240 µl (184 mg, 1.42 mmol, 35.0 eq) DIPEA in 1.5 ml NMP were added to the resin and shaken for 1 h. After washing, 3 × 6 ml 20 % piperidine in NMP were applied for 10 min each for Fmoc deprotection and the resin was washed again. Then, 63 mg (162 µmol, 4.00 eq) Fmoc-AEEA-COOH was coupled to the resin with 55 mg (146 µmol, 3.60 eq) HBTU, 22 mg (162 µmol, 4.00 eq) HOBt and 193 µl (147 mg, 1.14 mmol, 28.0 eq) DIPEA in 1 ml NMP for 1 h. After washing, 3 × 6 ml 20 % piperidine in NMP were applied for 10 min each for Fmoc deprotection and the resin was washed again. 59 mg (406 µmol, 10.0 eq) glutaric anhydride was coupled with 69 µl (52 mg, 406 µmol, 10.0 eq) DIPEA in 1 ml NMP for 30 min. The resin was washed again with a subsequent additional washing step with 1 % NaOH in dioxane/H_2O (1:1) for 1 min and thereafter washing 4 × each with DCM/NMP (1:1), DCM and NMP. For activation of the glutaric acid, 2 × 73 µl (119 mg, 426 µmol, 10.5 eq) Pfp-OTFA in 2 ml pyridine/DCM (1:1) were applied for 10 min and 20 min respectively. After washing 4 × with NMP only, 25 mg (112 µmol, 2.75 eq) chloroalkane-NH_2 with 250 µl (190 mg, 1.47 mmol, 36.2 eq) in 1 ml NMP were coupled to the resin overnight.

For Alloc deprotection, the resin was washed again, rendered inert under nitrogen atmosphere and additionally washed 5 × with anhydrous DCM for 30 s. First, 119 µl (105 mg, 975 µmol, 24.0 eq) $PhSiH_3$ in 1 ml anhydrous DCM were applied to the resin, then 4.7 mg (4.06 µmol, 0.10 eq) $Pd(PPh_3)_4$ in 1.5 ml NMP were added. After 10 min, the resin was washed 8 × with anhydrous DCM for 30 s and the procedure was repeated once.

63 mg (162 µmol, 4.00 eq) Fmoc-AEEA-COOH was coupled to the resin with 55 mg (146 µmol, 3.60 eq) HBTU, 22 mg (162 µmol, 4.00 eq) HOBt and 193 µl (147 mg, 1.14 mmol, 28.0 eq) DIPEA in 1 ml NMP for 1 h. After washing, 3 × 6 ml 20 % piperidine in NMP were applied for 10 min each for Fmoc deprotection and the resin was washed again. 59 mg (406 µmol, 10.0 eq) glutaric anhydride was coupled with 69 µl (52 mg, 406 µmol, 10.0 eq) DIPEA in 1 ml NMP for 30 min. The resin was washed again with a subsequent additional washing step with 1 % NaOH in dioxane/H_2O (1:1) for 1 min and thereafter washing 4 × each with DCM/NMP (1:1), DCM and NMP. For activation of the glutaric acid, 2 × 73 µl (119 mg, 426 µmol, 10.5 eq) Pfp-OTFA in 2 ml pyridine/DCM (1:1) were applied for 10 min and 20 min respectively. After washing 4 × with NMP only, 30 mg (112 µmol, 2.75 eq) BG-NH_2 in 1 ml DMSO/pyridine (20:1) were coupled to the resin overnight.

Finally, the resin was washed 4 × each with NMP/DCM (1:1), DCM, NMP and Et_2O, swelled 2 × in NMP for 5 min and washed 4 × with DCM. Cleavage from the resin was executed under continuous flow with 20 ml DCM/HFIP (8:2), which was removed under reduced pressure. The resulting crude product was dissolved in 30 % buffer B, filtered and purified via preparative HPLC (30 % B to 65 % B in 55 min), which yielded 15 mg (12.7 µmol, 31 %) chloroalkane-BG-linker-OH as a colorless powder after lyophilisation.

mp = 93.2 °C (H_2O); UV spectrum (PBS): λ_{max} = 283 nm, $\varepsilon_{260\ nm}$ = 2.50 $mM^{-1}cm^{-}1$; t_R = 10.5 min; *m/z* calculated for $[C_{53}H_{83}ClN_{12}O_{16}+H]^+$: 1179.58113, found: 1179.57942.

$(BG)_2$-linker-OH ($(snap)_2$)

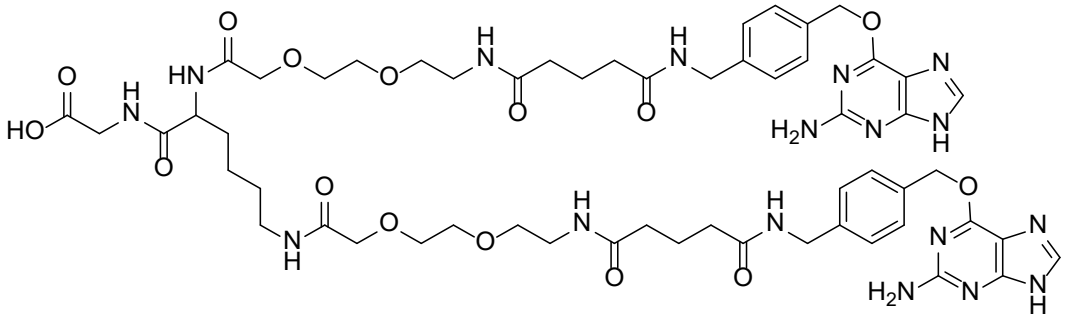

$(BG)_2$-linker-OH

Figure S2. Structure of $(BG)_2$-linker-OH ($(snap)_2$).

All reaction steps were performed at room temperature on a peptide shaker at 1000 rpm. Unless indicated otherwise, washing refers to washing 3 × each with 5 ml NMP/DCM (1:1), then DCM, then NMP.

In a 10 ml syringe with a polyethylene frit, 75 mg (40.6 µmol, 1.00 eq) H-Gly-2-chlorotrityl resin were swelled in NMP for 1 h. 120 mg (203 µmol, 5.00 eq) FmocLys(Fmoc)-OH, 69 mg (183 µmol, 4.50 eq) HBTU, 27 mg (203 µmol, 5.00 eq) and 240 µl (184 mg, 1.42 mmol, 35.0 eq) DIPEA in 1.5 ml NMP were added to the resin and shaken for 1 h. After washing, 3 × 6 ml 20 % piperidine in NMP were applied for 10 min each for Fmoc deprotection and the resin was washed again. Then, 125 mg (325 µmol, 8.00 eq) Fmoc-AEEA-COOH was coupled to the resin with 111 mg (292 µmol, 7.20 eq) HBTU, 44 mg (325 µmol, 8.00 eq) HOBt and 387 µl (294 mg, 2.27 mmol, 56.0 eq) DIPEA in 1.5 ml NMP for 1 h. After washing, 3 × 6 ml 20 % piperidine in NMP were applied for 10 min each for Fmoc deprotection and the resin was washed again. 93 mg (812 µmol, 20.0 eq) glutaric anhydride was coupled with 138 µl (105 mg, 812 µmol, 20.0 eq) DIPEA in 1 ml NMP for 30 min. The resin was washed again with a subsequent additional washing step with 1 % NaOH in dioxane/H_2O (1:1) for 1 min and thereafter washing 4 × each with DCM/NMP (1:1), DCM and NMP. For activation of the glutaric acid, 2 × 146 µl (238 mg, 850 µmol, 21.0 eq) Pfp-OTFA in 3.75 ml pyridine/DCM (1:1) were applied for 10 min and 20 min respectively. After washing 4 × with NMP only, 60 mg (224 µmol, 5.50 eq) BG-NH_2 in 2 ml DMSO/pyridine (20:1) were coupled to the resin overnight.

Finally, the resin was washed 4 × each with NMP/DCM (1:1), DCM, NMP and Et_2O, swelled 2 × in NMP for 5 min and washed 4 × with DCM. Cleavage from the resin was executed under continuous flow with DCM/HFIP/TFA (90:10:0.5), which was removed under reduced pressure. The resulting crude product was dissolved in 7 % buffer B supplemented with 10 % DMSO, filtered and purified via preparative HPLC (5 % B to 50 % B in 40 min), which yielded 25 mg (20.0 µmol, 36 %) $(BG)_2$-linker-OH as a colorless powder after lyophilisation.

UV spectrum (PBS): λ_{max} = 282 nm, $\varepsilon_{260\ nm}$ = 5.00 $mM^{-1}cm^{-1}$; t_R = 8.5 min; *m/z* calculated for $[C_{56}H_{75}N_{17}O_{15}+H]^+$: 1226.57013, found: 1226.57121.

(Chloroalkane)$_2$-linker-OH ((halo)$_2$)

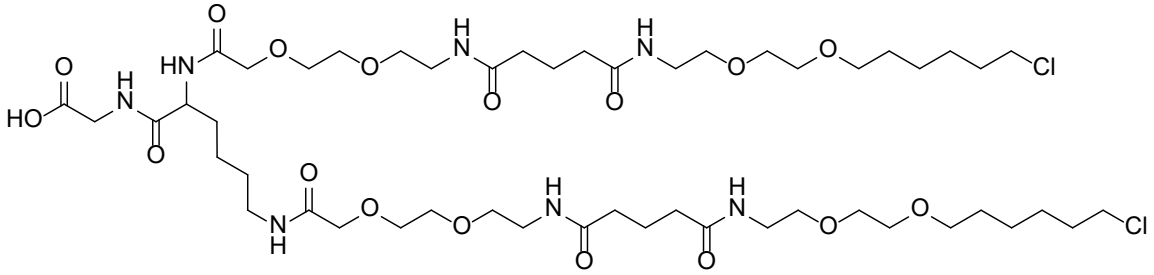

Figure S3. Structure of (chloroalkane)$_2$-linker-OH ((halo)$_2$).

(Chloroalkane)$_2$-linker-OH was obtained via the solid phase peptide synthesis protocol described for (BG)$_2$-linker-OH by coupling 50 mg (224 µmol, 5.50 eq) chloroalkane-NH_2 in 2 ml NMP instead of BG-NH_2. The resulting crude product was dissolved in 33 % buffer B, filtered and purified via preparative HPLC (35 % B to 70 % B in 40 min), which yielded 29 mg (25.7 µmol, 63 %) (chloroalkane)$_2$-linker-OH as a colorless oil after lyophilization.

t_R = 14.8 min; *m/z* calculated for $[C_{50}H_{91}Cl_2N_7O_{17}+Na]^+$: 1154.57407, found: 1154.57269.

TMR-chloroalkane

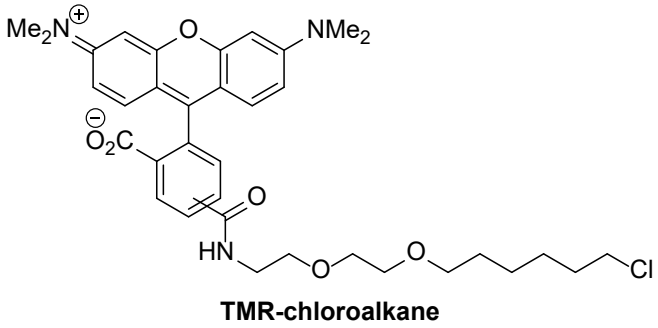

Figure S4. Structure of TMR-chloroalkane.

N-(2-(2-(6-Chloro-hexyloxy)-ethoxy)-ethyl)-tetramethylrhodamine-5(6)-amide (TMR-chloroalkane) was synthesized starting from chloroalkane-NH_2 and 5(6)-carboxytetramethylrhodamine *N*-succinimidyl ester according to literature.[7]

TMR-BG

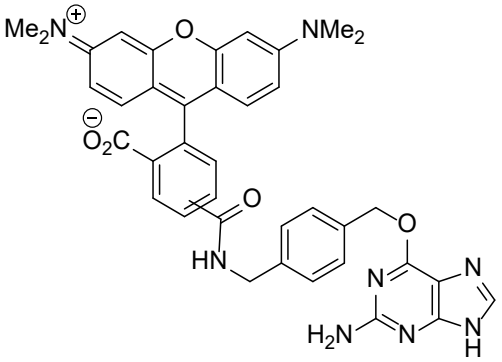

TMR-BG

Figure S5. Structure of TMR-BG.

TMR-BG was obtained via the protocol described for TMR-chloroalkane[7] by using BG-NH_2 instead of chloroalkane-NH_2 and replacing the solvent with DMSO.

UV spectrum (H_2O/MeCN): λ_{max} = 552 nm, $\varepsilon_{543\,nm}$ = 95.826 $mM^{-1}cm^{-1}$; t_R = 11.2 min; LCMS *m/z* found for $[C_{38}H_{34}N_8O_5+2H]^{2+}$: 342.35.

Generation of guideRNAs

As guideRNAs, 22 nt long RNAs with a 5'-C6-aminolinker (NH_2-guideRNAs) that were chemically stabilized in an antagomir-like fashion as described before[8] were applied. All guideRNAs were purchased either from BIOSPRING purified via ion exchange HPLC or from EUROGENTEC purified either via reverse phase HPLC or desalted. guideRNAs that were only desalted were further purified by precipitation with 0.1 volumes of 3 M NaCl and 3.0 volumes of EtOH prior to reaction with the respective self-labeling moiety.

Sequences and extinction coefficients at 260 nm of all guideRNAs used are displayed in Table S1.

Table S1. Sequences and $\varepsilon_{260\,nm}$ of used guideRNAs. Italics = 2'OMe, s = phosphorothioate linkage, lowercase = DNA base.

guideRNA	Target	Sequence	$\varepsilon_{260\,nm}$ / $mM^{-1}cm^{-1}$
NH_2-UAG	eGFP W58X	*UsAsUGUGUCGG* CCA *CGGAAsCsAsGsG*	226.00
snap-UAG	eGFP W58X	*UsAsUGUGUCGG* CCA *CGGAAsCsAsGsG*	228.50
clip-UAG	eGFP W58X	*UsAsUGUGUCGG* CCA *CGGAAsCsAsGsG*	230.24
halo-UAG	eGFP W58X	*UsAsUGUGUCGG* CCA *CGGAAsCsAsGsG*	226.00
NH_2-UAC	GAPDH T211A	*CsCsGAGCGCCA* GCA *GAGGCsAsGsGsG*	222.00
snap-UAC	GAPDH T211A	*CsCsGAGCGCCA* GCA *GAGGCsAsGsGsG*	224.50
halo-UAC	GAPDH T211A	*CsCsGAGCGCCA* GCA *GAGGCsAsGsGsG*	222.00
NH_2-UAU	GAPDH I30V	*CsUsAGGCAACA* ACA *UCCACsUsUsUsA*	224.00
snap-UAU	GAPDH I30V	*CsUsAGGCAACA* ACA *UCCACsUsUsUsA*	226.50
halo-UAU	GAPDH I30V	*CsUsAGGCAACA* ACA *UCCACsUsUsUsA*	224.00
NH_2-CAG	ACTB S323G	*GsAsACAUUGUG* CCG *GGUGCsCsAsGsG*	214.70
snap-CAG	ACTB S323G	*GsAsACAUUGUG* CCG *GGUGCsCsAsGsG*	217.20
halo-CAG	ACTB S323G	*GsAsACAUUGUG* CCG *GGUGCsCsAsGsG*	214.70
halo-snap-CAG	ACTB S323G	*GsAsACAUUGUG* CCG *GGUGCsCsAsGsG*	217.20
$(snap)_2$-CAG	ACTB S323G	*GsAsACAUUGUG* CCG *GGUGCsCsAsGsG*	219.70

(halo)$_2$-CAG	ACTB S323G	*GsAsACAUUGUG* CCG *GGUGCsCsAsGsG*	214.70
NH$_2$-CAG_2	GAPDH T177T	*UsAsCGCAUGGA* CCG *UGGUCsAsUsGsA*	226.00
snap-CAG_2	GAPDH T177T	*UsAsCGCAUGGA* CCG *UGGUCsAsUsGsA*	228.50
halo-CAG_2	GAPDH T177T	*UsAsCGCAUGGA* CCG *UGGUCsAsUsGsA*	226.00
NH$_2$-CAU	GAPDH I38V	*CsAsAGAGGUCA* ACG *AAGGGsGsUsCsA*	238.00
snap-CAU	GAPDH I38V	*CsAsAGAGGUCA* ACG *AAGGGsGsUsCsA*	240.50
halo-CAU	GAPDH I38V	*CsAsAGAGGUCA* ACG *AAGGGsGsUsCsA*	238.00
halo-snap-CAU	GAPDH I38V	*CsAsAGAGGUCA* ACG *AAGGGsGsUsCsA*	240.50
(snap)$_2$-CAU	GAPDH I38V	*CsAsAGAGGUCA* ACG *AAGGGsGsUsCsA*	243.00
(halo)$_2$-CAU	GAPDH I38V	*CsAsAGAGGUCA* ACG *AAGGGsGsUsCsA*	238.00
NH$_2$-eGFP	eGFP W58X + T63M	*GsUsGUAGUGUCGG* CCA *CGGAAsCsAsGsG*	249.00
snap-eGFP	eGFP W58X + T63M	*GsUsGUAGUGUCGG* CCA *CGGAAsCsAsGsG*	251.50
halo-eGFP	eGFP W58X + T63M	*GsUsGUAGUGUCGG* CCA *CGGAAsCsAsGsG*	249.00
halo-snap-GFP	eGFP W58X + T63M	*GsUsGUAGUGUCGG* CCA *CGGAAsCsAsGsG*	251.00
mod-NH$_2$-eGFP	eGFP T63M	*UUUUAGUGUCGGCCACGGAACAGG*	238.6
mod-snap-eGFP	eGFP T63M	*UUUUAGUGUCGGCCACGGAACAGG*	241.1
NH$_2$-UAU	ACTB I5V	*CsUsCCGCGGCG* ACA *UCAUCsAsUsCsC*	199.60
(halo)$_2$-UAU	ACTB I5V	*CsUsCCGCGGCG* ACA *UCAUCsAsUsCsC*	199.60
NH$_2$-ACC	GAPDH T52I	*CCUAUCAUAUUGGAACAUGUAAAC*	247.20
(snap)$_2$-ACC	GAPDH T52I	*CCUAUCAUAUUGGAACAUGUAAAC*	252.20
anti-(snap)$_2$-ACC		atggtttacatgttccaatatgatagg	
snap-UAG_2	ACTB 3'-UTR	*UsCsGAGCAAUG* CCA *UCACCsUsCsCsC*	209.50

Constructs for stable cell lines

The sequences of the respective constructs are attached as Appendix. Furthermore, full plasmid maps with assigned features and restriction sites are additionally supplied as SnapGene files.

Single cell lines

SA1Q, CA1Q and HA1Q were cloned in a pcDNA 5 vector under control of the CMV promoter followed by two copies of the *tet* operator (TetO$_2$) via restriction/ligation (BamHI/NotI, NEW ENGLAND BIOLABS). C-terminally, a Myc- and a His-tag, followed by the targeted UAG codon in the 3'-UTR, were attached.

HA1Q / SA2Q duo cell lines 1 – 5

Constructs for HA1Q / SA2Q duo cell lines **1** – **5** were cloned in a pcDNA 5 vector via restriction/ligation (BamHI/ApaI/NotI/ClaI for **1**, **2**; BamHI/PacI for **3**; ClaI/NotI/BamHI/PacI for **4**, **5**).

HA1Q / APO1S duo cell lines 6 – 9

Constructs for HA1Q / APO1S duo cell lines **6** – **9** were cloned in a pcDNA 5 vector via restriction/ligation (BamHI/ApaI/NotI/ClaI for **6**, **7**; ClaI/NotI/BamHI/PacI for **8**, **9**).

Immunostaining of single cell lines

Unless stated otherwise, incubation steps were performed at room temperature.

For immunostaining, coverslips in 4 wells of a 24 well plate were coated with 500 µl poly-D-lysine hydrobromide (0.1 mg/ml in Millipore water) for 30 min. After washing with 500 µl Millipore water and 500 µl PBS, the well plate was irradiated with a UV lamp for 30 min and subsequently allowed to dry for further 30 min. $1.2 \cdot 10^5$ SA1Q or HA1Q 293 Flp-In T-REx cells were seeded in 500 µl DMEM/FBS/B/H for – Dox samples or 500 µl DMEM/FBS/B/H/10 ng/ml doxycycline (DMEM/FBS/B/H/10 D) for + Dox samples respectively.

After 24 h, medium was removed and coverslips were washed wit 500 µl PBS. Cells were incubated with 500 µl 3.7 % formaldehyde in PBS for 20 min and washed 3 × with 500 µl PBS. For permeabilization, 500 µl 1 % Triton X-100 in PBS were added, incubated for 5 min and washed 3 × with 500 µl PBS. Then, cells were incubated with 500 µl 10 % FBS in PBS for 1.5 h and subsequently with 200 µl mouse α-Myc (1:1.000 in 10 % FBS in PBS, SIGMA ALDRICH M4439) for 2 h. Washing with 3 × 500 µl PBS was followed by incubation with 250 µl goat α-mouse Alexa Fluor 488 (1:1.000 in 10 % FBS in PBS, THERMO FISHER SCIENTIFIC A11001) for 1 h. After washing with 2 × 500 µl PBS, nuclei were stained with 200 µl NucBlue™ Live ReadyProbes™ Reagent Hoechst33342 (1:100 in PBS, THERMO FISHER SCIENTIFIC R37605) for 30 min and washed again with 2 × 500 µl PBS. Coverslips were then mounted to object slides with Fluorescence Mounting Medium by DAKO and dried overnight at 4 °C. Microscopy was performed with a ZEISS AXIO Observer.Z1 with a Colibri.2 light source under 63× magnification. For excitation and emission wavelengths, see *Table S2*.

Table S2. Excitation and emission wavelengths λ.

Channel	**green**		**blue**		**red**	
	λ	band pass filter	λ	band pass filter	λ	band pass filter
Excitation	488 nm	460 – 488 nm	353 nm	350 – 390 nm	587 nm	567 – 602 nm
Emission	509 nm	500 – 557 nm	465 nm	402 – 448 nm	610 nm	615 – 4095 nm

FITC-BG & TMR-chloroalkane staining of duo cell lines

Unless stated otherwise, incubation steps were performed at room temperature.

For FITC-BG and TMR-chloroalkane staining, coverslips in 10 wells of a 24 well plate were coated with 500 µl poly-D-lysine hydrobromide (0.1 mg/ml in Millipore water) for 30 min. After washing with 500 µl Millipore water and 500 µl PBS, the well plate was irradiated with a UV lamp for 30 min and subsequently allowed to dry for further 30 min. $5 \cdot 10^4$ 293 Flp-In T-REx cells from cell lines **1** – **5** were seeded in 500 µl DMEM/FBS/B/H for – Dox samples or 500 µl DMEM/FBS/B/H/10 D for + Dox samples respectively.

After 24 h, 303 µl of the medium were removed and replaced with 1 µl DMEM/FBS/B/H containing 0.4 mM FITC-BG and 1.0 mM TMR-chloroalkane and 2 µl NucBlue™ Live ReadyProbes™ Reagent Hoechst33342 (THERMO FISHER SCIENTIFIC R37605). After incubation for 30 min, 21.6 µl 37 % aqueous formaldehyde were added, cells were incubated for 3 min and subsequently washed 3 × with 200 µl PBS. For permeabilization, cells were incubated with 200 µl 0.1% Triton X-100 in PBS for 15 min and washed 3 × with 200 µl PBS. Coverslips were then mounted to object slides with Fluorescence Mounting Medium by DAKO and dried overnight at 4 °C. Microscopy was performed with a ZEISS AXIO Observer.Z1 with a Colibri.2 light source under 63× magnification. For excitation and emission wavelengths, see *Table S2*.

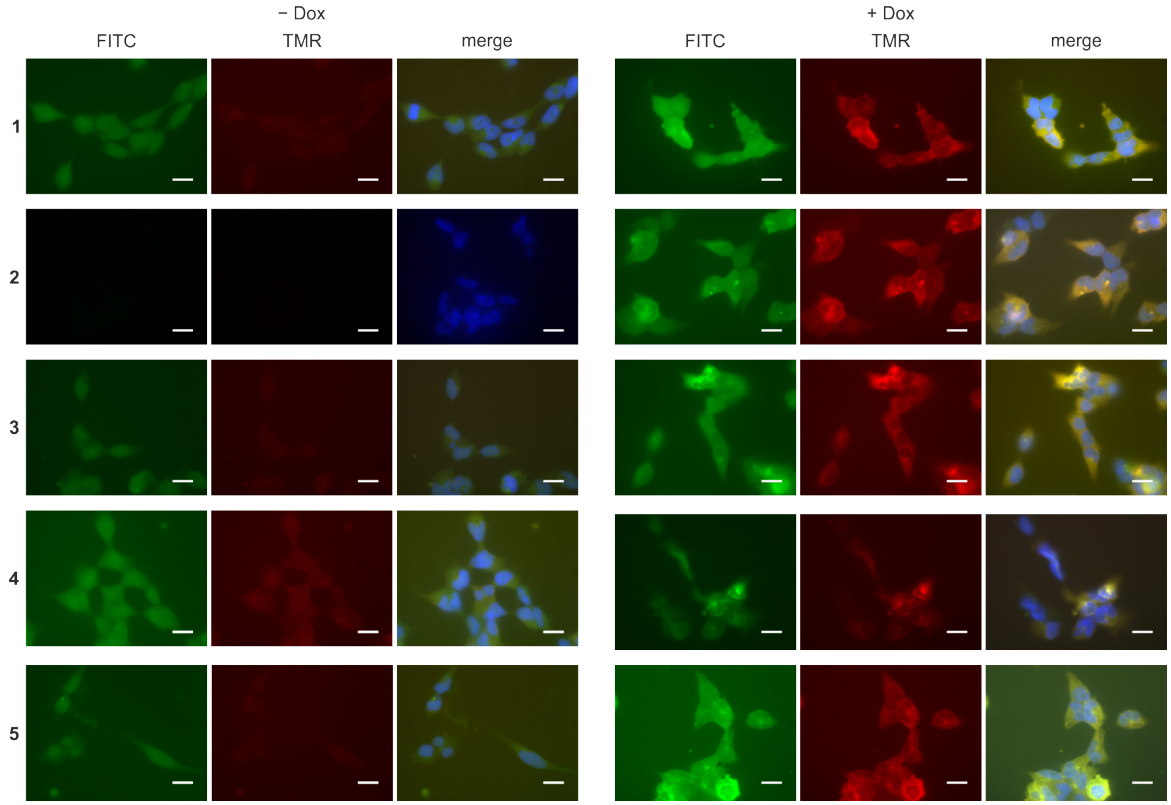

*Figure S6. FITC-BG (green channel) and TMR-chloroalkane (red channel) staining of cell lines **1** – **5** without (left panel) and with (right panel, same as Fig. 2b) doxycycline induction. Cell nuclei are stained with Hoechst33342 (blue channel).*

SDS-PAGE & Western Blotting

Expression in single cell lines

$1 \cdot 10^5$ SA1Q or HA1Q 293 Flp-In T-REx cells respectively were seeded in 500 µl medium in 2 wells per condition of a 24 well plate. For the uninduced samples (–) and the samples with 24 h of doxycycline induction (+), DMEM/FBS/B/H was used as medium; for the samples with 48 h of doxycycline induction (++) DMEM/FBS/B/H/10 D was used. After 24 h, the medium of the + samples was replaced by DMEM/FBS/B/H/10 D. After another 24 h, medium was removed and cells were washed with 500 µl PBS. After treatment with 60 µl trypsin-EDTA solution from SIGMA ALDRICH, 440 µl DMEM/FBS were added and cells were transferred to reaction tubes. Centrifugation for 5 min at 1.600 rpm was followed by washing with 500 µl PBS and resuspension of the cell pellets in 100 µl urea lysis buffer (8 M urea, 100 mM NaH_2PO_4, 10 mM Tris, pH 8.0). Cells were lysed via shear force by drawing the solution up and out a 19 gauge syringe 6×. After centrifugation for 15 min at 16.000 rpm and 4 °C, supernatants were transferred to fresh reaction tubes and total protein concentration of the samples was determined via Bradford assay from SIGMA ALDRICH.

7 µg protein lysate in 13.33 µl urea lysis buffer were heated with 4 µl 6× Laemmli buffer (0.4 M SDS, 60 mM Tris pH 6.8, 6.5 M glycerol, 0.6 M dithiothreitol, 0.9 mM bromophenol blue) for 5 min at 95 °C and 700 rpm and subsequently loaded to an SDS-PAGE, which was run at 80 V for 1.5 h followed by 120 V for 45 min. Transfer onto a PVDF membrane (BIO-RAD LABORATORIES) was performed at 30 V and 4 °C for 18 h. After blocking in 5 % dry milk in TBST containing 50 µg/ml avidin for 1 h, the blot was incubated with mouse α-Myc (1:5.000, SIGMA ALDRICH M4439) and mouse α-ACTB (1:40.000, SIGMA-

Aldrich A5441) in 5 % dry milk-TBST for 2 h at room temperature as primary antibodies. As secondary antibody, goat α-mouse HRP (1:10.000, JACKSON IMMUNORESEARCH 115-035-003) with added Precision Protein StrepTactin HRP conjugate (for visualisation of the Precision Plus Western C Standard, 1:25.000, BIO-RAD) in 5 % dry milk-TBST was applied for 2 h at room temperature. Chemiluminescence was measured with a FUSION FX by VILBER.

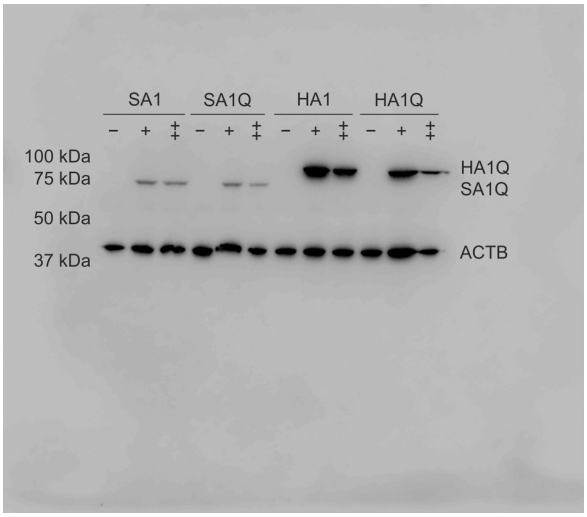

Figure S7. Full Western Blot (from Fig. 1c) of SA1, SA1Q, HA1 and HA1Q 293 Flp-In T-REx cells without (–), with 24 h (+) or 48 h (++) doxycycline induction. The different ADAR fusions were detected via a C-terminally attached Myc-tag, ACTB served as loading control.

GuideRNA-protein conjugation assay

For detection of the respective editing enzyme-guideRNA conjugate, SA1Q and HA1Q 293 Flp-In T-REx cells were transfected with varying amounts of snap- or halo-guideRNA, respectively, and characterized via Western Blot. For comparison, an additional serial dilution of the editing enzyme without guideRNA and an uninduced control sample (–) were loaded side by side. The experiment was conducted completely analogous to editing experiments of endogenous targets, differing only in the 5× greater scale to ensure sufficient protein amounts for Western Blot detection.

$2 \cdot 10^6$ SA1Q or HA1Q 293 Flp-In T-REx cells were seeded in a 6 well plate in 2.5 ml DMEM/FBS/B/H for – Dox samples or 2.5 ml DMEM/FBS/B/H/10 D for + Dox samples respectively. After 24 h, $4 \cdot 10^5$ cells were reverse transfected in a 24 well plate with 5.0, 25, 50 or 125 pmol (corresponding to 1.0, 5.0, 10 or 25 pmol per $8 \cdot 10^4$ cells on the editing experiment's scale) snap- or halo-ACC respectively with 2.5 µl Lipofectamine 2000. Doxycycline concentration for + Dox samples was kept at 10 ng/ml and after further 24 h medium was removed and cells were washed with 500 µl PBS. Cells were lysed with 70 µl 1× Laemmli (67 mM SDS, 10 mM Tris pH 6.8, 1.1 M glycerol, 0.10 M dithiothreitol, 0.15 mM bromophenol blue) in RIPA Lysis and Extraction Buffer (1 % NP-40, 150 mM NaCl, 25 mM Tris·HCl pH 7.6, 1 % sodium deoxycholate, 0.1 % SDS, THERMO FISHER SCIENTIFIC; supplemented with 1 tablet cOmplete™ Mini EDTA-free Protease Inhibitor Cocktail by ROCHE per 10 ml) and cell lysates were immediately frozen in liquid nitrogen. For SDS-PAGE, protein lysates were heated for 15 min at 95 °C and 1500 rpm and 20 µl of the respective lysate or the indicated dilution in 1× Laemmli in RIPA Lysis and Extraction buffer were loaded and run at 90 V for 5 min followed by 200 V for 110 min. Transfer onto a PVDF membrane (BIO-RAD LABORATORIES) was performed at 35 V and 4 °C for 16 h. After blocking in 5 % dry milk in TBST for 1 h, the blot was incubated with first rabbit α-ADAR1 (1:1.000, BETHYL LABORATORIES A303-884) in 5 % dry milk-TBST for 2 h at room temperature and subsequently with rabbit α-GAPDH (1:1.000, CELL SIGNALING

#5174) in 5 % dry milk-TBST overnight at 4 °C as primary antibodies. As secondary antibody, goat α-rabbit HRP (1:10.000, JACKSON IMMUNORESEARCH 111-035-003) in 5 % dry milk-TBST was applied for 2 h at room temperature. Chemiluminescence was measured with an Odyssey Fc Imaging System (LI-COR).

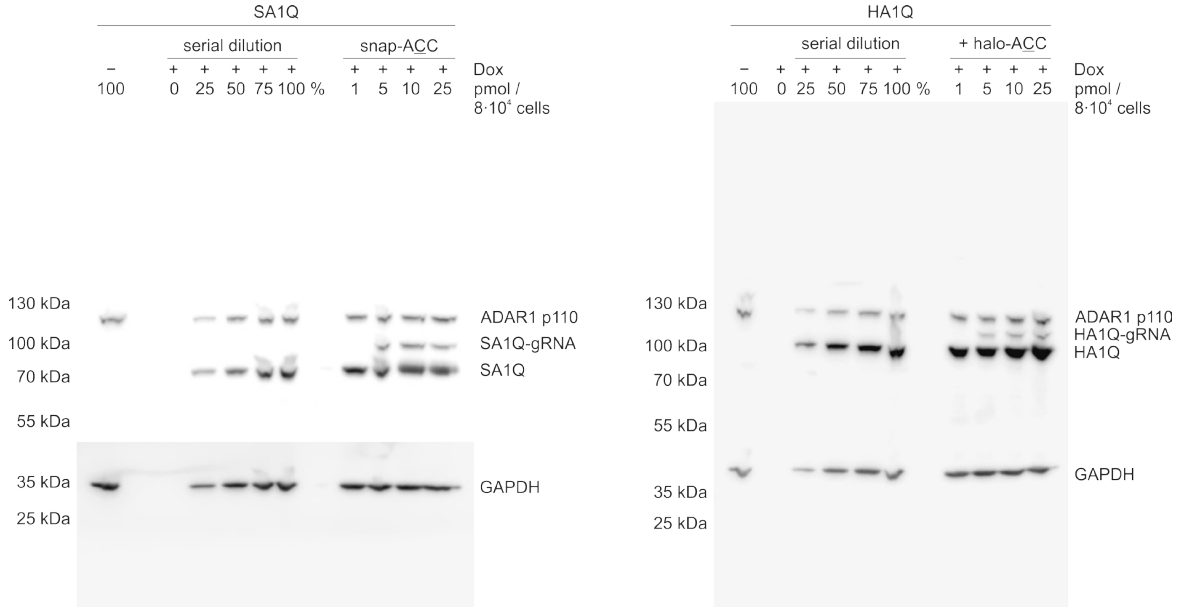

Figure S8. Full Western Blots (from Fig. 1e) of SA1Q and HA1Q 293 Flp-In T-REx cells after transfection of 1.0, 5.0, 10 or 25 pmol snap- or halo-ACC per 8·10⁴ cells, respectively. On the left, a sample without doxycycline induction (–) and a serial dilution of 0, 25, 50, 75 or 100 % lysate from cells induced with doxycycline (+), but without guideRNA are shown. For detection, an α-ADAR1 antibody was used, staining the different ADAR proteins (SA1Q, HA1Q), its guideRNA conjugates (SA1Q-gRNA, HA1Q-gRNA), but also endogenous ADAR1 p110; GAPDH served as loading control. The SA1Q blot was cut above GAPDH before detection.

Expression in duo cell lines

$2 \cdot 10^5$ 293 Flp-In T-REx cells from the respective duo cell line were seeded in 500 µl medium in 2 wells of a 24 well plate per condition. For the uninduced samples (– Dox) DMEM/FBS/B/H was used as medium, for the samples with doxycycline induction (+ Dox) DMEM/FBS/B/H/10 D was used. After 24 h, medium was removed and cells were first washed with 500 µl PBS and then detached and suspended in 500 µl fresh PBS per well. Centrifugation for 5 min at 1.600 rpm was followed by removal of PBS and resuspension of the cell pellets in 30 µl NP40 lysis buffer (1 % NP-40, 150 mM NaCl, 50 mM Tris pH 8.0; 1 tablet cOmplete™ Mini EDTA-free Protease Inhibitor Cocktail by ROCHE per 10 ml). After centrifugation for 15 min at 16.000 rpm and 4 °C, supernatants were transferred to fresh reaction tubes and total protein concentration of the samples was determined via Pierce BCA Protein Assay Kit by THERMO FISHER SCIENTIFIC.

For co-staining with TMR-BG and TMR-chloroalkane, 10 µg protein lysate was incubated with 5 µM TMR-BG and TMR-chloroalkane each in 13.33 µl NP40 lysis buffer for 30 min at 37 °C and 600 rpm. 4 µl 6× Laemmli buffer (0.4 M SDS, 60 mM Tris pH 6.8, 6.5 M glycerol, 0.6 M dithiothreitol, 0.9 mM bromophenol blue) were added, samples were heated for 5 min at 95 °C and 700 rpm and subsequently loaded to an SDS-PAGE. TMR staining on the completed SDS-PAGE was visualized on a FLA 5100 by FUJIFILM with excitation at 532 nm and emission at 557 nm (Cy3 filter set) and a resolution of 10 µm.

Transfer onto a PVDF membrane (BIO-RAD LABORATORIES) was performed at 28 V and 4 °C for 18.5 h. After blocking in 5 % dry milk in TBST containing 50 µg/ml avidin for 1 h, the blot was incubated with first mouse α-ACTB (1:40.000, SIGMA-Aldrich A5441) in 5 % dry milk-TBST for 2 h at room temperature and subsequently with rabbit α-SNAP-tag (1:1.000, NEW ENGLAND BIOLABS P9310S) and rabbit α-HaloTag (1:1.000, PROMEGA G9281) in 5 % dry milk-TBST overnight at 4 °C as primary antibodies. As secondary antibodies, first goat α-mouse HRP (1:5.000, JACKSON IMMUNORESEARCH 115-035-003) with added Precision Protein StrepTactin HRP conjugate (for visualisation of the Precision Plus Western C Standard, 1:25.000, BIO-RAD) in 5 % dry milk-TBST was applied for 2 h at room temperature, followed by goat α-rabbit HRP (1:5.000, JACKSON IMMUNORESEARCH 111-035-003) for 2 h at room temperature. Chemiluminescence was measured with a FUSION FX by VILBER.

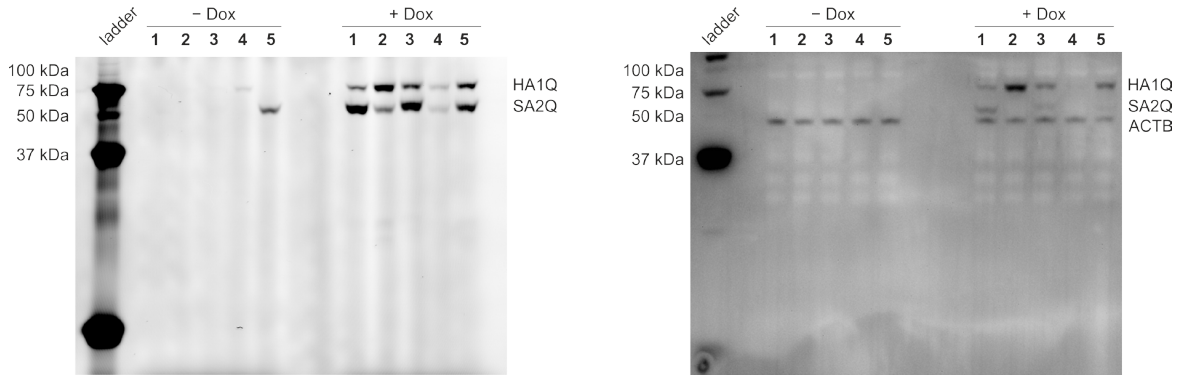

*Figure S9. TMR stained SDS-PAGE (left panel, from Fig. 2c) and Western Blot (right panel) of HA1Q / SA2Q 293 Flp-In T-REx duo cells **1** – **5** without (– Dox) and with (+ Dox) doxycycline induction. The different ADAR fusions were detected via co-staining with TMR-BG and TMR-chloroalkane or antibodies against SNAP-tag and HaloTag respectively, ACTB served as loading control.*

Editing experiments

All editing experiments depicted in bar graphs were conducted in biological triplicates and standard deviations are shown. The exact editing yields can also be found in tabular form as additional supporting file.

Editing under transient expression of editing enzymes

As a first test, editing of a premature stop codon (W58X) in eGFP with transiently expressed $SNAP_f$-, $CLIP_f$- and HALO-ADAR1 (wildtype deaminase domain) was compared.

$2 \cdot 10^5$ wildtype 293T cells were seeded in 500 µl DMEM/FBS/1 % penicillin/1 % streptomycin (DMEM/FBS/P/S) in a 24 well plate. After 24 h, medium was replaced with 450 µl DMEM/FBS and 500 ng eGFP W58X in pcDNA 3.1 plus either 100 ng $SNAP_f$-, $CLIP_f$- or HALO-ADAR1 in pcDNA 3.1 were forward transfected with 2.4 µl Lipofectamine 2000. 24 h thereafter, $6 \cdot 10^4$ cells were reverse transfected in a 96 well plate with 10 pmol of the respective guideRNA with 2.2 µl Lipofectamine 2000. After further 24 h, cells were examined under a ZEISS AXIO Observer.Z1 microscope with a Colibri.2 light source under 5× magnification for successfully edited and therefore fluorescent eGFP. For excitation and emission wavelengths, see *Table S2*. Then, cells were harvested and RNA isolation was performed with the Monarch® RNA cleanup kit from NEW ENGLAND BIOLABS, followed by DNase I digestion. eGFP RNA was reverse transcribed to cDNA, which was amplified via Taq PCR and subsequently analyzed with Sanger sequencing (either EUROFINS GENOMICS or MICROSYNTH). A-to-I

editing yields were determined by dividing the peak height for guanosine by the sum of the peak heights for both adenosine and guanosine.

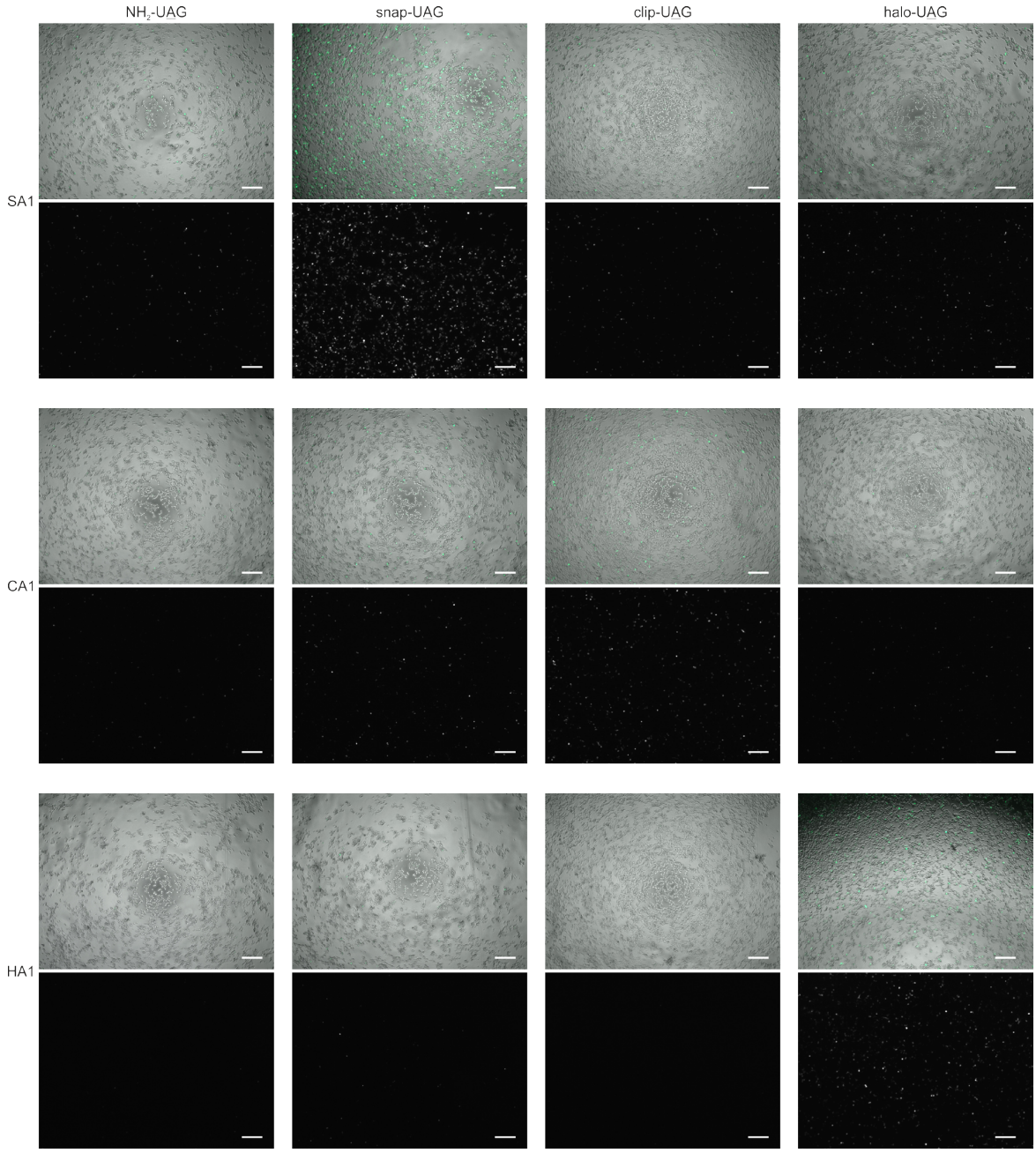

Figure S10. eGFP fluorescence (lower panels) and overlays with bright field images (upper panels) of wildtype 293T cells transiently transfected with eGFP W58X and either SA1, CA1 or HA1 after transfection of 10 pmol NH_2- (negative control), snap-, clip- or halo-UAG guideRNA. Scale bars correspond to 250 µm.

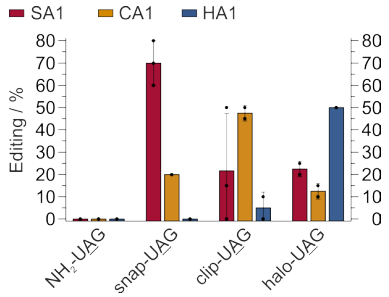

Figure S11. Editing efficiencies and orthogonality of NH_2- (negative control), snap-, clip- and halo-UAG targeting a premature W58X stop codon in eGFP in wildtype 293T cells transiently expressing either SA1, CA1 or HA1. The guideRNAs differ only in the indicated self-labeling moiety. The NH_2-guideRNA refers to a control guideRNA lacking a self-labeling moiety.

Editing of endogenous targets under genomic expression of editing enzymes

$4 \cdot 10^5$ of the respective 293 Flp-In T-REx cells were seeded in 500 µl DMEM/FBS/B/H/10 D in a 24 well plate. After 24 h, $8 \cdot 10^4$ cells were reverse transfected in a 96 well plate with the respective amount of the guideRNA to be examined with 0.5 µl Lipofectamine 2000. Doxycycline concentration was kept at 10 ng/ml and after further 24 h (or 48 h for cell lines expressing APO1S) cells were harvested. RNA isolation was performed with the Monarch® RNA cleanup kit from NEW ENGLAND BIOLABS, followed by DNase I digestion. Samples containing $(snap)_2$-ACC were treated with a DNA oligonucleotide of complementary sequence (anti-$(snap)_2$-ACC, 1 µM) at 95 °C for 3 min to trap the guideRNA. Purified RNA was then reverse transcribed to cDNA, which was amplified via Taq PCR and subsequently analyzed with Sanger sequencing (either EUROFINS GENOMICS or MICROSYNTH). A-to-I editing yields were determined by dividing the peak height for guanosine by the sum of the peak heights for both adenosine and guanosine, C-to-U editing yields by dividing the peak height for thymidine by the sum of the peak heights for both cytidine and thymidine.

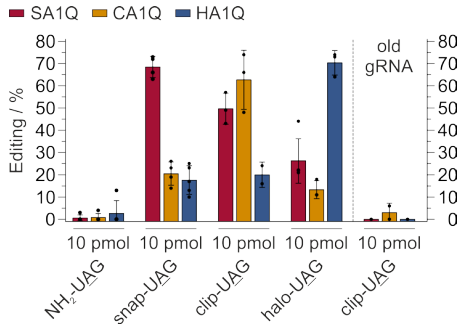

Figure S12. Editing efficiencies and orthogonality of NH_2- (negative control), snap-, clip- and halo-UAG targeting a 5´-UAG reporter codon in the 3'-UTR in three different cell lines, each expressing one ADAR1 fusion protein (SNAP-ADAR1Q (SA1Q), CLIP-ADAR1Q (CA1Q), HALO-ADAR1Q), as indicated. clip-guideRNA shows loss of activity upon long-term storage.

*Table S3. Screening of duo cell lines **1** – **5**. Maximum editing yield and selectivity after single or co-transfection of a snap- and/or a halo-guideRNA (snap-/halo-CAG_2 and snap-/halo-CAU, 5.0 pmol each) for a CAG and a CAU codon in the ORF of GAPDH.*

Cell line	**1**		**2**		**3**		**4**		**5**	
	CAG	CAU	CAG	CAU	CAG	CAU	CAG	CAU	CAG	CAU
Editing yield	50 %	10 %	35 %	35 %	45 %	15 %	7 %	5 %	45 %	30 %
Selectivity	3.3x	∞	-	∞	1.2x	6.8x	-	-	1.2x	∞

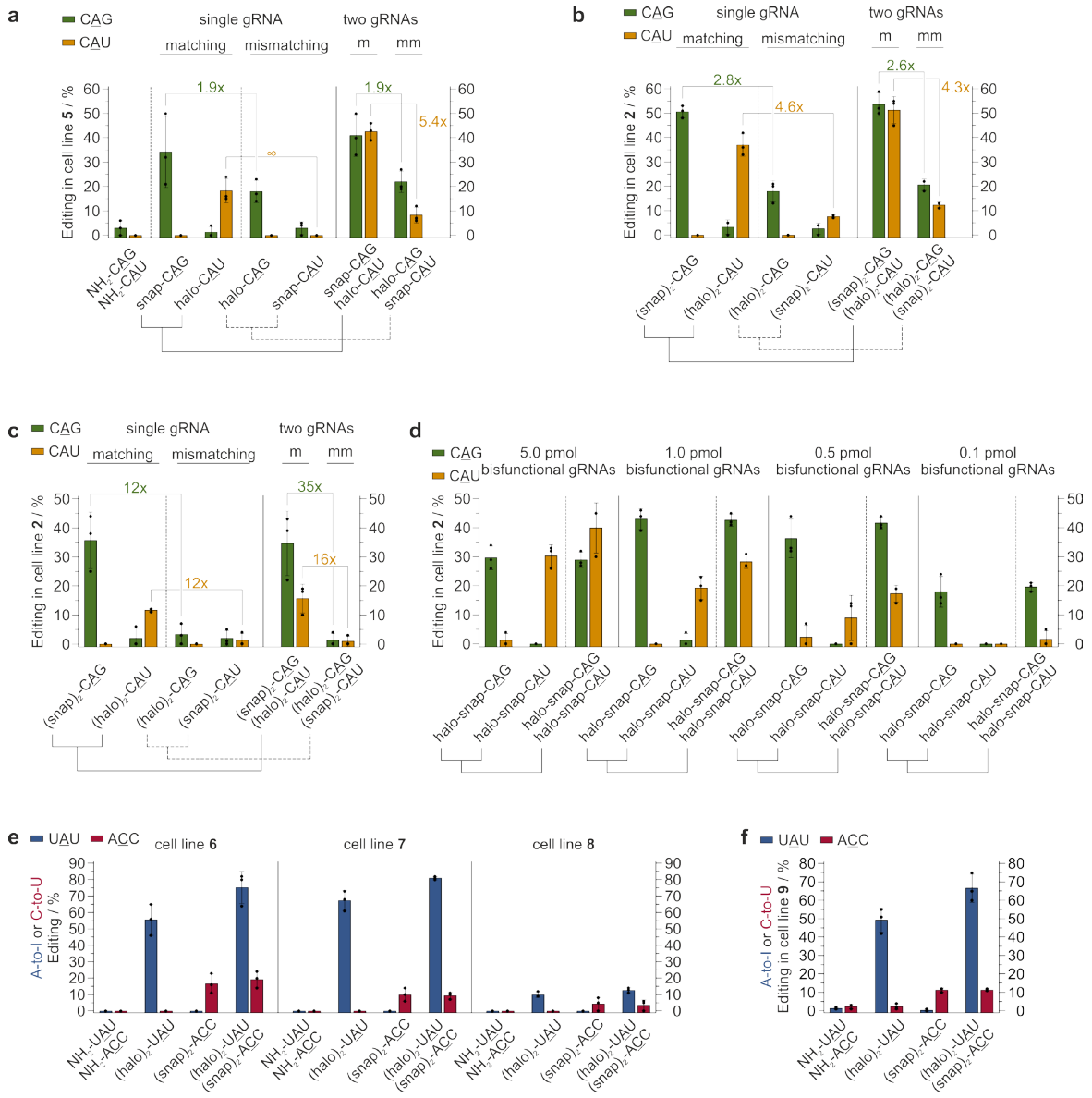

*Figure S13. **a)** Editing yield and selectivity after transfection of a single (5.0 pmol), matching or mismatching snap- or halo-guideRNA (left panel) into duo cell line **5** compared to the co-transfection of two guideRNAs (one snap- and one halo-guideRNA, each 5.0 pmol) either in matching (m) or in mismatching (mm) combination **b)** Editing yield and selectivity in duo cell line **2** after transfection of 1.0 pmol of a single $(snap)_2$- or $(halo)_2$-guideRNA or after co-transfection of a $(snap)_2$- and a $(halo)_2$-guideRNA, either in matching (m) or mismatching (mm) combination respectively. **c)** Same as b) but*

with 0.1 pmol guideRNAs. ***d)*** *Concentration dependency of editing yield in duo cell line* ***2*** *after transfection of either a single or two (same as Fig. 3h) bisfunctional halo-snap-guideRNAs.* ***e)*** *Editing yield in duo cell lines* ***6****,* ***7*** *and* ***8*** *after transfection of a single or cotransfection of two guideRNAs, one* $(halo)_2$*-guideRNA for A-to-I editing in ACTB and one* $(snap)_2$*-guideRNA for C-to-U editing in GAPDH (5.0 pmol each). As expected from the transgene expression, cell line* ***8*** *(construct analog to cell line* ***4****) shows only minor editing.* ***f)*** *Same as e) but with 2.5 pmol guideRNAs in duo cell line* ***9****.*

Editing of a transfected reporter transcript under genomic expression of editing enzymes

$2 \cdot 10^5$ of the respective 293 Flp-In T-REx cells were seeded in 500 µl DMEM/FBS/B/H/10 D in a 24 well plate. 24 h thereafter, each well was forward transfected with 300 ng pcDNA 3.1 containing the coding sequence for eGFP-W58X with 1.2 µl Lipofectamine 2000. After 24 h, $8 \cdot 10^4$ cells were reverse transfected in a 96 well plate with the respective amount of the guideRNA to be examined with 0.5 µl Lipofectamine 2000. Doxycycline concentration was kept at 10 ng/ml and after further 48 h cells were harvested. RNA isolation was performed with the Monarch® RNA cleanup kit from NEW ENGLAND BIOLABS, followed by DNase I digestion. RNA was then reverse transcribed to cDNA, which was amplified via Taq PCR and subsequently analyzed with Sanger sequencing (either EUROFINS GENOMICS or MICROSYNTH). A-to-I editing yields were determined by dividing the peak height for guanosine by the sum of the peak heights for both adenosine and guanosine, C-to-U editing yields by dividing the peak height for thymidine by the sum of the peak heights for both cytidine and thymidine.

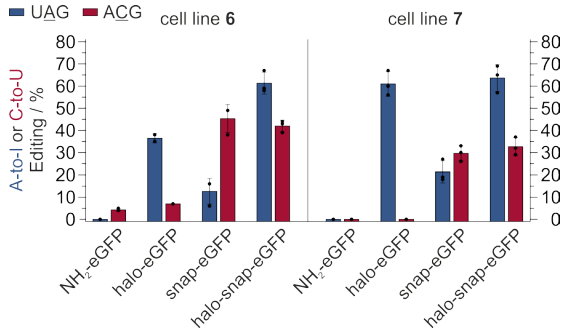

Figure S14. Editing yield in cell lines ***6*** *and* ***7*** *from concurrent A-to-I and C-to-U editing in an eGFP reporter transcript after transfection of a halo-, snap- or halo-snap-guideRNA (5.0 pmol).*

Benchmark with RESCUE

For guideRNA expression in RESCUE editing experiments, DNA oligonucleotides (Table S4) were golden-gate cloned into the guideRNA expression vector (Addgene #103852) as previously described.[9] As per requirement of the U6 promoter, a 5'-G was added in case the sequence did not start with one.

Table S4. Sequences and C or U flip positions of guideRNAs applied for editing with RESCUE. Sequences are shown in 5'-orientation. For cloning, the listed sequences and the complementary strands were preceded by a 5'-CACC or 5'-CAAC respectively.

Flip position	Target	Sequence
C flip 26	eGFP T63M	gcgt cct cactagtgtcggccacggaacagg
C flip 24	eGFP T63M	gagcgt cct cactagtgtcggccacggaaca
C flip 22	eGFP T63M	gagagcgt cct cactagtgtcggccacggaa
C flip 20	eGFP T63M	ggcagagcgt cct cactagtgtcggccacgg

C flip 26	GAPDH T52I	gatg gct ggaatcatattggaacatgtaaac
C flip 24	GAPDH T52I	gccatg gct ggaatcatattggaacatgtaa
C flip 22	GAPDH T52I	gtgccatg gct ggaatcatattggaacatgt
C flip 20	GAPDH T52I	gtttgccatg gct ggaatcatattggaacat
U flip 24	PPIB R7C	gtgttg ctt tcggagaggcgcagcatccaca
C flip 24	PPIB R7C	gtgttg cct tcggagaggcgcagcatccaca
C flip 22	PPIB R7C	gcatgttgc cct cggagaggcgcagcatcca
C flip 20	PPIB R7C	gttcatgttgc cct cggagaggcgcagcatc

Editing experiments were conducted as previously described.[9] Briefly, $2 \cdot 10^4$ 293FT cells were seeded in 150 µl DMEM/FBS in a 96 well plate. 16 h thereafter, cells were forward transfected with 150 ng RESCUEr16 expression vector (Addgene #130661), 300 ng corresponding guideRNA expression vector (sequences see Table S4) and 40 ng eGFP in pcDNA 3.1 with 0.5 µl Lipofectamine 2000. To ensure equal treatment of cells, eGFP in pcDNA 3.1 was also transfected to editing experiments targeting endogenous transcripts. After 48 h, cells were harvested and RNA isolation was performed with the Monarch® RNA cleanup kit from NEW ENGLAND BIOLABS, followed by DNase I digestion. RNA was then reverse transcribed to cDNA, which was amplified via Taq PCR and subsequently analyzed with Sanger sequencing (either EUROFINS GENOMICS or MICROSYNTH). C-to-U editing yields were determined by dividing the peak height for thymidine by the sum of the peak heights for both cytidine and thymidine, A-to-I bystander editing yields by dividing the peak height for guanosine by the sum of the peak heights for both adenosine and guanosine.

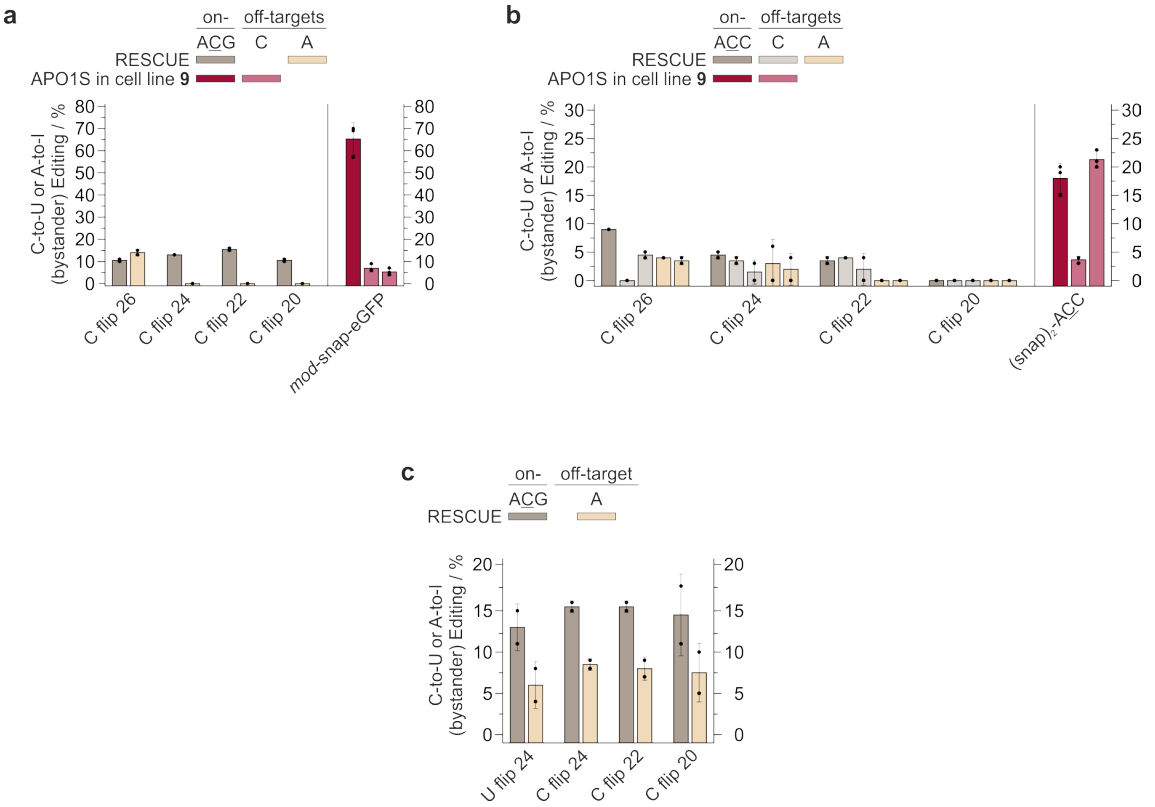

Figure S15. *Comparison of C-to-U editing yield on the same target C with RESCUEr16[9] vs. APO1S in cell line **9**. For RESCUE, four different guideRNA designs with a C or U flip at the indicated position were tested for each target, as recommended by Abudayyeh et al.[9] **a)** Editing of an eGFP reporter transcript*

with C flip 26 – 20 (300 ng) for RESCUEr16 and mod-snap-eGFP (5.0 pmol) for APO1S. ***b)*** *Editing of endogenous GAPDH with C flip 26 – 20 for RESCUEr16 (300 ng) and (snap)$_2$-ACC (5.0 pmol) for APO1S.* ***c)*** *Control for RESCUEr16 with editing in endogenous PPIB with U or C flip 24 – 20 (300 ng). The positions of the respective bystander off-targets are summarized in Table S5. Data shown as the mean ± s.d. of N = 2 – 3 independent experiments.*

Table S5. Positions of bystander off-targets in C-to-U editing with RESCUEr16 or APO1S in cell line ***9*** *from Figure S15.*

Target	Editase	Off-target	Distance to on-target / bp
eGFP T63M	RESCUE	A	– 5
	APO1S in cell line **9**	C #1	+ 30
		C #2	+ 46
GAPDH T52I	RESCUE	C #1	+ 1
		C #2	+ 21
		A #1	– 9
		A #2	– 6
	APO1S in cell line **9**	C #1	+ 21
		C #2	+ 253
PPIB R7C	RESCUE	A	– 4

Next generation sequencing

HA1Q / SA2Q duo cell line

For NGS, four samples were prepared, i.e. a duplicate of an empty transfection and a duplicate of a guideRNA transfection, both in doxycycline-induced cell line **2**. $2 \cdot 10^6$ cells from cell line **2** were seeded in 2.5 ml DMEM/FBS/B/H/10 D in a 6 well plate. After 24 h, $8 \cdot 10^4$ cells per well were reverse transfected in 5 wells of a 96 well plate per sample. For the duplicate of the empty transfection, the cells were treated with an empty reverse transfection with 0.5 µl Lipofectamine 2000 only. For the duplicate of the guideRNA transfection, cells were reverse transfected with 0.5 pmol (snap)$_2$-CAG and 0.5 pmol (halo)$_2$-CAU with 0.5 µl Lipofectamine 2000. Doxycycline concentration was kept at 10 ng/ml and after further 24 h cells were harvested. RNA isolation was performed with the RNeasy MinElute Cleanup Kit from QIAGEN, followed by DNase I digestion, which was again purified via RNeasy MinElute Cleanup Kit from QIAGEN. mRNA next generation sequencing was then performed by CEGAT. The library was prepared with the library preparation kit TruSeq Stranded mRNA by ILLUMINA starting from 100 ng RNA. Samples were then sequenced on a NovaSeq 6000 by ILLUMINA with 50 million reads and 2 × 100 bp paired end.

For comparison, data previously generated by Vogel *et al.*[10] was reanalyzed with the more sensitive pipeline applied here. Briefly, for the duplicate editing experiments of these samples, 5.0 pmol of a guideRNA targeting a 5'-UAG codon in the 3'-UTR of ACTB (snap-UAG_2, see Table S1) were transfected into 293 Flp-In T-REx cell lines either expressing SA1Q only (GSM3083480, SA1Q_rep1 & GSM3083481, SA1Q_rep2) or SA2Q only (GSM3083482, SA2Q_rep1 & GSM3083483, SA2Q_rep2). As negative control, an empty 293 Flp-In T-REx cell line expressing no artificial editing enzyme, treated with an empty transfection of Lipofectamine 2000 only (GSM3083474, ctrl_rep1 & GSM3083475, ctrl_rep2), was applied for all data sets. Data analysis is described in the Materials & Methods section.

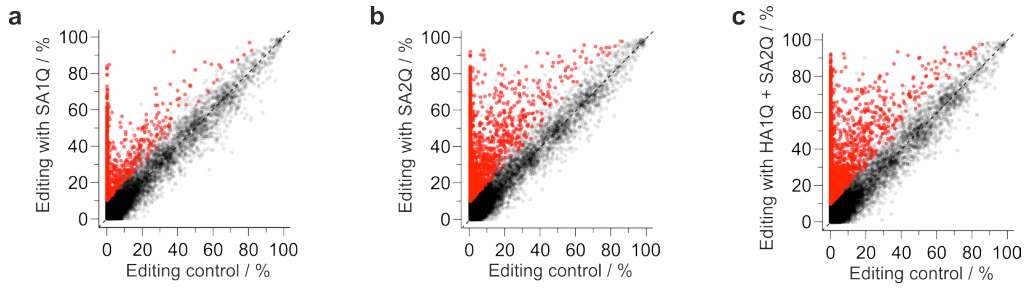

Figure S16. Scatter plots of total off-targets in editing experiments. Significantly differently edited sites are marked in red. ***a)*** *Cell line expressing SA1Q only after transfection of 5.0 pmol snap-UAG_2 versus empty 293 Flp-In T-REx.*[10] ***b)*** *Cell line expressing SA2Q only after transfection of 5.0 pmol snap-UAG_2 versus empty 293 Flp-In T-REx.*[10] ***c)*** *Cell line* ***2*** *(HA1Q + SA2Q) after transfection of 0.5 pmol (snap)$_2$-CAG and 0.5 pmol (halo)$_2$-CAU versus empty 293 Flp-In T-REx.*

Table S6. Number of significantly differently edited sites with editing difference ≥ 25 % found in editing experiments in mono cell lines SA1Q, SA2Q,[10] *and in duo cell line* ***2*** *(HA1Q + SA2Q) in comparison to a negative control cell line (293 Flp-In T-REx) not expressing any editing enzyme (Total off-targets with Δ ≥ 25 %). The last column shows the guideRNA-dependent fraction of the total off-targets with editing difference ≥ 25 % for duo cell line* ***2****.*

	Total off-targets with Δ ≥ 25 %			**gRNA-depend.**
	SA1Q	**SA2Q**	**HA1Q + SA2Q**	**HA1Q + SA2Q**
Total number	706	1423	2444	37
incl. Alu sites	75	411	418	14
5'UTR	25	46	72	1
Missense mutation	134	260	556	5
Nonstop mutation	9	10	20	0
Start codon SNP	0	0	2	0
Silent	102	143	314	0
3'UTR	332	662	1081	18
Noncoding	104	302	399	13

*Table S7. guideRNA-dependent off-target sites found by NGS in cell line **2**. Listed are significantly differently edited sites with an editing difference ≥ 25 % between duo cell line **2** with guideRNAs versus without guideRNAs. On-target sites targeted by (snap)$_2$-CAG and (halo)$_2$-CAU are shown on the top.*

Entry no.	Site	Localization	Editing / %		
			without gRNAs	with gRNAs	difference
On-target	ACTB	Missense Mutation	0	52	52
	GAPDH	Missense Mutation	0	41	41
1	UBA52	3'UTR	0	56	56
2	ACTA2	Missense Mutation	0	47	47
3	FAM50A	3'UTR	3	44	40
4	EGFL7	3'UTR	0	38	38
5	HNRNPA1L2	Noncoding	20	56	36
6	KLHDC3	3'UTR	24	58	34
7	LARP6	Noncoding	0	32	32
8	FAM129A	3'UTR	18	50	32
9	MAN2B2	Missense Mutation	5	37	32
10	UBIAD1	Noncoding	18	50	32
11	SYNGR1	Noncoding	0	31	31
12	KCNJ14	Noncoding	46	76	30
13	Unknown	Noncoding	20	50	30
14	COL4A1	3'UTR	0	30	30
15	RP13-36G14.4	Noncoding	23	53	30
16	TTC33	Noncoding	3	32	29
17	PAQR5	3'UTR	37	66	28
18	CDC42BPB	Missense Mutation	18	46	28
19	GOLGA8A	Noncoding	19	47	28
20	XRCC2	5'UTR	51	79	28
21	PVR	Noncoding	40	68	28
22	UGGT1	3'UTR	13	41	28
23	MTRF1L	Noncoding	28	55	27
24	HADHA	3'UTR	0	27	27
25	SCARB1	3'UTR	4	30	26
26	TMEM17	3'UTR	18	45	26
27	RP13-36G14.4	Noncoding	41	67	26
28	SYPL2	3'UTR	33	59	26
29	EPHB2	3'UTR	11	37	26
30	RCOR1	3'UTR	32	58	26
31	ZNF101	3'UTR	3	29	26
32	RPL28	3'UTR	28	54	26
33	WAC-AS1	Noncoding	38	64	26
34	PPDPF	3'UTR	0	26	26
35	MYL6B	Missense Mutation	0	26	26
36	ARHGAP44	Missense Mutation	10	35	25
37	SLC25A48	3'UTR	0	25	25

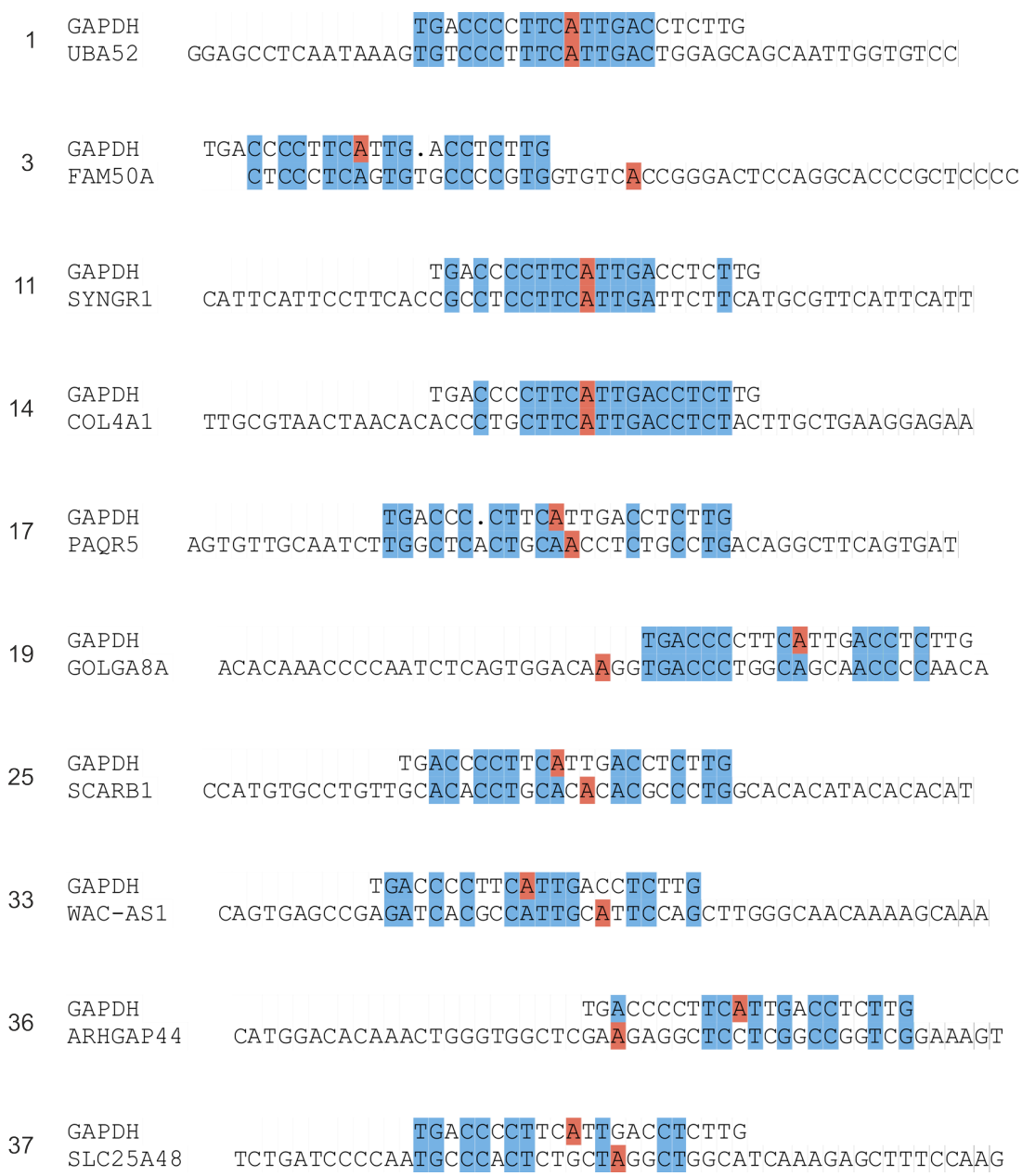

*Figure S17. Alignments of the regions around guideRNA-dependent off-target sites in duo cell line **2** (with entry no. corresponding to Table S7) to the guideRNA-interacting region of the targeted GAPDH transcript. Matching nucleotides are highlighted in blue, the deaminated adenosines in red.*

*Figure S18. Alignments of the regions around guideRNA-dependent off-target sites in duo cell line **2** (with entry no. corresponding to Table S7) to the guideRNA-interacting region of the targeted ACTB transcript. Matching nucleotides are highlighted in blue, the deaminated adenosines in red.*

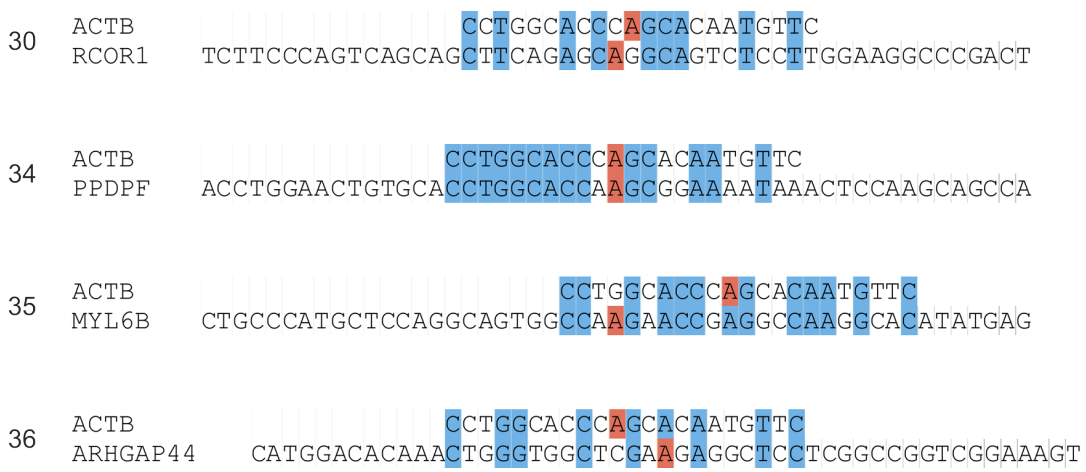

*Figure S18 (continued). Alignments of the regions around guideRNA-dependent off-target sites in duo cell line **2** (with entry no. corresponding to Table S7) to the guideRNA-interacting region of the targeted ACTB transcript. Matching nucleotides are highlighted in blue, the deaminated adenosines in red.*

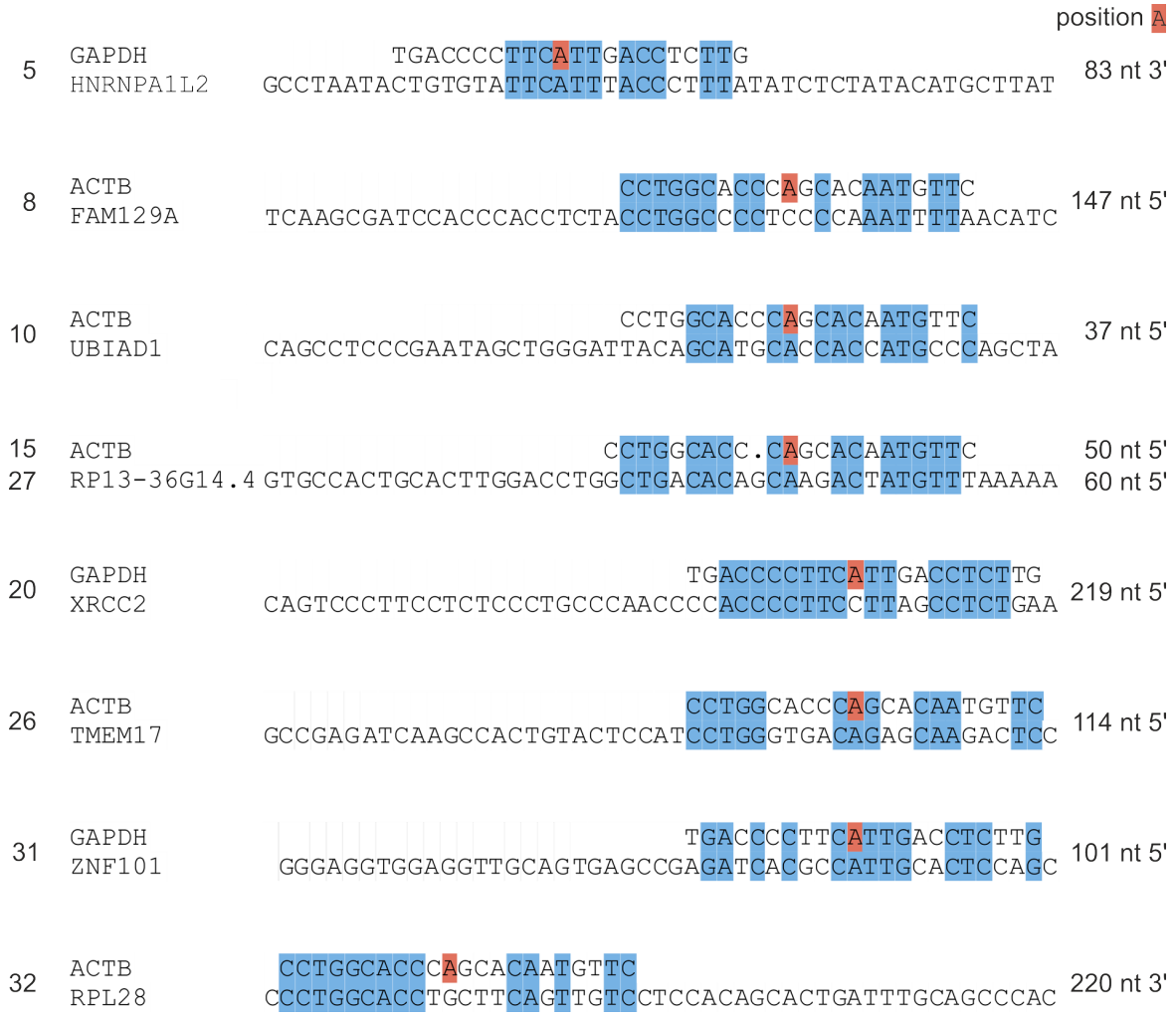

*Figure S19. Alignments of regions around guideRNA-dependent off-target sites in duo cell line **2** in Alu elements (with entry no. corresponding to Table S7) to the guideRNA-interacting regions of either the targeted GAPDH or ACTB transcript. It is likely that the secondary RNA structure within Alu elements*

leads to editable dsRNA once an ADAR is delivered nearby by a guideRNA. The relative position of the off-target site is indicated on the right. Matching nucleotides are highlighted in blue, the targeted adenosine in red.

*Table S8. Bystander editing found by NGS in cell line **2** in GAPDH. Listed are all significantly differently edited sites between duo cell line **2** with guideRNAs versus without guideRNAs within ± 500 bp of the on-target site, sorted by editing difference. In order to spot even minute editing, sites are included independent of editing difference. The on-target site targeted by $(halo)_2$-CAU is shown on the top.*

Entry no.	Distance to on-target / bp	Localization	Editing / % without gRNAs	with gRNAs	difference
On-target	± 0	Missense Mutation	0.0	40.8	40.8
1	+ 142	Missense Mutation	0.2	1.2	1.0
2	+ 187	Missense Mutation	0.0	0.2	0.2
3	+ 175	Missense Mutation	0.1	0.2	0.1
4	+ 141	Missense Mutation	0.0	0.1	0.1

*Table S9. Bystander editing found by NGS in cell line **2** in ACTB. Listed are all significantly differently edited sites between duo cell line **2** with guideRNAs versus without guideRNAs within ± 500 bp of the on-target site, sorted by editing difference. In order to spot even minute editing, sites are included independent of editing difference. The on-target site targeted by $(snap)_2$-CAG is shown on the top.*

Entry no.	Distance to on-target / bp	Localization	Editing / % without gRNAs	with gRNAs	difference
On-target	± 0	Missense Mutation	0.0	51.9	51.9
1	+ 220	Nonstop Mutation	3.7	19.7	16.0
2	+ 221	Missense Mutation	1.0	13.4	12.5
3	– 307	Missense Mutation	0.8	8.5	7.7
4	+ 336	3'UTR	0.0	3.0	3.0
5	+ 224	Missense Mutation	0.0	2.3	2.3
6	+ 425	3'UTR	0.0	1.3	1.3
7	– 325	Missense Mutation	0.1	0.4	0.3
8	– 26	Missense Mutation	0.0	0.1	0.1
9	– 35	Missense Mutation	0.0	0.1	0.1
10	– 365	Missense Mutation	0.0	0.1	0.1

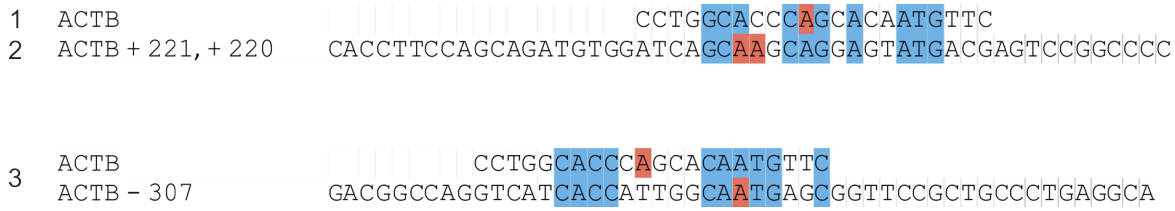

*Figure S20. Alignments of the regions around bystander sites in ACTB in duo cell line **2** with an editing difference ≥ 5 % (with entry no. corresponding to Table S9) to the guideRNA-interacting region of the targeted ACTB transcript. Matching nucleotides are highlighted in blue, the deaminated adenosines in red.*

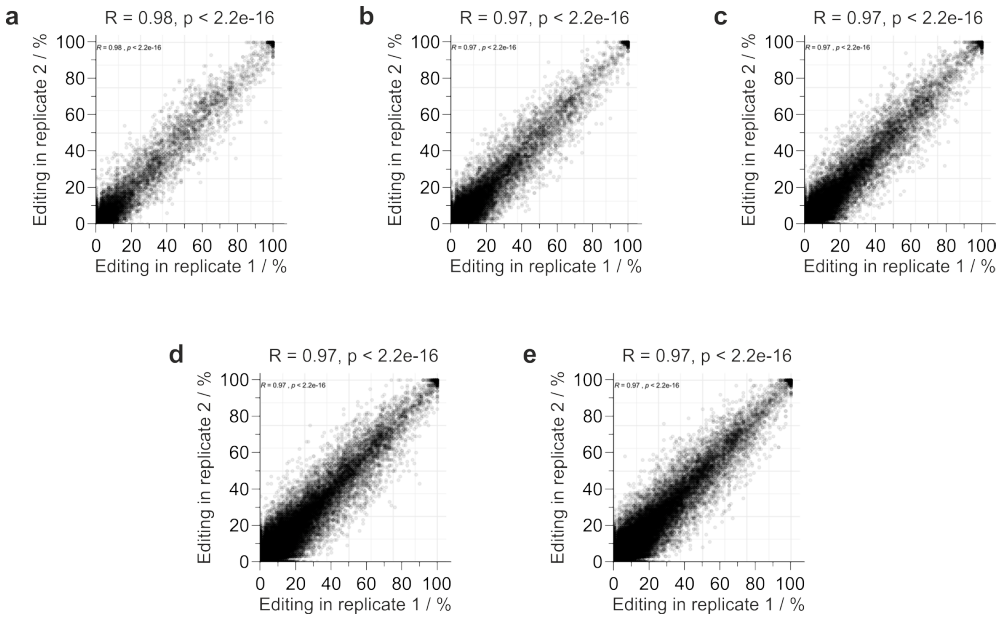

*Figure S21. Scatter plots of all called editing sites in duo cell line **2** in replicate 2 against replicate 1 respectively. **a)** empty 293 Flp-In T-REx. **b)** Cell line expressing SA1Q only after transfection of 5.0 pmol snap-UAG_2.[10] **c)** Cell line expressing SA2Q only after transfection of 5.0 pmol snap-UAG_2.[10] **d)** Cell line **2** (HA1Q + SA2Q) without guideRNA transfection. **e)** Cell line **2** (HA1Q + SA2Q) after transfection of 0.5 pmol $(snap)_2$-CAG and 0.5 pmol $(halo)_2$-CAU.*

HA1Q / APO1S duo cell line

For NGS of duo cell line **9**, again four samples, i.e. a duplicate of an empty transfection and a duplicate of a guideRNA transfection, were prepared analogous to NGS of duo cell line **2**. For the duplicate of the guideRNA transfection, cells were reverse transfected with 2.5 pmol $(halo)_2$-UAU and 2.5 pmol $(snap)_2$-ACC with 0.5 µl Lipofectamine 2000. Cells were harvested 48 h after transfection and subsequently treated as described for NGS of duo cell line **2**. The empty 293 Flp-In T-REx cell line expressing no artificial editing enzyme from Vogel *et al*.[10] (GSM3083474, ctrl_rep1 & GSM3083475, ctrl_rep2) was again applied as negative control. Data analysis is described in the Materials & Methods section.

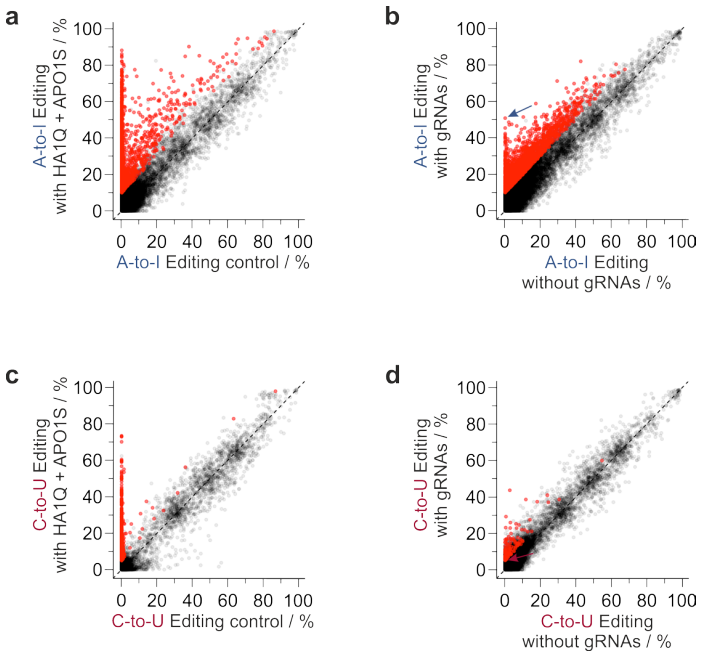

*Figure S22. Scatter plots of off-target analysis of duo cell line **9** (HA1Q + APO1S). Significantly differently edited sites are marked in red. **a)** Total A-to-I off-targets after transfection of 2.5 pmol (halo)$_2$-UAU and 2.5 (snap)$_2$-ACC versus empty 293 Flp-In T-REx.[10] **b)** guideRNA-dependent A-to-I off-targets. The UAU on-target site (ACTB) is marked by a blue arrow. **c)** Total C-to-U off-targets after transfection of 2.5 pmol (halo)$_2$-UAU and 2.5 (snap)$_2$-ACC versus empty 293 Flp-In T-REx.[10] **d)** guideRNA-dependent C-to-U off-targets. The ACC on-target site (GAPDH) is marked by a red arrow.*

*Table S10. Number of significantly differently edited A-to-I sites with editing difference ≥ 25 % found in editing experiments in duo cell line **9** (HA1Q + APO1S) in comparison to a negative control cell line (293 Flp-In T-REx) not expressing any editing enzyme (Total off-targets). The guideRNA-dependent fractions of the total off-targets are shown in the right column.*

	A-to-I (Δ ≥ 25 %)	
	Total off-targets	**gRNA-depend.**
Total number	1621	129
incl. Alu sites	207	8
5'UTR	54	7
Missense mutation	364	49
Nonsense mutation	0	0
Nonstop mutation	18	0
Start codon SNP	1	0
Silent	231	16
3'UTR	715	39
Noncoding	238	19

*Table S 11. Number of significantly differently edited C-to-U sites with editing difference ≥ 10 % and ≥ 25 % found in editing experiments in duo cell line **9** (HA1Q + APO1S) in comparison to a negative control cell line (293 Flp-In T-REx) not expressing any editing enzyme (Total off-targets). The guideRNA-dependent fractions of the total off-targets are shown in the right column respectively.*

	C-to-U (Δ ≥ 10 %)		**C-to-U** (Δ ≥ 25 %)	
	Total off-targets	**gRNA-depend.**	**Total off-targets**	**gRNA-depend.**
Total number	1009	44	129	3
incl. Alu sites	10	1	3	0
5'UTR	21	22	3	0
Missense mutation	7	0	0	0
Nonsense mutation	0	0	0	0
Nonstop mutation	0	0	0	0
Start codon SNP	0	0	0	0
Silent	2	0	0	0
3'UTR	846	33	109	3
Noncoding	133	9	17	0

*Table S12. C-to-U bystander editing found by NGS in cell line **9** in GAPDH. Listed are all significantly differently edited sites between duo cell line **9** with guideRNAs versus without guideRNAs within ± 500 bp of the on-target site, sorted by editing difference. In order to spot even minute editing, sites are included independent of editing difference. The on-target site targeted by $(snap)_2$-ACC is shown on the top, the bystander site at + 472 bp corresponds to one of the off-target sites also observed in Sanger sequencing (see Figure S15b, Table S5 C #2 at + 253, since RNA-seq data is aligned to the human reference genome hg19 including introns).*

Entry no.	**Distance to on-target / bp**	**Localization**	**Editing / % without gRNAs**	**with gRNAs**	**difference**
On-target	± 0	Missense Mutation	0.0	5.1	5.1
1	+ 472	Silent	0.0	6.8	6.8
2	+ 21	Missense Mutation	0.0	0.9	0.9
3	– 3	Missense Mutation	0.0	0.8	0.8
4	– 119	Noncoding	0.1	0.8	0.7
5	+ 25	Silent	0.0	0.7	0.7
6	– 122	Noncoding	0.1	0.8	0.7
7	+ 487	Silent	0.1	0.7	0.6
8	+ 473	Missense Mutation	0.0	0.5	0.5
9	+ 37	Silent	0.0	0.3	0.3
10	– 173	Noncoding	0.1	0.3	0.2
11	+ 49	Silent	0.0	0.2	0.2
12	– 140	Noncoding	0.0	0.2	0.2
13	+ 52	Silent	0.0	0.2	0.2
14	+ 62	Missense Mutation	0.0	0.2	0.2
15	+ 490	Silent	0.0	0.1	0.1
16	– 2	Silent	0.0	0.1	0.1
17	+ 270	Missense Mutation	0.0	0.1	0.1
18	+ 69	Missense Mutation	0.0	0.1	0.1
19	+ 496	Silent	0.0	0.1	0.1
20	+ 256	Silent	0.0	0.1	0.1
21	+ 13	Silent	0.0	0.1	0.1
22	+ 22	Silent	0.0	0.1	0.1

*Table S13. A-to-I bystander editing found by NGS in cell line **9** in ACTB. Listed are all significantly differently edited sites between duo cell line **9** with guideRNAs versus without guideRNAs within ± 500 bp of the on-target site, sorted by editing difference. In order to spot even minute editing, sites are included independent of editing difference. The on-target site targeted by (halo)$_2$-UAU is shown on the top.*

Entry no.	Distance to on-target / bp	Localization	Editing / % without gRNAs	with gRNAs	difference
On-target	± 0	Missense Mutation	0.0	50.8	50.8
22	– 350	Missense Mutation	0.0	0.9	0.9

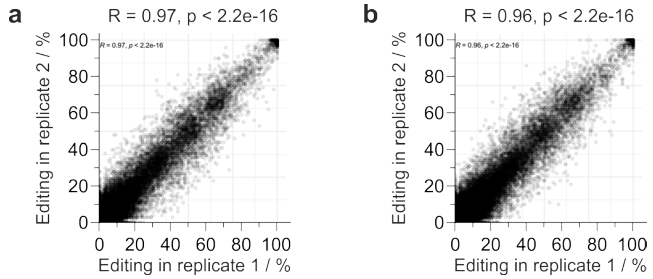

*Figure S23. Scatter plots of all called editing sites in duo cell line **9** in replicate 2 against replicate 1 respectively. **a)** Cell line **9** (HA1Q + APO1S) without guideRNA transfection. **b)** Cell line **9** (HA1Q + APO1S) after transfection of 2.5 pmol (halo)$_2$-UAU and 2.5 (snap)$_2$-ACC.*

Supporting literature

1. Keppler, A. et al. A general method for the covalent labeling of fusion proteins with small molecules *in vivo*. *Nat. Biotechnol.* **21**, 86–89 (2003).
2. Hanswillemenke, A. & Stafforst, T. Protocols for the generation of caged guideRNAs for light-triggered RNA-targeting with SNAP-ADARs. *Methods Enzymol.* **624**, 47–68 (2019).
3. Gautier, A. et al. An Engineered Protein Tag for Multiprotein Labeling in Living Cells. *Chem. Biol.* **15**, 128–136 (2008).
4. Keppler, A. et al. Labeling of fusion proteins of O^6-alkylguanine-DNA alkyltransferase with small molecules in vivo and in vitro. *Methods* **32**, 437–444 (2004).
5. Varga, N. et al. Selective Targeting of Dendritic Cell-Specific Intercellular Adhesion Molecule-3-Grabbing Nonintegrin (DC-SIGN) with Mannose-Based Glycomimetics: Synthesis and Interaction Studies of Bis(benzylamide) Derivatives of a Pseudomannobioside. *Chem. – Eur. J.* **19**, 4786–4797 (2013).
6. Singh, V., Wang, S. & Kool, E.T. Genetically Encoded Multispectral Labeling of Proteins with Polyfluorophores on a DNA Backbone. *J. Am. Chem. Soc.* **135**, 6184–6191 (2013).
7. Los, G.V. et al. HaloTag: A Novel Protein Labeling Technology for Cell Imaging and Protein Analysis. *ACS Chem. Biol.* **3**, 373–382 (2008).
8. Vogel, P. & Stafforst, T. Site-Directed RNA Editing with Antagomir Deaminases — A Tool to Study Protein and RNA Function. *ChemMedChem* **9**, 2021–2025 (2014).
9. Abudayyeh, O.O. et al. A cytosine deaminase for programmable single-base RNA editing. *Science* **365**, 382–386 (2019).
10. Vogel, P. et al. Efficient and precise editing of endogenous transcripts with SNAP-tagged ADARs. *Nat. Methods* **15**, 535–538 (2018).

Appendix

Constructs for single cell lines

Cell line SA1Q: CMV-enhancer – CMV promoter – $TetO_2$ – $SNAP_f$-tag – ADAR1Q – Myc-tag – His-tag – Stop – UAG – bGH

GACATTGATTATTGACTAGTTATTAATAGTAATCAATTACGGGGTCATTAGTTCATAGCCCATATATG
GAGTTCCGCGTTACATAACTTACGGTAAATGGCCCGCCTGGCTGACCGCCCAACGACCCCCGCCCATT
GACGTCAATAATGACGTATGTTCCCATAGTAACGCCAATAGGGACTTTCCATTGACGTCAATGGGTGG
AGTATTTACGGTAAACTGCCCACTTGGCAGTACATCAAGTGTATCATATGCCAAGTACGCCCCCTATT
GACGTCAATGACGGTAAATGGCCCGCCTGGCATTATGCCCAGTACATGACCTTATGGGACTTTCCTAC
TTGGCAGTACATCTACGTATTAGTCATCGCTATTACCATGGTGATGCGGTTTTGGCAGTACATCAATG
GGCGTGGATAGCGGTTTGACTCACGGGGATTTCCAAGTCTCCACCCCATTGACGTCAATGGGAGTTTG
TTTTGGCACCAAAATCAACGGGACTTTCCAAAATGTCGTAACAACTCCGCCCCATTGACGCAAATGGG
CGGTAGGCGTGTACGGTGGGAGGTCTATATAAGCAGAGCTCTCCCTATCAGTGATAGAGATCTCCCTA
TCAGTGATAGAGATCGTCGACGAGCTCGTTTAGTGAACCGTCAGATCGCCTGGAGACGCCATCCACGC
TGTTTTGACCTCCATAGAAGACACCGGGACCGATCCAGCCTCCGGACTCTAGCGTTTAAACTTAAGCT
TGGTACCGAGCTCGGATCCATGGACAAAGACTGCGAAATGAAGCGCACCACCCTGGATAGCCCTCTGG
GCAAGCTGGAACTGTCTGGGTGCGAACAGGGCCTGCACCGTATCATCTTCCTGGGCAAAGGAACATCT
GCCGCCGACGCCGTGGAAGTGCCTGCCCCAGCCGCCGTGCTGGGCGGACCAGAGCCACTGATGCAGGC
CACCGCCTGGCTCAACGCCTACTTTCACCAGCCTGAGGCCATCGAGGAGTTCCCTGTGCCAGCCCTGC
ACCACCCAGTGTTCCAGCAGGAGAGCTTTACCCGCCAGGTGCTGTGGAAACTGCTGAAAGTGGTGAAG
TTCGGAGAGGTCATCAGCTACAGCCACCTGGCCGCCCTGGCCGGCAATCCCGCCGCCACCGCCGCCGT
GAAAACCGCCCTGAGCGGAAATCCCGTGCCCATTCTGATCCCCTGCCACCGGGTGGTGCAGGGCGACC
TGGACGTGGGGGGCTACGAGGGCGGGCTCGCCGTGAAAGAGTGGCTGCTGGCCCACGAGGGCCACAGA
CTGGGCAAGCCTGGGCTGGGTCCTGCAGGCGGAGGCGCGCCAGGGTCTGGCGGCGGCAGTAAGGCAGA
ACGCATGGGTTTCACAGAGGTAACCCCAGTGACAGGGGCCAGTCTCAGAAGAACTATGCTCCTCCTCT
CAAGGTCCCCAGAAGCACAGCCAAAGACACTCCCTCTCACTGGCAGCACCTTCCATGACCAGATAGCC
ATGCTGAGCCACCGGTGCTTCAACACTCTGACTAACAGCTTCCAGCCCTCCTTGCTCGGCCGCAAGAT
TCTGGCCGCCATCATTATGAAAAAAGACTCTGAGGACATGGGTGTCGTCGTCAGCTTGGGAACAGGGA
ATCGCTGTGTAAAAGGAGATTCTCTCAGCCTAAAAGGAGAAACTGTCAATGACTGCCATGCAGAAATA
ATCTCCCGGAGAGGCTTCATCAGGTTTCTCTACAGTGAGTTAATGAAATACAACTCCCAGACTGCGAA
GGATAGTATATTTGAACCTGCTAAGGGAGGAGAAAAGCTCCAAATAAAAAAGACTGTGTCATTCCATC
TGTATATCAGCACTGCTCCGTGTGGAGATGGCGCCCTCTTTGACAAGTCCTGCAGCGACCGTGCTATG
GAAAGCACAGAATCCCGCCACTACCCTGTCTTCGAGAATCCCAAACAAGGAAAGCTCCGCACCAAGGT
GGAGAACGGACAAGGCACAATCCCTGTGGAATCCAGTGACATTGTGCCTACGTGGGATGGCATTCGGC
TCGGGGAGAGACTCCGTACCATGTCCTGTAGTGACAAAATCCTACGCTGGAACGTGCTGGGCCTGCAA
GGGGCACTGTTGACCCACTTCCTGCAGCCCATTTATCTCAAATCTGTCACATTGGGTTACCTTTTCAG
CCAAGGGCATCTGACCCGTGCTATTTGCTGTCGTGTGACAAGAGATGGGAGTGCATTTGAGGATGGAC
TACGACATCCCTTTATTGTCAACCACCCCAAGGTTGGCAGAGTCAGCATATATGATTCCAAAAGGCAA
TCCGGGAAGACTAAGGAGACAAGCGTCAACTGGTGTCTGGCTGATGGCTATGACCTGGAGATCCTGGA
CGGTACCAGAGGCACTGTGGATGGGCCACGGAATGAATTGTCCCGGGTCTCCAAAAAGAACATTTTTC
TTCTATTTAAGAAGCTCTGCTCCTTCCGTTACCGCAGGGATCTACTGAGACTCTCCTATGGTGAGGCC
AAGAAAGCTGCCCGTGACTACGAGACGGCCAAGAACTACTTCAAAAAAGGCCTGAAGGATATGGGCTA
TGGGAACTGGATTAGCAAACCCCAGGAGGAAAAGAACTTTTATCTCTGCCCAGTATCTAGAGGGCCCT
TCGAACAAAAACTCATCTCAGAAGAGGATCTGAATATGCATACCGGTCATCATCACCATCACCATTGA
CTGCCTGTTCCGTAGCCGACACGCGGCCGCTCGAGTCTAGAGGGCCCGTTTAAACCCGCTGATCAGCC
TCGACTGTGCCTTCTAGTTGCCAGCCATCTGTTGTTTGCCCCTCCCCCGTGCCTTCCTTGACCCTGGA
AGGTGCCACTCCCACTGTCCTTTCCTAATAAAATGAGGAAATTGCATCGCATTGTCTGAGTAGGTGTC
ATTCTATTCTGGGGGGTGGGGTGGGGCAGGACAGCAAGGGGGAGGATTGGGAAGACAATAGCAGGCAT
GCTGGGGATGCGGTGGGCTCTATGG

Cell line CA1Q: CMV-enhancer – CMV promoter – $TetO_2$ – $CLIP_f$-tag – ADAR1Q – Myc-tag – His-tag – Stop – UAG – bGH

GACATTGATTATTGACTAGTTATTAATAGTAATCAATTACGGGGTCATTAGTTCATAGCCCATATATG
GAGTTCCGCGTTACATAACTTACGGTAAATGGCCCGCCTGGCTGACCGCCCAACGACCCCCGCCCATT
GACGTCAATAATGACGTATGTTCCCATAGTAACGCCAATAGGGACTTTCCATTGACGTCAATGGGTGG
AGTATTTACGGTAAACTGCCCACTTGGCAGTACATCAAGTGTATCATATGCCAAGTACGCCCCCTATT
GACGTCAATGACGGTAAATGGCCCGCCTGGCATTATGCCCAGTACATGACCTTATGGGACTTTCCTAC
TTGGCAGTACATCTACGTATTAGTCATCGCTATTACCATGGTGATGCGGTTTTGGCAGTACATCAATG
GGCGTGGATAGCGGTTTGACTCACGGGGATTTCCAAGTCTCCACCCCATTGACGTCAATGGGAGTTTG
TTTTGGCACCAAAATCAACGGGACTTTCCAAAATGTCGTAACAACTCCGCCCCATTGACGCAAATGGG
CGGTAGGCGTGTACGGTGGGAGGTCTATATAAGCAGAGCTCTCCCTATCAGTGATAGAGATCTCCCTA
TCAGTGATAGAGATCGTCGACGAGCTCGTTTAGTGAACCGTCAGATCGCCTGGAGACGCCATCCACGC
TGTTTTGACCTCCATAGAAGACACCGGGACCGATCCAGCCTCCGGACTCTAGCGTTTAAACTTAAGCT
TGGTACCGAGCTCGGATCCATGGACAAAGACTGCGAAATGAAGCGCACCACCCTGGATAGCCCTCTGG
GCAAGCTGGAACTGTCTGGGTGCGAACAGGGCCTGCACCGTATCATCTTCCTGGGCAAAGGAACATCT
GCCGCCGACGCCGTGGAAGTGCCTGCCCCAGCCGCCGTGCTGGGCGGACCAGAGCCACTGATCCAGGC
CACCGCCTGGCTCAACGCCTACTTTCACCAGCCTGAGGCCATCGAGGAGTTCCCTGTGCCAGCCCTGC
ACCACCCAGTGTTCCAGCAGGAGAGCTTTACCCGCCAGGTGCTGTGGAAACTGCTGAAAGTGGTGAAG
TTCGGAGAGGTCATCAGCGAGAGCCACCTGGCCGCCCTGGTGGGCAATCCCGCCGCCACCGCCGCCGT
GAACACCGCCCTGGACGGAAATCCCGTGCCCATTCTGATCCCCTGCCACCGGGTGGTGCAGGGCGACA
GCGACGTGGGGCCCTACCTGGGCGGGCTCGCCGTGAAAGAGTGGCTGCTGGCCCACGAGGGCCACAGA
CTGGGCAAGCCTGGGCTGGGTCCTGCAGGCGGAGGCGCGCCAGGGTCTGGCGGCGGCAGTAAGGCAGA
ACGCATGGGTTTCACAGAGGTAACCCCAGTGACAGGGGCCAGTCTCAGAAGAACTATGCTCCTCCTCT
CAAGGTCCCCAGAAGCACAGCCAAAGACACTCCCTCTCACTGGCAGCACCTTCCATGACCAGATAGCC
ATGCTGAGCCACCGGTGCTTCAACACTCTGACTAACAGCTTCCAGCCCTCCTTGCTCGGCCGCAAGAT
TCTGGCCGCCATCATTATGAAAAAAGACTCTGAGGACATGGGTGTCGTCGTCAGCTTGGGAACAGGGA
ATCGCTGTGTAAAAGGAGATTCTCTCAGCCTAAAAGGAGAAACTGTCAATGACTGCCATGCAGAAATA
ATCTCCCGGAGAGGCTTCATCAGGTTTCTCTACAGTGAGTTAATGAAATACAACTCCCAGACTGCGAA
GGATAGTATATTTGAACCTGCTAAGGGAGGAGAAAAGCTCCAAATAAAAAAGACTGTGTCATTCCATC
TGTATATCAGCACTGCTCCGTGTGGAGATGGCGCCCTCTTTGACAAGTCCTGCAGCGACCGTGCTATG
GAAAGCACAGAATCCCGCCACTACCCTGTCTTCGAGAATCCCAAACAAGGAAAGCTCCGCACCAAGGT
GGAGAACGGACAAGGCACAATCCCTGTGGAATCCAGTGACATTGTGCCTACGTGGGATGGCATTCGGC
TCGGGGAGAGACTCCGTACCATGTCCTGTAGTGACAAAATCCTACGCTGGAACGTGCTGGGCCTGCAA
GGGGCACTGTTGACCCACTTCCTGCAGCCCATTTATCTCAAATCTGTCACATTGGGTTACCTTTTCAG
CCAAGGGCATCTGACCCGTGCTATTTGCTGTCGTGTGACAAGAGATGGGAGTGCATTTGAGGATGGAC
TACGACATCCCTTTATTGTCAACCACCCCAAGGTTGGCAGAGTCAGCATATATGATTCCAAAAGGCAA
TCCGGGAAGACTAAGGAGACAAGCGTCAACTGGTGTCTGGCTGATGGCTATGACCTGGAGATCCTGGA
CGGTACCAGAGGCACTGTGGATGGGCCACGGAATGAATTGTCCCGGGTCTCCAAAAAGAACATTTTTC
TTCTATTTAAGAAGCTCTGCTCCTTCCGTTACCGCAGGGATCTACTGAGACTCTCCTATGGTGAGGCC
AAGAAAGCTGCCCGTGACTACGAGACGGCCAAGAACTACTTCAAAAAAGGCCTGAAGGATATGGGCTA
TGGGAACTGGATTAGCAAACCCCAGGAGGAAAAGAACTTTTATCTCTGCCCAGTATCTAGAGGGCCCT
TCGAACAAAAACTCATCTCAGAAGAGGATCTGAATATGCATACCGGTCATCATCACCATCACCATTGA
CTGCCTGTTCCGTAGCCGACACGCGGCCGCTCGAGTCTAGAGGGCCCGTTTAAACCCGCTGATCAGCC
TCGACTGTGCCTTCTAGTTGCCAGCCATCTGTTGTTTGCCCCTCCCCCGTGCCTTCCTTGACCCTGGA
AGGTGCCACTCCCACTGTCCTTTCCTAATAAAATGAGGAAATTGCATCGCATTGTCTGAGTAGGTGTC
ATTCTATTCTGGGGGGTGGGGTGGGGCAGGACAGCAAGGGGGAGGATTGGGAAGACAATAGCAGGCAT
GCTGGGGATGCGGTGGGCTCTATGG

Cell line HA1Q: CMV-enhancer – CMV promoter – $TetO_2$ – HaloTag – ADAR1Q – Myc-tag – His-tag – Stop – UAG – bGH

GACATTGATTATTGACTAGTTATTAATAGTAATCAATTACGGGGTCATTAGTTCATAGCCCATATATG
GAGTTCCGCGTTACATAACTTACGGTAAATGGCCCGCCTGGCTGACCGCCCAACGACCCCCGCCCATT
GACGTCAATAATGACGTATGTTCCCATAGTAACGCCAATAGGGACTTTCCATTGACGTCAATGGGTGG
AGTATTTACGGTAAACTGCCCACTTGGCAGTACATCAAGTGTATCATATGCCAAGTACGCCCCCTATT
GACGTCAATGACGGTAAATGGCCCGCCTGGCATTATGCCCAGTACATGACCTTATGGGACTTTCCTAC
TTGGCAGTACATCTACGTATTAGTCATCGCTATTACCATGGTGATGCGGTTTTGGCAGTACATCAATG
GGCGTGGATAGCGGTTTGACTCACGGGGATTTCCAAGTCTCCACCCCATTGACGTCAATGGGAGTTTG
TTTTGGCACCAAAATCAACGGGACTTTCCAAAATGTCGTAACAACTCCGCCCCATTGACGCAAATGGG
CGGTAGGCGTGTACGGTGGGAGGTCTATATAAGCAGAGCTCTCCCTATCAGTGATAGAGATCTCCCTA
TCAGTGATAGAGATCGTCGACGAGCTCGTTTAGTGAACCGTCAGATCGCCTGGAGACGCCATCCACGC
TGTTTTGACCTCCATAGAAGACACCGGGACCGATCCAGCCTCCGGACTCTAGCGTTTAAACTTAAGCT
TGGTACCGAGCTCGGATCCATGGCAGAAATCGGTACTGGCTTTCCATTCGACCCCCATTATGTGGAAG
TCCTGGGCGAGCGCATGCACTACGTCGATGTTGGTCCGCGCGATGGCACCCCTGTGCTGTTCCTGCAC
GGTAACCCGACCTCCTCCTACGTGTGGCGCAACATCATCCCGCATGTTGCACCGACCCATCGCTGCAT
TGCTCCAGACCTGATCGGTATGGGCAAATCCGACAAACCAGACCTGGGTTATTTCTTCGACGACCACG
TCCGCTTCATGGATGCCTTCATCGAAGCCCTGGGTCTGGAAGAGGTCGTCCTGGTCATTCACGACTGG
GGCTCCGCTCTGGGTTTCCACTGGGCCAAGCGCAATCCAGAGCGCGTCAAAGGTATTGCATTTATGGA
GTTCATCCGCCCTATCCCGACCTGGGACGAATGGCCAGAATTTGCCCGCGAGACCTTCCAGGCCTTCC
GCACCACCGACGTCGGCCGCAAGCTGATCATCGATCAGAACGTTTTTATCGAGGGTACGCTGCCGATG
GGTGTCGTCCGCCCGCTGACTGAAGTCGAGATGGACCATTACCGCGAGCCGTTCCTGAATCCTGTTGA
CCGCGAGCCACTGTGGCGCTTCCCAAACGAGCTGCCAATCGCCGGTGAGCCAGCGAACATCGTCGCGC
TGGTCGAAGAATACATGGACTGGCTGCACCAGTCCCCTGTCCCGAAGCTGCTGTTCTGGGGCACCCCA
GGCGTTCTGATCCCACCGGCCGAAGCCGCTCGCCTGGCCAAAAGCCTGCCTAACTGCAAGGCTGTGGA
CATCGGCCCGGGTCTGAATCTGCTGCAAGAAGACAACCCGGACCTGATCGGCAGCGAGATCGCGCGCT
GGCTGTCGACGCTCGAGAAGCCAACCCCTGCAGGCGGAGGCGCGCCAGGGTCTGGCGGCGGCAGTAAG
GCAGAACGCATGGGTTTCACAGAGGTAACCCCAGTGACAGGGGCCAGTCTCAGAAGAACTATGCTCCT
CCTCTCAAGGTCCCCAGAAGCACAGCCAAAGACACTCCCTCTCACTGGCAGCACCTTCCATGACCAGA
TAGCCATGCTGAGCCACCGGTGCTTCAACACTCTGACTAACAGCTTCCAGCCCTCCTTGCTCGGCCGC
AAGATTCTGGCCGCCATCATTATGAAAAAAGACTCTGAGGACATGGGTGTCGTCGTCAGCTTGGGAAC
AGGGAATCGCTGTGTAAAAGGAGATTCTCTCAGCCTAAAAGGAGAAACTGTCAATGACTGCCATGCAG
AAATAATCTCCCGGAGAGGCTTCATCAGGTTTCTCTACAGTGAGTTAATGAAATACAACTCCCAGACT
GCGAAGGATAGTATATTTGAACCTGCTAAGGGAGGAGAAAAGCTCCAAATAAAAAAGACTGTGTCATT
CCATCTGTATATCAGCACTGCTCCGTGTGGAGATGGCGCCCTCTTTGACAAGTCCTGCAGCGACCGTG
CTATGGAAAGCACAGAATCCCGCCACTACCCTGTCTTCGAGAATCCCAAACAAGGAAAGCTCCGCACC
AAGGTGGAGAACGGACAAGGCACAATCCCTGTGGAATCCAGTGACATTGTGCCTACGTGGGATGGCAT
TCGGCTCGGGGAGAGACTCCGTACCATGTCCTGTAGTGACAAAATCCTACGCTGGAACGTGCTGGGCC
TGCAAGGGGCACTGTTGACCCACTTCCTGCAGCCCATTTATCTCAAATCTGTCACATTGGGTTACCTT
TTCAGCCAAGGGCATCTGACCCGTGCTATTTGCTGTCGTGTGACAAGAGATGGGAGTGCATTTGAGGA
TGGACTACGACATCCCTTTATTGTCAACCACCCCAAGGTTGGCAGAGTCAGCATATATGATTCCAAAA
GGCAATCCGGGAAGACTAAGGAGACAAGCGTCAACTGGTGTCTGGCTGATGGCTATGACCTGGAGATC
CTGGACGGTACCAGAGGCACTGTGGATGGGCCACGGAATGAATTGTCCCGGGTCTCCAAAAAGAACAT
TTTTCTTCTATTTAAGAAGCTCTGCTCCTTCCGTTACCGCAGGGATCTACTGAGACTCTCCTATGGTG
AGGCCAAGAAAGCTGCCCGTGACTACGAGACGGCCAAGAACTACTTCAAAAAAGGCCTGAAGGATATG
GGCTATGGGAACTGGATTAGCAAACCCCAGGAGGAAAAGAACTTTTATCTCTGCCCAGTATCTAGAGG
GCCCTTCGAACAAAAACTCATCTCAGAAGAGGATCTGAATATGCATACCGGTCATCATCACCATCACC
ATTGACTGCCTGTTCCGTAGCCGACACGCGGCCGCTCGAGTCTAGAGGGCCCGTTTAAACCCGCTGAT
CAGCCTCGACTGTGCCTTCTAGTTGCCAGCCATCTGTTGTTTGCCCCTCCCCCGTGCCTTCCTTGACC
CTGGAAGGTGCCACTCCCACTGTCCTTTCCTAATAAAATGAGGAAATTGCATCGCATTGTCTGAGTAG
GTGTCATTCTATTCTGGGGGGTGGGGTGGGGCAGGACAGCAAGGGGGAGGATTGGGAAGACAATAGCA
GGCATGCTGGGGATGCGGTGGGCTCTATGG

Constructs for HA1Q / SA2Q duo cell lines 1 – 5

Cell line **1**: CMV-enhancer – CMV promoter – $TetO_2$ – $SNAP_f$-tag – ADAR2Q – bGH – CMV-enhancer – CMV promoter – $TetO_2$ – HaloTag – ADAR1Q – bGH

GACATTGATTATTGACTAGTTATTAATAGTAATCAATTACGGGGTCATTAGTTCATAGCCCATATATG
GAGTTCCGCGTTACATAACTTACGGTAAATGGCCCGCCTGGCTGACCGCCCAACGACCCCCGCCCATT
GACGTCAATAATGACGTATGTTCCCATAGTAACGCCAATAGGGACTTTCCATTGACGTCAATGGGTGG
AGTATTTACGGTAAACTGCCCACTTGGCAGTACATCAAGTGTATCATATGCCAAGTACGCCCCCTATT
GACGTCAATGACGGTAAATGGCCCGCCTGGCATTATGCCCAGTACATGACCTTATGGGACTTTCCTAC
TTGGCAGTACATCTACGTATTAGTCATCGCTATTACCATGGTGATGCGGTTTTGGCAGTACATCAATG
GGCGTGGATAGCGGTTTGACTCACGGGGATTTCCAAGTCTCCACCCCATTGACGTCAATGGGAGTTTG
TTTTGGCACCAAAATCAACGGGACTTTCCAAAATGTCGTAACAACTCCGCCCCATTGACGCAAATGGG
CGGTAGGCGTGTACGGTGGGAGGTCTATATAAGCAGAGCTCTCCCTATCAGTGATAGAGATCTCCCTA
TCAGTGATAGAGATCGTCGACGAGCTCGTTTAGTGAACCGTCAGATCGCCTGGAGACGCCATCCACGC
TGTTTTGACCTCCATAGAAGACACCGGGACCGATCCAGCCTCCGGACTCTAGCGTTTAAACTTAAGCT
TGGTACCGAGCTCGGATCCCCACCATGGACAAAGACTGCGAAATGAAGCGCACCACCCTGGATAGCCC
TCTGGGCAAGCTGGAACTGTCTGGGTGCGAACAGGGCCTGCACCGTATCATCTTCCTGGGCAAAGGAA
CATCTGCCGCCGACGCCGTGGAAGTGCCTGCCCCAGCCGCCGTGCTGGGCGGACCAGAGCCACTGATG
CAGGCCACCGCCTGGCTCAACGCCTACTTTCACCAGCCTGAGGCCATCGAGGAGTTCCCTGTGCCAGC
CCTGCACCACCCAGTGTTCCAGCAGGAGAGCTTTACCCGCCAGGTGCTGTGGAAACTGCTGAAAGTGG
TGAAGTTCGGAGAGGTCATCAGCTACAGCCACCTGGCCGCCCTGGCCGGCAATCCCGCCGCCACCGCC
GCCGTGAAAACCGCCCTGAGCGGAAATCCCGTGCCCATTCTGATCCCCTGCCACCGGGTGGTGCAGGG
CGACCTGGACGTGGGGGGCTACGAGGGCGGGCTCGCCGTGAAAGAGTGGCTGCTGGCCCACGAGGGCC
ACAGACTGGGCAAGCCTGGGCTGGGTCCTGCAGGCGGAGGCGCGCCAGGGTCTGGCGGCGGCAGTAAG
AAGCTTGCCAAGGCCCGGGCTGCGCAGTCTGCCCTGGCCGCCATTTTTAACTTGCACTTGGATCAGAC
GCCATCTCGCCAGCCTATTCCCAGTGAGGGTCTTCAGCTGCATTTACCGCAGGTTTTAGCTGACGCTG
TCTCACGCCTGGTCCTGGGTAAGTTTGGTGACCTGACCGACAACTTCTCCTCCCCTCACGCTCGCAGA
AAAGTGCTGGCTGGAGTCGTCATGACAACAGGCACAGATGTTAAAGATGCCAAGGTGATAAGTGTTTC
TACAGGAACAAAATGTATTAATGGTGAATACATGAGTGATCGTGGCCTTGCATTAAATGACTGCCATG
CAGAAATAATATCTCGGAGATCCTTGCTCAGATTTCTTTATACACAACTTGAGCTTTACTTAAATAAC
AAAGATGATCAAAAAAGATCCATCTTTCAGAAATCAGAGCGAGGGGGGTTTAGGCTGAAGGAGAATGT
CCAGTTTCATCTGTACATCAGCACCTCTCCCTGTGGAGATGCCAGAATCTTCTCACCACATGAGCCAA
TCCTGGAAGAACCAGCAGATAGACACCCAAATCGTAAAGCAAGAGGACAGCTACGGACCAAAATAGAG
TCTGGTCAGGGGACGATTCCAGTGCGCTCCAATGCGAGCATCCAAACGTGGGACGGGGTGCTGCAAGG
GGAGCGGCTGCTCACCATGTCCTGCAGTGACAAGATTGCACGCTGGAACGTGGTGGGCATCCAGGGTT
CCCTGCTCAGCATTTTCGTGGAGCCCATTTACTTCTCGAGCATCATCCTGGGCAGCCTTTACCACGGG
GACCACCTTTCCAGGGCCATGTACCAGCGGATCTCCAACATAGAGGACCTGCCACCTCTCTACACCCT
CAACAAGCCTTTGCTCAGTGGCATCAGCAATGCAGAAGCACGGCAGCCAGGGAAGGCCCCCAACTTCA
GTGTCAACTGGACGGTAGGCGACTCCGCTATTGAGGTCATCAACGCCACGACTGGGAAGGATGAGCTG
GGCCGCGCGTCCCGCCTGTGTAAGCACGCGTTGTACTGTCGCTGGATGCGTGTGCACGGCAAGGTTCC
CTCCCACTTACTACGCTCCAAGATTACCAAACCCAACGTGTACCATGAGTCCAAGCTGGCGGCAAAGG
AGTACCAGGCCGCCAAGGCGCGTCTGTTCACAGCCTTCATCAAGGCGGGGCTGGGGGCCTGGGTGGAG
AAGCCCACCGAGCAGGACCAGTTCTCACTCACGCCCTGAGGGCCCATGTACGATTTAATTATGCGGAC
GTGATGAGCGAAGTACGATCCCACGACCGAGGCCCGTTTAAACCCGCTGATCAGCCTCGACTGTGCCT
TCTAGTTGCCAGCCATCTGTTGTTTGCCCCTCCCCCGTGCCTTCCTTGACCCTGGAAGGTGCCACTCC
CACTGTCCTTTCCTAATAAAATGAGGAAATTGCATCGCATTGTCTGAGTAGGTGTCATTCTATTCTGG
GGGGTGGGGTGGGGCAGGACAGCAAGGGGGAGGATTGGGAAGACAATAGCAGGCATGCTGGGGATGCG
GTGGGCTCTATGGCTTCTGAGGCGGAAAGAACCAGCTGGGGCTCTAGGGGGTATCCCCACGCGCCCTG
TAGCGGCGCATTAAGCGCGGCGGGTGTGGTGGTTACGCGCAGCGTGACCGCTACACTTGCCAGCGCCC
TAGCGCCCGCTCCTTTCGCTTTCTTCCCTTCCTTTCTCGCCACGTTCGCCGGTCGATGTACGGGCCAG
ATATACGCGTTGACATTGATTATTGACTAGTTATTAATAGTAATCAATTACGGGGTCATTAGTTCATA
GCCCATATATGGAGTTCCGCGTTACATAACTTACGGTAAATGGCCCGCCTGGCTGACCGCCCAACGAC

CCCCGCCCATTGACGTCAATAATGACGTATGTTCCCATAGTAACGCCAATAGGGACTTTCCATTGACG
TCAATGGGTGGAGTATTTACGGTAAACTGCCCACTTGGCAGTACATCAAGTGTATCATATGCCAAGTA
CGCCCCCTATTGACGTCAATGACGGTAAATGGCCCGCCTGGCATTATGCCCAGTACATGACCTTATGG
GACTTTCCTACTTGGCAGTACATCTACGTATTAGTCATCGCTATTACCATGGTGATGCGGTTTTGGCA
GTACATCAATGGGCGTGGATAGCGGTTTGACTCACGGGGATTTCCAAGTCTCCACCCCATTGACGTCA
ATGGGAGTTTGTTTTGGCACCAAAATCAACGGGACTTTCCAAAATGTCGTAACAACTCCGCCCCATTG
ACGCAAATGGGCGGTAGGCGTGTACGGTGGGAGGTCTATATAAGCAGAGCTCTCCCTATCAGTGATAG
AGATCTCCCTATCAGTGATAGAGAGCGTGCATAGGGAACATCCACCACTTTAGTGAATTGTAGCACGG
CTTCAGAAGCGGCCGCCCACCATGGCAGAAATCGGTACTGGCTTTCCATTCGACCCCCATTATGTGGA
AGTCCTGGGCGAGCGCATGCACTACGTCGATGTTGGTCCGCGCGATGGCACCCCTGTGCTGTTCCTGC
ACGGTAACCCGACCTCCTCCTACGTGTGGCGCAACATCATCCCGCATGTTGCACCGACCCATCGCTGC
ATTGCTCCAGACCTGATCGGTATGGGCAAATCCGACAAACCAGACCTGGGTTATTTCTTCGACGACCA
CGTCCGCTTCATGGATGCCTTCATCGAAGCCCTGGGTCTGGAAGAGGTCGTCCTGGTCATTCACGACT
GGGGCTCCGCTCTGGGTTTCCACTGGGCCAAGCGCAATCCAGAGCGCGTCAAAGGTATTGCATTTATG
GAGTTCATCCGCCCTATCCCGACCTGGGACGAATGGCCAGAATTTGCCCGCGAGACCTTCCAGGCCTT
CCGCACCACCGACGTCGGCCGCAAGCTGATCATTGATCAGAACGTTTTTATCGAGGGTACGCTGCCGA
TGGGTGTCGTCCGCCCGCTGACTGAAGTCGAGATGGACCATTACCGCGAGCCGTTCCTGAATCCTGTT
GACCGCGAGCCACTGTGGCGCTTCCCAAACGAGCTGCCAATCGCCGGTGAGCCAGCGAACATCGTCGC
GCTGGTCGAAGAATACATGGACTGGCTGCACCAGTCCCCTGTCCCGAAGCTGCTGTTCTGGGGCACCC
CAGGCGTTCTGATCCCACCGGCCGAAGCCGCTCGCCTGGCCAAAAGCCTGCCTAACTGCAAGGCTGTG
GACATCGGCCCGGGTCTGAATCTGCTGCAAGAAGACAACCCGGACCTGATCGGCAGCGAGATCGCGCG
CTGGCTGTCGACGCTCGAGATTTCCGGCCCTGCAGGCGGAGGCGCGCCAGGGTCTGGCGGCGGCAGTA
AGGCAGAACGCATGGGTTTCACAGAGGTAACCCCAGTGACAGGGGCCAGTCTCAGAAGAACTATGCTC
CTCCTCTCAAGGTCCCCAGAAGCACAGCCAAAGACACTCCCTCTCACTGGCAGCACCTTCCATGACCA
GATAGCCATGCTGAGCCACCGGTGCTTCAACACTCTGACTAACAGCTTCCAGCCCTCCTTGCTCGGCC
GCAAGATTCTGGCCGCCATCATTATGAAAAAAGACTCTGAGGACATGGGTGTCGTCGTCAGCTTGGGA
ACAGGGAATCGCTGTGTAAAAGGAGATTCTCTCAGCCTAAAAGGAGAAACTGTCAATGACTGCCATGC
AGAAATAATCTCCCGGAGAGGCTTCATCAGGTTTCTCTACAGTGAGTTAATGAAATACAACTCCCAGA
CTGCGAAGGATAGTATATTTGAACCTGCTAAGGGAGGAGAAAAGCTCCAAATAAAAAAGACTGTGTCA
TTCCATCTGTATATCAGCACTGCTCCGTGTGGAGATGGCGCCCTCTTTGACAAGTCCTGCAGCGACCG
TGCTATGGAAAGCACAGAATCCCGCCACTACCCTGTCTTCGAGAATCCCAAACAAGGAAAGCTCCGCA
CCAAGGTGGAGAACGGACAAGGCACAATCCCTGTGGAATCCAGTGACATTGTGCCTACGTGGGATGGC
ATTCGGCTCGGGGAGAGACTCCGTACCATGTCCTGTAGTGACAAAATCCTACGCTGGAACGTGCTGGG
CCTGCAAGGGGCACTGTTGACCCACTTCCTGCAGCCCATTTATCTCAAATCTGTCACATTGGGTTACC
TTTTCAGCCAAGGGCATCTGACCCGTGCTATTTGCTGTCGTGTGACAAGAGATGGGAGTGCATTTGAG
GATGGACTACGACATCCCTTTATTGTCAACCACCCCAAGGTTGGCAGAGTCAGCATATATGATTCCAA
AAGGCAATCCGGGAAGACTAAGGAGACAAGCGTCAACTGGTGTCTGGCTGATGGCTATGACCTGGAGA
TCCTGGACGGTACCAGAGGCACTGTGGATGGGCCACGGAATGAATTGTCCCGGGTCTCCAAAAAGAAC
ATTTTTCTTCTATTTAAGAAGCTCTGCTCCTTCCGTTACCGCAGGGATCTACTGAGACTCTCCTATGG
TGAGGCCAAGAAAGCTGCCCGTGACTACGAGACGGCCAAGAACTACTTCAAAAAAGGCCTGAAGGATA
TGGGCTATGGGAACTGGATTAGCAAACCCCAGGAGGAAAAGAACTTTTATCTCTGCCCAGTATGAATC
GATATTTTCAGATATCGTGTTAGTAGGGTTGCACCGACGCGCATGTGGATTAGTGCTGTGCCTTCTAG
TTGCCAGCCATCTGTTGTTTGCCCCTCCCCCGTGCCTTCCTTGACCCTGGAAGGTGCCACTCCCACTG
TCCTTTCCTAATAAAATGAGGAAATTGCATCGCATTGTCTGAGTAGGTGTCATTCTATTCTGGGGGGT
GGGGTGGGGCAGGACAGCAAGGGGGAGGATTGGGAAGACAATAGCAGGCATGCTGGGGATGCGGTGGG
CTCTATGG

Cell line **2**: CMV-enhancer – CMV promoter – $TetO_2$ – HaloTag – ADAR1Q – bGH – CMV-enhancer – CMV promoter – $TetO_2$ – $SNAP_f$-tag– ADAR2Q – bGH

GACATTGATTATTGACTAGTTATTAATAGTAATCAATTACGGGGTCATTAGTTCATAGCCCATATATG
GAGTTCCGCGTTACATAACTTACGGTAAATGGCCCGCCTGGCTGACCGCCCAACGACCCCCGCCCATT
GACGTCAATAATGACGTATGTTCCCATAGTAACGCCAATAGGGACTTTCCATTGACGTCAATGGGTGG
AGTATTTACGGTAAACTGCCCACTTGGCAGTACATCAAGTGTATCATATGCCAAGTACGCCCCCTATT
GACGTCAATGACGGTAAATGGCCCGCCTGGCATTATGCCCAGTACATGACCTTATGGGACTTTCCTAC
TTGGCAGTACATCTACGTATTAGTCATCGCTATTACCATGGTGATGCGGTTTTGGCAGTACATCAATG
GGCGTGGATAGCGGTTTGACTCACGGGGATTTCCAAGTCTCCACCCCATTGACGTCAATGGGAGTTTG
TTTTGGCACCAAAATCAACGGGACTTTCCAAAATGTCGTAACAACTCCGCCCCATTGACGCAAATGGG
CGGTAGGCGTGTACGGTGGGAGGTCTATATAAGCAGAGCTCTCCCTATCAGTGATAGAGATCTCCCTA
TCAGTGATAGAGATCGTCGACGAGCTCGTTTAGTGAACCGTCAGATCGCCTGGAGACGCCATCCACGC
TGTTTTGACCTCCATAGAAGACACCGGGACCGATCCAGCCTCCGGACTCTAGCGTTTAAACTTAAGCT
TGGTACCGAGCTCGGATCCCCACCATGGCAGAAATCGGTACTGGCTTTCCATTCGACCCCCATTATGT
GGAAGTCCTGGGCGAGCGCATGCACTACGTCGATGTTGGTCCGCGCGATGGCACCCCTGTGCTGTTCC
TGCACGGTAACCCGACCTCCTCCTACGTGTGGCGCAACATCATCCCGCATGTTGCACCGACCCATCGC
TGCATTGCTCCAGACCTGATCGGTATGGGCAAATCCGACAAACCAGACCTGGGTTATTTCTTCGACGA
CCACGTCCGCTTCATGGATGCCTTCATCGAAGCCCTGGGTCTGGAAGAGGTCGTCCTGGTCATTCACG
ACTGGGGCTCCGCTCTGGGTTTCCACTGGGCCAAGCGCAATCCAGAGCGCGTCAAAGGTATTGCATTT
ATGGAGTTCATCCGCCCTATCCCGACCTGGGACGAATGGCCAGAATTTGCCCGCGAGACCTTCCAGGC
CTTCCGCACCACCGACGTCGGCCGCAAGCTGATCATTGATCAGAACGTTTTTATCGAGGGTACGCTGC
CGATGGGTGTCGTCCGCCCGCTGACTGAAGTCGAGATGGACCATTACCGCGAGCCGTTCCTGAATCCT
GTTGACCGCGAGCCACTGTGGCGCTTCCCAAACGAGCTGCCAATCGCCGGTGAGCCAGCGAACATCGT
CGCGCTGGTCGAAGAATACATGGACTGGCTGCACCAGTCCCCTGTCCCGAAGCTGCTGTTCTGGGGCA
CCCCAGGCGTTCTGATCCCACCGGCCGAAGCCGCTCGCCTGGCCAAAAGCCTGCCTAACTGCAAGGCT
GTGGACATCGGCCCGGGTCTGAATCTGCTGCAAGAAGACAACCCGGACCTGATCGGCAGCGAGATCGC
GCGCTGGCTGTCGACGCTCGAGATTTCCGGCCCTGCAGGCGGAGGCGCGCCAGGGTCTGGCGGCGGCA
GTAAGGCAGAACGCATGGGTTTCACAGAGGTAACCCCAGTGACAGGGGCCAGTCTCAGAAGAACTATG
CTCCTCCTCTCAAGGTCCCCAGAAGCACAGCCAAAGACACTCCCTCTCACTGGCAGCACCTTCCATGA
CCAGATAGCCATGCTGAGCCACCGGTGCTTCAACACTCTGACTAACAGCTTCCAGCCCTCCTTGCTCG
GCCGCAAGATTCTGGCCGCCATCATTATGAAAAAAGACTCTGAGGACATGGGTGTCGTCGTCAGCTTG
GGAACAGGGAATCGCTGTGTAAAAGGAGATTCTCTCAGCCTAAAAGGAGAAACTGTCAATGACTGCCA
TGCAGAAATAATCTCCCGGAGAGGCTTCATCAGGTTTCTCTACAGTGAGTTAATGAAATACAACTCCC
AGACTGCGAAGGATAGTATATTTGAACCTGCTAAGGGAGGAGAAAAGCTCCAAATAAAAAAGACTGTG
TCATTCCATCTGTATATCAGCACTGCTCCGTGTGGAGATGGCGCCCTCTTTGACAAGTCCTGCAGCGA
CCGTGCTATGGAAAGCACAGAATCCCGCCACTACCCTGTCTTCGAGAATCCCAAACAAGGAAAGCTCC
GCACCAAGGTGGAGAACGGACAAGGCACAATCCCTGTGGAATCCAGTGACATTGTGCCTACGTGGGAT
GGCATTCGGCTCGGGGAGAGACTCCGTACCATGTCCTGTAGTGACAAAATCCTACGCTGGAACGTGCT
GGGCCTGCAAGGGGCACTGTTGACCCACTTCCTGCAGCCCATTTATCTCAAATCTGTCACATTGGGTT
ACCTTTTCAGCCAAGGGCATCTGACCCGTGCTATTTGCTGTCGTGTGACAAGAGATGGGAGTGCATTT
GAGGATGGACTACGACATCCCTTTATTGTCAACCACCCCAAGGTTGGCAGAGTCAGCATATATGATTC
CAAAAGGCAATCCGGGAAGACTAAGGAGACAAGCGTCAACTGGTGTCTGGCTGATGGCTATGACCTGG
AGATCCTGGACGGTACCAGAGGCACTGTGGATGGGCCACGGAATGAATTGTCCCGGGTCTCCAAAAAG
AACATTTTTCTTCTATTTAAGAAGCTCTGCTCCTTCCGTTACCGCAGGGATCTACTGAGACTCTCCTA
TGGTGAGGCCAAGAAAGCTGCCCGTGACTACGAGACGGCCAAGAACTACTTCAAAAAAGGCCTGAAGG
ATATGGGCTATGGGAACTGGATTAGCAAACCCCAGGAGGAAAAGAACTTTTATCTCTGCCCAGTATGA
GGGCCCATGTACGATTTAATTATGCGGACGTGATGAGCGAAGTACGATCCCACGACCGAGGCCCGTTT
AAACCCGCTGATCAGCCTCGACTGTGCCTTCTAGTTGCCAGCCATCTGTTGTTTGCCCCTCCCCCGTG
CCTTCCTTGACCCTGGAAGGTGCCACTCCCACTGTCCTTTCCTAATAAAATGAGGAAATTGCATCGCA
TTGTCTGAGTAGGTGTCATTCTATTCTGGGGGGTGGGGTGGGGCAGGACAGCAAGGGGGAGGATTGGG
AAGACAATAGCAGGCATGCTGGGGATGCGGTGGGCTCTATGGCTTCTGAGGCGGAAAGAACCAGCTGG
GGCTCTAGGGGGTATCCCCACGCGCCCTGTAGCGGCGCATTAAGCGCGGCGGGTGTGGTGGTTACGCG

CAGCGTGACCGCTACACTTGCCAGCGCCCTAGCGCCCGCTCCTTTCGCTTTCTTCCCTTCCTTTCTCG
CCACGTTCGCCGGTCGATGTACGGGCCAGATATACGCGTTGACATTGATTATTGACTAGTTATTAATA
GTAATCAATTACGGGGTCATTAGTTCATAGCCCATATATGGAGTTCCGCGTTACATAACTTACGGTAA
ATGGCCCGCCTGGCTGACCGCCCAACGACCCCCGCCCATTGACGTCAATAATGACGTATGTTCCCATA
GTAACGCCAATAGGGACTTTCCATTGACGTCAATGGGTGGAGTATTTACGGTAAACTGCCCACTTGGC
AGTACATCAAGTGTATCATATGCCAAGTACGCCCCCTATTGACGTCAATGACGGTAAATGGCCCGCCT
GGCATTATGCCCAGTACATGACCTTATGGGACTTTCCTACTTGGCAGTACATCTACGTATTAGTCATC
GCTATTACCATGGTGATGCGGTTTTGGCAGTACATCAATGGGCGTGGATAGCGGTTTGACTCACGGGG
ATTTCCAAGTCTCCACCCCATTGACGTCAATGGGAGTTTGTTTTGGCACCAAAATCAACGGGACTTTC
CAAAATGTCGTAACAACTCCGCCCCATTGACGCAAATGGGCGGTAGGCGTGTACGGTGGGAGGTCTAT
ATAAGCAGAGCTCTCCCTATCAGTGATAGAGATCTCCCTATCAGTGATAGAGAGCGTGCATAGGGAAC
ATCCACCACTTTAGTGAATTGTAGCACGGCTTCAGAAGCGGCCGCCCACCATGGACAAAGACTGCGAA
ATGAAGCGCACCACCCTGGATAGCCCTCTGGGCAAGCTGGAACTGTCTGGGTGCGAACAGGGCCTGCA
CCGTATCATCTTCCTGGGCAAAGGAACATCTGCCGCCGACGCCGTGGAAGTGCCTGCCCCAGCCGCCG
TGCTGGGCGGACCAGAGCCACTGATGCAGGCCACCGCCTGGCTCAACGCCTACTTTCACCAGCCTGAG
GCCATCGAGGAGTTCCCTGTGCCAGCCCTGCACCACCCAGTGTTCCAGCAGGAGAGCTTTACCCGCCA
GGTGCTGTGGAAACTGCTGAAAGTGGTGAAGTTCGGAGAGGTCATCAGCTACAGCCACCTGGCCGCCC
TGGCCGGCAATCCCGCCGCCACCGCCGCCGTGAAAACCGCCCTGAGCGGAAATCCCGTGCCCATTCTG
ATCCCCTGCCACCGGGTGGTGCAGGGCGACCTGGACGTGGGGGGCTACGAGGGCGGGCTCGCCGTGAA
AGAGTGGCTGCTGGCCCACGAGGGCCACAGACTGGGCAAGCCTGGGCTGGGTCCTGCAGGCGGAGGCG
CGCCAGGGTCTGGCGGCGGCAGTAAGAAGCTTGCCAAGGCCCGGGCTGCGCAGTCTGCCCTGGCCGCC
ATTTTTAACTTGCACTTGGATCAGACGCCATCTCGCCAGCCTATTCCCAGTGAGGGTCTTCAGCTGCA
TTTACCGCAGGTTTTAGCTGACGCTGTCTCACGCCTGGTCCTGGGTAAGTTTGGTGACCTGACCGACA
ACTTCTCCTCCCCTCACGCTCGCAGAAAAGTGCTGGCTGGAGTCGTCATGACAACAGGCACAGATGTT
AAAGATGCCAAGGTGATAAGTGTTTCTACAGGAACAAAATGTATTAATGGTGAATACATGAGTGATCG
TGGCCTTGCATTAAATGACTGCCATGCAGAAATAATATCTCGGAGATCCTTGCTCAGATTTCTTTATA
CACAACTTGAGCTTTACTTAAATAACAAAGATGATCAAAAAAGATCCATCTTTCAGAAATCAGAGCGA
GGGGGGTTTAGGCTGAAGGAGAATGTCCAGTTTCATCTGTACATCAGCACCTCTCCCTGTGGAGATGC
CAGAATCTTCTCACCACATGAGCCAATCCTGGAAGAACCAGCAGATAGACACCCAAATCGTAAAGCAA
GAGGACAGCTACGGACCAAAATAGAGTCTGGTCAGGGGACGATTCCAGTGCGCTCCAATGCGAGCATC
CAAACGTGGGACGGGGTGCTGCAAGGGGAGCGGCTGCTCACCATGTCCTGCAGTGACAAGATTGCACG
CTGGAACGTGGTGGGCATCCAGGGTTCCCTGCTCAGCATTTTCGTGGAGCCCATTTACTTCTCGAGCA
TCATCCTGGGCAGCCTTTACCACGGGGACCACCTTTCCAGGGCCATGTACCAGCGGATCTCCAACATA
GAGGACCTGCCACCTCTCTACACCCTCAACAAGCCTTTGCTCAGTGGCATCAGCAATGCAGAAGCACG
GCAGCCAGGGAAGGCCCCCAACTTCAGTGTCAACTGGACGGTAGGCGACTCCGCTATTGAGGTCATCA
ACGCCACGACTGGGAAGGATGAGCTGGGCCGCGCGTCCCGCCTGTGTAAGCACGCGTTGTACTGTCGC
TGGATGCGTGTGCACGGCAAGGTTCCCTCCCACTTACTACGCTCCAAGATTACCAAACCCAACGTGTA
CCATGAGTCCAAGCTGGCGGCAAAGGAGTACCAGGCCGCCAAGGCGCGTCTGTTCACAGCCTTCATCA
AGGCGGGGCTGGGGGCCTGGGTGGAGAAGCCCACCGAGCAGGACCAGTTCTCACTCACGCCCTGAATC
GATATTTTCAGATATCGTGTTAGTAGGGTTGCACCGACGCGCATGTGGATTAGTGCTGTGCCTTCTAG
TTGCCAGCCATCTGTTGTTTGCCCCTCCCCCGTGCCTTCCTTGACCCTGGAAGGTGCCACTCCCACTG
TCCTTTCCTAATAAAATGAGGAAATTGCATCGCATTGTCTGAGTAGGTGTCATTCTATTCTGGGGGGT
GGGGTGGGGCAGGACAGCAAGGGGGAGGATTGGGAAGACAATAGCAGGCATGCTGGGGATGCGGTGGG
CTCTATGG

Cell line **3**: CMV-enhancer – CMV promoter – $TetO_2$ – $SNAP_f$-tag – ADAR2Q – P2A – HaloTag – ADAR1Q – bGH

GACATTGATTATTGACTAGTTATTAATAGTAATCAATTACGGGGTCATTAGTTCATAGCCCATATATG
GAGTTCCGCGTTACATAACTTACGGTAAATGGCCCGCCTGGCTGACCGCCCAACGACCCCCGCCCATT
GACGTCAATAATGACGTATGTTCCCATAGTAACGCCAATAGGGACTTTCCATTGACGTCAATGGGTGG
AGTATTTACGGTAAACTGCCCACTTGGCAGTACATCAAGTGTATCATATGCCAAGTACGCCCCCTATT
GACGTCAATGACGGTAAATGGCCCGCCTGGCATTATGCCCAGTACATGACCTTATGGGACTTTCCTAC
TTGGCAGTACATCTACGTATTAGTCATCGCTATTACCATGGTGATGCGGTTTTGGCAGTACATCAATG
GGCGTGGATAGCGGTTTGACTCACGGGGATTTCCAAGTCTCCACCCCATTGACGTCAATGGGAGTTTG
TTTTGGCACCAAAATCAACGGGACTTTCCAAAATGTCGTAACAACTCCGCCCCATTGACGCAAATGGG
CGGTAGGCGTGTACGGTGGGAGGTCTATATAAGCAGAGCTCTCCCTATCAGTGATAGAGATCTCCCTA
TCAGTGATAGAGATCGTCGACGAGCTCGTTTAGTGAACCGTCAGATCGCCTGGAGACGCCATCCACGC
TGTTTTGACCTCCATAGAAGACACCGGGACCGATCCAGCCTCCGGACTCTAGCGTTTAAACTTAAGCT
TGGTACCGAGCTCGGATCCCCACCATGGACAAAGACTGCGAAATGAAGCGCACCACCCTGGATAGCCC
TCTGGGCAAGCTGGAACTGTCTGGGTGCGAACAGGGCCTGCACCGTATCATCTTCCTGGGCAAAGGAA
CATCTGCCGCCGACGCCGTGGAAGTGCCTGCCCCAGCCGCCGTGCTGGGCGGACCAGAGCCACTGATG
CAGGCCACCGCCTGGCTCAACGCCTACTTTCACCAGCCTGAGGCCATCGAGGAGTTCCCTGTGCCAGC
CCTGCACCACCCAGTGTTCCAGCAGGAGAGCTTTACCCGCCAGGTGCTGTGGAAACTGCTGAAAGTGG
TGAAGTTCGGAGAGGTCATCAGCTACAGCCACCTGGCCGCCCTGGCCGGCAATCCCGCCGCCACCGCC
GCCGTGAAAACCGCCCTGAGCGGAAATCCCGTGCCCATTCTGATCCCCTGCCACCGGGTGGTGCAGGG
CGACCTGGACGTGGGGGGCTACGAGGGCGGGCTCGCCGTGAAAGAGTGGCTGCTGGCCCACGAGGGCC
ACAGACTGGGCAAGCCTGGGCTGGGTCCTGCAGGCGGAGGCGCGCCAGGGTCTGGCGGCGGCAGTAAG
AAGCTTGCCAAGGCCCGGGCTGCGCAGTCTGCCCTGGCCGCCATTTTTAACTTGCACTTGGATCAGAC
GCCATCTCGCCAGCCTATTCCCAGTGAGGGTCTTCAGCTGCATTTACCGCAGGTTTTAGCTGACGCTG
TCTCACGCCTGGTCCTGGGTAAGTTTGGTGACCTGACCGACAACTTCTCCTCCCCTCACGCTCGCAGA
AAAGTGCTGGCTGGAGTCGTCATGACAACAGGCACAGATGTTAAAGATGCCAAGGTGATAAGTGTTTC
TACAGGAACAAAATGTATTAATGGTGAATACATGAGTGATCGTGGCCTTGCATTAAATGACTGCCATG
CAGAAATAATATCTCGGAGATCCTTGCTCAGATTTCTTTATACACAACTTGAGCTTTACTTAAATAAC
AAAGATGATCAAAAAAGATCCATCTTTCAGAAATCAGAGCGAGGGGGGTTTAGGCTGAAGGAGAATGT
CCAGTTTCATCTGTACATCAGCACCTCTCCCTGTGGAGATGCCAGAATCTTCTCACCACATGAGCCAA
TCCTGGAAGAACCAGCAGATAGACACCCAAATCGTAAAGCAAGAGGACAGCTACGGACCAAAATAGAG
TCTGGTCAGGGGACGATTCCAGTGCGCTCCAATGCGAGCATCCAAACGTGGGACGGGGTGCTGCAAGG
GGAGCGGCTGCTCACCATGTCCTGCAGTGACAAGATTGCACGCTGGAACGTGGTGGGCATCCAGGGTT
CCCTGCTCAGCATTTTCGTGGAGCCCATTTACTTCTCGAGCATCATCCTGGGCAGCCTTTACCACGGG
GACCACCTTTCCAGGGCCATGTACCAGCGGATCTCCAACATAGAGGACCTGCCACCTCTCTACACCCT
CAACAAGCCTTTGCTCAGTGGCATCAGCAATGCAGAAGCACGGCAGCCAGGGAAGGCCCCCAACTTCA
GTGTCAACTGGACGGTAGGCGACTCCGCTATTGAGGTCATCAACGCCACGACTGGGAAGGATGAGCTG
GGCCGCGCGTCCCGCCTGTGTAAGCACGCGTTGTACTGTCGCTGGATGCGTGTGCACGGCAAGGTTCC
CTCCCACTTACTACGCTCCAAGATTACCAAACCCAACGTGTACCATGAGTCCAAGCTGGCGGCAAAGG
AGTACCAGGCCGCCAAGGCGCGTCTGTTCACAGCCTTCATCAAGGCGGGGCTGGGGGCCTGGGTGGAG
AAGCCCACCGAGCAGGACCAGTTCTCACTCACGCCCGGCGGCCGCGGAAGCGGAGCTACTAACTTCAG
CCTGCTGAAGCAGGCTGGAGACGTGGAGGAGAACCCTGGACCTCTCGAGATGGCAGAAATCGGTACTG
GCTTTCCATTCGACCCCCATTATGTGGAAGTCCTGGGCGAGCGCATGCACTACGTCGATGTTGGTCCG
CGCGATGGCACCCCTGTGCTGTTCCTGCACGGTAACCCGACCTCCTCCTACGTGTGGCGCAACATCAT
CCCGCATGTTGCACCGACCCATCGCTGCATTGCTCCAGACCTGATCGGTATGGGCAAATCCGACAAAC
CAGACCTGGGTTATTTCTTCGACGACCACGTCCGCTTCATGGATGCCTTCATCGAAGCCCTGGGTCTG
GAAGAGGTCGTCCTGGTCATTCACGACTGGGGCTCCGCTCTGGGTTTCCACTGGGCCAAGCGCAATCC
AGAGCGCGTCAAAGGTATTGCATTTATGGAGTTCATCCGCCCTATCCCGACCTGGGACGAATGGCCAG
AATTTGCCCGCGAGACCTTCCAGGCCTTCCGCACCACCGACGTCGGCCGCAAGCTGATCATCGATCAG
AACGTTTTTATCGAGGGTACGCTGCCGATGGGTGTCGTCCGCCCGCTGACTGAAGTCGAGATGGACCA
TTACCGCGAGCCGTTCCTGAATCCTGTTGACCGCGAGCCACTGTGGCGCTTCCCAAACGAGCTGCCAA
TCGCCGGTGAGCCAGCGAACATCGTCGCGCTGGTCGAAGAATACATGGACTGGCTGCACCAGTCCCCT

GTCCCGAAGCTGCTGTTCTGGGGCACCCCAGGCGTTCTGATCCCACCGGCCGAAGCCGCTCGCCTGGC
CAAAAGCCTGCCTAACTGCAAGGCTGTGGACATCGGCCCGGGTCTGAATCTGCTGCAAGAAGACAACC
CGGACCTGATCGGCAGCGAGATCGCGCGCTGGCTGTCGACGCTGGAGATTTCCGGCCCTGCAGGCGGA
GGCGCGCCAGGGTCTGGCGGCGGCAGTAAGGCAGAACGCATGGGTTTCACAGAGGTAACCCCAGTGAC
AGGGGCCAGTCTCAGAAGAACTATGCTCCTCCTCTCAAGGTCCCCAGAAGCACAGCCAAAGACACTCC
CTCTCACTGGCAGCACCTTCCATGACCAGATAGCCATGCTGAGCCACCGGTGCTTCAACACTCTGACT
AACAGCTTCCAGCCCTCCTTGCTCGGCCGCAAGATTCTGGCCGCCATCATTATGAAAAAAGACTCTGA
GGACATGGGTGTCGTCGTCAGCTTGGGAACAGGGAATCGCTGTGTAAAAGGAGATTCTCTCAGCCTAA
AAGGAGAAACTGTCAATGACTGCCATGCAGAAATAATCTCCCGGAGAGGCTTCATCAGGTTTCTCTAC
AGTGAGTTAATGAAATACAACTCCCAGACTGCGAAGGATAGTATATTTGAACCTGCTAAGGGAGGAGA
AAAGCTCCAAATAAAAAAGACTGTGTCATTCCATCTGTATATCAGCACTGCTCCGTGTGGAGATGGCG
CCCTCTTTGACAAGTCCTGCAGCGACCGTGCTATGGAAAGCACAGAATCCCGCCACTACCCTGTCTTC
GAGAATCCCAAACAAGGAAAGCTCCGCACCAAGGTGGAGAACGGACAAGGCACAATCCCTGTGGAATC
CAGTGACATTGTGCCTACGTGGGATGGCATTCGGCTCGGGGAGAGACTCCGTACCATGTCCTGTAGTG
ACAAAATCCTACGCTGGAACGTGCTGGGCCTGCAAGGGGCACTGTTGACCCACTTCCTGCAGCCCATT
TATCTCAAATCTGTCACATTGGGTTACCTTTTCAGCCAAGGGCATCTGACCCGTGCTATTTGCTGTCG
TGTGACAAGAGATGGGAGTGCATTTGAGGATGGACTACGACATCCCTTTATTGTCAACCACCCCAAGG
TTGGCAGAGTCAGCATATATGATTCCAAAAGGCAATCCGGGAAGACTAAGGAGACAAGCGTCAACTGG
TGTCTGGCTGATGGCTATGACCTGGAGATCCTGGACGGTACCAGAGGCACTGTGGATGGGCCACGGAA
TGAATTGTCCCGGGTCTCCAAAAAGAACATTTTTCTTCTATTTAAGAAGCTCTGCTCCTTCCGTTACC
GCAGGGATCTACTGAGACTCTCCTATGGTGAGGCCAAGAAAGCTGCCCGTGACTACGAGACGGCCAAG
AACTACTTCAAAAAAGGCCTGAAGGATATGGGCTATGGGAACTGGATTAGCAAACCCCAGGAGGAAAA
GAACTTTTATCTCTGCCCAGTATGATTAATTAAGTTTAAACCCGCTGATCAGCCTCGACTGTGCCTTC
TAGTTGCCAGCCATCTGTTGTTTGCCCCTCCCCCGTGCCTTCCTTGACCCTGGAAGGTGCCACTCCCA
CTGTCCTTTCCTAATAAAATGAGGAAATTGCATCGCATTGTCTGAGTAGGTGTCATTCTATTCTGGGG
GGTGGGGTGGGGCAGGACAGCAAGGGGGAGGATTGGGAAGACAATAGCAGGCATGCTGGGGATGCGGT
GGGCTCTATGG

Cell line **4**: bGH – ADAR2Q – $SNAP_f$-tag – $TetO_2$ – CMV promoter – EF1α core promoter – $TetO_2$ – HaloTag – ADAR1Q – bGH

CCATAGAGCCCACCGCATCCCCAGCATGCCTGCTATTGTCTTCCCAATCCTCCCCCTTGCTGTCCTGC
CCCACCCCACCCCCCAGAATAGAATGACACCTACTCAGACAATGCGATGCAATTTCCTCATTTTATTA
GGAAAGGACAGTGGGAGTGGCACCTTCCAGGGTCAAGGAAGGCACGGGGGAGGGGCAAACAACAGATG
GCTGGCAACTAGAAGGCACAGTCGAGGCTGATCAGCGGGTTTAAACATCGATTCAGGGCGTGAGTGAG
AACTGGTCCTGCTCGGTGGGCTTCTCCACCCAGGCCCCCAGCCCCGCCTTGATGAAGGCTGTGAACAG
ACGCGCCTTGGCGGCCTGGTACTCCTTTGCCGCCAGCTTGGACTCATGGTACACGTTGGGTTTGGTAA
TCTTGGAGCGTAGTAAGTGGGAGGGAACCTTGCCGTGCACACGCATCCAGCGACAGTACAACGCGTGC
TTACACAGGCGGGACGCGCGGCCCAGCTCATCCTTCCCAGTCGTGGCGTTGATGACCTCAATAGCGGA
GTCGCCTACCGTCCAGTTGACACTGAAGTTGGGGGCCTTCCCTGGCTGCCGTGCTTCTGCATTGCTGA
TGCCACTGAGCAAAGGCTTGTTGAGGGTGTAGAGAGGTGGCAGGTCCTCTATGTTGGAGATCCGCTGG
TACATGGCCCTGGAAAGGTGGTCCCCGTGGTAAAGGCTGCCCAGGATGATGCTCGAGAAGTAAATGGG
CTCCACGAAAATGCTGAGCAGGGAACCCTGGATGCCCACCACGTTCCAGCGTGCAATCTTGTCACTGC
AGGACATGGTGAGCAGCCGCTCCCCTTGCAGCACCCCGTCCCACGTTTGGATGCTCGCATTGGAGCGC
ACTGGAATCGTCCCCTGACCAGACTCTATTTTGGTCCGTAGCTGTCCTCTTGCTTTACGATTTGGGTG
TCTATCTGCTGGTTCTTCCAGGATTGGCTCATGTGGTGAGAAGATTCTGGCATCTCCACAGGGAGAGG
TGCTGATGTACAGATGAAACTGGACATTCTCCTTCAGCCTAAACCCCCCTCGCTCTGATTTCTGAAAG
ATGGATCTTTTTTGATCATCTTTGTTATTTAAGTAAAGCTCAAGTTGTGTATAAAGAAATCTGAGCAA
GGATCTCCGAGATATTATTTCTGCATGGCAGTCATTTAATGCAAGGCCACGATCACTCATGTATTCAC
CATTAATACATTTTGTTCCTGTAGAAACACTTATCACCTTGGCATCTTTAACATCTGTGCCTGTTGTC
ATGACGACTCCAGCCAGCACTTTTCTGCGAGCGTGAGGGGAGGAGAAGTTGTCGGTCAGGTCACCAAA

CTTACCCAGGACCAGGCGTGAGACAGCGTCAGCTAAAACCTGCGGTAAATGCAGCTGAAGACCCTCAC
TGGGAATAGGCTGGCGAGATGGCGTCTGATCCAAGTGCAAGTTAAAAATGGCGGCCAGGGCAGACTGC
GCAGCCCGGGCCTTGGCAAGCTTCTTACTGCCGCCGCCAGACCCTGGCGCGCCTCCGCCTGCAGGACC
CAGCCCAGGCTTGCCCAGTCTGTGGCCCTCGTGGGCCAGCAGCCACTCTTTCACGGCGAGCCCGCCCT
CGTAGCCCCCCACGTCCAGGTCGCCCTGCACCACCCGGTGGCAGGGGATCAGAATGGGCACGGGATTT
CCGCTCAGGGCGGTTTTCACGGCGGCGGTGGCGGCGGGATTGCCGGCCAGGGCGGCCAGGTGGCTGTA
GCTGATGACCTCTCCGAACTTCACCACTTTCAGCAGTTTCCACAGCACCTGGCGGGTAAAGCTCTCCT
GCTGGAACACTGGGTGGTGCAGGGCTGGCACAGGGAACTCCTCGATGGCCTCAGGCTGGTGAAAGTAG
GCGTTGAGCCAGGCGGTGGCCTGCATCAGTGGCTCTGGTCCGCCCAGCACGGCGGCTGGGGCAGGCAC
TTCCACGGCGTCGGCGGCAGATGTTCCTTTGCCCAGGAAGATGATACGGTGCAGGCCCTGTTCGCACC
CAGACAGTTCCAGCTTGCCCAGAGGGCTATCCAGGGTGGTGCGCTTCATTTCGCAGTCTTTGTCCATG
GTGGGCGGCCGCCCCAGAGTAAAGCTATTCGGTAATTCGTCACCCAAGAGATCAATCGGTCTCTCTCT
ATCACTGATAGGGAGATCTCTATCACTGATAGGGAGAGCTCTGCTTATATAGACCTCCCACCGTACAC
GCCTACCGCCCATTTGCGTCAATGGGGCGGAGTTGTTACGACATTTTGGAAAGTCCCGTTGATTTTGG
TGCCAAAACAAACTCCCATTGACGTCAATGGGGTGGAGACTTGGAAATCCCCGTGAGTCAAACCGCTA
TCCACGCCCATTGATGTACTGCCAAAACCGCATCACCATGGACGTGTCGAGGTGATAATTCCACTCGA
GTGGCTCCGGTGCCCGTCAGTGGGCAGAGCGCACATCGCCCACAGTCCCCGAGAAGTTGGGGGGAGGG
GTCGGCAATTGAACCGGTGCCTAGAGAAGGTGGCGCGGGGTAAACTGGGAAAGTGATGTCGTGTACTG
GCTCCGCCTTTTTCCCGAGGGTGGGGGAGAACCGTATATAAGTGCAGTAGTCGCCGTGAACGTTCTTT
TTCGCAACGGGTTTGCCGCCAGAACACAGGTCCCTATCAGTGATAGAGATCTCCCTATCAGTGATAGA
GATCGTCGACGAGCTCGTTTAGTGAACCGTCAGATCGCCTGGAGACGCCATCGGATCCCCACCATGGC
AGAAATCGGTACTGGCTTTCCATTCGACCCCCATTATGTGGAAGTCCTGGGCGAGCGCATGCACTACG
TCGATGTTGGTCCGCGCGATGGCACCCCTGTGCTGTTCCTGCACGGTAACCCGACCTCCTCCTACGTG
TGGCGCAACATCATCCCGCATGTTGCACCGACCCATCGCTGCATTGCTCCAGACCTGATCGGTATGGG
CAAATCCGACAAACCAGACCTGGGTTATTTCTTCGACGACCACGTCCGCTTCATGGATGCCTTCATCG
AAGCCCTGGGTCTGGAAGAGGTCGTCCTGGTCATTCACGACTGGGGCTCCGCTCTGGGTTTCCACTGG
GCCAAGCGCAATCCAGAGCGCGTCAAAGGTATTGCATTTATGGAGTTCATCCGCCCTATCCCGACCTG
GGACGAATGGCCAGAATTTGCCCGCGAGACCTTCCAGGCCTTCCGCACCACCGACGTCGGCCGCAAGC
TGATCATTGATCAGAACGTTTTTATCGAGGGTACGCTGCCGATGGGTGTCGTCCGCCCGCTGACTGAA
GTCGAGATGGACCATTACCGCGAGCCGTTCCTGAATCCTGTTGACCGCGAGCCACTGTGGCGCTTCCC
AAACGAGCTGCCAATCGCCGGTGAGCCAGCGAACATCGTCGCGCTGGTCGAAGAATACATGGACTGGC
TGCACCAGTCCCCTGTCCCGAAGCTGCTGTTCTGGGGCACCCCAGGCGTTCTGATCCCACCGGCCGAA
GCCGCTCGCCTGGCCAAAAGCCTGCCTAACTGCAAGGCTGTGGACATCGGCCCGGGTCTGAATCTGCT
GCAAGAAGACAACCCGGACCTGATCGGCAGCGAGATCGCGCGCTGGCTGTCGACGCTCGAGATTTCCG
GCCCTGCAGGCGGAGGCGCGCCAGGGTCTGGCGGCGGCAGTAAGGCAGAACGCATGGGTTTCACAGAG
GTAACCCCAGTGACAGGGGCCAGTCTCAGAAGAACTATGCTCCTCCTCTCAAGGTCCCCAGAAGCACA
GCCAAAGACACTCCCTCTCACTGGCAGCACCTTCCATGACCAGATAGCCATGCTGAGCCACCGGTGCT
TCAACACTCTGACTAACAGCTTCCAGCCCTCCTTGCTCGGCCGCAAGATTCTGGCCGCCATCATTATG
AAAAAAGACTCTGAGGACATGGGTGTCGTCGTCAGCTTGGGAACAGGGAATCGCTGTGTAAAAGGAGA
TTCTCTCAGCCTAAAAGGAGAAACTGTCAATGACTGCCATGCAGAAATAATCTCCCGGAGAGGCTTCA
TCAGGTTTCTCTACAGTGAGTTAATGAAATACAACTCCCAGACTGCGAAGGATAGTATATTTGAACCT
GCTAAGGGAGGAGAAAAGCTCCAAATAAAAAAGACTGTGTCATTCCATCTGTATATCAGCACTGCTCC
GTGTGGAGATGGCGCCCTCTTTGACAAGTCCTGCAGCGACCGTGCTATGGAAAGCACAGAATCCCGCC
ACTACCCTGTCTTCGAGAATCCCAAACAAGGAAAGCTCCGCACCAAGGTGGAGAACGGACAAGGCACA
ATCCCTGTGGAATCCAGTGACATTGTGCCTACGTGGGATGGCATTCGGCTCGGGGAGAGACTCCGTAC
CATGTCCTGTAGTGACAAAATCCTACGCTGGAACGTGCTGGGCCTGCAAGGGGCACTGTTGACCCACT
TCCTGCAGCCCATTTATCTCAAATCTGTCACATTGGGTTACCTTTTCAGCCAAGGGCATCTGACCCGT
GCTATTTGCTGTCGTGTGACAAGAGATGGGAGTGCATTTGAGGATGGACTACGACATCCCTTTATTGT
CAACCACCCCAAGGTTGGCAGAGTCAGCATATATGATTCCAAAAGGCAATCCGGGAAGACTAAGGAGA
CAAGCGTCAACTGGTGTCTGGCTGATGGCTATGACCTGGAGATCCTGGACGGTACCAGAGGCACTGTG
GATGGGCCACGGAATGAATTGTCCCGGGTCTCCAAAAAGAACATTTTTCTTCTATTTAAGAAGCTCTG
CTCCTTCCGTTACCGCAGGGATCTACTGAGACTCTCCTATGGTGAGGCCAAGAAAGCTGCCCGTGACT

ACGAGACGGCCAAGAACTACTTCAAAAAAGGCCTGAAGGATATGGGCTATGGGAACTGGATTAGCAAA
CCCCAGGAGGAAAAGAACTTTTATCTCTGCCCAGTATGATTAATTAAGTTTAAACCCGCTGATCAGCC
TCGACTGTGCCTTCTAGTTGCCAGCCATCTGTTGTTTGCCCCTCCCCCGTGCCTTCCTTGACCCTGGA
AGGTGCCACTCCCACTGTCCTTTCCTAATAAAATGAGGAAATTGCATCGCATTGTCTGAGTAGGTGTC
ATTCTATTCTGGGGGGTGGGGTGGGGCAGGACAGCAAGGGGGAGGATTGGGAAGACAATAGCAGGCAT
GCTGGGGATGCGGTGGGCTCTATGG

Cell line **5**: bGH – ADAR1Q – HaloTag – $TetO_2$ – CMV promoter – EF1α core promoter – $TetO_2$ – $SNAP_f$-tag – ADAR2Q – bGH

CCATAGAGCCCACCGCATCCCCAGCATGCCTGCTATTGTCTTCCCAATCCTCCCCCTTGCTGTCCTGC
CCCACCCCACCCCCCAGAATAGAATGACACCTACTCAGACAATGCGATGCAATTTCCTCATTTTATTA
GGAAAGGACAGTGGGAGTGGCACCTTCCAGGGTCAAGGAAGGCACGGGGGAGGGGCAAACAACAGATG
GCTGGCAACTAGAAGGCACAGTCGAGGCTGATCAGCGGGTTTAAACATCGATTCATACTGGGCAGAGA
TAAAAGTTCTTTTCCTCCTGGGGTTTGCTAATCCAGTTCCCATAGCCCATATCCTTCAGGCCTTTTTT
GAAGTAGTTCTTGGCCGTCTCGTAGTCACGGGCAGCTTTCTTGGCCTCACCATAGGAGAGTCTCAGTA
GATCCCTGCGGTAACGGAAGGAGCAGAGCTTCTTAAATAGAAGAAAAATGTTCTTTTTGGAGACCCGG
GACAATTCATTCCGTGGCCCATCCACAGTGCCTCTGGTACCGTCCAGGATCTCCAGGTCATAGCCATC
AGCCAGACACCAGTTGACGCTTGTCTCCTTAGTCTTCCCGGATTGCCTTTTGGAATCATATATGCTGA
CTCTGCCAACCTTGGGGTGGTTGACAATAAAGGGATGTCGTAGTCCATCCTCAAATGCACTCCCATCT
CTTGTCACACGACAGCAAATAGCACGGGTCAGATGCCCTTGGCTGAAAAGGTAACCCAATGTGACAGA
TTTGAGATAAATGGGCTGCAGGAAGTGGGTCAACAGTGCCCCTTGCAGGCCCAGCACGTTCCAGCGTA
GGATTTTGTCACTACAGGACATGGTACGGAGTCTCTCCCCGAGCCGAATGCCATCCCACGTAGGCACA
ATGTCACTGGATTCCACAGGGATTGTGCCTTGTCCGTTCTCCACCTTGGTGCGGAGCTTTCCTTGTTT
GGGATTCTCGAAGACAGGGTAGTGGCGGGATTCTGTGCTTTCCATAGCACGGTCGCTGCAGGACTTGT
CAAAGAGGGCGCCATCTCCACACGGAGCAGTGCTGATATACAGATGGAATGACACAGTCTTTTTTATT
TGGAGCTTTTCTCCTCCCTTAGCAGGTTCAAATATACTATCCTTCGCAGTCTGGGAGTTGTATTTCAT
TAACTCACTGTAGAGAAACCTGATGAAGCCTCTCCGGGAGATTATTTCTGCATGGCAGTCATTGACAG
TTTCTCCTTTTAGGCTGAGAGAATCTCCTTTTACACAGCGATTCCCTGTTCCCAAGCTGACGACGACA
CCCATGTCCTCAGAGTCTTTTTTCATAATGATGGCGGCCAGAATCTTGCGGCCGAGCAAGGAGGGCTG
GAAGCTGTTAGTCAGAGTGTTGAAGCACCGGTGGCTCAGCATGGCTATCTGGTCATGGAAGGTGCTGC
CAGTGAGAGGGAGTGTCTTTGGCTGTGCTTCTGGGGACCTTGAGAGGAGGAGCATAGTTCTTCTGAGA
CTGGCCCCTGTCACTGGGGTTACCTCTGTGAAACCCATGCGTTCTGCCTTACTGCCGCCGCCAGACCC
TGGCGCGCCTCCGCCTGCAGGGCCGGAAATCTCGAGCGTCGACAGCCAGCGCGCGATCTCGCTGCCGA
TCAGGTCCGGGTTGTCTTCTTGCAGCAGATTCAGACCCGGGCCGATGTCCACAGCCTTGCAGTTAGGC
AGGCTTTTGGCCAGGCGAGCGGCTTCGGCCGGTGGGATCAGAACGCCTGGGGTGCCCCAGAACAGCAG
CTTCGGGACAGGGGACTGGTGCAGCCAGTCCATGTATTCTTCGACCAGCGCGACGATGTTCGCTGGCT
CACCGGCGATTGGCAGCTCGTTTGGGAAGCGCCACAGTGGCTCGCGGTCAACAGGATTCAGGAACGGC
TCGCGGTAATGGTCCATCTCGACTTCAGTCAGCGGGCGGACGACACCCATCGGCAGCGTACCCTCGAT
AAAAACGTTCTGATCAATGATCAGCTTGCGGCCGACGTCGGTGGTGCGGAAGGCCTGGAAGGTCTCGC
GGGCAAATTCTGGCCATTCGTCCCAGGTCGGGATAGGGCGGATGAACTCCATAAATGCAATACCTTTG
ACGCGCTCTGGATTGCGCTTGGCCCAGTGGAAACCCAGAGCGGAGCCCCAGTCGTGAATGACCAGGAC
GACCTCTTCCAGACCCAGGGCTTCGATGAAGGCATCCATGAAGCGGACGTGGTCGTCGAAGAAATAAC
CCAGGTCTGGTTTGTCGGATTTGCCCATACCGATCAGGTCTGGAGCAATGCAGCGATGGGTCGGTGCA
ACATGCGGGATGATGTTGCGCCACACGTAGGAGGAGGTCGGGTTACCGTGCAGGAACAGCACAGGGGT
GCCATCGCGCGGACCAACATCGACGTAGTGCATGCGCTCGCCCAGGACTTCCACATAATGGGGGTCGA
ATGGAAAGCCAGTACCGATTTCTGCCATGGTGGGCGGCCGCCCCAGAGTAAAGCTATTCGGTAATTCG
TCACCCAAGAGATCAATCGGTCTCTCTCTATCACTGATAGGGAGATCTCTATCACTGATAGGGAGAGC
TCTGCTTATATAGACCTCCCACCGTACACGCCTACCGCCCATTTGCGTCAATGGGGCGGAGTTGTTAC
GACATTTTGGAAAGTCCCGTTGATTTTGGTGCCAAAACAAACTCCCATTGACGTCAATGGGGTGGAGA
CTTGGAAATCCCCGTGAGTCAAACCGCTATCCACGCCCATTGATGTACTGCCAAAACCGCATCACCAT

GGACGTGTCGAGGTGATAATTCCACTCGAGTGGCTCCGGTGCCCGTCAGTGGGCAGAGCGCACATCGC
CCACAGTCCCCGAGAAGTTGGGGGGAGGGGTCGGCAATTGAACCGGTGCCTAGAGAAGGTGGCGCGGG
GTAAACTGGGAAAGTGATGTCGTGTACTGGCTCCGCCTTTTTCCCGAGGGTGGGGGAGAACCGTATAT
AAGTGCAGTAGTCGCCGTGAACGTTCTTTTTCGCAACGGGTTTGCCGCCAGAACACAGGTCCCTATCA
GTGATAGAGATCTCCCTATCAGTGATAGAGATCGTCGACGAGCTCGTTTAGTGAACCGTCAGATCGCC
TGGAGACGCCATCGGATCCCCACCATGGACAAAGACTGCGAAATGAAGCGCACCACCCTGGATAGCCC
TCTGGGCAAGCTGGAACTGTCTGGGTGCGAACAGGGCCTGCACCGTATCATCTTCCTGGGCAAAGGAA
CATCTGCCGCCGACGCCGTGGAAGTGCCTGCCCCAGCCGCCGTGCTGGGCGGACCAGAGCCACTGATG
CAGGCCACCGCCTGGCTCAACGCCTACTTTCACCAGCCTGAGGCCATCGAGGAGTTCCCTGTGCCAGC
CCTGCACCACCCAGTGTTCCAGCAGGAGAGCTTTACCCGCCAGGTGCTGTGGAAACTGCTGAAAGTGG
TGAAGTTCGGAGAGGTCATCAGCTACAGCCACCTGGCCGCCCTGGCCGGCAATCCCGCCGCCACCGCC
GCCGTGAAAACCGCCCTGAGCGGAAATCCCGTGCCCATTCTGATCCCCTGCCACCGGGTGGTGCAGGG
CGACCTGGACGTGGGGGGCTACGAGGGCGGGCTCGCCGTGAAAGAGTGGCTGCTGGCCCACGAGGGCC
ACAGACTGGGCAAGCCTGGGCTGGGTCCTGCAGGCGGAGGCGCGCCAGGGTCTGGCGGCGGCAGTAAG
AAGCTTGCCAAGGCCCGGGCTGCGCAGTCTGCCCTGGCCGCCATTTTTAACTTGCACTTGGATCAGAC
GCCATCTCGCCAGCCTATTCCCAGTGAGGGTCTTCAGCTGCATTTACCGCAGGTTTTAGCTGACGCTG
TCTCACGCCTGGTCCTGGGTAAGTTTGGTGACCTGACCGACAACTTCTCCTCCCCTCACGCTCGCAGA
AAAGTGCTGGCTGGAGTCGTCATGACAACAGGCACAGATGTTAAAGATGCCAAGGTGATAAGTGTTTC
TACAGGAACAAAATGTATTAATGGTGAATACATGAGTGATCGTGGCCTTGCATTAAATGACTGCCATG
CAGAAATAATATCTCGGAGATCCTTGCTCAGATTTCTTTATACACAACTTGAGCTTTACTTAAATAAC
AAAGATGATCAAAAAAGATCCATCTTTCAGAAATCAGAGCGAGGGGGGTTTAGGCTGAAGGAGAATGT
CCAGTTTCATCTGTACATCAGCACCTCTCCCTGTGGAGATGCCAGAATCTTCTCACCACATGAGCCAA
TCCTGGAAGAACCAGCAGATAGACACCCAAATCGTAAAGCAAGAGGACAGCTACGGACCAAAATAGAG
TCTGGTCAGGGGACGATTCCAGTGCGCTCCAATGCGAGCATCCAAACGTGGGACGGGGTGCTGCAAGG
GGAGCGGCTGCTCACCATGTCCTGCAGTGACAAGATTGCACGCTGGAACGTGGTGGGCATCCAGGGTT
CCCTGCTCAGCATTTTCGTGGAGCCCATTTACTTCTCGAGCATCATCCTGGGCAGCCTTTACCACGGG
GACCACCTTTCCAGGGCCATGTACCAGCGGATCTCCAACATAGAGGACCTGCCACCTCTCTACACCCT
CAACAAGCCTTTGCTCAGTGGCATCAGCAATGCAGAAGCACGGCAGCCAGGGAAGGCCCCCAACTTCA
GTGTCAACTGGACGGTAGGCGACTCCGCTATTGAGGTCATCAACGCCACGACTGGGAAGGATGAGCTG
GGCCGCGCGTCCCGCCTGTGTAAGCACGCGTTGTACTGTCGCTGGATGCGTGTGCACGGCAAGGTTCC
CTCCCACTTACTACGCTCCAAGATTACCAAACCCAACGTGTACCATGAGTCCAAGCTGGCGGCAAAGG
AGTACCAGGCCGCCAAGGCGCGTCTGTTCACAGCCTTCATCAAGGCGGGGCTGGGGGCCTGGGTGGAG
AAGCCCACCGAGCAGGACCAGTTCTCACTCACGCCCTGATTAATTAAGTTTAAACCCGCTGATCAGCC
TCGACTGTGCCTTCTAGTTGCCAGCCATCTGTTGTTTGCCCCTCCCCCGTGCCTTCCTTGACCCTGGA
AGGTGCCACTCCCACTGTCCTTTCCTAATAAAATGAGGAAATTGCATCGCATTGTCTGAGTAGGTGTC
ATTCTATTCTGGGGGGTGGGGTGGGGCAGGACAGCAAGGGGGAGGATTGGGAAGACAATAGCAGGCAT
GCTGGGGATGCGGTGGGCTCTATGG

Constructs for HA1Q / APO1S duo cell lines 6 – 9

Cell line **6**: CMV-enhancer – CMV promoter – $TetO_2$ – mAPOBEC1 – $SNAP_f$-tag – NES – bGH – CMV-enhancer – CMV promoter – $TetO_2$ – HaloTag – ADAR1Q – bGH

GACATTGATTATTGACTAGTTATTAATAGTAATCAATTACGGGGTCATTAGTTCATAGCCCATATATG
GAGTTCCGCGTTACATAACTTACGGTAAATGGCCCGCCTGGCTGACCGCCCAACGACCCCCGCCCATT
GACGTCAATAATGACGTATGTTCCCATAGTAACGCCAATAGGGACTTTCCATTGACGTCAATGGGTGG
AGTATTTACGGTAAACTGCCCACTTGGCAGTACATCAAGTGTATCATATGCCAAGTACGCCCCCTATT
GACGTCAATGACGGTAAATGGCCCGCCTGGCATTATGCCCAGTACATGACCTTATGGGACTTTCCTAC
TTGGCAGTACATCTACGTATTAGTCATCGCTATTACCATGGTGATGCGGTTTTGGCAGTACATCAATG
GGCGTGGATAGCGGTTTGACTCACGGGGATTTCCAAGTCTCCACCCCATTGACGTCAATGGGAGTTTG
TTTTGGCACCAAAATCAACGGGACTTTCCAAAATGTCGTAACAACTCCGCCCCATTGACGCAAATGGG
CGGTAGGCGTGTACGGTGGGAGGTCTATATAAGCAGAGCTCTCCCTATCAGTGATAGAGATCTCCCTA

TCAGTGATAGAGATCGTCGACGAGCTCGTTTAGTGAACCGTCAGATCGCCTGGAGACGCCATCCACGC
TGTTTTGACCTCCATAGAAGACACCGGGACCGATCCAGCCTCCGGACTCTAGCGTTTAAACTTAAGCT
TGGTACCGAGCTCGGATCCGCCACCATGAGTTCCGAGACAGGCCCTGTAGCTGTTGATCCCACTCTGA
GGAGAAGAATTGAGCCCCACGAGTTTGAAGTCTTCTTTGACCCCCGGGAGCTTCGGAAAGAGACCTGT
CTGCTGTATGAGATCAACTGGGGTGGAAGGCACAGTGTCTGGCGACACACGAGCCAAAACACCAGCAA
CCACGTTGAAGTCAACTTCTTAGAAAAATTTACTACAGAAAGATACTTTCGTCCGAACACCAGATGCT
CCATTACCTGGTTCCTGTCCTGGAGTCCCTGCGGGGAGTGCTCCAGGGCCATTACAGAGTTTCTGAGC
CGACACCCCTATGTAACTCTGTTTATTTACATAGCACGGCTTTATCACCACACGGATCAGCGAAACCG
CCAAGGACTCAGGGACCTTATTAGCAGCGGTGTGACTATCCAGATCATGACAGAGCAAGAGTATTGTT
ACTGCTGGAGGAATTTCGTCAACTACCCCCCTTCAAACGAAGCATATTGGCCAAGGTACCCCCATCTG
TGGGTGAAACTGTATGTACTGGAGCTCTACTGCATCATTTTAGGACTTCCACCCTGTTTAAAAATTTT
AAGAAGAAAGCAACCTCAACTCACGTTTTTCACAATTACTCTTCAAACCTGCCATTACCAAAGGATAC
CACCCCATCTCCTTTGGGCTACAGGGTTGAAAGGAGCGGCGGCGACTGGCGCGCCAGGGCCTGCCGCG
ACTGGCGCGCCAGGGTCTGGCGGCTCCATGGACAAAGACTGCGAAATGAAGCGCACCACCCTGGATAG
CCCTCTGGGCAAGCTGGAACTGTCTGGGTGCGAACAGGGCCTGCACCGTATCATCTTCCTGGGCAAAG
GAACATCTGCCGCCGACGCCGTGGAAGTGCCTGCCCCAGCCGCCGTGCTGGGCGGACCAGAGCCACTG
ATGCAGGCCACCGCCTGGCTCAACGCCTACTTTCACCAGCCTGAGGCCATCGAGGAGTTCCCTGTGCC
AGCCCTGCACCACCCAGTGTTCCAGCAGGAGAGCTTTACCCGCCAGGTGCTGTGGAAACTGCTGAAAG
TGGTGAAGTTCGGAGAGGTCATCAGCTACAGCCACCTGGCCGCCCTGGCCGGCAATCCCGCCGCCACC
GCCGCCGTGAAAACCGCCCTGAGCGGAAATCCCGTGCCCATTCTGATCCCCTGCCACCGGGTGGTGCA
GGGCGACCTGGACGTGGGGGGCTACGAGGGCGGGCTCGCCGTGAAAGAGTGGCTGCTGGCCCACGAGG
GCCACAGACTGGGCAAGCCTGGGCTGGGTACCGGTCTGCCTCCACTTGAAAGACTGACACTGTAAGGG
CCCATGTACGATTTAATTATGCGGACGTGATGAGCGAAGTACGATCCCACGACCGAGGCCCGTTTAAA
CCCGCTGATCAGCCTCGACTGTGCCTTCTAGTTGCCAGCCATCTGTTGTTTGCCCCTCCCCCGTGCCT
TCCTTGACCCTGGAAGGTGCCACTCCCACTGTCCTTTCCTAATAAAATGAGGAAATTGCATCGCATTG
TCTGAGTAGGTGTCATTCTATTCTGGGGGGTGGGGTGGGGCAGGACAGCAAGGGGGAGGATTGGGAAG
ACAATAGCAGGCATGCTGGGGATGCGGTGGGCTCTATGGCTTCTGAGGCGGAAAGAACCAGCTGGGGC
TCTAGGGGGTATCCCCACGCGCCCTGTAGCGGCGCATTAAGCGCGGCGGGTGTGGTGGTTACGCGCAG
CGTGACCGCTACACTTGCCAGCGCCCTAGCGCCCGCTCCTTTCGCTTTCTTCCCTTCCTTTCTCGCCA
CGTTCGCCGGTCGATGTACGGGCCAGATATACGCGTTGACATTGATTATTGACTAGTTATTAATAGTA
ATCAATTACGGGGTCATTAGTTCATAGCCCATATATGGAGTTCCGCGTTACATAACTTACGGTAAATG
GCCCGCCTGGCTGACCGCCCAACGACCCCCGCCCATTGACGTCAATAATGACGTATGTTCCCATAGTA
ACGCCAATAGGGACTTTCCATTGACGTCAATGGGTGGAGTATTTACGGTAAACTGCCCACTTGGCAGT
ACATCAAGTGTATCATATGCCAAGTACGCCCCCTATTGACGTCAATGACGGTAAATGGCCCGCCTGGC
ATTATGCCCAGTACATGACCTTATGGGACTTTCCTACTTGGCAGTACATCTACGTATTAGTCATCGCT
ATTACCATGGTGATGCGGTTTTGGCAGTACATCAATGGGCGTGGATAGCGGTTTGACTCACGGGGATT
TCCAAGTCTCCACCCCATTGACGTCAATGGGAGTTTGTTTTGGCACCAAAATCAACGGGACTTTCCAA
AATGTCGTAACAACTCCGCCCCATTGACGCAAATGGGCGGTAGGCGTGTACGGTGGGAGGTCTATATA
AGCAGAGCTCTCCCTATCAGTGATAGAGATCTCCCTATCAGTGATAGAGAGCGTGCATAGGGAACATC
CACCACTTTAGTGAATTGTAGCACGGCTTCAGAAGCGGCCGCCCACCATGGCAGAAATCGGTACTGGC
TTTCCATTCGACCCCCATTATGTGGAAGTCCTGGGCGAGCGCATGCACTACGTCGATGTTGGTCCGCG
CGATGGCACCCCTGTGCTGTTCCTGCACGGTAACCCGACCTCCTCCTACGTGTGGCGCAACATCATCC
CGCATGTTGCACCGACCCATCGCTGCATTGCTCCAGACCTGATCGGTATGGGCAAATCCGACAAACCA
GACCTGGGTTATTTCTTCGACGACCACGTCCGCTTCATGGATGCCTTCATCGAAGCCCTGGGTCTGGA
AGAGGTCGTCCTGGTCATTCACGACTGGGGCTCCGCTCTGGGTTTCCACTGGGCCAAGCGCAATCCAG
AGCGCGTCAAAGGTATTGCATTTATGGAGTTCATCCGCCCTATCCCGACCTGGGACGAATGGCCAGAA
TTTGCCCGCGAGACCTTCCAGGCCTTCCGCACCACCGACGTCGGCCGCAAGCTGATCATTGATCAGAA
CGTTTTTATCGAGGGTACGCTGCCGATGGGTGTCGTCCGCCCGCTGACTGAAGTCGAGATGGACCATT
ACCGCGAGCCGTTCCTGAATCCTGTTGACCGCGAGCCACTGTGGCGCTTCCCAAACGAGCTGCCAATC
GCCGGTGAGCCAGCGAACATCGTCGCGCTGGTCGAAGAATACATGGACTGGCTGCACCAGTCCCCTGT
CCCGAAGCTGCTGTTCTGGGGCACCCCAGGCGTTCTGATCCCACCGGCCGAAGCCGCTCGCCTGGCCA
AAAGCCTGCCTAACTGCAAGGCTGTGGACATCGGCCCGGGTCTGAATCTGCTGCAAGAAGACAACCCG

GACCTGATCGGCAGCGAGATCGCGCGCTGGCTGTCGACGCTCGAGATTTCCGGCCCTGCAGGCGGAGG
CGCGCCAGGGTCTGGCGGCGGCAGTAAGGCAGAACGCATGGGTTTCACAGAGGTAACCCCAGTGACAG
GGGCCAGTCTCAGAAGAACTATGCTCCTCCTCTCAAGGTCCCCAGAAGCACAGCCAAAGACACTCCCT
CTCACTGGCAGCACCTTCCATGACCAGATAGCCATGCTGAGCCACCGGTGCTTCAACACTCTGACTAA
CAGCTTCCAGCCCTCCTTGCTCGGCCGCAAGATTCTGGCCGCCATCATTATGAAAAAAGACTCTGAGG
ACATGGGTGTCGTCGTCAGCTTGGGAACAGGGAATCGCTGTGTAAAAGGAGATTCTCTCAGCCTAAAA
GGAGAAACTGTCAATGACTGCCATGCAGAAATAATCTCCCGGAGAGGCTTCATCAGGTTTCTCTACAG
TGAGTTAATGAAATACAACTCCCAGACTGCGAAGGATAGTATATTTGAACCTGCTAAGGGAGGAGAAA
AGCTCCAAATAAAAAAGACTGTGTCATTCCATCTGTATATCAGCACTGCTCCGTGTGGAGATGGCGCC
CTCTTTGACAAGTCCTGCAGCGACCGTGCTATGGAAAGCACAGAATCCCGCCACTACCCTGTCTTCGA
GAATCCCAAACAAGGAAAGCTCCGCACCAAGGTGGAGAACGGACAAGGCACAATCCCTGTGGAATCCA
GTGACATTGTGCCTACGTGGGATGGCATTCGGCTCGGGGAGAGACTCCGTACCATGTCCTGTAGTGAC
AAAATCCTACGCTGGAACGTGCTGGGCCTGCAAGGGGCACTGTTGACCCACTTCCTGCAGCCCATTTA
TCTCAAATCTGTCACATTGGGTTACCTTTTCAGCCAAGGGCATCTGACCCGTGCTATTTGCTGTCGTG
TGACAAGAGATGGGAGTGCATTTGAGGATGGACTACGACATCCCTTTATTGTCAACCACCCCAAGGTT
GGCAGAGTCAGCATATATGATTCCAAAAGGCAATCCGGGAAGACTAAGGAGACAAGCGTCAACTGGTG
TCTGGCTGATGGCTATGACCTGGAGATCCTGGACGGTACCAGAGGCACTGTGGATGGGCCACGGAATG
AATTGTCCCGGGTCTCCAAAAAGAACATTTTTCTTCTATTTAAGAAGCTCTGCTCCTTCCGTTACCGC
AGGGATCTACTGAGACTCTCCTATGGTGAGGCCAAGAAAGCTGCCCGTGACTACGAGACGGCCAAGAA
CTACTTCAAAAAAGGCCTGAAGGATATGGGCTATGGGAACTGGATTAGCAAACCCCAGGAGGAAAAGA
ACTTTTATCTCTGCCCAGTATGAATCGATATTTTCAGATATCGTGTTAGTAGGGTTGCACCGACGCGC
ATGTGGATTAGTGCTGTGCCTTCTAGTTGCCAGCCATCTGTTGTTTGCCCCTCCCCCGTGCCTTCCTT
GACCCTGGAAGGTGCCACTCCCACTGTCCTTTCCTAATAAAATGAGGAAATTGCATCGCATTGTCTGA
GTAGGTGTCATTCTATTCTGGGGGGTGGGGTGGGGCAGGACAGCAAGGGGGAGGATTGGGAAGACAAT
AGCAGGCATGCTGGGGATGCGGTGGGCTCTATGG

Cell line **7**: CMV-enhancer – CMV promoter – $TetO_2$ – HaloTag – ADAR1Q – bGH – CMV-enhancer – CMV promoter – $TetO_2$ – mAPOBEC1 – $SNAP_f$-tag – NES – bGH

GACATTGATTATTGACTAGTTATTAATAGTAATCAATTACGGGGTCATTAGTTCATAGCCCATATATG
GAGTTCCGCGTTACATAACTTACGGTAAATGGCCCGCCTGGCTGACCGCCCAACGACCCCCGCCCATT
GACGTCAATAATGACGTATGTTCCCATAGTAACGCCAATAGGGACTTTCCATTGACGTCAATGGGTGG
AGTATTTACGGTAAACTGCCCACTTGGCAGTACATCAAGTGTATCATATGCCAAGTACGCCCCCTATT
GACGTCAATGACGGTAAATGGCCCGCCTGGCATTATGCCCAGTACATGACCTTATGGGACTTTCCTAC
TTGGCAGTACATCTACGTATTAGTCATCGCTATTACCATGGTGATGCGGTTTTGGCAGTACATCAATG
GGCGTGGATAGCGGTTTGACTCACGGGGATTTCCAAGTCTCCACCCCATTGACGTCAATGGGAGTTTG
TTTTGGCACCAAAATCAACGGGACTTTCCAAAATGTCGTAACAACTCCGCCCCATTGACGCAAATGGG
CGGTAGGCGTGTACGGTGGGAGGTCTATATAAGCAGAGCTCTCCCTATCAGTGATAGAGATCTCCCTA
TCAGTGATAGAGATCGTCGACGAGCTCGTTTAGTGAACCGTCAGATCGCCTGGAGACGCCATCCACGC
TGTTTTGACCTCCATAGAAGACACCGGGACCGATCCAGCCTCCGGACTCTAGCGTTTAAACTTAAGCT
TGGTACCGAGCTCGGATCCCCACCATGGCAGAAATCGGTACTGGCTTTCCATTCGACCCCCATTATGT
GGAAGTCCTGGGCGAGCGCATGCACTACGTCGATGTTGGTCCGCGCGATGGCACCCCTGTGCTGTTCC
TGCACGGTAACCCGACCTCCTCCTACGTGTGGCGCAACATCATCCCGCATGTTGCACCGACCCATCGC
TGCATTGCTCCAGACCTGATCGGTATGGGCAAATCCGACAAACCAGACCTGGGTTATTTCTTCGACGA
CCACGTCCGCTTCATGGATGCCTTCATCGAAGCCCTGGGTCTGGAAGAGGTCGTCCTGGTCATTCACG
ACTGGGGCTCCGCTCTGGGTTTCCACTGGGCCAAGCGCAATCCAGAGCGCGTCAAAGGTATTGCATTT
ATGGAGTTCATCCGCCCTATCCCGACCTGGGACGAATGGCCAGAATTTGCCCGCGAGACCTTCCAGGC
CTTCCGCACCACCGACGTCGGCCGCAAGCTGATCATTGATCAGAACGTTTTTATCGAGGGTACGCTGC
CGATGGGTGTCGTCCGCCCGCTGACTGAAGTCGAGATGGACCATTACCGCGAGCCGTTCCTGAATCCT
GTTGACCGCGAGCCACTGTGGCGCTTCCCAAACGAGCTGCCAATCGCCGGTGAGCCAGCGAACATCGT
CGCGCTGGTCGAAGAATACATGGACTGGCTGCACCAGTCCCCTGTCCCGAAGCTGCTGTTCTGGGGCA

CCCCAGGCGTTCTGATCCCACCGGCCGAAGCCGCTCGCCTGGCCAAAAGCCTGCCTAACTGCAAGGCT
GTGGACATCGGCCCGGGTCTGAATCTGCTGCAAGAAGACAACCCGGACCTGATCGGCAGCGAGATCGC
GCGCTGGCTGTCGACGCTCGAGATTTCCGGCCCTGCAGGCGGAGGCGCGCCAGGGTCTGGCGGCGGCA
GTAAGGCAGAACGCATGGGTTTCACAGAGGTAACCCCAGTGACAGGGGCCAGTCTCAGAAGAACTATG
CTCCTCCTCTCAAGGTCCCCAGAAGCACAGCCAAAGACACTCCCTCTCACTGGCAGCACCTTCCATGA
CCAGATAGCCATGCTGAGCCACCGGTGCTTCAACACTCTGACTAACAGCTTCCAGCCCTCCTTGCTCG
GCCGCAAGATTCTGGCCGCCATCATTATGAAAAAAGACTCTGAGGACATGGGTGTCGTCGTCAGCTTG
GGAACAGGGAATCGCTGTGTAAAAGGAGATTCTCTCAGCCTAAAAGGAGAAACTGTCAATGACTGCCA
TGCAGAAATAATCTCCCGGAGAGGCTTCATCAGGTTTCTCTACAGTGAGTTAATGAAATACAACTCCC
AGACTGCGAAGGATAGTATATTTGAACCTGCTAAGGGAGGAGAAAAGCTCCAAATAAAAAAGACTGTG
TCATTCCATCTGTATATCAGCACTGCTCCGTGTGGAGATGGCGCCCTCTTTGACAAGTCCTGCAGCGA
CCGTGCTATGGAAAGCACAGAATCCCGCCACTACCCTGTCTTCGAGAATCCCAAACAAGGAAAGCTCC
GCACCAAGGTGGAGAACGGACAAGGCACAATCCCTGTGGAATCCAGTGACATTGTGCCTACGTGGGAT
GGCATTCGGCTCGGGGAGAGACTCCGTACCATGTCCTGTAGTGACAAAATCCTACGCTGGAACGTGCT
GGGCCTGCAAGGGGCACTGTTGACCCACTTCCTGCAGCCCATTTATCTCAAATCTGTCACATTGGGTT
ACCTTTTCAGCCAAGGGCATCTGACCCGTGCTATTTGCTGTCGTGTGACAAGAGATGGGAGTGCATTT
GAGGATGGACTACGACATCCCTTTATTGTCAACCACCCCAAGGTTGGCAGAGTCAGCATATATGATTC
CAAAAGGCAATCCGGGAAGACTAAGGAGACAAGCGTCAACTGGTGTCTGGCTGATGGCTATGACCTGG
AGATCCTGGACGGTACCAGAGGCACTGTGGATGGGCCACGGAATGAATTGTCCCGGGTCTCCAAAAAG
AACATTTTTCTTCTATTTAAGAAGCTCTGCTCCTTCCGTTACCGCAGGGATCTACTGAGACTCTCCTA
TGGTGAGGCCAAGAAAGCTGCCCGTGACTACGAGACGGCCAAGAACTACTTCAAAAAAGGCCTGAAGG
ATATGGGCTATGGGAACTGGATTAGCAAACCCCAGGAGGAAAAGAACTTTTATCTCTGCCCAGTATGA
GGGCCCATGTACGATTTAATTATGCGGACGTGATGAGCGAAGTACGATCCCACGACCGAGGCCCGTTT
AAACCCGCTGATCAGCCTCGACTGTGCCTTCTAGTTGCCAGCCATCTGTTGTTTGCCCCTCCCCCGTG
CCTTCCTTGACCCTGGAAGGTGCCACTCCCACTGTCCTTTCCTAATAAAATGAGGAAATTGCATCGCA
TTGTCTGAGTAGGTGTCATTCTATTCTGGGGGGTGGGGTGGGGCAGGACAGCAAGGGGGAGGATTGGG
AAGACAATAGCAGGCATGCTGGGGATGCGGTGGGCTCTATGGCTTCTGAGGCGGAAAGAACCAGCTGG
GGCTCTAGGGGGTATCCCCACGCGCCCTGTAGCGGCGCATTAAGCGCGGCGGGTGTGGTGGTTACGCG
CAGCGTGACCGCTACACTTGCCAGCGCCCTAGCGCCCGCTCCTTTCGCTTTCTTCCCTTCCTTTCTCG
CCACGTTCGCCGGTCGATGTACGGGCCAGATATACGCGTTGACATTGATTATTGACTAGTTATTAATA
GTAATCAATTACGGGGTCATTAGTTCATAGCCCATATATGGAGTTCCGCGTTACATAACTTACGGTAA
ATGGCCCGCCTGGCTGACCGCCCAACGACCCCCGCCCATTGACGTCAATAATGACGTATGTTCCCATA
GTAACGCCAATAGGGACTTTCCATTGACGTCAATGGGTGGAGTATTTACGGTAAACTGCCCACTTGGC
AGTACATCAAGTGTATCATATGCCAAGTACGCCCCCTATTGACGTCAATGACGGTAAATGGCCCGCCT
GGCATTATGCCCAGTACATGACCTTATGGGACTTTCCTACTTGGCAGTACATCTACGTATTAGTCATC
GCTATTACCATGGTGATGCGGTTTTGGCAGTACATCAATGGGCGTGGATAGCGGTTTGACTCACGGGG
ATTTCCAAGTCTCCACCCCATTGACGTCAATGGGAGTTTGTTTTGGCACCAAAATCAACGGGACTTTC
CAAAATGTCGTAACAACTCCGCCCCATTGACGCAAATGGGCGGTAGGCGTGTACGGTGGGAGGTCTAT
ATAAGCAGAGCTCTCCCTATCAGTGATAGAGATCTCCCTATCAGTGATAGAGAGCGTGCATAGGGAAC
ATCCACCACTTTAGTGAATTGTAGCACGGCTTCAGAAGCGGCCGCGCCACCATGAGTTCCGAGACAGG
CCCTGTAGCTGTTGATCCCACTCTGAGGAGAAGAATTGAGCCCCACGAGTTTGAAGTCTTCTTTGACC
CCCGGGAGCTTCGGAAAGAGACCTGTCTGCTGTATGAGATCAACTGGGGTGGAAGGCACAGTGTCTGG
CGACACACGAGCCAAAACACCAGCAACCACGTTGAAGTCAACTTCTTAGAAAAATTTACTACAGAAAG
ATACTTTCGTCCGAACACCAGATGCTCCATTACCTGGTTCCTGTCCTGGAGTCCCTGCGGGGAGTGCT
CCAGGGCCATTACAGAGTTTCTGAGCCGACACCCCTATGTAACTCTGTTTATTTACATAGCACGGCTT
TATCACCACACGGATCAGCGAAACCGCCAAGGACTCAGGGACCTTATTAGCAGCGGTGTGACTATCCA
GATCATGACAGAGCAAGAGTATTGTTACTGCTGGAGGAATTTCGTCAACTACCCCCCTTCAAACGAAG
CATATTGGCCAAGGTACCCCCATCTGTGGGTGAAACTGTATGTACTGGAGCTCTACTGCATCATTTTA
GGACTTCCACCCTGTTTAAAAATTTTAAGAAGAAAGCAACCTCAACTCACGTTTTTCACAATTACTCT
TCAAACCTGCCATTACCAAAGGATACCACCCCATCTCCTTTGGGCTACAGGGTTGAAAGGAGCGGCGG
CGACTGGCGCGCCAGGGCCTGCCGCGACTGGCGCGCCAGGGTCTGGCGGCTCCATGGACAAAGACTGC
GAAATGAAGCGCACCACCCTGGATAGCCCTCTGGGCAAGCTGGAACTGTCTGGGTGCGAACAGGGCCT

GCACCGTATCATCTTCCTGGGCAAAGGAACATCTGCCGCCGACGCCGTGGAAGTGCCTGCCCCAGCCG
CCGTGCTGGGCGGACCAGAGCCACTGATGCAGGCCACCGCCTGGCTCAACGCCTACTTTCACCAGCCT
GAGGCCATCGAGGAGTTCCCTGTGCCAGCCCTGCACCACCCAGTGTTCCAGCAGGAGAGCTTTACCCG
CCAGGTGCTGTGGAAACTGCTGAAAGTGGTGAAGTTCGGAGAGGTCATCAGCTACAGCCACCTGGCCG
CCCTGGCCGGCAATCCCGCCGCCACCGCCGCCGTGAAAACCGCCCTGAGCGGAAATCCCGTGCCCATT
CTGATCCCCTGCCACCGGGTGGTGCAGGGCGACCTGGACGTGGGGGGCTACGAGGGCGGGCTCGCCGT
GAAAGAGTGGCTGCTGGCCCACGAGGGCCACAGACTGGGCAAGCCTGGGCTGGGTACCGGTCTGCCTC
CACTTGAAAGACTGACACTGTAA

Cell line **8**: bGH – NES – $SNAP_f$-tag – mAPOBEC1 – $TetO_2$ – CMV promoter – EF1α core promoter – $TetO_2$ – HaloTag – ADAR1Q – bGH

CCATAGAGCCCACCGCATCCCCAGCATGCCTGCTATTGTCTTCCCAATCCTCCCCCTTGCTGTCCTGC
CCCACCCCACCCCCCAGAATAGAATGACACCTACTCAGACAATGCGATGCAATTTCCTCATTTTATTA
GGAAAGGACAGTGGGAGTGGCACCTTCCAGGGTCAAGGAAGGCACGGGGGAGGGGCAAACAACAGATG
GCTGGCAACTAGAAGGCACAGTCGAGGCTGATCAGCGGGTTTAAACATCGATTTACAGTGTCAGTCTT
TCAAGTGGAGGCAGACCGGTACCCAGCCCAGGCTTGCCCAGTCTGTGGCCCTCGTGGGCCAGCAGCCA
CTCTTTCACGGCGAGCCCGCCCTCGTAGCCCCCCACGTCCAGGTCGCCCTGCACCACCCGGTGGCAGG
GGATCAGAATGGGCACGGGATTTCCGCTCAGGGCGGTTTTCACGGCGGCGGTGGCGGCGGGATTGCCG
GCCAGGGCGGCCAGGTGGCTGTAGCTGATGACCTCTCCGAACTTCACCACTTTCAGCAGTTTCCACAG
CACCTGGCGGGTAAAGCTCTCCTGCTGGAACACTGGGTGGTGCAGGGCTGGCACAGGGAACTCCTCGA
TGGCCTCAGGCTGGTGAAAGTAGGCGTTGAGCCAGGCGGTGGCCTGCATCAGTGGCTCTGGTCCGCCC
AGCACGGCGGCTGGGGCAGGCACTTCCACGGCGTCGGCGGCAGATGTTCCTTTGCCCAGGAAGATGAT
ACGGTGCAGGCCCTGTTCGCACCCAGACAGTTCCAGCTTGCCCAGAGGGCTATCCAGGGTGGTGCGCT
TCATTTCGCAGTCTTTGTCCATGGAGCCGCCAGACCCTGGCGCGCCAGTCGCGGCAGGCCCTGGCGCG
CCAGTCGCCGCCGCTCCTTTCAACCCTGTAGCCCAAAGGAGATGGGGTGGTATCCTTTGGTAATGGCA
GGTTTGAAGAGTAATTGTGAAAAACGTGAGTTGAGGTTGCTTTCTTCTTAAAATTTTTAAACAGGGTG
GAAGTCCTAAAATGATGCAGTAGAGCTCCAGTACATACAGTTTCACCCACAGATGGGGGTACCTTGGC
CAATATGCTTCGTTTGAAGGGGGGTAGTTGACGAAATTCCTCCAGCAGTAACAATACTCTTGCTCTGT
CATGATCTGGATAGTCACACCGCTGCTAATAAGGTCCCTGAGTCCTTGGCGGTTTCGCTGATCCGTGT
GGTGATAAAGCCGTGCTATGTAAATAAACAGAGTTACATAGGGGTGTCGGCTCAGAAACTCTGTAATG
GCCCTGGAGCACTCCCCGCAGGGACTCCAGGACAGGAACCAGGTAATGGAGCATCTGGTGTTCGGACG
AAAGTATCTTTCTGTAGTAAATTTTTCTAAGAAGTTGACTTCAACGTGGTTGCTGGTGTTTTGGCTCG
TGTGTCGCCAGACACTGTGCCTTCCACCCCAGTTGATCTCATACAGCAGACAGGTCTCTTTCCGAAGC
TCCCGGGGGTCAAAGAAGACTTCAAACTCGTGGGGCTCAATTCTTCTCCTCAGAGTGGGATCAACAGC
TACAGGGCCTGTCTCGGAACTCATGGTGGCGCGGCCGCCCCAGAGTAAAGCTATTCGGTAATTCGTCA
CCCAAGAGATCAATCGGTCTCTCTCTATCACTGATAGGGAGATCTCTATCACTGATAGGGAGAGCTCT
GCTTATATAGACCTCCCACCGTACACGCCTACCGCCCATTTGCGTCAATGGGGCGGAGTTGTTACGAC
ATTTTGGAAAGTCCCGTTGATTTTGGTGCCAAAACAAACTCCCATTGACGTCAATGGGGTGGAGACTT
GGAAATCCCCGTGAGTCAAACCGCTATCCACGCCCATTGATGTACTGCCAAAACCGCATCACCATGGA
CGTGTCGAGGTGATAATTCCACTCGAGTGGCTCCGGTGCCCGTCAGTGGGCAGAGCGCACATCGCCCA
CAGTCCCCGAGAAGTTGGGGGGAGGGGTCGGCAATTGAACCGGTGCCTAGAGAAGGTGGCGCGGGGTA
AACTGGGAAAGTGATGTCGTGTACTGGCTCCGCCTTTTTCCCGAGGGTGGGGGAGAACCGTATATAAG
TGCAGTAGTCGCCGTGAACGTTCTTTTTCGCAACGGGTTTGCCGCCAGAACACAGGTCCCTATCAGTG
ATAGAGATCTCCCTATCAGTGATAGAGATCGTCGACGAGCTCGTTTAGTGAACCGTCAGATCGCCTGG
AGACGCCATCGGATCCCCACCATGGCAGAAATCGGTACTGGCTTTCCATTCGACCCCCATTATGTGGA
AGTCCTGGGCGAGCGCATGCACTACGTCGATGTTGGTCCGCGCGATGGCACCCCTGTGCTGTTCCTGC
ACGGTAACCCGACCTCCTCCTACGTGTGGCGCAACATCATCCCGCATGTTGCACCGACCCATCGCTGC
ATTGCTCCAGACCTGATCGGTATGGGCAAATCCGACAAACCAGACCTGGGTTATTTCTTCGACGACCA
CGTCCGCTTCATGGATGCCTTCATCGAAGCCCTGGGTCTGGAAGAGGTCGTCCTGGTCATTCACGACT
GGGGCTCCGCTCTGGGTTTCCACTGGGCCAAGCGCAATCCAGAGCGCGTCAAAGGTATTGCATTTATG

GAGTTCATCCGCCCTATCCCGACCTGGGACGAATGGCCAGAATTTGCCCGCGAGACCTTCCAGGCCTT
CCGCACCACCGACGTCGGCCGCAAGCTGATCATTGATCAGAACGTTTTTATCGAGGGTACGCTGCCGA
TGGGTGTCGTCCGCCCGCTGACTGAAGTCGAGATGGACCATTACCGCGAGCCGTTCCTGAATCCTGTT
GACCGCGAGCCACTGTGGCGCTTCCCAAACGAGCTGCCAATCGCCGGTGAGCCAGCGAACATCGTCGC
GCTGGTCGAAGAATACATGGACTGGCTGCACCAGTCCCCTGTCCCGAAGCTGCTGTTCTGGGGCACCC
CAGGCGTTCTGATCCCACCGGCCGAAGCCGCTCGCCTGGCCAAAAGCCTGCCTAACTGCAAGGCTGTG
GACATCGGCCCGGGTCTGAATCTGCTGCAAGAAGACAACCCGGACCTGATCGGCAGCGAGATCGCGCG
CTGGCTGTCGACGCTCGAGATTTCCGGCCCTGCAGGCGGAGGCGCGCCAGGGTCTGGCGGCGGCAGTA
AGGCAGAACGCATGGGTTTCACAGAGGTAACCCCAGTGACAGGGGCCAGTCTCAGAAGAACTATGCTC
CTCCTCTCAAGGTCCCCAGAAGCACAGCCAAAGACACTCCCTCTCACTGGCAGCACCTTCCATGACCA
GATAGCCATGCTGAGCCACCGGTGCTTCAACACTCTGACTAACAGCTTCCAGCCCTCCTTGCTCGGCC
GCAAGATTCTGGCCGCCATCATTATGAAAAAAGACTCTGAGGACATGGGTGTCGTCGTCAGCTTGGGA
ACAGGGAATCGCTGTGTAAAAGGAGATTCTCTCAGCCTAAAAGGAGAAACTGTCAATGACTGCCATGC
AGAAATAATCTCCCGGAGAGGCTTCATCAGGTTTCTCTACAGTGAGTTAATGAAATACAACTCCCAGA
CTGCGAAGGATAGTATATTTGAACCTGCTAAGGGAGGAGAAAAGCTCCAAATAAAAAAGACTGTGTCA
TTCCATCTGTATATCAGCACTGCTCCGTGTGGAGATGGCGCCCTCTTTGACAAGTCCTGCAGCGACCG
TGCTATGGAAAGCACAGAATCCCGCCACTACCCTGTCTTCGAGAATCCCAAACAAGGAAAGCTCCGCA
CCAAGGTGGAGAACGGACAAGGCACAATCCCTGTGGAATCCAGTGACATTGTGCCTACGTGGGATGGC
ATTCGGCTCGGGGAGAGACTCCGTACCATGTCCTGTAGTGACAAAATCCTACGCTGGAACGTGCTGGG
CCTGCAAGGGGCACTGTTGACCCACTTCCTGCAGCCCATTTATCTCAAATCTGTCACATTGGGTTACC
TTTTCAGCCAAGGGCATCTGACCCGTGCTATTTGCTGTCGTGTGACAAGAGATGGGAGTGCATTTGAG
GATGGACTACGACATCCCTTTATTGTCAACCACCCCAAGGTTGGCAGAGTCAGCATATATGATTCCAA
AAGGCAATCCGGGAAGACTAAGGAGACAAGCGTCAACTGGTGTCTGGCTGATGGCTATGACCTGGAGA
TCCTGGACGGTACCAGAGGCACTGTGGATGGGCCACGGAATGAATTGTCCCGGGTCTCCAAAAAGAAC
ATTTTTCTTCTATTTAAGAAGCTCTGCTCCTTCCGTTACCGCAGGGATCTACTGAGACTCTCCTATGG
TGAGGCCAAGAAAGCTGCCCGTGACTACGAGACGGCCAAGAACTACTTCAAAAAAGGCCTGAAGGATA
TGGGCTATGGGAACTGGATTAGCAAACCCCAGGAGGAAAAGAACTTTTATCTCTGCCCAGTATGATTA
ATTAAGTTTAAACCCGCTGATCAGCCTCGACTGTGCCTTCTAGTTGCCAGCCATCTGTTGTTTGCCCC
TCCCCCGTGCCTTCCTTGACCCTGGAAGGTGCCACTCCCACTGTCCTTTCCTAATAAAATGAGGAAAT
TGCATCGCATTGTCTGAGTAGGTGTCATTCTATTCTGGGGGGTGGGGTGGGGCAGGACAGCAAGGGGG
AGGATTGGGAAGACAATAGCAGGCATGCTGGGGATGCGGTGGGCTCTATGG

Cell line **9**: bGH – ADAR1Q – HaloTag – $TetO_2$ – CMV promoter – EF1α core promoter – $TetO_2$ – mAPOBEC1 – $SNAP_f$-tag – NES – bGH

CCATAGAGCCCACCGCATCCCCAGCATGCCTGCTATTGTCTTCCCAATCCTCCCCCTTGCTGTCCTGC
CCCACCCCACCCCCCAGAATAGAATGACACCTACTCAGACAATGCGATGCAATTTCCTCATTTTATTA
GGAAAGGACAGTGGGAGTGGCACCTTCCAGGGTCAAGGAAGGCACGGGGGAGGGGCAAACAACAGATG
GCTGGCAACTAGAAGGCACAGTCGAGGCTGATCAGCGGGTTTAAACATCGATTCATACTGGGCAGAGA
TAAAAGTTCTTTTCCTCCTGGGGTTTGCTAATCCAGTTCCCATAGCCCATATCCTTCAGGCCTTTTTT
GAAGTAGTTCTTGGCCGTCTCGTAGTCACGGGCAGCTTTCTTGGCCTCACCATAGGAGAGTCTCAGTA
GATCCCTGCGGTAACGGAAGGAGCAGAGCTTCTTAAATAGAAGAAAAATGTTCTTTTTGGAGACCCGG
GACAATTCATTCCGTGGCCCATCCACAGTGCCTCTGGTACCGTCCAGGATCTCCAGGTCATAGCCATC
AGCCAGACACCAGTTGACGCTTGTCTCCTTAGTCTTCCCGGATTGCCTTTTGGAATCATATATGCTGA
CTCTGCCAACCTTGGGGTGGTTGACAATAAAGGGATGTCGTAGTCCATCCTCAAATGCACTCCCATCT
CTTGTCACACGACAGCAAATAGCACGGGTCAGATGCCCTTGGCTGAAAAGGTAACCCAATGTGACAGA
TTTGAGATAAATGGGCTGCAGGAAGTGGGTCAACAGTGCCCCTTGCAGGCCCAGCACGTTCCAGCGTA
GGATTTTGTCACTACAGGACATGGTACGGAGTCTCTCCCCGAGCCGAATGCCATCCCACGTAGGCACA
ATGTCACTGGATTCCACAGGGATTGTGCCTTGTCCGTTCTCCACCTTGGTGCGGAGCTTTCCTTGTTT
GGGATTCTCGAAGACAGGGTAGTGGCGGGATTCTGTGCTTTCCATAGCACGGTCGCTGCAGGACTTGT
CAAAGAGGGCGCCATCTCCACACGGAGCAGTGCTGATATACAGATGGAATGACACAGTCTTTTTTATT

TGGAGCTTTTCTCCTCCCTTAGCAGGTTCAAATATACTATCCTTCGCAGTCTGGGAGTTGTATTTCAT
TAACTCACTGTAGAGAAACCTGATGAAGCCTCTCCGGGAGATTATTTCTGCATGGCAGTCATTGACAG
TTTCTCCTTTTAGGCTGAGAGAATCTCCTTTTACACAGCGATTCCCTGTTCCCAAGCTGACGACGACA
CCCATGTCCTCAGAGTCTTTTTTCATAATGATGGCGGCCAGAATCTTGCGGCCGAGCAAGGAGGGCTG
GAAGCTGTTAGTCAGAGTGTTGAAGCACCGGTGGCTCAGCATGGCTATCTGGTCATGGAAGGTGCTGC
CAGTGAGAGGGAGTGTCTTTGGCTGTGCTTCTGGGGACCTTGAGAGGAGGAGCATAGTTCTTCTGAGA
CTGGCCCCTGTCACTGGGGTTACCTCTGTGAAACCCATGCGTTCTGCCTTACTGCCGCCGCCAGACCC
TGGCGCGCCTCCGCCTGCAGGGCCGGAAATCTCGAGCGTCGACAGCCAGCGCGCGATCTCGCTGCCGA
TCAGGTCCGGGTTGTCTTCTTGCAGCAGATTCAGACCCGGGCCGATGTCCACAGCCTTGCAGTTAGGC
AGGCTTTTGGCCAGGCGAGCGGCTTCGGCCGGTGGGATCAGAACGCCTGGGGTGCCCCAGAACAGCAG
CTTCGGGACAGGGGACTGGTGCAGCCAGTCCATGTATTCTTCGACCAGCGCGACGATGTTCGCTGGCT
CACCGGCGATTGGCAGCTCGTTTGGGAAGCGCCACAGTGGCTCGCGGTCAACAGGATTCAGGAACGGC
TCGCGGTAATGGTCCATCTCGACTTCAGTCAGCGGGCGGACGACACCCATCGGCAGCGTACCCTCGAT
AAAAACGTTCTGATCAATGATCAGCTTGCGGCCGACGTCGGTGGTGCGGAAGGCCTGGAAGGTCTCGC
GGGCAAATTCTGGCCATTCGTCCCAGGTCGGGATAGGGCGGATGAACTCCATAAATGCAATACCTTTG
ACGCGCTCTGGATTGCGCTTGGCCCAGTGGAAACCCAGAGCGGAGCCCCAGTCGTGAATGACCAGGAC
GACCTCTTCCAGACCCAGGGCTTCGATGAAGGCATCCATGAAGCGGACGTGGTCGTCGAAGAAATAAC
CCAGGTCTGGTTTGTCGGATTTGCCCATACCGATCAGGTCTGGAGCAATGCAGCGATGGGTCGGTGCA
ACATGCGGGATGATGTTGCGCCACACGTAGGAGGAGGTCGGGTTACCGTGCAGGAACAGCACAGGGGT
GCCATCGCGCGGACCAACATCGACGTAGTGCATGCGCTCGCCCAGGACTTCCACATAATGGGGGTCGA
ATGGAAAGCCAGTACCGATTTCTGCCATGGTGGGCGGCCGCCCCAGAGTAAAGCTATTCGGTAATTCG
TCACCCAAGAGATCAATCGGTCTCTCTCTATCACTGATAGGGAGATCTCTATCACTGATAGGGAGAGC
TCTGCTTATATAGACCTCCCACCGTACACGCCTACCGCCCATTTGCGTCAATGGGGCGGAGTTGTTAC
GACATTTTGGAAAGTCCCGTTGATTTTGGTGCCAAAACAAACTCCCATTGACGTCAATGGGGTGGAGA
CTTGGAAATCCCCGTGAGTCAAACCGCTATCCACGCCCATTGATGTACTGCCAAAACCGCATCACCAT
GGACGTGTCGAGGTGATAATTCCACTCGAGTGGCTCCGGTGCCCGTCAGTGGGCAGAGCGCACATCGC
CCACAGTCCCCGAGAAGTTGGGGGGAGGGGTCGGCAATTGAACCGGTGCCTAGAGAAGGTGGCGCGGG
GTAAACTGGGAAAGTGATGTCGTGTACTGGCTCCGCCTTTTTCCCGAGGGTGGGGGAGAACCGTATAT
AAGTGCAGTAGTCGCCGTGAACGTTCTTTTTCGCAACGGGTTTGCCGCCAGAACACAGGTCCCTATCA
GTGATAGAGATCTCCCTATCAGTGATAGAGATCGTCGACGAGCTCGTTTAGTGAACCGTCAGATCGCC
TGGAGACGCCATCGGATCCGCCACCATGAGTTCCGAGACAGGCCCTGTAGCTGTTGATCCCACTCTGA
GGAGAAGAATTGAGCCCCACGAGTTTGAAGTCTTCTTTGACCCCCGGGAGCTTCGGAAAGAGACCTGT
CTGCTGTATGAGATCAACTGGGGTGGAAGGCACAGTGTCTGGCGACACACGAGCCAAAACACCAGCAA
CCACGTTGAAGTCAACTTCTTAGAAAAATTTACTACAGAAAGATACTTTCGTCCGAACACCAGATGCT
CCATTACCTGGTTCCTGTCCTGGAGTCCCTGCGGGGAGTGCTCCAGGGCCATTACAGAGTTTCTGAGC
CGACACCCCTATGTAACTCTGTTTATTTACATAGCACGGCTTTATCACCACACGGATCAGCGAAACCG
CCAAGGACTCAGGGACCTTATTAGCAGCGGTGTGACTATCCAGATCATGACAGAGCAAGAGTATTGTT
ACTGCTGGAGGAATTTCGTCAACTACCCCCCTTCAAACGAAGCATATTGGCCAAGGTACCCCCATCTG
TGGGTGAAACTGTATGTACTGGAGCTCTACTGCATCATTTTAGGACTTCCACCCTGTTTAAAAATTTT
AAGAAGAAAGCAACCTCAACTCACGTTTTTCACAATTACTCTTCAAACCTGCCATTACCAAAGGATAC
CACCCCATCTCCTTTGGGCTACAGGGTTGAAAGGAGCGGCGGCGACTGGCGCGCCAGGGCCTGCCGCG
ACTGGCGCGCCAGGGTCTGGCGGCTCCATGGACAAAGACTGCGAAATGAAGCGCACCACCCTGGATAG
CCCTCTGGGCAAGCTGGAACTGTCTGGGTGCGAACAGGGCCTGCACCGTATCATCTTCCTGGGCAAAG
GAACATCTGCCGCCGACGCCGTGGAAGTGCCTGCCCCAGCCGCCGTGCTGGGCGGACCAGAGCCACTG
ATGCAGGCCACCGCCTGGCTCAACGCCTACTTTCACCAGCCTGAGGCCATCGAGGAGTTCCCTGTGCC
AGCCCTGCACCACCCAGTGTTCCAGCAGGAGAGCTTTACCCGCCAGGTGCTGTGGAAACTGCTGAAAG
TGGTGAAGTTCGGAGAGGTCATCAGCTACAGCCACCTGGCCGCCCTGGCCGGCAATCCCGCCGCCACC
GCCGCCGTGAAAACCGCCCTGAGCGGAAATCCCGTGCCCATTCTGATCCCCTGCCACCGGGTGGTGCA
GGGCGACCTGGACGTGGGGGGCTACGAGGGCGGGCTCGCCGTGAAAGAGTGGCTGCTGGCCCACGAGG
GCCACAGACTGGGCAAGCCTGGGCTGGGTACCGGTCTGCCTCCACTTGAAAGACTGACACTGTAATTA
ATTAAGTTTAAACCCGCTGATCAGCCTCGACTGTGCCTTCTAGTTGCCAGCCATCTGTTGTTTGCCCC
TCCCCCGTGCCTTCCTTGACCCTGGAAGGTGCCACTCCCACTGTCCTTTCCTAATAAAATGAGGAAAT

TGCATCGCATTGTCTGAGTAGGTGTCATTCTATTCTGGGGGGTGGGGTGGGGCAGGACAGCAAGGGGG
AGGATTGGGAAGACAATAGCAGGCATGCTGGGGATGCGGTGGGCTCTATGG

A.2.2 Publication 2 (published)

Controlling Site-Directed RNA Editing by Chemically Induced Dimerization

Anna S. Stroppel, Ruth Lappalainen, Thorsten Stafforst, *Chem. – Eur. J.* **2021**, *27*, 12 300 – 12 304.

Chemistry–A European Journal | Communication
doi.org/10.1002/chem.202101985

Chemistry Europe
European Chemical Societies Publishing

Controlling Site-Directed RNA Editing by Chemically Induced Dimerization

Anna S. Stroppel,[a] Ruth Lappalainen,[a] and Thorsten Stafforst*[a]

Abstract: Various RNA-targeting approaches have been engineered to modify specific sites on endogenous transcripts, breaking new ground for a variety of basic research tools and promising clinical applications in the future. Here, we combine site-directed adenosine-to-inosine RNA editing with chemically induced dimerization. Specifically, we achieve tight and dose-dependent control of the editing reaction with gibberellic acid, and obtain editing yields up to 20% and 44% in the endogenous STAT1 and GAPDH transcript in cell culture. Furthermore, the disease-relevant MECP2 R106Q mutation was repaired with editing yields up to 42%. The introduced principle will enable new applications where temporal or spatiotemporal control of an RNA-targeting mechanism is desired.

RNA base editing enables the rewriting of genetic information with high efficiency and without the risk of permanent off-target effects and thus has high prospects for clinical application.[1] Furthermore, the reversibility of an editing event on the transient (m)RNA copy allows to tune the yield of base exchange and might be used to introduce otherwise lethal mutations suddenly and/or temporally restricted.[2] The SNAP-ADAR approach was engineered for site-directed adenosine-to-inosine (A-to-I) RNA editing.[3] For this, the dsRNA binding domains responsible for substrate recognition in wildtype adenosine deaminase acting on RNA (ADAR)[4] are replaced by the self-labeling SNAP-tag. The SNAP-tag binds covalently to guideRNAs carrying its substrate, O^6-benzylguanine[5] (BG, snap-guideRNAs), which then allows for recruitment of the fused ADAR deaminase domain to a specific target via Watson-Crick base pairing. The approach has been shown to be rationally programmable, to achieve high editing yields in cell culture and in vivo,[6] to be very precise,[2] and to be efficient enough to enable concurrent editing.[6] The extension of the approach by further layers of control is desirable. Recently, we achieved photo-control in developing embryos by application of guide-RNAs carrying a nitropiperonyloxymethyl-protected BG moiety.[7] Here, we now include control of the editing reaction by chemically induced dimerization[8] with a small molecule. This opens many new opportunities to run editing under temporal, spatial or dose control.

Specifically, we decided to use gibberellic acid (GA_3) for chemically induced dimerization. GA_3 is a plant hormone that can be delivered as a cell-permeable prodrug (GA_3–AM), that has been shown to induce the heterodimerization of the two plant proteins GAI (gibberellic acid insensitive) and GID1A (gibberellin insensitive dwarf 1A, Figure 1) on a timescale of seconds to minutes inside live cells.[9] Binding of GA_3 to GID1A induces a conformational change that leads to recruitment of GAI. In order to control the SNAP-ADAR-based editing reaction by GA_3-induced dimerization, the SNAP-tag and the ADAR deaminase domain needed engineering into two separate fusion proteins with GAI and GID1A, respectively. We decided to use a GAI_{1-92}–ADAR1 fusion, applying a 92 amino acid fragment of GAI sufficient for dimerization,[9] and a SNAP-GID1A fusion. In our design, we kept the SNAP-tag and ADAR deaminase domain at their respective N- and C-terminal position. We combined the ADAR deaminase domain with the GAI fragment to also place the latter in accordance with its native N-terminal position. The GID1A protein has recently been applied in fusion with an N-terminal eGFP-tag.[9–10] We expected that the exchange of the eGFP-tag with a SNAP-tag will not interfere with the function of the plant protein. Finally, both transgenes have the same size (59 kDa). We engineered four plasmid constructs (**I**–**IV**) that contain both transgenes in one expression cassette (Figure 2a). This design was chosen to obtain a balanced expression of both transgenes after stable genetic integration of the respective single plasmid into a cell line. Furthermore, under transient expression conditions such constructs would help to reduce the transfection bias and to improve the balance in the expression of both transgenes. The two transgenes were either put consecutively, each with its own CMV promotor and bGH terminator, or they were expressed as a single P2A[11] construct from one promotor using a translational skipping mechanism to create two separate proteins from one transcript in a nearly 1:1 stoichiometry. For the editase fusion, we either chose the catalytic deaminase domain of wildtype human ADAR1 (GAI_{1-92}–ADAR1) or of a hyperactive mutant (GAI_{1-92}–ADAR1Q), carrying a well-known E>Q single point mutation.[12] To create duo cell lines expressing both transgenes stably under doxycycline induction,

[a] A. S. Stroppel, R. Lappalainen, Prof. T. Stafforst
Interfaculty Institute of Biochemistry
University of Tübingen
Auf der Morgenstelle 15, 72076 Tübingen (Germany)
E-mail: thorsten.stafforst@uni-tuebingen.de

Supporting information for this article is available on the WWW under https://doi.org/10.1002/chem.202101985

Chemistry–A European Journal | Communication
doi.org/10.1002/chem.202101985
Chemistry Europe
European Chemical Societies Publishing

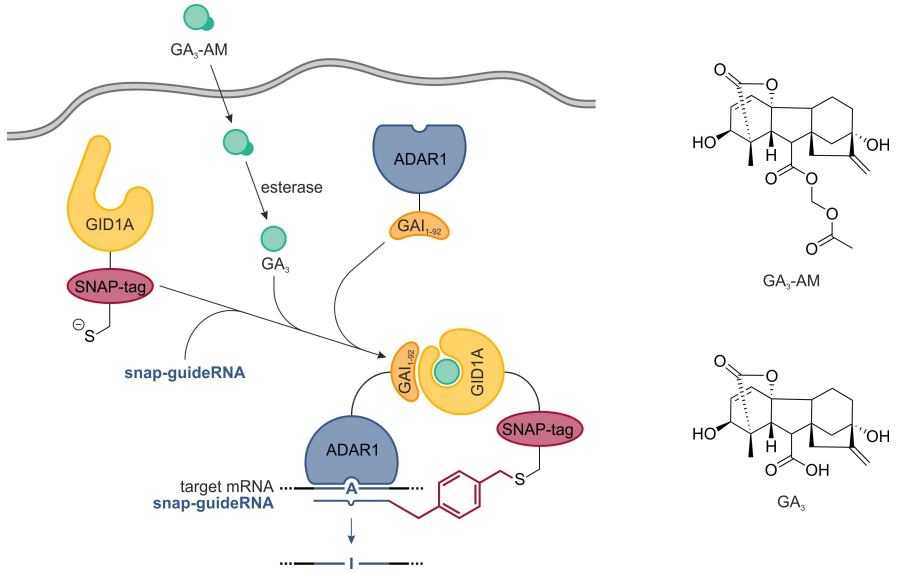

Figure 1. Principle of gibberellic acid-induced site-directed RNA editing with the SNAP-ADAR platform. Covalent conjugation of an O^6-benzylguanosine (BG)-modified guideRNA (snap-guideRNA) with the SNAP-tagged deaminase ADAR enables the steering of A-to-I deaminase activity to any arbitrary mRNA to achieve programmable, RNA-guided site-specific RNA editing. To place the process under control of gibberellic acid, the SNAP-ADAR protein is split into a GAI_{1-92}–ADAR and a SNAP-GID1A fusion, separating the editing activity from the RNA-targeting mechanism. Gibberellic acid, delivered in the form of a cell-permeable acetoxymethyl ester (GA_3–AM), enforces heterodimerization of GAI_{1-92} and GID1A by binding to the latter, and thereby recruits the ADAR deaminase to the guideRNA/mRNA substrate duplex.

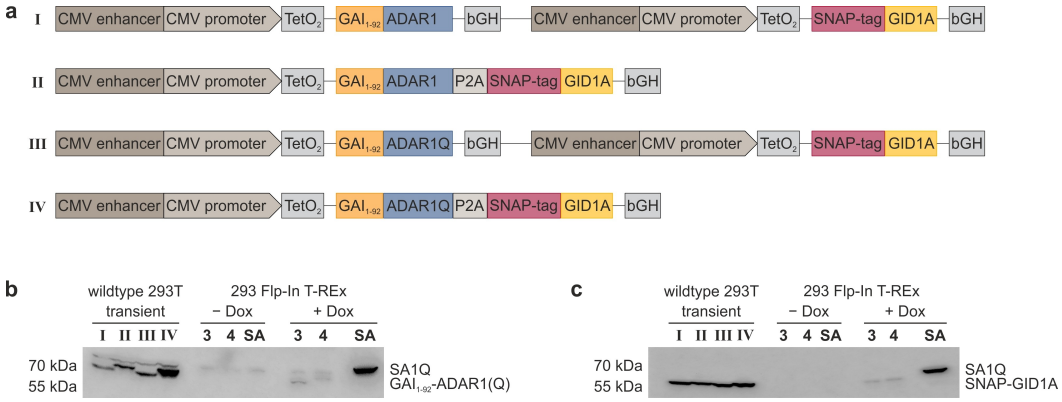

Figure 2. Expression constructs for gibberellic acid-induced RNA editing with SNAP-ADAR and analysis of transgene expression. a) Constructs **I**–**IV** were designed to create transgenic 293 Flp-In T-REx cell lines **1**–**4**, stably co-expressing GAI_{1-92}–ADAR1(Q) and SNAP-GID1A from one cassette under doxycycline control. $TetO_2$: tet operator, leads to repression of expression in the absence of a tetracycline;[13] bGH: bovine growth hormone terminator; P2A: porcine teschovirus-1 self-cleaving 2A peptide.[11] The protocol for the generation of stable cell lines **1**–**4** from constructs **I**–**IV** and details on the constructs can be found in the Supporting Information. b) Characterization of GAI_{1-92}–ADAR1(Q) expression via Western Blot (α-ADAR1 deaminase domain). Wildtype 293T cells were transiently transfected with constructs **I**–**IV** and stable cell lines **3** and **4** were examined without (−Dox) and with 24 h (+Dox) doxycycline induction. Previously established SA1Q 293 Flp-In T-REx cell line (**SA**) shown for comparison. c) Same as (b) but for expression analysis of SNAP-GID1A (α-SNAP-tag).

we applied the 293 Flp-In T-REx system. For each construct, **I**–**IV**, we generated a separate duo cell line, **1**–**4**, by a plasmid transfection and antibiotic selection procedure, as described before.[6] The doxycycline-dependent expression of both transgenes was confirmed by Western blot with antibodies against ADAR1 deaminase (Figure 2b) and SNAP-tag (Figure 2c). Notably, the expression levels were comparably low in relation to the stable expression of SNAP-ADAR1Q after integration into the 293 Flp-In T-REx cell line (Figure 2b,c).[6]

First, we tested the editing reaction in cell lines **3** and **4** expressing the hyperactive ADAR1Q fusion. Specifically, we targeted a 5′-UAG codon in the 3′ untranslated region (UTR) of

Chemistry–A European Journal | Communication doi.org/10.1002/chem.202101985 | Chemistry Europe European Chemical Societies Publishing

the endogenous GAPDH transcript (Figure 3a). Beside the snap-GAPDH guideRNA, carrying the BG moiety required for covalent reaction with the SNAP-tag, we also applied an NH_2–GAPDH guideRNA as control, comprising of the same sequence and modification pattern, but lacking the BG moiety, thus incompetent of forming a conjugate. The control guideRNA (NH_2–GAPDH) gave no detectable editing, highlighting the requirement for covalent guideRNA attachment to recruit ADAR deaminase activity. This clean negative control is a hallmark of RNA-targeting with the SNAP-ADAR approach.[2,6] Notably, in the absence of the inducer GA_3–AM, no GAPDH editing above the threshold for accurate detection (5%) was detected with the snap-GAPDH guideRNA. However, in presence of 10 μM GA_3–AM in the medium, editing levels of 29±9% and 44±4% were achieved in cell line **3** and **4**, respectively. We therefore estimate the dynamic change of the editing yield by GA_3–AM induction to be >10 fold. Nevertheless, the editing efficiency stayed clearly below the one obtained with the analogous SNAP-ADAR1Q cell line,[6] which, as expected, yielded high editing independent of GA_3–AM (74±3% versus 76±3%, Figure 3a). This loss of efficiency might be either due to the low expression of the GAI and GID1A fusion proteins compared to the SNAP-ADAR1Q fusion (Figure 2b,c), or it could be a drawback resulting from the necessity to bring not only one, but two proteins, a guideRNA, and an mRNA together for editing. To make sure that the applied GA_3–AM amount was sufficient to induce maximum editing, we determined the dose-response of the editing yield in cell line **4** over a concentration range from 10 nM to 100 μM GA_3–AM (Figure 3b). We determined the EC_{50} to approximately 290 nM, indicating that the editing yield was already close to saturation at 10 μM GA_3–AM. The determined EC_{50} value fits to earlier reports from different applications in literature.[9]

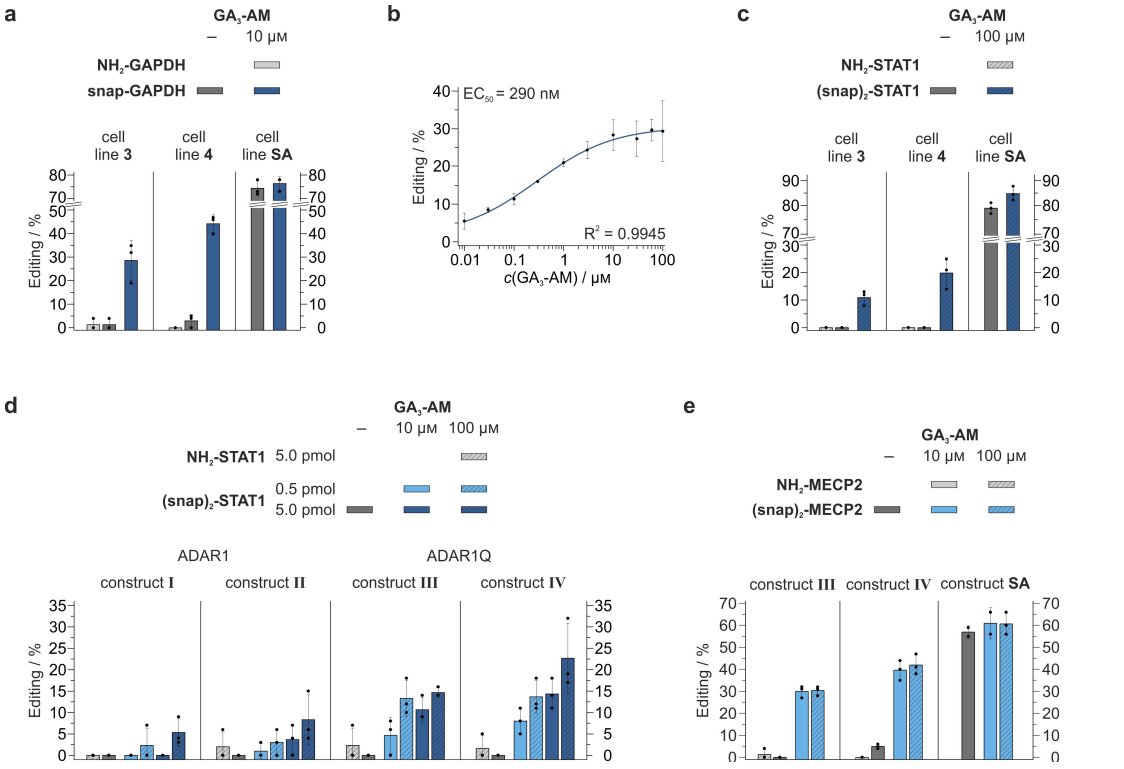

Figure 3. Controlling site-directed RNA editing with gibberellic acid. a) A snap-GAPDH guideRNA (5.0 pmol) targeting a 5′-UAG codon in the 3′-UTR of endogenous GAPDH was transfected into cell lines **3** and **4**, as indicated. An NH_2-guideRNA lacking the BG moiety required for covalent conjugation to the SNAP-GID1A fusion served as negative control. Simultaneously, GA_3–AM (10 μM) was added to the medium, as indicated. RNA editing yields were determined 24 h after transfection by RT-PCR and Sanger sequencing, as described in the Supporting Information. Editing clearly depended on GA_3–AM. b) Determination of the dose-response to GA_3–AM effecting the RNA editing yield in cell line **4**. Editing was performed as described in panel a) on endogenous GAPDH, but with GA_3–AM concentrations ranging from 10 nM to 100 μM. The EC_{50} was determined to 290 nM by applying a logistic fit. c) Analogous to panel a), but with a $(snap)_2$-STAT1 guideRNA (5.0 pmol) targeting the phosphorylation site Tyr(Y)701 (5′-UAU codon) in the endogenous STAT1 transcript in cell lines **3** and **4**, induced with 100 μM GA_3–AM, as indicated. d) Editing of Y701 in endogenous STAT1 in wildtype 293T cells and under transient plasmid transfection of the expression cassettes **I**–**IV** (300 ng/well). Cells were treated with GA_3–AM and guideRNAs in indicated concentrations and amounts. e) Repair of transiently plasmid transfected MECP2 R106Q in wildtype 293T cells under transient plasmid transfection of expression cassette **III** or **IV** with a $(snap)_2$-MECP2 guideRNA (1.0 pmol) targeting the disease relevant R106Q mutation, induced with 10 μM or 100 μM GA_3–AM as indicated. In panel (a)–(e), the data is shown as the mean±s.d. of N=3 independent experiments.

Chemistry–A European Journal | Communication doi.org/10.1002/chem.202101985 | Chemistry Europe European Chemical Societies Publishing

In the past, we found A-to-I RNA editing in the open reading frame (ORF) considerably more challenging compared to editing in the 3′-UTR.[6] Thus, we tested editing in the ORF of the endogenous STAT1 transcript (Figure 3c). Specifically, we designed a guideRNA targeting the phosphorylation site Tyr(Y) 701 (5′-UAU codon), which is important for activation of said transcription factor upon interferon signaling.[14] Again, we found no detectable editing with an NH_2-guideRNA lacking the self-labeling moiety. However, we obtained reasonable editing levels when applying the $(snap)_2$–STAT1 guideRNA, able to recruit two SNAP-GID1A proteins per guideRNA. In presence of 100 μM GA_3–AM, editing levels of 11 ± 3% and 20 ± 6% were achieved in cell line **3** and **4**, respectively. Again, cell line **4** outperformed cell line **3** by means of editing yields. Due to the lack of detectable editing in absence of GA_3–AM, the dynamic range for the induction with GA_3–AM was estimated to be very high again. However, the overall editing yields were moderate compared to levels obtained in the analogous SNAP-ADAR1Q 293 Flp-In T-REx cell line (79 ± 2% and 84 ± 3%, without versus with GA_3–AM, Figure 3c).[6] We wondered if this was due to the low expression levels of the GAI and GID1A fusion proteins, and if editing could be fostered by stronger expression of the fusion proteins and further optimization of conditions. We thus tested the editing of all four constructs under transient transfection into wildtype 293T cells, and varied the amount of $(snap)_2$–STAT1 guideRNA (0.5 pmol versus 5.0 pmol) and of the inducer (10 μM versus 100 μM, Figure 3d). We made several observations. First, we found wildtype constructs **I** and **II** to give considerably less editing than the hyperactive constructs **III** and **IV**. This is in accordance with literature for the analogous SNAP-ADAR1 293 Flp-In T-REx cells.[6] Second, editing worked better with higher amounts of guideRNA. Third, higher amounts of inducer also fostered editing. Similar to what we had seen for cell line **4** versus cell line **3**, construct **IV** gave better editing yields than construct **III** under most conditions. Taken together, the data suggests that editing yield is boosted by every component that assists in the formation of the tertiary complex (guideRNA + mRNA + two proteins), for example, more guideRNA, more inducer, and higher protein expression. The latter was supported by Western blot (Figure 2b), showing that more GAI_{1-92}–ADAR1Q was expressed by construct **IV** than by construct **III**. Notably, the editing yields at endogenous STAT1 under transient transgene expression did hardly exceed the levels obtained in the stable cell lines (Figure 3c,d). Obviously, the balanced transgene expression in the stable cell lines, even at very low expression levels, is more powerful for targeting endogenous transcripts than the strong, but uneven transgene expression upon plasmid transfection.

Finally, we aimed to repair the R106Q mutation in the transcription factor Methyl CpG Binding Protein 2 (MECP2), which is known to cause Rett syndrome. The underlying G-to-A mutation is located in the DNA binding domain of MECP2 and leads to reduced protein stability and therefore decreased expression levels, as well as reduced binding to heterochromatin.[15] Since healthy expression levels of MECP2 vary between different neural cell types[16] and duplication of MECP2 causes MECP2 duplication syndrome,[17] repair of R106Q under tight, precisely doseable control at the transcript level is highly desirable. We thus transfected wildtype 293T cells with MECP2 R106Q and either construct **III** or **IV** and tested a guideRNA targeting the R106Q site. Upon induction with 10 μM or 100 μM GA_3–AM, we achieved good editing yields for both construct **III** (30 ± 3% and 30 ± 2%, respectively) and construct **IV** (40 ± 5% and 42 ± 5%, respectively, Figure 3e). Contrary to the editing in the STAT1 transcript (Figure 3d), the editing yields for MECP2 in presence of 10 μM and 100 μM GA_3–AM were equal, indicating saturation at 10 μM inducer for this target, which fits well to the dose-dependence curve shown for the GAPDH target (Figure 3b). Once again, construct **IV** performed better than construct **III**. Notably, the MECP2 editing levels of our constructs came close to the editing levels with the transfected SNAP-ADAR1Q construct (57 ± 3%, 61 ± 7% and 60 ± 5% without, with 10 μM and with 100 μM GA_3–AM, respectively). Importantly, the editing yields obtained with construct **IV** are in the range of editing yields reported to suffice for significant enrichment of heterochromatic MECP2 (37–52%) in vivo in murine neural cells[18] with the λN-ADAR2Q system[19] and therefore might lead to significant diminution of the Rett syndrome phenotype.

In summary, we achieved tight control of site-directed RNA editing by chemically induced dimerization with a small molecule plant hormone. The dimerization occurs promptly (seconds to minutes) after addition of the inducer[9] and elicits a tunable, dose-dependent response. This temporal and dose-dependent control of the RNA editing reaction may break new ground for attractive applications, for example, to trigger targeted editing during embryogenesis after microinjection of all components,[7] to trigger editing to measure RNA lifetimes with RNA timestamp approaches more accurately,[20] or to modulate the pharmacological (adverse) effect of targeted editing.[21] Importantly, we demonstrated that our engineered system, based on the SNAP-ADAR approach in combination with gibberellic acid-induced GID1A-GAI heterodimerization, works not only via transient overexpression, but also under stable genetic integration of the components, which, as we had shown before, reduces artifacts[22] and global off-target editing.[2,6] Furthermore, the editing reaction was strongly dependent on the small molecule – virtually lacking any reaction in the absence of gibberellic acid. Even though the splitting of the SNAP-ADAR editing enzyme into two separate fusion proteins was required to engineer small molecule control, editing of lowly expressed endogenous transcripts was possible in reasonable yields, as demonstrated for the editing of the functionally important phosphorylation site Y701 in STAT1. This is even more remarkable given the comparably low expression levels of the engineered components. We assume that the SNAP-ADAR RNA-targeting approach is particularly suited for the engineering of this kind of small molecule-control as the covalent conjugation of guideRNA and SNAP-tag pre-organizes two components permanently, thus reducing the number of components which need to encounter for editing. Additionally, the disease-relevant R106Q mutation in MECP2 could be repaired to an extent that has been reported[18] to significantly enhance MECP2 function. We expect that the

Chemistry–A European Journal | Communication doi.org/10.1002/chem.202101985 | Chemistry Europe European Chemical Societies Publishing

approach can be further improved, for example the editing yields may be amplified by optimizing the expression levels of the fusion proteins. Furthermore, the approach could be extended by one- or two photon-decaging of gibberellic acid[10] to enable spatiotemporal control in the future.[8,23] Finally, the design principle could be included into further tools that apply RNA-guided proteins to manipulate the (epi)transcriptome[24] or could be integrated into existing SNAP-tag-based sensors[25] to include a further layer of control.

Experimental Section

Detailed experimental procedures for Western Blotting (including full blots) and editing experiments, as well as further details on constructs **I**–**IV**, the generation of stable cell lines and guideRNAs along with their sequences can be found in the Supporting Information.

Acknowledgements

We gratefully acknowledge funding by the Deutsche Forschungsgemeinschaft (DFG, German Research Foundation) – projects 430214260, STA1053/7-1, STA1053/11-1 for TS. The work was supported by the European Research Council (ERC) under the European Union's Horizon 2020 research and innovation program (grant agreement no. 647328 to TS). We thank Richard Wombacher and Gail Mandel for kindly providing GAI_{1-92} and GID1A coding sequences and mMECP2 R106Q in pEGFP–N3, respectively. Open access funding enabled and organized by Projekt DEAL.

Conflict of Interest

T.S. holds patents on site-directed RNA editing.

Keywords: ADAR · chemically induced dimerization · gibberellic acid · RNA targeting · site-directed RNA editing

[1] H. A. Rees, D. R. Liu, *Nat. Rev. Genet.* **2018**, *19*, 770–788.
[2] P. Vogel, T. Stafforst, *Curr. Opin. Biotechnol.* **2019**, *55*, 74–80.
[3] T. Stafforst, M. F. Schneider, *Angew. Chem. Int. Ed.* **2012**, *51*, 11166–11169; *Angew. Chem.* **2012**, *124*, 11329–11332.
[4] K. Nishikura, *Annu. Rev. Biochem.* **2010**, *79*, 321–349.
[5] A. Keppler, S. Gendreizig, T. Gronemeyer, H. Pick, H. Vogel, K. Johnsson, *Nat. Biotechnol.* **2003**, *21*, 86–89.
[6] P. Vogel, M. Moschref, Q. Li, T. Merkle, K. D. Selvasaravanan, J. B. Li, T. Stafforst, *Nat. Methods* **2018**, *15*, 535–538.
[7] A. Hanswillemenke, T. Kuzdere, P. Vogel, G. Jékely, T. Stafforst, *J. Am. Chem. Soc.* **2015**, *137*, 15875–15881.
[8] S. Voß, L. Klewer, Y.-W. Wu, *Curr. Opin. Chem. Biol.* **2015**, *28*, 194–201.
[9] T. Miyamoto, R. DeRose, A. Suarez, T. Ueno, M. Chen, T.-p. Sun, M. J. Wolfgang, C. Mukherjee, D. J. Meyers, T. Inoue, *Nat. Chem. Biol.* **2012**, *8*, 465–470.
[10] K. M. Schelkle, T. Griesbaum, D. Ollech, S. Becht, T. Buckup, M. Hamburger, R. Wombacher, *Angew. Chem. Int. Ed.* **2015**, *54*, 2825–2829; *Angew. Chem.* **2015**, *127*, 2867–2871.
[11] J. H. Kim, S.-R. Lee, L.-H. Li, H.-J. Park, J.-H. Park, K. Y. Lee, M.-K. Kim, B. A. Shin, S.-Y. Choi, *PLoS One* **2011**, *6*, e18556.
[12] A. Kuttan, B. L. Bass, *Proc. Natl. Acad. Sci. USA* **2012**, *109*, E3295–E3304.
[13] F. Yao, T. Svensjö, T. Winkler, M. Lu, C. Eriksson, E. Eriksson, *Hum. Gene Ther.* **1998**, *9*, 1939–1950.
[14] J. E. Darnell, I. M. Kerr, G. R. Stark, *Science* **1994**, *264*, 1415–1421.
[15] J. R. Sinnamon, S. Y. Kim, G. M. Corson, Z. Song, H. Nakai, J. P. Adelman, G. Mandel, *Proc. Natl. Acad. Sci. USA* **2017**, *114*, E9395–E9402.
[16] M. D. Shahbazian, B. Antalffy, D. L. Armstrong, H. Y. Zoghbi, *Hum. Mol. Genet.* **2002**, *11*, 115–124.
[17] H. Van Esch, M. Bauters, J. Ignatius, M. Jansen, M. Raynaud, K. Hollanders, D. Lugtenberg, T. Bienvenu, L. R. Jensen, J. Gécz, C. Moraine, P. Marynen, J.-P. Fryns, G. Froyen, *Am. J. Hum. Genet.* **2005**, *77*, 442–453.
[18] J. R. Sinnamon, S. Y. Kim, J. R. Fisk, Z. Song, H. Nakai, S. Jeng, S. K. McWeeney, G. Mandel, *Cell Rep.* **2020**, *32*, 107878.
[19] M. F. Montiel-Gonzalez, I. Vallecillo-Viejo, G. A. Yudowski, J. J. C. Rosenthal, *Proc. Natl. Acad. Sci. USA* **2013**, *110*, 18285–18290.
[20] S. G. Rodriques, L. M. Chen, S. Liu, E. D. Zhong, J. R. Scherrer, E. S. Boyden, F. Chen, *Nat. Biotechnol.* **2020**, *39*, 320–325.
[21] V. M. Rivera, T. Clackson, S. Natesan, R. Pollock, J. F. Amara, T. Keenan, S. R. Magari, T. Phillips, N. L. Courage, F. C. Jr, D. A. Holt, M. Gilman, *Nat. Med.* **1996**, *2*, 1028–1032.
[22] P. Vogel, A. Hanswillemenke, T. Stafforst, *ACS Synth. Biol.* **2017**, *6*, 1642–1649.
[23] N. Ankenbruck, T. Courtney, Y. Naro, A. Deiters, *Angew. Chem. Int. Ed.* **2018**, *57*, 2768–2798; *Angew. Chem.* **2018**, *130*, 2816–2848.
[24] a) X.-M. Liu, J. Zhou, Y. Mao, Q. Ji, S.-B. Qian, *Nat. Chem. Biol.* **2019**, *15*, 865–871; b) K. Rau, L. Rösner, A. Rentmeister, *RNA* **2019**, *25*, 1311–1323; c) B. S. Zhao, I. A. Roundtree, C. He, *Nat. Rev. Mol. Cell Biol.* **2017**, *18*, 31–42.
[25] a) Q. Yu, L. Xue, J. Hiblot, R. Griss, S. Fabritz, C. Roux, P.-A. Binz, D. Haas, J. G. Okun, K. Johnsson, *Science* **2018**, *361*, 1122–1126; b) T. Podewin, J. Ast, J. Broichhagen, N. H. F. Fine, D. Nasteska, P. Leippe, M. Gailer, T. Buenaventura, N. Kanda, B. J. Jones, C. M'Kadmi, J.-L. Baneres, J. Marie, A. Tomas, D. Trauner, A. Hoffmann-Röder, D. J. Hodson, *ACS Cent. Sci.* **2018**, *4*, 166–179.

Manuscript received: June 6, 2021
Accepted manuscript online: June 25, 2021
Version of record online: July 26, 2021

Chemistry–A European Journal

Supporting Information

Controlling Site-Directed RNA Editing by Chemically Induced Dimerization

Anna S. Stroppel, Ruth Lappalainen, and Thorsten Stafforst*

Contents

List of Figures

List of Tables

Cloning of editase constructs **I – IV**

Constructs **I – IV** for co-expression of GAI_{1-92}-ADAR1(Q) and $SNAP_f$-GID1A were cloned in a pcDNA 5 vector via restriction/ligation. ADAR1(Q) and $SNAP_f$ were amplified from our own plasmids, GAI_{1-92} and GID1A coding sequences were kindly provided by Dr. R. Wombacher, Ruprecht Karls University, Heidelberg, Germany.[1] GAI_{1-92}-ADAR1(Q) and $SNAP_f$-GID1A were then successively ligated into one common pcDNA 5 vector. Constructs **I** and **III** were generated by ligation into a vector with two consecutive CMV enhancers and CMV promoters, each followed by two copies of the *tet* operator ($TetO_2$) via BamHI/AscI/ApaI and NotI/NheI/ClaI. Constructs **II** and **IV** were generated by ligation into a vector with one CMV enhancer and CMV promoter, followed by two copies of the *tet* operator ($TetO_2$) and a central self-cleaving P2A via BamHI/AscI/NotI and XhoI/NheI/PacI. The sequences of the respective constructs are attached as Appendix.

General cultivation & generation of stable cell lines

In general, cells were cultivated in Dulbecco's Modified Eagle Medium (DMEM, LIFE TECHNOLOGIES) supplemented with 10 % fetal bovine serum (FBS, LIFE TECHNOLOGIES) and 100 U/ml penicillin-streptomycin (LIFE TECHNOLOGIES), short DMEM/FBS/P/S, at 37 °C with 5 % CO_2 in a water saturated steam atmosphere. Stable, inducible cell lines **1 – 4** with integrated constructs **I – IV** respectively were generated with the Flp-In™ T-REx™ system by LIFE TECHNOLOGIES. $4 \cdot 10^6$ 293 Flp-In™ T-REx™ cells were seeded in 10 ml DMEM/10 % FBS/100 µg/ml zeocin/15 µg/ml blasticidin (DMEM/FBS/Z/B) in a 10 cm dish. After 23 h, medium was replaced with DMEM/10 % FBS (DMEM/FBS) and 1 h later 9 µg pOG 44 and 1 µg of the respective construct in a pcDNA 5 vector were forward transfected with 30 µl Lipofectamine 2000 (THERMO FISHER SCIENTIFIC). After 24 h, medium was replaced with 15 ml DMEM/FBS/15 µg/ml blasticidin/100 µg/ml hygromycin (DMEM/FBS/B/H), followed by selection for approximately two weeks. Then, the stable cell lines were transferred to a 75 cm^2 cell culture flask and subsequently cultivated in DMEM/FBS/B/H.

Western Blotting

Preparation of lysates from wildtype 293T cells transiently expressing constructs **I – IV**

$2 \cdot 10^5$ wildtype 293T cells were seeded in 500 µl DMEM/FBS/P/S in 3 wells of a 24 well plate per condition. After 24 h, medium was replaced with 450 µl DMEM/FBS and 300 ng of constructs **I – IV** in pcDNA 5 respectively were forward transfected with 1.2 µl Lipofectamine 2000 (LIFE TECHNOLOGIES). 24 h thereafter, medium was removed and cells were first washed with 500 µl PBS and then detached and suspended in 500 µl fresh PBS per well. Cells from one condition were combined and then centrifuged for 5 min at 1.600 rpm, followed by removal of PBS and resuspension of the cell pellets in 75 µl urea lysis buffer (8 M urea, 100 mM NaH_2PO_4, 10 mM Tris, pH 8.0). Cells were then lysed via shear force by drawing the solution 15× up and out a 19 gauge syringe. After centrifugation for 15 min at 16.000 rpm and 4 °C, the supernatant lysates were transferred to fresh reaction tubes.

Preparation of lysates from 293 Flp-In™ T-REx™ cell lines 3 & 4

Lysates from stable, inducible cell lines **3** and **4** expressing the hyperactive ADAR1Q were also analyzed via Western Blot. For comparison, our previously established SNAP-ADAR1Q 293 Flp-In™ T-REx™ cell line (SA1Q)[2] was examined in parallel. $1 \cdot 10^6$ 293 Flp-In™ T-REx™ cells from the respective cell line were seeded in 2500 µl medium in one well of a 6 well plate per condition. For the uninduced samples (– Dox) DMEM/FBS/B/H was used as medium, for the samples with doxycycline induction (+ Dox)

DMEM/FBS/B/H/ 10 ng/ml doxycycline (DMEM/FBS/B/H/D) was used. After 24 h, medium was removed and cells were first washed with 1000 µl PBS and then detached and suspended in 1000 µl fresh PBS. Centrifugation for 5 min at 1.600 rpm was followed by removal of PBS and resuspension of the cell pellets in 75 µl urea lysis buffer (8 M urea, 100 mM NaH_2PO_4, 10 mM Tris, pH 8.0). Cells were then again lysed via shear force by drawing the solution 15× up and out a 19-gauge syringe. After centrifugation for 15 min at 16.000 rpm and 4 °C, the supernatant lysates were transferred to fresh reaction tubes.

PAGE & Western Blot

Total protein concentrations of all samples were determined via Bradford assay (SIGMA ALDRICH B6916) and equal amounts of proteins in 16.66 µl urea lysis buffer were heated with 3.33 µl 6× Laemmli buffer (0.4 M SDS, 60 mM Tris pH 6.8, 6.5 M glycerol, 0.6 M dithiothreitol, 0.9 mM bromophenol blue) for 5 min at 95 °C and 700 rpm. Subsequently, samples and PageRuler™ Plus protein ladder (THERMO FISHER 26620) were loaded to a Novex™ WedgeWell™ 8–16 % Tris-Glycine gel (THERHMO FISHER XP08165BOX), which was run at 90 V for 5 min followed by 160 V for 90 min. Proteins were transferred onto a PVDF membrane (BIO-RAD LABORATORIES) at 30 V and 4 °C for 18 h, followed by blocking in 5 % dry milk in TBST for 1 h. For characterization of $GAI_{1\text{-}92}$-ADAR1(Q) expression, the respective blot was incubated with rabbit α-ADAR1 (1:1.000, BETHYL LABORATORIES A303-884A) in 5 % DryMilk-TBST at 4 °C overnight as primary antibody. For characterization of SNAP-GID1A expression, the respective blot was incubated with rabbit α-SNAP-tag (1:1.000, NEW ENGLAND BIOLABS P9310S) in 5 % DryMilk-TBST at room temperature for 2 h. In both cases, this was followed by incubation with goat α-rabbit HRP (1:5.000, JACKSON IMMUNORESEARCH 111-035-003) for 2 h at room temperature as secondary antibody. Chemiluminescence was measured with a FUSION FX by VILBER. As loading control, α-GAPDH (1:3.333, THERMO FISHER AM4300) in 5 % DryMilk-TBST was applied at 4 °C overnight, followed by goat α-mouse HRP (1:5.000, JACKSON IMMUNORESEARCH 115-035-003) in 5 % DryMilk-TBST for 2 h at room temperature. Chemiluminescence was again measured with a FUSION FX by VILBER.

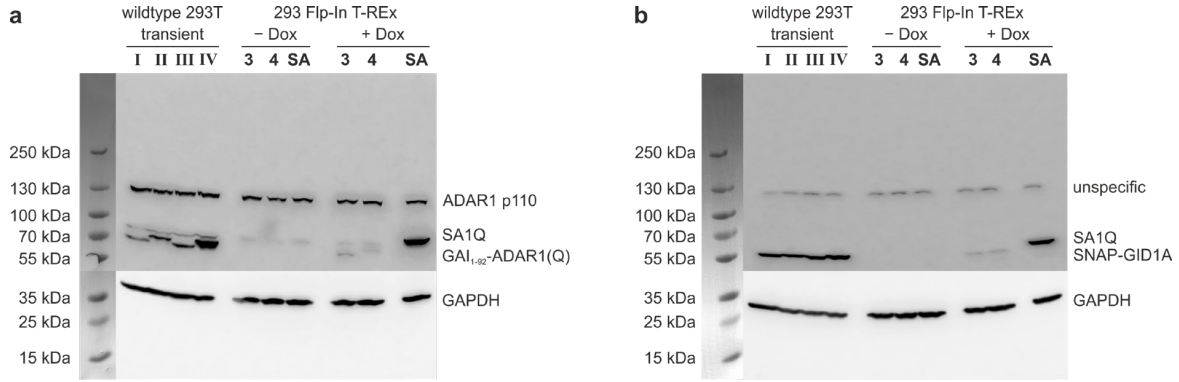

Figure S1. Full Western Blots (corresponding to sections shown in Figure 2b,c) of wildtype 293T cells transiently transfected with constructs ***I – IV****, as well as $GAI_{1\text{-}92}$-ADAR1Q/SNAP-GID1A 293 Flp-In T-REx cell lines* ***3*** *and* ***4*** *without (– Dox) and with 24 h (+ Dox) doxycycline induction. SA1Q 293 Flp-In T-REx cell line (****SA****) shown for comparison.* ***a)*** *Detection of the different ADAR1 proteins with α-ADAR1. $GAI_{1\text{-}92}$-ADAR1(Q) from constructs* ***II*** *and* ***IV*** *is of slightly larger size due to the residual P2A peptide. An additional band originating from endogenous ADAR1 p110 can be observed equally for all samples.* ***b)*** *Detection of different SNAP proteins with α-SNAP-tag. Blots were cut above the GAPDH loading control before detection.*

Generation of guideRNAs

NH_2-guideRNAs were purchased from BIOSPRING in ion exchange HPLC-purified quality. guideRNAs were 22 to 25 nt long, containing a 5'-C6-aminolinker, and were chemically stabilized similar as described before.[3] Table S1 provides the sequences, modification patterns and extinction coefficients at 260 nm of all guideRNAs. The snap-GAPDH guideRNA was generated from the NH_2-GAPDH guideRNA by a post-synthesis labeling protocol analogous to a previously published protocol,[4] by applying snap (35 eq). $(snap)_2$-STAT1 and $(snap)_2$-MECP2 were produced analogous to the previously reported improved protocol with DIC activation,[5] using $(snap)_2$ (17.5 eq).

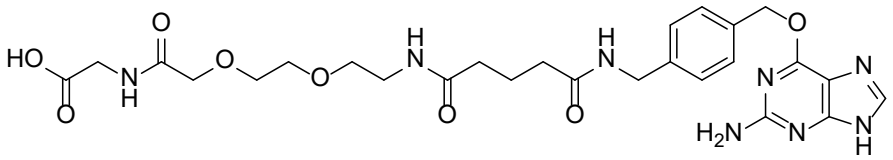

snap

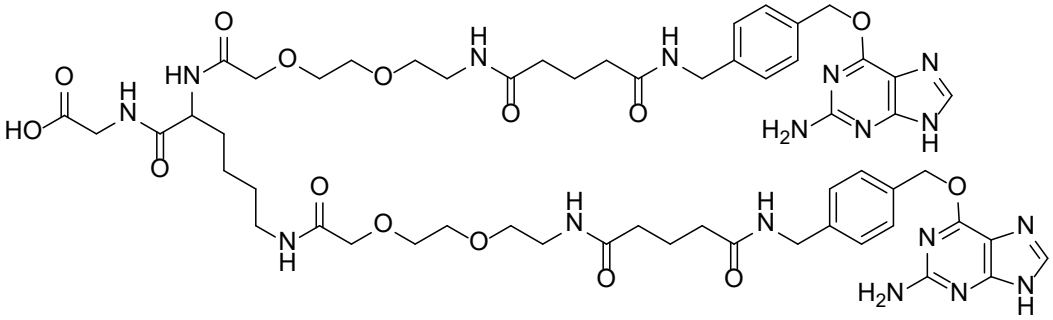

$(snap)_2$

Figure S2. Structures of snap and $(snap)_2$, which were pre-activated at their carboxylic acids and coupled to the 5'-C6-aminolinker of NH_2-guideRNA.

Table S1. Sequences and $\varepsilon_{260\,nm}$ of used guideRNAs. Normal uppercase = ribonucleotide, italics = 2'OMe, bold = LNA, s = phosphorothioate linkage.

guideRNA	Target	Sequence	$\varepsilon_{260\,nm}$ / $mM^{-1}cm^{-1}$
NH_2-GAPDH	GAPDH 3'-UTR	*AsAsUAAGGGGU* CCA *CAUGGsCsAsAsC*	232.00
snap-GAPDH	GAPDH 3'-UTR	*AsAsUAAGGGGU* CCA *CAUGGsCsAsAsC*	234.50
NH_2-STAT1	STAT1 Y701C	*AsGsU***G***U***C***UUGAU* ACA *UCCAGUU*sC*s***C***s*U*s***T**	246.50
$(snap)_2$-STAT1	STAT1 Y701C	*AsGsU***G***U***C***UUGAU* ACA *UCCAGUU*sC*s***C***s*U*s***T**	251.50
NH_2-MECP2	MECP2 R106Q	*AsCsA***T***U***A***AGCUU* UCG *UGUCCAAsCs***C**s*Us***T**	245.65
$(snap)_2$-MECP2	MECP2 R106Q	*AsCsA***T***U***A***AGCUU* UCG *UGUCCAAsCs***C**s*Us***T**	250.65

Editing experiments

All editing experiments depicted in bar graphs were conducted in biological triplicates and standard deviations are shown.

Editing of endogenous GAPDH under genomic expression of editase constructs

$4 \cdot 10^5$ of the respective 293 Flp-In™ T-REx™ cells were seeded in 500 µl DMEM/FBS/B/H/D in a 24 well plate. After 24 h, $8 \cdot 10^4$ cells were reverse transfected in a 96 well plate with 5.0 pmol of the respective guideRNA with 0.5 µl Lipofectamine 2000 and 10 µM GA_3-AM (from a 10 mM stock in DMSO) were added to the medium of the indicated samples. Doxycycline concentration was kept at 10 ng/ml and after further 24 h cells were harvested. RNA isolation was performed with the Monarch® RNA cleanup kit from NEW ENGLAND BIOLABS, followed by DNase I digestion. Purified RNA was then reverse transcribed and amplified with the One Step RT-PCR Kit from BIOTECHRABBIT and subsequently analyzed with Sanger sequencing (MICROSYNTH). A-to-I editing yields were determined by dividing the peak height for guanosine by the sum of the peak heights for both adenosine and guanosine.

Determination of dose-response to GA_3-AM

To determine the dose-response to GA_3-AM, editing experiments were performed in 293 Flp-In™ T-REx™ cells from cell line **4** as described for the editing of endogenous GAPDH. 0.01, 0.03, 0.1, 0.3, 1, 3, 10, 30, 60 or 100 µM GA_3-AM were applied from the respective 1000× stocks in DMSO. As negative controls, cells were treated with NH_2-GAPDH without GA_3-AM, NH_2-GAPDH + 100 µM GA_3-AM and snap-GAPDH without GA_3-AM, none of which showed substantial editing.

The experiment was conducted in biological triplicates and the mean editing yields after treatment with snap-GAPDH and the respective concentration of GA_3-AM were plotted on a logarithmic scale against the concentration of GA_3-AM. The following logistic dose response curve was fitted to the data:

$$editing\ e\ /\ \% = \frac{e_{min} - e_{max}}{1 + \left(\frac{x}{x_0}\right)^p} + e_{max}$$

with e_{min} = 1.5 %: minimal editing, e_{max} = 31 %: maximal editing, x: c(GA_3-AM), x_0 = 0.29: center, p = 0.56: power and corrected R^2 = 0.9945. The resulting half maximal effective concentration of GA_3-AM is $EC_{50} \approx 290$ nM.

Editing of endogenous STAT1 under genomic expression of editase constructs

$4 \cdot 10^5$ of the respective 293 Flp-In™ T-REx™ cells were seeded in 500 µl DMEM/FBS/B/H/D in a 24 well plate. After 24 h, $8 \cdot 10^4$ cells were reverse transfected in a 96 well plate with 5.0 pmol of the respective guideRNA with 0.5 µl Lipofectamine 2000 and 100 µM GA_3-AM (from a 100 mM stock in DMSO) were added to the medium of the indicated samples. Doxycycline concentration was kept at 10 ng/ml and after further 24 h cells were harvested. RNA isolation was performed with the Monarch® RNA cleanup kit from NEW ENGLAND BIOLABS. Purified RNA was then treated with a DNA oligonucleotide of complementary sequence to the STAT1 guideRNA (5'-aaggaactggatctatcaagacacc, 1 µM) at 95 °C for 1 min to trap the guideRNA, followed by reverse transcription and amplification with the One Step RT-PCR Kit from BIOTECHRABBIT. A-to-I editing yields were again determined by Sanger sequencing (MICROSYNTH) by dividing the peak height for guanosine by the sum of the peak heights for both adenosine and guanosine.

Editing of endogenous STAT1 under transient expression of editase constructs

$2 \cdot 10^5$ wildtype 293T cells were seeded in 500 µl DMEM/FBS/P/S in a 24 well plate. After 24 h, medium was replaced with 450 µl DMEM/FBS and 300 ng of either construct **I**, **II**, **III** or **IV** in pcDNA 5 were forward transfected with 1.2 µl Lipofectamine 2000. After further 24 h, $8 \cdot 10^4$ cells were reverse transfected in a 96 well plate with the respective amount of the indicated guideRNA with 0.5 µl Lipofectamine 2000 and 10 µM or 100 µM GA_3-AM (from a 10 mM or 100 mM stock in DMSO) were added to the medium as indicated. Doxycycline concentration was kept at 10 ng/ml and after further 24 h cells were harvested and proceeded as for the editing of STAT1 under genomic expression of the editase constructs.

Editing of transfected MECP2 under transient expression of editase constructs

$2 \cdot 10^5$ wildtype 293T cells were seeded in 500 µl DMEM/FBS/P/S in a 24 well plate. After 24 h, medium was replaced with 450 µl DMEM/FBS and 300 ng mMECP2 R106Q in pEGFP-N3 (kindly provided by Dr. G. Mandel, Oregon Health and Science University, Portland, USA)[6] together with 300 ng of either construct **III**, **IV** or SNAP-ADAR1Q in pcDNA 5 were forward transfected with 2.4 µl Lipofectamine 2000. After further 24 h, $8 \cdot 10^4$ cells were reverse transfected in a 96 well plate with 1.0 pmol of the indicated guideRNA with 0.5 µl Lipofectamine 2000 and 10 µM or 100 µM GA_3-AM (from a 10 mM or 100 mM stock in DMSO) were added to the medium as indicated. Doxycycline concentration was kept at 10 ng/ml and after further 24 h cells were harvested and proceeded as for the editing of GAPDH.

Supporting literature

[1] K. M. Schelkle, T. Griesbaum, D. Ollech, S. Becht, T. Buckup, M. Hamburger, R. Wombacher, *Angew. Chem. Int. Ed.* **2015**, *54*, 2825–2829; *Angew. Chem.* **2015**, *127*, 2867–2871.

[2] P. Vogel, M. Moschref, Q. Li, T. Merkle, K. D. Selvasaravanan, J. B. Li, T. Stafforst, *Nat. Methods* **2018**, *15*, 535–538.

[3] P. Vogel, T. Stafforst, *ChemMedChem* **2014**, *9*, 2021–2025.

[4] A. Hanswillemenke, T. Kuzdere, P. Vogel, G. Jékely, T. Stafforst, *J. Am. Chem. Soc.* **2015**, *137*, 15875–15881.

[5] A. Hanswillemenke, T. Stafforst, *Methods Enzymol.* **2019**, *624*, 47–68.

[6] J. R. Sinnamon, S. Y. Kim, G. M. Corson, Z. Song, H. Nakai, J. P. Adelman, G. Mandel, *Proc. Natl. Acad. Sci. U. S. A.* **2017**, *114*, E9395–E9402.

Appendix

Constructs I – IV

Construct **I**: CMV-enhancer – CMV promoter – $TetO_2$ – GAI_{1-92} – ADAR1 – bGH – CMV-enhancer – CMV promoter – $TetO_2$ – $SNAP_f$-tag – GID1A – bGH

GACATTGATTATTGACTAGTTATTAATAGTAATCAATTACGGGGTCATTAGTTCATAGCCCATATATG
GAGTTCCGCGTTACATAACTTACGGTAAATGGCCCGCCTGGCTGACCGCCCAACGACCCCCGCCCATT
GACGTCAATAATGACGTATGTTCCCATAGTAACGCCAATAGGGACTTTCCATTGACGTCAATGGGTGG
AGTATTTACGGTAAACTGCCCACTTGGCAGTACATCAAGTGTATCATATGCCAAGTACGCCCCCTATT
GACGTCAATGACGGTAAATGGCCCGCCTGGCATTATGCCCAGTACATGACCTTATGGGACTTTCCTAC
TTGGCAGTACATCTACGTATTAGTCATCGCTATTACCATGGTGATGCGGTTTTGGCAGTACATCAATG
GGCGTGGATAGCGGTTTGACTCACGGGGATTTCCAAGTCTCCACCCCATTGACGTCAATGGGAGTTTG
TTTTGGCACCAAAATCAACGGGACTTTCCAAAATGTCGTAACAACTCCGCCCCATTGACGCAAATGGG
CGGTAGGCGTGTACGGTGGGAGGTCTATATAAGCAGAGCTCTCCCTATCAGTGATAGAGATCTCCCTA
TCAGTGATAGAGATCGTCGACGAGCTCGTTTAGTGAACCGTCAGATCGCCTGGAGACGCCATCCACGC
TGTTTTGACCTCCATAGAAGACACCGGGACCGATCCAGCCTCCGGACTCTAGCGTTTAAACTTAAGCT
TGGTACCGAGCTCGGATCCCCACCATGAAGAGAGATCATCATCATCATCATCATCAAGATAAGAAGAC
TATGATGATGAATGAAGAAGACGACGGTAACGGCATGGATGAGCTTCTAGCTGTTCTTGGTTACAAGG
TTAGGTCATCCGAAATGGCTGATGTTGCTCAGAAACTTGAGCAGCTTGAAGTTATGATGTCTAATGTT
CAAGAAGACGATCTTTCTCAACTCGCTACTGAGACTGTTCACTATAATCCGGCGGAGCTTTACACGTG
GCTTGATTCTATGCTCACCGACCTTAATCCTGCAGGCGGAGGCGCGCCAGGGTCTGGCGGCGGCAGTA
AGGCAGAACGCATGGGTTTCACAGAGGTAACCCCAGTGACAGGGGCCAGTCTCAGAAGAACTATGCTC
CTCCTCTCAAGGTCCCCAGAAGCACAGCCAAAGACACTCCCTCTCACTGGCAGCACCTTCCATGACCA
GATAGCCATGCTGAGCCACCGGTGCTTCAACACTCTGACTAACAGCTTCCAGCCCTCCTTGCTCGGCC
GCAAGATTCTGGCCGCCATCATTATGAAAAAAGACTCTGAGGACATGGGTGTCGTCGTCAGCTTGGGA
ACAGGGAATCGCTGTGTAAAAGGAGATTCTCTCAGCCTAAAAGGAGAAACTGTCAATGACTGCCATGC
AGAAATAATCTCCCGGAGAGGCTTCATCAGGTTTCTCTACAGTGAGTTAATGAAATACAACTCCCAGA
CTGCGAAGGATAGTATATTTGAACCTGCTAAGGGAGGAGAAAAGCTCCAAATAAAAAAGACTGTGTCA
TTCCATCTGTATATCAGCACTGCTCCGTGTGGAGATGGCGCCCTCTTTGACAAGTCCTGCAGCGACCG
TGCTATGGAAAGCACAGAATCCCGCCACTACCCTGTCTTCGAGAATCCCAAACAAGGAAAGCTCCGCA
CCAAGGTGGAGAACGGAGAAGGCACAATCCCTGTGGAATCCAGTGACATTGTGCCTACGTGGGATGGC
ATTCGGCTCGGGGAGAGACTCCGTACCATGTCCTGTAGTGACAAAATCCTACGCTGGAACGTGCTGGG
CCTGCAAGGGGCACTGTTGACCCACTTCCTGCAGCCCATTTATCTCAAATCTGTCACATTGGGTTACC
TTTTCAGCCAAGGGCATCTGACCCGTGCTATTTGCTGTCGTGTGACAAGAGATGGGAGTGCATTTGAG
GATGGACTACGACATCCCTTTATTGTCAACCACCCCAAGGTTGGCAGAGTCAGCATATATGATTCCAA
AAGGCAATCCGGGAAGACTAAGGAGACAAGCGTCAACTGGTGTCTGGCTGATGGCTATGACCTGGAGA
TCCTGGACGGTACCAGAGGCACTGTGGATGGGCCACGGAATGAATTGTCCCGGGTCTCCAAAAAGAAC
ATTTTTCTTCTATTTAAGAAGCTCTGCTCCTTCCGTTACCGCAGGGATCTACTGAGACTCTCCTATGG
TGAGGCCAAGAAAGCTGCCCGTGACTACGAGACGGCCAAGAACTACTTCAAAAAAGGCCTGAAGGATA
TGGGCTATGGGAACTGGATTAGCAAACCCCAGGAGGAAAAGAACTTTTATCTCTGCCCAGTATAGGGG
CCCATGTACGATTTAATTATGCGGACGTGATGAGCGAAGTACGATCCCACGACCGAGGCCCGTTTAAA
CCCGCTGATCAGCCTCGACTGTGCCTTCTAGTTGCCAGCCATCTGTTGTTTGCCCCTCCCCCGTGCCT
TCCTTGACCCTGGAAGGTGCCACTCCCACTGTCCTTTCCTAATAAAATGAGGAAATTGCATCGCATTG
TCTGAGTAGGTGTCATTCTATTCTGGGGGGTGGGGTGGGGCAGGACAGCAAGGGGGAGGATTGGGAAG
ACAATAGCAGGCATGCTGGGGATGCGGTGGGCTCTATGGCTTCTGAGGCGGAAAGAACCAGCTGGGGC
TCTAGGGGGTATCCCCACGCGCCCTGTAGCGGCGCATTAAGCGCGGCGGGTGTGGTGGTTACGCGCAG
CGTGACCGCTACACTTGCCAGCGCCCTAGCGCCCGCTCCTTTCGCTTTCTTCCCTTCCTTTCTCGCCA
CGTTCGCCGGTCGATGTACGGGCCAGATATACGCGTTGACATTGATTATTGACTAGTTATTAATAGTA
ATCAATTACGGGGTCATTAGTTCATAGCCCATATATGGAGTTCCGCGTTACATAACTTACGGTAAATG
GCCCGCCTGGCTGACCGCCCAACGACCCCCGCCCATTGACGTCAATAATGACGTATGTTCCCATAGTA
ACGCCAATAGGGACTTTCCATTGACGTCAATGGGTGGAGTATTTACGGTAAACTGCCCACTTGGCAGT
ACATCAAGTGTATCATATGCCAAGTACGCCCCCTATTGACGTCAATGACGGTAAATGGCCCGCCTGGC

ATTATGCCCAGTACATGACCTTATGGGACTTTCCTACTTGGCAGTACATCTACGTATTAGTCATCGCT
ATTACCATGGTGATGCGGTTTTGGCAGTACATCAATGGGCGTGGATAGCGGTTTGACTCACGGGGATT
TCCAAGTCTCCACCCCATTGACGTCAATGGGAGTTTGTTTTGGCACCAAAATCAACGGGACTTTCCAA
AATGTCGTAACAACTCCGCCCCATTGACGCAAATGGGCGGTAGGCGTGTACGGTGGGAGGTCTATATA
AGCAGAGCTCTCCCTATCAGTGATAGAGATCTCCCTATCAGTGATAGAGAGCGTGCATAGGGAACATC
CACCACTTTAGTGAATTGTAGCACGGCTTCAGAAGCGGCCGCCCACCATGGACAAAGACTGCGAAATG
AAGCGCACCACCCTGGATAGCCCTCTGGGCAAGCTGGAACTGTCTGGGTGCGAACAGGGCCTGCACCG
TATCATCTTCCTGGGCAAAGGAACATCTGCCGCCGACGCCGTGGAAGTGCCTGCCCCAGCCGCCGTGC
TGGGCGGACCAGAGCCACTGATGCAGGCCACCGCCTGGCTCAACGCCTACTTTCACCAGCCTGAGGCC
ATCGAGGAGTTCCCTGTGCCAGCCCTGCACCACCCAGTGTTCCAGCAGGAGAGCTTTACCCGCCAGGT
GCTGTGGAAACTGCTGAAAGTGGTGAAGTTCGGAGAGGTCATCAGCTACAGCCACCTGGCCGCCCTGG
CCGGCAATCCCGCCGCCACCGCCGCCGTGAAAACCGCCCTGAGCGGAAATCCCGTGCCCATTCTGATC
CCCTGCCACCGGGTGGTGCAGGGCGACCTGGACGTGGGGGGCTACGAGGGCGGGCTCGCCGTGAAAGA
GTGGCTGCTGGCCCACGAGGGCCACAGACTGGGCAAGCCTGGGCTGGGTCCAGGAGCCGGAGCTAGCG
GCCCAACAGGAATGGCTGCGAGCGATGAAGTTAATCTTATTGAGAGCAGAACAGTGGTTCCTCTCAAT
ACATGGGTTTTAATATCCAACTTCAAAGTAGCCTACAATATCCTTCGTCGCCCTGATGGAACCTTTAA
CCGACACTTAGCTGAGTATCTAGACCGTAAAGTCACTGCAAACGCCAATCCGGTTGATGGGGTTTTCT
CGTTCGATGTCTTGATTGATCGCAGGATCAATCTTCTAAGCAGAGTCTATAGACCAGCTTATGCAGAT
CAAGAGCAACCTCCTAGTATTTTAGATCTGGAGAAGCCTGTTGATGGCGACATTGTCCCTGTTATATT
GTTCTTCCATGGAGGTAGCTTTGCTCATTCTTCTGCAAACAGTGCCATCTACGATACTCTTTGTCGCA
GGCTTGTTGGTTTGTGCAAGTGTGTTGTTGTCTCTGTGAATTATCGGCGTGCACCAGAGAATCCATAC
CCTTGTGCTTATGATGATGGTTGGATTGCTCTTAATTGGGTTAACTCCAGATCTTGGCTTAAATCCAA
GAAAGACTCAAAGGTCCATATTTTCTTGGCTGGTGATAGCTCTGGAGGTAACATCGCGCATAATGTGG
CTTTAAGAGCGGGTGAATCGGGAATTGATGTTTTGGGGAACATTCTGCTGAATCCTATGTTTGGTGGG
AATGAGAGAACGGAGTCTGAGAAAAGTTTGGATGGGAAATACTTTGTGACGGTTAGAGACCGCGATTG
GTACTGGAAAGCGTTTTTACCCGAGGGAGAAGATAGAGAGCATCCAGCGTGTAATCCGTTTAGCCCGA
GAGGGAAAAGCTTAGAAGGAGTGAGTTTCCCCAAGAGTCTTGTGGTTGTCGCGGGTTTGGATTTGATT
AGAGATTGGCAGTTGGCATACGCGGAAGGGCTCAAGAAAGCGGGTCAAGAGGTTAAGCTTATGCATTT
AGAGAAAGCAACTGTTGGGTTTTACCTCTTGCCTAATAACAATCATTTCCATAATGTTATGGATGAGA
TTTCGGCGTTTGTAAACGCGGAATGTTGAATCGATATTTTCAGATATCGTGTTAGTAGGGTTGCACCG
ACGCGCATGTGGATTAGTGCTGTGCCTTCTAGTTGCCAGCCATCTGTTGTTTGCCCCTCCCCCGTGCC
TTCCTTGACCCTGGAAGGTGCCACTCCCACTGTCCTTTCCTAATAAAATGAGGAAATTGCATCGCATT
GTCTGAGTAGGTGTCATTCTATTCTGGGGGGTGGGGTGGGGCAGGACAGCAAGGGGGAGGATTGGGAA
GACAATAGCAGGCATGCTGGGGATGCGGTGGGCTCTATGG

Construct **II**: CMV-enhancer – CMV promoter – $TetO_2$ – GAI_{1-92} – ADAR1 – P2A – $SNAP_f$-tag – GID1A– bGH

GACATTGATTATTGACTAGTTATTAATAGTAATCAATTACGGGGTCATTAGTTCATAGCCCATATATG
GAGTTCCGCGTTACATAACTTACGGTAAATGGCCCGCCTGGCTGACCGCCCAACGACCCCCGCCCATT
GACGTCAATAATGACGTATGTTCCCATAGTAACGCCAATAGGGACTTTCCATTGACGTCAATGGGTGG
AGTATTTACGGTAAACTGCCCACTTGGCAGTACATCAAGTGTATCATATGCCAAGTACGCCCCCTATT
GACGTCAATGACGGTAAATGGCCCGCCTGGCATTATGCCCAGTACATGACCTTATGGGACTTTCCTAC
TTGGCAGTACATCTACGTATTAGTCATCGCTATTACCATGGTGATGCGGTTTTGGCAGTACATCAATG
GGCGTGGATAGCGGTTTGACTCACGGGGATTTCCAAGTCTCCACCCCATTGACGTCAATGGGAGTTTG
TTTTGGCACCAAAATCAACGGGACTTTCCAAAATGTCGTAACAACTCCGCCCCATTGACGCAAATGGG
CGGTAGGCGTGTACGGTGGGAGGTCTATATAAGCAGAGCTCTCCCTATCAGTGATAGAGATCTCCCTA
TCAGTGATAGAGATCGTCGACGAGCTCGTTTAGTGAACCGTCAGATCGCCTGGAGACGCCATCCACGC
TGTTTTGACCTCCATAGAAGACACCGGGACCGATCCAGCCTCCGGACTCTAGCGTTTAAACTTAAGCT
TGGTACCGAGCTCGGATCCCCACCATGAAGAGAGATCATCATCATCATCATCATCAAGATAAGAAGAC
TATGATGATGAATGAAGAAGACGACGGTAACGGCATGGATGAGCTTCTAGCTGTTCTTGGTTACAAGG

TTAGGTCATCCGAAATGGCTGATGTTGCTCAGAAACTTGAGCAGCTTGAAGTTATGATGTCTAATGTT
CAAGAAGACGATCTTTCTCAACTCGCTACTGAGACTGTTCACTATAATCCGGCGGAGCTTTACACGTG
GCTTGATTCTATGCTCACCGACCTTAATCCTGCAGGCGGAGGCGCGCCAGGGTCTGGCGGCGGCAGTA
AGGCAGAACGCATGGGTTTCACAGAGGTAACCCCAGTGACAGGGGCCAGTCTCAGAAGAACTATGCTC
CTCCTCTCAAGGTCCCCAGAAGCACAGCCAAAGACACTCCCTCTCACTGGCAGCACCTTCCATGACCA
GATAGCCATGCTGAGCCACCGGTGCTTCAACACTCTGACTAACAGCTTCCAGCCCTCCTTGCTCGGCC
GCAAGATTCTGGCCGCCATCATTATGAAAAAAGACTCTGAGGACATGGGTGTCGTCGTCAGCTTGGGA
ACAGGGAATCGCTGTGTAAAAGGAGATTCTCTCAGCCTAAAAGGAGAAACTGTCAATGACTGCCATGC
AGAAATAATCTCCCGGAGAGGCTTCATCAGGTTTCTCTACAGTGAGTTAATGAAATACAACTCCCAGA
CTGCGAAGGATAGTATATTTGAACCTGCTAAGGGAGGAGAAAAGCTCCAAATAAAAAAGACTGTGTCA
TTCCATCTGTATATCAGCACTGCTCCGTGTGGAGATGGCGCCCTCTTTGACAAGTCCTGCAGCGACCG
TGCTATGGAAAGCACAGAATCCCGCCACTACCCTGTCTTCGAGAATCCCAAACAAGGAAAGCTCCGCA
CCAAGGTGGAGAACGGAGAAGGCACAATCCCTGTGGAATCCAGTGACATTGTGCCTACGTGGGATGGC
ATTCGGCTCGGGGAGAGACTCCGTACCATGTCCTGTAGTGACAAAATCCTACGCTGGAACGTGCTGGG
CCTGCAAGGGGCACTGTTGACCCACTTCCTGCAGCCCATTTATCTCAAATCTGTCACATTGGGTTACC
TTTTCAGCCAAGGGCATCTGACCCGTGCTATTTGCTGTCGTGTGACAAGAGATGGGAGTGCATTTGAG
GATGGACTACGACATCCCTTTATTGTCAACCACCCCAAGGTTGGCAGAGTCAGCATATATGATTCCAA
AAGGCAATCCGGGAAGACTAAGGAGACAAGCGTCAACTGGTGTCTGGCTGATGGCTATGACCTGGAGA
TCCTGGACGGTACCAGAGGCACTGTGGATGGGCCACGGAATGAATTGTCCCGGGTCTCCAAAAAGAAC
ATTTTTCTTCTATTTAAGAAGCTCTGCTCCTTCCGTTACCGCAGGGATCTACTGAGACTCTCCTATGG
TGAGGCCAAGAAAGCTGCCCGTGACTACGAGACGGCCAAGAACTACTTCAAAAAAGGCCTGAAGGATA
TGGGCTATGGGAACTGGATTAGCAAACCCCAGGAGGAAAAGAACTTTTATCTCTGCCCAGTAGGCGGC
CGCGGAAGCGGAGCTACTAACTTCAGCCTGCTGAAGCAGGCTGGAGACGTGGAGGAGAACCCTGGACC
TCTCGAGATGGACAAAGACTGCGAAATGAAGCGCACCACCCTGGATAGCCCTCTGGGCAAGCTGGAAC
TGTCTGGGTGCGAACAGGGCCTGCACCGTATCATCTTCCTGGGCAAAGGAACATCTGCCGCCGACGCC
GTGGAAGTGCCTGCCCCAGCCGCCGTGCTGGGCGGACCAGAGCCACTGATGCAGGCCACCGCCTGGCT
CAACGCCTACTTTCACCAGCCTGAGGCCATCGAGGAGTTCCCTGTGCCAGCCCTGCACCACCCAGTGT
TCCAGCAGGAGAGCTTTACCCGCCAGGTGCTGTGGAAACTGCTGAAAGTGGTGAAGTTCGGAGAGGTC
ATCAGCTACAGCCACCTGGCCGCCCTGGCCGGCAATCCCGCCGCCACCGCCGCCGTGAAAACCGCCCT
GAGCGGAAATCCCGTGCCCATTCTGATCCCCTGCCACCGGGTGGTGCAGGGCGACCTGGACGTGGGGG
GCTACGAGGGCGGGCTCGCCGTGAAAGAGTGGCTGCTGGCCCACGAGGGCCACAGACTGGGCAAGCCT
GGGCTGGGTCCAGGAGCCGGAGCTAGCGGCCCAACAGGAATGGCTGCGAGCGATGAAGTTAATCTTAT
TGAGAGCAGAACAGTGGTTCCTCTCAATACATGGGTTTTAATATCCAACTTCAAAGTAGCCTACAATA
TCCTTCGTCGCCCTGATGGAACCTTTAACCGACACTTAGCTGAGTATCTAGACCGTAAAGTCACTGCA
AACGCCAATCCGGTTGATGGGGTTTTCTCGTTCGATGTCTTGATTGATCGCAGGATCAATCTTCTAAG
CAGAGTCTATAGACCAGCTTATGCAGATCAAGAGCAACCTCCTAGTATTTTAGATCTGGAGAAGCCTG
TTGATGGCGACATTGTCCCTGTTATATTGTTCTTCCATGGAGGTAGCTTTGCTCATTCTTCTGCAAAC
AGTGCCATCTACGATACTCTTTGTCGCAGGCTTGTTGGTTTGTGCAAGTGTGTTGTTGTCTCTGTGAA
TTATCGGCGTGCACCAGAGAATCCATACCCTTGTGCTTATGATGATGGTTGGATTGCTCTTAATTGGG
TTAACTCCAGATCTTGGCTTAAATCCAAGAAAGACTCAAAGGTCCATATTTTCTTGGCTGGTGATAGC
TCTGGAGGTAACATCGCGCATAATGTGGCTTTAAGAGCGGGTGAATCGGGAATTGATGTTTTGGGGAA
CATTCTGCTGAATCCTATGTTTGGTGGGAATGAGAGAACGGAGTCTGAGAAAAGTTTGGATGGGAAAT
ACTTTGTGACGGTTAGAGACCGCGATTGGTACTGGAAAGCGTTTTTACCCGAGGGAGAAGATAGAGAG
CATCCAGCGTGTAATCCGTTTAGCCCGAGAGGGAAAAGCTTAGAAGGAGTGAGTTTCCCCAAGAGTCT
TGTGGTTGTCGCGGGTTTGGATTTGATTAGAGATTGGCAGTTGGCATACGCGGAAGGGCTCAAGAAAG
CGGGTCAAGAGGTTAAGCTTATGCATTTAGAGAAAGCAACTGTTGGGTTTTACCTCTTGCCTAATAAC
AATCATTTCCATAATGTTATGGATGAGATTTCGGCGTTTGTAAACGCGGAATGTTGATTAATTAAGTT
TAAACCCGCTGATCAGCCTCGACTGTGCCTTCTAGTTGCCAGCCATCTGTTGTTTGCCCCTCCCCCGT
GCCTTCCTTGACCCTGGAAGGTGCCACTCCCACTGTCCTTTCCTAATAAAATGAGGAAATTGCATCGC
ATTGTCTGAGTAGGTGTCATTCTATTCTGGGGGGTGGGGTGGGGCAGGACAGCAAGGGGGAGGATTGG
GAAGACAATAGCAGGCATGCTGGGGATGCGGTGGGCTCTATGG

Construct **III**: CMV-enhancer – CMV promoter – $TetO_2$ – GAI_{1-92} – ADAR1Q – bGH – CMV-enhancer – CMV promoter – $TetO_2$ – $SNAP_f$-tag – GID1A – bGH

GACATTGATTATTGACTAGTTATTAATAGTAATCAATTACGGGGTCATTAGTTCATAGCCCATATATG
GAGTTCCGCGTTACATAACTTACGGTAAATGGCCCGCCTGGCTGACCGCCCAACGACCCCCGCCCATT
GACGTCAATAATGACGTATGTTCCCATAGTAACGCCAATAGGGACTTTCCATTGACGTCAATGGGTGG
AGTATTTACGGTAAACTGCCCACTTGGCAGTACATCAAGTGTATCATATGCCAAGTACGCCCCCTATT
GACGTCAATGACGGTAAATGGCCCGCCTGGCATTATGCCCAGTACATGACCTTATGGGACTTTCCTAC
TTGGCAGTACATCTACGTATTAGTCATCGCTATTACCATGGTGATGCGGTTTTGGCAGTACATCAATG
GGCGTGGATAGCGGTTTGACTCACGGGGATTTCCAAGTCTCCACCCCATTGACGTCAATGGGAGTTTG
TTTTGGCACCAAAATCAACGGGACTTTCCAAAATGTCGTAACAACTCCGCCCCATTGACGCAAATGGG
CGGTAGGCGTGTACGGTGGGAGGTCTATATAAGCAGAGCTCTCCCTATCAGTGATAGAGATCTCCCTA
TCAGTGATAGAGATCGTCGACGAGCTCGTTTAGTGAACCGTCAGATCGCCTGGAGACGCCATCCACGC
TGTTTTGACCTCCATAGAAGACACCGGGACCGATCCAGCCTCCGGACTCTAGCGTTTAAACTTAAGCT
TGGTACCGAGCTCGGATCCCCACCATGAAGAGAGATCATCATCATCATCATCATCAAGATAAGAAGAC
TATGATGATGAATGAAGAAGACGACGGTAACGGCATGGATGAGCTTCTAGCTGTTCTTGGTTACAAGG
TTAGGTCATCCGAAATGGCTGATGTTGCTCAGAAACTTGAGCAGCTTGAAGTTATGATGTCTAATGTT
CAAGAAGACGATCTTTCTCAACTCGCTACTGAGACTGTTCACTATAATCCGGCGGAGCTTTACACGTG
GCTTGATTCTATGCTCACCGACCTTAATCCTGCAGGCGGAGGCGCGCCAGGGTCTGGCGGCGGCAGTA
AGGCAGAACGCATGGGTTTCACAGAGGTAACCCCAGTGACAGGGGCCAGTCTCAGAAGAACTATGCTC
CTCCTCTCAAGGTCCCCAGAAGCACAGCCAAAGACACTCCCTCTCACTGGCAGCACCTTCCATGACCA
GATAGCCATGCTGAGCCACCGGTGCTTCAACACTCTGACTAACAGCTTCCAGCCCTCCTTGCTCGGCC
GCAAGATTCTGGCCGCCATCATTATGAAAAAAGACTCTGAGGACATGGGTGTCGTCGTCAGCTTGGGA
ACAGGGAATCGCTGTGTAAAAGGAGATTCTCTCAGCCTAAAAGGAGAAACTGTCAATGACTGCCATGC
AGAAATAATCTCCCGGAGAGGCTTCATCAGGTTTCTCTACAGTGAGTTAATGAAATACAACTCCCAGA
CTGCGAAGGATAGTATATTTGAACCTGCTAAGGGAGGAGAAAAGCTCCAAATAAAAAAGACTGTGTCA
TTCCATCTGTATATCAGCACTGCTCCGTGTGGAGATGGCGCCCTCTTTGACAAGTCCTGCAGCGACCG
TGCTATGGAAAGCACAGAATCCCGCCACTACCCTGTCTTCGAGAATCCCAAACAAGGAAAGCTCCGCA
CCAAGGTGGAGAACGGACAAGGCACAATCCCTGTGGAATCCAGTGACATTGTGCCTACGTGGGATGGC
ATTCGGCTCGGGGAGAGACTCCGTACCATGTCCTGTAGTGACAAAATCCTACGCTGGAACGTGCTGGG
CCTGCAAGGGGCACTGTTGACCCACTTCCTGCAGCCCATTTATCTCAAATCTGTCACATTGGGTTACC
TTTTCAGCCAAGGGCATCTGACCCGTGCTATTTGCTGTCGTGTGACAAGAGATGGGAGTGCATTTGAG
GATGGACTACGACATCCCTTTATTGTCAACCACCCCAAGGTTGGCAGAGTCAGCATATATGATTCCAA
AAGGCAATCCGGGAAGACTAAGGAGACAAGCGTCAACTGGTGTCTGGCTGATGGCTATGACCTGGAGA
TCCTGGACGGTACCAGAGGCACTGTGGATGGGCCACGGAATGAATTGTCCCGGGTCTCCAAAAAGAAC
ATTTTTCTTCTATTTAAGAAGCTCTGCTCCTTCCGTTACCGCAGGGATCTACTGAGACTCTCCTATGG
TGAGGCCAAGAAAGCTGCCCGTGACTACGAGACGGCCAAGAACTACTTCAAAAAAGGCCTGAAGGATA
TGGGCTATGGGAACTGGATTAGCAAACCCCAGGAGGAAAAGAACTTTTATCTCTGCCCAGTATGAGGG
CCCATGTACGATTTAATTATGCGGACGTGATGAGCGAAGTACGATCCCACGACCGAGGCCCGTTTAAA
CCCGCTGATCAGCCTCGACTGTGCCTTCTAGTTGCCAGCCATCTGTTGTTTGCCCCTCCCCCGTGCCT
TCCTTGACCCTGGAAGGTGCCACTCCCACTGTCCTTTCCTAATAAAATGAGGAAATTGCATCGCATTG
TCTGAGTAGGTGTCATTCTATTCTGGGGGGTGGGGTGGGGCAGGACAGCAAGGGGGAGGATTGGGAAG
ACAATAGCAGGCATGCTGGGGATGCGGTGGGCTCTATGGCTTCTGAGGCGGAAAGAACCAGCTGGGGC
TCTAGGGGGTATCCCCACGCGCCCTGTAGCGGCGCATTAAGCGCGGCGGGTGTGGTGGTTACGCGCAG
CGTGACCGCTACACTTGCCAGCGCCCTAGCGCCCGCTCCTTTCGCTTTCTTCCCTTCCTTTCTCGCCA
CGTTCGCCGGTCGATGTACGGGCCAGATATACGCGTTGACATTGATTATTGACTAGTTATTAATAGTA
ATCAATTACGGGGTCATTAGTTCATAGCCCATATATGGAGTTCCGCGTTACATAACTTACGGTAAATG
GCCCGCCTGGCTGACCGCCCAACGACCCCCGCCCATTGACGTCAATAATGACGTATGTTCCCATAGTA
ACGCCAATAGGGACTTTCCATTGACGTCAATGGGTGGAGTATTTACGGTAAACTGCCCACTTGGCAGT
ACATCAAGTGTATCATATGCCAAGTACGCCCCCTATTGACGTCAATGACGGTAAATGGCCCGCCTGGC
ATTATGCCCAGTACATGACCTTATGGGACTTTCCTACTTGGCAGTACATCTACGTATTAGTCATCGCT
ATTACCATGGTGATGCGGTTTTGGCAGTACATCAATGGGCGTGGATAGCGGTTTGACTCACGGGGATT
TCCAAGTCTCCACCCCATTGACGTCAATGGGAGTTTGTTTTGGCACCAAAATCAACGGGACTTTCCAA

AATGTCGTAACAACTCCGCCCCATTGACGCAAATGGGCGGTAGGCGTGTACGGTGGGAGGTCTATATA
AGCAGAGCTCTCCCTATCAGTGATAGAGATCTCCCTATCAGTGATAGAGAGCGTGCATAGGGAACATC
CACCACTTTAGTGAATTGTAGCACGGCTTCAGAAGCGGCCGCCCACCATGGACAAAGACTGCGAAATG
AAGCGCACCACCCTGGATAGCCCTCTGGGCAAGCTGGAACTGTCTGGGTGCGAACAGGGCCTGCACCG
TATCATCTTCCTGGGCAAAGGAACATCTGCCGCCGACGCCGTGGAAGTGCCTGCCCCAGCCGCCGTGC
TGGGCGGACCAGAGCCACTGATGCAGGCCACCGCCTGGCTCAACGCCTACTTTCACCAGCCTGAGGCC
ATCGAGGAGTTCCCTGTGCCAGCCCTGCACCACCCAGTGTTCCAGCAGGAGAGCTTTACCCGCCAGGT
GCTGTGGAAACTGCTGAAAGTGGTGAAGTTCGGAGAGGTCATCAGCTACAGCCACCTGGCCGCCCTGG
CCGGCAATCCCGCCGCCACCGCCGCCGTGAAAACCGCCCTGAGCGGAAATCCCGTGCCCATTCTGATC
CCCTGCCACCGGGTGGTGCAGGGCGACCTGGACGTGGGGGGCTACGAGGGCGGGCTCGCCGTGAAAGA
GTGGCTGCTGGCCCACGAGGGCCACAGACTGGGCAAGCCTGGGCTGGGTCCAGGAGCCGGAGCTAGCG
GCCCAACAGGAATGGCTGCGAGCGATGAAGTTAATCTTATTGAGAGCAGAACAGTGGTTCCTCTCAAT
ACATGGGTTTTAATATCCAACTTCAAAGTAGCCTACAATATCCTTCGTCGCCCTGATGGAACCTTTAA
CCGACACTTAGCTGAGTATCTAGACCGTAAAGTCACTGCAAACGCCAATCCGGTTGATGGGGTTTTCT
CGTTCGATGTCTTGATTGATCGCAGGATCAATCTTCTAAGCAGAGTCTATAGACCAGCTTATGCAGAT
CAAGAGCAACCTCCTAGTATTTTAGATCTGGAGAAGCCTGTTGATGGCGACATTGTCCCTGTTATATT
GTTCTTCCATGGAGGTAGCTTTGCTCATTCTTCTGCAAACAGTGCCATCTACGATACTCTTTGTCGCA
GGCTTGTTGGTTTGTGCAAGTGTGTTGTTGTCTCTGTGAATTATCGGCGTGCACCAGAGAATCCATAC
CCTTGTGCTTATGATGATGGTTGGATTGCTCTTAATTGGGTTAACTCCAGATCTTGGCTTAAATCCAA
GAAAGACTCAAAGGTCCATATTTTCTTGGCTGGTGATAGCTCTGGAGGTAACATCGCGCATAATGTGG
CTTTAAGAGCGGGTGAATCGGGAATTGATGTTTTGGGGAACATTCTGCTGAATCCTATGTTTGGTGGG
AATGAGAGAACGGAGTCTGAGAAAAGTTTGGATGGGAAATACTTTGTGACGGTTAGAGACCGCGATTG
GTACTGGAAAGCGTTTTTACCCGAGGGAGAAGATAGAGAGCATCCAGCGTGTAATCCGTTTAGCCCGA
GAGGGAAAAGCTTAGAAGGAGTGAGTTTCCCCAAGAGTCTTGTGGTTGTCGCGGGTTTGGATTTGATT
AGAGATTGGCAGTTGGCATACGCGGAAGGGCTCAAGAAAGCGGGTCAAGAGGTTAAGCTTATGCATTT
AGAGAAAGCAACTGTTGGGTTTTACCTCTTGCCTAATAACAATCATTTCCATAATGTTATGGATGAGA
TTTCGGCGTTTGTAAACGCGGAATGTTGAATCGATATTTTCAGATATCGTGTTAGTAGGGTTGCACCG
ACGCGCATGTGGATTAGTGCTGTGCCTTCTAGTTGCCAGCCATCTGTTGTTTGCCCCTCCCCCGTGCC
TTCCTTGACCCTGGAAGGTGCCACTCCCACTGTCCTTTCCTAATAAAATGAGGAAATTGCATCGCATT
GTCTGAGTAGGTGTCATTCTATTCTGGGGGGTGGGGTGGGGCAGGACAGCAAGGGGGAGGATTGGGAA
GACAATAGCAGGCATGCTGGGGATGCGGTGGGCTCTATGG

Construct **IV**: CMV-enhancer – CMV promoter – $TetO_2$ – $GAI_{1\text{-}92}$ – ADAR1Q – P2A – $SNAP_f$-tag – GID1A– bGH

GACATTGATTATTGACTAGTTATTAATAGTAATCAATTACGGGGTCATTAGTTCATAGCCCATATATG
GAGTTCCGCGTTACATAACTTACGGTAAATGGCCCGCCTGGCTGACCGCCCAACGACCCCCGCCCATT
GACGTCAATAATGACGTATGTTCCCATAGTAACGCCAATAGGGACTTTCCATTGACGTCAATGGGTGG
AGTATTTACGGTAAACTGCCCACTTGGCAGTACATCAAGTGTATCATATGCCAAGTACGCCCCCTATT
GACGTCAATGACGGTAAATGGCCCGCCTGGCATTATGCCCAGTACATGACCTTATGGGACTTTCCTAC
TTGGCAGTACATCTACGTATTAGTCATCGCTATTACCATGGTGATGCGGTTTTGGCAGTACATCAATG
GGCGTGGATAGCGGTTTGACTCACGGGGATTTCCAAGTCTCCACCCCATTGACGTCAATGGGAGTTTG
TTTTGGCACCAAAATCAACGGGACTTTCCAAAATGTCGTAACAACTCCGCCCCATTGACGCAAATGGG
CGGTAGGCGTGTACGGTGGGAGGTCTATATAAGCAGAGCTCTCCCTATCAGTGATAGAGATCTCCCTA
TCAGTGATAGAGATCGTCGACGAGCTCGTTTAGTGAACCGTCAGATCGCCTGGAGACGCCATCCACGC
TGTTTTGACCTCCATAGAAGACACCGGGACCGATCCAGCCTCCGGACTCTAGCGTTTAAACTTAAGCT
TGGTACCGAGCTCGGATCCCCACCATGAAGAGAGATCATCATCATCATCATCATCAAGATAAGAAGAC
TATGATGATGAATGAAGAAGACGACGGTAACGGCATGGATGAGCTTCTAGCTGTTCTTGGTTACAAGG
TTAGGTCATCCGAAATGGCTGATGTTGCTCAGAAACTTGAGCAGCTTGAAGTTATGATGTCTAATGTT
CAAGAAGACGATCTTTCTCAACTCGCTACTGAGACTGTTCACTATAATCCGGCGGAGCTTTACACGTG
GCTTGATTCTATGCTCACCGACCTTAATCCTGCAGGCGGAGGCGCGCCAGGGTCTGGCGGCGGCAGTA

AGGCAGAACGCATGGGTTTCACAGAGGTAACCCCAGTGACAGGGGCCAGTCTCAGAAGAACTATGCTC
CTCCTCTCAAGGTCCCCAGAAGCACAGCCAAAGACACTCCCTCTCACTGGCAGCACCTTCCATGACCA
GATAGCCATGCTGAGCCACCGGTGCTTCAACACTCTGACTAACAGCTTCCAGCCCTCCTTGCTCGGCC
GCAAGATTCTGGCCGCCATCATTATGAAAAAAGACTCTGAGGACATGGGTGTCGTCGTCAGCTTGGGA
ACAGGGAATCGCTGTGTAAAAGGAGATTCTCTCAGCCTAAAAGGAGAAACTGTCAATGACTGCCATGC
AGAAATAATCTCCCGGAGAGGCTTCATCAGGTTTCTCTACAGTGAGTTAATGAAATACAACTCCCAGA
CTGCGAAGGATAGTATATTTGAACCTGCTAAGGGAGGAGAAAAGCTCCAAATAAAAAAGACTGTGTCA
TTCCATCTGTATATCAGCACTGCTCCGTGTGGAGATGGCGCCCTCTTTGACAAGTCCTGCAGCGACCG
TGCTATGGAAAGCACAGAATCCCGCCACTACCCTGTCTTCGAGAATCCCAAACAAGGAAAGCTCCGCA
CCAAGGTGGAGAACGGACAAGGCACAATCCCTGTGGAATCCAGTGACATTGTGCCTACGTGGGATGGC
ATTCGGCTCGGGGAGAGACTCCGTACCATGTCCTGTAGTGACAAAATCCTACGCTGGAACGTGCTGGG
CCTGCAAGGGGCACTGTTGACCCACTTCCTGCAGCCCATTTATCTCAAATCTGTCACATTGGGTTACC
TTTTCAGCCAAGGGCATCTGACCCGTGCTATTTGCTGTCGTGTGACAAGAGATGGGAGTGCATTTGAG
GATGGACTACGACATCCCTTTATTGTCAACCACCCCAAGGTTGGCAGAGTCAGCATATATGATTCCAA
AAGGCAATCCGGGAAGACTAAGGAGACAAGCGTCAACTGGTGTCTGGCTGATGGCTATGACCTGGAGA
TCCTGGACGGTACCAGAGGCACTGTGGATGGGCCACGGAATGAATTGTCCCGGGTCTCCAAAAAGAAC
ATTTTTCTTCTATTTAAGAAGCTCTGCTCCTTCCGTTACCGCAGGGATCTACTGAGACTCTCCTATGG
TGAGGCCAAGAAAGCTGCCCGTGACTACGAGACGGCCAAGAACTACTTCAAAAAAGGCCTGAAGGATA
TGGGCTATGGGAACTGGATTAGCAAACCCCAGGAGGAAAAGAACTTTTATCTCTGCCCAGTAGGCGGC
CGCGGAAGCGGAGCTACTAACTTCAGCCTGCTGAAGCAGGCTGGAGACGTGGAGGAGAACCCTGGACC
TCTCGAGATGGACAAAGACTGCGAAATGAAGCGCACCACCCTGGATAGCCCTCTGGGCAAGCTGGAAC
TGTCTGGGTGCGAACAGGGCCTGCACCGTATCATCTTCCTGGGCAAAGGAACATCTGCCGCCGACGCC
GTGGAAGTGCCTGCCCCAGCCGCCGTGCTGGGCGGACCAGAGCCACTGATGCAGGCCACCGCCTGGCT
CAACGCCTACTTTCACCAGCCTGAGGCCATCGAGGAGTTCCCTGTGCCAGCCCTGCACCACCCAGTGT
TCCAGCAGGAGAGCTTTACCCGCCAGGTGCTGTGGAAACTGCTGAAAGTGGTGAAGTTCGGAGAGGTC
ATCAGCTACAGCCACCTGGCCGCCCTGGCCGGCAATCCCGCCGCCACCGCCGCCGTGAAAACCGCCCT
GAGCGGAAATCCCGTGCCCATTCTGATCCCCTGCCACCGGGTGGTGCAGGGCGACCTGGACGTGGGGG
GCTACGAGGGCGGGCTCGCCGTGAAAGAGTGGCTGCTGGCCCACGAGGGCCACAGACTGGGCAAGCCT
GGGCTGGGTCCAGGAGCCGGAGCTAGCGGCCCAACAGGAATGGCTGCGAGCGATGAAGTTAATCTTAT
TGAGAGCAGAACAGTGGTTCCTCTCAATACATGGGTTTTAATATCCAACTTCAAAGTAGCCTACAATA
TCCTTCGTCGCCCTGATGGAACCTTTAACCGACACTTAGCTGAGTATCTAGACCGTAAAGTCACTGCA
AACGCCAATCCGGTTGATGGGGTTTTCTCGTTCGATGTCTTGATTGATCGCAGGATCAATCTTCTAAG
CAGAGTCTATAGACCAGCTTATGCAGATCAAGAGCAACCTCCTAGTATTTTAGATCTGGAGAAGCCTG
TTGATGGCGACATTGTCCCTGTTATATTGTTCTTCCATGGAGGTAGCTTTGCTCATTCTTCTGCAAAC
AGTGCCATCTACGATACTCTTTGTCGCAGGCTTGTTGGTTTGTGCAAGTGTGTTGTTGTCTCTGTGAA
TTATCGGCGTGCACCAGAGAATCCATACCCTTGTGCTTATGATGATGGTTGGATTGCTCTTAATTGGG
TTAACTCCAGATCTTGGCTTAAATCCAAGAAAGACTCAAAGGTCCATATTTTCTTGGCTGGTGATAGC
TCTGGAGGTAACATCGCGCATAATGTGGCTTTAAGAGCGGGTGAATCGGGAATTGATGTTTTGGGGAA
CATTCTGCTGAATCCTATGTTTGGTGGGAATGAGAGAACGGAGTCTGAGAAAAGTTTGGATGGGAAAT
ACTTTGTGACGGTTAGAGACCGCGATTGGTACTGGAAAGCGTTTTTACCCGAGGGAGAAGATAGAGAG
CATCCAGCGTGTAATCCGTTTAGCCCGAGAGGGAAAAGCTTAGAAGGAGTGAGTTTCCCCAAGAGTCT
TGTGGTTGTCGCGGGTTTGGATTTGATTAGAGATTGGCAGTTGGCATACGCGGAAGGGCTCAAGAAAG
CGGGTCAAGAGGTTAAGCTTATGCATTTAGAGAAAGCAACTGTTGGGTTTTACCTCTTGCCTAATAAC
AATCATTTCCATAATGTTATGGATGAGATTTCGGCGTTTGTAAACGCGGAATGTTGATTAATTAAGTT
TAAACCCGCTGATCAGCCTCGACTGTGCCTTCTAGTTGCCAGCCATCTGTTGTTTGCCCCTCCCCCGT
GCCTTCCTTGACCCTGGAAGGTGCCACTCCCACTGTCCTTTCCTAATAAAATGAGGAAATTGCATCGC
ATTGTCTGAGTAGGTGTCATTCTATTCTGGGGGGTGGGGTGGGGCAGGACAGCAAGGGGGAGGATTGG
GAAGACAATAGCAGGCATGCTGGGGATGCGGTGGGCTCTATGG

A.2.3 Publication 3 (published)

Npom-Protected NONOate Enables Light-Triggered NO/cGMP Signalling in Primary Vascular Smooth Muscle Cells

Anna S. Stroppel, Michael Paolillo, Thomas Ziegler, Robert Feil, Thorsten Stafforst, *ChemBioChem* **2018**, *19*, 1312 – 1318.

Highlighted as "Very important paper".

Highlighted in *Chemistry Views*.

ChemPubSoc Europe

DOI: 10.1002/cbic.201700683

CHEMBIOCHEM Full Papers

VIP *Very Important Paper*

SPECIAL ISSUE

Npom-Protected NONOate Enables Light-Triggered NO/cGMP Signalling in Primary Vascular Smooth Muscle Cells

Anna S. Stroppel,[a] Michael Paolillo,[b] Thomas Ziegler,[c] Robert Feil,[b] and Thorsten Stafforst*[a]

Diazeniumdiolates (NONOates) are a class of nitric-oxide-releasing substances widely used in studies of NO/cGMP signalling. Because spatiotemporal control is highly desirable for such purposes, we have synthesised a new Npom-caged pyrrolidine NONOate. A kinetic analysis together with a Griess assay showed the photodependent release of NO with high quantum yield (UV light). In primary vascular smooth muscle cells (VSMCs), our compound was reliably able to induce fast increases in cGMP, as measured with a genetically encoded FRET-based cGMP sensor and further validated by the phosphorylation of the downstream target vasodilator-stimulated phosphoprotein (VASP). Thanks to their facile synthesis, good decaging kinetics and capability to activate cGMP signalling in a fast and efficient manner, Npom-protected NONOates allow for improved spatiotemporal control of NO/cGMP signalling.

Introduction

Nitric oxide (NO) is the subject of numerous studies, due to its role in regulating several (patho)physiological processes, including vasodilation, neurotransmission, hormone secretion and platelet aggregation, among others.[1,2] NO is a potent drug with unique pharmacokinetics. It is small, gaseous and uncharged, and can thus freely diffuse into tissue. However, because of its short half-life (seconds) its effects are restricted locally.[3] Consequently, NO-releasing drugs such as glyceryl trinitrate are in clinical use and under further development.[4]

Many (patho)physiological effects of NO are related to the elevation of cGMP levels by direct activation of NO-sensitive soluble guanylate cyclase (sGC). Activation of the NO/cGMP cascade in blood vessels results in acute vasodilation and might also contribute to vascular proliferative disorders such as atherosclerosis and restenosis.[5]

Diazeniumdiolates (also called NONOates) are a particularly interesting class of NO-releasing substances widely used to study NO- and cGMP-related processes.[6–9] They are stable enough to have long shelf-lives but can be designed to release NO with half-lives ranging from 3 s to 20 h under physiological conditions.[10] NONOates have been further modified, to improve, for example, cellular uptake, which results in more potent prodrugs.[11] In this respect β-Gal-NONOate is notable, because it is readily taken up by the cell and releases NO in a β-galactosidase-dependent manner, allowing the tissue-specific activation of the NO/cGMP cascade in cells.[12]

To aid study of cGMP biology, mouse models that express genetically encoded FRET-based sensors for cGMP visualisation have been created.[13] These biosensors are well characterised and allow monitoring of cGMP concentration changes in intact cells in real time, in response to, for example, NO-releasing drugs or other drugs that interfere with cGMP metabolism, such as phosphodiesterase (PDE) inhibitors.[13]

Here we describe the synthesis of a new α-methyl-6-nitropiperonyloxymethyl-photocaged (Npom-photocaged) NONOate based on pyrrolidine and characterise its ability to photostimulate cGMP signalling in primary vascular smooth muscle cells (VSMCs).

Results and Discussion

The photocaged NONOate **1** was synthesised from pyrrolidine-based NONOate **2** and Npom chloride (**3**) in good yields (Scheme 1). The starting materials **2** and **3** are accessible from commercially available compounds in one and two steps, respectively, by literature protocols.[10,14]

We characterised the photolytic decaging of **1** in phosphate buffer at pH 7.4 by means of HPLC (Figure 1 A). Irradiation was performed in the presence of air at 365 nm with a standard transilluminator. The peak area of **1** was plotted against the irradiation time to extract a first-order exponential decay rate of (0.39 ± 0.02) min, which corresponds to a quantum yield of ≈0.66 (Figure 1 B). The HPLC analysis showed the formation of one new main product that was assigned as nitroso acetophe-

[a] *A. S. Stroppel, Prof. Dr. T. Stafforst*
Interfaculty Institute of Biochemistry, University of Tübingen
Auf der Morgenstelle 15, 72076 Tübingen (Germany)
E-mail: thorsten.stafforst@uni-tuebingen.de

[b] *M. Paolillo, Prof. Dr. R. Feil*
Interfaculty Institute of Biochemistry, University of Tübingen
Hoppe-Seyler-Strasse 4, 72076 Tübingen (Germany)

[c] *Prof. Dr. T. Ziegler*
Institute of Organic Chemistry, University of Tübingen
Auf der Morgenstelle 18, 72076 Tübingen (Germany)

Supporting information and the ORCID identification numbers for the authors of this article can be found under https://doi.org/10.1002/cbic.201700683.

This article is part of a Special Issue on the Optical Control of Biological Processes.

ChemPubSoc Europe

CHEMBIOCHEM Full Papers

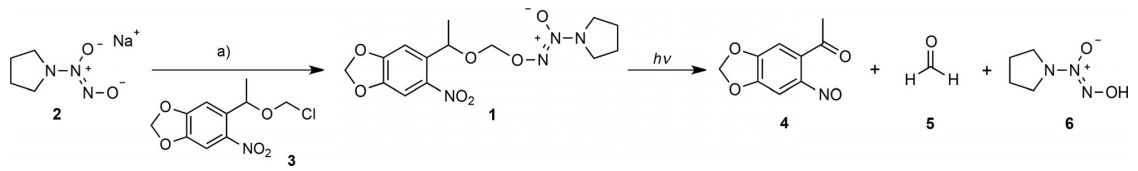

Scheme 1. Synthesis and expected photolysis route of Npom-protected NONOate **1**. Nitroso acetophenone **4**, formaldehyde (**5**), and deprotected NONOate **6** would be expected to be formed upon irradiation with UV light, with **6** being known to release NO with a half-life of 3 s at 37 °C and pH 7.4.[15] a) DBU, **3**, DMF, RT, 3 h (78 %).

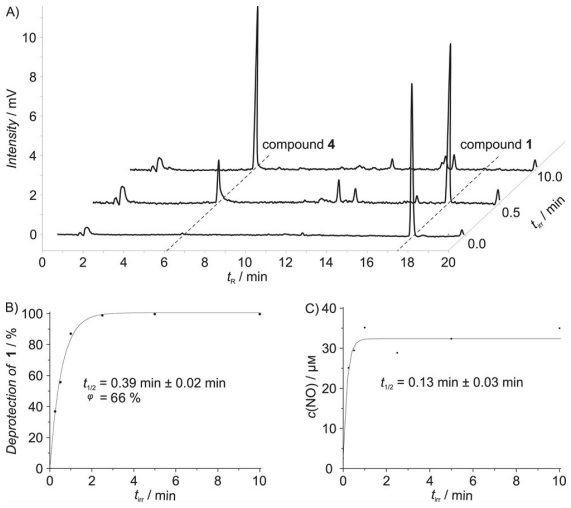

Figure 1. Photolytic decaging properties of NONOate **1**. A) Time course of HPLC traces (365 nm detection) of **1** after different irradiation times t_{irr} (with 365 nm light). Starting material **1** has a retention time $t_R = 17.50$ min; the main product nitroso acetophenone **4** has a $t_R = 6.10$ min and is gradually formed upon irradiation. B) The decay of starting material **1** was fitted to a first-order exponential fit by using the areas of HPLC traces shown in (A). Half-life ($t_{1/2}$) and quantum yield (φ) were determined as described in the Experimental Section. C) The photostimulated release of NO was similarly fitted to a first-order exponential function. NO was formed by UV irradiation (365 nm) of NONOate **1** (100 µM) for different irradiation times (t_{irr}). NO concentrations were determined by using the Griess assay as described in the Experimental Section.

none **4** by coinjection of an illuminated reference compound (^{N9}Npom-BG-TFA) known to release compound **4**.[16] We were unable to detect any hydrolysis in the dark when NONOate **1** was kept in physiological buffer at pH 7.4 at room temperature for seven days, thus demonstrating the inertness desirable for a caged compound.

Formation of NO cannot be followed by HPLC, and so we analysed the photodependent NO release from NONOate **1** (100 µM) by using the Griess assay (Figure 1 C). As expected, there was no detectable NO release in the dark. Upon irradiation, however, there was a rapid rise in NO to concentrations up to 30 µM, though with high variance. Unexpectedly, with 30 µM NO only one sixth of the maximal theoretical NO concentration was obtained.[17] However, control assays starting from 100 µM diethylamine NONOate diethylammonium salt (DEA/NO) or 100 µM unprotected NONOate **2** both also yielded lower values than expected (i.e., only 100 µM, Scheme S2 in the Supporting Information), and again produced high variance (Tables S1 and S2). The high variance might be a consequence of the long waiting time (20 min) between irradiation and assay treatment, and in the case of compound **1** could also be a result of its limited solubility in the Griess assay reaction buffer. Nevertheless, NO was clearly released, and the irradiation kinetics were in accordance with the decaging kinetics of NONOate **1**. The promising decaging characteristics of NONOate **1** in terms of quantum yield, hydrolytic stability in the dark and the clear release of NO in the presence of UV light encouraged us to test the compound in primary VSMCs obtained from transgenic mice that express the FRET-based cGMP sensor cGi500 (Scheme 2).

Primary VSMCs were isolated from aortae of cGi500 sensor mice and examined in superfusion imaging chambers, as described previously.[13] This setup allows for the continuous perfusion of cells and the successive application of various sets of conditions (such as different amounts of **1**, different substan-

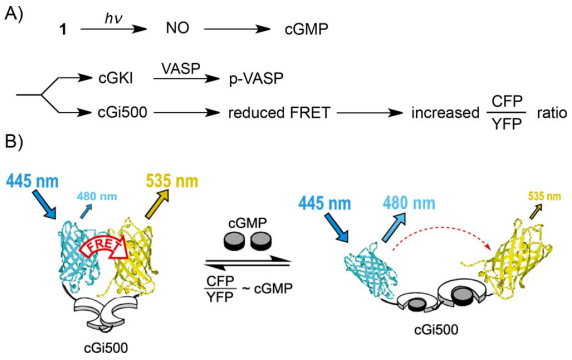

Scheme 2. A) NO-dependent signalling leads to the phosphorylation of vasodilator-stimulated phosphoprotein (VASP). In VSMCs obtained from cGi500 transgenic mice, the change in concentration of the signalling molecule cGMP can be monitored in real time by measuring FRET changes by fluorescence microscopy. Upon UV irradiation of Npom-protected NONOate **1** NO is released, and this stimulates soluble guanylate cyclase (sGC) to produce cGMP from GTP. cGMP either activates cGMP-dependent protein kinase type I (cGKI), resulting in VASP phosphorylation, or binds to the cGi500 sensor, resulting in an increased CFP/YFP ratio. B) The cGi500 sensor consists of the tandem cGMP binding sites of the bovine cGKI (white) flanked by CFP and YFP,[18] adapted from ref. [13]. In the absence of cGMP, efficient FRET from CFP to YFP takes place after CFP excitation at 445 nm, resulting in YFP co-emission at 535 nm. Binding of cGMP leads to a conformational change increasing the distance between CFP and YFP, which results in a reduced FRET efficiency.

ChemPubSoc Europe

CHEMBIOCHEM Full Papers

ces etc.) while the cGMP responses of the cells are simultaneously examined live under the fluorescence microscope. In one field of view, the fluorescence of ≈20 VSMCs was typically recorded for the fluorescence of cyan fluorescent protein (CFP) and yellow fluorescent protein (YFP) over the whole experiment. Each experiment started with a negative control in which cells were irradiated in the absence of any compound to make sure that FRET changes were not caused by photobleaching of the FRET sensor or direct photoinduced cGMP formation. Aside from some rare and inconsistent small reductions in FRET, cells showed no reaction to UV light alone. To demonstrate the functionality of the FRET cGMP sensor, each experiment was finished with a positive control by perfusion of 0.1 μM DEA/NO over the cells. The applied substances were perfused over the cells for 240 s under each set of conditions. For the first 25 s of perfusion under a new set of conditions, VSMCs were always kept in the dark; this confirmed the inertness of unexposed compound **1**. After a short pulse of UV light (5–30 s), NO release was triggered and cGMP signals could be observed.

Firstly, we held the irradiation time constant (340 nm, 5 s, applying the DAPI filter of the microscope), but varied the concentration of NONOate **1** between 0.1 and 100 μM (Figure 2 A). For the low concentrations (0.1–1 μM), little to no FRET change was found, depending on the specific cell. However, on application of 5 μM **1** a strong and fast FRET change became visible. The signal went back to base line within about 50 s after termination of irradiation. With further increases in the concentration of NONOate **1** both the maximum FRET change and the duration of the signal remained relatively unchanged. This suggests that the full cGMP signal (equivalent to a full cGi500 sensor activation) is achieved when a particular amount of NO is released in a burst-like manner. Thus we would expect that an increase in the irradiation time (equivalent to more applied

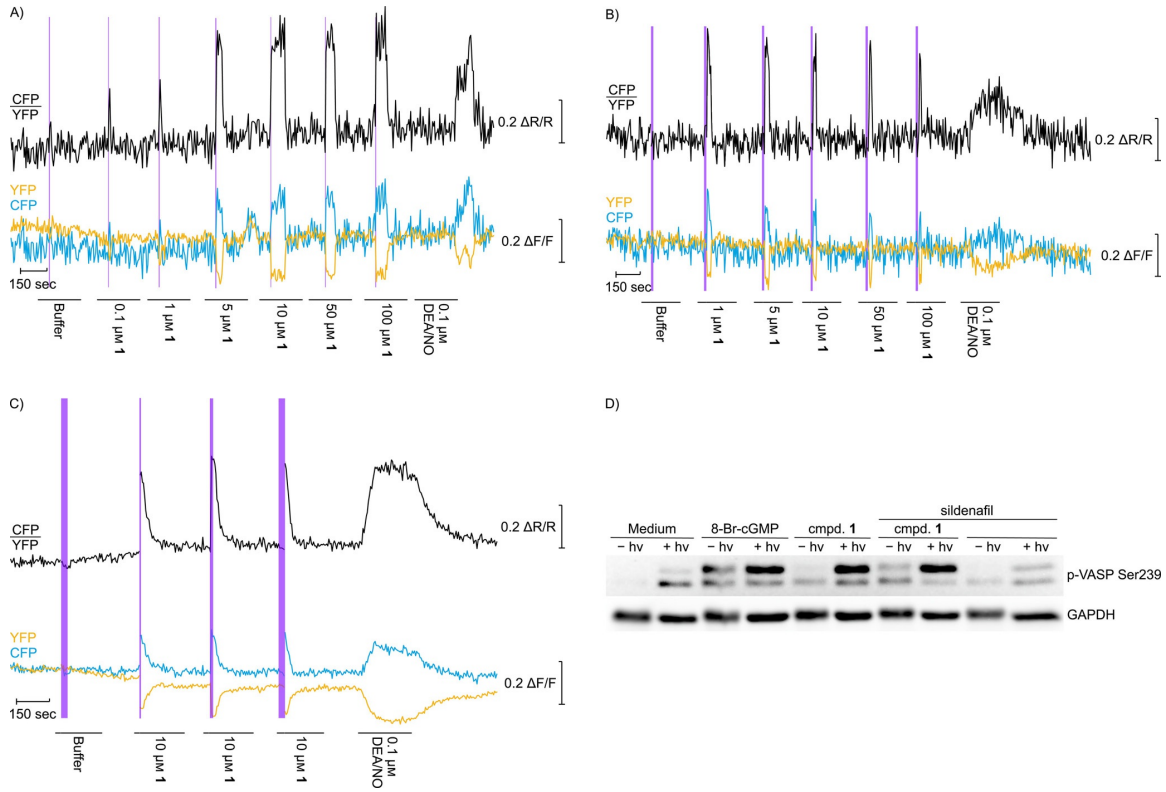

Figure 2. Imaging of photoinduced NO-dependent cGMP signalling in primary VSMCs with the cGi500 sensor. The fluorescence emission time traces of YFP (yellow) and CFP (cyan) in $\Delta F/F$ are shown, together with the calculated CFP/YFP emission ratios in $\Delta R/R$ (black). Fluorescence emission intensities and ratios were normalised to averaged baseline signals. Time traces of individual cells are shown. Average time traces of 10–25 cells are shown in the Supporting Information (Figures S8 and S9). In each graph, the time window when specific compounds were perfused over the cells is indicated. The corresponding illumination times (at 340 nm) are indicated by purple bars. In each experiment, addition of buffer served as negative control, and DEA/NO (as diethylammonium salt) served as a positive NO control. A) Concentration series of compound **1** (0.1–100 μM) with constant irradiation time (5 s). Traces for one representative cell are shown. B) Concentration series of compound **1** (1–100 μM) with increased but constant irradiation time (15 s). Traces for one representative cell are shown. C) Series of increasing irradiation times (5–30 s) with concentration of **1** kept constant (10 μM). Traces for one representative cell are shown. For further description, see the Experimental Section. D) Western blot of VASP phosphorylation detected by a primary antibody specific for Ser239 phosphorylation ($n=1$). $\pm h\nu$ indicates illumination for 15 s with 365 nm light; compound **1** (100 μM) was applied for 5 min; medium serves as a negative control; 8-Br-cGMP (100 μM, incubation for 5 min) as a positive control; sildenafil (30 μM, incubation for 5 min) blocks cGMP degradation; GAPDH serves as a loading control. For further description and analysis, see the Experimental Section and Figure S12.

ChemPubSoc Europe

CHEMBIOCHEM Full Papers

photons) would not further increase the overall cGMP signal but would rather already result in a full signal at a lower concentration of compound **1**.

To test this, we performed the same experiment but irradiated for 15 s instead of 5 s (Figure 2B). Indeed, the full cGMP signal was then already achieved at a NONOate **1** concentration of 1 μM.

If a short UV burst (5 s) is sufficient to activate the cGi500 sensor fully to its highest FRET reduction with 10 μM NONOate **1**, then this would mean that more light would not result in a stronger cGMP signal. We tested this behaviour by holding the concentration of **1** constant (10 μM) and varying the irradiation time (5, 15, 30 s, Figure 2C). As expected, the same cGMP signal was generated for all three sets of irradiation conditions. Taken together, the cGMP activation profiles were very constant and reproducible once a certain threshold in the amount of compound **1** and UV photons was exceeded. Such robust behaviour—insensitivity to fluctuations in the concentration of NONOate **1** or the photon flux—is highly desirable for potential in vivo applications.

Also notable is the shape of the cGMP signal upon photoactivation, which differs greatly from the positive cGMP control when DEA/NO is used (at the end of each experiment in Figure 2A–C). The shape after photorelease of NO is very steep, both on the side reflecting cGMP build-up as well as on the side reflecting cGMP decay. Clearly, the shape is dominated by the kinetics of NO release and the enzymatic formation (sGC) and decay (PDE) of cGMP. The shape is not dominated by the pharmacokinetics of the applied compound as in the case of NO control with DEA/NO.

Finally, to ensure that the FRET reporter had truly sensed changes in cGMP levels, we performed an assay to verify cGMP formation independently, through the activation of a downstream target. cGMP is known to activate the protein kinase cGKI in VSMCs, and cGKI then phosphorylates various protein substrates including VASP (Scheme 2). This is readily detectable by western blot. To detect the generation of phosphorylated VASP (*p*-VASP), we isolated protein from wild-type VSMCs after treatment with **1** in the presence or in the absence of UV illumination (15 s at 365 nm). As controls, we compared cells treated with medium only or with the membrane-permeable cGKI activator 8-Br-cGMP, again with and without illumination. As an additional control, we tested the effect of treatment with the phosphodiesterase 5 (PDE 5) inhibitor sildenafil, which blocks the degradation of cGMP in VSMCs.

Using an antibody that specifically detects VASP when phosphorylated at Ser239, we detected some phosphorylation for unexposed **1**, but this was still comparable with our observations for the unexposed negative controls with medium only or with sildenafil only (Figure 2D). Upon irradiation of **1**, VASP phosphorylation achieved the level of the positive control (8-Br-cGMP), which always showed strong phosphorylation independent of irradiation. Both negative controls showed a subtle effect of UV irradiation on phosphorylation, but to a much lower extent than compound **1**. During the cGMP imaging experiments (FRET-based sensor), small reductions in FRET were rarely and inconsistently observed, thus indicating that UV light alone might influence cGMP levels (Figure S9). Overall, analysis of VASP phosphorylation was consistent with the data obtained by FRET imaging and confirmed the sufficient inertness of Npom-protected NONOate **1** in the dark, as well as the NO-mediated build-up of cGMP after UV decaging of compound **1**.

Conclusion

NONOates are particularly useful NO-releasing substances and have been used widely in NO and cGMP research.[6–9] To study the mechanisms of NO-dependent signalling, but also to generate smart drugs, potential means for the release of NO with high temporal and spatial control have been explored. These also include various classes of light-activated NO donors.[19–23] The advantages of NONOates over other NO-releasing substances include the lack of metals, their ease of synthesis, their tunable properties (such as speed of NO release) and the possibility to generate them as membrane-permeable prodrugs.[24] However, the direct caging of NONOates with a photoprotection group at their terminal oxygen atom has been problematic in the past. Such compounds were typically characterised by low decaging quantum yields, unwanted pH dependency and decomposition routes that were nonproductive in terms of NO release due to direct, photodependent decomposition of the NONOate moiety itself.[25] Here, we now show for the first time that the Npom protection group allows for direct photocaging of typical NONOates to afford NO-releasing substances. The Npom protection group was initially developed for the caging of heterocycles that are difficult to cage stably or to photoreactivate with classical carbamates (such as the Nvoc group) or classical nitrobenzyl groups (such as the DMNB group).[14] The Npom group has been used in nucleic acid chemistry by others,[26] and we have used it successfully for the caging of O^6-benzylguanine.[16] In comparison with the classical caging groups described above, the Npom group features an additional oxymethylene bridge between the light antenna and the protected moiety. On one hand this puts additional space between the part where the photochemistry takes place and the caged moiety. On the other hand, Npom-protected substances decay into three molecules upon irradiation. This fragmentation mechanism might be particularly suited for the generation of NO from caged NONOates. Interestingly, while we were writing this manuscript, Behara et al. published an analogous caging strategy for a similar NONOate in which a fluorogenic coumarin bridge is released upon irradiation, which was applied at high doses and enduring irradiation to elicit NO-dependent anticancer activity.[27] In contrast, we apply our substance for the burst-like release of NO just enough to activate cGMP signalling. The FRET-based cGMP sensing would not be compatible with coumarin release. Our data show that our Npom-protected NONOate allows for the strong activation of cGMP signalling within seconds in live primary VSMCs. The cGMP imaging experiments were not limited either by solubility or by cytotoxicity of our compound (see the Supporting Information and Figures S10 and S11). Npom-protected NONO-

ChemPubSoc Europe

CHEMBIOCHEM Full Papers

ates should enable the study of NO/cGMP signalling with better spatiotemporal control than before.

Experimental Section

Instrumental setup: NMR spectra were measured with a Bruker Avance III HDX 400 spectrometer at 400.16 MHz for ^{1}H spectra and 100.62 MHz for ^{13}C spectra. Chemical shifts are given in ppm and were calibrated to the peak of the solvent in question; ^{13}C spectra are broadband decoupled. The signals of compound **1** were assigned by ^{1}H,^{1}H COSY and ^{13}C,^{1}H HSQC measurements. The mass spectrum of **1** was recorded with a Bruker Daltonics maxis 4G high-resolution (HR) mass spectrometer with electrospray ionisation (ESI) source and time-of-flight (TOF) analyser. For elemental analysis of compound **1** an elemental analyser (Euro EA 3000) from HEKAtech, GmbH was used. Analytical HPLC was performed with a Shimadzu system with an SPD-20AV Prominence UV/VIS detector and an EC 125/4 Nucleodur 100-5 C18 ec-column from Macherey–Nagel. Buffer A consisted of H_2O/trifluoroacetic acid (TFA) 100:0.1, buffer B of MeCN/H_2O/TFA 90:10:0.1. Spectra were measured with a linear gradient of buffer B (5%) to buffer B (95%) over 25 min. UV spectra were measured with a Cary 300 Scan UV/Visible spectrophotometer from Agilent. The microscopy setup used was as previously described by Thunemann et al.,[13] with minor changes. It was composed of an Axiovert 200 inverted microscope with EC Plan NeoFluar 10×/0.30 air or 40×/1.30 oil objectives and optional 1.6× Optovar magnification (Carl Zeiss Microscopy), a light source with excitation filter switching device (FEI GmbH, Munich, Germany), a DualView DV2 beam splitter from Photometrics with 516 nm dichroic mirror and CFP and YFP emission filters (480/30 nm and 535/30 nm, respectively), and a Retiga R1 CCD digital camera from QImaging. The system was operated with VisiView4 software (Visitron Systems GmbH, Puchheim, Germany).

Synthesis of photoprotected NONOate 1

*Sodium 1-(pyrrolidin-1-yl)diazen-1-ium-1,2-diolate (**2**):* NONOate **2** was synthesised by a modified route similar to that already described by Konter et al.[10] but with reduced pressure and a simplified experimental setup. Pyrrolidine (1.0 mL, 12.00 mmol, 1.0 equiv) and sodium methoxide in methanol (25 wt%, 2.7 mL, 12.00 mmol, 1.0 equiv) were dissolved in methanol (20 mL) under nitrogen in a heavy-walled Schlenk tube with additional gas inlet. The solution was degassed and subsequently stirred under nitric oxide (1.7 bar) at room temperature for 5 h. The mixture was concentrated in vacuo, and the product was precipitated with diethyl ether, filtered, and dried in vacuo, resulting in NONOate **2** (545 mg, 3.56 mmol, 30%) as a white powder. R_f [cyclohexane (CH)/ethyl acetate (EA) 3:2]: 0.15; ^{1}H NMR (400 MHz, CD_3OD): δ = 1.89–1.92 (m, 4H), 3.24–3.28 ppm (m, 4H); ^{13}C NMR (100 MHz, CD_3OD): δ = 23.9, 52.5 ppm. Spectroscopic data are in agreement with the literature.[28]

*2-{[1-(6-Nitrobenzo[d][1,3]dioxol-5-yl)ethoxy]methoxy}-1-(pyrrolidin-1-yl)diazene 1-oxide (**1**):* DBU (97 μL, 0.65 mmol, 1.0 equiv) was added under nitrogen to a solution of NONOate **2** (100.0 mg, 0.65 mmol, 1.0 equiv) in dimethylformamide (2.5 mL). Subsequently, 5-[1-(chloromethoxy)ethyl]-6-nitrobenzo[1,3]dioxole (**3**, 270.0 mg, 1.04 mmol, 1.6 equiv), synthesised according to published literature,[29,14] in dimethylformamide (3.0 mL) was added dropwise, and the mixture was stirred at room temperature for 3 h. After addition of an aqueous solution of citric acid (1%) the aqueous layer was extracted three times with ethyl acetate. The combined organic layers were washed with aqueous solutions (1%) of citric acid (1×), saturated $NaHCO_3$ (1×) and saturated NaCl (3×) and were dried over Na_2SO_4, and the solvents were removed in vacuo. Double purification by flash column chromatography (CH/EA 2:1 and $CHCl_3$) yielded Npom-protected NONOate **1** as a light yellow solid (180 mg, 0.51 mmol, 78%). R_f (CH/EA 3:2): 0.28. ^{1}H NMR (400 MHz, $CDCl_3$): δ = 1.53 (d, J = 6.3 Hz, 3H; 14-H), 1.93–1.97 (m, 4H; 12-H, 11-H), 3.49–3.53 (m, 4H; 13-H, 10-H), 5.13 (d, J = 8.0 Hz, 1H; 9-H), 5.25 (d, J = 8.0 Hz, 1H; 9-H), 5.52 (q, J = 6.3 Hz, 1H; 8-H), 6.10 (s, 2H; 1-H), 7.19 (s, 1H; 3-H or 6-H), 7.48 ppm (s, 1H; 3-H or 6-H); ^{13}C NMR (100 MHz, $CDCl_3$): δ = 22.8 (C-12, C-11), 23.6 (C-14), 50.6 (C-13, C-10), 73.4 (C-8), 95.1 (C-9), 102.9 (C-1), 104.9 (C-3 or C-6), 106.6 (C-3 or C-6), 137.4 (C_q), 141.4 (C_q), 146.9 (C_q), 152.3 ppm (C_q); UV [NaCl (100.0 mM), KH_2PO_4 (10.0 mM), K_2HPO_4 (10.0 mM), DMSO (0.2%), pH 7.4]: λ_{max} = 357 nm, $\varepsilon_{357\,nm}$ = 4.44 mM^{-1} cm^{-1}; HRMS (ESI-TOF): *m/z* calcd for $C_{14}H_{18}N_4O_7Na$: 377.10677 $[M+Na]^+$; found: 377.10670; elemental analysis calcd (%) for $C_{14}H_{18}N_4O_7$: C 47.46, H 5.12, N 15.81; found: C 47.86, H: 5.20, N: 15.48. For atom numbering and spectra, see Scheme S1 and Figures S1–S4.

Determination of deprotection kinetics of 1 by HPLC: Eight samples of photoprotected NONOate **1** [60 μL, 10 μM in buffer, pH 7.4, containing NaCl (100.0 mM), KH_2PO_4 (10.0 mM), and K_2HPO_4 (10.0 mM)] were illuminated with a UVP high-performance UV transilluminator (25 W) at 365 nm for 0.00 min, 0.25 min, 0.50 min, 1.00 min, 2.50 min, 5.00 min, 10.00 min, and 20.00 min, respectively, and subsequently subjected to analytical HPLC. Plotting of the areas under the curves of the peaks of **1** against the irradiation time and fitting of an exponential decay resulted in a half-life of $t_{1/2}$ = (0.39 ± 0.02) min (Figure 1B). For two compounds M and N under identical measuring conditions the quantum yields φ relate by [Equation (1)]

$$\varepsilon_{365\,nm}(M)\varphi(M) = \varepsilon_{365\,nm}(N)\varphi(N)\frac{t_{1/2}(N)}{t_{1/2}(M)} \quad (1)$$

so the quantum yield of the deprotection of **1** could be determined to be φ(**1**) = 66% by comparison with the previously published[16] values for ^{N7}Npom-BG-TFA. For further information, see the Supporting Information and Figures S5 and S6.

Griess assay for NO determination: The Griess assay was conducted with the "Nitric Oxide (total) detection kit" from Enzo according to the manufacturer's manual. Briefly, the Griess assay reaction buffer (as a blank), nitrate standards of known concentrations, and DEA/NO (as the diethylammonium salt), unprotected NONOate **2** and protected NONOate **1** (all NONOates at 100 μM in reaction buffer) were used as samples. Each sample was assayed in duplicate. Samples of DEA/NO, **2** and **1** were irradiated side-by-side with a UVP high-performance UV transilluminator (25 W) at 365 nm for 0.00, 0.25, 0.50, 1.00, 2.50, 5.00, 10.00 or 20.00 min. After 20 min, nicotinamide adenine dinucleotide (NADH), nitrate reductase and the Griess reagents I and II were added to all samples according to the manual, and the absorbance of the samples at 540 nm was measured with a Spark 10M TECAN reader. The standard curve obtained from the average net absorbance intensities of the nitrate standards, absorbance values and concentrations of NO determined from average net absorbance intensities of the NONOate samples are shown in Figure S7 and Tables S1 and S2. The resulting concentrations of nitric oxide were plotted against the irradiation time and an exponential growth was fitted, showing a half-life of $t_{1/2}$ = (0.13 ± 0.03) min (Figure 1C).

Primary culture of vascular smooth muscle cells (VSMCs): All animal procedures were performed in compliance with the standards for humane care and use of laboratory animals. VSMCs were

ChemPubSoc Europe

CHEMBIOCHEM Full Papers

isolated from mice as previously described by Thunemann et al.[13] Briefly, two to five aortae from wild-type or transgenic cGi500 mice[13] (5–10 weeks old) were isolated and collected on ice-cold PBS. Surrounding fat and connective tissue were removed from the aorta. The tissues were then cut into 5 mm pieces and incubated at 37 °C for 60 min with papain (0.7 mg mL^{-1}), followed by 15 min with collagenase and hyaluronidase (1.0 mg mL^{-1} each); tissues were dissociated by pipetting through a 1 mL pipette tip. Cells (viability 90% as measured by trypan blue exclusion) were suspended in culture medium consisting of Dulbecco's modified Eagle's medium (DMEM) with foetal bovine serum (10%), glucose (4.5 g L^{-1}), penicillin (100 U mL^{-1}) and streptomycin (100 μg mL^{-1}). Cells for imaging were plated into 24-well plates equipped with glass coverslips (55 k VSMCs per well), cells for protein isolation into six-well plates (150 k VSMCs per well). After the cells had been grown at 37 °C under CO_2 (5%) for three days, medium was exchanged. Cells were grown for an additional one to four days in culture medium before being serum-starved in culture medium without serum for 24 h prior to imaging experiments or protein isolation.

Real-time imaging of cGMP in VSMCs: As previously described by Thunemann et al,[13] for cGMP imaging of primary cells, cGi500 VSMCs were grown on glass coverslips and mounted into a Warner Instrument SA-20LZ superfusion imaging chamber from Harvard Bioscience. Samples were continuously superfused with Tyrode buffer (pH 7.4) containing NaCl (140.0 mM), KCl (5.0 mM), $MgSO_4$ (1.2 mM), $CaCl_2$ (2.5 mM), glucose (5.0 mM), and HEPES (5.0 mM) by using a Pharmacia P-500 pump from GE Healthcare set to 0.5 mL min^{-1} and Pharmacia IV-7 injection valves (GE Healthcare) with a 2.0 mL sample loop to apply solutions of test compounds in Tyrode buffer. Compound **1** was diluted in Tyrode buffer from a stock solution in DMSO (50 mM), and the solutions were warmed to 37 °C in the imaging chamber. cGi500 fluorescence was observed through a YFP filter set (excitation filter 497/16 nm, 516 nm dichroic mirror, emission filter 535/22 nm). For FRET measurements, a CFP excitation filter (445/20 nm) was used together with a 470 nm dichroic mirror and the beam splitter device. Illumination was performed with the Oligochrome light source and a 340 nm excitation filter (340/26 nm). Images were analysed as previously described[13] with Fiji[30] and Microsoft Excel; graphs were produced with OriginPro 2017.

VASP phosphorylation assay

Preparation of cell extracts: For protein isolation, separate 6-well plates with wild-type cells were prepared: one for the samples without and one for the samples with illumination. On these plates, two wells were treated according to each set of conditions. Firstly, the cells were washed with PBS (pH 7.4) containing NaCl (135.0 mM), KCl (3.0 mM), Na_2HPO_4 (8.0 mM), and KH_2PO_4 (2.0 mM). Then, serum-free culture medium supplemented variously with 8-Br-cGMP (100 μM), with protected NONOate **1** [100 μM, diluted from a stock solution in DMSO (50 mM)], with sildenafil (30 μM) in combination with protected NONOate **1** (100 mM), or only with sildenafil (30 μM) was added. After 5 min, one of the plates was irradiated with a Nitechore Chameleon Series CU6 UV lamp for 15 s at 365 nm (3000 mW), while the other plate was incubated in the dark. Subsequently, medium was removed, and cells were washed again with PBS and lysed with lysis buffer (100 μL) containing sodium dodecyl sulfate (SDS, 0.67%, *w/v*), tris(hydroxymethyl)aminomethane·HCl (pH 8.3, 21 mM), phenylmethylsulfonyl fluoride (0.2 mM), and one tablet of PhosSTOP phosphatase inhibitor cocktail (Roche) per 10 mL. Cells from the two wells with identical conditions were pooled. After incubation at 95 °C for 10 min, cells were stored at −20 °C until performance of the Lowry assay.

Lowry assay: The Lowry assay was performed with the "Total protein kit, Micro Lowry, Peterson's Modification" from Sigma according to the manufacturer's manual. Briefly, samples were diluted 1:6.6, Lowry Reagent Solution and Folin & Ciocalteu's Phenol Reagent Working Solution were added to the standard solutions of known protein concentrations and samples as stated in the manual, and absorbance at 620 nm was measured with a Multiskan EX multi-well plate reader (Thermo Fisher). Water and lysis buffer were used as negative controls. Absorbance of standards was measured in duplicate, absorbance of samples in triplicate. Protein concentrations of the samples were determined by comparison with the standard curve produced from the standards and multiplication with the dilution factor.

SDS-PAGE and western blot: After the Lowry assay, SDS-PAGE and western blotting were performed according to standard procedures; protein (17 μg) was loaded onto each lane. After semi-dry blotting, polyvinylidene fluoride membranes were blocked in milk powder (5%) in TBS-T [Tris·HCl (pH 8.2, 5 mM), NaCl (75 mM), Tween 20 (0.1%)] for 1 h followed by incubation overnight at 4 °C with primary rabbit antibodies detecting *p*-VASP (Ser239) (1:1000, Cell Signaling 3114) or GAPDH (1:1000, Cell Signaling 2118). Antibody binding was detected by using horseradish-peroxidase-conjugated secondary antibodies (goat anti-rabbit IgG, 1:2000, Cell Signaling 7074) and the chemiluminescent substrate WesternBright ECL (Advansta). Signals were recorded with a cooled CCD Alpha-Imager camera (Bio-Rad Laboratories), image processing and analysis of band intensities were carried out with Fiji,[30] and band intensities of both bands for *p*-VASP were combined for each lane. Quantification of band intensities is shown in Figure S12.

Acknowledgements

We thank Dr. Gregor Lemanski for his help with the nitric oxide gas reaction, Alfred Hanswillemenke for providing the kinetic data for DMNB-cAMP and ^{N7}Npom-BG-TFA, and Hyazinth Dobrowinski for his help with the VSMC cultures. We gratefully acknowledge support from the Deutsche Forschungsgemeinschaft to T.S. (STA 1053/3-2; STA 1053/7-1) and R.F. (FOR 2060 projects FE 438/5-2 and FE 438/6-2). M.P. is affiliated with the Graduate School of Cellular and Molecular Neuroscience, University of Tübingen.

Conflict of Interest

The authors declare no conflict of interest.

Keywords: biosensors · cGMP · nitric oxide · photocaging · signal transduction

[1] D. S. Bredt, S. H. Snyder, *Annu. Rev. Biochem.* **1994**, *63*, 175–195.
[2] V. Calabrese, C. Mancuso, M. Calvani, E. Rizzarelli, D. A. Butterfield, A. M. G. Stella, *Nat. Rev. Neurosci.* **2007**, *8*, 766–775.
[3] E. M. Hetrick, M. H. Schoenfisch, *Annu. Rev. Anal. Chem.* **2009**, *2*, 409–433.
[4] C. Napoli, L. J. Ignarro, *Annu. Rev. Pharmacol. Toxicol.* **2003**, *43*, 97–123.
[5] R. Feil, S. Feil, F. Hofmann, *Trends Mol. Med.* **2005**, *11*, 71–75.

ChemPubSoc Europe

CHEMBIOCHEM Full Papers

[6] R. Feil, N. Gappa, M. Rutz, J. Schlossmann, C. R. Rose, A. Konnerth, S. Brummer, S. Kühbandner, F. Hofmann, *Circ. Res.* **2002**, *90*, 1080 – 1086.
[7] A. M. Kitay, A. Link, J. Geibel, *Cell. Physiol. Biochem.* **2017**, *44*, 1606 – 1615.
[8] L. A. Ridnour, A. N. Windhausen, J. S. Isenberg, N. Yeung, D. D. Thomas, M. P. Vitek, D. D. Roberts, D. A. Wink, *Proc. Natl. Acad. Sci. USA* **2007**, *104*, 16898 – 16903.
[9] J. C. Irvine, N. Cao, S. Gossain, A. E. Alexander, J. E. Love, C. Qin, J. D. Horowitz, B. K. Kemp-Harper, R. H. Ritchie, *Am. J. Physiol. Heart. Circ. Physiol.* **2013**, *305*, H365 – H377.
[10] J. Konter, G. E.-D. A. A. H. Abuo-Rahma, A. El-Emam, J. Lehmann, *Methods Enzymol.* **2005**, *396*, 17 – 26.
[11] G. Cantuaria, A. Magalhaes, R. Angioli, L. Mendez, R. Mirhashemi, J. Wang, P. Wang, M. Penalver, H. Averette, P. Braunschweiger, *Cancer* **2000**, *88*, 381 – 388.
[12] X. Wu, X. Tang, M. Xian, P. G. Wang, *Tetrahedron Lett.* **2001**, *42*, 3779 – 3782.
[13] M. Thunemann, L. Wen, M. Hillenbrand, A. Vachaviolos, S. Feil, T. Ott, X. Han, D. Fukumura, R. K. Jain, M. Russwurm, C. de Wit, R. Feil, *Circ. Res.* **2013**, *113*, 365 – 371.
[14] H. Lusic, A. Deiters, *Synthesis* **2006**, *13*, 2147 – 2150.
[15] J. E. Saavedra, T. R. Billiar, D. L. Williams, Y.-M. Kim, S. C. Watkins, L. K. Keefer, *J. Med. Chem.* **1997**, *40*, 1947 – 1954.
[16] A. Hanswillemenke, T. Kuzdere, P. Vogel, G. Jékely, T. Stafforst, *J. Am. Chem. Soc.* **2015**, *137*, 15875 – 15881.
[17] L. K. Keefer, R. W. Nims, K. M. Davies, D. A. Wink, *Methods Enzymol.* **1996**, *268*, 281 – 293.
[18] M. Russwurm, F. Mullershausen, A. Friebe, R. Jäger, C. Russwurm, D. Koesling, *Biochem. J.* **2007**, *407*, 69 – 77.
[19] M. Blangetti, A. Fraix, L. Lazzarato, E. Marini, B. Rolando, F. Sodano, R. Fruttero, A. Gasco, S. Sortino, *Chem. Eur. J.* **2017**, *23*, 9026 – 9029.
[20] N. L. Fry, P. K. Mascharak, *Acc. Chem. Res.* **2011**, *44*, 289 – 298.
[21] P. C. Ford, *Acc. Chem. Res.* **2008**, *41*, 190 – 200.
[22] G. M. Halpenny, B. Heilman, P. K. Mascharak, *Chem. Biodiversity* **2012**, *9*, 1829 – 1839.
[23] A. Fraix, S. Sortino, *Chem. Asian J.* **2015**, *10*, 1116 – 1125.
[24] L. Keefer, *Curr. Top. Med. Chem.* **2005**, *5*, 625 – 636.
[25] C. M. Pavlos, H. Xu, J. P. Toscano, *Curr. Top. Med. Chem.* **2005**, *5*, 637 – 647.
[26] H. Lusic, D. D. Young, M. O. Lively, A. Deiters, *Org. Lett.* **2007**, *9*, 1903 – 1906.
[27] K. K. Behara, Y. Rajesh, Y. Venkatesh, B. R. Pinninti, M. Mandal, N. D. P. Singh, *Chem. Commun.* **2017**, *53*, 9470 – 9473.
[28] T. B. Cai, D. Lu, M. Landerholm, P. G. Wang, *Org. Lett.* **2004**, *6*, 4203 – 4205.
[29] G. H. McGall, A. D. Barone, M. Diggelmann, S. P. A. Fodor, E. Gentalen, N. Ngo, *J. Am. Chem. Soc.* **1997**, *119*, 5081 – 5090.
[30] J. Schindelin, I. Arganda-Carreras, E. Frise, V. Kaynig, M. Longair, T. Pietzsch, S. Preibisch, C. Rueden, S. Saalfeld, B. Schmid, J.-Y. Tinevez, D. J. White, V. Hartenstein, K. Eliceiri, P. Tomancak, A. Cardona, *Nat. Methods* **2012**, *9*, 676 – 682.

Manuscript received: December 22, 2017
Accepted manuscript online: February 8, 2018
Version of record online: March 27, 2018

CHEMBIOCHEM

Supporting Information

Npom-Protected NONOate Enables Light-Triggered NO/cGMP Signalling in Primary Vascular Smooth Muscle Cells

Anna S. Stroppel,[a] Michael Paolillo,[b] Thomas Ziegler,[c] Robert Feil,[b] and Thorsten Stafforst*[a]

cbic_201700683_sm_miscellaneous_information.pdf

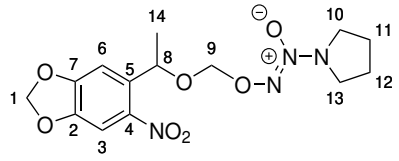

1

Scheme S1. Atom numbering of compound **1**.

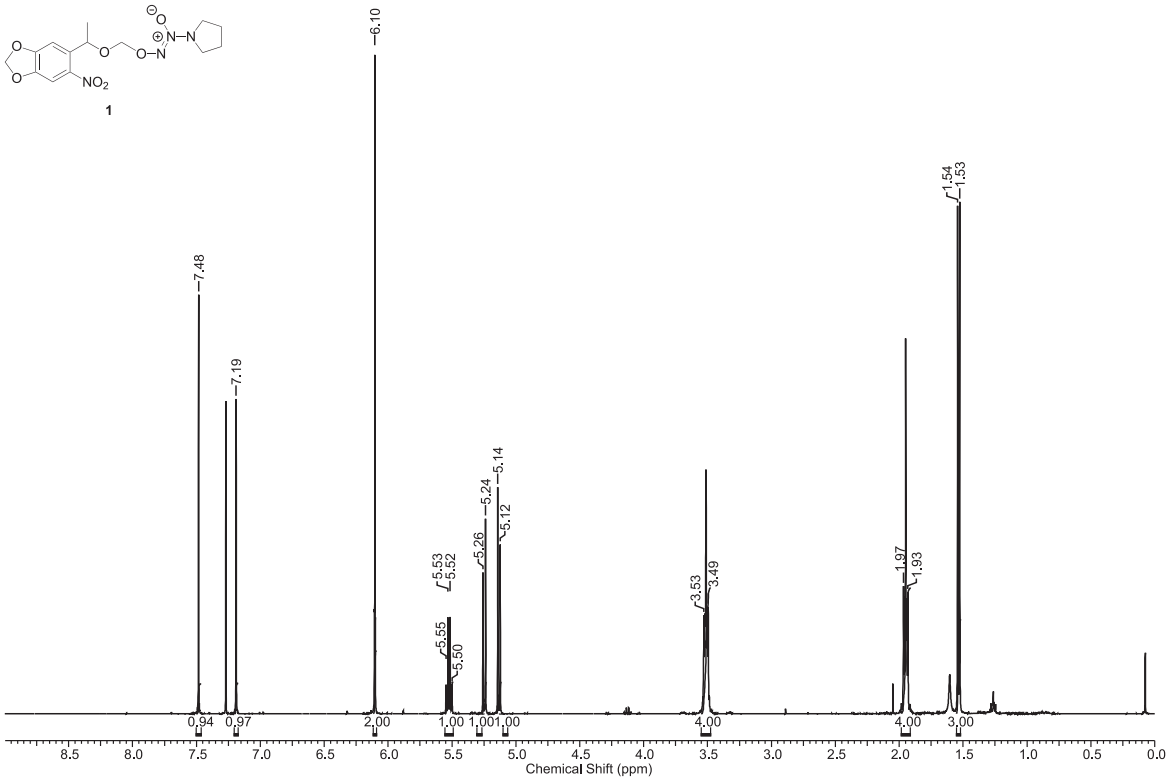

Figure S1. ^{1}H-NMR spectrum (400 MHz, $CDCl_3$) of Npom-protected NONOate **1**.

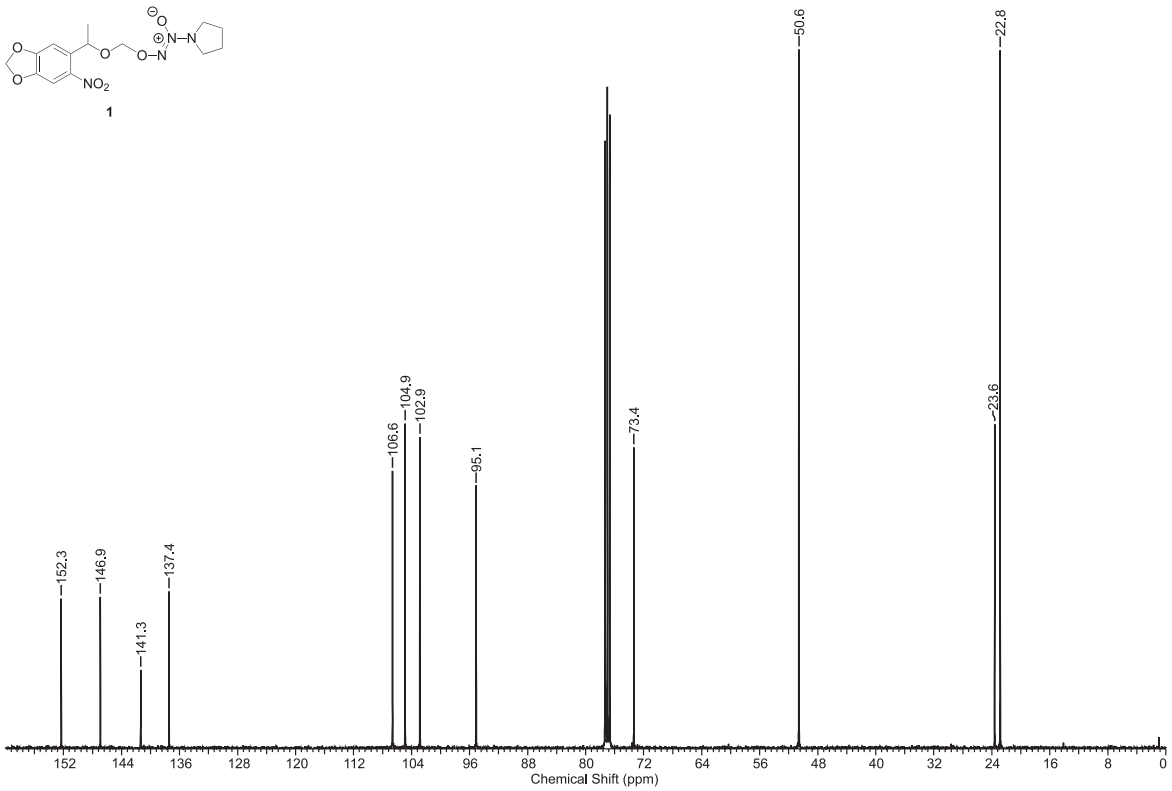

Figure S2. ^{13}C-NMR spectrum (400 MHz, $CDCl_3$) of Npom-protected NONOate **1**.

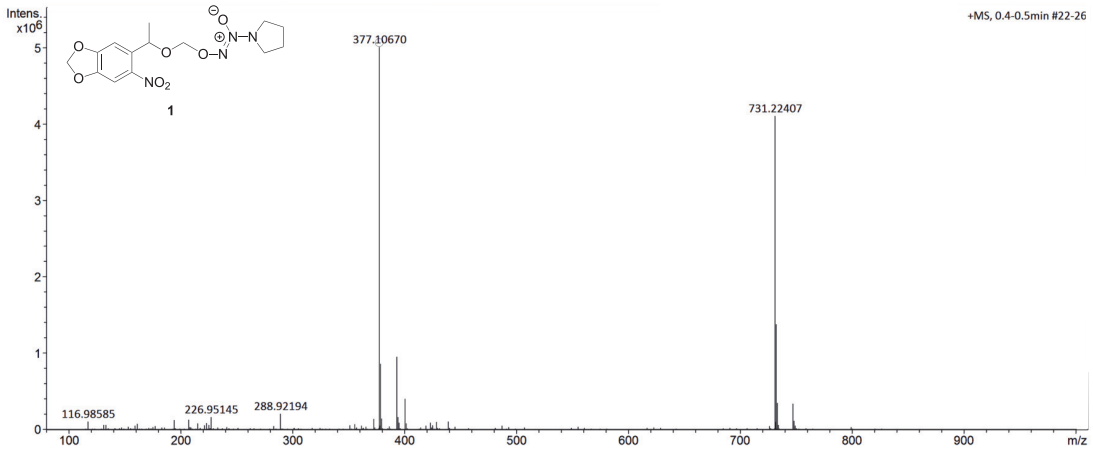

Figure S3. HR-ESI-TOF-MS of Npom-protected NONOate **1**. *m/z* calculated for $[C_{14}H_{18}N_4O_7+Na]^+$: 377.10677, found: 377.10670.

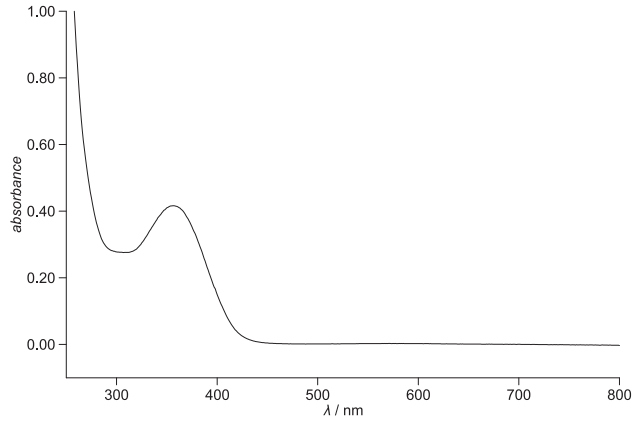

Figure S4: UV-spectrum of Npom-protected NONOate **1** (100 µM in buffer at pH 7.4 containing NaCl (100.0 mM), KH_2PO_4 (10.0 mM), and K_2HPO_4 (10.0 mM), and DMSO (0.2 %)). λ_{max} = 357 nm, $\varepsilon_{357\ nm}$ = 4.44 $mM^{-1}cm^{-1}$.

Determination of quantum yield of Npom-protected NONOate 1

For two compounds M and N under identical measuring conditions the quantum yields φ relate by $\varepsilon_{365\,nm}(M)\varphi(M) = \varepsilon_{365\,nm}(N)\varphi(N)\cdot\frac{t_{1/2}(N)}{t_{1/2}(M)}$. As previously published,[S1] the quantum yield of ^{N7}Npom-BG-TFA has been determined under identical measuring conditions as the deprotection kinetics of **1** by comparison with DMNB-cAMP as reference compound with known quantum yield. Briefly, eight or seven samples of DMNB-cAMP or ^{N7}Npom-BG-TFA (60 µl, 10 µM in buffer at pH 7.4 containing NaCl (100.0 mM), KH_2PO_4 (10.0 mM), and K_2HPO_4 (10.0 mM)) in PCR tubes respectively were illuminated on an UVP high performance UV transilluminator with 25 W at 365 nm for 0.00 min, 0.25 min, 0.50 min, 1.00 min, 2.50 min, 5.00 min, 10.00 min, and 20.00 min (only for DMNB-cAMP) respectively and subsequently submitted to analytical HPLC with detection at 260 nm or 280 nm and 365 nm. Plotting of the areas under the curve of the peaks of cAMP and BG-TFA against the irradiation time and fitting of 1st-order exponential functions resulted in a half-life of $t_{1/2}$ = 5.54 min ± 0.43 min for DMNB-cAMP and $t_{1/2}$ = 0.57 min ± 0.04 min for ^{N7}Npom-BG-TFA respectively. Exemplary chromatograms and deprotection kinetics are shown in Figures S5, S6. With the known quantum yield φ = 5 %[S2] and a determined extinction coefficient of $\varepsilon_{365\ nm}$ = 4.00 $mM^{-1}cm^{-1}$ for DMNB-cAMP, the quantum yield of ^{N7}Npom-BG-TFA with $\varepsilon_{365\,nm}$ = 4.00 $mM^{-1}cm^{-1}$ was determined to be φ = 50 %.

Now, the deprotection kinetics of compound **1** were measured as described above and its extinction coefficient at 365 nm determined to be $\varepsilon_{365\ nm}$ = 4.30 $mM^{-1}cm^{-1}$. Comparison with the values for ^{N7}Npom-BG-TFA results in a quantum yield φ = 66 %.

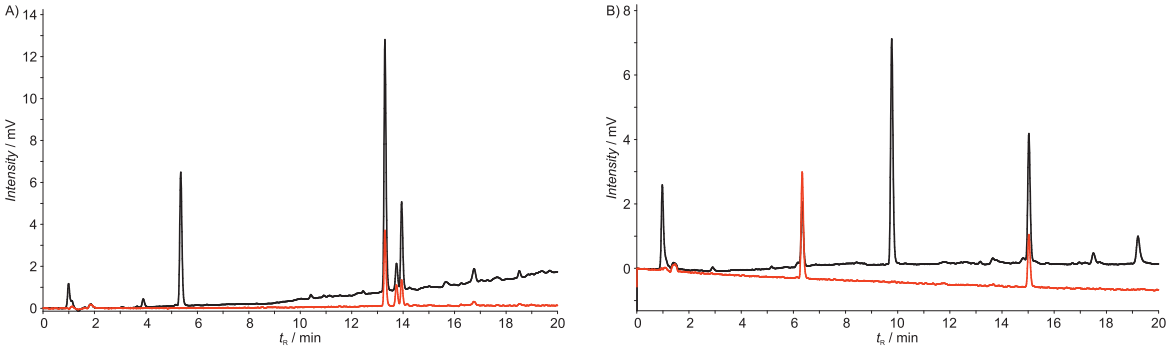

Figure S5. HPLC traces of illuminated DMNB-cAMP and ^{N7}Npom-BG-TFA. A) DMNB-cAMP after irradiation at 365 nm for 2.5 min. Detection at 260 nm and 365 nm is depicted in black and red respectively. Starting material DMNB-cAMP consists of two isomers with retention times t_R = 13.30 min and t_R = 13.90 min, cAMP with t_R = 5.40 min is gradually formed upon irradiation. B) ^{N7}Npom-BG-TFA after irradiation at 365 nm for 0.5 min. Detection at 280 nm and 365 nm is depicted in black and red respectively. Starting material ^{N7}Npom-BG-TFA has a retention time t_R = 15.10 min, BG-TFA with t_R = 9.80 min and nitroso acetophenone **4** with t_R = 6.10 min are gradually formed upon irradiation.

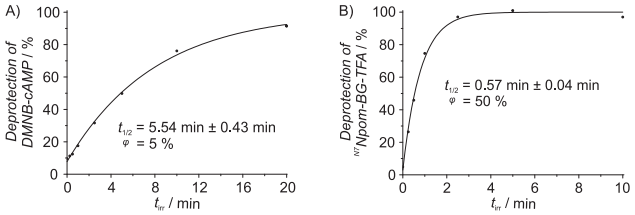

Figure S6. The decay of DMNB-cAMP (A) and ^{N7}Npom-BG-TFA (B) was fitted to a 1st-order exponential function by using the areas of HPLC traces as the ones shown in Figure S5.

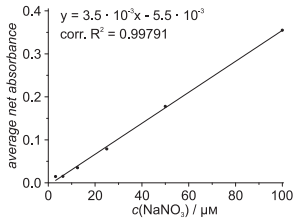

Figure S7. Standard curve of the Griess assay. Plotted are the average absorbance values (at 540 nm) obtained with a series of the nitrate standards of known concentrations c($NaNO_3$).

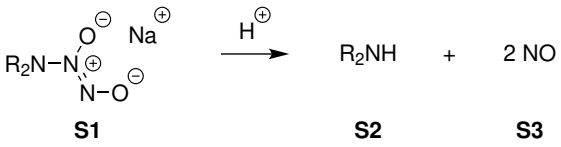

S1 **S2** **S3**

Scheme S2. Decay of one equivalent NONOate **S1** should result in one equivalent of the corresponding amine **S2** and two equivalents of nitric oxide (**S3**).[S3]

Table S1. Absorbance values at 540 nm measured by the Griess assay. Solutions of DEA/NO, unprotected NONOate **2**, and Npom-protected NONOate **1** (100 µM in Griess assay's reaction buffer each) were irradiated for different irradiation times t_{irr} and subsequently submitted to the Griess assay. Each sample was assayed in duplicates. The absorbance value for the zero standard with reaction buffer instead of a sample was 0.0785.

t_{irr} / min	DEA/NO		cmpd. **2**		cmpd. **1**	
0.00	0.5833	0.4380	0.2852	0.4599	0.0869	0.0995
0.25	0.4423	0.5018	0.3289	0.4544	0.1658	0.1831
0.50	0.4124	0.4641	0.2942	0.3651	0.1519	0.2282
1.00	0.4546	0.5221	0.3672	0.4812	0.2659	0.1553
2.50	0.3816	0.3329	0.5031	0.4782	0.1761	0.1997
5.00	0.2897	0.2870	0.5800	0.6468	0.1833	0.2178
10.00	0.3827	0.4383	0.6285	0.7037	0.2014	0.2186
20.00	0.2841	0.5338	0.3619	0.5099	0.1886	0.2037

Table S2. NO concentrations in µM derived from the Griess assay. Solutions of DEA/NO, unprotected NONOate **2**, and Npom-protected NONOate **1** (100 µM in Griess assay's reaction buffer each) were irradiated for different irradiation times t_{irr} and subsequently submitted to the Griess assay. Net absorbance values (of duplicate samples) were calculated by subtraction of the zero standard value from the averages of the absorbance values (Table S1); NO concentrations were calculated from net absorbance values applying the linear fit from the standard curve above (Figure S7). Mean value of NO concentrations derived from DEA/NO: 93.79 µM, from cmpd. **2**: 105.93 µM, expected: 200 µM each (see Scheme S2).

t_{irr} / min	DEA/NO	cmpd. **2**	cmpd. **1**
0.00	118.47	80.12	2.55
0.25	107.75	85.42	25.11
0.50	98.36	68.21	29.44
1.00	112.27	94.46	35.15
2.50	75.87	112.91	28.84
5.00	56.74	147.00	32.36
10.00	90.66	161.63	34.98
20.00	90.23	97.71	31.14

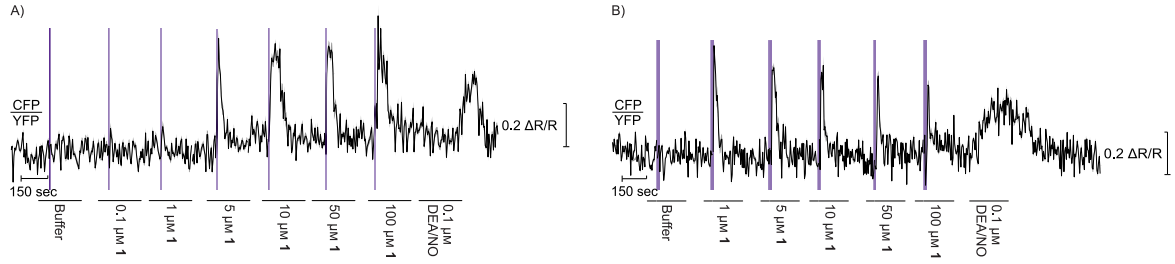

Figure S8. Averaged time traces from cGMP imaging with the cGi500 sensor shown in Figure 2A–B. Shown are the calculated CFP/YFP emission ratios in ΔR/R (black), normalised to averaged baseline signals. Mean values and standard deviations (grey) were calculated by OriginPro 2017. In each graph, the time window is indicated when specific compounds were perfused over the cells. The respective illumination times (at 340 nm) are indicated by purple bars. In each experiment, addition of buffer served as negative control, DEA/NO served as a positive NO control. A) Concentration series of compound **1** (0.1 µM – 100 µM) with constant irradiation time (5 s). Averaged traces of 12 cells are shown. B) Concentration series of compound **1** (1 µM – 100 µM) with increased but constant irradiation time (15 s). Averaged traces of 20 cells are shown.

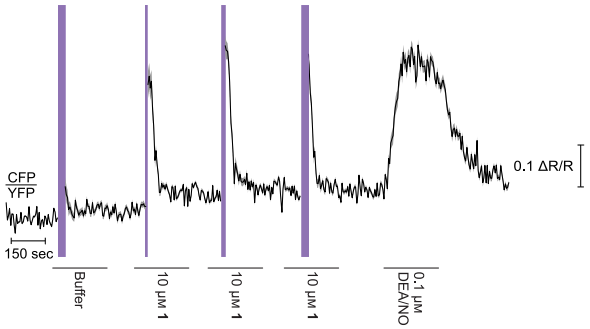

Figure S9. Averaged time traces from cGMP imaging with the cGi500 sensor shown in Figure 2C. Shown are the calculated CFP/YFP emission ratios in ΔR/R (black), normalised to averaged baseline signals. Mean values and standard deviations (grey) were calculated by OriginPro 2017. The time window is indicated when specific compounds were perfused over the cells. The respective illumination times (5 s, 15 s, 30 s, at 340 nm) are indicated by purple bars. Addition of buffer served as negative control; in this experiment we observed a small reduction in FRET upon illumination of only buffer, indicating UV light alone might influence cGMP levels. DEA/NO served as a positive NO control. Shown are the averaged time traces of 25 cells of a series of increasing irradiation times (5 s – 30 s) keeping concentration of **1** constant (10 µM).

Examination of cytotoxicity of Npom-protected NONOate 1

In order to test for potential cytotoxicity of our compound **1**, we submitted HEK 293T cells to different amounts of **1** for different periods of time and subsequently checked the viability of the cells by microscopy. HEK 293T cells were grown in a 25 cm^2 cell culture flask in DMEM with 10% fetal bovine serum, penicillin (100 U/ml), and streptomycin (100 µg/ml) at 37 °C and with 5 % CO_2 in a water saturated steam atmosphere. At the start of the experiment, medium was removed, cells were washed with 5.0 ml PBS, incubated with 500 µl trypsin/ethylene-diaminetetraacetic acid for 2 min, and 4.5 ml medium were added. The cell number was determined by incubation with trypan blue for 2 min and counting in a hemacytometer, then 10 000 cells per well were seeded into 45 wells of a 96 well plate.

After 24 h, medium was replaced by DMEM with 10 % fetal bovine serum without phenol red and cells were examined under the microscope with 10x magnification (Figure S10, A). Subsequently, medium was replaced with medium containing substances, at which all samples were conducted in triplicates. Only medium and medium supplemented with 0.1 % DMSO served as negative controls, blasticidin (15 µg/ml) as positive control, compound **1** was added in three concentrations (10 µM, 25 µM, and 50 µM). After additional 20 h and 23 h, compound **1** (10 µM, 25 µM, and 50 µM) was added to further wells.

24 h after preceding microscopy, cells were again examined under the microscope with 10x magnification. Representative images of the triplicate samples of negative and positive controls (panels B–D), cells treated with 10 µM **1** for 1 h, 4 h, or 24 h (panels E, F, G, respectively), with 25 µM **1** for 1 h, 4 h, or 24 h (panels H, I, J, respectively), and with 50 µM **1** for 1 h, 4 h, or 24 h (panels K, L, M, respectively) are shown in Figure S10. It is apparent that after treatment with compound **1**, there was no change in morphology of the cells or cell number in comparison to the negative controls, whereas death of all cells occurred in the positive control (panel D).

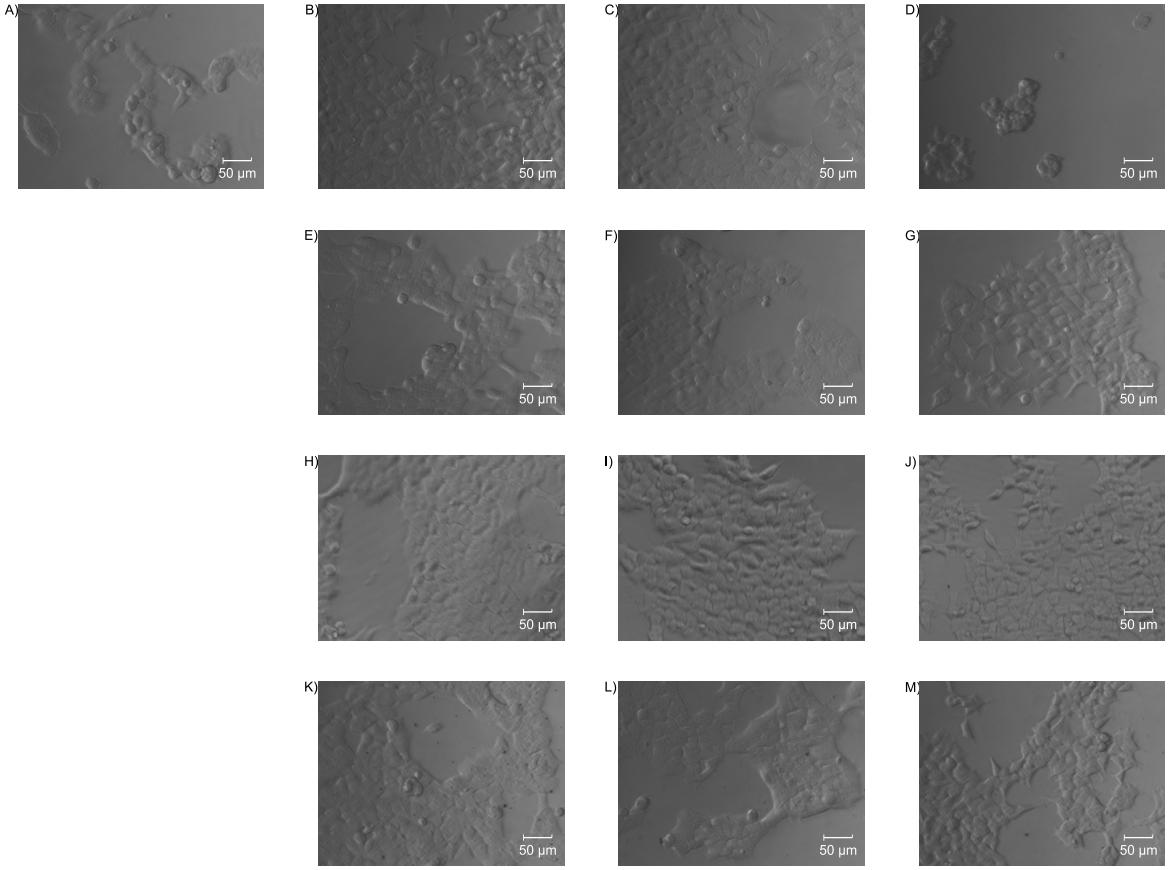

Figure S10. Microscopy images (10x magnification) of cytotoxitcity test of Npom-protected NONOate **1** in HEK 293T cells. A) Untreated cells at the beginning of the experiment. B) – J) Cells after 24 h with different treatments. B) Medium as negative control. C) Medium supplemented with 0.1 % DMSO as additional negative control. D) Blasticidin (15 µg/ml) as positive control. E) 10 µM **1** for 1 h. F) 10 µM **1** for 4 h. G) 10 µM **1** for 24 h. H) 25 µM **1** for 1 h. I) 25 µM **1** for 4 h. J) 25 µM **1** for 24 h. K) 50 µM **1** for 1 h. L) 50 µM **1** for 4 h. M) 50 µM **1** for 24 h.

The irradiation at 340 nm and the products of the deprotection of compound **1**, e.g. nitroso acetophenone **4**, formaldehyde (**5**), and unprotected NONOate **6** and consequentially generated pyrrolidine and NO could also possibly be cytotoxic. However, VSMCs were permanently observed during cGMP imaging measurements. As shown in Figure S11, VSMCs did not display any morphological signs of damage at the end of the respective measurement and looked as viable as at the beginning of the respective experiment. Furthermore, VSMCs were stimulated with DEA/NO (0.1 µM) at the end of each experiment to ensure the cells were still alive and capable of generating a cGMP response, which was always the case (see Figures S8, S9). In conclusion, cytotoxicity did not restrict cGMP imaging experiments with our Npom-protected NONOate **1** in any way.

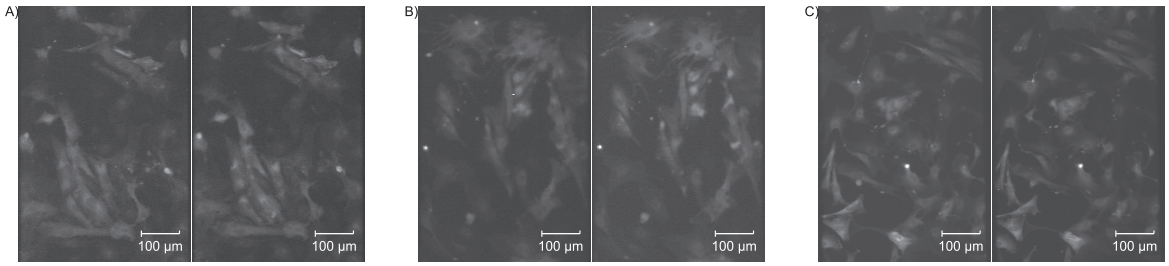

Figure S11. YFP emission microscopy images (10x magnification) of VSMCs at the beginning and at the end of each cGMP imaging experiment. The first (each left panel) and the last (each right panel) five frames were compiled for each experiment (A–C, respectively). A) VSMCs of concentration series of compound **1** (0.1 µM – 100 µM) with constant irradiation time (5 s) shown in Figure 2A. B) VSMCs of concentration series of compound **1** (1 µM – 100 µM) with increased but constant irradiation time (15 s) shown in Figure 2B. C) VSMCs of series of increasing irradiation times (5 s – 30 s) keeping concentration of **1** constant (10 µM) shown in Figure 2C.

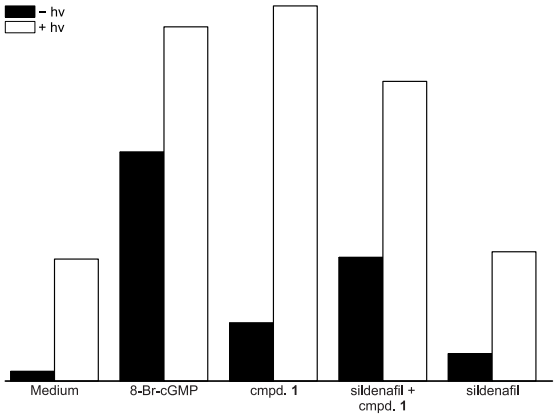

Figure S12. Intensity ratios of p-VASP bands (primary antibody: Phospho-VASP Ser239) of the Western blot shown in Figure 2D. Band intensities of both bands for p-VASP were combined for each lane. ± hv indicates illumination for 15 s with 365 nm light; compound **1** (100 µM) was applied for 5 min; medium served as a negative control, 8-Br-cGMP (100 µM, incubation for 5 min) as a positive control; sildenafil (30 µM, incubation for 5 min) blocks cGMP degradation. Intensities were calculated with Fiji.[S4]

Literature

[S1] A. Hanswillemenke, T. Kuzdere, P. Vogel, G. Jékely, T. Stafforst, *J. Am. Chem. Soc.* **2015**, *137*, 15875–15881.

[S2] Y. Zhu, T. Wang, F. Gai, S. I. Chan, J. J.-T. Huang, R. W. Larsen, R. S. Rock, K. C. Hansen, S. G. Chaulk, O. A. Kent, A. M. Macmillan, W. T. Monroe, F. R. Haselton, S. B. Cambridge, *Dynamic Studies in Biology: Phototriggers, Photoswitches and Caged Biomolecules* (Eds.: M. Goeldner, R. S. Givens), Wiley-VCH, Weinheim, **2005**, p. 159.

[S3] L. K. Keefer, R. W. Nims, K. M. Davies, D. A. Wink, *Methods Enzymol.* **1996**, *268*, 281–293.

[S4] J. Schindelin, I. Arganda-Carreras, E. Frise, V. Kaynig, M. Longair, T. Pietzsch, S. Preibisch, C. Rueden, S. Saalfeld, B. Schmid, J.-Y. Tinevez, D. J. White, V. Hartenstein, K. Eliceiri, P. Tomancak, A. Cardona, *Nat. Methods* **2012**, *9*, 676–682.

A.2.4 Publication 4 (submitted)

Light-controlled RNA-Targeting with Two Self-Labeling Enzymes

Alfred Hanswillemenke, Tim Stefan Berneiser, Marius Blackholm, Johann Kaiser, Anna S. Stroppel, Karthika D. Kiran Kumar, Thorsten Stafforst.

Light-controlled RNA-Targeting with Two Self-Labeling Enzymes

Alfred Hanswillemenke[1], Tim Stefan Berneiser[1], Marius Blackholm[1], Johann Kaiser[1], Anna Sofia Stroppel[1], Karthika D. Kiran Kumar[1] and Thorsten Stafforst[1,2]*

[1]University of Tübingen, Interfaculty Institute of Biochemistry, Auf der Morgenstelle 15, 72076 Tübingen (Germany)

[2]Gene and RNA Therapy Center (GRTC), Faculty of Medicine University Tübingen

*correspondence to thorsten.stafforst@uni-tuebingen.de

Abstract

Rationally programmable RNA-targeting strategies are a prerequisite for the precise and efficient manipulation of information encoded in the (epi)transcriptome of the cell. Besides Cas-based tools, self-labeling enzymes have been applied for that purpose with high versatility. The latter strategy benefits in particular from the engineering capability of the small molecule-based self-labeling moieties. Here, we further engineered that approach to control RNA-targeting and RNA editing with light and applied it to swap between two RNA editing events inside the living cell with light. Furthermore, we combined two orthogonal self-labeling enzymes for the recruitment of two distinct fusion proteins to a target RNA inside the cell, showing the approach's versatility and paving the way for further tool development in RNA imaging and transcript engineering.

Introduction

Genetic information is commonly diversified at the transcript level, e.g., by mRNA splicing and modification,[1,2] leading to a mixture of protein isoforms originating from one gene. Due to the short half-life of an mRNA, the derived mixture of protein isoforms can quickly vary over time, e.g., transcription factors in response to external stimuli. Engineering the transcriptome by site-directed targeting of RNA editing enzymes is a recent field of research that aims at manipulating the balance of protein isoforms. One example is site-directed A(denosine)-to-I(nosine) RNA editing.[3] As inosine is biochemically read as guanosine, protein isoforms with altered function can be created in a highly rational manner.[4] To target particular sites on specific mRNA transcripts, we engineered an artificial RNA editing system called SNAP-ADAR,[5] which is based on the fusion of the self-labeling SNAP-tag[6] domain with the catalytic deaminase domain from the RNA editing enzyme ADAR (adenosine deaminase acting on RNA). The SNAP-tag catalyzes the transfer of a single guideRNA to itself, provided the latter is modified with the O^6-benzylguanine (BG) moiety. The covalently attached guideRNA then steers the SNAP-ADAR to its target (m)RNA in a programmable way following Watson-Crick base-pairing rules. The SNAP-ADAR approach applies a unique RNA-targeting mechanism, which enables the use of chemically densely modified guideRNAs.[4] These chemical modifications allow for controlling bystander editing in adenosine-rich targets.[7] Furthermore, the RNA-targeting mechanism works very well even under low expression of the artificial editing enzyme, markedly reducing global off-target effects.[8] Editing with a SNAP-ADAR is fully dependent on the SNAP-tag-mediated, covalent assembly of guideRNA and SNAP-ADAR. This conjugation reaction can

be exploited to include further layers of control. By installing an Npom (6-nitropiperonyloxymethyl) photo-caging group at the *N*7 of the BG moiety on the guideRNA, we previously were able to implement a photo-triggered on-switch of RNA editing activity.[9] Light is a highly attractive trigger to study the dynamics of biochemical processes in cell culture and in transparent animals or their developing embryos.[10] Considerable efforts have been made to control RNA-guided proteins, e.g., the RNA-induced silencing complex (RISC) or the CRISPR-Cas system. For this, laboratories have developed caged nucleotides and amino acids to block functionally important sites temporarily,[11,12,13] and control over genome editing with caged nucleotides has been described recently in vitro and in vivo[14,15,16].

Here, we now report the light-triggered off-switch of RNA editing. In combination with the established on-switch,[9] this was used to perturb the balance of two editing events with opposite effects on the endogenous *STAT1* transcript. Furthermore, we combined two orthogonal self-labeling enzymes, SNAP- and CLIP-tag, and achieved simultaneous (photo-)control of the recruitment and disassembly process of two different proteins inside the living cell. This highlights the versatility of this RNA-guided RNA-targeting platform, which relies on the chemical engineering of the self-labeling moieties at the guideRNA component.

Results and Discussion

RNA editing can be switched on and off by light

The editing reaction is strictly dependent on the covalent assembly of guideRNA and SNAP-ADAR.[8,9] We reasoned that introducing a photo-cleavable group between the guideRNA and the self-labeling BG moiety would enable the light-induced off-switch of RNA editing (Figure 1a). For this, we conceived a new photo-cleavable amino acid based on 6-nitropiperonyl alcohol.[17] In a simple five-step synthesis starting from 4',5'-methylenedioxy-2'-nitroacetophenone, the photo-cleavable moiety was incorporated into the Fmoc-protected amino acid Fmoc-^{UV}X-OH (Figure 1b). Through solid-phase peptide synthesis, Fmoc-^{UV}X-OH was included in a photo-cleavable BG-linker (BG-^{UV}X-OH) containing a terminal carboxyl group for subsequent attachment to a guideRNA. At this stage, the products and kinetics of photo-cleavage were determined (Figure 1c). We compared the cleavage of BG-^{UV}X-OH side-by-side with the decaging of $^{N7\text{-}Npom}$BG-TFA[9]. We expected very similar key properties of both molecules (e.g., UV spectra, quantum yield). Indeed, BG-^{UV}X-OH decomposed under formation of the respective nitrosoacetophenone and (4-hydroxybenzoyl)-glycine, as confirmed by HPLC-MS and comparison to reference samples (Supporting Figure 1). The absorbance spectra >340 nm of both photo-labile molecules overlapped almost perfectly, and both reacted upon irradiation (transilluminator, 365 nm at 7.9±0.2 mW/cm^2, PBS buffer pH 7, HPLC assay) with very similar kinetics, e.g., $t_{1/2}$ = 17±2 s (BG-^{UV}X-OH) and 15±3 s ($^{N7\text{-}Npom}$BG-TFA). We then activated BG-^{UV}X-OH as an hydroxysuccinimide ester, coupled it to a guideRNA carrying a 5´-terminal amino linker, and purified the product by PAGE following a recently described procedure.[18] The BG-^{UV}X-guideRNA was incubated *in vitro* with purified SNAP-ADAR protein, and the assembly reaction was readily followed as a band shift of the SNAP-ADAR protein via SDS-PAGE, similar as before.[9] Within 60 s of irradiation (365 nm), the SNAP-ADAR-guideRNA conjugate almost entirely released SNAP-ADAR in a light-dose-dependent manner, demonstrating the photo-triggered disassembly of guideRNA and SNAP-ADAR protein (Figure 1d).

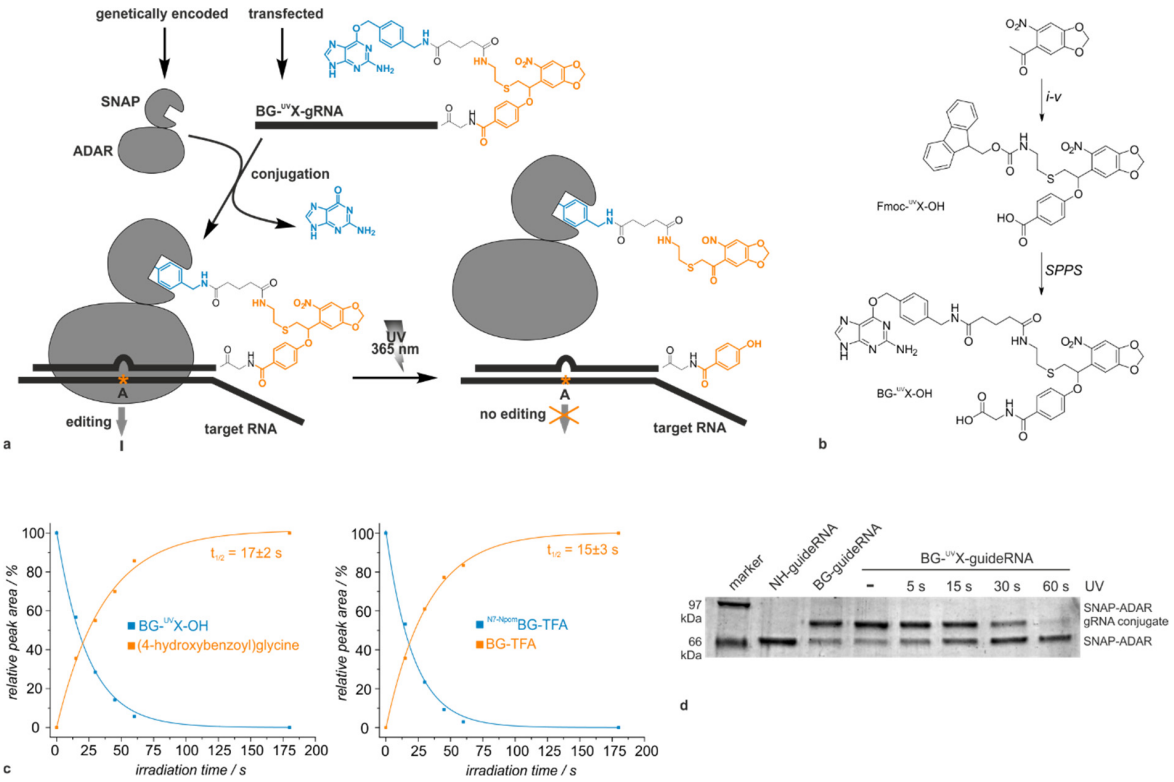

Figure 1. Engineering of the light-triggered disassembly of a guideRNA-effector protein conjugate. a) *Schematic overview. The self-labeling BG moiety (blue) mediates the covalent assembly between guideRNA and SNAP-tagged effector protein, here, the editing enzyme ADAR, which leads to site-directed A-to-I RNA editing (orange asterisk). The BG-^{UV}X-guideRNA contains a photosensitive moiety (orange), which can be used to photo-disassemble the guideRNA-SNAP-ADAR conjugate, stopping targeted RNA editing abruptly.* ***b)*** *Synthesis of the photo-cleavable, Fmoc-protected amino acid Fmoc-^{UV}X-OH, and structure of the photo-cleavable linker BG-^{UV}X-OH. i) Br_2, dioxane, 67%; ii) (9H-Fluoren-9-yl)methyl (2-mercaptoethyl)carbamate, TEA, THF, 90%; iii) $NaBH_4$, MeOH, 98%; iv) methyl paraben, PPh_3, DIAD, THF, 28%; v) LiOH, K_2CO_3, Fmoc-OSu, THF, ACN, H_2O, 50%, yield SPPS: 71%.* ***c)*** *Photo-cleavage kinetics of BG-^{UV}X-OH and $^{N7\text{-}Npom}$BG-TFA monitored by HPLC. For more details, see Supporting Information and Supporting Figure S1.* ***d)*** *In-vitro assay of assembly and light-triggered disassembly of the SNAP-ADAR-guideRNA conjugate. A BG-^{UV}X-guideRNA was incubated with purified SNAP-ADAR3 for conjugation and treated with 365 nm light (transilluminator; light intensity 7.9±0.2 mW/cm^2) for various amounts of time (0-60 s) prior to SDS-PAGE analysis. As controls, the analog photo-insensitive BG-guideRNA and the conjugation-incompetent NH-guideRNA were loaded, defining the position of the free and guideRNA-conjugated SNAP-ADAR band, respectively. For more details on the experimental setup, see Supplementary Information.*

We then tested the photo-controlled editing of the endogenous *STAT1* transcript in Flp-In 293T-REx cells stably expressing[8] the SNAP-ADAR1Q editase (Figure 2). STAT1 is an essential transcription factor in pathogen defense and cell homeostasis and is activated by phosphorylation of tyrosine 701 (Y701) in response to cytokines and growth factors.[19] After phosphorylation, STAT1 dimerizes, enters the nucleus, and acts as a transcription factor. We had shown before that Y701 in STAT1 can be defunctionalized to cysteine (C) by RNA editing,[8] mimicking a naturally occurring genetic variant related to predisposition to mycobacterial diseases[20]. To follow the photo-manipulation, we took a time profile of the editing reaction. With a standard BG-modified guideRNA, the maximum editing yield (~70%) was obtained 12 h post transfection; after 48 h, the editing yield was reduced by half. This effect was independent of the irradiation of the cells. The same trend was observed for the photo-cleavable BG-^{UV}X-guideRNA in the absence of light. However, when the cells were irradiated

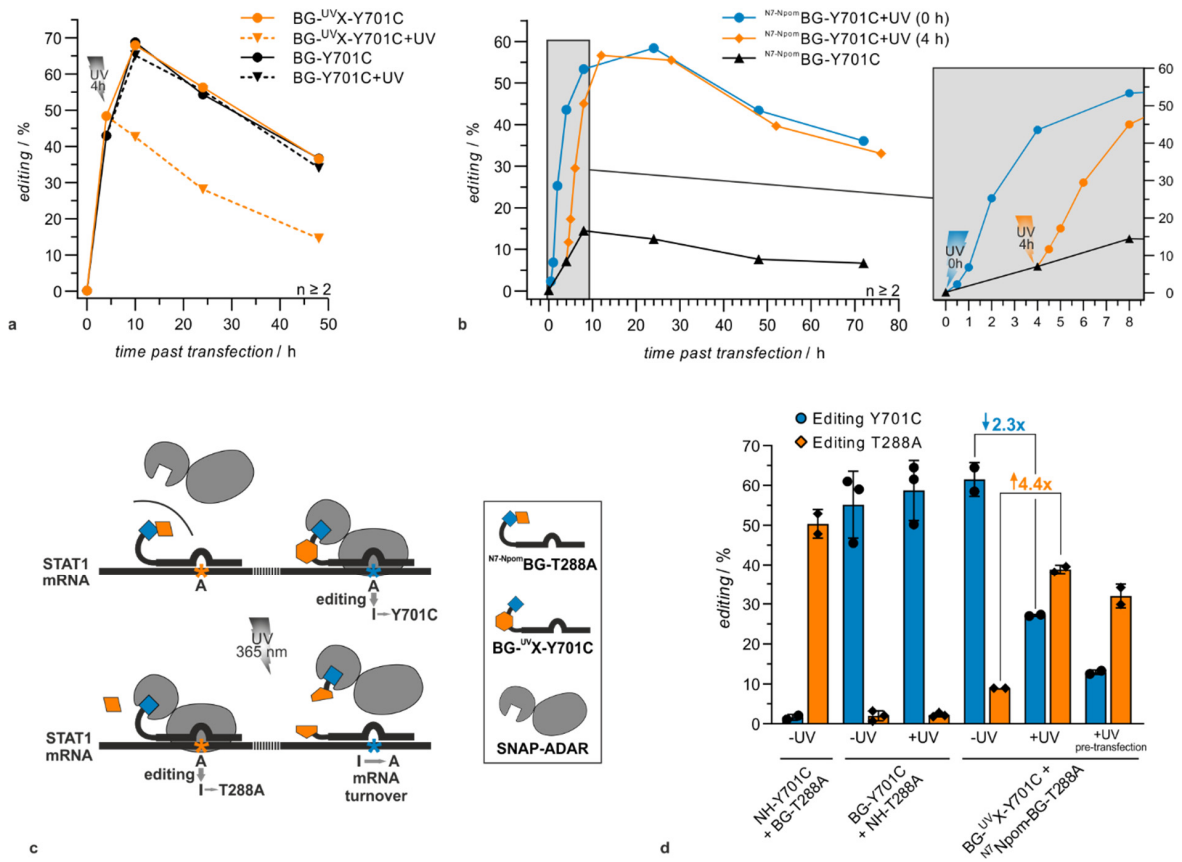

Figure 2. Photo-control of RNA editing at two different sites in the endogenous STAT1 transcript. a) *Photo off-switch of STAT1 editing. Shown is the editing yield at the endogenous STAT1 transcript (Y701C) over 72 h, with either a photo-cleavable BG-^{UV}X- or a normal BG-guideRNA, in the absence or presence of a light trigger (+UV, 365 nm), which was applied for 3 min, 4 h after guideRNA transfection, as indicated.* ***b)*** *Photo on-switch of STAT1 editing. Shown is the editing yield at the endogenous STAT1 transcript (Y701C) over 48 h, in the presence of a photo-activatable $^{N7\text{-}Npom}$BG- guideRNA, absence or presence of a light trigger (+UV). The light trigger was applied for 2 min (365 nm) either prior to guideRNA transfection (0 h) or 4 h afterwards (4 h).* ***c)*** *Concept of photo-swapping between two editing events on endogenous STAT1. Two guideRNAs, one with a photo-activatable, one with a photocleavable linker, are co-transfected. Before irradiation, editing takes place at Y701 but not at T288. After irradiation, editing activity swaps, and T288 but not Y701 is edited.* ***d)*** *Photo-swap is achieved by co-transfection of a photo-sensitive BG-^{UV}X-guideRNA for Y701C and a photo-activatable $^{N7\text{-}Npom}$BG-guideRNA for T288A editing. Shown are controls with and without photo-trigger (365 nm, 3 min), control guideRNAs with and without self-labeling moiety (NH vs. BG), control guideRNAs with and without photo-control (BG vs. $^{N7\text{-}Npom}$BG vs. BG-^{UV}X).* For more details on the experimental setup, see Supplementary Information and Supporting Figure S2.

on a transilluminator (3 min, 365 nm) 4 h post transfection, the time profiles of the cleavable and non-cleavable guideRNA clearly segregated after irradiation, indicating a sudden stop of the editing reaction via photo-cleavage of guideRNA and SNAP-ADAR1Q, followed by a slow replacement of the edited transcript with newly synthesized unedited RNA (Figure 2a). We also tested the on-switch of RNA editing by transfecting a caged $^{N7\text{-}Npom}$BG-guideRNA[9] with or without irradiation prior to transfection. As expected, the editing performance clearly differed, achieving editing yields >60% with the pre-irradiated guideRNA, while the untreated, caged guideRNA gave only minor yields <15% (Figure 2b). However, when the caged guideRNA was irradiated 4 h post transfection (2 min, 365 nm), editing levels increased abruptly to a maximum yield of ≈60%, and the profile matched that of

the uncaged control guideRNA. This validates our previous results obtained on a fluorescent reporter gene, on an endogenous target.

The transient manipulation of the STAT1 transcript by RNA editing could become an attractive application for photo-triggered spatiotemporal control, as many heterozygous STAT1 mutations have been reported with clear clinical phenotypes.[20,21] To test this concept, we conceived the photo-triggered swap between two editing events, Tyr701>Cys and Thre288>Ala. While the first mutation is reported as a loss-of-function mutation, the latter is a known gain-of-function mutation.[21] For this, the cleavable BG-^{UV}X-guideRNA for Y701C editing was co-transfected with a caged $^{N7\text{-}Npom}$BG-guideRNA for T288A editing. In the absence of light, an editing level of >50% was obtained at Y701 24 h post transfection, similar to the one of the positive control (BG). In contrast, the editing level at T288 stayed <15%. However, when the cells were irradiated (3 min, 365 nm) 4 h post transfection, the editing levels at Y701 and T288 had swapped 20 h later (Figure 2d), demonstrating the feasibility of the concept. However, the light-driven off-switch was not complete. Control experiments simulating a photo-disassembly yield of 97% (Supporting Fig. S3) gave residual editing yields up to 10% showing that the high editing efficiency of the SNAP-ADAR tool is causing that problem.

Two RNA-guided proteins can be controlled by light

To further characterize the achieved photo-control, we photo-triggered the (dis)assembly reaction and followed the process inside the living cell by fluorescence microscopy. First, we expressed a plasma membrane-bound SNAP-tag fusion[22] and labeled it with BG-^{UV}X-Atto488, giving rise to intensive green staining of the cell surface (Supporting Fig. 2). As expected, the Atto488 stain was efficiently removed with a short pulse (100 ms) of UV light (390 nm, lumencor® AuraII), indicating that the engineered photo-labile linker is applicable to achieve fast disassembly of the fluorescence dye-protein conjugates on the living cell. To visualize the RNA-guided steering of proteins inside the living cell, we created a HeLa cell line stably expressing the green fluorescent reporter protein SNAP-$(eGFP)_3$ and the blue fluorescent stress granule marker BFP-G3BP1[23] (Figure 3a). We transfected a BG-poly(U)-guideRNA into these cells to recruit the SNAP-$(eGFP)_3$ reporter protein in a guideRNA-dependent manner into arsenite-induced stress granules, which contain a bulk of polyadenylated mRNA[24]. Indeed, only in presence of a BG-poly(U)-guideRNA a strong co-localization (Pearson coefficient 0.7) of the green (GFP) and blue (BFP) channel was detected (Figure 3b). A poly(U)-guideRNA carrying the O^2-benzylcytosine (BC) moiety served as a negative control. Notably, the BC moiety could not induce a strong green-blue correlation (Pearson coefficient <0.1). The BC moiety is the substrate for the self-labeling CLIP-tag.[25] Hence, the results indicated that the orthogonality between BG/SNAP- and BC/CLIP-tag might be sufficient to exploit them for the concurrent control of two different proteins inside the living cell. To further elucidate this, we created cell lines stably expressing the red fluorescent NLS-CLIP-$(mCherry)_3$ reporter protein beside NLS-SNAP-$(eGFP)_3$ and transfected them with poly(U)-guideRNAs either carrying the BG or BC self-labeling moiety (Figure 3d). Each guideRNA resulted in the respective coloring of arsenite-induced stress granules. The BG-guideRNA colored them predominantly green, the BC-guideRNA red. To better compare the fluorescence intensities of the red and green channel, we synthesized a bifunctional linker comprising of both, one BG and one BC moiety, and attached it to the poly(U)-guideRNA (Figure 3c). The BG/BC-poly(U)-guideRNA consistently recruited both fluorescent proteins, presumably in a 1:1: stoichiometry, into the stress granules and achieved a stable green-to-red fluorescence intensity of 0.78. For comparison, the monofunctional BC-guideRNA recruited significantly less GFP resulting in a green-to-red intensity ratio of only 0.11 (Figure 3d).

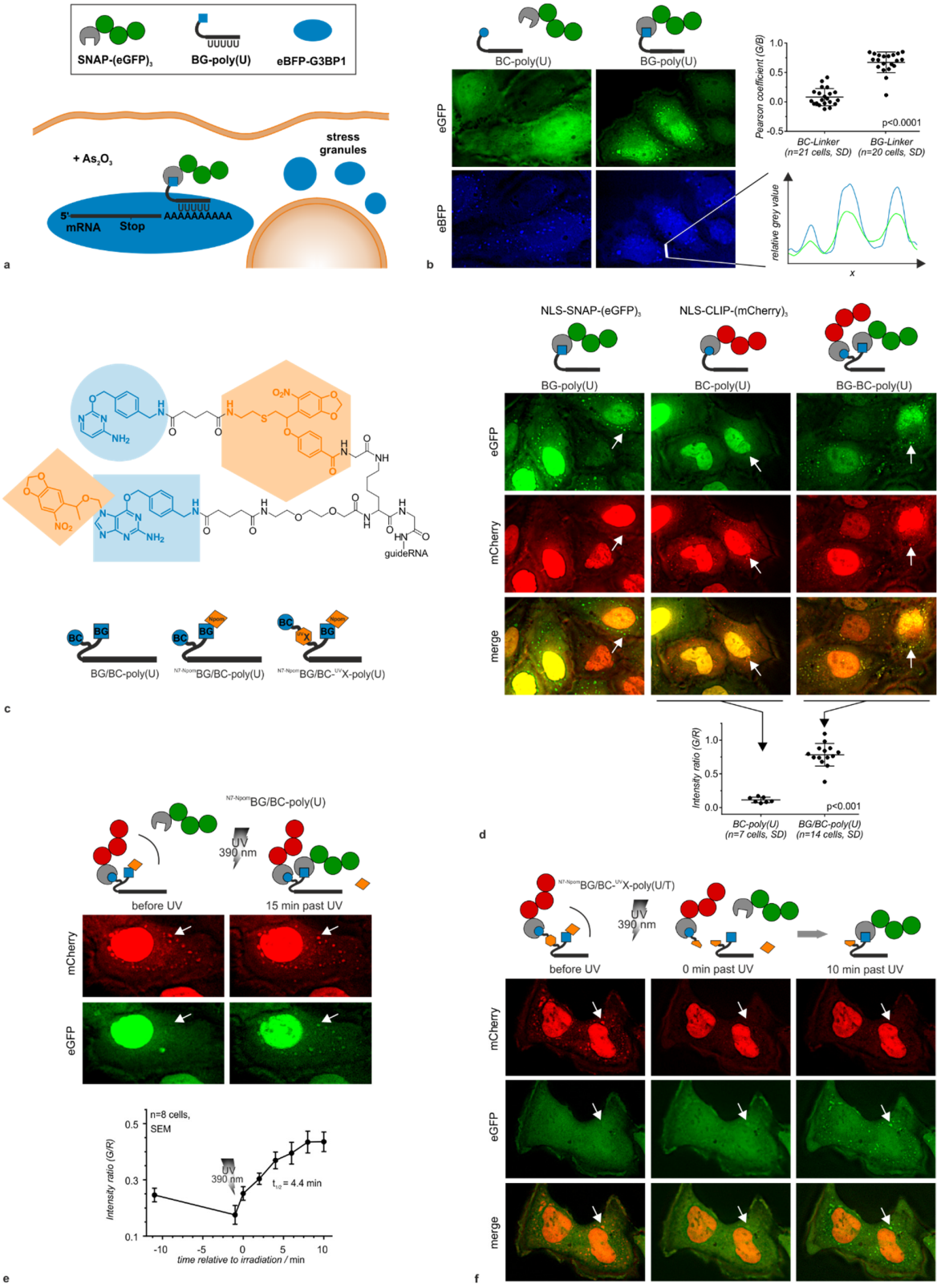

Figure 3. Orthogonal recruitment of two different proteins under photo-control. a) *Scheme of the staining of polyadenylated mRNAs in arsenite-induced stress granules with guideRNAs conjugated to fluorescent reporter proteins.* ***b)*** *Recruitment of a BG-poly(U)-guideRNA into arsenite-induced stress granules (50 µM As_2O_3, 30 min) in a transgenic HeLa cell line, stably expressing a SNAP-$(eGFP)_3$ reporter and a BFP-G3BP1 stress granule marker. Arsenite-induced stress granules appear as blue foci. The BG-poly(U)-guideRNA gives co-staining in the*

green channel, whereas the control BC-poly(U)-guideRNA does less, as indicated by the Pearson coefficient for the correlation of green and blue fluorescence at blue foci in N ≥20 cells. Statistical significance was calculated by an unpaired Welch's t-test. ***c)*** *Highly functionalized linkers engineered to provide photo-control over the concurrent and orthogonal RNA-guided steering of two different proteins based on the self-labeling enzymes SNAP- and CLIP-tag.* ***d)*** *Orthogonal recruitment of two proteins. Transgenic HeLa cells, stably co-expressing SNAP-(eGFP)$_3$ and CLIP-(mCherry)$_3$, were either transfected with a poly(U)-guideRNA carrying the BG, BC, or bifunctional BG/BC self-labeling moieties. The red channel monitors recruitment of mCherry; the green channel monitors recruitment of eGFP upon arsenite-induced stress granule formation. The intensity ratio (green/red) was measured at red foci in N=7-14 cells. Statistical significance was calculated by an unpaired Welch's t-test.* ***e)*** *Light-triggered recruitment of a protein into stress granules. A bifunctional, photo-caged $^{N7\text{-}Npom}$BG/BC-poly(U)-guideRNA was transfected into a eGFP/mCherry transgenic HeLa reporter cell line. After arsenite treatment, the light-induced (390 nm, 100 ms, lumencor® AuraII) recruitment of eGFP to mCherry-stained stress granules was monitored over time. Conjugation kinetics have been obtained from following the green/red ratios over 10 min. Error bars indicate standard error of the mean (SEM) for measurements in N=8 cells.* ***f)*** *Light-triggered swapping of two different proteins in stress granules. A bifunctional, photosensitive, and photo-caged $^{N7\text{-}Npom}$BG/BC-^{UV}-X-poly(U)-guideRNA was transfected into the eGFP/mCherry transgenic HeLa reporter cell line. After arsenite treatment, stress granules appear red (mCherry) but not green (eGFP). After light-treatment (390 nm, 100 ms, lumencor® AuraII), mCherry fluorescence (red channel) disappears immediately and is replaced by eGFP fluorescence (green channel) over the course of several minutes. For more detail on cell line creation and experimental setup see the Supplementary Information.*

Next, we included photo-control into the orthogonal assembly reaction. By combining solid and liquid phase peptide chemistry, we synthesized the photo-caged, bifunctional linker $^{N7\text{-}Npom}$BG/BC, carrying an *N7*-Npom photo-caged BG moiety and a regular BC moiety, and attached it to the 5´-terminus of a poly(U)-guideRNA (Figure 3c). As the BG moiety is photo-caged at the beginning, the respective $^{N7\text{-}Npom}$BG/BC-poly(U)-guideRNA stained arsenite-induced stress granules preferentially red before irradiation, resulting in an initial green-to-red ratio of ≈0.2. However, after a short pulse of 390 nm light (100 ms, lumencor® AuraII), the green-to-red ratio increased to a final value of ≈0.45 after 10 min, demonstrating the light-induced, covalent co-recruitment of the free-floating SNAP-tagged GFP protein (Figure 3e). The kinetics of the SNAP-(eGFP)$_3$ recruitment into the stress granules could be followed live by fluorescence microscopy. From the slope of the green-to-red ratio change over time, a half-life of ≈ 4.4 min was estimated, defining the time frame for photo-driven assembly reactions that can be realized with the SNAP-/CLIP-tag RNA-targeting approach. Finally, we combined photo-triggered on- and off-switch within one guideRNA. For this, we synthesized the highly complex $^{N7\text{-}Npom}$BG/BC-^{UV}X-Linker comprising of the photo-caged BG moiety in combination with a photo-cleavable BC moiety, and attached it to a poly(U)-guideRNA. As expected, arsenite-induced stress granules turned red but not green after transfection of this guideRNA, indicating the preferred recruitment of CLIP-(mCherry)$_3$. However, triggered by a short UV light pulse (390nm 100 ms, lumencor® AuraII), the red fluorescence disappeared within seconds, followed by a slow recruitment of green fluorescence over several minutes, indicating the exchange of the RNA-targeted protein from CLIP-(mCherry)$_3$ to SNAP-(eGFP)$_3$ inside stress granules (Figure 3f).

Conclusions

In summary, we demonstrated the general versatility of the RNA-guided RNA-targeting strategy based on self-labeling enzymes like SNAP[6]- and CLIP-tag[25]. Self-labeling enzymes have unique and advantageous properties compared to competing strategies that rely on Cas9[26]- or Cas13[3,27]. First, SNAP- and CLIP-tag are small proteins (28 kDa), engineered from a human *O*^{6}-methylguanine-DNA-methyltransferase, and are ready for C- and N-terminal tagging.[6,25] They are readily cloned and stably

integrated into cell lines, as demonstrated here by the generation of cell lines co-expressing SNAP- and CLIP-tagged reporter fusion proteins. Second, self-labeling enzymes apply a covalent mechanism for the assembly of functional RNA-protein conjugates.[4] Importantly, different self-labeling enzymes can be combined for the orthogonal and concurrent recruitment of two different proteins in a defined stoichiometry inside the living cell, as we have demonstrated here. Furthermore, the unique covalent assembly mechanism allows to rationally engineer further layers of control into the linker that mediates the assembly reaction. Specifically, we now demonstrated both, the inclusion of a photo on- and a photo off-switch into the assembly reaction. This was then applied to photo-swap between two different RNA editing events on the endogenous *STAT1* transcript, highlighting novel opportunities for the targeted engineering of the transcriptome.[3,4] With a pair of orthogonal caging groups, a sequential photo-control would also be conceivable in the future.[12,13] Off-target editing is a major limitation of current RNA and DNA editing tools.[3,4] Importantly, the SNAP-ADAR system is characterized by rather low levels of global off-target editing and good control over bystander editing in the mRNA/guideRNA duplex.[8] Accordingly, we found no bystander editing at both STAT1 target sites (Y701, T288) even though highly adenosine-rich sequences were addressed (Supporting Information pp.64 ff). Our strategy will enable and inspire new applications to photo-control biochemical processes,[10] e.g., it might become useful to transiently manipulate specific transcripts with sufficient spatiotemporal control in quickly developing embryos, like zebrafish or Platynereis dumerilii,[9] or as a trigger in novel applications like RNA timestamp[28]. The presented microscopy data suggests that our RNA-targeting platform could also be used to manipulate the transcriptome on a much faster time scale, e.g., seconds to minutes. Finally, we have shown the recruitment of two different fusion proteins inside the living cell. This may enable the use of guideRNAs to steer two different enzymes independently inside living cells in the future, e.g. two RNA editases or other writers and erasers of epitranscriptomic marks.

Acknowledgement

We gratefully acknowledge support from the University of Tübingen and the Deutsche Forschungsgemeinschaft (STA1053/3-2; STA1053/4-1; SPP1784: STA1053/8-1; Heisenberg-Program: STA1053/7-1, STA1053/11-1). This work has received funding from the European Research Council (ERC) under the European Union's Horizon 2020 research and innovation program (grant agreement No 647328).

Materials and Methods

Please find detailed information on the procedures of syntheses, editing experiments, irradiation experiments, microscopy experiments, cloning, and sequences of applied oligonucleotides and transgenes in the online Supplementary Information.

Keywords

RNA editing, RNA targeting, Clip-tag, Snap-tag, photo-control

Conflict of Interest

T.S. holds patents on site-directed RNA base editing and is cofounder of, shareholder of and consultant to AIRNA Bio Inc.

References

1. J.D. Keene. RNA regulons: coordination of post-transcriptional events. Nature Reviews Genetics 8, 533–543 (2007).

2. B.S. Zhao, I.A. Roundtree, C. He. Post-transcriptional gene regulation by mRNA modifications. Nat Rev Mol Cell Biol 18, 31-42 (2017).

3. H.A. Rees, D.R. Liu, Base editing: precision chemistry on the genome and transcriptome of living cells. Nat Rev Genet. 19, 770–788 (2018).

4. Vogel, P. & Stafforst, T. Critical review on engineering deaminases for site-directed RNA editing. Curr. Opin. Biotechnol. 55, 74–80 (2019).

5. Stafforst, T. & Schneider, M. F. An RNA-deaminase conjugate selectively repairs point mutations. Angew. Chem. Int. Ed. 51, 11166–11169 (2012).

6. Keppler, A. et al. A general method for the covalent labeling of fusion proteins with small molecules in vivo. Nat. Biotechnol. 21, 86–89 (2003).

7. P. Vogel, M.F. Schneider, J. Wettengel, T. Stafforst. Improving site-directed RNA editing in vitro and in cell culture by chemical modification of the guideRNA. Angew Chem Int Ed Engl 53, 6267-71 (2014).

8. Vogel, P. et al. Efficient and Precise Editing of Endogenous Transcripts with SNAP-tagged ADARs. Nat. Methods 15, 535–38 (2018).

9. Hanswillemenke, A., Kuzdere, T., Vogel, P., Jékely, G. & Stafforst, T. Site-Directed RNA Editing in Vivo Can Be Triggered by the Light-Driven Assembly of an Artificial Riboprotein. J. Am. Chem. Soc. 137, 15875–15881 (2015).

10. N. Ankenbruck, T. Courtney, Y. Naro, A. Deiters. Optochemical Control of Biological Processes in Cells and Animals. Angew Chem Int Ed Engl. 57, 2768–2798 (2018).

11. K. Lenz, A. Heckel. Photoinduced transcription by using temporarily mismatched caged oligonucleotides. Angew Chem Int Ed Engl 44, 471-3 (2005).

12. C. Brieke, et al. Light-controlled tools. Angew Chem Int Ed Engl 51, 8446-76 (2012).

13. N. Ankenbruck, et al. Optochemical Control of Biological Processes in Cells and Animals. Angew Chem Int Ed Engl 57, 2768–2798 (2018).

14. W. Zhou, A. Deiters. Conditional Control of CRISPR/Cas9 Function. Angew Chem Int Ed Engl 55, 5394-9 (2016).

15. E.V. Moroz-Omori, et al. Photoswitchable gRNAs for Spatiotemporally Controlled CRISPR-Cas-Based Genomic Regulation. ACS Cent Sci 6(5), 695-703 (2020).

16. W. Zhou, et al. Spatiotemporal Control of CRISPR/Cas9 Function in Cells and Zebrafish using Light-Activated Guide RNA. Angew Chem Int Ed Engl 59, 8998-9003 (2020).

17. H. Lusic, A. Deiters. A New Photocaging Group for Aromatic N-Heterocycles. Synthesis 13, 2147-2150 (2006).

18. A. Hanswillemenke, T. Stafforst. Protocols for the generation of caged guideRNAs for light-triggered RNA-targeting with SNAP-ADARs. Methods in Enzymology 624, 47-68 (2019).

19. Y.E. Chin, et al. Cell growth arrest and induction of cyclin-dependent kinase inhibitor p21 WAF1/CIP1 mediated by STAT1. Science 272, 719-22 (1996).

20. O. Hirata, et al. Heterozygosity for the Y701C STAT1 mutation in a multiplex kindred with multifocal osteomyelitis. Haematologica 98, 1641–1649 (2013).

21. L. Liu et al. Gain-of-function human STAT1 mutations impair IL-17 immunity and underlie chronic mucocutaneous candidiasis. J Exp Med. 208, 1635-48 (2011).

22. M.A. Brun, et al. Semisynthesis of fluorescent metabolite sensors on cell surfaces. J Am Chem Soc 133, 16235-42 (2011).

23. H. Tourrièr, et al. The RasGAP-associated endoribonuclease G3BP assembles stress granules. J Cell Biol 160, 823-31 (2003).

24. A. Khong, et al. The Stress Granule Transcriptome Reveals Principles of mRNA Accumulation in Stress Granules. Mol Cell 68, 808-820 (2017).

25. Gautier, A. et al. An engineered protein tag for multiprotein labeling in living cells. Chem. Biol. 15, 128–136 (2008).

26. R. J. Marina, et al. Evaluation of Engineered CRISPR-Cas-Mediated Systems for Site-Specific RNA Editing. Cell Rep 33, 108350 (2020).

27. D.B.T. Cox, et al. RNA Editing with CRISPR-Cas13. Science 358, 1019–1027 (2017).

28. S.G. Rodriques, et al. RNA timestamps identify the age of single molecules in RNA sequencing. Nat. Biotechnology 39, 320-325 (2021.)

Supplementary Information

Light-controlled RNA-Targeting with Two Self-Labeling Enzymes

Alfred Hanswillemenke[1], Tim Stefan Berneiser[1], Marius Blackholm[1], Johann Kaiser[1], Anna Sofia Stroppel[1], Karthika D. Kiran Kumar[1] and Thorsten Stafforst[1,2]*

[1]Interfaculty Institute of Biochemistry; University of Tübingen
Auf der Morgenstelle 15; 72076 Tübingen (Germany)

[2]Gene and RNA Therapy Center (GRTC), Faculty of Medicine University Tübingen

**correspondence to thorsten.stafforst@uni-tuebingen.de*

Content:

Extended data

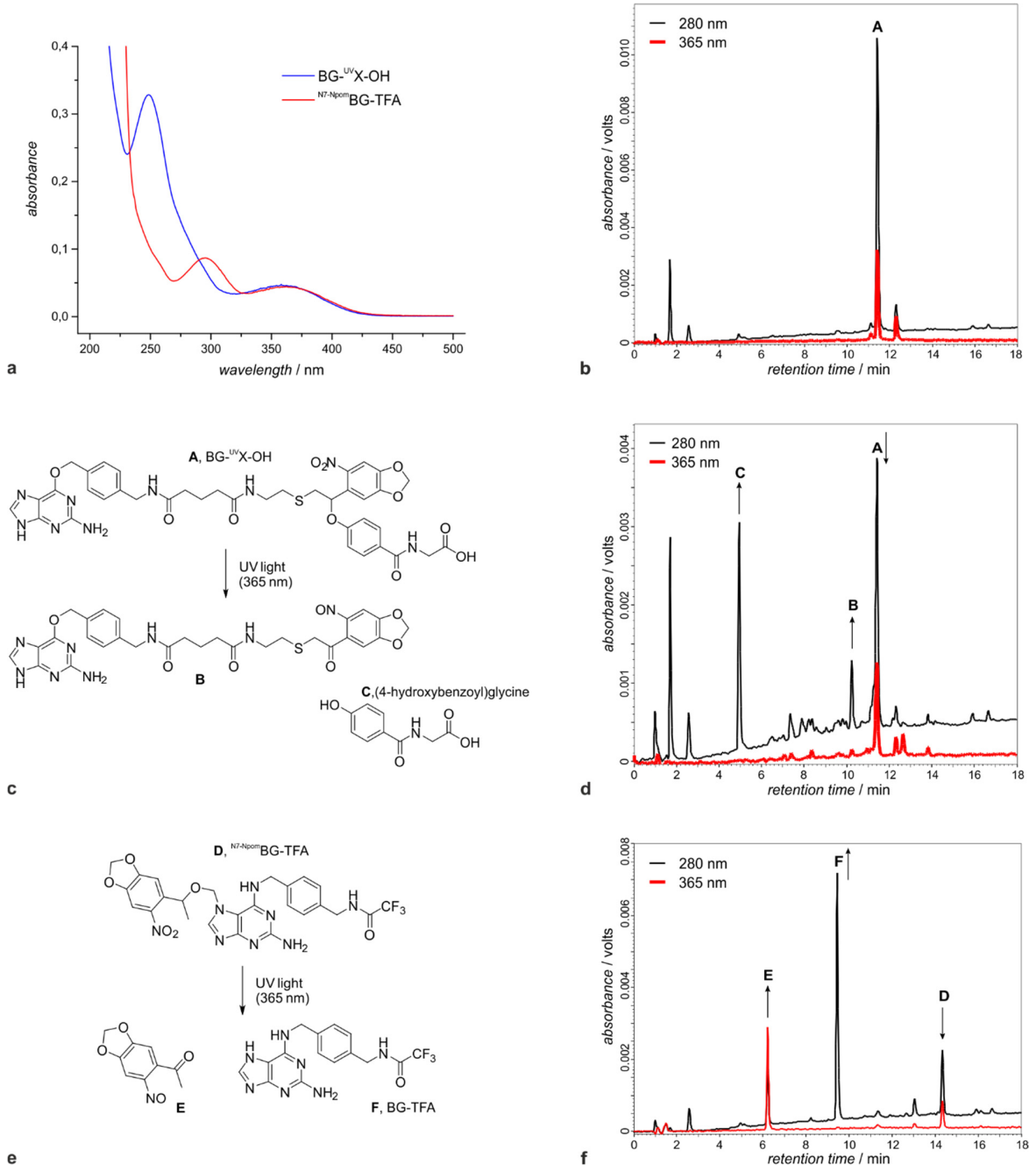

Figure S1. **Photo-dissociation kinetics of BG-^{UV}X-OH.** ***a)*** *Absorption spectra of BG-^{UV}X-OH and $^{N7\text{-}Npom}$BG-TFA.* ***b)*** *Analytical HPLC of BG-^{UV}X-OH before irradiation.* ***c)*** *Expected photo-dissociation products (**B+C**) of BG-^{UV}X-OH (**A**).* ***d)*** *Analytical HPLC of BG-^{UV}X-OH after partial photo-dissociation. Peaks are labeled according to Fig.S1c* ***e)*** *Reference substance $^{N7\text{-}Npom}$BG-TFA (**D**) and the expected decaging products (**E+F**)* ***f)*** *Analytical HPLC of $^{N7\text{-}Npom}$BG-TFA after partial decaging. Peaks are labeled according to Fig.S1e.*

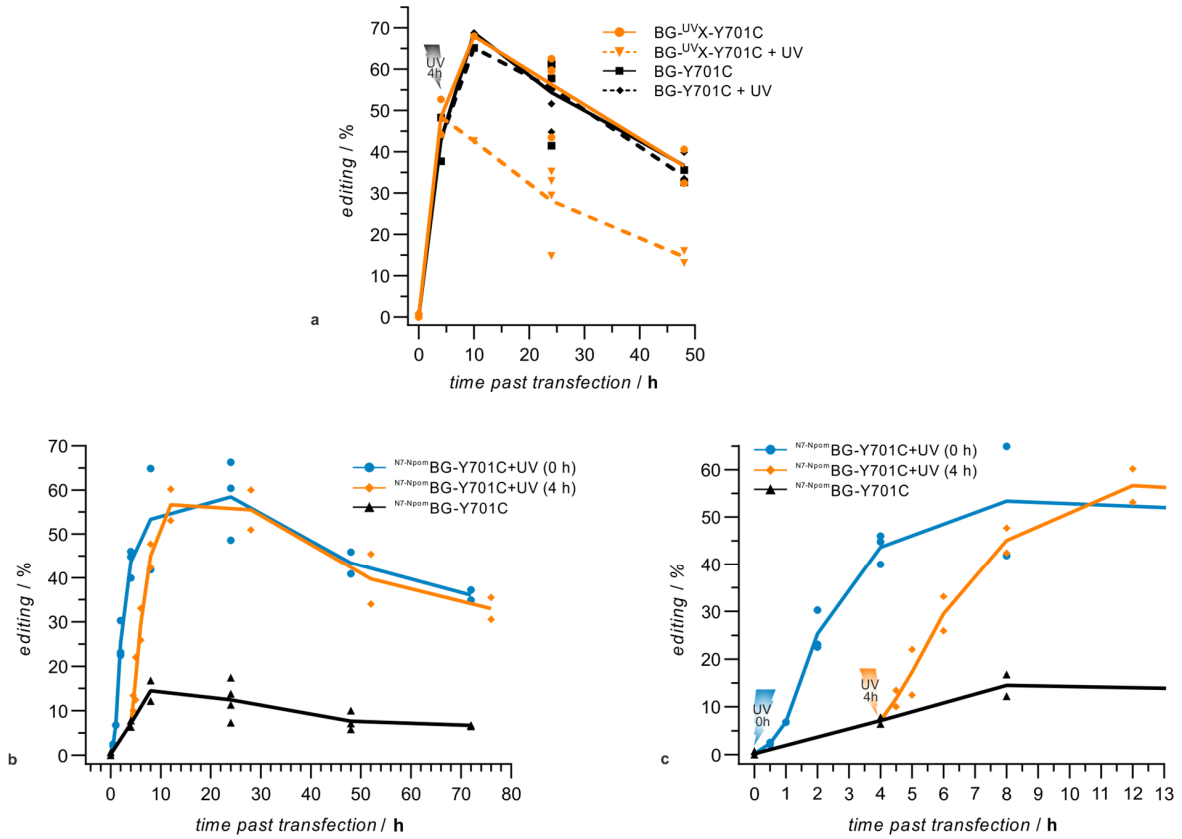

Figure S2. **Editing yields of independent biological replicates of photo-controlled RNA editing at the Y701C site in the endogenous STAT1 transcript.** ***a)*** *and* ***b)*** *Photo off-switch of STAT1 editing as shown in Figure 2a. Shown is the editing yield of independent biological experiments, with either a photo-cleavable BG-*^{UV}*X- or a normal BG-guideRNA, in the absence or presence of a light trigger (+UV, 365 nm), which was applied for 3 min, 4 h after guideRNA transfection, as indicated.* ***c)*** *Photo on-switch of STAT1 editing as shown in Figure 2b. Shown is the editing yield of independent biological experiments over 72 h, in the presence of a photo-activatable* $^{N7\text{-}Npom}$*BG-guideRNA, absence or presence of a light trigger (+UV). The light trigger was applied for 2 min (365 nm) either prior to guideRNA transfection (0 h) or 4 h afterwards (4 h).*

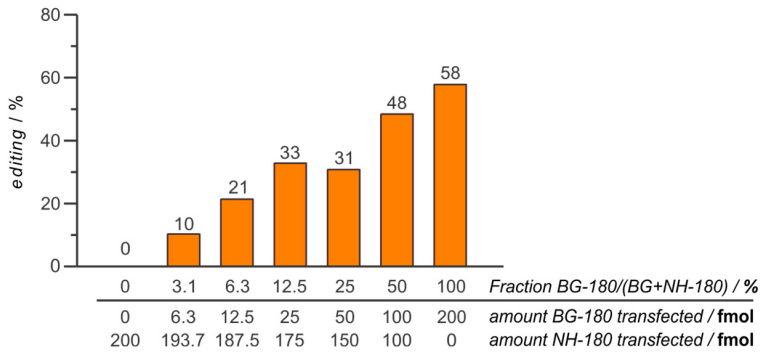

Figure S3. **Correlation of editing and the amount of functional, conjugation-competent BG-guideRNA.** *BG-guideRNA (conjugation-competent) and NH-guideRNA (nonfunctional control, conjugation-incompetent) targeting the Y701C site within the endogenous STAT1 transcript were mixed at different ratios and transfected into SNAP-ADAR-expressing Hek293T cells. Shown is the editing yield obtained upon transfection of 200 fmol total guideRNA containing 3.1% to 100% of conjugation-competent BG-guideRNA. Notably, editing does not show a linear correlation with the fraction of BG-guideRNA, but already 6.3 fmol BG-guideRNA were able to induce significant editing (10%) even in the presence of 30fold excess NH-guideRNA. The setup mimics a situation where a tiny fraction of* $^{N7\text{-}Npom}$*BG-guideRNA is decaged by ambient light or dark hydrolysis in an on-switch editing experiment, or it mimics the result of incomplete cleavage of BG-*^{UV}*X-guideRNA in an off-switch editing experiment. In both situations, tiny amounts of conjugation-competent guideRNA can account for the observed premature editing (on-switch) or residual editing (off-switch) due to the high efficiency of the SNAP-ADAR enzyme for targeted editing.*

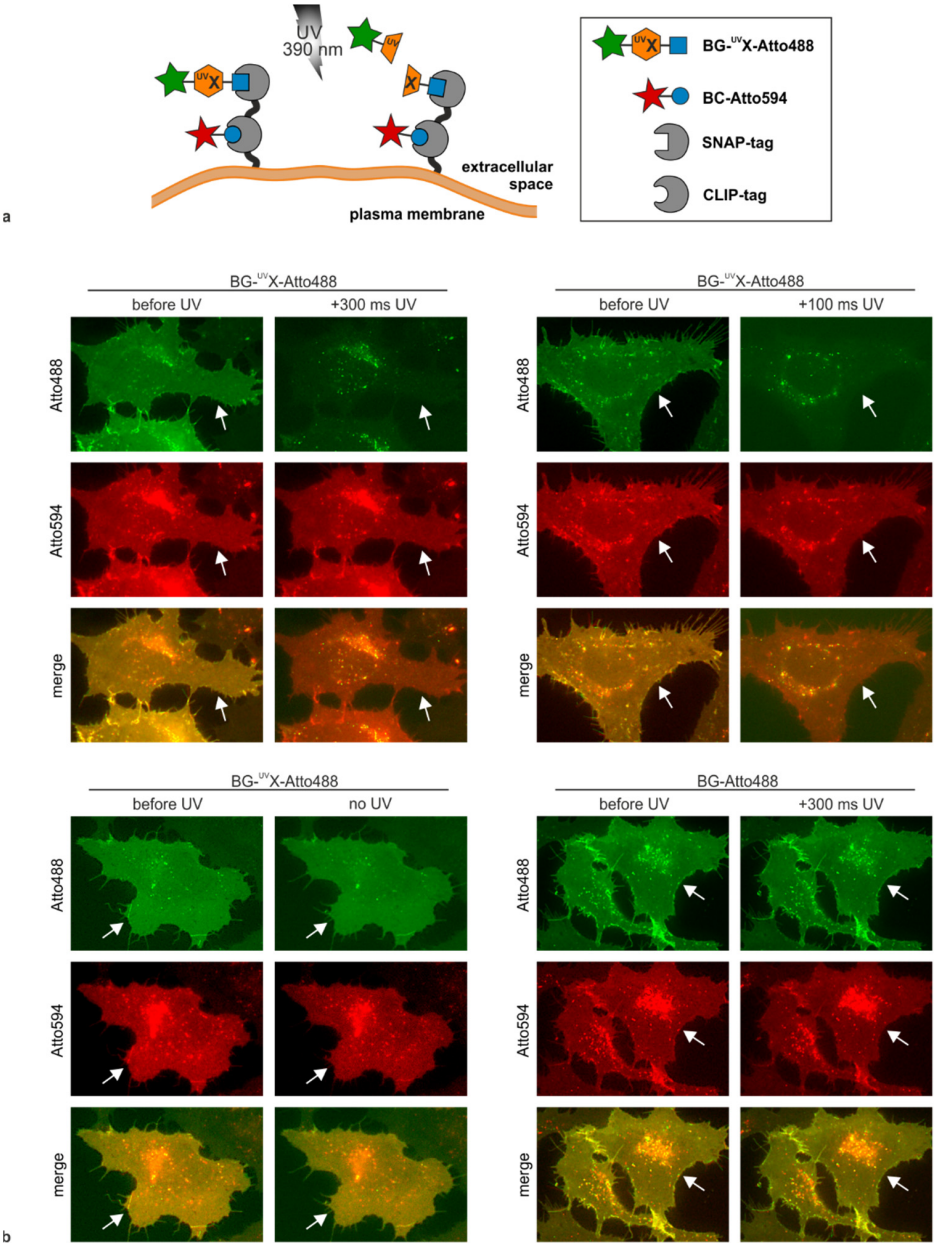

Figure S4. **Characterization of the light-triggered cleavage reaction.** ***a)*** *Scheme of cell surface labeling with BG-^{UV}X-Atto488 and BC-Atto594. A fusion protein containing SNAP-tag and CLIP-tag (SNAP-CLIP display) was localized to the plasma membrane of HeLa cells.[15] A CLIP-tag substrate carrying a red fluorescent dye (BC-Atto594) and a SNAP-tag substrate carrying a green fluorescent dye (BG-Atto488,* ***16****) are added to the medium. If a photocleavable linker is placed between benzyl guanine and Atto488 (BG-^{UV}X-Atto488,* ***17****) the green surface stain can be removed under the microscope by a short UV light pulse.* ***b)*** *Live cells expressing the SNAP-CLIP display construct were stained with BC-Atto594 and BG-Atto488 or BG-^{UV}X-Atto488. Both dyes successfully stained the cell surface (marked on one edge with a white arrow for orientation). Upon UV irradiation (390 nm, lumencor® AuraII, 100 ms or 300 ms) the red signal (BC-Atto594) remains unaffected, but the green signal (BG-^{UV}X-Atto488) is removed immediately. This is not the case in the absence of UV light or if the non-cleavable BG-Atto488 is used.*

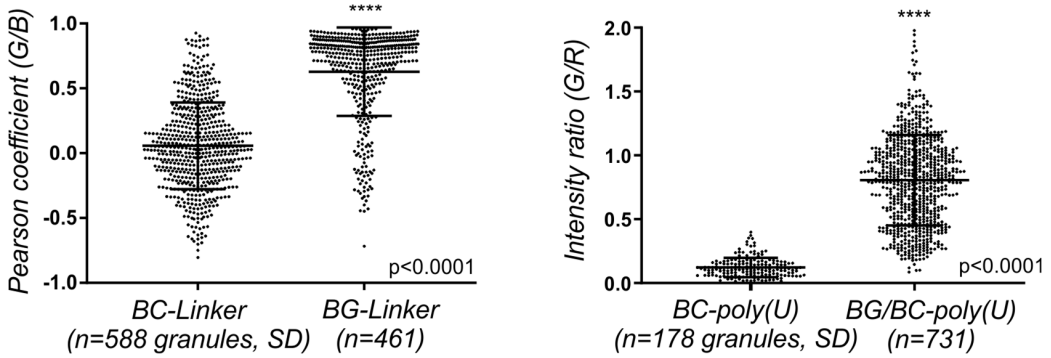

Figure S5. Quantification of orthogonal recruitment of two different proteins to stress granules. a) *Recruitment of a BG-poly(U)-guideRNA into arsenite-induced stress granules (50 µM As_2O_3, 30 min) in a transgenic HeLa cell line, stably expressing a SNAP-$(eGFP)_3$ reporter and a BFP-G3BP1 stress granule marker. Arsenite-induced stress granules appear as blue foci. The BG-poly(U)-guideRNA gives co-staining in the green channel, whereas the control BC-poly(U)-guideRNA does less, as indicated by the Pearson coefficient for the correlation of green (G) and blue (B) fluorescence at N ≥461 blue foci. Statistical significance was calculated by an unpaired Welch's t-test. Details of experimental procedures and image processing can be found in the supplementary information.* ***b)*** *Orthogonal recruitment of two proteins. Transgenic HeLa cells, stably co-expressing SNAP-$(eGFP)_3$ and CLIP-$(mCherry)_3$, were either transfected with a poly(U)-guideRNA carrying the BG, BC, or bifunctional BG/BC self-labeling moieties. The red channel (R) monitors recruitment of mCherry; the green channel (G) monitors recruitment of eGFP upon arsenite-induced stress granule formation. The intensity ratio (green/red; G/R) was measured at N ≥178 red foci. Statistical significance was calculated by an unpaired Welch's t-test. Details of experimental procedures and image processing can be found in the supplementary information.*

Photodissociation Kinetics of BG-^{UV}X-OH

*To determine the decaging efficiency εΦ, the decay of BG-^{UV}X-OH (**8**) was compared to the decaging of the previously characterized $^{N7\text{-}Npom}$BG-TFA as described before.[8] The latter was chosen because of the similar absorbance properties of their photocleavable moieties (see supporting Figure S1a). For both substances the extinction coefficient was estimated to be ε_{365nm} = 4.3 $mM^{-1}cm^{-1}$ as determined for Npom-OH.[8] Stock solutions of BG-^{UV}X-OH and $^{N7\text{-}Npom}$BG-TFA were prepared in DMSO and diluted in PBS (137 mM NaCl, 2.7 mM KCl, 12 mM K_2HPO_4, 12 mM KH_2PO_4, pH = 7.4) to a final concentration of 10 µM (DMSO < 0.02%). Decaging was performed in PCR tubes by irradiation with 365 nm light on a UV transilluminator (UVP TFL-40V, 25 W power, intensity high, giving 7.9±0.2 mW/cm² on the sample) for the indicated amount of time at room temperature. Samples were covered with aluminium foil and stored at –20°C until they were applied to analytical HPLC with UV detection at 280nm and 365 nm (see supporting Figures S1d and S1f). Decomposition of $^{N7\text{-}Npom}$BG-TFA (**D**) results in two clean products, BG-TFA (**F**) which shows high absorption at 280nm but no absorption at 365 nm and the released caging group (**E**) that shows high absorbance at 365nm (see supporting Figures S1e and S1f). The photocleavable linker BG-^{UV}X-OH (**A**) decomposed to several peaks on the HPLC (see supporting Figures S1c and S1d), one of which can be assigned to be (4-hydroxybenzoyl)glycine (**C**) by LC-MS and comparison to the reference substance synthesized (spectra below). (4-Hydroxybenzoyl)glycine is the cleavage product that remains on a guideRNA after irradiation in editing experiments and therefore demonstration of its timely release is most relevant for this study. Another peak could be assigned to be the nitroso acetophenone product (**B**) containing the benzyl guanine by LC-MS which shows absorption at 365 nm (spectra below). The peaks were integrated with the Shimadzu VP-Class software.*

The peak area of the cleavage products was plotted against irradiation time (see Figure 1c) and by logarithmic fit the half-time was determined to be $t_{1/2}$ = 17±2 s for (4-hydroxybenzoyl)glycine and $t_{1/2}$ = 15±3 s for BG-TFA. With the quantum yield of the reference substance ($^{N7\text{-}Npom}$BG-TFA Φ ≈ 0.5), the quantum yield of BG-^{UV}X-OH can be calculated to be Φ ≈ 0.4 according to following formula:

$$\Phi_{BG-^{UV}X-OH} = \Phi_{Reference} \times \frac{t_{1/2\,reference}}{t_{1/2\,BG-^{UV}X-OH}} \times \frac{\varepsilon_{reference}}{\varepsilon_{BG-^{UV}X-OH}} = 0.41$$

Table of the relative peak area of BG-^{UV}X-OH and $^{N7\text{-}Npom}$BG-TFA and their cleavage products upon UV irradiation as determined in analytical HPLC:

	relative peak area			
time [s]	BG-^{UV}X-OH	(4-hydroxy-benzoyl)glycine	$^{N7\text{-}Npom}$BG-TFA	BG-TFA
0	100.0	0.0	100.0	0.0
15	56.7	35.6	53.2	35.7
30	28.4	55.0	23.3	70.0
45	14.2	69.9	9.3	77.3
60	5.7	85.7	2.9	83.5
180	0.0	100.0	0.0	100.0

*UV chromatogram of the LC-MS analysis of BG-^{UV}X-OH after partial photo-dissociation (corresponds to supporting Figure S1d). Peaks corresponding to BG-^{UV}X-OH (**A**) and its decay products (**B**) and (**C**, (4-hydroxybenzoyl)glycine) are marked. See also supporting Figure S1c.*

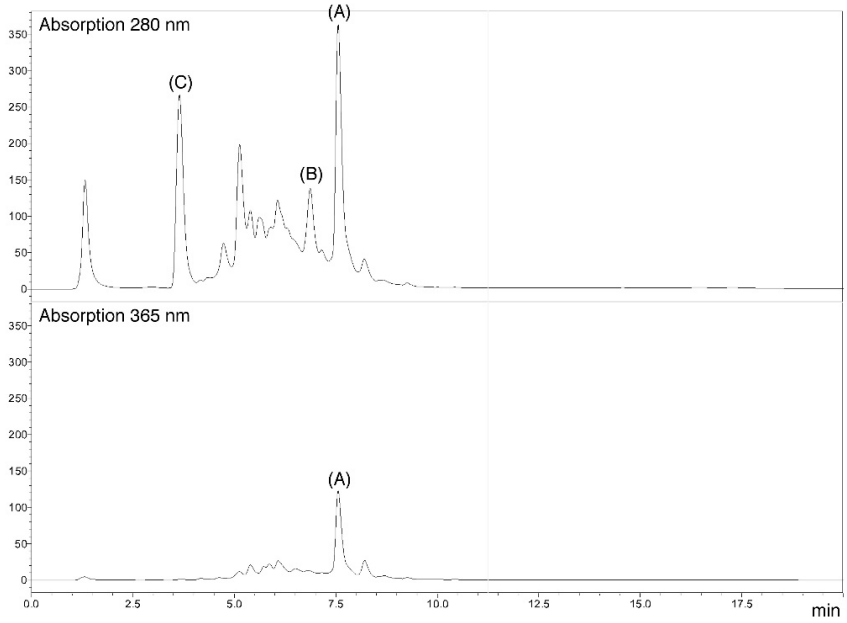

*Extracted MS spectrum of BG-^{UV}X-OH (**A**), positive mode (top) and negative mode (bottom)*

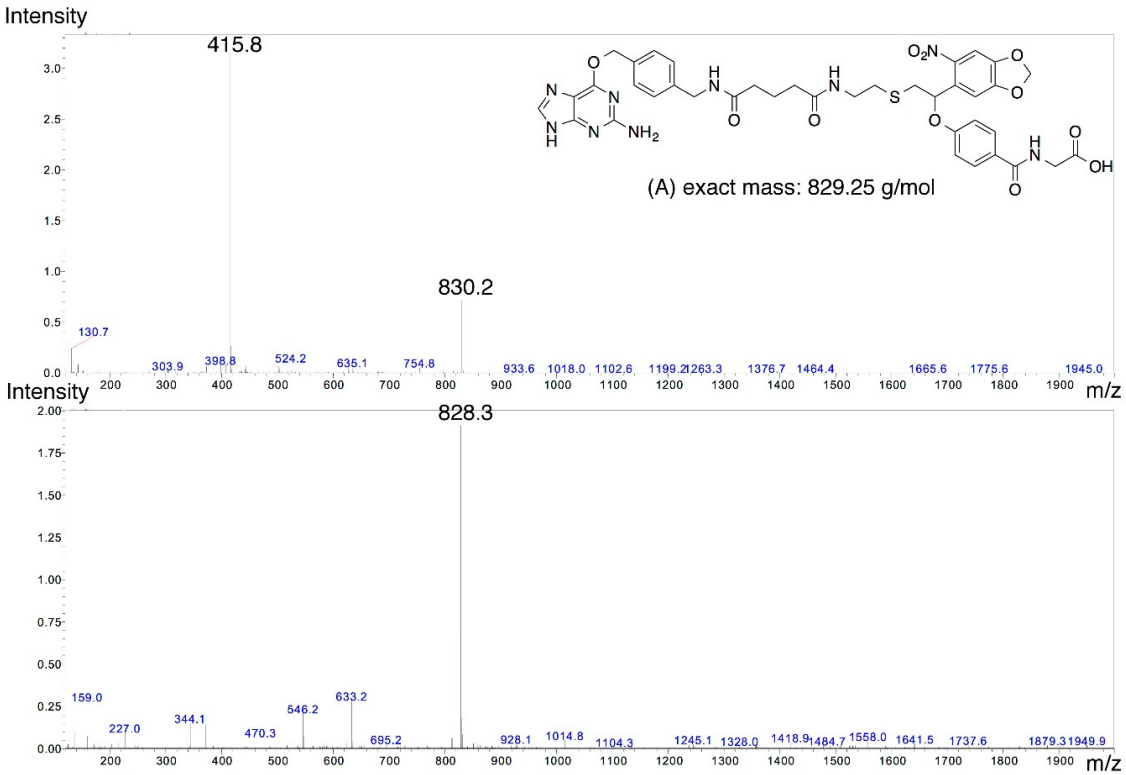

*Extracted MS spectrum of peak (**B**), corresponding to the nitroso acetophenone decay product of BG-^{UV}X-OH, positive mode (top) and negative mode (bottom)*

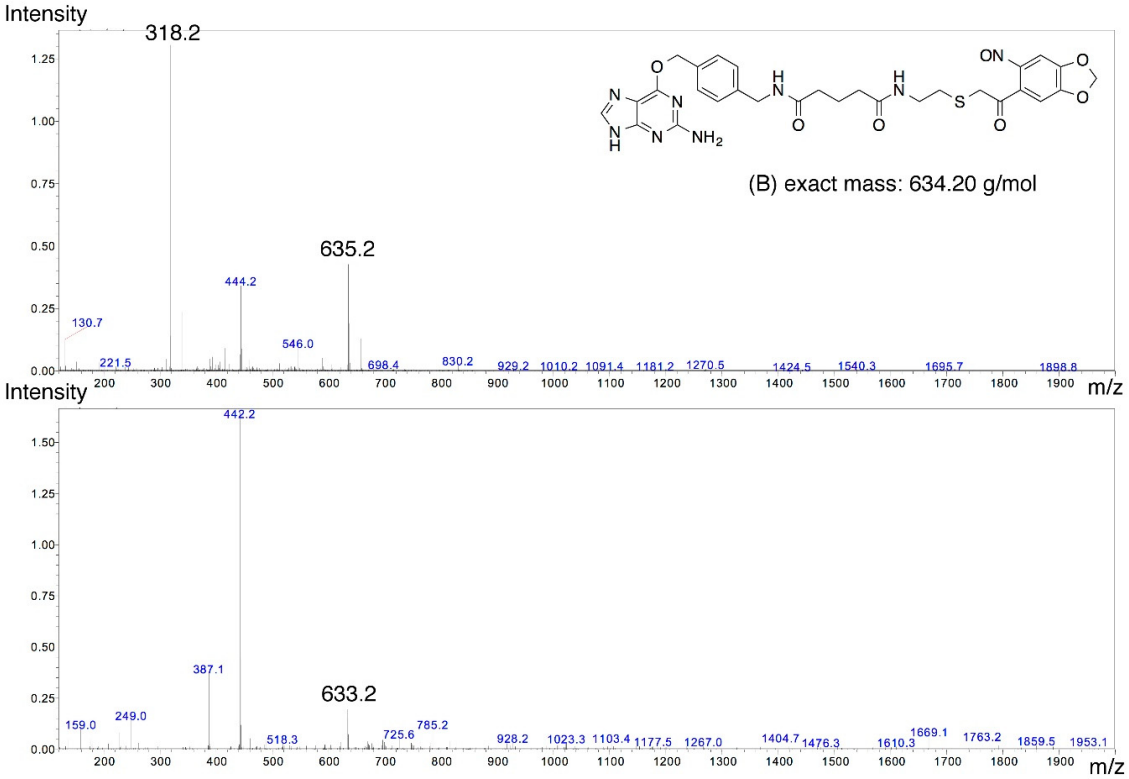

*Extracted MS spectrum of peak (**C**), corresponding to (4-hydroxybenzoyl)glycine, positive mode (top) and negative mode (bottom)*

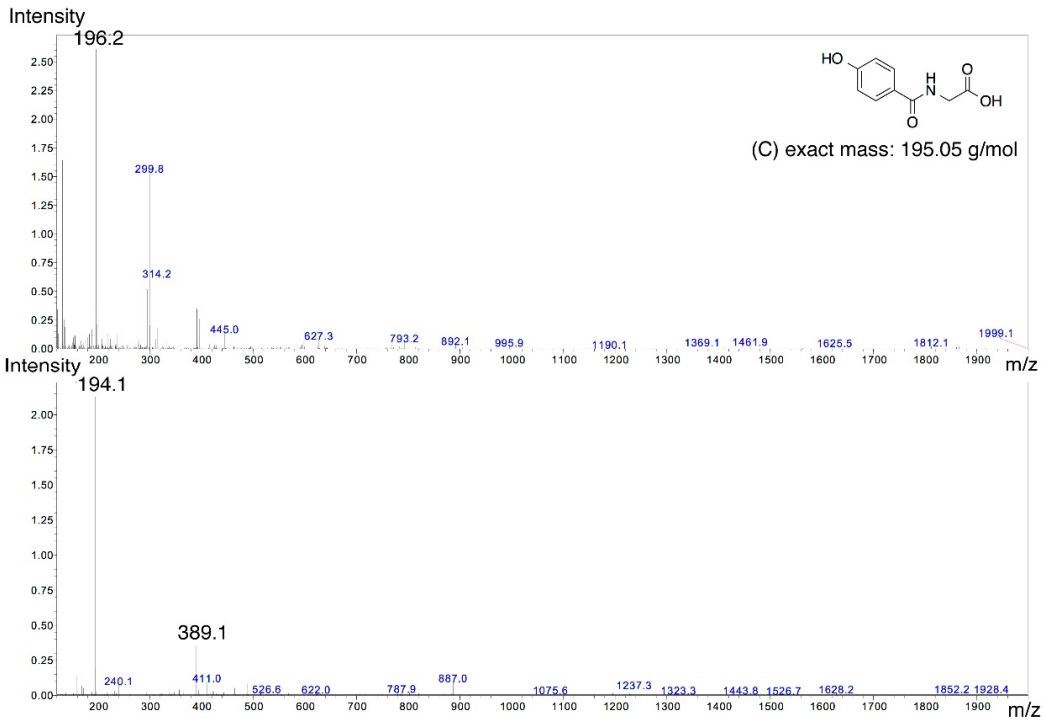

*UV chromatogram of LC-MS analysis and extracted MS spectrum of synthesized (4-hydroxybenzoyl)glycine (**10**), positive mode (top) and negative mode (bottom). Elution time and detected m/z ratios correspond to decaging product (**C**) detected in the LC-MS analysis of partially photo-cleaved BG-^{UV}X-OH.*

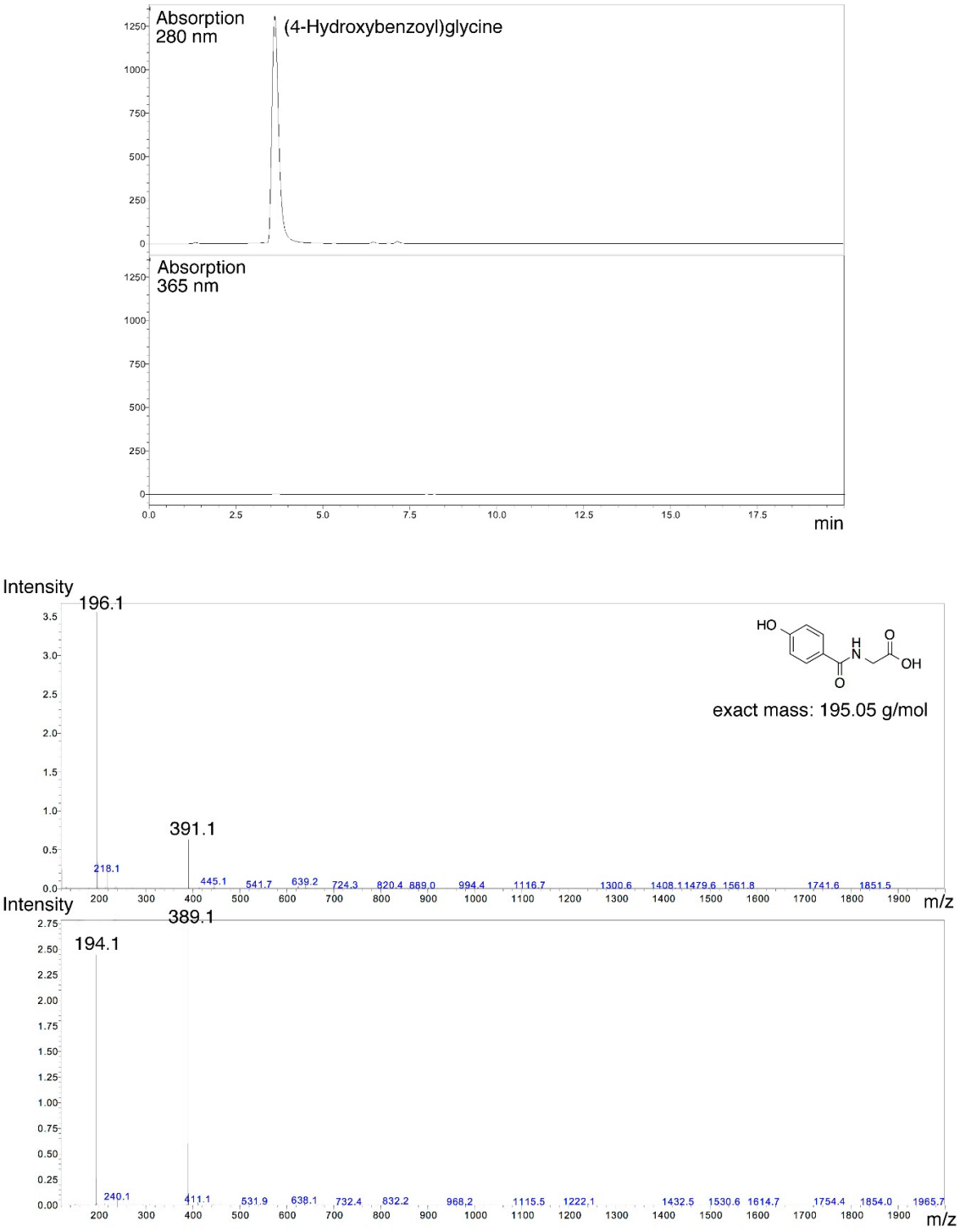

Chemical synthesis

Chemicals

If not stated otherwise, all substrates and reagents required for synthesis and biochemical studies were purchased from commercial providers and used without further purification.

O^6-(4-aminomethyl-benzyl)guanine (BG-NH_2) was synthesized as described in literature.[1] 2-(4-(Aminomethyl)-benzyloxy)-4-aminopyrimidine (BC-NH_2) was prepared from commercially available methyl-4-(aminomethyl) benzoate hydrochloride according to literature.[2-4] We recently described a detailed synthesis of $^{N7\text{-}Npom}$BG-TFA and $^{N7\text{-}Npom}$BG-NH_2.[5]

General Methods

All column chromatographic purifications were carried out on self-packed columns of silica gel (0.04-0.063 mm/230-240 mesh). Thin-layer chromatography (TLC) was performed on silica gel sheets (60 F254, 0.2 mm, 5 x 10 cm, Merck) and visualized under UV light (254 nm). All analytical and preparative HPLC runs were performed on a Shimadzu system (SCL-10A VP, SPD-20AV, LC-20AT) running with 0.1% TFA in water (eluent A) and 0.1% TFA in acetonitrile/water (9:1, eluent B). Analytical HPLC was performed using an EC 125/4 Nucleodur C18 column by Machery + Nagel with a linear gradient from 5% eluent B (starting after 1 min) to 95% eluent B (ending after 25 min). Preparative HPLC was performed using a VP 250/10 Nucleodur C18 column by Machery + Nagel. High resolution mass spectrometry was performed on a maXis4G ESI-TOF-MS by Bruker Daltonics. LC-MS analyses were conducted on a LC-MS2020 (Shimadzu) with a Kinetex C18 column (Phenomonex). 0.1% formid acid in water (eluent A) and 0.1% formic acid in acetonitrile/water (4:1, eluent B) were used as eluents. A linear gradient from 5% eluent B (starting after 1 min) to 95% eluent B (ending after 11 min) was used. NMR spectra were recorded on a Bruker ARX 250 spectrometer at 250 MHz for ^{1}H spectra and 63 MHz for ^{13}C spectra or a Bruker Avance 400 spectrometer at 400MHz for ^{1}H spectra and 101 MHz for ^{13}C spectra. 2D-NMR spectra were recorded with a Bruker Avance 400 at 400 MHz/101 MHz.

Synthesis of Fmoc-^{UV}X-OH

The photo-cleavable amino acid Fmoc-^{UV}X-OH was synthesized in a five-step synthesis starting with the bromination of 4',5'-methylenedioxy-2'- nitroacetophenone which was carried out following the description of Pendrak et al.[6] The brominated product was reacted with Fmoc-protected cysteamine which was synthesized following to the protocol of Miura et al.[7] The full synthesis scheme is shown below.

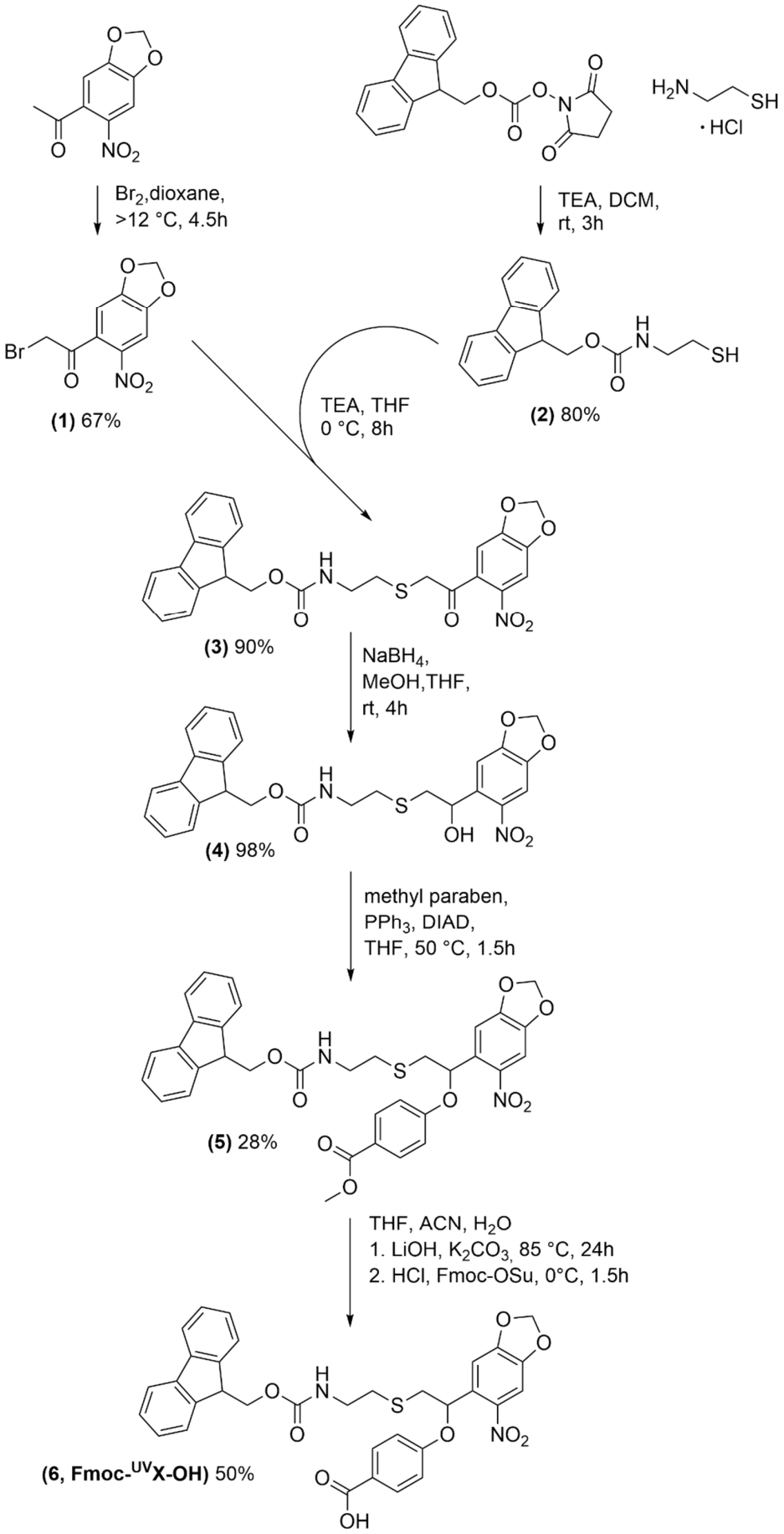
Br2,dioxane,
>12 °C, 4.5h
TEA, DCM,
rt, 3h
(1) 67%
(2) 80%
TEA, THF
0 °C, 8h
(3) 90%
NaBH4,
MeOH,THF,
rt, 4h
(4) 98%
methyl paraben,
PPh3, DIAD,
THF, 50 °C, 1.5h
(5) 28%
THF, ACN, H2O
1. LiOH, K2CO3, 85 °C, 24h
2. HCl, Fmoc-OSu, 0°C, 1.5h
(6, Fmoc-UVX-OH) 50%

2-Bromo-1-(6-nitrobenzo[d][1,3]dioxol-5-yl)ethan-1-one (1)

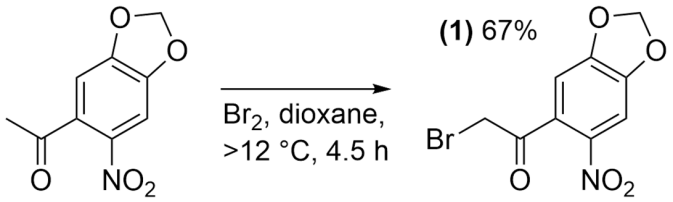

A solution of 4',5'-methylenedioxy-2'-nitroacetophenone (4 g, 19.12 mmol, 1.0 eq) in dioxane (12 ml) was stirred on ice and a solution of bromine (1.1 ml, 21.03 mmol, 1.1 eq) in dioxane (44 ml) was added dropwise. The reaction was stirred for 4.5 h with occasional cooling. The solvent was evaporated, and the residue was solved in Et_2O, washed with sodium thiosulfate and brine, and dried over Na_2SO_4. The solvent was removed in vacuo and the crude product was crystallized from cyclohexane (110 ml) and DCM (45 ml). Evaporation of the solvents resulted in 3.8 g (67%) of **1** *as a yellow solid.*

R_f (CH/Et_2O, 7:5) = 0.21

^{1}H-NMR (250 MHz, $CDCl_3$) δ [ppm] = 7.63 (s, 1H), 6.83 (s, 1H), 6.22 (s, 2H), 4.24 (s, 2H).

^{13}C-NMR (63 MHz, $CDCl_3$) δ [ppm] = 193.5, 153.0, 149.5, 131.7, 108.2, 104.7, 140.0, 97.8, 33.8.

Analytical HPLC of **1** *after crystallization*

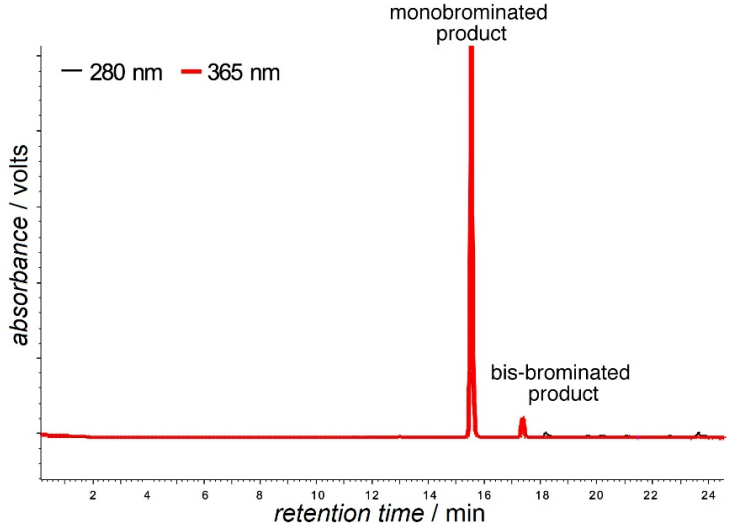

^{1}H-NMR (250 MHz, $CDCl_3$) of **1**

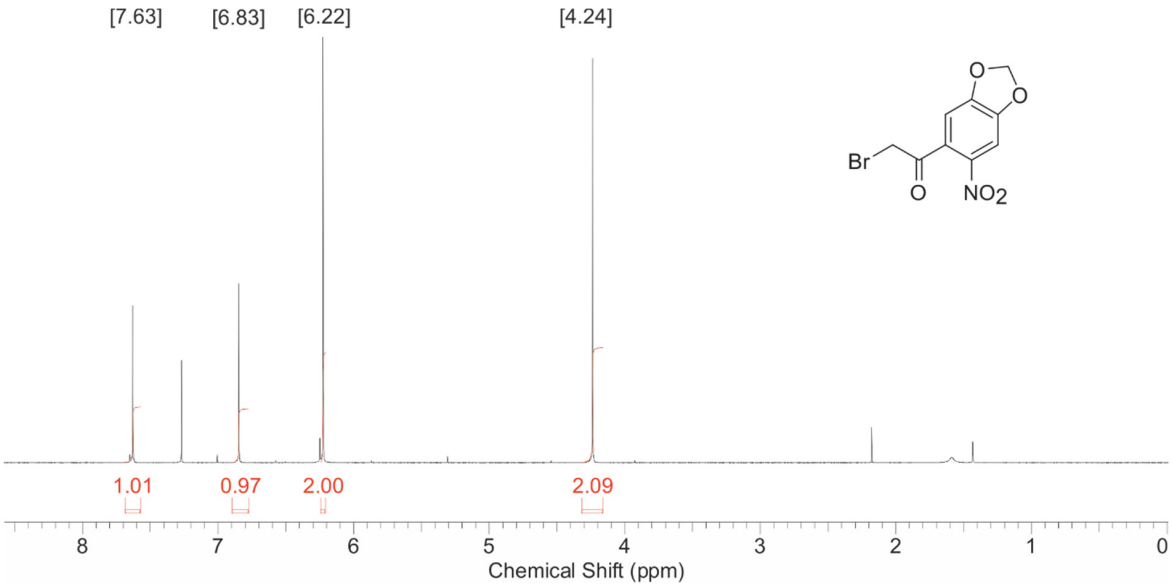

^{13}C-NMR (63 MHz, $CDCl_3$) of **1**

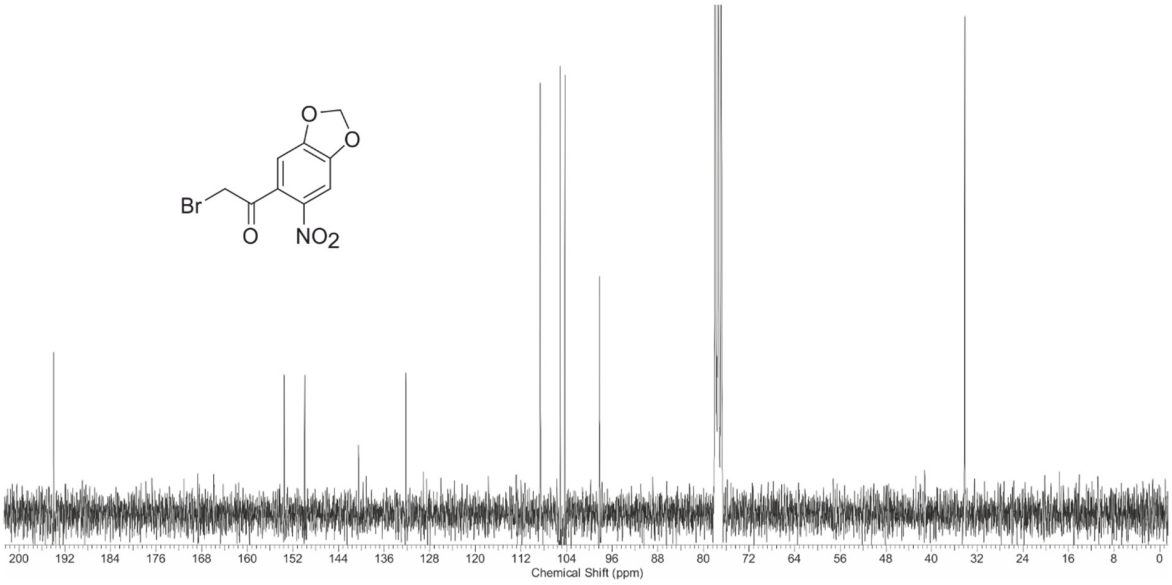

(9H-Fluoren-9-yl)methyl (2-mercaptoethyl)carbamate (2)

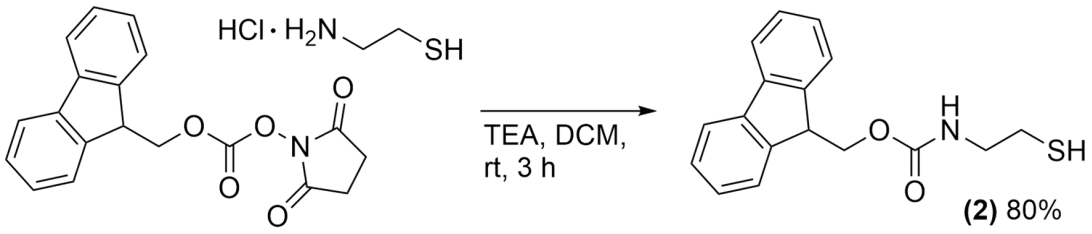

Fmoc-OSu (10.0 g, 29.6 mmol, 1.0 eq) was solved in DCM (40 ml) and stirred on ice under an argon atmosphere. Cysteamine hydrochloride (3.34 g, 29.4 mmol, 1.0 eq) in DCM (40 ml) and TEA (8.15 ml, 58.8 mmol, 2.0 eq) were added to the reaction mixture. After 3 h, the solution was washed with 0.1 M HCl and brine and the organic phase was dried over Na_2SO_4. After evaporation of the solvent, 7.08 g (80%) of a white solid were obtained. The product showed little impurities in HPLC and was used for the next reactions without further purification.

R_f (CH/EA, 2:1) = 0.53

^{1}H-NMR (250 MHz, $CDCl_3$) δ [ppm] = 7.79 (d, J = 7.1 Hz, 2H), 7.61 (d, J = 7.3 Hz, 2H), 7.38 (m, 4H), 5.14 (br s, 1H), 4.45 (d, J = 6.6 Hz, 2H), 4.24 (t, J = 6.6 Hz, 1H), 3.38 (q, J = 6.0 Hz, 2H), 2.66 (q, J = 7.2 Hz, 2H), 1.34 (t, J = 8.5 Hz,1H).

Analytical HPLC of crude product of **2**

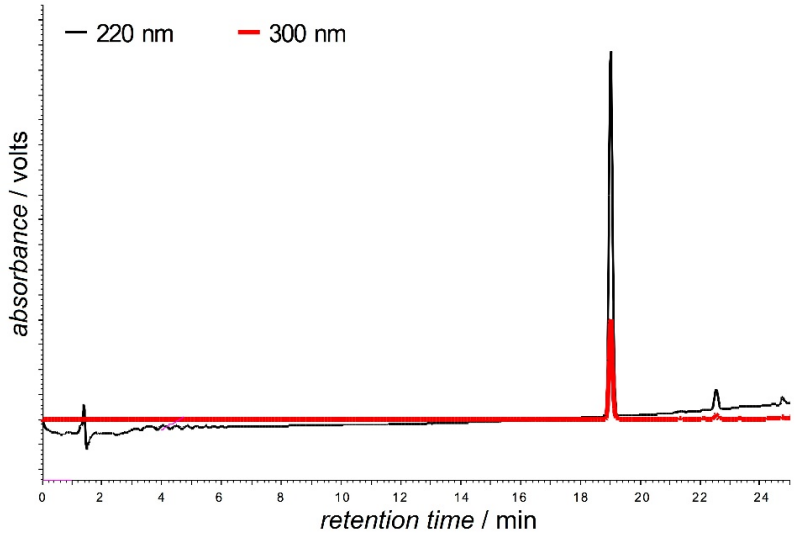

15

^{1}H-NMR (250 MHz, $CDCl_3$) of **2**

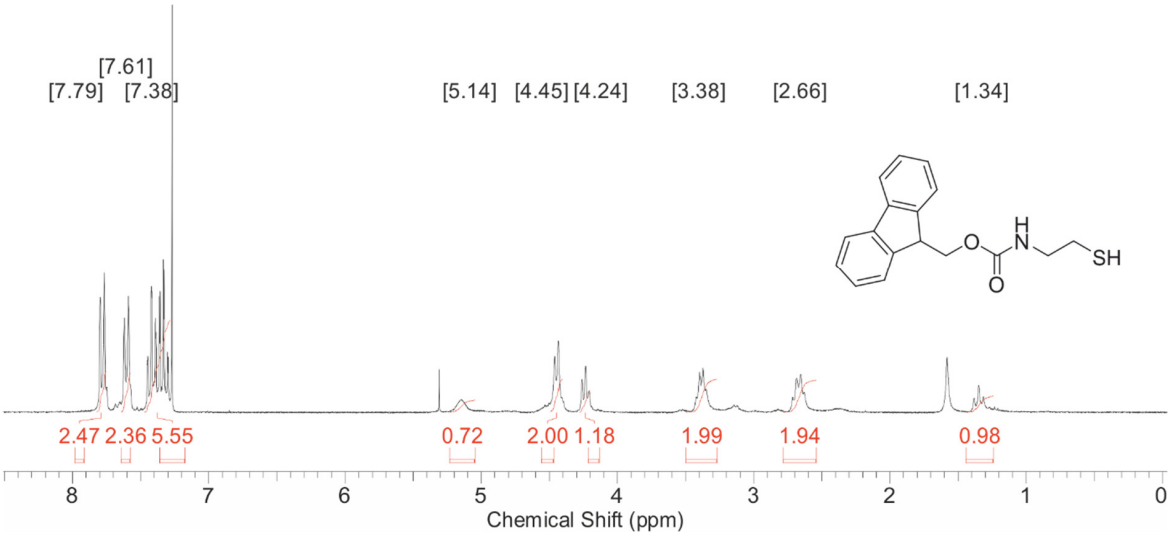

(9H-Fluoren-9-yl)methyl (2-((2-(6-nitrobenzo[d][1,3]dioxol-5-yl)-2-oxoethyl)-thio)ethyl)carbamate (3)

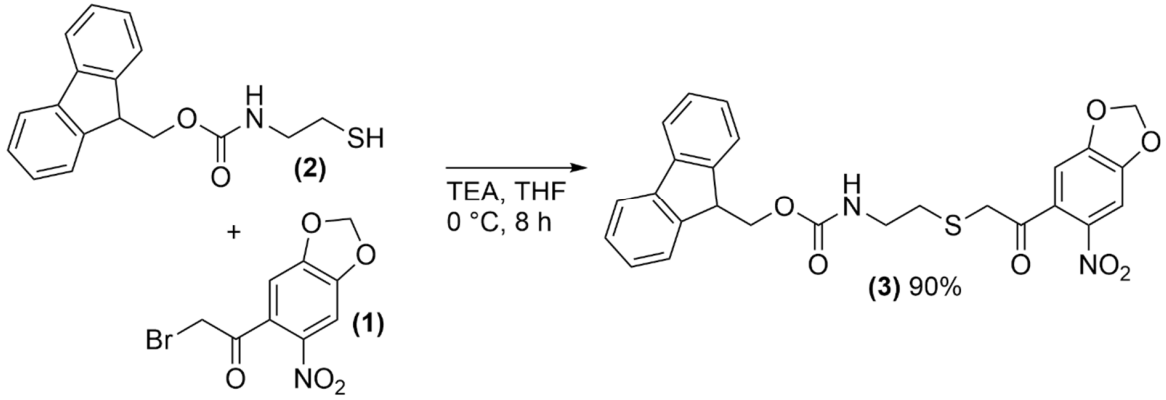

Compound **2** *(3.9 g, 13.0 mmol, 1.0 eq) was solved in THF (100 ml) under argon atmosphere and TEA (2 ml, 14.3 mmol, 1.1 eq) was added dropwise while cooling the reaction on ice. Afterwards the mixture was added to a solution of* **1** *(3.75 g, 13.0 mmol, 1.0 eq) in THF (200 ml). After 4 h, another 0.5 eq of* **1** *(1.88 g, 6.5 mmol) and 0.5 eq of TEA (0.91 ml, 6.5 mmol) were added and the reaction was stirred for another 4 h. The solvent was removed in vacuo and the residue dissolved in EA, washed with 0.1 M HCl and brine, and dried over Na_2SO_4. The removal of the solvent yielded 10.2 g brownish raw product, which was purified by flash column chromatography (CH/EA, 2:1–1:2). 6.7 g (90%) of a yellow-orange solid were obtained.*

R_f (CH/EA, 2:1) = 0.15

^{1}H-NMR (250 MHz, $CDCl_3$) δ [ppm] = 7.78 (d, J = 7.6 Hz, 2H), 7.60 (d, J = 7.6 Hz, 2H), 7.60 (s, 1H), 7.38 (m, 4H), 6.85 (s, 1H), 6.17 (s, 2H), 5.22 (br s, 1H), 4.45 (d, J = 7.1 Hz, 2H), 4.25 (t, J = 6.8 Hz, 1H), 3.65 (s, 2H), 3.46 (q, J = 5.9 Hz, 2H), 2.77 (t, J = 6.1 Hz, 2H).

^{13}C-NMR (63 MHz, $CDCl_3$) δ [ppm] = 195.9, 156.3, 152.9, 149.3, 143.9, 141.3, 127.6, 126.8, 125.1, 120.0, 108.0, 104.6, 103.8, 66.9, 60.5, 47.3, 40.7, 32.3, 21.1, 14.2.

HR-ESI-MS: $[M+Na]^{+}_{(theor.)}$ = 529.10399, $[M+Na]^{+}_{(meas.)}$ = 529.10439.

^{1}H-NMR (250 MHz, $CDCl_3$) of **3**

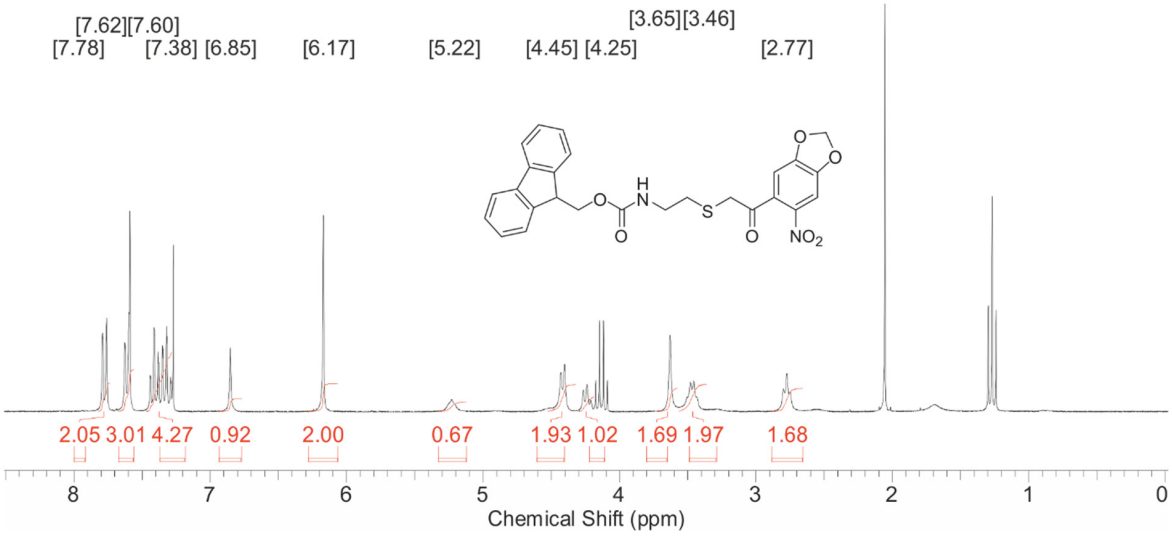

^{13}C-NMR (63 MHz, $CDCl_3$) of **3**

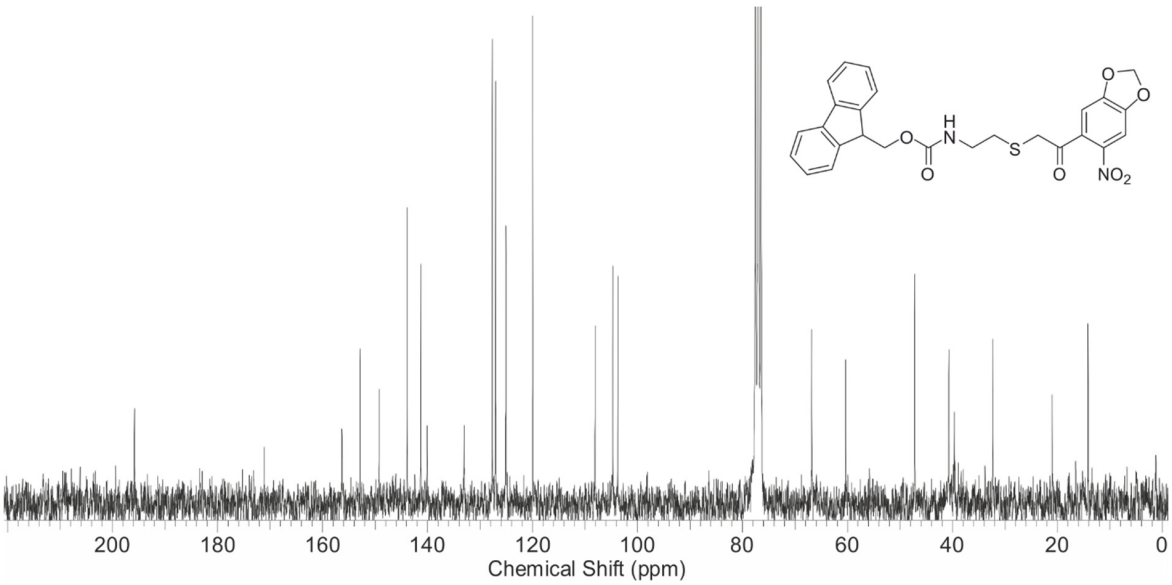

17

((9H-Fluoren-9-yl)methyl (2-((2-hydroxy-2-(6-nitrobenzo[d][1,3]dioxol-5-yl)ethyl)thio)ethyl)carbamate (4)

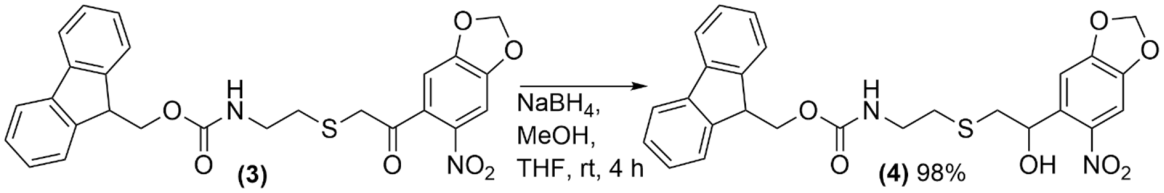

3 *(6.5 g, 12.8 mmol, 1.0 eq) was solved in MeOH (350 ml), THF (50 ml) and $NaBH_4$ (0.49 g, 12.8 mmol, 1.0 eq) and the reaction was stirred for 4 hours at room temperature. The solvation was facilitated by sonication. Subsequently, the reaction was quenched with a saturated solution of NH_4Cl and the product extracted with EA. The organic phase was washed with brine and dried over Na_2SO_4. After removal of the solvent, 6.4 g (98%) of yellow-brown product were obtained which was used in the following reactions without further purification.*

R_f (CH/EA, 2:1) = 0.23

^{1}H-NMR (400 MHz, $CDCl_3$) δ [ppm] = 7.77 (d, J = 7.6 Hz, 2H), 7.60 (d, J = 7.3 Hz, 2H), 7.51 (s, 1H), 7.36 (m, 4H), 7.36 (s, 1H), 6.11 (d, J = 6.1 Hz, 2H), 5.43 (d, J = 8.8 Hz, 1H), 5.22 (t, J = 4.0 Hz, 1H), 4.46 (d, J = 6.3 Hz, 2H), 4.23 (t, J = 6.8 Hz, 1H), 3.51 (m, 2H), 3.19 (d, J = 14.2 Hz, 1H), 2.84 (m, 2H), 2.53 (m, 2H).

^{13}C-NMR (101 MHz, $CDCl_3$) δ [ppm] = 156.6, 152.7, 147.2, 143.9, 141.3, 136.0, 127.6, 127.1, 125.0, 119.9, 106.7, 105.2, 103.0, 67.7, 66.8, 53.5, 47.3, 40.8, 40.5, 32.1.

HR-ESI-MS: $[M+Na]^+_{(theor.)}$ = 531.11964, $[M+Na]^+_{(meas.)}$ = 531.11969.

^{1}H-NMR (400 MHz, $CDCl_3$) of **4**

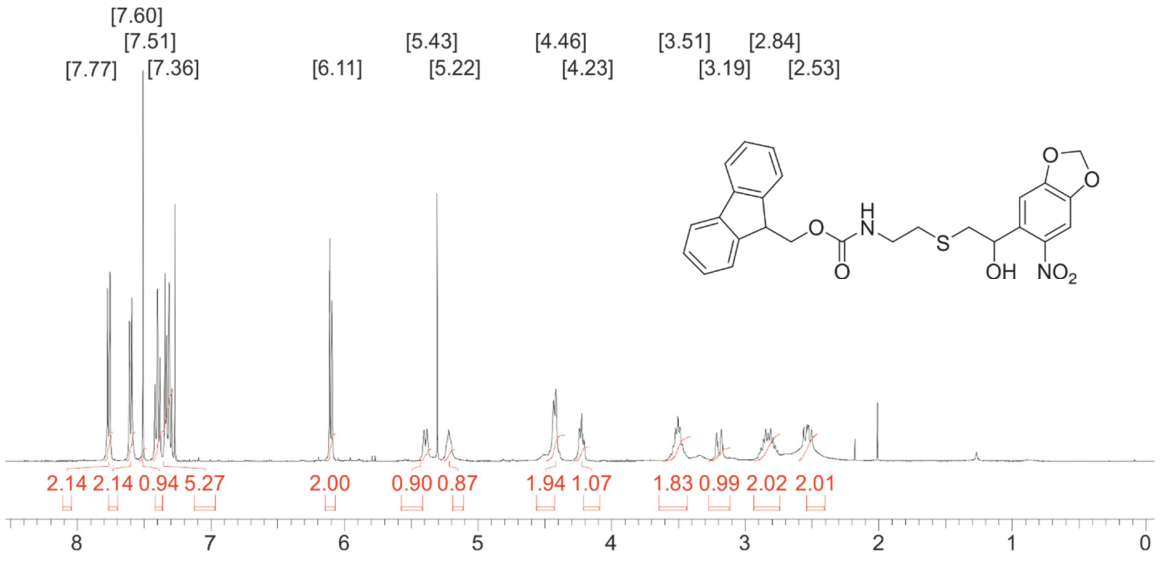

^{13}C-NMR (101 MHz, $CDCl_3$) of **4**

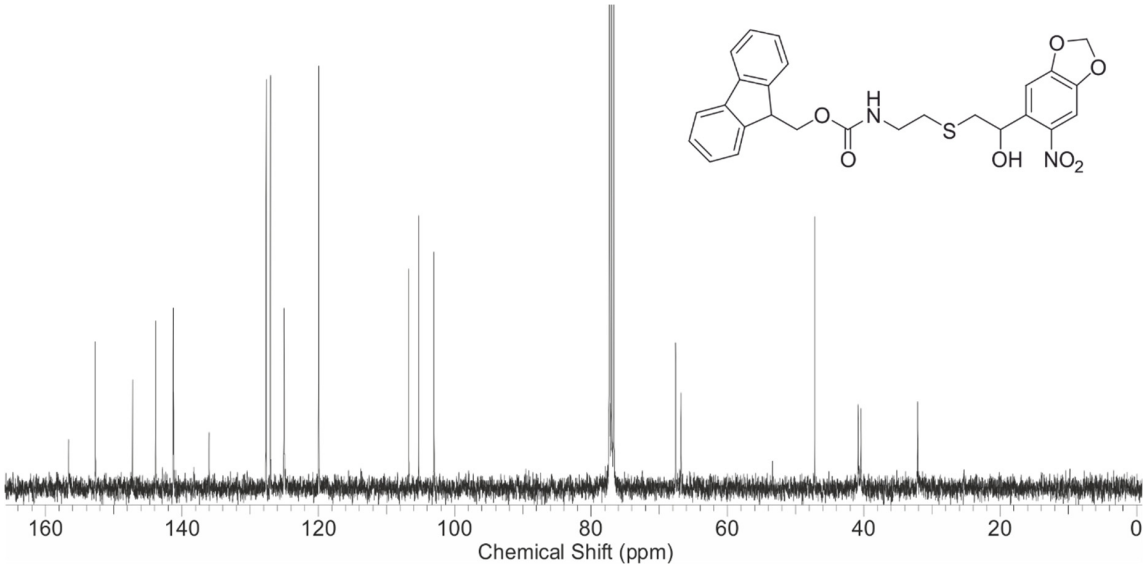

2D-NMR ^{1}H,^{1}H-COSY of **4**

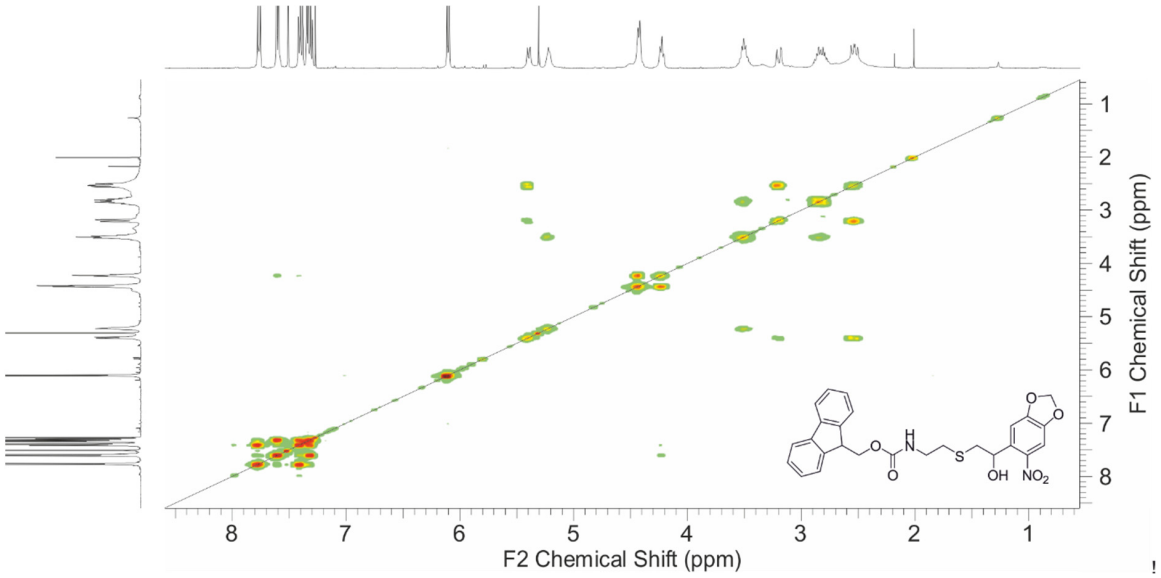

19

2D-NMR $^{1}H,^{13}C$-HSQC of **4**

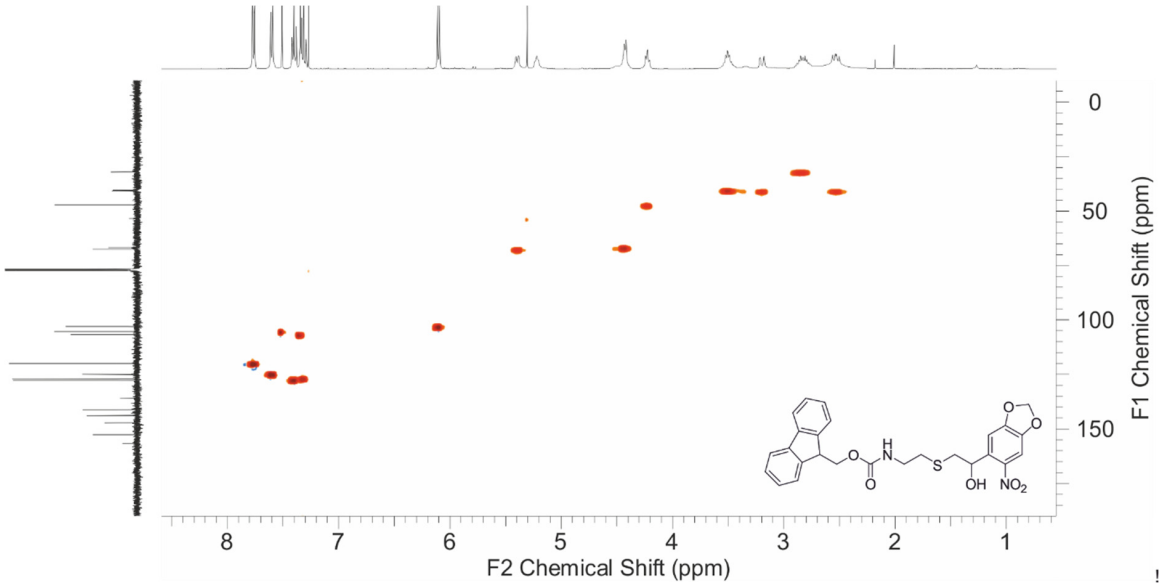

Methyl 4-(2-((2-((((9H-fluoren-9-yl)methoxy)carbonyl)amino)ethyl)thio)-1-(6-nitrobenzo[d][1,3]dioxol-5-yl)ethoxy)benzoate (5)

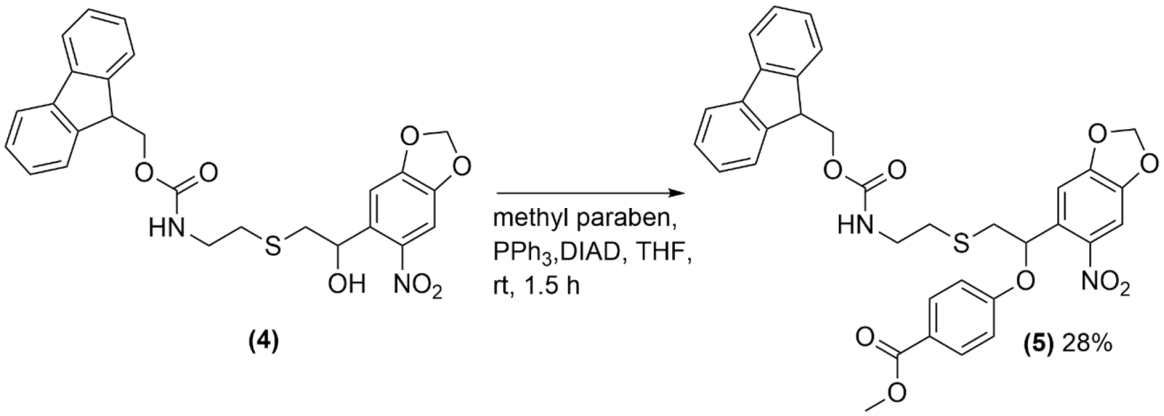

4 *was coupled to methyl paraben in a Mitsunobu reaction. Due to the UV light sensitivity of the product the reaction vessel was protected from light with aluminium foil. Compound* **4** *(5.05 g, 9.9 mmol, 1.0 eq), methyl paraben (1.59 g, 10.4 mmol, 1.05 eq) and PPh_3 (2.74 g, 10.4 mmol, 1.05 eq) were dissolved in THF (4 ml) under argon atmosphere and sonicated in an ultrasonic bath (Bandelin electronic water bath sonicator, 320 W, 35 KHz) for three minutes, resulting in a brown viscous solution. DIAD (2.14 ml, 10.9 mmol, 1.1 eq) was added and the reaction mixture was sonicated for 1.5 h allowing the ultrasonic bath to heat up to 50 °C. The raw product was purified by flash column chromatography twice. First purification with CH/EA 2:1 yielded 7.7 g of a yellow-brown solid which was applied again to flash column chromatography using DCM/MeOH 100:1 as eluent. 1.12 g (18%) of a clean yellow solid were obtained and 5.19 g of an impure brownish. Repeated purification yielded further 630 mg (10%) of clean product.*

R_f (CH/EA, 2:1) = 0.21

^{1}H-NMR (400 MHz, $CDCl_3$) δ [ppm] = 7.91 (d, J = 9.1 Hz, 2H), 7.76 (d, J = 7.6 Hz, 2H), 7.59 (d, J = 7.3 Hz, 2H), 7.59 (s, 1H), 7.40 (m, 2H), 7.31 (m, 2H), 7.09 (s, 1H), 6.83 (d, J = 8.8 Hz, 2H), 6.15 (dd, J = 6.7, 3.8 Hz, 1H), 6.08 (d, J = 8.3 Hz, 2H), 5.17 (m, 1H), 4.38 (d, J = 7.0 Hz, 2H), 4.20 (t, J = 7.0 Hz, 1H), 3.85 (s, 3H), 3. 46 (q, J = 5.9 Hz, 2H), 3.09 (m, 2H), 2.84 (m, 2H).

^{13}C-NMR (101 MHz, $CDCl_3$) δ [ppm] = 166.5, 160.7, 156.3, 153.0, 147.9, 143.8, 141.7, 141.3, 133.1, 131.7, 127.6, 127.0, 125.1, 123.7, 120.0, 115.2, 106.4, 105.7, 103.3, 75.9, 66.7, 51.9, 47.2, 40.2, 38.5, 33.1.

HR-ESI-MS: $[M+Na]^+_{(theor.)}$ = 665.15642, $[M+Na]^+_{(meas.)}$ = 665.15657.

^{1}H-NMR (400 MHz, $CDCl_3$) of **5**

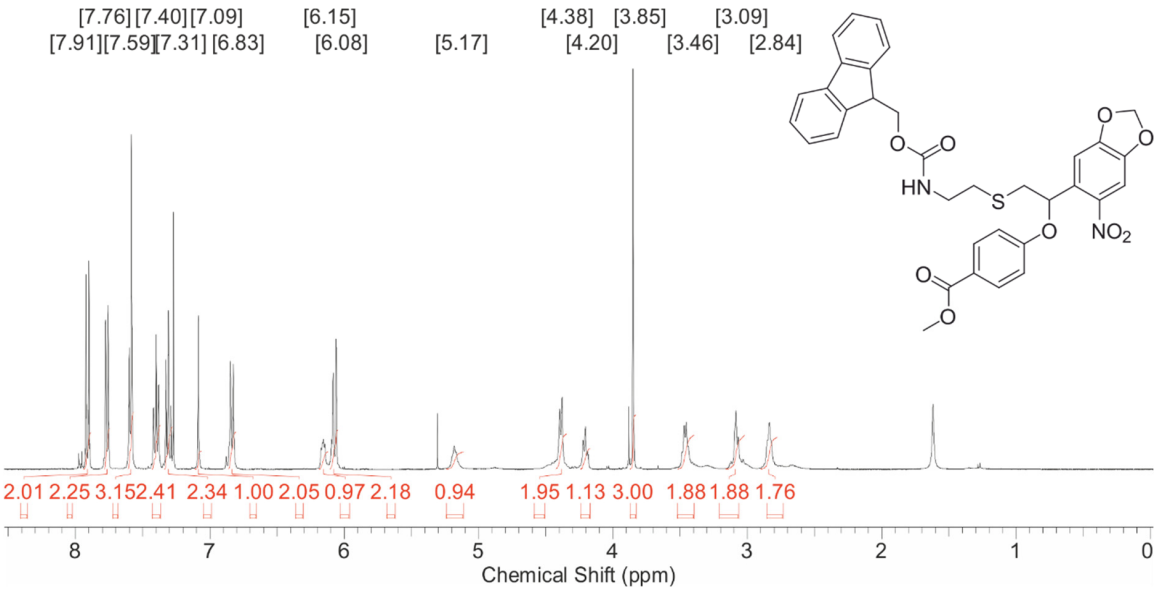

^{13}C-NMR (101 MHz, $CDCl_3$) of **5**

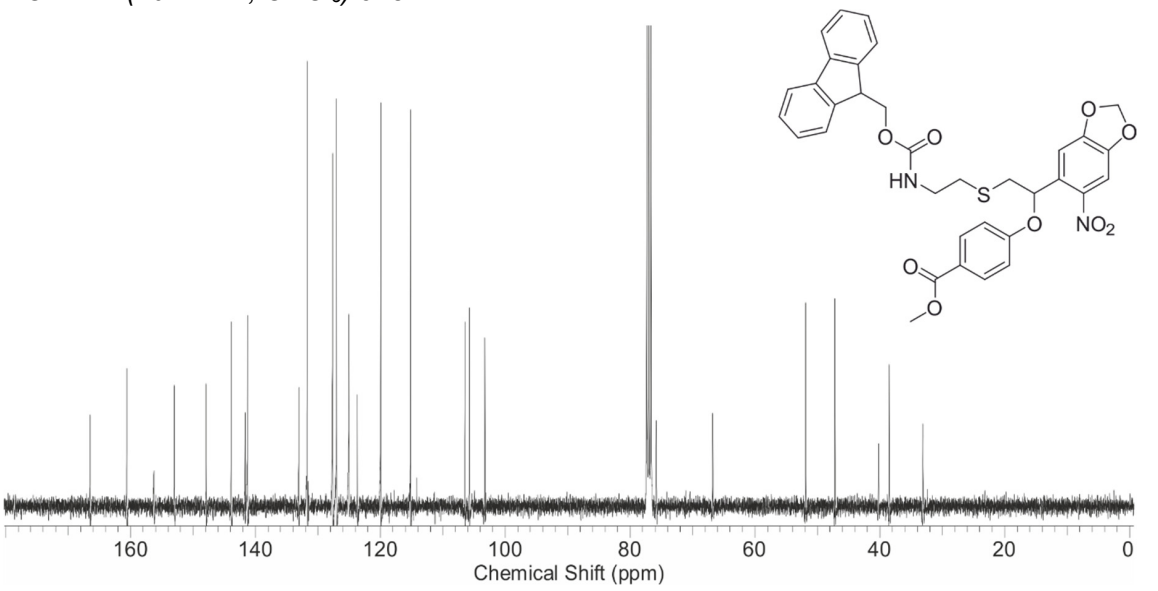

21

2D-NMR $^{1}H,^{1}H$-COSY of **5**

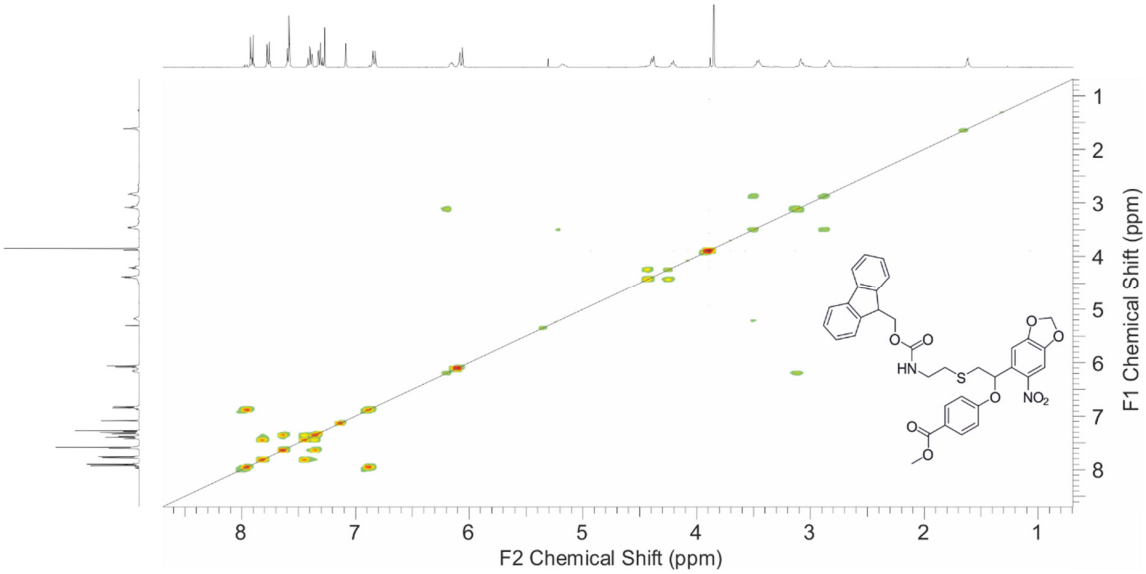

2D-NMR $^{1}H,^{13}C$-HSQC of **5**

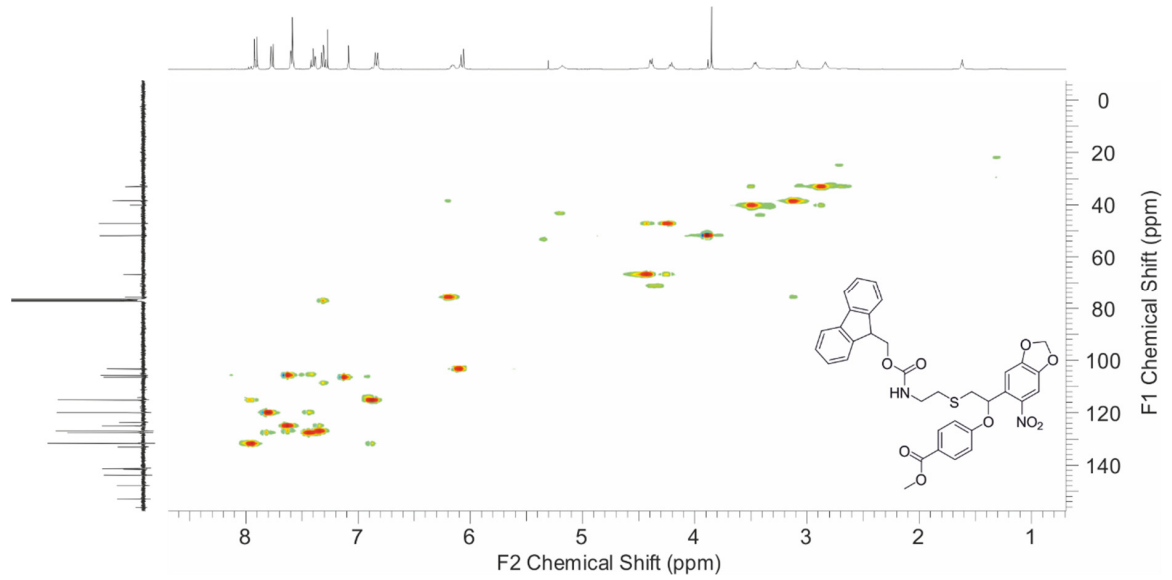

4-(2-((2-((((9H-Fluoren-9-yl)methoxy)carbonyl)amino)ethyl)thio)-1-(6-nitrobenzo[d][1,3]dioxol-5-yl)ethoxy)benzoic acid (6)

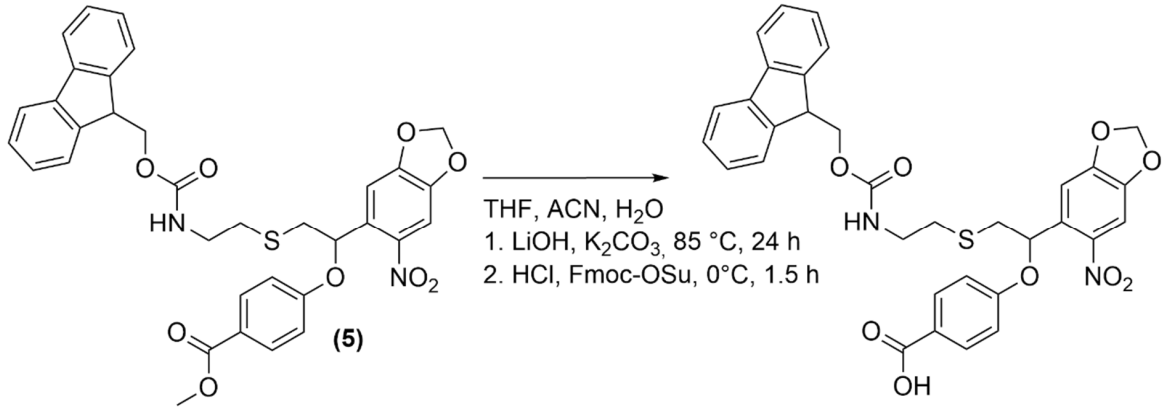

5 *(0.93 g, 1.5 mmol, 1.0 eq) was suspended in THF (40 ml) and stirred under argon atmosphere. LiOH (0.07 g, 5.8 mmol, 4.0 eq) in water (5.8 ml), K_2CO_3 (0.2 g, 2.9 mmol, 2.0 eq) and ACN (40 ml) were added, and the mixture was heated to 85 °C (reflux, 24 h). The saponification was stopped by adjusting the pH value to 8–9 with 1 M HCl under ice cooling. Since the Fmoc-group was cleaved under basic conditions, Fmoc-OSu (0.49 g, 1.5 mmol, 1.0 eq) was added at 0 °C. After stirring for 1.5 h at rt, the solvent was removed in vacuo. EA was added, and the organic layer was washed with brine and dried over Na_2SO_4. After evaporation of the solvent, the crude product was purified by flash column chromatography (CH/EA 2:3 + 0.1% AcOH) to yield 0.45 g (50%) clean product.*

R_f (CH/EA, 2:3 + 0.1% AcOH) = 0.37

^{1}H-NMR (400 MHz, $CDCl_3$) δ [ppm] = 7.96 (d, J = 8.8 Hz, 2H), 7.76 (d, J = 7.6 Hz, 2H), 7.59 (d, J = 7.3 Hz, 2H), 7.59 (s, 1H), 7.40 (m, 2H), 7.31 (m, 2H), 7.08 (s, 1H), 6.85 (d, J = 8.7 Hz, 2H), 6.17 (dd, J = 6.6, 3.9 Hz, 1H), 6.08 (d, J = 8.2 Hz, 2H), 5,17 (m, 1H), 4.39 (d, J = 7.0 Hz, 2H), 4.20 (t, J = 6.9 Hz, 1H), 3. 46 (q, J = 5.9 Hz, 2H), 3.08 (m, 2H), 2.83 (m, 2H).

^{13}C-NMR (101 MHz, $CDCl_3$) δ [ppm] = 167.0, 161.2, 153.0, 147.9, 143.9, 141.6, 141.2, 133.0, 132.5, 127.7, 127.0, 125.1, 122.7, 120.0, 115.3, 106.4, 105.8, 103.4, 81.4, 75.9, 66.8, 47.2, 40.2, 38.4, 33.1.

HR-ESI-MS: $[M+Na]^+_{(theor.)}$ = 651.14077, $[M+Na]^+_{(meas.)}$ = 651.14100.

^{1}H-NMR (400 MHz, $CDCl_3$) of **6**

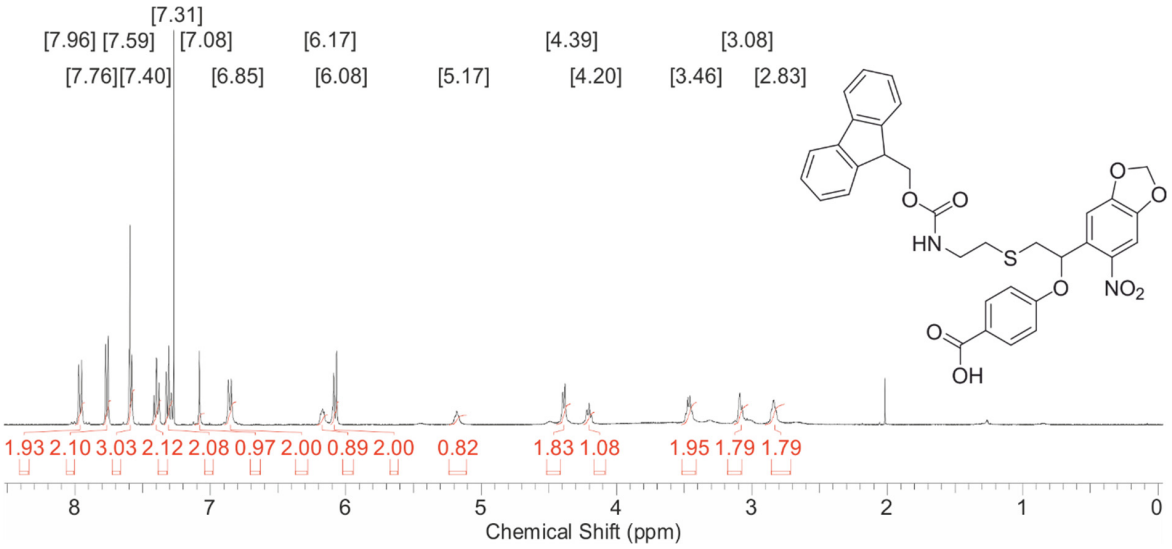

^{13}C-NMR (101 MHz, $CDCl_3$) of **6**

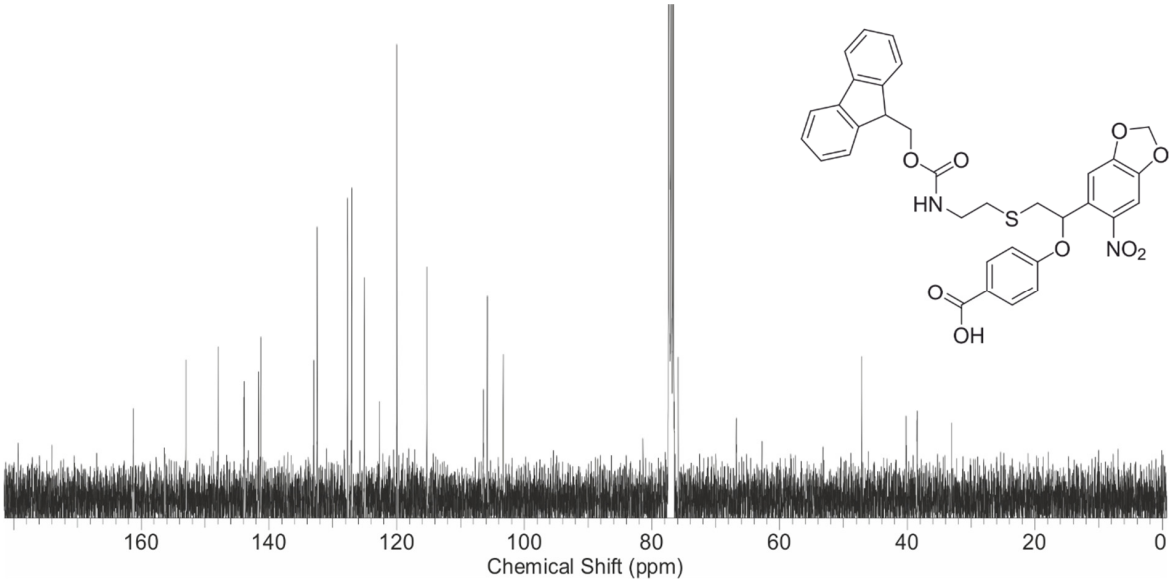

2D-NMR $^{1}H,^{1}H$-COSY of **6**

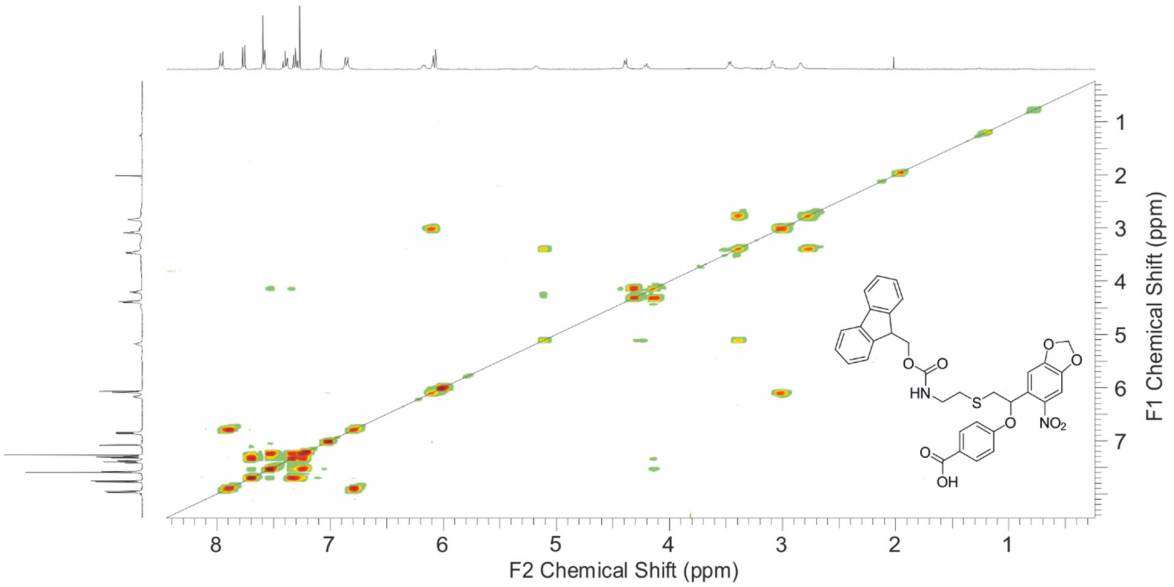

2D-NMR $^{1}H,^{13}C$-HSQC of **6**

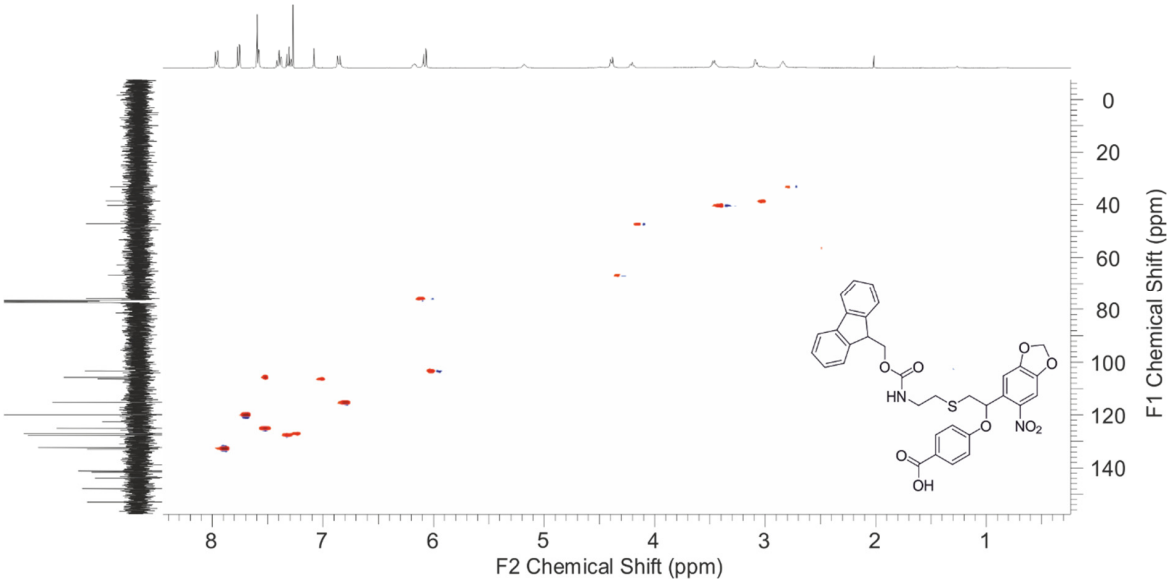

25

Solid-phase peptide synthesis (SPPS)

The general SPPS setup used here was recently described in detail.[5] In short manual synthesis was performed in polypropylene/polyethylene syringes equipped with a polyether sulfone frit. Incubation was carried out on a VIBRAX VXR basic (IKA) shaker (1500 rpm) at room temperature. If not indicated otherwise the resin was washed after each coupling, capping or deprotection step with NMP/DCM 1:1 (3 times 5 ml), DCM (3 times 5 ml) and NMP (3 times 5 ml). If not indicated otherwise all amino acids were pre-activated with HBTU/HOBt for 5-15 min at room temperature before being added to the resin.

BG-OH and $^{N7\text{-}Npom}$BG-OH were synthesized as previously described.[5]

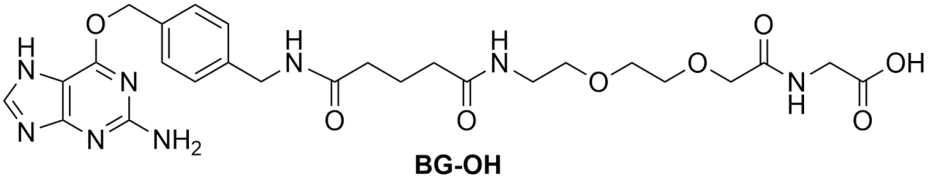

BG-OH

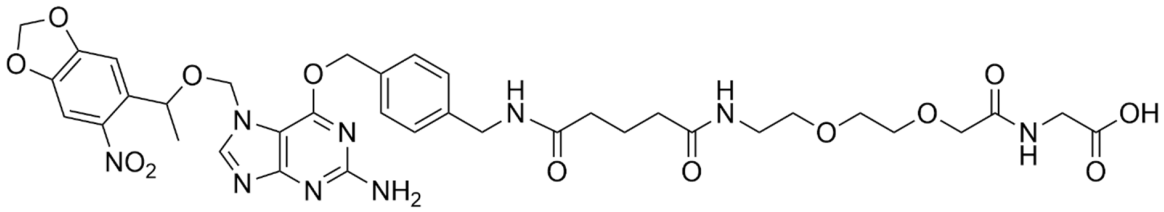

$^{N7\text{-}Npom}$BG-OH

BC-OH (7)

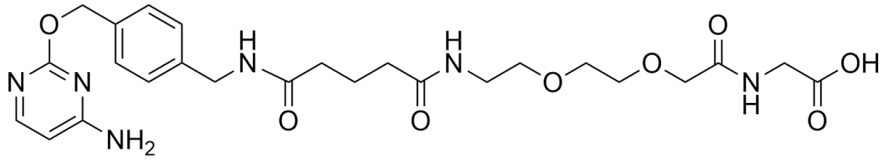

(7, BC-OH) 65%

BC-OH was obtained via solid-phase peptide synthesis as described for BG-OH starting from 413 mg (260 µmol, 1 eq) H-Gly-2-Cl-Trt resin and using 20 mg (87.0 µmol, 0.33 eq) BC-NH_2.[2] The resulting crude product was dissolved in 20 % buffer B, filtered, and purified via preparative HPLC, which yielded 31 mg (58.8 µmol, 65 %) BC-OH after lyophilization.

HR-ESI-MS: $[M+H]^+_{(theor.)}$ = 547.25109 $[M+H]^+_{(meas.)}$ = 547.25159.

BG-^{UV}X-OH (8)

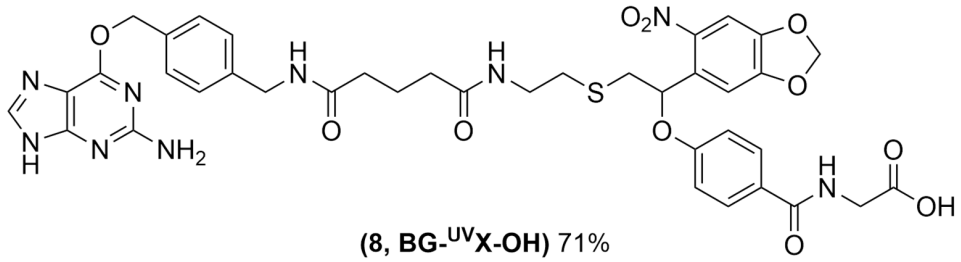

(8, BG-^{UV}X-OH) 71%

*Fmoc-^{UV}X-OH (**6**, 140 mg, 170 µmol, 1.7 eq) was coupled to the H-Gly-2-Cl-Trt resin (Merck, 171 mg, 100 µmol, 1eq) with HBTU (57 mg, 150 µmol, 1.5 eq) and HOBt (31 mg, 200 µmol, 2 eq) in 1,4 ml NMP and 120 µl DIPEA for 1 hour. After washing the resin was capped two times with 6 ml acetic anhydride/DIPEA/NMP 1:1:10 for 10 min. The resin was deprotected using NMP/piperidine 5:1 (3 times 3 ml for 7 min). Glutaric anhydride (114 mg, 1 mmol, 10 eq) in 1,5 ml NMP and 150 µl DIPEA was coupled for 20 minutes. To activate the terminal carboxyl group, the linker was incubated with HBTU (380 mg, 1 mmol, 10 eq) and HOBt (230mg, 1.5 mmol, 1.5 eq) in 4.3 ml NMP and 0.7 ml DIPEA for 10 minutes. The resin was washed with dried NMP only (4 times). BG-NH_2 (20 mg, 75 µmol, 0.75 eq) in 3 ml DMF/DMSO 1:3 with 50 µl DIPEA was added and reacted for 3 hours. Afterwards the resin was washed with DCM/NMP, DCM, NMP and Et_2O (each 3 times, 5 ml). After swelling in DCM, the resin was cleaved in 15 ml DCM/HFIP/TFA 9:1:0.05 under continuous flow. The cleavage solution was dried in vacuo resulting in 126 mg of a yellow solid. The crude product was solved in eluent A and B. Preparative HPLC yielded 42.5 mg (51.8 µmol, 71%) BG-^{UV}X-OH.*

HR-ESI-MS: $[M+H]^+_{(theor.)}$ = 830.25625 $[M+H]^+_{(meas.)}$ = 830.25666

$[M-H]^-_{(theor.)}$ = 828.24170 $[M-H]^-_{(meas.)}$ = 828.24108.

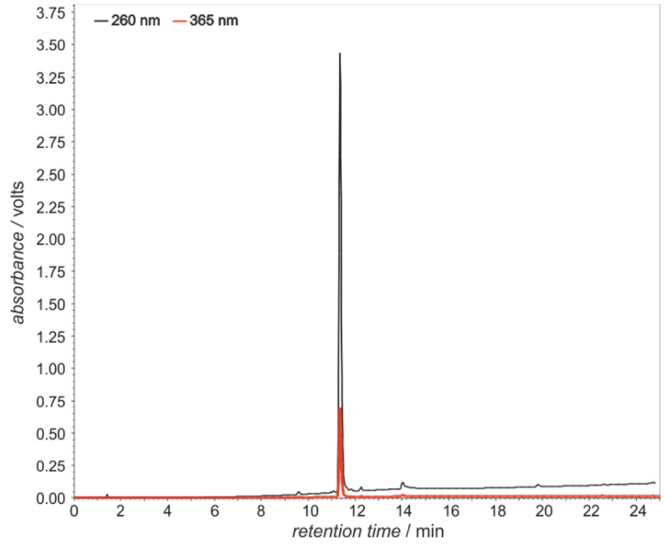

BC-^{UV}X-OH (9)

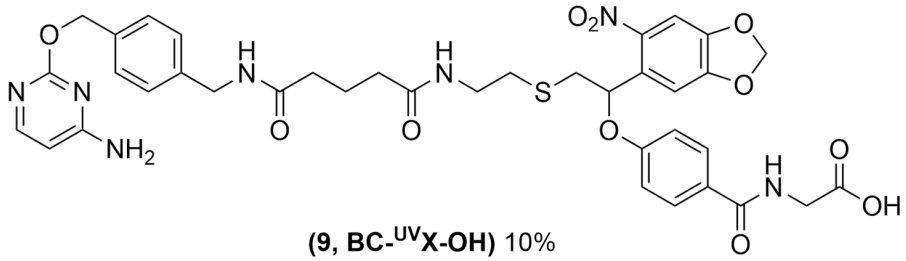

(9, BC-^{UV}X-OH) 10%

*Fmoc-^{UV}X-OH (**6**, 70 mg, 85 µmol, 1.7 eq) was coupled to the H-Gly-2-Cl-Trt resin (Merck, 86.2 mg, 50 µmol, 1 eq) with HBTU (28.5 mg, 75 µmol, 1.5 eq) and HOBt (15.5 mg, 100 µmol, 2 eq) in 700 µl NMP and 60 µl DIPEA for 1 hour. The resin was deprotected using NMP/piperidine 5:1 (3 times 5 ml for 10 min). Next, glutaric anhydride (57 mg, 0.5 mmol, 10 eq) in 750 µl NMP and 75 µL DIPEA was coupled for 20 minutes. To activate the terminal carboxyl group, the linker was incubated with HBTU (190 mg, 0.5 mmol, 10 eq) and HOBt (115 mg, 0.75 mmol, 1.5 eq) in 2.2 ml NMP and 350 µl DIPEA for 10 minutes. The resin was washed with dried NMP only (4 times). BC-NH_2 (8.6 mg, 37.5 µmol, 0.75 eq) in 500 µl NMP and 125 µl DIPEA was added and reacted for 4 hours. Test cleavage showed a low coupling efficiency. Therefore, the resin was activated again with EDCI (500 µmol, 10 eq) and NHS (750 µmol, 15 eq) in NMP/DIPEA 17:3. BC-NH_2 (8.6 mg, 37.5 µmol, 0.75 eq) was added and incubated for another 3 hours. Afterwards the resin was washed with DCM/NMP, DCM, NMP and Et_2O (each 3 times, 5 ml). After swelling in DCM, the resin was cleaved with 30 ml DCM/HFIP/TFA 9:1:0.05 under continuous flow. The crude product was dried in vacuo and solved in eluent A and B for HPLC. Preparative HPLC yielded 3.0 mg (3.8 µmol, 10%) BC-^{UV}X-OH.*

HR-ESI-MS: $[M+H]^+_{(theor.)}$ = 790.25010 $[M+H]^+_{(meas.)}$ = 790.24965.

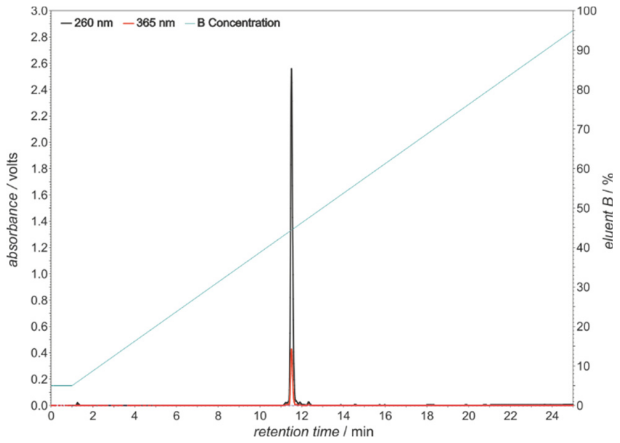

Note: We have recently published an optimized protocol for the synthesis of $^{N7\text{-}Npom}$BG-OH and BG-OH linker.[5] There we recommend an activation of the glutaric anhydride on the resin using pentafluorphenyl-trifluoracetat. To our experience this yields higher coupling efficiency and allows to store the activated resin for at least 3 months at -20°C. However, we do not recommend applying this protocol for linker containing the Fmoc-^{UV}X-OH building block since it results in strong formation of a side product with an oxidized sulfur (data not shown).

(4-Hydroxybenzoyl)glycine (10)

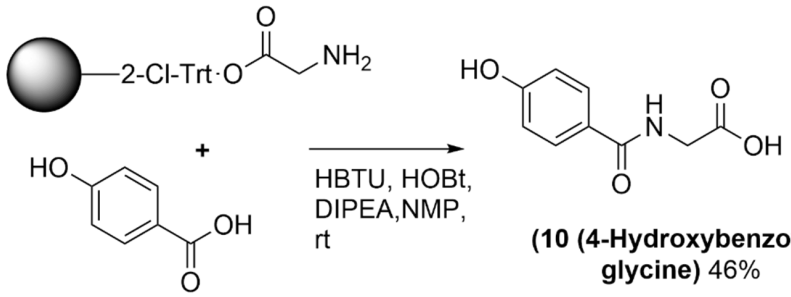

H-Gly-2-Cl-Trt resin (Merck, 71 mg, 45 µmol, 1.0 eq) was swelled in NMP (2 ml) for 10 min. 4-hydroxybenzoic acid (25 mg, 0.18 mmol, 4.0 eq), was preactivated with HBTU (83 mg, 0.18 mmol, 4.0 eq) and HOBt (33 mg, 0.18 mmol, 4.0 eq) in 2 ml NMP/DIPEA 8:1 for 5 min. The preactivation was added to the resin and shaken for 30 min. The resin was washed with DCM/NMP 1:1 (4x), DCM (4x), NMP (4x) and DCM (4x). Cleavage was performed with DCM + 0.5% TFA (15 ml). The cleavage solution was evaporated, and the crude product applied to preparative HPLC. 4 mg (46%) of a white solid were obtained.

^{1}H-NMR (250 MHz, DMSO-d_6) δ [ppm] = 9.97 (br s, 1H), 8.54 (t, J = 5.9 Hz, 1H), 7.73 (d, J = 8.8 Hz, 2H), 6.79 (d, J = 8.8 Hz, 2H), 3.89 (d, J = 5.9 Hz, 2H).

LC-MS: $[M+H]^+$ = 196.1, $[2M+H]^+$ = 391.1, $[M-H]^-$ = 194.1, $[2M-H]^-$ = 389.1.

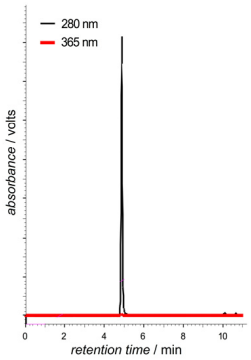

1H-NMR (250 MHz, CDCl3) of **10**

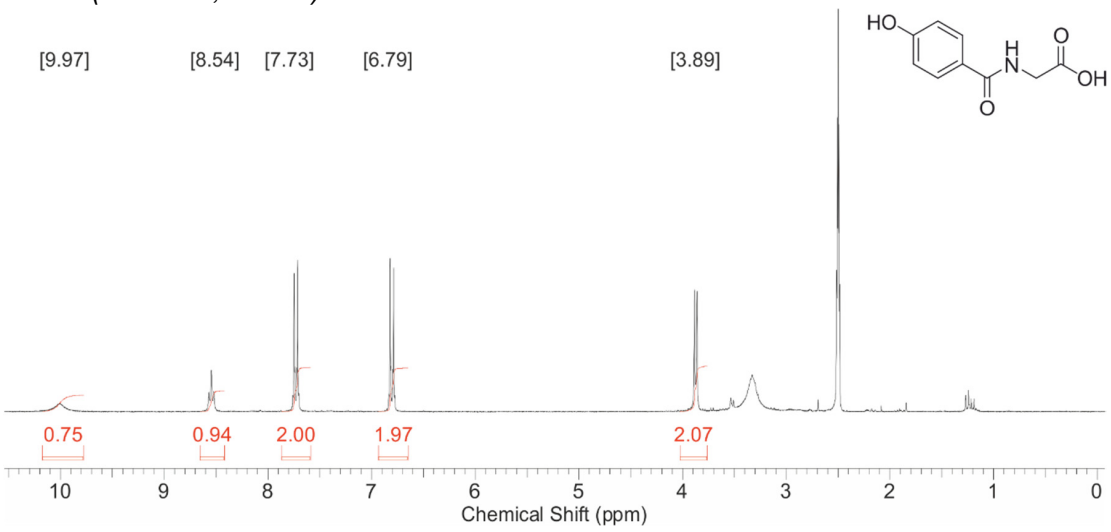

29

BG-Lys(NH_2)-OH and $^{N7\text{-}Npom}$BG-Lys(NH_2)-OH (11,12)

The SPPS of the linker for BG-Lys(NH_2)-OH and $^{N7\text{-}Npom}$BG-Lys(NH_2)-OH was carried out in parallel until the final coupling step. Of 0.71 mg of H-Gly-2-Cl-Trt-resin (450 µmol) initially used, one quarter (112.5 µmol) was used for the synthesis BG-Lys(NH_2)-OH and one quarter (112.5 µmol) was used for the synthesis $^{N7\text{-}Npom}$BG-Lys(NH_2)-OH. The remaining resin was stored at -20°C after pentafluorphenyl activation and used for later syntheses.

Fmoc-Lys(Mtt)-OH (845 mg, 1.35 mmol, 3 eq) was coupled to the H-Gly-2-Cl-Trt resin (Merck, 705 mg, 450 µmol, 1 eq) with HBTU (455 mg, 1.2 mmol, 2.7 eq) and HOBt (182 mg, 1.35 mmol, 3 eq) in 6 ml NMP and 1.5 ml DIPEA for 1 hour. After washing the resin was capped two times with 12 ml acetic anhydride/DIPEA/NMP 1:1:10 for 10 min. The resin was deprotected using NMP/piperidine 5:1 (3 times 5 ml for 10 min) and Fmoc-AEEA-OH (520 mg, 1.35 mmol, 3 eq) was coupled with HBTU (455 mg, 1.2 mmol, 2.7 eq) and HOBt (182 mg, 1.35 mmol, 1 eq) in 6 ml DMSO and 1.5 ml DIPEA for 1 hour. The resin was capped and deprotected as described above and glutaric anhydride (500 mg, 4.4 mmol, 10 eq) in 10 ml NMP/DIPEA 5:1 was coupled for 30 min. An additional washing step with 0.1% NaOH in Dioxan/H_2O 1:1 was performed, and the resin was washed again to remove remaining H_2O. To activate the terminal carboxyl group, pentafluorphenyl-trifluoracetat (Pfp-TFA, 373 µL, 2.2 mmol, 5 eq) in 5 ml pyridine/DCM 1:1 was incubated with the resin two times (10 min + 20 min). The resin was washed as described above and followed by additional washing with DCM (3 times). The resin was dried in vacuo and split into 4 equal portions according to weight.

BG-Lys(NH_2)-OH (11)

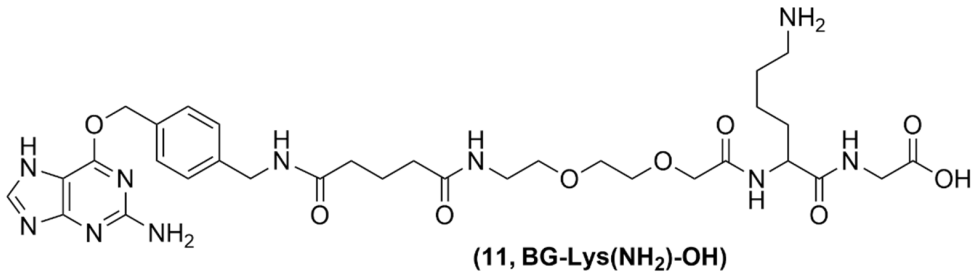

(11, BG-Lys(NH_2)-OH)

For synthesis of BG-Lys(NH_2)-OH, BG-NH_2 (10 mg, 37.5 µmol, 0.33 eq) was solved in 3 ml NMP/DMSO 1:3 with 50 µl DIPEA and incubated with Pfp-glutaric anhydride-AEEA-Lys(Mtt)-Gly-2-Cl-Trt resin (112.5 µmol, 1 eq) for 18 hours at room temperature. The resin was washed with DCM/NMP, DCM, NMP and Et_2O (each 3 times, 5 ml). After swelling in DCM, the resin was cleaved with 30 ml DCM/HFIP/TIPS/TFA 9:1:0.05:0.1 under continuous flow. The crude product was dried in vacuo and purified by preparative HPLC.

HR-ESI-MS: $[M+H]^+_{(theor.)}$ = 715.35220, $[M+H]^+_{(meas.)}$ = 715.35235.

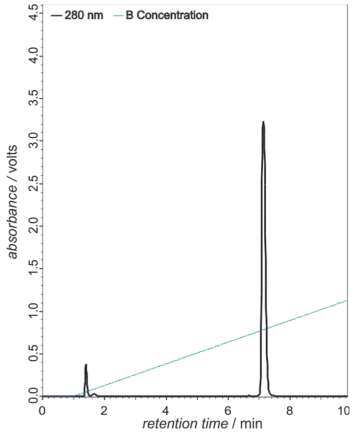

$^{N7\text{-}Npom}$BG-Lys(NH_2)-OH (12)

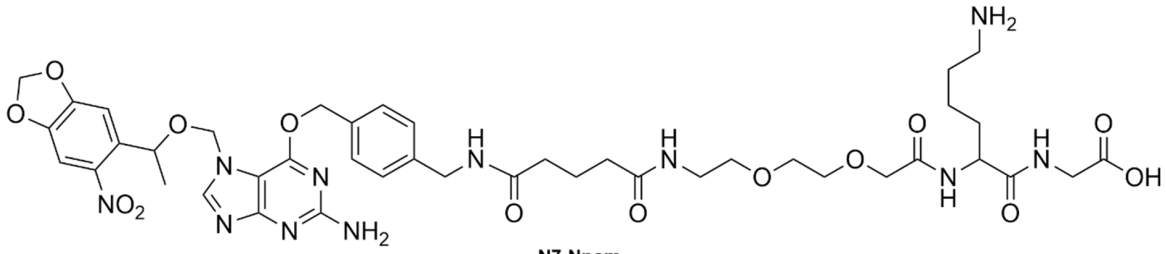

(12, $^{N7\text{-}Npom}$BG-Lys(NH_2)-OH) 50%

*For synthesis of $^{N7\text{-}Npom}$BG-Lys(NH_2)-OH, $^{N7\text{-}Npom}$BG-NH_2 (16 mg, 33 µmol, 0.3 eq) was solved in 1.5 ml NMP/DMSO/DIPEA 100:15:8 and incubated with Pfp-glutaric anhydride-AEEA-Lys(Mtt)-Gly-2-Cl-Trt resin (112.5 µmol) for 18 hours at room temperature. The resin was washed with DCM/NMP, DCM, NMP and Et_2O (each 3 times, 5 ml). After swelling in DCM, the resin was cleaved with 30 ml DCM/HFIP/TIPS/TFA 9:1:0.05:0.1 under continuous flow. The crude product was dried in vacuo and purified by preparative HPLC, yielding 8.5 mg (**12**, 9 µmol, 27%).*

HR-ESI-MS: $[M+H]^+_{(theor.)}$ = 938.40027, $[M+H]^+_{(meas.)}$ = 938.39942.

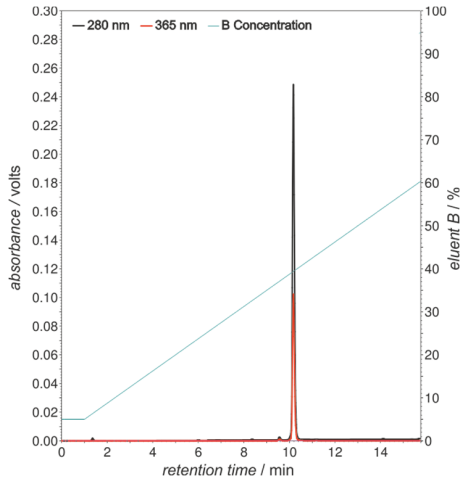

Synthesis of bifunctional linker

For the synthesis of the bifunctional linkers BC-OH or BC-^{UV}X-OH were activated with N,N'-diisopropylcarbodiimide (DIC) and N-hydroxysuccinimide (NHS) to form the corresponding NHS ester. The NHS esters were used in situ to react either with BG-Lys(NH_2)-OH or $^{N7\text{-}Npom}$Bg-Lys(NH_2)-OH.

For preactivation the following solutions were freshly prepared and used within a day:

- *DIC in DMSO (34 mg/ml, 270 mM)*
- *NHS in DMSO (53.1 mg/ml, 450 mM)*
- *DIPEA/DMSO 1:20*
- *All linker molecules were solved in DMSO to a concentration of 60 mM*

The amount of BC-OH or BC-^{UV}X-OH linker activated for each synthesis is listed for the respective molecule below. Equal volumes of the above mentioned four solutions were mixed and the reaction was carried out for 15-18 hours at 40°C on a shaker at 900 rpm. The solution was then freeze dried overnight using a Christ Alpha 2-4 LDplus lyophilizer to remove solvent and excess DIC. The resulting oil was solved in 140 µl DMSO and 100 µl $NaHCO_3$ (0.2 M in H_2O), and added to the indicated amount of BG-Lys(NH_2)-OH or $^{N7\text{-}Npom}$Bg-Lys(NH_2)-OH linker.

BG/BC-OH linker (13)

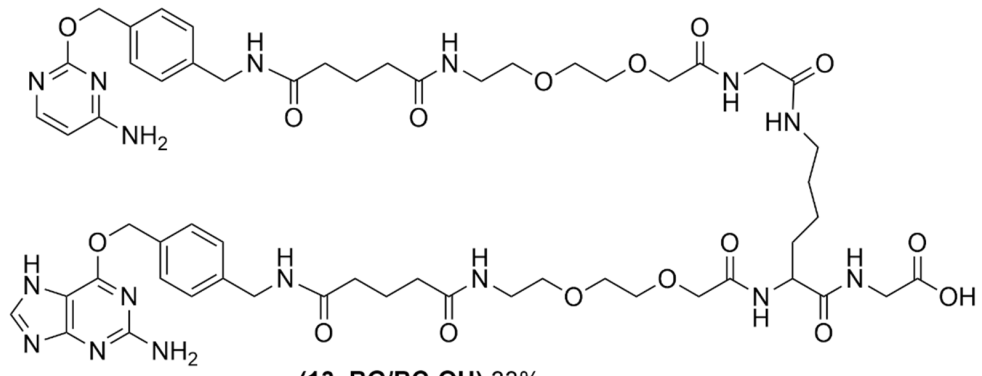

(13, BG/BC-OH) 33%

*BC-OH linker (**7**, 60 mM in DMSO, 60 µl, 3.6 µmol, 1 eq) was preactivated and reacted with BG-Lys(NH_2)-OH linker (**11**, 60 mM in DMSO, 90 µl, 5.4 µmol, 1.5 eq) for 35 min. The reaction was stopped by the addition of 2.5 ml of HPLC eluent A/B 5:1. The linker was purified by preparative HPLC, yielding 1.5 mg BG/BC-OH linker (1.2 µmol, 33%).*

LC-MS: $[M+2H]^{2+}_{(theor.)}$ = 621.29 $[M+2H]^{2+}_{(meas.)}$ = 622.40, $[M+3H]^{3+}_{(meas.)}$ = 415.25, $[M+4H]^{4+}_{(meas.)}$ = 311.65.

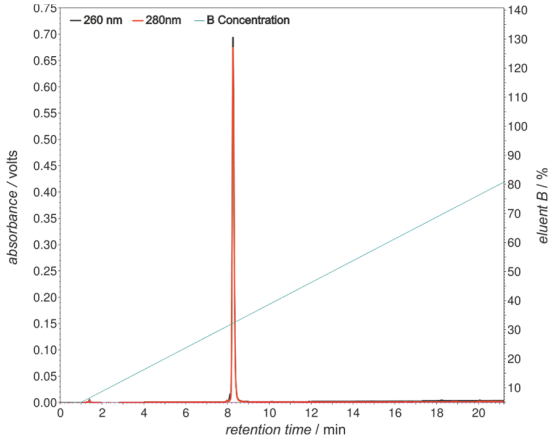

$^{N7\text{-}Npom}$BG/BC-OH linker (14)

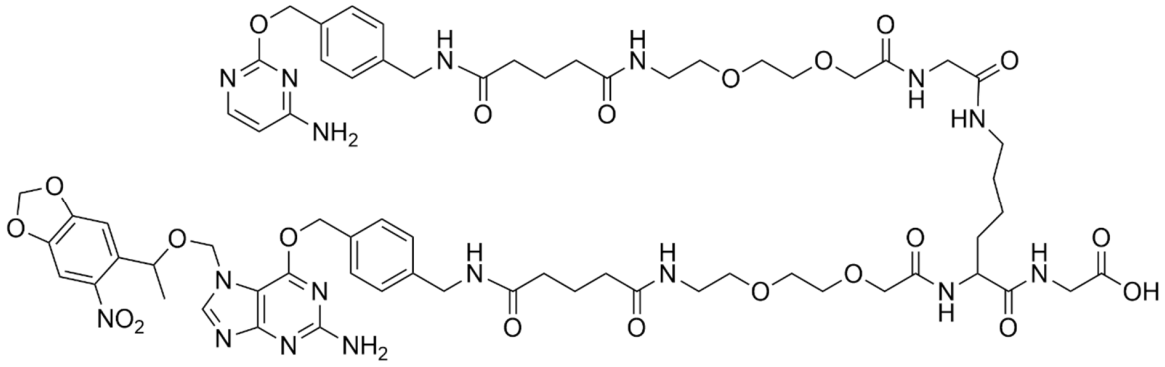

(14, $^{N7\text{-}Npom}$BG/BC-OH) 31%

*BC-OH linker (**7**, 60 mM in DMSO, 60 µl, 3.6 µmol, 1 eq) was preactivated and reacted with $^{N7\text{-}Npom}$BG-Lys(NH_2)-OH linker (**12**, 60 mM in DMSO, 65 µl, 3.9 µmol, 1.08 eq) for 30 min. The reaction was stopped by the addition of 2.5 ml of HPLC eluent A/B 5:1. The linker was purified by preparative HPLC, yielding 1.6 mg $^{N7\text{-}Npom}$BG/BC-OH linker (1.1 µmol, 31%).*

HR-ESI-MS: $[M+H]^{+}_{(theor.)}$ = 1466.63352, $[M+H]^{+}_{(meas.)}$ = 1466.63192
HR-ESI-MS: $[M+2H]^{2+}_{(theor.)}$ = 733.82040, $[M+2H]^{2+}_{(meas.)}$ = 733.82055.

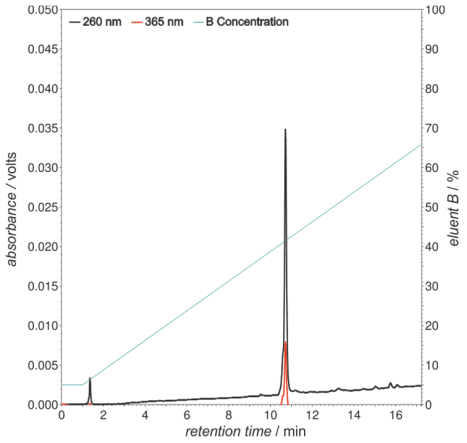

$^{N7\text{-}Npom}$BG/BC-^{UV}X-OH linker (15)

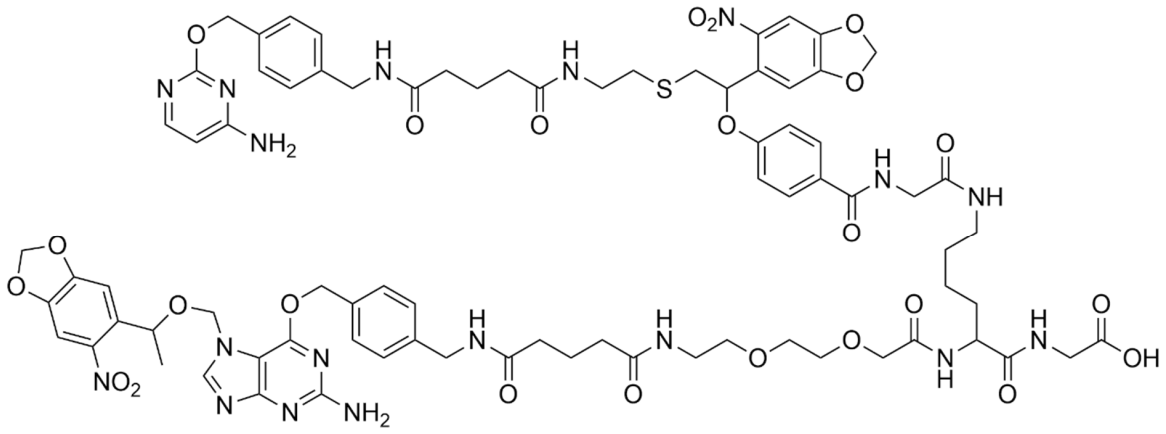

(15, $^{N7\text{-}Npom}$BG/BC-^{UV}X-OH) 11%

*BC-^{UV}X-OH linker (**9**, 60 mM in DMSO, 60 µl, 3.6 µmol, 1 eq) was preactivated and reacted with $^{N7\text{-}Npom}$BG-Lys(NH_2)-OH linker (**12**, 60 mM in DMSO, 65 µl, 3.9 µmol, 1.08 eq) for 30 min. The reaction was stopped by the addition of 2.5 ml of HPLC eluent A/B 5:1. The linker was purified by preparative HPLC, yielding 0.7 mg $^{N7\text{-}Npom}$BG/BC-^{UV}X-OH linker (0.41 µmol, 11%).*

LC-MS: $[M+2H]^{2+}_{(theor.)}$ = 854.31 $[M+2H]^{2+}$ = 855.75, $[M+3H]^{3+}$ = 570.80, $[M+4H]^{4+}$ = 428.25.

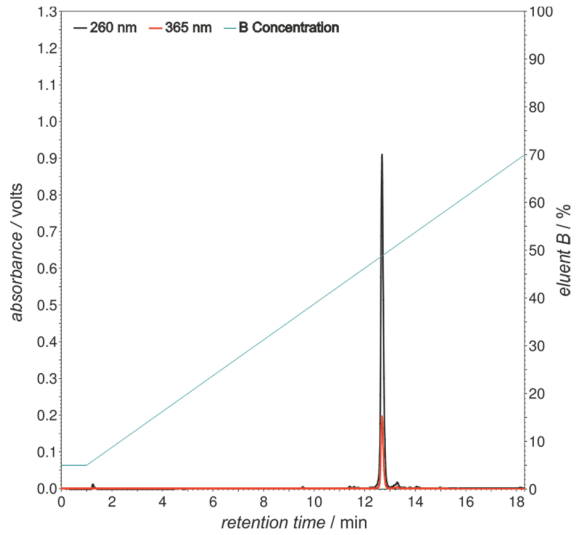

Synthesis of BG-Atto488 and BG-^{UV}X-Atto488

For the synthesis of the fluorophore conjugates BG-OH and BG-^{UV}X-OH were activated with 1-ethyl-3-(3-dimethylaminopropyl)carbodiimide (EDCI) and N-hydroxysuccinimide (NHS) to form the corresponding NHS ester. The NHS esters were used in situ to react with Atto488-amine (Atto-tec GmbH, Germany).

For preactivation the following solutions were freshly prepared and used within a day:

- *EDCI·HCl in DMSO (52.2 mg/ml, 270 mM)*
- *NHS in DMSO (53.1 mg/ml, 460 mM)*
- *DIPEA/DMSO 1:20*
- *All linker molecules were solved in DMSO to a concentration of 60 mM*

The amount of BG-OH and BG-^{UV}X-OH linker activated for each synthesis is listed for the respective molecule below. Equal volumes of the above mentioned four solutions were mixed and the reaction was carried out for 15-18 hours at 37°C on a shaker (900 rpm).

BG-Atto488 (16)

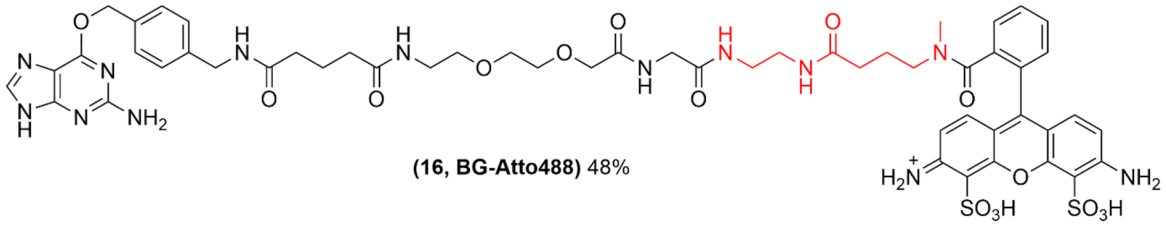

(16, BG-Atto488) 48%

BG-OH linker (60 mM in DMSO, 20 µl, 1.2 µmol, 4 eq) was preactivated and reacted with Atto488-amine (11.6 mM in DMSO, 25 µl, 0.29 µmol, 1 eq) for 60 min at 37°C on a shaker at 900 rpm. The reaction was stopped by the addition of 2.5 ml of HPLC eluent A and followed by HPLC purification yielding 170 µg BG-Atto488 (0.14 µmol, 48 %). The yield was determined by solving the product in DMSO, dilution in phosphate buffered saline (PBS) and measurement of the absorbance at 500 nm ($\varepsilon_{500\ nm}$ = 90.000 $M^{-1}cm^{-1}$). Note: the full structure of Atto488-amine is not available from the supplier. The substructure marked in red within the structural formula is therefore not confirmed but fits to the HR-MS analysis.

HR-ESI-MS: $[M+2H]^{2+}_{(theor.)}$ = 600.69731, $[M+2H]^{2+}_{(meas.)}$ = 600.69664.

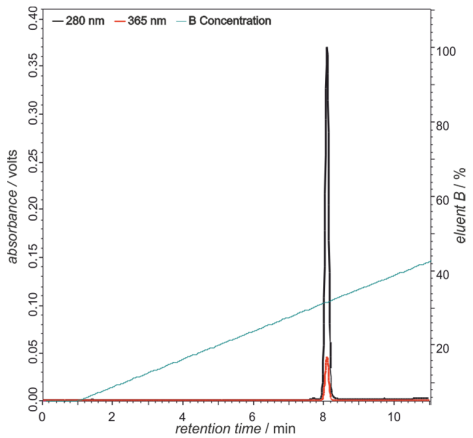

BG-^{UV}X-Atto488 (17)

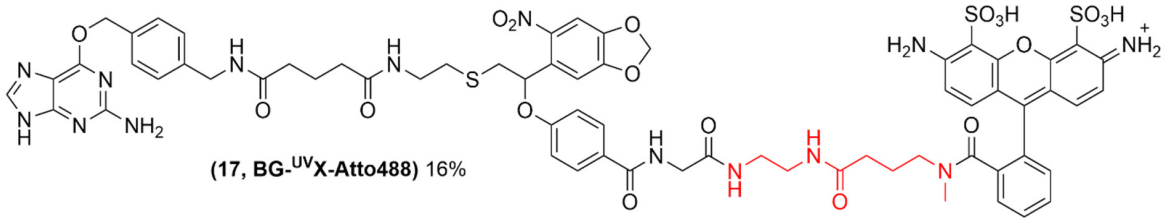

*BG-^{UV}X-OH linker (**8**, 60 mM in DMSO, 30 µl, 1.8 µmol, 4.4 eq) was preactivated and reacted with Atto488-amine (11.6 mM in DMSO, 35 µl, 0.41 µmol, 1 eq) for 60 min at 37°C on a shaker at 900 rpm. The reaction was stopped by the addition of 2.5 ml of HPLC eluent A and followed by HPLC purification yielding 91 µg BG-^{UV}X-Atto488 (63 nmol, 16%). The yield was determined by solving the product in DMSO, dilution in phosphate buffered saline (PBS) and measurement of the absorbance at 500 nm ($\varepsilon_{500\ nm}$ = 90.000 $M^{-1}cm^{-1}$). Note: the full structure of Atto488-amine is not available from the supplier. The substructure marked in red within the structural formula is therefore not confirmed but fits to the HR-MS analysis.*

HR-ESI-MS: $[M+2H]^{2+}_{(theor.)}$ = 722.19682, $[M+2H]^{2+}_{(meas.)}$ = 722.19613.

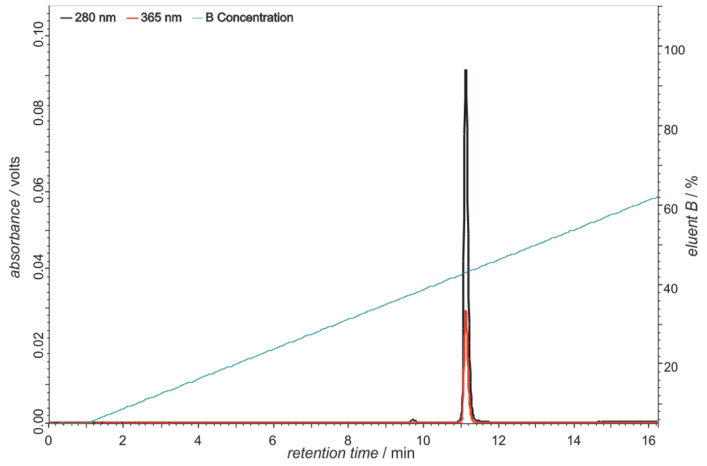

guideRNA synthesis

NH-Stop-66 guideRNA was obtained from Eurofins in HPLC-purified quality carrying a 5´-C6-aminolinker. NH-Y701C and NH-T288A were obtained from Biospring (Frankfurt, Germany) in HPLC-purified quality carrying a 5´-C6-aminolinker. OMe modified poly(U) was obtained from Sigma Aldrich in desalted quality carrying a 5´-C6-aminolinker and OMe/LNA modified poly(U) was obtained from Eurogentec in desalted quality carrying a 5´-C6-aminolinker and a 3'-C7-aminolinker. NH-Y701C and NH-T288A guideRNAs were solved in RNase free water to a concentration of 6 µg/µl. NH-Stop66 and NH-poly(U) were precipitated with 0.1 volumes of 3 M NaCl and 3 volumes of 100% EtOH, washed with 70% EtOH and dissolved in RNase free water (6 µg/µl) prior to coupling. We recently described the guideRNA synthesis in detail.[5] In short the respective linker (BG-OH, BC-OH, $^{N7\text{-}Npom}$BG-OH, BG-^{UV}X-OH, BC-^{UV}X-OH, BG/BC-

OH, $^{N7\text{-}Npom}$BG/BC-OH or $^{N7\text{-}Npom}$BG/BC-^{UV}X-OH) was activated with DIC, NHS and DIPEA in DMSO according to the protocol for the synthesis of bifunctional linker described above. For all linker containing photo-sensitive moieties the reaction was performed protected from light. The resulting NHS ester was then reacted with the corresponding NH_2-guideRNA in DMSO/H_2O/DIPEA 66:33:1 and purified on a 20% UREA-PAGE. For all linker containing photo-sensitive moieties, the UREA-PAGE was performed in the dark. While the main part of the gel was protected with aluminum foil one lane containing ca. 10% of the crude guideRNA was analyzed on a TLC plate under 254 nm UV light. The migration of NH_2-guideRNA and modified gRNA were noted, and the analyzed lane was discarded. The region corresponding to migration of the modified gRNA was cut out from the remaining lanes and was transferred to an amber reaction tube. guideRNAs were extracted from the gel slices by shaking overnight at 4°C with nuclease free water and precipitated with 0.1 volumes sodium acetate (NaOAc, 3 M) and 3 volumes of EtOH 100% (incubation at -20°C for >4 h). After centrifugation (17,000 g, -4°C, >45 min) the guideRNA pellet was washed with 70% EtOH and dissolved in nuclease free water. Concentrations were determined photometrically by absorption at 260 nm. The extinction coefficients were estimated from the $\varepsilon_{260\ nm}$ provided from the commercial supplier and the sum of the following moieties incorporated into the terminal modification: BG ($\varepsilon_{260\ nm}$ ~ 2.5 $mM^{-1}cm^{-1}$), BC ($\varepsilon_{260\ nm}$ ~ 4.2 $mM^{-1}cm^{-1}$), $^{N7\text{-}Npom}$BG ($\varepsilon_{260\ nm}$ ~6.5 $mM^{-1}cm^{-1}$) and ^{UV}X ($\varepsilon_{260\ nm}$ ~ 23 $mM^{-1}cm^{-1}$).

The synthesis BG-guideRNAs and $^{N7\text{-}Npom}$BG-guideRNAs has been well established in previous publications.[5,8] By our experience the same protocol also achieves good yields of BG-^{UV}X and bifunctional guideRNAs. Shown below on the left panel is the image of an exemplary preparative UREA-PAGE of the crude BG-^{UV}X-guideRNA (BG-^{UV}X-Stop66 used in figure 1d). Two guideRNAs-containing bands are observed with the faster migrating band corresponding to unreacted NH_2-guideRNA followed by the BG-^{UV}X-guideRNA. Scalpel cuts indicate the areas of the UREA- PAGE that were excised for purification and analysis. Excess of BG-^{UV}X-OH can be easily identified by its absorbance spectrum after extraction (see figure S1a). On the right panel, the MALDI-MS spectrum of the pure BG-^{UV}X-Stop66 guideRNA obtained from this synthesis is shown. The two highest peaks correlate to the expected single ionized ($[M–H]^-$ = 7360) and double ionized ($[M–2H]^{2-}$ = 3680) product. No signal corresponding to NH-guideRNA (Mw = 6550 g/mol) was observed.

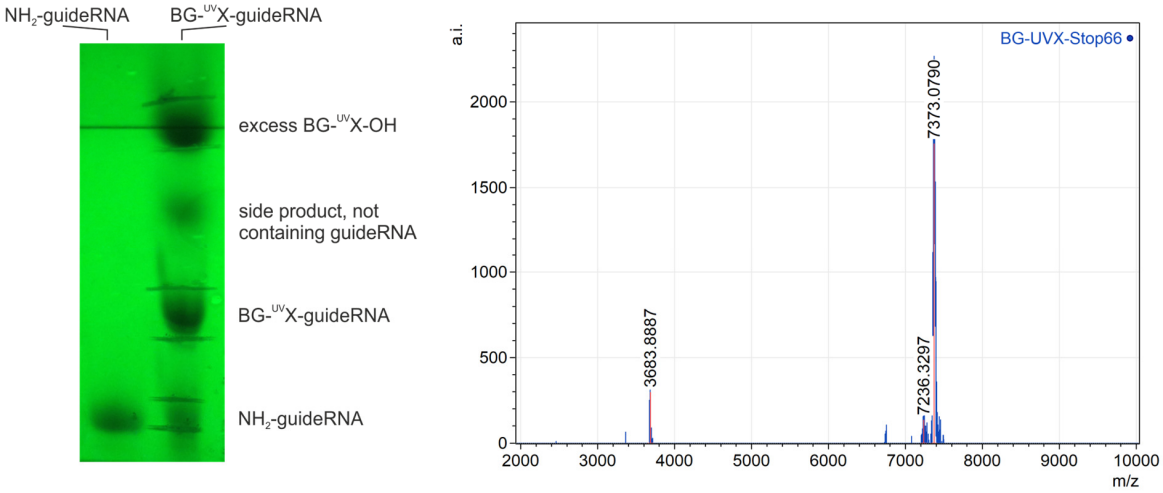

Sequences and modification patterns of guideRNAs used. 2'-OMe modified nucleotides are shown in italic, unmodified RNA bases are shown in bold. LNA bases are underlined. Phosphorothioate linkages have been marked with a star (*). All 5' modifications have been attached via a 6-carbon atom linker at the 5'-terminus.

terminal modification /guideRNA	*sequence*	*Used in Figure*
NH-Stop66	*5´-***UCGGAACACCCCAGCACAGA***-3´*	*1d*
BG-Stop66		*1d*
BG-^{UV}X-Stop66		*1d*
NH-Y701C	*5´-A*G*U**G**U**C**UUGAU* **ACA** *UCCAGUU*C*C*U*T-3´*	*2d*
BG-Y701C		*2a,2d*
$^{N7\text{-}Npom}$BG-Y701C		*2b,*
BG-^{UV}X-Y701C		*2a, 2d*
NH-T288A	*5´-G*U*A**G**U**T**CGUAG* **GCG** *UAUUUCU*G*T*U*C-3´*	*2d*
BG-T288A		*2d*
$^{N7\text{-}Npom}$BG-T288A		*2d*
BG-poly(U)	*5´-UUUUUUUUUUUUUUUUUUUUUUUUUUUUUU -3´*	*3b, 3d*
BC-poly(U)		*3b, 3d*
BG-BC-poly(U)		*3d*
$^{N7\text{-}Npom}$BG-BC-poly(U)		*3e*
$^{N7\text{-}Npom}$BG-BC-^{UV}X-poly(U)	*5´-U**T**UU**T**UU**T**UUU**T**UU**T**UUU**T**UU**T**UUU**T**U -3´*	*3f*

ADAR SDS-PAGE Shift Assay

Expression and purification of SNAP-ADAR3 was performed as previously described.[9] SNAP-ADAR 3 (0.5 µM) and guideRNAs (2 µM) were diluted in 8 µl reaction buffer (10 mM Tris-HCl, 100 mM NaCl, 5% glycerol at pH 8.0). The reaction was carried out in PCR tubes which were wrapped in aluminum foil for light protection. After incubating for 30 min at 30 °C, the samples were irradiated on an UV table (UVP high performance UV transilluminator, 365 nm). 4 µl 4x SDS loading buffer (SDS (8% w/v), glycerol (40% v/v) and bromophenol blue (0,015% w/v) was added, and the samples were applied to SDS-PAGE gel electrophoresis (4% stacking gel, 12% loading gel, gel was run in the dark). GE Healthcare LMW protein marker was applied as size marker and the proteins were visualized by Coomassie staining. The staining solution was composed of Coomassie Brilliant Blue G-250 (0.02% w/v), $Al_2(SO_4)_3$ (5% w/v), EtOH (10% v/v) and phosphoric acid (2% v/v).

Cloning

The full sequence of all previously unpublished plasmids used in this study can be found in the appendix of the supplementary information and plasmid maps are found below.

eBFP-G3BP1 was created by amplifying the coding sequence of G3BP1 from the cDNA of Flp-In 293T-REx cells and fusing it with eBFP2 (obtained from Addgene, Cat.No.54595, https://www.addgene.org/54595/)[10] by primer extension and restriction cloning. SNAP-(eGFP)$_3$ and NLS-SNAP-(eGFP)$_3$ were created by primer extension PCR of the mammalian cell optimized SNAPf-tag (New England Biolabs) and fusion to three copies of eGFP by restriction cloning. NLS-CLIP-(mCherry)$_3$ was created by primer extension PCR of the CLIPf tag (New England Biolabs) and fusion to three copies of the red fluorescent protein mCherry by restriction cloning.

For generating stable HeLa cell lines expressing two transgenes we used the PiggyBac transposase approach.[11] The carrier plasmid PB-CA was obtained from Addgene (Cat.No.20960, https://www.addgene.org/20960/)[12] and the CA resistance was exchanged with a puromycin resistance gene (PuroR). The CMV promoter was replaced by an expression cassette containing a bidirectional tetracycline responsive promoter.[13] Subcloning of eBFP-G3BP1 and SNAP-(eGFP)$_3$ followed by a SV40 polyadenylation signal resulted in PiggyBac-Puro_SNAP-(eGFP)$_3$_eBFP-G3BP1 (used in fig.3b). Subcloning of NLS-CLIP-(mCherry)$_3$ and NLS-SNAP-(eGFP)$_3$ followed by a SV40 polyadenylation signal resulted in PiggyBac-Puro_NLS-SNAP-(eGFP)$_3$_NLS-CLIP-(mCherry)$_3$ (used in fig.3d and 3e). Subcloning of NLS-CLIP-(mCherry)$_3$ and SNAP-(eGFP)$_3$ followed by a SV40 polyadenylation signal resulted in PiggyBac-Puro_SNAP-(eGFP)$_3$_NLS-CLIP-(mCherry)$_3$ (used in fig.3f).

Note: The expression of the transgenes by the bidirectional promoter can be strongly enhanced in the presence of reverse tetracycline-controlled transactivator (rtTA) protein and doxycycline (Tet-On System). However, we found the basal expression of the minimal CMV promoters completely sufficient for the expression of (NLS)-SNAP-(eGFP)$_3$ and NLS-CLIP-(mCherry)$_3$. The expression of eBFP-G3BP1 is relatively low and showed more variation between cells. Since we observed that transient overexpression of eBFP-G3BP1 can trigger stress granules even in the absence of oxidative stress (data not shown) we also proceeded the experiments with the low basal expression of the minimal CMV.

For generating a stable, doxycycline-inducible HeLa cell line expressing the SNAP and CLIP tag on the plasma membrane surface, we used the previously described all-in-one, Tet-On 3G inducible PiggyBac plasmid XLone.[14] XLone-GFP was obtained from Addgene (Cat.No. 96930, https://www.addgene.org/96930/) and the ORF of the blasticidin resistance gene (Bsd) was replaced with a puromycin resistance gene (PuroR) by restriction cloning. Afterwards GFP was entirely replaced by the SNAP-CLIP-display fusion protein which was a kind gift from Kai Johnssons laboratory (now Heidelberg) [15], resulting in the XLone-Puro_SNAP-CLIP-display plasmid.

A mammalian codon-optimized PiggyBac-transposase (mPB) gene[11] was subcloned into the commercial pcDNA3.1 backbone resulting in the pcDNA3.1_mPB plasmid.

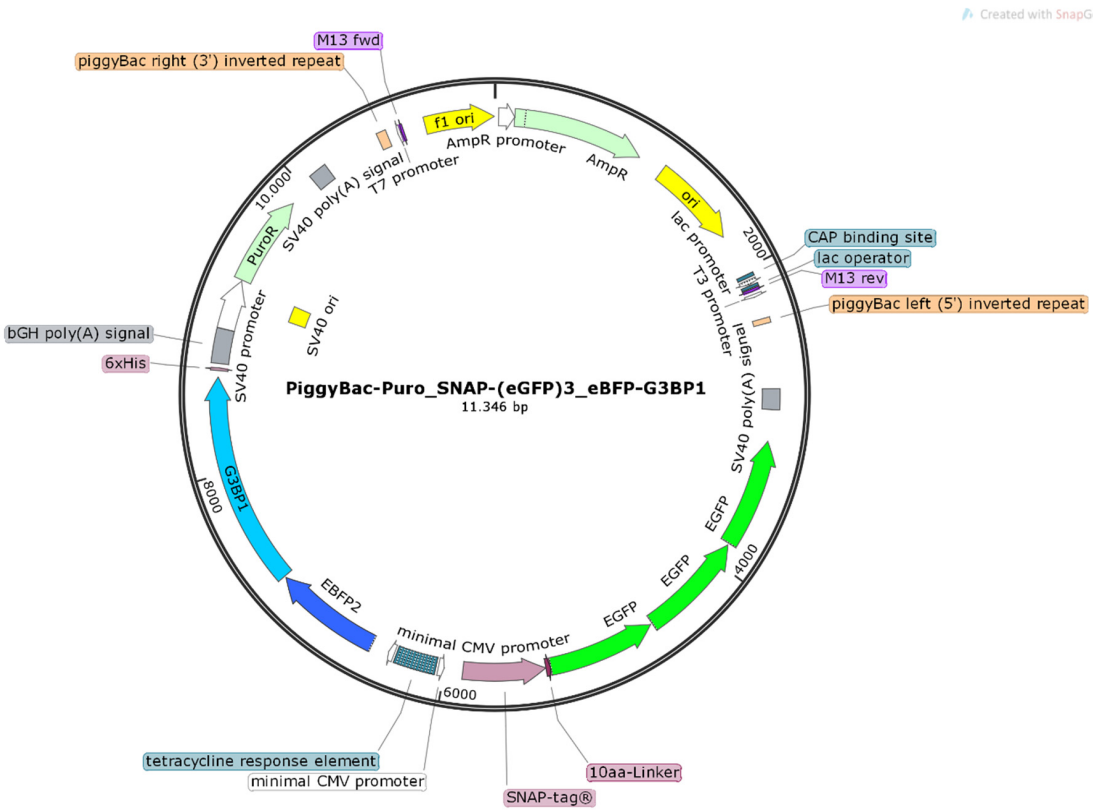
Created with SnapGene®
M13 fwd
piggyBac right (3') inverted repeat
f1 ori
AmpR promoter
AmpR
ori
lac promoter
T3 promoter
CAP binding site
lac operator
M13 rev
piggyBac left (5') inverted repeat
SV40 poly(A) signal
EGFP
EGFP
EGFP
minimal CMV promoter
EBFP2
G3BP1
SV40 promoter
SV40 ori
T7 promoter
SV40 poly(A) signal
PuroR
bGH poly(A) signal
6xHis
PiggyBac-Puro_SNAP-(eGFP)3_eBFP-G3BP1
11.346 bp
2000
4000
6000
8000
10.000
tetracycline response element
minimal CMV promoter
10aa-Linker
SNAP-tag®

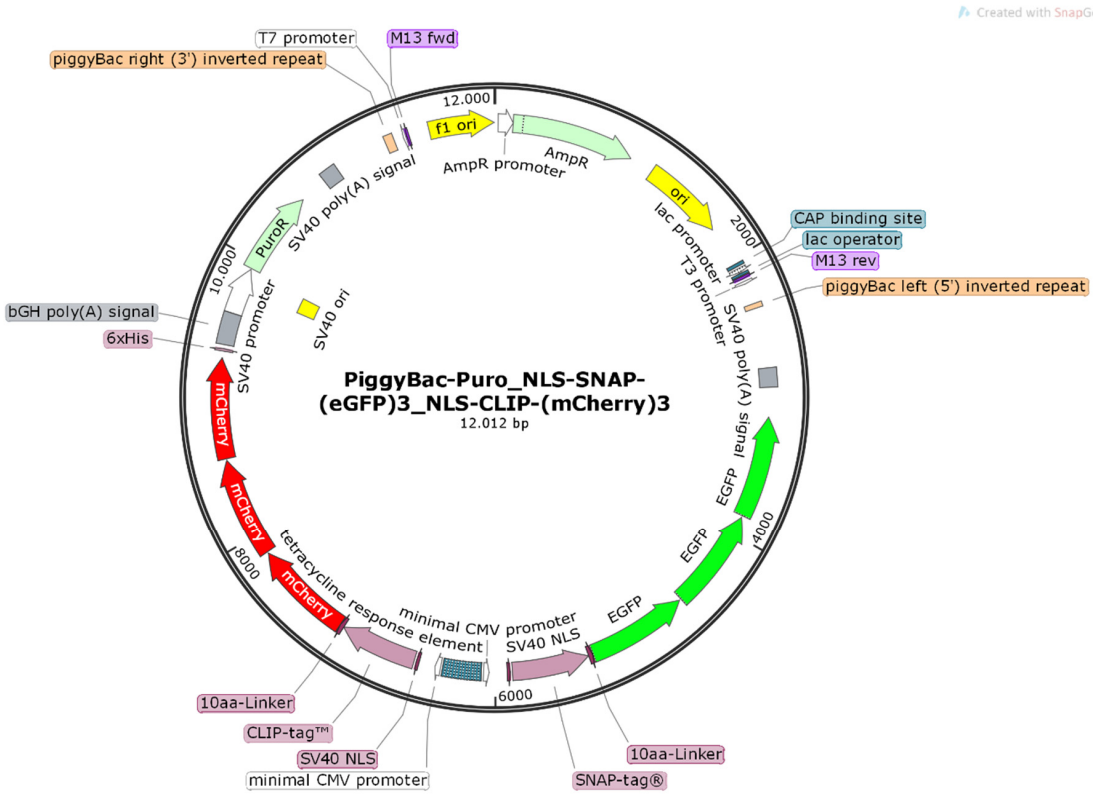
Created with SnapGene®
T7 promoter
M13 fwd
piggyBac right (3') inverted repeat
12.000
f1 ori
AmpR promoter
AmpR
ori
lac promoter
T3 promoter
CAP binding site
lac operator
M13 rev
piggyBac left (5') inverted repeat
SV40 poly(A) signal
EGFP
EGFP
EGFP
minimal CMV promoter
SV40 NLS
tetracycline response element
mCherry
mCherry
mCherry
SV40 promoter
SV40 ori
SV40 poly(A) signal
PuroR
bGH poly(A) signal
6xHis
PiggyBac-Puro_NLS-SNAP-
(eGFP)3_NLS-CLIP-(mCherry)3
12.012 bp
2000
4000
6000
8000
10.000
10aa-Linker
CLIP-tag™
SV40 NLS
minimal CMV promoter
10aa-Linker
SNAP-tag®

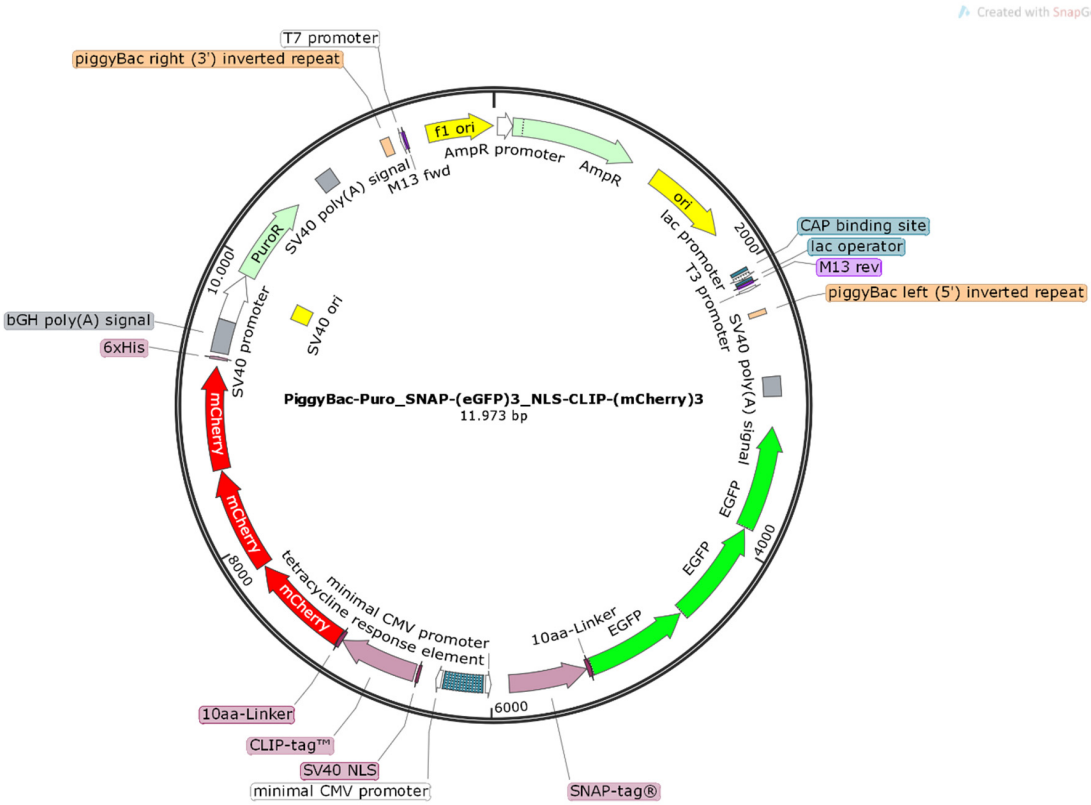
Created with SnapGene®
T7 promoter
piggyBac right (3') inverted repeat
f1 ori
AmpR promoter
AmpR
ori
lac promoter
T3 promoter
CAP binding site
lac operator
M13 rev
piggyBac left (5') inverted repeat
SV40 poly(A) signal
EGFP
EGFP
10aa-Linker
SNAP-tag®
minimal CMV promoter
tetracycline response element
mCherry
mCherry
mCherry
CLIP-tag™
10aa-Linker
SV40 NLS
minimal CMV promoter
SV40 promoter
6xHis
bGH poly(A) signal
PuroR
SV40 poly(A) signal
M13 fwd
SV40 ori
PiggyBac-Puro_SNAP-(eGFP)3_NLS-CLIP-(mCherry)3
11.973 bp
2000
4000
6000
8000
10.000

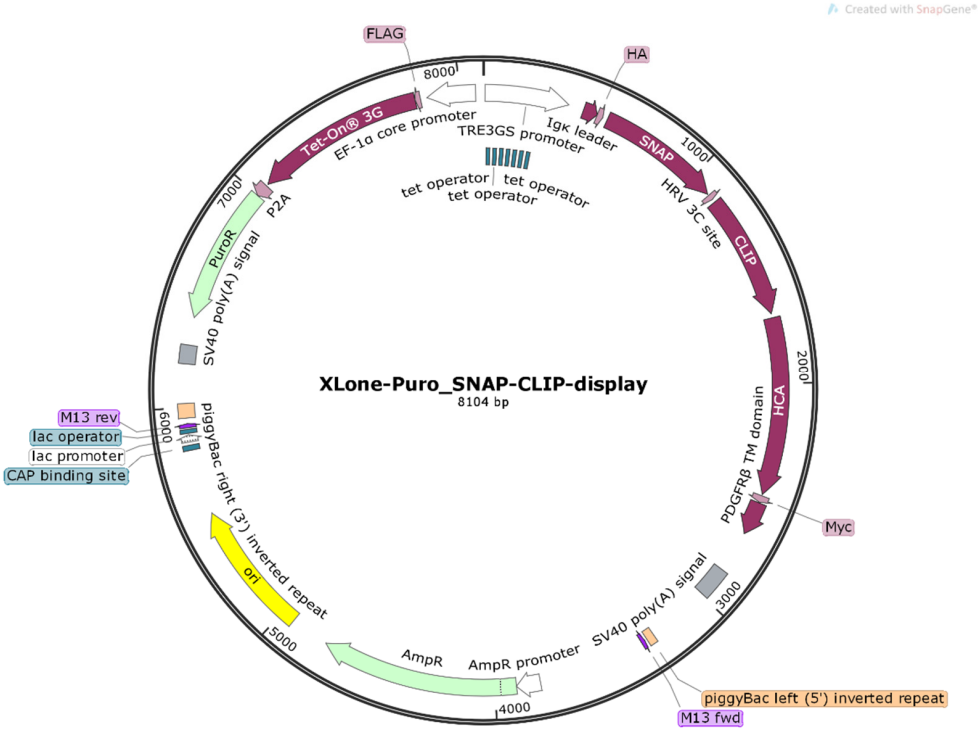
Created with SnapGene®
FLAG
HA
Tet-On® 3G
EF-1α core promoter
TRE3GS promoter
Igκ leader
SNAP
HRV 3C site
CLIP
HCA
PDGFRβ TM domain
Myc
tet operator
tet operator
tet operator
P2A
PuroR
SV40 poly(A) signal
M13 rev
lac operator
lac promoter
CAP binding site
piggyBac right (3') inverted repeat
ori
AmpR
AmpR promoter
SV40 poly(A) signal
piggyBac left (5') inverted repeat
M13 fwd
XLone-Puro_SNAP-CLIP-display
8104 bp
1000
2000
3000
4000
5000
6000
7000
8000

Cell culture

If not stated otherwise, cells were cultivated in Dulbecco's Modified Eagle Medium (DMEM, Thermo Fisher Scientific) supplemented with 10 % fetal bovine serum (FBS, Thermo Fisher Scientific) at 37 °C with 5 % CO_2 in a water saturated steam atmosphere. For sub cultivation and seeding, cells were washed with phosphate-buffered saline (PBS), detached with 0.25 % trypsin/EDTA (Sigma Aldrich), and resuspended in fresh DMEM/FBS. Sub cultivation was performed every 3-5 days. For editing experiments Flp-In 293T-REx cells, stably expressing SNAP-ADAR1Q were used. The creation and sub cultivation of this cell line has been previously described.[16,17]

Creation of HeLa PiggyBac cells

We used the previously described mPB PiggyBac transposase for generating stable transgenic HeLa cell lines.[11] For this, 1×10^5 HeLa cells (DSMZ, Braunschweig, Germany, no: ACC 57) were seeded in 0.5 ml DMEM/FBS in a 24-well plate. After 24 h, medium was replaced with 0.4 ml fresh DMEM/FBS, and 800 ng of the respective PiggyBac carrier plasmid and 200 ng pcDNA3.1_mPB were transfected with 3 µl Fugene6 (Promega) in 100 µl OptiMEM according to the manual. After 24 h, the cells were transferred to two wells of a 6 well plate. 48 h later, the medium was replaced with DMEM/10% FBS/5 µg/ml puromycin. After 12 days of selection, the medium was replaced by DMEM/FBS. Cells were used without monoclonal selection and subsequently cultured in DMEM/FBS.

RNA editing experiments

Induction, transfection, and irradiation

Transgene expression in Flp-In T-REx SNAP-ADAR1Q cells was induced by seeding 1.5 x 10^6 cells in a 6 well in 2.5 ml DMEM/FBS +15 µg/ml blasticidin +100 µg/ml hygromycin (DMEM/FBS/B/H) containing 10 ng/ml doxycycline. After 24 hours cells were washed with PBS, trypsinated, and taken up in fresh DMEM/FBS. Cells were pelleted (300 g, 5 min) and resuspended to a concentration of 800,000 cells/ml in DMEM/FBS+HEPES without phenol red (Thermo Fisher Scientific) containing 15 ng/ml doxycycline.

Per 96-well 0.5 µl Lipofectamine 2000 (Thermo Fisher Scientific) was diluted in 25 µl OptiMEM (Thermo Fisher Scientific). After 5 min of incubation the solution was added to a predilution of guideRNA (0.5 pmol for Y701C guideRNAs and 2 pmol for T288A guideRNAs) in 25 µl OptiMEM and the mix was incubated another 15 min. 50 µl guideRNA/Lipofectamine mix was transferred to a well of a 96-well plate and 100 µl cell suspension were added for a final amount of 80,000 cells per well. For every sample, two wells were used and processed in parallel. The cells were kept in the incubator and protected from light until harvest.

For UV irradiation, the plate was sealed with parafilm and placed on a High-Performance UV Transilluminator (UVP, setting = high, 7.9±0.2 mW/cm^2 light with 365 nm wavelength) for 2 or 3 min at the indicated time point.

Note: If guideRNA was irradiated before transfection, the guideRNA dilution in OptiMEM was transferred to a 96-well plate and irradiated as described above and afterwards transferred back to a reaction tube for incubation with transfection reagent.

Cell harvest, RNA isolation, RT-PCR and sequencing

Cells were harvested at the indicated time point by discarding the medium and adding 50 µl RLT lysis buffer (Qiagen) per well. Lysate from two wells with the same treatment was pooled and RNA isolation was performed with Monarch RNA Cleanup Kit (New England Biolabs) according to the manual. Total RNA was eluted with 30 µl RNase free water and concentration was determined by measuring the absorbance at 260 nm.

STAT1 Y701C editing site was amplified using the following primer set:
fw = GCTTCATCAGCAAGGAGCGAGAGCG, rev = CTTCAGACACAGAAATCAACTCATTC.

STAT1 T228A editing site was amplified using the following primer set:
fw = GAATGTCACTGAACTTACCCAGAATGC, rev = CACCAACAGTCTCAACTTCACAGTG.

If both sites were detected from one sample two separate RT-PCR reactions were setup. Reverse transcription and PCR were performed using the One-Step RT PCR Kit (biotech-rabbit GmbH). Typically 500 ng RNA were diluted with nuclease free water to 9.25 µl. 1 µl reverse primer (10 µM) was added and the reaction mix was incubated for 1 min at 90 °C. 1 µl forward primer (10 µM), 12.5 µl One Step Mix (2x) and 1.25 µl RT-RI Blend (20x) were added. RT-PCR was carried out in a PCR cycler starting with reverse transcription at 50°C for 30 min and an initial denaturation step at 95°C. 35 cycles of denaturation (95°C, 15 s), annealing (51°C, 30 s) and elongation (72°C, 40 s) were performed, followed by a final extension step (68°C, 10 min).

The resulting PCR fragments (~400 bp) were loaded on a 1.4% TAE-agarose gel and purified using the NucleoSpin Gel and PCR Cleanup Set (Macherey Nagel). 120 ng DNA were sent to sequencing (Eurofins Genomics, primer STAT1 Y701C: GGCTGCTGAGAA-TATTCCTGAGAATC, primer STAT1 T288A: GAATGTCACTGAACTTACCCAGAATGC). A-to-I editing yields were determined by dividing the peak height for guanosine by the sum of the peak heights for both adenosine and guanosine.

Stress granule imaging experiments

50,000 Hela PiggyBac cells were reverse transfected with 25 pmol guideRNA and 0.25 µl Lipofectamine 2000 (Thermo Fisher Scientific) in 50 µl OptiMem (Thermo Fisher Scientific) into a 96-well cell culture-treated plate. Cell concentration prior transfection was adjusted to 500,000 cells per ml in DMEM/FBS. After 4 hours, cells were washed with PBS, trypsinated and re-suspended in 300 µl DMEM/FBS. 3x100 µl were transferred into three wells of a 96-well imaging plate with a 170 µm glass bottom (Eppendorf). The cells were kept in the incubator and protected from light for 24 hours. Stress granule formation was induced by changing the medium to DMEM/FBS containing 50 µM As_2O_3 for 30 min. For imaging the medium was changed to 100 µl DMEM/FBS+HEPES without phenol red (Thermo Fisher Scientific). Irradiation was performed on a Nikon Elipse Ti2-E microscope equipped with a lumencor® AuraII light engine and a 60X oil objective (numerical aperture 1.4). 390 nM light (source intensity 100%) and a quad band excitation filter (Chroma 89402x) were used. Irradiation time was typically 100 or 300 ms.

Note: Performing reverse transfection directly in glass bottom plates resulted in lower viability of the cells (data not shown). Furthermore, a low density of cells is required for imaging (~10-15.000 cells per 96-well). However, reverse transfection at such low cell density resulted in low viablity. Performing transfection in a regular cell culture-treated plastic well plate and at high concentration (50.000 cells per 96-well) increased the viability of the cells. The additional trypsination step that is required to transfer them to the imaging plate later, also reduces the number of liposomes seen in microscopy.

Surface labeling experiments

10,000 HeLa XLone-Puro SNAP-CLIP-display cells were seeded into a 96-well imaging plate with a 170 µm glass bottom (Eppendorf) in 100 µl DMEM/FBS containing 500 ng/µl doxycycline to induce transgene expression. After 16 h, 50 µl of DMEM/FBS were added, containing 1.5% NucBlue (Thermo Fisher Scientific),15 µM BC-Atto594, and 15 µM BG-Atto488 or BG-^{UV}X-Atto488. The cells were kept in the incubator and protected from light for 15-30 min and washed twice with 100 µl DMEM/FBS+HEPES without phenol red (Thermo Fisher Scientific). Irradiation was performed as described above for stress granule imaging experiments.

Microscopy

Microscopy was performed on a Nikon Elipse Ti2-E inverted fluorescent microscope equipped with a photometrics® Prime 95B camera and a lumencor® AuraII light engine. All pictures were recorded using a 60X oil objective (numerical aperture 1.4) and Olympus IMMOIL-F30CC immersion oil. The excitation wavelengths and corresponding filter sets used to record each channel are specified in the following table. Typically, a z-stack covering 6 µm (0.2 µm steps) was recorded. The images were deconvoluted using Nikon NIS-Elements software and a single layer (z resolution ~0.6 µM) is displayed. Assignment of lookup tables, contrast settings and cropping were performed in FIJI ImageJ.[18] The same acquisition settings were chosen for every channel within one subfigure.

Fluorophore	*Excitation*	*Filter*
eGFP	*475 nM*	*Excitation: Chroma 89402x* *Beamsplitter: Chroma 89402bs* *Emission: Chroma 89402m*
mCherry	*575 nM*	*F66-016NXL CFP/YFP/mCherry/Cy7 Quad filter (AHF, Germany)*
Atto488	*475 nM*	*Excitation: Chroma ET500/20x* *Beamsplitter: Chroma T515lp* *Emission: Chroma ET535/30m*
Atto594	*575 nM*	*Excitation: Semrock 585/29 BrightLine HC* *Beamsplitter: Chroma T610LPXR* *Emission: Semrock 650/60 BrightLine HC*
eBFP, NucBlue, Irradiation	*390 nM*	*Excitation: Chroma 89402x* *Beamsplitter: Chroma 89402bs* *Emission: Chroma 89402m*

Quantification of fluorescent signal in stress granules

Quantification of the red and green signal in stress granules was performed in Nikon NIS-Elements software using a maximum projection in z. The experiments were performed with the NLS-SNAP-(eGFP)$_3$+NLS-CLIP-(mCherry)$_3$ cell line, due to the low background signal in the cytoplasm. Since the NLS-CLIP-(mCherry)$_3$ signal served as reference, we manually chose cells with clearly visible stress granules in the red channel for quantification. The cytoplasm was defined as region of interest (ROI) by manually outlining the cells. The nucleus was detected in the red channel and excluded using the bright spot detection function of Nikon NIS-Elements software (minimal ⌀ set to 15 µM, example seen below in **a***). Background was subtracted using rolling ball correction (ball size = 1.5 µM, example seen below in* **b***) and stress granules were detected using bright spot detection in NIS-Elements software (settings: growing 400-600, example seen below in* **c***). The mean intensity of eGFP and mCherry signal for each spot was measured and the ratio calculated. For each cell the mean of the ratios of all quantified granules is shown (figure 3d and figure 3e). The values for all individual granules quantified are shown below in figure S5b. Significance was calculated in GraphPad Prism 8 (version 8.4.3) using an unpaired Welch's t test.*

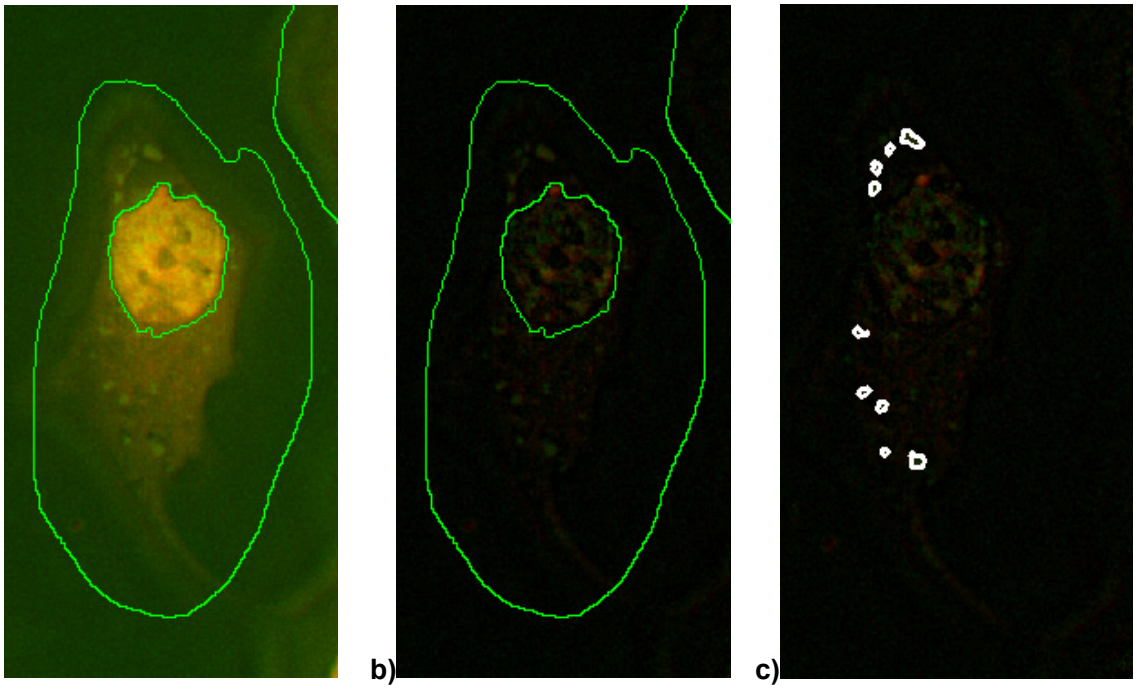

a) **b)** **c)**

The same quantification could not be applied to the correlation of SNAP-(eGFP)$_3$ and G3BP1 since the expression levels of eBFP-G3BP1 varied stronger and the transfection efficiency influenced the amount of SNAP-(eGFP)$_3$ in the granules relative to eBFP-G3BP1. Instead, the local correlation of eBFP-G3BP1 and SNAP-(eGFP)$_3$ was determined (figure 3b).

Since the eBFP-G3BP1 signal served as reference, we manually chose cells with clearly visible stress granules in the blue channel for quantification. The cells were manually outlined and defined as region of interest (ROI). An example is shown below in **d**. *Stress granules were selected using bright spot detection in NIS-Elements software (1-1.2 µM size) and a circular selection (⌀ 15px) around each granule was analyzed (example shown below in* **e**). *Pearson correlation was determined for the eGFP and G3BP1 channel within each of the selections (figure S5a) and averaged for all stress granules of one cell (figure 3b). Significance was calculated in GraphPad Prism 8 (version 8.4.3) using an unpaired Welch's t test.*
Note: If the Pearson correlation is determined for the whole cell it will mainly reflect whether both signals are cytoplasmatic or if one of them is nuclear. Determining the Pearson correlation within a defined radius surrounding each granule circumvents this problem. However, it is important to ensure that the area analyzed is bigger than the average granule size).

d)

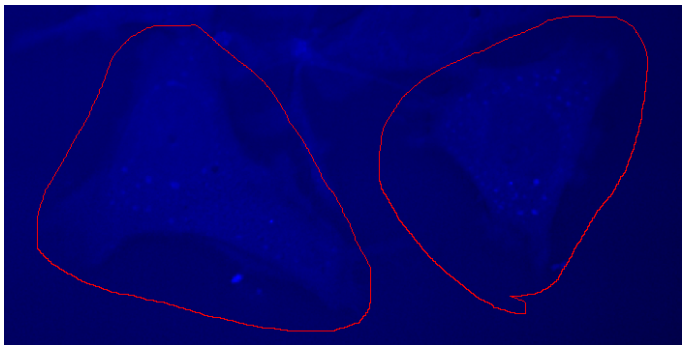

e)

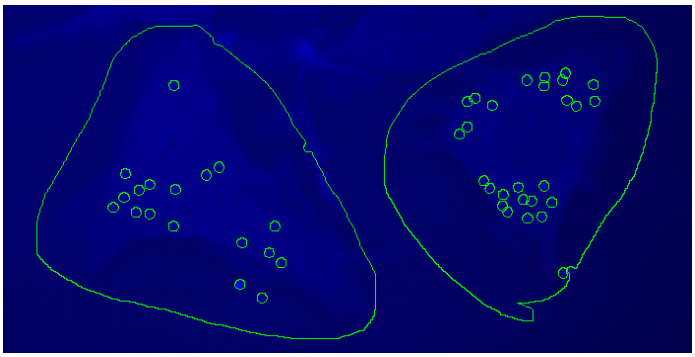

Supporting literature

1. Keppler, A. et al. A general method for the covalent labeling of fusion proteins with small molecules in vivo. Nat. Biotechnol. 21, 86–89 (2003).
2. Gautier, A. et al. An Engineered Protein Tag for Multiprotein Labeling in Living Cells. Chem. Biol. 15, 128–136 (2008).
3. Keppler, A. et al. Labeling of fusion proteins of O6-alkylguanine-DNA alkyl-transferase with small molecules in vivo and in vitro. Methods 32, 437–444 (2004).
4. Varga, N. et al. Selective Targeting of Dendritic Cell-Specific Intercellular Adhesion Molecule-3-Grabbing Nonintegrin (DC-SIGN) with Mannose-Based Glycomimetics: Synthesis and Interaction Studies of Bis(benzylamide) Derivatives of a Pseudomannobioside. Chem. – Eur. J. 19, 4786–4797 (2013).
5. Hanswillemenke, A. & Stafforst, T. Protocols for the generation of caged guide-RNAs for light-triggered RNA-targeting with SNAP-ADARs. Methods Enzymol. 624, 47–68 (2019).
6. Pendrak, I. et al. Synthesis and Anti-HSV Activity of Methylenedioxy Mappicine Ketone Analogs. The Journal of Organic Chemistry, 60 (9), 2912-2915 (1995).
7. Miura, Y. et al. Synthesis of amphiphilic lactosides that possess a lactosyl-ceramide-mimicking N-acyl structure: Alternative universal substrates for endo-type glycosylceramidases, Carbohydrate Research, 289, 193-199 (1996).
8. Hanswillemenke, A. et al. Site-Directed RNA Editing in Vivo Can Be Triggered by the Light-Driven Assembly of an Artificial Riboprotein. J. Am. Chem. Soc. 137, 15875–15881 (2015).
9. Schneider, M.F. et al. Optimal guideRNAs for re-directing deaminase activity of hADAR1 and hADAR2 in trans. Nucl. Acids Res. 42, e87 (2014).
10. EBFP2-N1 was a gift from Michael Davidson (Addgene plasmid # 54595; http://n2t.net/addgene:54595; RRID: Addgene_54595)
11. Cadiñanos J & Bradley A. Generation of an inducible and optimized piggyBac transposon system. Nucl. Acids Res., 35(12), e87 (2007)
12. Woltjen, K. et al. piggyBac transposition reprograms fibroblasts to induced pluripotent stem cells. Nature 458, 766–770 (2009).
13. Schopp, I. et al. Split-BioID a conditional proteomics approach to monitor the composition of spatiotemporally defined protein complexes. Nat Commun., 8, 15690 (2017).
14. Randolph, L.N. et al., An all-in-one, Tet-On 3G inducible PiggyBac system for human pluripotent stem cells and derivatives. Sci Rep. 7(1), 1549 (2017).
15. Brun, A.M. et al. Semisynthesis of Fluorescent Metabolite Sensors on Cell Surfaces. J. Am. Chem. Soc. 133, 16235-16242 (2011).
16. Vogel, P. et al. Efficient and Precise Editing of Endogenous Transcripts with SNAP-tagged ADARs. Nat. Methods 15, 535–38 (2018).
17. Vogel, P. et al. Switching protein localization by site-directed RNA editing under control of light. ACS Synth. Biol. 6, 1642-9 (2017).
18. Schindelin, J. et al. Fiji: an open-source platform for biological-image analysis. Nat Methods 9, 676–682 (2012).

Appendix

Unedited image of SDS-PAGE, Fig. 1d

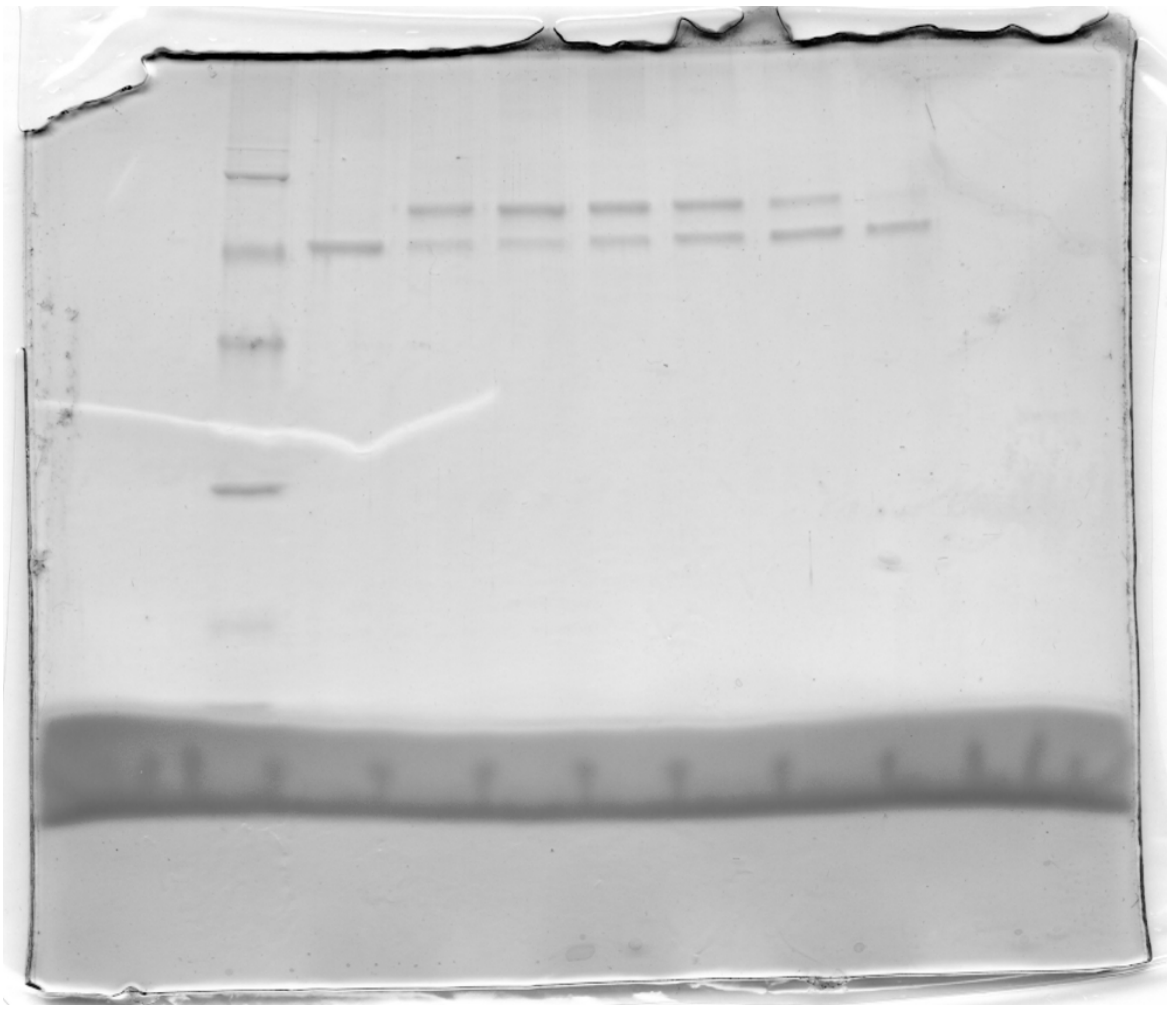

Full sequences of plasmids used in this study

PiggyBac-Puro_SNAPf-3xeGFP+BFP-G3BP

CAGGTGGCACTTTTCGGGGAAATGTGCGCGGAACCCCTATTTGTTTATTTTTCTAAATACATTCAAAT
ATGTATCCGCTCATGAGACAATAACCCTGATAAATGCTTCAATAATATTGAAAAAGGAAGAGTATGAG
TATTCAACATTTCCGTGTCGCCCTTATTCCCTTTTTTGCGGCATTTTGCCTTCCTGTTTTTGCTCACC
CAGAAACGCTGGTGAAAGTAAAAGATGCTGAAGATCAGTTGGGTGCACGAGTGGGTTACATCGAACTG
GATCTCAACAGCGGTAAGATCCTTGAGAGTTTTCGCCCCGAAGAACGTTTTCCAATGATGAGCACTTT
TAAAGTTCTGCTATGTGGCGCGGTATTATCCCGTATTGACGCCGGGCAAGAGCAACTCGGTCGCCGCA
TACACTATTCTCAGAATGACTTGGTTGAGTACTCACCAGTCACAGAAAAGCATCTTACGGATGGCATG
ACAGTAAGAGAATTATGCAGTGCTGCCATAACCATGAGTGATAACACTGCGGCCAACTTACTTCTGAC
AACGATCGGAGGACCGAAGGAGCTAACCGCTTTTTTGCACAACATGGGGGATCATGTAACTCGCCTTG
ATCGTTGGGAACCGGAGCTGAATGAAGCCATACCAAACGACGAGCGTGACACCACGATGCCTGTAGCA
ATGGCAACAACGTTGCGCAAACTATTAACTGGCGAACTACTTACTCTAGCTTCCCGGCAACAATTAAT
AGACTGGATGGAGGCGGATAAAGTTGCAGGACCACTTCTGCGCTCGGCCCTTCCGGCTGGCTGGTTTA
TTGCTGATAAATCTGGAGCCGGTGAGCGTGGGTCTCGCGGTATCATTGCAGCACTGGGGCCAGATGGT
AAGCCCTCCCGTATCGTAGTTATCTACACGACGGGGAGTCAGGCAACTATGGATGAACGAAATAGACA
GATCGCTGAGATAGGTGCCTCACTGATTAAGCATTGGTAACTGTCAGACCAAGTTTACTCATATATAC
TTTAGATTGATTTAAAACTTCATTTTTAATTTAAAAGGATCTAGGTGAAGATCCTTTTTGATAATCTC
ATGACCAAAATCCCTTAACGTGAGTTTTCGTTCCACTGAGCGTCAGACCCCGTAGAAAAGATCAAAGG
ATCTTCTTGAGATCCTTTTTTTCTGCGCGTAATCTGCTGCTTGCAAACAAAAAAACCACCGCTACCAG
CGGTGGTTTGTTTGCCGGATCAAGAGCTACCAACTCTTTTTCCGAAGGTAACTGGCTTCAGCAGAGCG
CAGATACCAAATACTGTCCTTCTAGTGTAGCCGTAGTTAGGCCACCACTTCAAGAACTCTGTAGCACC
GCCTACATACCTCGCTCTGCTAATCCTGTTACCAGTGGCTGCTGCCAGTGGCGATAAGTCGTGTCTTA
CCGGGTTGGACTCAAGACGATAGTTACCGGATAAGGCGCAGCGGTCGGGCTGAACGGGGGGTTCGTGC
ACACAGCCCAGCTTGGAGCGAACGACCTACACCGAACTGAGATACCTACAGCGTGAGCTATGAGAAAG
CGCCACGCTTCCCGAAGGGAGAAAGGCGGACAGGTATCCGGTAAGCGGCAGGGTCGGAACAGGAGAGC
GCACGAGGGAGCTTCCAGGGGGAAACGCCTGGTATCTTTATAGTCCTGTCGGGTTTCGCCACCTCTGA
CTTGAGCGTCGATTTTTGTGATGCTCGTCAGGGGGGCGGAGCCTATGGAAAAACGCCAGCAACGCGGC
CTTTTTACGGTTCCTGGCCTTTTGCTGGCCTTTTGCTCACATGTTCTTTCCTGCGTTATCCCCTGATT
CTGTGGATAACCGTATTACCGCCTTTGAGTGAGCTGATACCGCTCGCCGCAGCCGAACGACCGAGCGC
AGCGAGTCAGTGAGCGAGGAAGCGGAAGAGCGCCCAATACGCAAACCGCCTCTCCCCGCGCGTTGGCC
GATTCATTAATGCAGCTGGCACGACAGGTTTCCCGACTGGAAAGCGGGCAGTGAGCGCAACGCAATTA
ATGTGAGTTAGCTCACTCATTAGGCACCCCAGGCTTTACACTTTATGCTTCCGGCTCGTATGTTGTGT
GGAATTGTGAGCGGATAACAATTTCACACAGGAAACAGCTATGACCATGATTACGCCAAGCTCGGAAT
TAACCCTCACTAAAGGGAACAAAAGCTGGGTACCTCGCGCGACTTGGTTTGCCATTCTTTAGCGCGCG
TCGCGTCACACAGCTTGGCCACAATGTGGTTTTTGTCAAACGAAGATTCTATGACGTGTTTAAAGTTT
AGGTCGAGTAAAGCGCAAATCTTTTTTAACCCTAGAAAGATAGTCTGCGTAAAATTGACGCATGCATT
CTTGAAATATTGCTCTCTCTTTCTAAATAGCGCGAATCCGTCGCTGTGCATTTAGGACATCTCAGTCG
CCGCTTGGAGCTCCCGTGAGGCGTGCTTGTCAATGCGGTAAGTGTCACTGATTTTGAACTATAACGAC
CGCGTGAGTCAAAATGACGCATGATTATCTTTTACGTGACTTTTAAGATTTAACTCATACGATAATTA
TATTGTTATTTCATGTTCTACTTACGTGATAACTTATTATATATATATTTTCTTGTTATAGATATCGT
GACTAATATATAATAAAATGGGTAGTTCTTTAGACGATGAGCATATCCTCTCTGCTCTTCTGCAAAGC
GATGACGAGCTTGTTGGCTAGCGCGCTGCTTCGCGATGTACGGGCCAGATATACGCGTTGACATTGAT
TATTGACTAGTAACTTGTTTATTGCAGCTTATAATGGTTACAAATAAGGCAATAGCATCACAAATTTC
ACAAATAAGGCATTTTTTTCACTGCATTCTAGTTTTGGTTTGTCCAAACTCATCAATGTATCTTATCA
TGTCTGGATCTCAAATCCCTCGGAAGCTGCGCCTGTCTTAGGTTGGAGTGATACATTTTTATCACTTT
TACCCGTCTTTGGATTAGGCAGTAGCTCTGACGGCCCTCCTGTCTTAGGTTAGTGAAAAATGTCACTC
TCTTACCCGTCATTGGCTGTCCAGCTTAGCTCGCAGGGGAGGTGGTCTGGGCCCATCGATTCTAGAAT
TAACCGGTGACCGGCTTGTACAGCTCGTCCATGCCGAGAGTGATCCCGGCGGCGGTCACGAACTCCAG
CAGGACCATGTGATCGCGCTTCTCGTTGGGGTCTTTGCTCAGGGCGGACTGGGTGCTCAGGTAGTGGT

TGTCGGGCAGCAGCACGGGGCCGTCGCCGATGGGGGTGTTCTGCTGGTAGTGGTCGGCGAGCTGCACG
CTGCCGTCCTCGATGTTGTGGCGGATCTTGAAGTTCACCTTGATGCCGTTCTTCTGCTTGTCGGCCAT
GATATAGACGTTGTGGCTGTTGTAGTTGTACTCCAGCTTGTGCCCCAGGATGTTGCCGTCCTCCTTGA
AGTCGATGCCCTTCAGCTCGATGCGGTTCACCAGGGTGTCGCCCTCGAACTTCACCTCGGCGCGGGTC
TTGTAGTTGCCGTCGTCCTTGAAGAAGATGGTGCGCTCCTGGACGTAGCCTTCGGGCATGGCGGACTT
GAAGAAGTCGTGCTGCTTCATGTGGTCGGGGTAGCGGCTGAAGCACTGCACGCCGTAGGTCAGGGTGG
TCACGAGGGTGGGCCAGGGCACGGGCAGCTTGCCGGTGGTGCAGATGAACTTCAGGGTCAGCTTGCCG
TAGGTGGCATCGCCCTCGCCCTCGCCGGACACGCTGAACTTGTGGCCGTTTACGTCGCCGTCCAGCTC
GACCAGGATGGGCACCACCCCGGTGAACAGCTCCTCGCCCTTGCTCACGCCGGTGACCGGCTTGTACA
GCTCGTCCATGCCGAGAGTGATCCCGGCGGCGGTCACGAACTCCAGCAGGACCATGTGATCGCGCTTC
TCGTTGGGGTCTTTGCTCAGGGCGGACTGGGTGCTCAGGTAGTGGTTGTCGGGCAGCAGCACGGGGCC
GTCGCCGATGGGGGTGTTCTGCTGGTAGTGGTCGGCGAGCTGCACGCTGCCGTCCTCGATGTTGTGGC
GGATCTTGAAGTTCACCTTGATGCCGTTCTTCTGCTTGTCGGCCATGATATAGACGTTGTGGCTGTTG
TAGTTGTACTCCAGCTTGTGCCCCAGGATGTTGCCGTCCTCCTTGAAGTCGATGCCCTTCAGCTCGAT
GCGGTTCACCAGGGTGTCGCCCTCGAACTTCACCTCGGCGCGGGTCTTGTAGTTGCCGTCGTCCTTGA
AGAAGATGGTGCGCTCCTGGACGTAGCCTTCGGGCATGGCGGACTTGAAGAAGTCGTGCTGCTTCATG
TGGTCGGGGTAGCGGCTGAAGCACTGCACGCCGTAGGTCAGGGTGGTCACGAGGGTGGGCCAGGGCAC
GGGCAGCTTGCCGGTGGTGCAGATGAACTTCAGGGTCAGCTTGCCGTAGGTGGCATCGCCCTCGCCCT
CGCCGGACACGCTGAACTTGTGGCCGTTTACGTCGCCGTCCAGCTCGACCAGGATGGGCACCACCCCG
GTGAACAGCTCCTCGCCCTTGCTCACGCCGGTGACCGGCTTGTACAGCTCGTCCATGCCGAGAGTGAT
CCCGGCGGCGGTCACGAACTCCAGCAGGACCATGTGATCGCGCTTCTCGTTGGGGTCTTTGCTCAGGG
CGGACTGGGTGCTCAGGTAGTGGTTGTCGGGCAGCAGCACGGGGCCGTCGCCGATGGGGGTGTTCTGC
TGGTAGTGGTCGGCGAGCTGCACGCTGCCGTCCTCGATGTTGTGGCGGATCTTGAAGTTCACCTTGAT
GCCGTTCTTCTGCTTGTCGGCCATGATATAGACGTTGTGGCTGTTGTAGTTGTACTCCAGCTTGTGCC
CCAGGATGTTGCCGTCCTCCTTGAAGTCGATGCCCTTCAGCTCGATGCGGTTCACCAGGGTGTCGCCC
TCGAACTTCACCTCGGCGCGGGTCTTGTAGTTGCCGTCGTCCTTGAAGAAGATGGTGCGCTCCTGGAC
GTAGCCTTCGGGCATGGCGGACTTGAAGAAGTCGTGCTGCTTCATGTGGTCGGGGTAGCGGCTGAAGC
ACTGCACGCCGTAGGTCAGGGTGGTCACGAGGGTGGGCCAGGGCACGGGCAGCTTGCCGGTGGTGCAG
ATGAACTTCAGGGTCAGCTTGCCGTAGGTGGCATCGCCCTCGCCCTCGCCGGACACGCTGAACTTGTG
GCCGTTTACGTCGCCGTCCAGCTCGACCAGGATGGGCACCACCCCGGTGAACAGCTCCTCGCCCTTGC
TCACGCCGGTCCCTGGCGCGCCTCCGCCTGCAGGACCCAGCCCAGGCTTGCCCAGTCTGTGGCCCTCG
TGGGCCAGCAGCCACTCTTTCACGGCGAGCCCGCCCTCGTAGCCCCCCACGTCCAGGTCGCCCTGCAC
CACCCGGTGGCAGGGGATCAGAATGGGCACGGGATTTCCGCTCAGGGCGGTTTTCACGGCGGCGGTGG
CGGCGGGATTGCCGGCCAGGGCGGCCAGGTGGCTGTAGCTGATGACCTCTCCGAACTTCACCACTTTC
AGCAGTTTCCACAGCACCTGGCGGGTAAAGCTCTCCTGCTGGAACACTGGGTGGTGCAGGGCTGGCAC
AGGGAACTCCTCGATGGCCTCAGGCTGGTGAAAGTAGGCGTTGAGCCAGGCGGTGGCCTGCATCAGTG
GCTCTGGTCCGCCCAGCACGGCGGCTGGGGCAGGCACTTCCACGGCGTCGGCGGCAGATGTTCCTTTG
CCCAGGAAGATGATACGGTGCAGGCCCTGTTCGCACCCAGACAGTTCCAGCTTGCCCAGAGGGCTATC
CAGGGTGGTGCGCTTCATTTCGCAGTCTTTGTCGCCGGCCATGCGGCCGCCGCGTCCTAGGTTTCGAC
CGCGGAGGCTGGATCGGTCCCGGTGTCTTCTATGGAGGTCAAAACAGCGTGGATGGCGTCTCCAGGCG
ATCTGACGGTTCACTAAACGAGCTCTGCTTATATAGGCCTCCCACCGTACACGCCTACAAGCTTCTTT
CACTTTTCTCTATCACTGATAGGGAGTGGTAAACTCGACTTTCACTTTTCTCTATCACTGATAGGGAG
TGGTAAACTCGACTTTCACTTTTCTCTATCACTGATAGGGAGTGGTAAACTCGACTTTCACTTTTCTC
TATCACTGATAGGGAGTGGTAAACTCGACTTTCACTTTTCTCTATCACTGATAGGGAGTGGTAAACTC
GACTTTCACTTTTCTCTATCACTGATAGGGAGTGGTAAACTCGACTTTCACTTTTCTCTATCACTGAT
AGGGAGTGGTAAACTCGAGGGTAGGCGTGTACGGTGGGAGGCCTATATAAGCAGAGCTCGTTTAGTGA
ACCGTCAGATCGCCTGGAGACGCCATCCACGCTGTTTTGACCTCCATAGAAGACACCGGGACCGATCC
AGCCTCCGCGGAATTCTTAATAGCGGCCGCATGGCCGGCGTGAGCAAGGGCGAGGAGCTGTTCACCGG
GGTGGTGCCCATCCTGGTCGAGCTGGACGGCGACGTAAACGGCCACAAGTTCAGCGTGAGGGGCGAGG
GCGAGGGCGATGCCACCAACGGCAAGCTGACCCTGAAGTTCATCTGCACCACCGGCAAGCTGCCCGTG
CCCTGGCCCACCCTCGTGACCACCCTGAGCCACGGCGTGCAGTGCTTCGCCCGCTACCCCGACCACAT
GAAGCAGCACGACTTCTTCAAGTCCGCCATGCCCGAAGGCTACGTCCAGGAGCGCACCATCTTCTTCA
AGGACGACGGCAACCTACAAGACCCGCGCCGAGGTGAAGTTCGAGGGCGACACCCTGGTGAACCGCATC
GAGCTGAAGGGCGTCGACTTCAAGGAGGACGGCAACATCCTGGGGCACAAGCTGGAGTACAACTTCAA

51

CAGCCACAACATCTATATCATGGCCGTCAAGCAGAAGAACGGCATCAAGGTGAACTTCAAGATCCGCC
ACAACGTGGAGGACGGCAGCGTGCAGCTCGCCGACCACTACCAGCAGAACACCCCCATCGGCGACGGC
CCCGTGCTGCTGCCCGACAGCCACTACCTGAGCACCCAGTCCGTGCTGAGCAAAGACCCCAACGAGAA
GCGCGATCACATGGTCCTGCTGGAGTTCCGCACCGCCGCCGGGATCACTCTCGGCATGGACGAGCTGT
ACAAGCCGGTCACCGGCGTGATGGAGAAGCCTAGTCCCCTGCTGGTCGGGCGGGAATTTGTGAGACAG
TATTACACACTGCTGAACCAGGCCCCAGACATGCTGCATAGATTTTATGGAAAGAACTCTTCTTATGT
CCATGGGGGATTGGATTCAAATGGAAAGCCAGCAGATGCAGTCTACGGACAGAAAGAAATCCACAGGA
AAGTGATGTCACAAAACTTCACCAACTGCCACACCAAGATTCGCCATGTTGATGCTCATGCCACGCTA
AATGATGGTGTGGTAGTCCAGGTGATGGGGCTTCTCTCTAACAACAACCAGGCTTTGAGGAGATTCAT
GCAAACGTTTGTCCTTGCTCCTGAGGGGTCTGTTGCAAATAAATTCTATGTTCACAATGATATCTTCA
GATACCAAGATGAGGTCTTTGGTGGGTTTGTCACTGAGCCTCAGGAGGAGTCTGAAGAAGAAGTAGAG
GAACCTGAAGAAAGACAGCAAACACCTGAGGTGGTACCTGATGATTCTGGAACTTTCTATGATCAGGC
AGTTGTCAGTAATGACATGGAAGAACATTTAGAGGAGCCTGTTGCTGAACCAGAGCCTGATCCTGAAC
CAGAACCAGAACAAGAACCTGTATCTGAAATCCAAGAGGAAAAGCCTGAGCCAGTATTAGAAGAAACT
GCCCCTGAGGATGCTCAGAAGAGTTCTTCTCCAGCACCTGCAGACATAGCTCAGACAGTACAGGAAGA
CTTGAGGACATTTTCTTGGGCATCTGTGACCAGTAAGAATCTTCCACCCAGTGGAGCTGTTCCAGTTA
CTGGGATACCACCTCATGTTGTTAAAGTACCAGCTTCACAGCCCCGTCCAGAGTCTAAGCCTGAATCT
CAGATTCCACCACAAAGACCTCAGCGGGATCAAAGAGTGCGAGAACAACGAATAAATATTCCTCCCCA
AAGGGGACCCAGACCAATCCGTGAGGCTGGTGAGCAAGGTGACATTGAACCCCGAAGAATGGTGAGAC
ACCCTGACAGTCACCAACTCTTCATTGGCAACCTGCCTCATGAAGTGGACAAATCAGAGCTTAAAGAT
TTCTTTCAAAGTTATGGAAACGTGGTGGAGTTGCGCATTAACAGTGGTGGGAAATTACCCAATTTTGG
TTTTGTTGTGTTTGATGATTCTGAGCCTGTTCAGAAAGTCCTTAGCAACAGGCCCATCATGTTCAGAG
GTGAGGTCCGTCTGAATGTCGAAGAGAAGAAGACTCGAGCTGCCAGGGAAGGCGACCGACGAGATAAT
CGCCTTCGGGGACCTGGAGGCCCTCGAGGTGGGCTGGGTGGTGGAATGAGAGGCCCTCCCCGTGGAGG
CATGGTGCAGAAACCAGGATTTGGAGTGGGAAGGGGGCTTGCGCCACGGCAGTGAACCGGTTAATTCT
AGAATCGATGTAGGAGGTACTAAGCCGGTCATCATCACCATCACCATTGAGTTTAAACCCGCTGATCA
GCCTCGACTGTGCCTTCTAGTTGCCAGCCATCTGTTGTTTGCCCCTCCCCCGTGCCTTCCTTGACCCT
GGAAGGTGCCACTCCCACTGTCCTTTCCTAATAAAATGAGGAAATTGCATCGCATTGTCTGAGTAGGT
GTCATTCTATTCTGGGGGGTGGGGTGGGGCAGGACAGCAAGGGGGAGGATTGGGAAGACAATAGCAGG
CATGCTGGGGATGCGGTGGGCTCTATGGCGTGTGTCAGTTAGGGTGTGGAAAGTCCCCAGGCTCCCCA
GCAGGCAGAAGTATGCAAAGCATGCATCTCAATTAGTCAGCAACCAGGTGTGGAAAGTCCCCAGGCTC
CCCAGCAGGCAGAAGTATGCAAAGCATGCATCTCAATTAGTCAGCAACCATAGTCCCGCCCCTAACTC
CGCCCATCCCGCCCCTAACTCCGCCCAGTTCCGCCCATTCTCCGCCCCATGGCTGACTAATTTTTTTT
ATTTATGCAGAGGCCGAGGCCGCCTCTGCCTCTGAGCTATTCCAGAAGTAGTGAGGAGGCTTTTTTGG
AGGCCTAGGCTTTTGCAAAAAGCTCCCATGACCGAGTACAAGCCCACGGTGCGCCTCGCCACCCGCGA
CGACGTCCCCAGGGCCGTACGCACCCTCGCCGCCGCGTTCGCCGACTACCCCGCCACGCGCCACACCG
TCGATCCGGACCGCCACATCGAGCGGGTCACCGAGCTGCAAGAACTCTTCCTCACGCGCGTCGGGCTC
GACATCGGCAAGGTGTGGGTCGCGGACGACGGCGCCGCGGTGGCGGTCTGGACCACGCCGGAGAGCGT
CGAAGCGGGGGCGGTGTTCGCCGAGATCGGCCCGCGCATGGCCGAGTTGAGCGGTTCCCGGCTGGCCG
CGCAGCAACAGATGGAAGGCCTCCTGGCGCCGCACCGGCCCAAGGAGCCCGCGTGGTTCCTGGCCACC
GTCGGCGTCTCGCCCGACCACCAGGGCAAGGGTCTGGGCAGCGCCGTCGTGCTCCCCGGAGTGGAGGC
GGCCGAGCGCGCCGGGGTGCCCGCCTTCCTGGAGACCTCCGCGCCCCGCAACCTCCCCTTCTACGAGC
GGCTCGGCTTCACCGTCACCGCCGACGTCGAGGTGCCCGAAGGACCGCGCACCTGGTGCATGACCCGC
AAGCCCGGTGCCTGAGCGGGACTCTGGGGTTCGAAATGACCGACCAAGCGACGCCCGAAATGACCGAC
CAAGCGACGCCCAACCTGCCATCACGAGATTTCGATTCCACCGCCGCCTTCTATGAAAGGTTGGGCTT
CGGAATCGTTTTCCGGGACGCCGGCTGGATGATCCTCCAGCGCGGGGATCTCATGCTGGAGTTCTTCG
CCCACCCCAACTTGTTTATTGCAGCTTATAATGGTTACAAATAAAGCAATAGCATCACAAATTTCACA
AATAAAGCATTTTTTTCACTGCATTCTAGTTGTGGTTTGTCCAAACTCATCAATGTATCTTATCATGT
CTGTATACCGTCGACCTCTAGCTAGTCGAGTTAATTAACGAGAGCATAATATTGATATGTGCCAAAGT
TGTTTCTGACTGACTAATAAGTATAATTTGTTTCTATTATGTATAGGTTAAGCTAATTACTTATTTTA
TAATACAACATGACTGTTTTTAAAGTACAAAATAAGTTTATTTTTGTAAAAGAGAGAATGTTTAAAAG
TTTTGTTACTTTATAGAAGAAATTTTGAGTTTTTGTTTTTTTTTAATAAATAAATAAACATAAATAAA
TTGTTTGTTGAATTTATTATTAGTATGTAAGTGTAAATATAATAAAACTTAATATCTATTCAAATTAA
TAAATAAACCTCGATATACAGACCGATAAAACACATGCGTCAATTTTACGCATGATTATCTTTAACGT

ACGTCACAATATGATTATCTTTCTAGGGTTAAATAATAGTTTCTAATTTTTTTATTATTCAGCCTGCT
GTCGTGAATACCGAGCTCCAATTCGCCCTATAGTGAGTCGTATTACAATTCACTGGCCGTCGTTTTAC
AACGTCGTGACTGGGAAAACCCTGGCGTTACCCAACTTAATCGCCTTGCAGCACATCCCCCTTTCGCC
AGCTGGCGTAATAGCGAAGAGGCCCGCACCGATCGCCCTTCCCAACAGTTGCGCAGCCTGAATGGCGA
ATGGCGCGACGCGCCCTGTAGCGGCGCATTAAGCGCGGCGGGTGTGGTGGTTACGCGCAGCGTGACCG
CTACACTTGCCAGCGCCCTAGCGCCCGCTCCTTTCGCTTTCTTCCCTTCCTTTCTCGCCACGTTCGCC
GGCTTTCCCCGTCAAGCTCTAAATCGGGGGCTCCCTTTAGGGTTCCGATTTAGTGCTTTACGGCACCT
CGACCCCAAAAAACTTGATTAGGGTGATGGTTCACGTAGTGGGCCATCGCCCTGATAGACGGTTTTTC
GCCCTTTGACGTTGGAGTCCACGTTCTTTAATAGTGGACTCTTGTTCCAAACTGGAACAACACTCAAC
CCTATCTCGGTCTATTCTTTTGATTTATAAGGGATTTTGCCGATTTCGGCCTATTGGTTAAAAAATGA
GCTGATTTAACAAAAATTTAACGCGAATTTTAACAAAATATTAACGTTTACAATTTCC

PiggyBac-Puro_NLS-SNAPf-3xeGFP+NLS-CLIP-3xmCherry

CAGGTGGCACTTTTCGGGGAAATGTGCGCGGAACCCCTATTTGTTTATTTTTCTAAATACATTCAAAT
ATGTATCCGCTCATGAGACAATAACCCTGATAAATGCTTCAATAATATTGAAAAAGGAAGAGTATGAG
TATTCAACATTTCCGTGTCGCCCTTATTCCCTTTTTTGCGGCATTTTGCCTTCCTGTTTTTGCTCACC
CAGAAACGCTGGTGAAAGTAAAAGATGCTGAAGATCAGTTGGGTGCACGAGTGGGTTACATCGAACTG
GATCTCAACAGCGGTAAGATCCTTGAGAGTTTTCGCCCCGAAGAACGTTTTCCAATGATGAGCACTTT
TAAAGTTCTGCTATGTGGCGCGGTATTATCCCGTATTGACGCCGGGCAAGAGCAACTCGGTCGCCGCA
TACACTATTCTCAGAATGACTTGGTTGAGTACTCACCAGTCACAGAAAAGCATCTTACGGATGGCATG
ACAGTAAGAGAATTATGCAGTGCTGCCATAACCATGAGTGATAACACTGCGGCCAACTTACTTCTGAC
AACGATCGGAGGACCGAAGGAGCTAACCGCTTTTTTGCACAACATGGGGGATCATGTAACTCGCCTTG
ATCGTTGGGAACCGGAGCTGAATGAAGCCATACCAAACGACGAGCGTGACACCACGATGCCTGTAGCA
ATGGCAACAACGTTGCGCAAACTATTAACTGGCGAACTACTTACTCTAGCTTCCCGGCAACAATTAAT
AGACTGGATGGAGGCGGATAAAGTTGCAGGACCACTTCTGCGCTCGGCCCTTCCGGCTGGCTGGTTTA
TTGCTGATAAATCTGGAGCCGGTGAGCGTGGGTCTCGCGGTATCATTGCAGCACTGGGGCCAGATGGT
AAGCCCTCCCGTATCGTAGTTATCTACACGACGGGGAGTCAGGCAACTATGGATGAACGAAATAGACA
GATCGCTGAGATAGGTGCCTCACTGATTAAGCATTGGTAACTGTCAGACCAAGTTTACTCATATATAC
TTTAGATTGATTTAAAACTTCATTTTTAATTTAAAAGGATCTAGGTGAAGATCCTTTTTGATAATCTC
ATGACCAAAATCCCTTAACGTGAGTTTTCGTTCCACTGAGCGTCAGACCCCGTAGAAAAGATCAAAGG
ATCTTCTTGAGATCCTTTTTTTCTGCGCGTAATCTGCTGCTTGCAAACAAAAAAACCACCGCTACCAG
CGGTGGTTTGTTTGCCGGATCAAGAGCTACCAACTCTTTTTCCGAAGGTAACTGGCTTCAGCAGAGCG
CAGATACCAAATACTGTCCTTCTAGTGTAGCCGTAGTTAGGCCACCACTTCAAGAACTCTGTAGCACC
GCCTACATACCTCGCTCTGCTAATCCTGTTACCAGTGGCTGCTGCCAGTGGCGATAAGTCGTGTCTTA
CCGGGTTGGACTCAAGACGATAGTTACCGGATAAGGCGCAGCGGTCGGGCTGAACGGGGGGTTCGTGC
ACACAGCCCAGCTTGGAGCGAACGACCTACACCGAACTGAGATACCTACAGCGTGAGCTATGAGAAAG
CGCCACGCTTCCCGAAGGGAGAAAGGCGGACAGGTATCCGGTAAGCGGCAGGGTCGGAACAGGAGAGC
GCACGAGGGAGCTTCCAGGGGGAAACGCCTGGTATCTTTATAGTCCTGTCGGGTTTCGCCACCTCTGA
CTTGAGCGTCGATTTTTGTGATGCTCGTCAGGGGGGCGGAGCCTATGGAAAAACGCCAGCAACGCGGC
CTTTTTACGGTTCCTGGCCTTTTGCTGGCCTTTTGCTCACATGTTCTTTCCTGCGTTATCCCCTGATT
CTGTGGATAACCGTATTACCGCCTTTGAGTGAGCTGATACCGCTCGCCGCAGCCGAACGACCGAGCGC
AGCGAGTCAGTGAGCGAGGAAGCGGAAGAGCGCCCAATACGCAAACCGCCTCTCCCCGCGCGTTGGCC
GATTCATTAATGCAGCTGGCACGACAGGTTTCCCGACTGGAAAGCGGGCAGTGAGCGCAACGCAATTA
ATGTGAGTTAGCTCACTCATTAGGCACCCCAGGCTTTACACTTTATGCTTCCGGCTCGTATGTTGTGT
GGAATTGTGAGCGGATAACAATTTCACACAGGAAACAGCTATGACCATGATTACGCCAAGCTCGGAAT
TAACCCTCACTAAAGGGAACAAAAGCTGGGTACCTCGCGCGACTTGGTTTGCCATTCTTTAGCGCGCG
TCGCGTCACACAGCTTGGCCACAATGTGGTTTTTGTCAAACGAAGATTCTATGACGTGTTTAAAGTTT
AGGTCGAGTAAAGCGCAAATCTTTTTTAACCCTAGAAAGATAGTCTGCGTAAAATTGACGCATGCATT
CTTGAAATATTGCTCTCTCTTTCTAAATAGCGCGAATCCGTCGCTGTGCATTTAGGACATCTCAGTCG
CCGCTTGGAGCTCCCGTGAGGCGTGCTTGTCAATGCGGTAAGTGTCACTGATTTTGAACTATAACGAC
CGCGTGAGTCAAAATGACGCATGATTATCTTTTACGTGACTTTTAAGATTTAACTCATACGATAATTA
TATTGTTATTTCATGTTCTACTTACGTGATAACTTATTATATATATATTTTCTTGTTATAGATATCGT

GACTAATATATAATAAAATGGGTAGTTCTTTAGACGATGAGCATATCCTCTCTGCTCTTCTGCAAAGC
GATGACGAGCTTGTTGGCTAGCGCGCTGCTTCGCGATGTACGGGCCAGATATACGCGTTGACATTGAT
TATTGACTAGTAACTTGTTTATTGCAGCTTATAATGGTTACAAATAAGGCAATAGCATCACAAATTTC
ACAAATAAGGCATTTTTTTCACTGCATTCTAGTTTTGGTTTGTCCAAACTCATCAATGTATCTTATCA
TGTCTGGATCTCAAATCCCTCGGAAGCTGCGCCTGTCTTAGGTTGGAGTGATACATTTTTATCACTTT
TACCCGTCTTTGGATTAGGCAGTAGCTCTGACGGCCCTCCTGTCTTAGGTTAGTGAAAAATGTCACTC
TCTTACCCGTCATTGGCTGTCCAGCTTAGCTCGCAGGGGAGGTGGTCTGGGCCCATCGATTCTAGAAT
TAACCGGTGACCGGCTTGTACAGCTCGTCCATGCCGAGAGTGATCCCGGCGGCGGTCACGAACTCCAG
CAGGACCATGTGATCGCGCTTCTCGTTGGGGTCTTTGCTCAGGGCGGACTGGGTGCTCAGGTAGTGGT
TGTCGGGCAGCAGCACGGGGCCGTCGCCGATGGGGGTGTTCTGCTGGTAGTGGTCGGCGAGCTGCACG
CTGCCGTCCTCGATGTTGTGGCGGATCTTGAAGTTCACCTTGATGCCGTTCTTCTGCTTGTCGGCCAT
GATATAGACGTTGTGGCTGTTGTAGTTGTACTCCAGCTTGTGCCCCAGGATGTTGCCGTCCTCCTTGA
AGTCGATGCCCTTCAGCTCGATGCGGTTCACCAGGGTGTCGCCCTCGAACTTCACCTCGGCGCGGGTC
TTGTAGTTGCCGTCGTCCTTGAAGAAGATGGTGCGCTCCTGGACGTAGCCTTCGGGCATGGCGGACTT
GAAGAAGTCGTGCTGCTTCATGTGGTCGGGGTAGCGGCTGAAGCACTGCACGCCGTAGGTCAGGGTGG
TCACGAGGGTGGGCCAGGGCACGGGCAGCTTGCCGGTGGTGCAGATGAACTTCAGGGTCAGCTTGCCG
TAGGTGGCATCGCCCTCGCCCTCGCCGGACACGCTGAACTTGTGGCCGTTTACGTCGCCGTCCAGCTC
GACCAGGATGGGCACCACCCCGGTGAACAGCTCCTCGCCCTTGCTCACGCCGGTGACCGGCTTGTACA
GCTCGTCCATGCCGAGAGTGATCCCGGCGGCGGTCACGAACTCCAGCAGGACCATGTGATCGCGCTTC
TCGTTGGGGTCTTTGCTCAGGGCGGACTGGGTGCTCAGGTAGTGGTTGTCGGGCAGCAGCACGGGGCC
GTCGCCGATGGGGGTGTTCTGCTGGTAGTGGTCGGCGAGCTGCACGCTGCCGTCCTCGATGTTGTGGC
GGATCTTGAAGTTCACCTTGATGCCGTTCTTCTGCTTGTCGGCCATGATATAGACGTTGTGGCTGTTG
TAGTTGTACTCCAGCTTGTGCCCCAGGATGTTGCCGTCCTCCTTGAAGTCGATGCCCTTCAGCTCGAT
GCGGTTCACCAGGGTGTCGCCCTCGAACTTCACCTCGGCGCGGGTCTTGTAGTTGCCGTCGTCCTTGA
AGAAGATGGTGCGCTCCTGGACGTAGCCTTCGGGCATGGCGGACTTGAAGAAGTCGTGCTGCTTCATG
TGGTCGGGGTAGCGGCTGAAGCACTGCACGCCGTAGGTCAGGGTGGTCACGAGGGTGGGCCAGGGCAC
GGGCAGCTTGCCGGTGGTGCAGATGAACTTCAGGGTCAGCTTGCCGTAGGTGGCATCGCCCTCGCCCT
CGCCGGACACGCTGAACTTGTGGCCGTTTACGTCGCCGTCCAGCTCGACCAGGATGGGCACCACCCCG
GTGAACAGCTCCTCGCCCTTGCTCACGCCGGTGACCGGCTTGTACAGCTCGTCCATGCCGAGAGTGAT
CCCGGCGGCGGTCACGAACTCCAGCAGGACCATGTGATCGCGCTTCTCGTTGGGGTCTTTGCTCAGGG
CGGACTGGGTGCTCAGGTAGTGGTTGTCGGGCAGCAGCACGGGGCCGTCGCCGATGGGGGTGTTCTGC
TGGTAGTGGTCGGCGAGCTGCACGCTGCCGTCCTCGATGTTGTGGCGGATCTTGAAGTTCACCTTGAT
GCCGTTCTTCTGCTTGTCGGCCATGATATAGACGTTGTGGCTGTTGTAGTTGTACTCCAGCTTGTGCC
CCAGGATGTTGCCGTCCTCCTTGAAGTCGATGCCCTTCAGCTCGATGCGGTTCACCAGGGTGTCGCCC
TCGAACTTCACCTCGGCGCGGGTCTTGTAGTTGCCGTCGTCCTTGAAGAAGATGGTGCGCTCCTGGAC
GTAGCCTTCGGGCATGGCGGACTTGAAGAAGTCGTGCTGCTTCATGTGGTCGGGGTAGCGGCTGAAGC
ACTGCACGCCGTAGGTCAGGGTGGTCACGAGGGTGGGCCAGGGCACGGGCAGCTTGCCGGTGGTGCAG
ATGAACTTCAGGGTCAGCTTGCCGTAGGTGGCATCGCCCTCGCCCTCGCCGGACACGCTGAACTTGTG
GCCGTTTACGTCGCCGTCCAGCTCGACCAGGATGGGCACCACCCCGGTGAACAGCTCCTCGCCCTTGC
TCACGCCGGTCCCTGGCGCGCCTCCGCCTGCAGGACCCAGCCCAGGCTTGCCCAGTCTGTGGCCCTCG
TGGGCCAGCAGCCACTCTTTCACGGCGAGCCCGCCCTCGTAGCCCCCCACGTCCAGGTCGCCCTGCAC
CACCCGGTGGCAGGGGATCAGAATGGGCACGGGATTTCCGCTCAGGGCGGTTTTCACGGCGGCGGTGG
CGGCGGGATTGCCGGCCAGGGCGGCCAGGTGGCTGTAGCTGATGACCTCTCCGAACTTCACCACTTTC
AGCAGTTTCCACAGCACCTGGCGGGTAAAGCTCTCCTGCTGGAACACTGGGTGGTGCAGGGCTGGCAC
AGGGAACTCCTCGATGGCCTCAGGCTGGTGAAAGTAGGCGTTGAGCCAGGCGGTGGCCTGCATCAGTG
GCTCTGGTCCGCCCAGCACGGCGGCTGGGGCAGGCACTTCCACGGCGTCGGCGGCAGATGTTCCTTTG
CCCAGGAAGATGATACGGTGCAGGCCCTGTTCGCACCCAGACAGTTCCAGCTTGCCCAGAGGGCTATC
CAGGGTGGTGCGCTTCATTTCGCAGTCTTTGTCACCTGAGCCTGGAGCAACTTTTCTTTTCTTTTTTG
GTCCCATGCGGCCGCGGATCCCGCGTCCTAGGTTTCGACCGCGGAGGCTGGATCGGTCCCGGTGTCTT
CTATGGAGGTCAAAACAGCGTGGATGGCGTCTCCAGGCGATCTGACGGTTCACTAAACGAGCTCTGCT
TATATAGGCCTCCCACCGTACACGCCTACAAGCTTCTTTCACTTTTCTCTATCACTGATAGGGAGTGG
TAAACTCGACTTTCACTTTTCTCTATCACTGATAGGGAGTGGTAAACTCGACTTTCACTTTTCTCTAT
CACTGATAGGGAGTGGTAAACTCGACTTTCACTTTTCTCTATCACTGATAGGGAGTGGTAAACTCGAC
TTTCACTTTTCTCTATCACTGATAGGGAGTGGTAAACTCGACTTTCACTTTTCTCTATCACTGATAGG

54

GAGTGGTAAACTCGACTTTCACTTTTCTCTATCACTGATAGGGAGTGGTAAACTCGAGGGTAGGCGTG
TACGGTGGGAGGCCTATATAAGCAGAGCTCGTTTAGTGAACCGTCAGATCGCCTGGAGACGCCATCCA
CGCTGTTTTGACCTCCATAGAAGACACCGGGACCGATCCAGCCTCCGCGGAATTCTTAATAGCGGCCG
CATGGGACCAAAAAAGAAAAGAAAAGTTGCTCCAGGCTCAGGTGACAAAGACTGCGAAATGAAGCGCA
CCACCCTGGATAGCCCTCTGGGCAAGCTGGAACTGTCTGGGTGCGAACAGGGCCTGCACCGTATCATC
TTCCTGGGCAAAGGAACATCTGCCGCCGACGCCGTGGAAGTGCCTGCCCCAGCCGCCGTGCTGGGCGG
ACCAGAGCCACTGATCCAGGCCACCGCCTGGCTCAACGCCTACTTTCACCAGCCTGAGGCCATCGAGG
AGTTCCCTGTGCCAGCCCTGCACCACCCAGTGTTCCAGCAGGAGAGCTTTACCCGCCAGGTGCTGTGG
AAACTGCTGAAAGTGGTGAAGTTCGGAGAGGTCATCAGCGAGAGCCACCTGGCCGCCCTGGTGGGCAA
TCCCGCCGCCACCGCCGCCGTGAACACCGCCCTGGACGGAAATCCCGTGCCCATTCTGATCCCCTGCC
ACCGGGTGGTGCAGGGCGACAGCGACGTGGGGCCCTACCTGGGCGGGCTCGCCGTGAAAGAGTGGCTG
CTGGCCCACGAGGGCCACAGACTGGGCAAGCCTGGGCTGGGTCCTGCAGGCGGAGGCGCGCCAGGGAC
CGGCGTGAGCAAGGGCGAGGAGGATAACATGGCCATCATCAAGGAGTTCATGCGCTTCAAGGTGCACA
TGGAGGGCTCCGTGAACGGCCACGAGTTCGAGATCGAGGGCGAGGGCGAGGGCCGCCCCTACGAGGGC
ACCCAGACCGCCAAGCTGAAGGTGACCAAGGGTGGCCCCCTGCCCTTCGCCTGGGACATCCTGTCCCC
TCAGTTCATGTACGGCTCCAAGGCCTACGTGAAGCACCCCGCCGACATCCCCGACTACTTGAAGCTGT
CCTTCCCCGAGGGCTTCAAGTGGGAGCGCGTGATGAACTTCGAGGACGGCGGCGTGGTGACCGTGACC
CAGGACTCCTCCCTGCAGGACGGCGAGTTCATCTACAAGGTGAAGCTGCGCGGCACCAACTTCCCCTC
CGACGGCCCCGTAATGCAGAAGAAGACCATGGGCTGGGAGGCCTCCTCCGAGCGGATGTACCCCGAGG
ACGGCGCCCTGAAGGGCGAGATCAAGCAGAGGCTGAAGCTGAAGGACGGCGGCCACTACGACGCTGAG
GTCAAGACCACCTACAAGGCCAAGAAGCCCGTGCAGCTGCCCGGCGCCTACAACGTCAACATCAAGTT
GGACATCACCTCCCACAACGAGGACTACACCATCGTGGAACAGTACGAACGCGCCGAGGGCCGCCACT
CCACCGGCGGCATGGACGAGCTGTACAAGCCGGTCACCGGCGTGAGCAAGGGCGAGGAGGATAACATG
GCCATCATCAAGGAGTTCATGCGCTTCAAGGTGCACATGGAGGGCTCCGTGAACGGCCACGAGTTCGA
GATCGAGGGCGAGGGCGAGGGCCGCCCCTACGAGGGCACCCAGACCGCCAAGCTGAAGGTGACCAAGG
GTGGCCCCCTGCCCTTCGCCTGGGACATCCTGTCCCCTCAGTTCATGTACGGCTCCAAGGCCTACGTG
AAGCACCCCGCCGACATCCCCGACTACTTGAAGCTGTCCTTCCCCGAGGGCTTCAAGTGGGAGCGCGT
GATGAACTTCGAGGACGGCGGCGTGGTGACCGTGACCCAGGACTCCTCCCTGCAGGACGGCGAGTTCA
TCTACAAGGTGAAGCTGCGCGGCACCAACTTCCCCTCCGACGGCCCCGTAATGCAGAAGAAGACCATG
GGCTGGGAGGCCTCCTCCGAGCGGATGTACCCCGAGGACGGCGCCCTGAAGGGCGAGATCAAGCAGAG
GCTGAAGCTGAAGGACGGCGGCCACTACGACGCTGAGGTCAAGACCACCTACAAGGCCAAGAAGCCCG
TGCAGCTGCCCGGCGCCTACAACGTCAACATCAAGTTGGACATCACCTCCCACAACGAGGACTACACC
ATCGTGGAACAGTACGAACGCGCCGAGGGCCGCCACTCCACCGGCGGCATGGACGAGCTGTACAAGCC
GGTCACCGGCGTGAGCAAGGGCGAGGAGGATAACATGGCCATCATCAAGGAGTTCATGCGCTTCAAGG
TGCACATGGAGGGCTCCGTGAACGGCCACGAGTTCGAGATCGAGGGCGAGGGCGAGGGCCGCCCCTAC
GAGGGCACCCAGACCGCCAAGCTGAAGGTGACCAAGGGTGGCCCCCTGCCCTTCGCCTGGGACATCCT
GTCCCCTCAGTTCATGTACGGCTCCAAGGCCTACGTGAAGCACCCCGCCGACATCCCCGACTACTTGA
AGCTGTCCTTCCCCGAGGGCTTCAAGTGGGAGCGCGTGATGAACTTCGAGGACGGCGGCGTGGTGACC
GTGACCCAGGACTCCTCCCTGCAGGACGGCGAGTTCATCTACAAGGTGAAGCTGCGCGGCACCAACTT
CCCCTCCGACGGCCCCGTAATGCAGAAGAAGACCATGGGCTGGGAGGCCTCCTCCGAGCGGATGTACC
CCGAGGACGGCGCCCTGAAGGGCGAGATCAAGCAGAGGCTGAAGCTGAAGGACGGCGGCCACTACGAC
GCTGAGGTCAAGACCACCTACAAGGCCAAGAAGCCCGTGCAGCTGCCCGGCGCCTACAACGTCAACAT
CAAGTTGGACATCACCTCCCACAACGAGGACTACACCATCGTGGAACAGTACGAACGCGCCGAGGGCC
GCCACTCCACCGGCGGCATGGACGAGCTGTACAAGCCGGTCACCGGTTAATTCTAGAATCGATGTAGG
AGGTACTAAGCCGGTCATCATCACCATCACCATTGAGTTTAAACCCGCTGATCAGCCTCGACTGTGCC
TTCTAGTTGCCAGCCATCTGTTGTTTGCCCCTCCCCCGTGCCTTCCTTGACCCTGGAAGGTGCCACTC
CCACTGTCCTTTCCTAATAAAATGAGGAAATTGCATCGCATTGTCTGAGTAGGTGTCATTCTATTCTG
GGGGGTGGGGTGGGGCAGGACAGCAAGGGGGAGGATTGGGAAGACAATAGCAGGCATGCTGGGGATGC
GGTGGGCTCTATGGCGTGTGTCAGTTAGGGTGTGGAAAGTCCCCAGGCTCCCCAGCAGGCAGAAGTAT
GCAAAGCATGCATCTCAATTAGTCAGCAACCAGGTGTGGAAAGTCCCCAGGCTCCCCAGCAGGCAGAA
GTATGCAAAGCATGCATCTCAATTAGTCAGCAACCATAGTCCCGCCCCTAACTCCGCCCATCCCGCCC
CTAACTCCGCCCAGTTCCGCCCATTCTCCGCCCCATGGCTGACTAATTTTTTTTATTTATGCAGAGGC
CGAGGCCGCCTCTGCCTCTGAGCTATTCCAGAAGTAGTGAGGAGGCTTTTTTGGAGGCCTAGGCTTTT
GCAAAAAGCTCCCATGACCGAGTACAAGCCCACGGTGCGCCTCGCCACCCGCGACGACGTCCCCAGGG

55

CCGTACGCACCCTCGCCGCCGCGTTCGCCGACTACCCCGCCACGCGCCACACCGTCGATCCGGACCGC
CACATCGAGCGGGTCACCGAGCTGCAAGAACTCTTCCTCACGCGCGTCGGGCTCGACATCGGCAAGGT
GTGGGTCGCGGACGACGGCGCCGCGGTGGCGGTCTGGACCACGCCGGAGAGCGTCGAAGCGGGGGCGG
TGTTCGCCGAGATCGGCCCGCGCATGGCCGAGTTGAGCGGTTCCCGGCTGGCCGCGCAGCAACAGATG
GAAGGCCTCCTGGCGCCGCACCGGCCCAAGGAGCCCGCGTGGTTCCTGGCCACCGTCGGCGTCTCGCC
CGACCACCAGGGCAAGGGTCTGGGCAGCGCCGTCGTGCTCCCCGGAGTGGAGGCGGCCGAGCGCGCCG
GGGTGCCCGCCTTCCTGGAGACCTCCGCGCCCCGCAACCTCCCCTTCTACGAGCGGCTCGGCTTCACC
GTCACCGCCGACGTCGAGGTGCCCGAAGGACCGCGCACCTGGTGCATGACCCGCAAGCCCGGTGCCTG
AGCGGGACTCTGGGGTTCGAAATGACCGACCAAGCGACGCCCGAAATGACCGACCAAGCGACGCCCAA
CCTGCCATCACGAGATTTCGATTCCACCGCCGCCTTCTATGAAAGGTTGGGCTTCGGAATCGTTTTCC
GGGACGCCGGCTGGATGATCCTCCAGCGCGGGGATCTCATGCTGGAGTTCTTCGCCCACCCCAACTTG
TTTATTGCAGCTTATAATGGTTACAAATAAAGCAATAGCATCACAAATTTCACAAATAAAGCATTTTT
TTCACTGCATTCTAGTTGTGGTTTGTCCAAACTCATCAATGTATCTTATCATGTCTGTATACCGTCGA
CCTCTAGCTAGTCGAGTTAATTAACGAGAGCATAATATTGATATGTGCCAAAGTTGTTTCTGACTGAC
TAATAAGTATAATTTGTTTCTATTATGTATAGGTTAAGCTAATTACTTATTTTATAATACAACATGAC
TGTTTTTAAAGTACAAAATAAGTTTATTTTTGTAAAAGAGAGAATGTTTAAAAGTTTTGTTACTTTAT
AGAAGAAATTTTGAGTTTTTGTTTTTTTTTAATAAATAAATAAACATAAATAAATTGTTTGTTGAATT
TATTATTAGTATGTAAGTGTAAATATAATAAAACTTAATATCTATTCAAATTAATAAATAAACCTCGA
TATACAGACCGATAAAACACATGCGTCAATTTTACGCATGATTATCTTTAACGTACGTCACAATATGA
TTATCTTTCTAGGGTTAAATAATAGTTTCTAATTTTTTTATTATTCAGCCTGCTGTCGTGAATACCGA
GCTCCAATTCGCCCTATAGTGAGTCGTATTACAATTCACTGGCCGTCGTTTTACAACGTCGTGACTGG
GAAAACCCTGGCGTTACCCAACTTAATCGCCTTGCAGCACATCCCCCTTTCGCCAGCTGGCGTAATAG
CGAAGAGGCCCGCACCGATCGCCCTTCCCAACAGTTGCGCAGCCTGAATGGCGAATGGCGCGACGCGC
CCTGTAGCGGCGCATTAAGCGCGGCGGGTGTGGTGGTTACGCGCAGCGTGACCGCTACACTTGCCAGC
GCCCTAGCGCCCGCTCCTTTCGCTTTCTTCCCTTCCTTTCTCGCCACGTTCGCCGGCTTTCCCCGTCA
AGCTCTAAATCGGGGGCTCCCTTTAGGGTTCCGATTTAGTGCTTTACGGCACCTCGACCCCAAAAAAC
TTGATTAGGGTGATGGTTCACGTAGTGGGCCATCGCCCTGATAGACGGTTTTTCGCCCTTTGACGTTG
GAGTCCACGTTCTTTAATAGTGGACTCTTGTTCCAAACTGGAACAACACTCAACCCTATCTCGGTCTA
TTCTTTTGATTTATAAGGGATTTTGCCGATTTCGGCCTATTGGTTAAAAAATGAGCTGATTTAACAAA
AATTTAACGCGAATTTTAACAAAATATTAACGTTTACAATTTCC

PiggyBac-Puro_SNAPf-3xeGFP+NLS-CLIP-3xmCherry

CAGGTGGCACTTTTCGGGGAAATGTGCGCGGAACCCCTATTTGTTTATTTTTCTAAATACATTCAAAT
ATGTATCCGCTCATGAGACAATAACCCTGATAAATGCTTCAATAATATTGAAAAAGGAAGAGTATGAG
TATTCAACATTTCCGTGTCGCCCTTATTCCCTTTTTTGCGGCATTTTGCCTTCCTGTTTTTGCTCACC
CAGAAACGCTGGTGAAAGTAAAAGATGCTGAAGATCAGTTGGGTGCACGAGTGGGTTACATCGAACTG
GATCTCAACAGCGGTAAGATCCTTGAGAGTTTTCGCCCCGAAGAACGTTTTCCAATGATGAGCACTTT
TAAAGTTCTGCTATGTGGCGCGGTATTATCCCGTATTGACGCCGGGCAAGAGCAACTCGGTCGCCGCA
TACACTATTCTCAGAATGACTTGGTTGAGTACTCACCAGTCACAGAAAAGCATCTTACGGATGGCATG
ACAGTAAGAGAATTATGCAGTGCTGCCATAACCATGAGTGATAACACTGCGGCCAACTTACTTCTGAC
AACGATCGGAGGACCGAAGGAGCTAACCGCTTTTTTGCACAACATGGGGGATCATGTAACTCGCCTTG
ATCGTTGGGAACCGGAGCTGAATGAAGCCATACCAAACGACGAGCGTGACACCACGATGCCTGTAGCA
ATGGCAACAACGTTGCGCAAACTATTAACTGGCGAACTACTTACTCTAGCTTCCCGGCAACAATTAAT
AGACTGGATGGAGGCGGATAAAGTTGCAGGACCACTTCTGCGCTCGGCCCTTCCGGCTGGCTGGTTTA
TTGCTGATAAATCTGGAGCCGGTGAGCGTGGGTCTCGCGGTATCATTGCAGCACTGGGGCCAGATGGT
AAGCCCTCCCGTATCGTAGTTATCTACACGACGGGGAGTCAGGCAACTATGGATGAACGAAATAGACA
GATCGCTGAGATAGGTGCCTCACTGATTAAGCATTGGTAACTGTCAGACCAAGTTTACTCATATATAC
TTTAGATTGATTTAAAACTTCATTTTTAATTTAAAAGGATCTAGGTGAAGATCCTTTTTGATAATCTC
ATGACCAAAATCCCTTAACGTGAGTTTTCGTTCCACTGAGCGTCAGACCCCGTAGAAAAGATCAAAGG
ATCTTCTTGAGATCCTTTTTTTCTGCGCGTAATCTGCTGCTTGCAAACAAAAAAACCACCGCTACCAG
CGGTGGTTTGTTTGCCGGATCAAGAGCTACCAACTCTTTTTCCGAAGGTAACTGGCTTCAGCAGAGCG
CAGATACCAAATACTGTCCTTCTAGTGTAGCCGTAGTTAGGCCACCACTTCAAGAACTCTGTAGCACC

GCCTACATACCTCGCTCTGCTAATCCTGTTACCAGTGGCTGCTGCCAGTGGCGATAAGTCGTGTCTTA
CCGGGTTGGACTCAAGACGATAGTTACCGGATAAGGCGCAGCGGTCGGGCTGAACGGGGGGTTCGTGC
ACACAGCCCAGCTTGGAGCGAACGACCTACACCGAACTGAGATACCTACAGCGTGAGCTATGAGAAAG
CGCCACGCTTCCCGAAGGGAGAAAGGCGGACAGGTATCCGGTAAGCGGCAGGGTCGGAACAGGAGAGC
GCACGAGGGAGCTTCCAGGGGGAAACGCCTGGTATCTTTATAGTCCTGTCGGGTTTCGCCACCTCTGA
CTTGAGCGTCGATTTTTGTGATGCTCGTCAGGGGGGCGGAGCCTATGGAAAAACGCCAGCAACGCGGC
CTTTTTACGGTTCCTGGCCTTTTGCTGGCCTTTTGCTCACATGTTCTTTCCTGCGTTATCCCCTGATT
CTGTGGATAACCGTATTACCGCCTTTGAGTGAGCTGATACCGCTCGCCGCAGCCGAACGACCGAGCGC
AGCGAGTCAGTGAGCGAGGAAGCGGAAGAGCGCCCAATACGCAAACCGCCTCTCCCCGCGCGTTGGCC
GATTCATTAATGCAGCTGGCACGACAGGTTTCCCGACTGGAAAGCGGGCAGTGAGCGCAACGCAATTA
ATGTGAGTTAGCTCACTCATTAGGCACCCCAGGCTTTACACTTTATGCTTCCGGCTCGTATGTTGTGT
GGAATTGTGAGCGGATAACAATTTCACACAGGAAACAGCTATGACCATGATTACGCCAAGCTCGGAAT
TAACCCTCACTAAAGGGAACAAAAGCTGGGTACCTCGCGCGACTTGGTTTGCCATTCTTTAGCGCGCG
TCGCGTCACACAGCTTGGCCACAATGTGGTTTTTGTCAAACGAAGATTCTATGACGTGTTTAAAGTTT
AGGTCGAGTAAAGCGCAAATCTTTTTTAACCCTAGAAAGATAGTCTGCGTAAAATTGACGCATGCATT
CTTGAAATATTGCTCTCTCTTTCTAAATAGCGCGAATCCGTCGCTGTGCATTTAGGACATCTCAGTCG
CCGCTTGGAGCTCCCGTGAGGCGTGCTTGTCAATGCGGTAAGTGTCACTGATTTTGAACTATAACGAC
CGCGTGAGTCAAAATGACGCATGATTATCTTTTACGTGACTTTTAAGATTTAACTCATACGATAATTA
TATTGTTATTTCATGTTCTACTTACGTGATAACTTATTATATATATATTTTCTTGTTATAGATATCGT
GACTAATATATAATAAAATGGGTAGTTCTTTAGACGATGAGCATATCCTCTCTGCTCTTCTGCAAAGC
GATGACGAGCTTGTTGGCTAGCGCGCTGCTTCGCGATGTACGGGCCAGATATACGCGTTGACATTGAT
TATTGACTAGTAACTTGTTTATTGCAGCTTATAATGGTTACAAATAAGGCAATAGCATCACAAATTTC
ACAAATAAGGCATTTTTTTCACTGCATTCTAGTTTTGGTTTGTCCAAACTCATCAATGTATCTTATCA
TGTCTGGATCTCAAATCCCTCGGAAGCTGCGCCTGTCTTAGGTTGGAGTGATACATTTTTATCACTTT
TACCCGTCTTTGGATTAGGCAGTAGCTCTGACGGCCCTCCTGTCTTAGGTTAGTGAAAAATGTCACTC
TCTTACCCGTCATTGGCTGTCCAGCTTAGCTCGCAGGGGAGGTGGTCTGGGCCCATCGATTCTAGAAT
TAACCGGTGACCGGCTTGTACAGCTCGTCCATGCCGAGAGTGATCCCGGCGGCGGTCACGAACTCCAG
CAGGACCATGTGATCGCGCTTCTCGTTGGGGTCTTTGCTCAGGGCGGACTGGGTGCTCAGGTAGTGGT
TGTCGGGCAGCAGCACGGGGCCGTCGCCGATGGGGGTGTTCTGCTGGTAGTGGTCGGCGAGCTGCACG
CTGCCGTCCTCGATGTTGTGGCGGATCTTGAAGTTCACCTTGATGCCGTTCTTCTGCTTGTCGGCCAT
GATATAGACGTTGTGGCTGTTGTAGTTGTACTCCAGCTTGTGCCCCAGGATGTTGCCGTCCTCCTTGA
AGTCGATGCCCTTCAGCTCGATGCGGTTCACCAGGGTGTCGCCCTCGAACTTCACCTCGGCGCGGGTC
TTGTAGTTGCCGTCGTCCTTGAAGAAGATGGTGCGCTCCTGGACGTAGCCTTCGGGCATGGCGGACTT
GAAGAAGTCGTGCTGCTTCATGTGGTCGGGGTAGCGGCTGAAGCACTGCACGCCGTAGGTCAGGGTGG
TCACGAGGGTGGGCCAGGGCACGGGCAGCTTGCCGGTGGTGCAGATGAACTTCAGGGTCAGCTTGCCG
TAGGTGGCATCGCCCTCGCCCTCGCCGGACACGCTGAACTTGTGGCCGTTTACGTCGCCGTCCAGCTC
GACCAGGATGGGCACCACCCCGGTGAACAGCTCCTCGCCCTTGCTCACGCCGGTGACCGGCTTGTACA
GCTCGTCCATGCCGAGAGTGATCCCGGCGGCGGTCACGAACTCCAGCAGGACCATGTGATCGCGCTTC
TCGTTGGGGTCTTTGCTCAGGGCGGACTGGGTGCTCAGGTAGTGGTTGTCGGGCAGCAGCACGGGGCC
GTCGCCGATGGGGGTGTTCTGCTGGTAGTGGTCGGCGAGCTGCACGCTGCCGTCCTCGATGTTGTGGC
GGATCTTGAAGTTCACCTTGATGCCGTTCTTCTGCTTGTCGGCCATGATATAGACGTTGTGGCTGTTG
TAGTTGTACTCCAGCTTGTGCCCCAGGATGTTGCCGTCCTCCTTGAAGTCGATGCCCTTCAGCTCGAT
GCGGTTCACCAGGGTGTCGCCCTCGAACTTCACCTCGGCGCGGGTCTTGTAGTTGCCGTCGTCCTTGA
AGAAGATGGTGCGCTCCTGGACGTAGCCTTCGGGCATGGCGGACTTGAAGAAGTCGTGCTGCTTCATG
TGGTCGGGGTAGCGGCTGAAGCACTGCACGCCGTAGGTCAGGGTGGTCACGAGGGTGGGCCAGGGCAC
GGGCAGCTTGCCGGTGGTGCAGATGAACTTCAGGGTCAGCTTGCCGTAGGTGGCATCGCCCTCGCCCT
CGCCGGACACGCTGAACTTGTGGCCGTTTACGTCGCCGTCCAGCTCGACCAGGATGGGCACCACCCCG
GTGAACAGCTCCTCGCCCTTGCTCACGCCGGTGACCGGCTTGTACAGCTCGTCCATGCCGAGAGTGAT
CCCGGCGGCGGTCACGAACTCCAGCAGGACCATGTGATCGCGCTTCTCGTTGGGGTCTTTGCTCAGGG
CGGACTGGGTGCTCAGGTAGTGGTTGTCGGGCAGCAGCACGGGGCCGTCGCCGATGGGGGTGTTCTGC
TGGTAGTGGTCGGCGAGCTGCACGCTGCCGTCCTCGATGTTGTGGCGGATCTTGAAGTTCACCTTGAT
GCCGTTCTTCTGCTTGTCGGCCATGATATAGACGTTGTGGCTGTTGTAGTTGTACTCCAGCTTGTGCC
CCAGGATGTTGCCGTCCTCCTTGAAGTCGATGCCCTTCAGCTCGATGCGGTTCACCAGGGTGTCGCCC
TCGAACTTCACCTCGGCGCGGGTCTTGTAGTTGCCGTCGTCCTTGAAGAAGATGGTGCGCTCCTGGAC

57

GTAGCCTTCGGGCATGGCGGACTTGAAGAAGTCGTGCTGCTTCATGTGGTCGGGGTAGCGGCTGAAGC
ACTGCACGCCGTAGGTCAGGGTGGTCACGAGGGTGGGCCAGGGCACGGGCAGCTTGCCGGTGGTGCAG
ATGAACTTCAGGGTCAGCTTGCCGTAGGTGGCATCGCCCTCGCCCTCGCCGGACACGCTGAACTTGTG
GCCGTTTACGTCGCCGTCCAGCTCGACCAGGATGGGCACCACCCCGGTGAACAGCTCCTCGCCCTTGC
TCACGCCGGTCCCTGGCGCGCCTCCGCCTGCAGGACCCAGCCCAGGCTTGCCCAGTCTGTGGCCCTCG
TGGGCCAGCAGCCACTCTTTCACGGCGAGCCCGCCCTCGTAGCCCCCCACGTCCAGGTCGCCCTGCAC
CACCCGGTGGCAGGGGATCAGAATGGGCACGGGATTTCCGCTCAGGGCGGTTTTCACGGCGGCGGTGG
CGGCGGGATTGCCGGCCAGGGCGGCCAGGTGGCTGTAGCTGATGACCTCTCCGAACTTCACCACTTTC
AGCAGTTTCCACAGCACCTGGCGGGTAAAGCTCTCCTGCTGGAACACTGGGTGGTGCAGGGCTGGCAC
AGGGAACTCCTCGATGGCCTCAGGCTGGTGAAAGTAGGCGTTGAGCCAGGCGGTGGCCTGCATCAGTG
GCTCTGGTCCGCCCAGCACGGCGGCTGGGGCAGGCACTTCCACGGCGTCGGCGGCAGATGTTCCTTTG
CCCAGGAAGATGATACGGTGCAGGCCCTGTTCGCACCCAGACAGTTCCAGCTTGCCCAGAGGGCTATC
CAGGGTGGTGCGCTTCATTTCGCAGTCTTTGTCGCCGGCCATGCGGCCGCCGCGTCCTAGGTTTCGAC
CGCGGAGGCTGGATCGGTCCCGGTGTCTTCTATGGAGGTCAAAACAGCGTGGATGGCGTCTCCAGGCG
ATCTGACGGTTCACTAAACGAGCTCTGCTTATATAGGCCTCCCACCGTACACGCCTACAAGCTTCTTT
CACTTTTCTCTATCACTGATAGGGAGTGGTAAACTCGACTTTCACTTTTCTCTATCACTGATAGGGAG
TGGTAAACTCGACTTTCACTTTTCTCTATCACTGATAGGGAGTGGTAAACTCGACTTTCACTTTTCTC
TATCACTGATAGGGAGTGGTAAACTCGACTTTCACTTTTCTCTATCACTGATAGGGAGTGGTAAACTC
GACTTTCACTTTTCTCTATCACTGATAGGGAGTGGTAAACTCGACTTTCACTTTTCTCTATCACTGAT
AGGGAGTGGTAAACTCGAGGGTAGGCGTGTACGGTGGGAGGCCTATATAAGCAGAGCTCGTTTAGTGA
ACCGTCAGATCGCCTGGAGACGCCATCCACGCTGTTTTGACCTCCATAGAAGACACCGGGACCGATCC
AGCCTCCGCGGAATTCTTAATAGCGGCCGCATGGGACCAAAAAAGAAAAGAAAAGTTGCTCCAGGCTC
AGGTGACAAAGACTGCGAAATGAAGCGCACCACCCTGGATAGCCCTCTGGGCAAGCTGGAACTGTCTG
GGTGCGAACAGGGCCTGCACCGTATCATCTTCCTGGGCAAAGGAACATCTGCCGCCGACGCCGTGGAA
GTGCCTGCCCCAGCCGCCGTGCTGGGCGGACCAGAGCCACTGATCCAGGCCACCGCCTGGCTCAACGC
CTACTTTCACCAGCCTGAGGCCATCGAGGAGTTCCCTGTGCCAGCCCTGCACCACCCAGTGTTCCAGC
AGGAGAGCTTTACCCGCCAGGTGCTGTGGAAACTGCTGAAAGTGGTGAAGTTCGGAGAGGTCATCAGC
GAGAGCCACCTGGCCGCCCTGGTGGGCAATCCCGCCGCCACCGCCGCCGTGAACACCGCCCTGGACGG
AAATCCCGTGCCCATTCTGATCCCCTGCCACCGGGTGGTGCAGGGCGACAGCGACGTGGGGCCCTACC
TGGGCGGGCTCGCCGTGAAAGAGTGGCTGCTGGCCCACGAGGGCCACAGACTGGGCAAGCCTGGGCTG
GGTCCTGCAGGCGGAGGCGCGCCAGGGACCGGCGTGAGCAAGGGCGAGGAGGATAACATGGCCATCAT
CAAGGAGTTCATGCGCTTCAAGGTGCACATGGAGGGCTCCGTGAACGGCCACGAGTTCGAGATCGAGG
GCGAGGGCGAGGGCCGCCCCTACGAGGGCACCCAGACCGCCAAGCTGAAGGTGACCAAGGGTGGCCCC
CTGCCCTTCGCCTGGGACATCCTGTCCCCTCAGTTCATGTACGGCTCCAAGGCCTACGTGAAGCACCC
CGCCGACATCCCCGACTACTTGAAGCTGTCCTTCCCCGAGGGCTTCAAGTGGGAGCGCGTGATGAACT
TCGAGGACGGCGGCGTGGTGACCGTGACCCAGGACTCCTCCCTGCAGGACGGCGAGTTCATCTACAAG
GTGAAGCTGCGCGGCACCAACTTCCCCTCCGACGGCCCCGTAATGCAGAAGAAGACCATGGGCTGGGA
GGCCTCCTCCGAGCGGATGTACCCCGAGGACGGCGCCCTGAAGGGCGAGATCAAGCAGAGGCTGAAGC
TGAAGGACGGCGGCCACTACGACGCTGAGGTCAAGACCACCTACAAGGCCAAGAAGCCCGTGCAGCTG
CCCGGCGCCTACAACGTCAACATCAAGTTGGACATCACCTCCCACAACGAGGACTACACCATCGTGGA
ACAGTACGAACGCGCCGAGGGCCGCCACTCCACCGGCGGCATGGACGAGCTGTACAAGCCGGTCACCG
GCGTGAGCAAGGGCGAGGAGGATAACATGGCCATCATCAAGGAGTTCATGCGCTTCAAGGTGCACATG
GAGGGCTCCGTGAACGGCCACGAGTTCGAGATCGAGGGCGAGGGCGAGGGCCGCCCCTACGAGGGCAC
CCAGACCGCCAAGCTGAAGGTGACCAAGGGTGGCCCCCTGCCCTTCGCCTGGGACATCCTGTCCCCTC
AGTTCATGTACGGCTCCAAGGCCTACGTGAAGCACCCCGCCGACATCCCCGACTACTTGAAGCTGTCC
TTCCCCGAGGGCTTCAAGTGGGAGCGCGTGATGAACTTCGAGGACGGCGGCGTGGTGACCGTGACCCA
GGACTCCTCCCTGCAGGACGGCGAGTTCATCTACAAGGTGAAGCTGCGCGGCACCAACTTCCCCTCCG
ACGGCCCCGTAATGCAGAAGAAGACCATGGGCTGGGAGGCCTCCTCCGAGCGGATGTACCCCGAGGAC
GGCGCCCTGAAGGGCGAGATCAAGCAGAGGCTGAAGCTGAAGGACGGCGGCCACTACGACGCTGAGGT
CAAGACCACCTACAAGGCCAAGAAGCCCGTGCAGCTGCCCGGCGCCTACAACGTCAACATCAAGTTGG
ACATCACCTCCCACAACGAGGACTACACCATCGTGGAACAGTACGAACGCGCCGAGGGCCGCCACTCC
ACCGGCGGCATGGACGAGCTGTACAAGCCGGTCACCGGCGTGAGCAAGGGCGAGGAGGATAACATGGC
CATCATCAAGGAGTTCATGCGCTTCAAGGTGCACATGGAGGGCTCCGTGAACGGCCACGAGTTCGAGA
TCGAGGGCGAGGGCGAGGGCCGCCCCTACGAGGGCACCCAGACCGCCAAGCTGAAGGTGACCAAGGGT

GGCCCCCTGCCCTTCGCCTGGGACATCCTGTCCCCTCAGTTCATGTACGGCTCCAAGGCCTACGTGAA
GCACCCCGCCGACATCCCCGACTACTTGAAGCTGTCCTTCCCCGAGGGCTTCAAGTGGGAGCGCGTGA
TGAACTTCGAGGACGGCGGCGTGGTGACCGTGACCCAGGACTCCTCCCTGCAGGACGGCGAGTTCATC
TACAAGGTGAAGCTGCGCGGCACCAACTTCCCCTCCGACGGCCCCGTAATGCAGAAGAAGACCATGGG
CTGGGAGGCCTCCTCCGAGCGGATGTACCCCGAGGACGGCGCCCTGAAGGGCGAGATCAAGCAGAGGC
TGAAGCTGAAGGACGGCGGCCACTACGACGCTGAGGTCAAGACCACCTACAAGGCCAAGAAGCCCGTG
CAGCTGCCCGGCGCCTACAACGTCAACATCAAGTTGGACATCACCTCCCACAACGAGGACTACACCAT
CGTGGAACAGTACGAACGCGCCGAGGGCCGCCACTCCACCGGCGGCATGGACGAGCTGTACAAGCCGG
TCACCGGTTAATTCTAGAATCGATGTAGGAGGTACTAAGCCGGTCATCATCACCATCACCATTGAGTT
TAAACCCGCTGATCAGCCTCGACTGTGCCTTCTAGTTGCCAGCCATCTGTTGTTTGCCCCTCCCCCGT
GCCTTCCTTGACCCTGGAAGGTGCCACTCCCACTGTCCTTTCCTAATAAAATGAGGAAATTGCATCGC
ATTGTCTGAGTAGGTGTCATTCTATTCTGGGGGGTGGGGTGGGGCAGGACAGCAAGGGGGAGGATTGG
GAAGACAATAGCAGGCATGCTGGGGATGCGGTGGGCTCTATGGCGTGTGTCAGTTAGGGTGTGGAAAG
TCCCCAGGCTCCCCAGCAGGCAGAAGTATGCAAAGCATGCATCTCAATTAGTCAGCAACCAGGTGTGG
AAAGTCCCCAGGCTCCCCAGCAGGCAGAAGTATGCAAAGCATGCATCTCAATTAGTCAGCAACCATAG
TCCCGCCCCTAACTCCGCCCATCCCGCCCCTAACTCCGCCCAGTTCCGCCCATTCTCCGCCCCATGGC
TGACTAATTTTTTTTATTTATGCAGAGGCCGAGGCCGCCTCTGCCTCTGAGCTATTCCAGAAGTAGTG
AGGAGGCTTTTTTGGAGGCCTAGGCTTTTGCAAAAAGCTCCCATGACCGAGTACAAGCCCACGGTGCG
CCTCGCCACCCGCGACGACGTCCCCAGGGCCGTACGCACCCTCGCCGCCGCGTTCGCCGACTACCCCG
CCACGCGCCACACCGTCGATCCGGACCGCCACATCGAGCGGGTCACCGAGCTGCAAGAACTCTTCCTC
ACGCGCGTCGGGCTCGACATCGGCAAGGTGTGGGTCGCGGACGACGGCGCCGCGGTGGCGGTCTGGAC
CACGCCGGAGAGCGTCGAAGCGGGGGCGGTGTTCGCCGAGATCGGCCCGCGCATGGCCGAGTTGAGCG
GTTCCCGGCTGGCCGCGCAGCAACAGATGGAAGGCCTCCTGGCGCCGCACCGGCCCAAGGAGCCCGCG
TGGTTCCTGGCCACCGTCGGCGTCTCGCCCGACCACCAGGGCAAGGGTCTGGGCAGCGCCGTCGTGCT
CCCCGGAGTGGAGGCGGCCGAGCGCGCCGGGGTGCCCGCCTTCCTGGAGACCTCCGCGCCCCGCAACC
TCCCCTTCTACGAGCGGCTCGGCTTCACCGTCACCGCCGACGTCGAGGTGCCCGAAGGACCGCGCACC
TGGTGCATGACCCGCAAGCCCGGTGCCTGAGCGGGACTCTGGGGTTCGAAATGACCGACCAAGCGACG
CCCGAAATGACCGACCAAGCGACGCCCAACCTGCCATCACGAGATTTCGATTCCACCGCCGCCTTCTA
TGAAAGGTTGGGCTTCGGAATCGTTTTCCGGGACGCCGGCTGGATGATCCTCCAGCGCGGGGATCTCA
TGCTGGAGTTCTTCGCCCACCCCAACTTGTTTATTGCAGCTTATAATGGTTACAAATAAAGCAATAGC
ATCACAAATTTCACAAATAAAGCATTTTTTTCACTGCATTCTAGTTGTGGTTTGTCCAAACTCATCAA
TGTATCTTATCATGTCTGTATACCGTCGACCTCTAGCTAGTCGAGTTAATTAACGAGAGCATAATATT
GATATGTGCCAAAGTTGTTTCTGACTGACTAATAAGTATAATTTGTTTCTATTATGTATAGGTTAAGC
TAATTACTTATTTTATAATACAACATGACTGTTTTTAAAGTACAAAATAAGTTTATTTTTGTAAAAGA
GAGAATGTTTAAAAGTTTTGTTACTTTATAGAAGAAATTTTGAGTTTTTGTTTTTTTTTAATAAATAA
ATAAACATAAATAAATTGTTTGTTGAATTTATTATTAGTATGTAAGTGTAAATATAATAAAACTTAAT
ATCTATTCAAATTAATAAATAAACCTCGATATACAGACCGATAAAACACATGCGTCAATTTTACGCAT
GATTATCTTTAACGTACGTCACAATATGATTATCTTTCTAGGGTTAAATAATAGTTTCTAATTTTTTT
ATTATTCAGCCTGCTGTCGTGAATACCGAGCTCCAATTCGCCCTATAGTGAGTCGTATTACAATTCAC
TGGCCGTCGTTTTACAACGTCGTGACTGGGAAAACCCTGGCGTTACCCAACTTAATCGCCTTGCAGCA
CATCCCCCTTTCGCCAGCTGGCGTAATAGCGAAGAGGCCCGCACCGATCGCCCTTCCCAACAGTTGCG
CAGCCTGAATGGCGAATGGCGCGACGCGCCCTGTAGCGGCGCATTAAGCGCGGCGGGTGTGGTGGTTA
CGCGCAGCGTGACCGCTACACTTGCCAGCGCCCTAGCGCCCGCTCCTTTCGCTTTCTTCCCTTCCTTT
CTCGCCACGTTCGCCGGCTTTCCCCGTCAAGCTCTAAATCGGGGGCTCCCTTTAGGGTTCCGATTTAG
TGCTTTACGGCACCTCGACCCCAAAAAACTTGATTAGGGTGATGGTTCACGTAGTGGGCCATCGCCCT
GATAGACGGTTTTTCGCCCTTTGACGTTGGAGTCCACGTTCTTTAATAGTGGACTCTTGTTCCAAACT
GGAACAACACTCAACCCTATCTCGGTCTATTCTTTTGATTTATAAGGGATTTTGCCGATTTCGGCCTA
TTGGTTAAAAAATGAGCTGATTTAACAAAAATTTAACGCGAATTTTAACAAAATATTAACGTTTACAA
TTTCC

Xlone-Puro_SNAP-CLIP-display

ATCACCTCGAGTTTACTCCCTATCAGTGATAGAGAACGTATGAAGAGTTTACTCCCTATCAGTGATAG
AGAACGTATGCAGACTTTACTCCCTATCAGTGATAGAGAACGTATAAGGAGTTTACTCCCTATCAGTG
ATAGAGAACGTATGACCAGTTTACTCCCTATCAGTGATAGAGAACGTATCTACAGTTTACTCCCTATC
AGTGATAGAGAACGTATATCCAGTTTACTCCCTATCAGTGATAGAGAACGTATAAGCTTTGCTTATGT
AAACCAGGGCGCCTATAAAAGAGTGCTGATTTTTTGAGTAAACTTCAATTCCACAACACTTTTGTCTT
ATACCAACTTTCCGTACCACTTCCTACCCTCGTAAAGGTACCGAGCTCGGATCCACTAGTAACGGCCG
CCAGTGTGCTGGAATTCGGCTTGGGGATATCCACCATGGAGACAGACACACTCCTGCTATGGGTACTG
CTGCTCTGGGTTCCAGGTTCCACTGGTGACTATCCATATGATGTTCCAGATTATGCTGGGGCCCAGCC
GGCCAGATCTATGGATAAAGACTGCGAAATGAAACGCACTACCCTGGACAGCCCGCTGGGTAAACTGG
AACTGAGCGGTTGCGAGCAGGGCCTGCACGAAATCATTTTCCTGGGCAAAGGTACGAGCGCTGCGGAT
GCGGTCGAAGTACCGGCTCCGGCTGCGGTTCTGGGTGGCCCGGAGCCGCTGATGCAGGCTACCGCATG
GCTGAACGCATATTTTCACCAGCCAGAGGCGATTGAAGAGTTCCCTGTACCGGCCCTGCATCACCCGG
TATTTCAGCAGGAATCCTTTACCCGTCAGGTACTGTGGAAACTGCTGAAAGTAGTGAAATTCGGCGAG
GTGATCTCCTATTCCCATCTGGCGGCGCTGGCTGGCAACCCAGCGGCAACTGCGGCGGTGAAAACCGC
TCTGTCTGGTAATCCGGTGCCAATTCTGATCCCGTGCCACCGTGTGGTTCAGGGCGACCTGGACGTAG
GTGGCTACGAAGGCGGCCTGGCTGTGAAAGAATGGCTGCTGGCGCACGAAGGTCACCGTCTGGGTAAA
CCAGGCCTGGGCGGCCGCCTGGAAGTTCTGTTCCAGGGCCCGAAAGCTTTCCTCGAGATGGACAAGGA
TTGTGAGATGAAGCGTACCACTCTGGATTCTCCACTGGGCAAGCTGGAGCTGTCTGGCTGTGAACAAG
GTCTGCATGAGATTATCTTTCTGGGTAAGGGCACCTCCGCGGCGGATGCTGTTGAGGTTCCAGCGCCA
GCGGCTGTGCTGGGCGGTCCAGAACCACTGATCCAAGCGACTGCGTGGCTGAATGCGTACTTCCATCA
ACCGGAAGCTATCGAGGAATTTCCGGTTCCAGCGCTGCACCATCCAGTTTTCCAACAAGAGAGCTTCA
CTCGCCAAGTTCTGTGGAAGCTGCTGAAGGTTGTTAAGTTTGGTGAAGTTATTAGCGAGAGCCACCTG
GCTGCTCTGGTTGGTAATCCGGCTGCGACCGCTGCTGTTAACACTGCGCTGGACGGCAACCCAGTTCC
GATCCTGATTCCATGTCATCGCGTTGTGCAAGGTGATTCCGATGTTGGCCCATATCTGGGTGGTCTGG
CGGTTAAGGAGTGGCTGCTGGCTCATGAGGGCCATCGCCTGGGCAAGCCGGGTCTGGGTGGAGCTCTG
GCCGGAGGCATGTCCCATCACTGGGGGTACGGCAAACACAACGGACCTGAGCACTGGCATAAGGACTT
CCCCATTGCCAAGGGAGAGCGCCAGTCCCCTGTTGACATCGACACTCATACAGCCAAGTATGACCCTT
CCCTGAAGCCCCTGTCTGTTTCCTATGATCAAGCAACTTCCCTGAGGATCCTCAACAATGGTCATGCT
TTCAACGTGGAGTTTGATGACTCTCAGGACAAAGCAGTGCTCAAGGGAGGACCCCTGGATGGCACTTA
CAGATTGATTCAGTTTCACTTTCACTGGGGTTCACTTGATGGACAAGGTTCAGAGCATACTGTGGATA
AAAAGAAATATGCTGCAGAACTTCACTTGGTTCACTGGAACACCAAATATGGGGATTTTGGGAAAGCT
GTGCAGCAACCTGATGGACTGGCCGTTCTAGGTATTTTTTTGAAGGTTGGCAGCGCTAAACCGGGCCT
TCAGAAAGTTGTTGACGTGCTGGATTCCATTAAAACAAAGGGCAAGAGTGCTGACTTCACTAACTTCG
ATCCTCGTGGCCTCCTTCCTGAATCCCTGGATTACTGGACCTACCCAGGCTCACTGACCACCCCTCCT
CTTCTGGAATGTGTGACCTGGATTGTGCTCAAGGAACCCATCAGCGTCAGCAGCGAGCAGGTGTTGAA
ATTCCGTAAACTTAACTTCAATGGGGAGGGTGAACCCGAAGAACTGATGGTGGACAACTGGCGCCCAG
CTCAGCCACTGAAGAACAGGCAAATCAAAGCTTCCTTCAAAGTCGACGAACAAAAACTCATCTCAGAA
GAGGATCTGAATGCTGTGGGCCAGGACACGCAGGAGGTCATCGTGGTGCCACACTCCTTGCCCTTTAA
GGTGGTGGTGATCTCAGCCATCCTGGCCCTGGTGGTGCTCACCATCATCTCCCTTATCATCCTCATCA
TGCTTTGGCAGAAGAAGCCACGTTAGTCTAGTAGACCACCTCCCCTGCGAGCTAAGCTGGACAGCCAA
TGACGGGTAAGAGAGTGACATTTTTCACTAACCTAAGACAGGAGGGCCGTCAGAGCTACTGCCTAATC
CAAAGACGGGTAAAAGTGATAAAAATGTATCACTCCAACCTAAGACAGGCGCAGCTTCCGAGGGATTT
GAGATCCAGACATGATAAGATACATTGATGAGTTTGGACAAACCAAAACTAGAATGCAGTGAAAAAAA
TGCCTTATTTGTGAAATTTGTGATGCTATTGCCTTATTTGTAACCATTATAAGCTGCAATAAACAAGT
TTGATATCTATAACAAGAAAATATATATATAATAAGTTATCACGTAAGTAGAACATGAAATAACAATA
TAATTATCGTATGAGTTAAATCTTAAAAGTCACGTAAAAGATAATCATGCGTCATTTTGACTCACGCG
GTCGTTATAGTTCAAAATCAGTGACACTTACCGCATTGACAAGCACGCCTCACGGGAGCTCCAAGCGG
CGACTGAGATGTCCTAAATGCACAGCGACGGATTCGCGCTATTTAGAAAGAGAGAGCAATATTTCAAG
AATGCATGCGTCAATTTTACGCAGACTATCTTTCTAGGGTTAAGAATTCACTGGCCGTCGTTTTACAA
CGTCGTGACTGGGAAAACCCTGGCGTTACCCAACTTAATCGCCTTGCAGCACATCCCCCTTTCGCCAG
CTGGCGTAATAGCGAAGAGGCCCGCACCGATCGCCCTTCCCAACAGTTGCGCAGCCTGAATGGCGAAT
GGCGCCTGATGCGGTATTTTCTCCTTACGCATCTGTGCGGTATTTCACACCGCATATGGTGCACTCTC

60

AGTACAATCTGCTCTGATGCCGCATAGTTAAGCCAGCCCCGACACCCGCCAACACCCGCTGACGCGCC
CTGACGGGCTTGTCTGCTCCCGGCATCCGCTTACAGACAAGCTGTGACCGTCTCCGGGAGCTGCATGT
GTCAGAGGTTTTCACCGTCATCACCGAAACGCGCGAGACGAAAGGGCCTCGTGATACGCCTATTTTTA
TAGGTTAATGTCATGATAATAATGGTTTCTTAGACGTCAGGTGGCACTTTTCGGGGAAATGTGCGCGG
AACCCCTATTTGTTTATTTTTCTAAATACATTCAAATATGTATCCGCTCATGAGACAATAACCCTGAT
AAATGCTTCAATAATATTGAAAAAGGAAGAGTATGAGTATTCAACATTTCCGTGTCGCCCTTATTCCC
TTTTTTGCGGCATTTTGCCTTCCTGTTTTTGCTCACCCAGAAACGCTGGTGAAAGTAAAAGATGCTGA
AGATCAGTTGGGTGCACGAGTGGGTTACATCGAACTGGATCTCAACAGCGGTAAGATCCTTGAGAGTT
TTCGCCCCGAAGAACGTTTTCCAATGATGAGCACTTTTAAAGTTCTGCTATGTGGCGCGGTATTATCC
CGTATTGACGCCGGGCAAGAGCAACTCGGTCGCCGCATACACTATTCTCAGAATGACTTGGTTGAGTA
CTCACCAGTCACAGAAAAGCATCTTACGGATGGCATGACAGTAAGAGAATTATGCAGTGCTGCCATAA
CCATGAGTGATAACACTGCGGCCAACTTACTTCTGACAACGATCGGAGGACCGAAGGAGCTAACCGCT
TTTTTGCACAACATGGGGGATCATGTAACTCGCCTTGATCGTTGGGAACCGGAGCTGAATGAAGCCAT
ACCAAACGACGAGCGTGACACCACGATGCCTGTAGCAATGGCAACAACGTTGCGCAAACTATTAACTG
GCGAACTACTTACTCTAGCTTCCCGGCAACAATTAATAGACTGGATGGAGGCGGATAAAGTTGCAGGA
CCACTTCTGCGCTCGGCCCTTCCGGCTGGCTGGTTTATTGCTGATAAATCTGGAGCCGGTGAGCGTGG
GTCTCGCGGTATCATTGCAGCACTGGGGCCAGATGGTAAGCCCTCCCGTATCGTAGTTATCTACACGA
CGGGGAGTCAGGCAACTATGGATGAACGAAATAGACAGATCGCTGAGATAGGTGCCTCACTGATTAAG
CATTGGTAACTGTCAGACCAAGTTTACTCATATATACTTTAGATTGATTTAAAACTTCATTTTTAATT
TAAAAGGATCTAGGTGAAGATCCTTTTTGATAATCTCATGACCAAAATCCCTTAACGTGAGTTTTCGT
TCCACTGAGCGTCAGACCCCGTAGAAAAGATCAAAGGATCTTCTTGAGATCCTTTTTTTCTGCGCGTA
ATCTGCTGCTTGCAAACAAAAAAACCACCGCTACCAGCGGTGGTTTGTTTGCCGGATCAAGAGCTACC
AACTCTTTTTCCGAAGGTAACTGGCTTCAGCAGAGCGCAGATACCAAATACTGTTCTTCTAGTGTAGC
CGTAGTTAGGCCACCACTTCAAGAACTCTGTAGCACCGCCTACATACCTCGCTCTGCTAATCCTGTTA
CCAGTGGCTGCTGCCAGTGGCGATAAGTCGTGTCTTACCGGGTTGGACTCAAGACGATAGTTACCGGA
TAAGGCGCAGCGGTCGGGCTGAACGGGGGGTTCGTGCACACAGCCCAGCTTGGAGCGAACGACCTACA
CCGAACTGAGATACCTACAGCGTGAGCTATGAGAAAGCGCCACGCTTCCCGAAGGGAGAAAGGCGGAC
AGGTATCCGGTAAGCGGCAGGGTCGGAACAGGAGAGCGCACGAGGGAGCTTCCAGGGGGAAACGCCTG
GTATCTTTATAGTCCTGTCGGGTTTCGCCACCTCTGACTTGAGCGTCGATTTTTGTGATGCTCGTCAG
GGGGGCGGAGCCTATGGAAAAACGCCAGCAACGCGGCCTTTTTACGGTTCCTGGCCTTTTGCTGGCCT
TTTGCTCACATGTTCTTTCCTGCGTTATCCCCTGATTCTGTGGATAACCGTATTACCGCCTTTGAGTG
AGCTGATACCGCTCGCCGCAGCCGAACGACCGAGCGCAGCGAGTCAGTGAGCGAGGAAGCGGAAGAGC
GCCCAATACGCAAACCGCCTCTCCCCGCGCGTTGGCCGATTCATTAATGCAGCTGGCACGACAGGTTT
CCCGACTGGAAAGCGGGCAGTGAGCGCAACGCAATTAATGTGAGTTAGCTCACTCATTAGGCACCCCA
GGCTTTACACTTTATGCTTCCGGCTCGTATGTTGTGTGGAATTGTGAGCGGATAACAATTTCACACAG
GAAACAGCTATGACCATGATTACGCCAAGGTCGACTTAACCCTAGAAAGATAATCATATTGTGACGTA
CGTTAAAGATAATCATGCGTAAAATTGACGCATGTGTTTTATCGGTCTGTATATCGAGGTTTATTTAT
TAATTTGAATAGATATTAAGTTTTATTATATTTACACTTACATACTAATAATAAATTCAACAAACAAT
TTATTTATGTTTATTTATTTATTAAAAAAAAACAAAAACTCAAAATTTCTTCTATAAAGTAACAAAAC
TTTTAGCAGTGAAAAAAATGCTTTATTTGTGAAATTTGTGATGCTATTGCTTTATTTGTAACCATTAT
AAGCTGCAATAAACAAGTTAACAACAACAATTGCATTCATTTTATGTTTCAGGTTCAGGGGGAGGTGT
GGGAGGTTTTTTAAAGCAAGTAAAACCTCTACAAATGTGGTATGGCTGATTATGATCCTCTGGAGATC
CTAGGCTAGGCACCGGGCTTGCGGGTCATGCACCAGGTGCGCGGTCCTTCGGGCACCTCGACGTCGGC
GGTGACGGTGAAGCCGAGCCGCTCGTAGAAGGGGAGGTTGCGGGGCGCGGAGGTCTCCAGGAAGGCGG
GCACCCCGGCGCGCTCGGCCGCCTCCACTCCGGGGAGCACGACGGCGCTGCCCAGACCCTTGCCCTGG
TGGTCGGGCGAGACGCCGACGGTGGCCAGGAACCACGCGGGCTCCTTGGGCCGGTGCGGCGCCAGGAG
GCCTTCCATCTGTTGCTGCGCGGCCAGCCGGGAACCGCTCAACTCGGCCATGCGCGGGCCGATCTCGG
CGAACACCGCCCCCGCTTCGACGCTCTCCGGCGTGGTCCAGACCGCCACCGCGGCGCCGTCGTCCGCG
ACCCACACCTTGCCGATGTCGAGCCCGACGCGCGTGAGGAAGAGTTCTTGCAGCTCGGTGACCCGCTC
GATGTGGCGGTCCGGATCGACGGTGTGGCGCGTGGCGGGGTAGTCGGCGAACGCGGCGGCGAGGGTGC
GTACGGCCCTGGGGACGTCGTCGCGGGTGGCGAGGCGCACCGTGGGCTTGTACTCGGTCATGGGGCCG
GGGTTCTCCTCCACGTCGCCGGCCTGCTTCAGCAGGCTGAAGTTGGTGGCGCCGCTGCCCCCGGGGAG
CATGTCAAGGTCAAAATCGTCAAGAGCGTCAGCAGGCAGCATATCAAGGTCAAAGTCGTCAAGGGCAT
CGGCTGGGAGCATGTCTAAGTCAAAATCGTCAAGGGCGTCGGTCGGCCCGCCGCTTTCGCACTTTAGC

61

TGTTTCTCCAGGCCACATATGATTAGTTCCAGGCCGAAAAGGAAGGCAGGTTCGGCTCCCTGCCGGTC
GAACAGCTCAATTGCTTGTTTCAGAAGTGGGGGCATAGAATCGGTGGTAGGTGTCTCTCTTTCCTCTT
TTGCTACTTGATGCTCCTGTTCCTCCAATACGCAGCCCAGTGTAAAGTGGCCCACGGCGGACAGAGCG
TACAGTGCGTTCTCCAGGGAGAAGCCTTGCTGACACAGGAACGCGAGCTGATTTTCCAGGGTTTCGTA
CTGTTTCTCTGTTGGGCGGGTGCCGAGATGCACTTTAGCCCCGTCGCGATGTGAGAGGAGAGCACAGC
GGTATGACTTGGCGTTGTTCCGCAGAAAGTCTTGCCATGACTCGCCTTCCAGGGGGCAGGAGTGGGTA
TGATGCCTGTCCAGCATCTCGATTGGCAGGGCATCGAGCAGGGCCCGCTTGTTCTTCACGTGCCAGTA
CAGGGTAGGCTGCTCAACTCCCAGCTTTTGAGCGAGTTTCCTTGTCGTCAGGCCTTCGATACCGACTC
CATTGAGTAATTCCAGAGCAGAGTTTATGACTTTGCTCTTGTCCAGTCTAGACATCTTATCGTCATCG
TCTTTGTAATCCATGGTGGCGGATCCCGCGTCACGACACCTGTGTTCTGGCGGCAAACCCGTTGCGAA
AAAGAACGTTCACGGCGACTACTGCACTTATATACGGTTCTCCCCCACCCTCGGGAAAAAGGCGGAGC
CAGTACACGACATCACTTTCCCAGTTTACCCCGCGCCACCTTCTCTAGGCACCGGTTCAATTGCCGAC
CCCTCCCCCCAACTTCTCGGGGACTGTGGGCGATGTGCGCTCTGCCCACTGACGGGCACCGGAGCCAC
TCGAGTGGAATT

pcDNA3.1_mBP

GACGGATCGGGAGATCTCCCGATCCCCTATGGTGCACTCTCAGTACAATCTGCTCTGATGCCGCATAG
TTAAGCCAGTATCTGCTCCCTGCTTGTGTGTTGGAGGTCGCTGAGTAGTGCGCGAGCAAAATTTAAGC
TACAACAAGGCAAGGCTTGACCGACAATTGCATGAAGAATCTGCTTAGGGTTAGGCGTTTTGCGCTGC
TTCGCGATGTACGGGCCAGATATACGCGTTGACATTGATTATTGACTAGTGATTATTGAGCCATAGAA
TTCGAGCTTGCATGCCTGCAGGTCGTTACATAACTTACGGTAAATGGCCCGCCTGGCTGACCGCCCAA
CGACCCCCGCCCATTGACGTCAATAATGACGTATGTTCCCATAGTAACGCCAATAGGGACTTTCCATT
GACGTCAATGGGTGGAGTATTTACGGTAAACTGCCCACTTGGCAGTACATCAAGTGTATCATATGCCA
AGTACGCCCCCTATTGACGTCAATGACGGTAAATGGCCCGCCTGGCATTATGCCCAGTACATGACCTT
ATGGGACTTTCCTACTTGGCAGTACATCTACGTATTAGTCATCGCTATTACCATGGTGATGCGGTTTT
GGCAGTACATCAATGGGCGTGGATAGCGGTTTGACTCACGGGGATTTCCAAGTCTCCACCCCATTGAC
GTCAATGGGAGTTTGTTTTGGCACCAAAATCAACGGGACTTTCCAAAATGTCGTAACAACTCCGCCCC
ATTGACGCAAATGGGCGGTAGGCGTGTACGGTGGGAGGTCTATATAAGCAGAGCTCGTTTAGTGAACC
GTCAGATCGCCTGGAGACGCCATCCACGCTGTTTTGACCTCCATAGAAGACACCGGGACCGATCCAGC
CTCCGGACTCTAGAGGATCCGGTACTCGAGGAACTGAAAAACCAGAAAGTTAACTGGTAAGTTTAGTC
TTTTTGTCTTTTATTTCAGGTCCCGGATCCGGTGGTGGTGCAAATCAAAGAACTGCTCCTCAGTGGAT
GTTGCCTTTACTTCTAGGCCTGTACGGAAGTGTTACTTCTGCTCTAAAAGCTGCGGAATTGTACCCAA
TTCGTTAAGGCCAAATTGGCCACCATGGGCTCTAGCCTGGACGACGAGCACATCCTGAGCGCCCTGCT
GCAGAGCGACGACGAACTGGTGGGCGAGGACAGCGACAGCGAGGTCAGCGACCACGTGTCCGAGGACG
ACGTGCAGTCCGACACCGAGGAAGCCTTCATCGACGAGGTGCACGAAGTGCAGCCTACCAGCAGCGGC
TCCGAGATCCTGGACGAGCAGAACGTGATCGAGCAGCCTGGCAGCTCCCTGGCCAGCAACAGAATCCT
GACCCTGCCCCAGAGAACCATCAGAGGCAAGAACAAGCACTGCTGGTCCACCTCCAAGAGCACCAGGC
GGAGCAGAGTGTCCGCCCTGAACATCGTGCGGAGCCAGAGGGGCCCCACCAGAATGTGCAGAAACATC
TACGACCCCCTGCTGTGCTTCAAGCTGTTCTTCACCGACGAGATCATCAGCGAGATCGTGAAGTGGAC
CAACGCCGAGATCAGCCTGAAGAGGCGGGAGAGCATGACCAGCGCCACCTTCAGAGACACCAACGAGG
ACGAGATCTACGCCTTCTTCGGCATCCTGGTGATGACCGCCGTGAGAAAGGACAACCACATGAGCACC
GACGACCTGTTCGACAGATCCCTGAGCATGGTGTACGTGTCCGTGATGAGCAGAGACAGATTCGACTT
CCTGATCAGATGCCTGAGAATGGACGACAAGAGCATCAGACCCACCCTGCGGGAGAACGACGTGTTCA
CCCCCGTGCGGAAGATCTGGGACCTGTTCATCCACCAGTGCATCCAGAACTACACCCCTGGCGCCCAC
CTGACCATCGATGAGCAGCTGCTGGGCTTCAGAGGCAGATGCCCCTTCAGAGTGTACATCCCCAACAA
GCCCAGCAAGTACGGCATCAAGATCCTGATGATGTGCGACAGCGGCACCAAGTACATGATCAACGGCA
TGCCCTACCTGGGCAGAGGCACCCAGACAAACGGCGTGCCCCTGGGCGAGTACTACGTGAAAGAACTG
AGCAAGCCTGTGCATGGCAGCTGCAGGAACATCACCTGCGACAACTGGTTCACCAGCATCCCCCTGGC
CAAGAACCTGCTGCAGGAACCCTACAAGCTGACCATCGTGGGCACCGTGCGGAGCAACAAGCGGGAGA
TCCCAGAGGTGCTGAAGAACAGCAGATCCAGACCTGTGGGAACAAGCATGTTCTGCTTCGACGGCCCC
CTGACCCTGGTGTCCTACAAGCCCAAGCCCGCCAAGATGGTGTACCTGCTGTCCAGCTGCGACGAGGA
CGCCAGCATCAACGAGAGCACCGGCAAGCCCCAGATGGTGATGTACTACAACCAGACCAAGGGCGGCG

TGGACACCCTGGACCAGATGTGCAGCGTGATGACCTGCAGCAGAAAGACCAACAGATGGCCCATGGCC
CTGCTGTACGGCATGATCAATATCGCCTGCATCAACAGCTTCATCATCTACAGCCACAACGTGTCCAG
CAAGGGCGAGAAGGTGCAGAGCCGGAAGAAATTCATGCGGAACCTGTACATGAGCCTGACCTCCAGCT
TCATGAGAAAGAGACTGGAAGCCCCCACCCTGAAGAGATACCTGCGGGACAACATCAGCAACATCCTG
CCCAAGGAAGTGCCAGGAACAAGCGACGACAGCACCGAGGAACCCGTGATGAAGAAGAGGACCTACTG
CACCTACTGTCCCAGCAAGATCAGAAGAAAGGCCAACGCCAGCTGCAAGAAATGCAAAAAAGTGATCT
GCCGGGAGCACAACATCGACATGTGCCAGAGCTGTTTCTGAGGCCGTAACGGCCGCCAGAATTGGGGA
TCCAGACATGATAAGATACATTGATGAGTTTGGACAAACCACAACTAGAATGCAGTGAAAAAAATGCT
TTATTTGTGAAATTTGTGATGCTATTGCTTTATTTGTAACCATTATAAGCTGCAATAAACAAGTTAAC
GCGGAAGCTTGGTACCGAGCTCGGATCCACTAGCGGCCGCTCGAGTCTAGAGGGCCCTTCGAACAAAA
ACTCATCTCAGAAGAGGATCTGAATATGCATACCGGTCATCATCACCATCACCATTGAGTTTAAACCC
GCTGATCAGCCTCGACTGTGCCTTCTAGTTGCCAGCCATCTGTTGTTTGCCCCTCCCCCGTGCCTTCC
TTGACCCTGGAAGGTGCCACTCCCACTGTCCTTTCCTAATAAAATGAGGAAATTGCATCGCATTGTCT
GAGTAGGTGTCATTCTATTCTGGGGGGTGGGGTGGGGCAGGACAGCAAGGGGGAGGATTGGGAAGACA
ATAGCAGGCATGCTGGGGATGCGGTGGGCTCTATGGCTTCTGAGGCGGAAAGAACCAGCTGGGGCTCT
AGGGGGTATCCCCACGCGCCCTGTAGCGGCGCATTAAGCGCGGCGGGTGTGGTGGTTACGCGCAGCGT
GACCGCTACACTTGCCAGCGCCCTAGCGCCCGCTCCTTTCGCTTTCTTCCCTTCCTTTCTCGCCACGT
TCGCCGGCTTTCCCCGTCAAGCTCTAAATCGGGGGCTCCCTTTAGGGTTCCGATTTAGTGCTTTACGG
CACCTCGACCCCAAAAAACTTGATTAGGGTGATGGTTCACGTAGTGGGCCATCGCCCTGATAGACGGT
TTTTCGCCCTTTGACGTTGGAGTCCACGTTCTTTAATAGTGGACTCTTGTTCCAAACTGGAACAACAC
TCAACCCTATCTCGGTCTATTCTTTTGATTTATAAGGGATTTTGCCGATTTCGGCCTATTGGTTAAAA
AATGAGCTGATTTAACAAAAATTTAACGCGAATTAATTCTGTGGAATGTGTGTCAGTTAGGGTGTGGA
AAGTCCCCAGGCTCCCCAGCAGGCAGAAGTATGCAAAGCATGCATCTCAATTAGTCAGCAACCAGGTG
TGGAAAGTCCCCAGGCTCCCCAGCAGGCAGAAGTATGCAAAGCATGCATCTCAATTAGTCAGCAACCA
TAGTCCCGCCCCTAACTCCGCCCATCCCGCCCCTAACTCCGCCCAGTTCCGCCCATTCTCCGCCCCAT
GGCTGACTAATTTTTTTTATTTATGCAGAGGCCGAGGCCGCCTCTGCCTCTGAGCTATTCCAGAAGTA
GTGAGGAGGCTTTTTTGGAGGCCTAGGCTTTTGCAAAAAGCTCCCGGGAGCTTGTATATCCATTTTCG
GATCTGATCAAGAGACAGGATGAGGATCGTTTCGCATGATTGAACAAGATGGATTGCACGCAGGTTCT
CCGGCCGCTTGGGTGGAGAGGCTATTCGGCTATGACTGGGCACAACAGACAATCGGCTGCTCTGATGC
CGCCGTGTTCCGGCTGTCAGCGCAGGGGCGCCCGGTTCTTTTTGTCAAGACCGACCTGTCCGGTGCCC
TGAATGAACTGCAGGACGAGGCAGCGCGGCTATCGTGGCTGGCCACGACGGGCGTTCCTTGCGCAGCT
GTGCTCGACGTTGTCACTGAAGCGGGAAGGGACTGGCTGCTATTGGGCGAAGTGCCGGGGCAGGATCT
CCTGTCATCTCACCTTGCTCCTGCCGAGAAAGTATCCATCATGGCTGATGCAATGCGGCGGCTGCATA
CGCTTGATCCGGCTACCTGCCCATTCGACCACCAAGCGAAACATCGCATCGAGCGAGCACGTACTCGG
ATGGAAGCCGGTCTTGTCGATCAGGATGATCTGGACGAAGAGCATCAGGGGCTCGCGCCAGCCGAACT
GTTCGCCAGGCTCAAGGCGCGCATGCCCGACGGCGAGGATCTCGTCGTGACCCATGGCGATGCCTGCT
TGCCGAATATCATGGTGGAAAATGGCCGCTTTTCTGGATTCATCGACTGTGGCCGGCTGGGTGTGGCG
GACCGCTATCAGGACATAGCGTTGGCTACCCGTGATATTGCTGAAGAGCTTGGCGGCGAATGGGCTGA
CCGCTTCCTCGTGCTTTACGGTATCGCCGCTCCCGATTCGCAGCGCATCGCCTTCTATCGCCTTCTTG
ACGAGTTCTTCTGAGCGGGACTCTGGGGTTCGAAATGACCGACCAAGCGACGCCCAACCTGCCATCAC
GAGATTTCGATTCCACCGCCGCCTTCTATGAAAGGTTGGGCTTCGGAATCGTTTTCCGGGACGCCGGC
TGGATGATCCTCCAGCGCGGGGATCTCATGCTGGAGTTCTTCGCCCACCCCAACTTGTTTATTGCAGC
TTATAATGGTTACAAATAAAGCAATAGCATCACAAATTTCACAAATAAAGCATTTTTTTCACTGCATT
CTAGTTGTGGTTTGTCCAAACTCATCAATGTATCTTATCATGTCTGTATACCGTCGACCTCTAGCTAG
AGCTTGGCGTAATCATGGTCATAGCTGTTTCCTGTGTGAAATTGTTATCCGCTCACAATTCCACACAA
CATACGAGCCGGAAGCATAAAGTGTAAAGCCTGGGGTGCCTAATGAGTGAGCTAACTCACATTAATTG
CGTTGCGCTCACTGCCCGCTTTCCAGTCGGGAAACCTGTCGTGCCAGCTGCATTAATGAATCGGCCAA
CGCGCGGGGAGAGGCGGTTTGCGTATTGGGCGCTCTTCCGCTTCCTCGCTCACTGACTCGCTGCGCTC
GGTCGTTCGGCTGCGGCGAGCGGTATCAGCTCACTCAAAGGCGGTAATACGGTTATCCACAGAATCAG
GGGATAACGCAGGAAAGAACATGTGAGCAAAAGGCCAGCAAAAGGCCAGGAACCGTAAAAAGGCCGCG
TTGCTGGCGTTTTTCCATAGGCTCCGCCCCCCTGACGAGCATCACAAAAATCGACGCTCAAGTCAGAG
GTGGCGAAACCCGACAGGACTATAAAGATACCAGGCGTTTCCCCCTGGAAGCTCCCTCGTGCGCTCTC
CTGTTCCGACCCTGCCGCTTACCGGATACCTGTCCGCCTTTCTCCCTTCGGGAAGCGTGGCGCTTTCT
CATAGCTCACGCTGTAGGTATCTCAGTTCGGTGTAGGTCGTTCGCTCCAAGCTGGGCTGTGTGCACGA

63

ACCCCCCGTTCAGCCCGACCGCTGCGCCTTATCCGGTAACTATCGTCTTGAGTCCAACCCGGTAAGAC
ACGACTTATCGCCACTGGCAGCAGCCACTGGTAACAGGATTAGCAGAGCGAGGTATGTAGGCGGTGCT
ACAGAGTTCTTGAAGTGGTGGCCTAACTACGGCTACACTAGAAGAACAGTATTTGGTATCTGCGCTCT
GCTGAAGCCAGTTACCTTCGGAAAAAGAGTTGGTAGCTCTTGATCCGGCAAACAAACCACCGCTGGTA
GCGGTTTTTTTGTTTGCAAGCAGCAGATTACGCGCAGAAAAAAAGGATCTCAAGAAGATCCTTTGATC
TTTTCTACGGGGTCTGACGCTCAGTGGAACGAAAACTCACGTTAAGGGATTTTGGTCATGAGATTATC
AAAAAGGATCTTCACCTAGATCCTTTTAAATTAAAAATGAAGTTTTAAATCAATCTAAAGTATATATG
AGTAAACTTGGTCTGACAGTTACCAATGCTTAATCAGTGAGGCACCTATCTCAGCGATCTGTCTATTT
CGTTCATCCATAGTTGCCTGACTCCCCGTCGTGTAGATAACTACGATACGGGAGGGCTTACCATCTGG
CCCCAGTGCTGCAATGATACCGCGAGACCCACGCTCACCGGCTCCAGATTTATCAGCAATAAACCAGC
CAGCCGGAAGGGCCGAGCGCAGAAGTGGTCCTGCAACTTTATCCGCCTCCATCCAGTCTATTAATTGT
TGCCGGGAAGCTAGAGTAAGTAGTTCGCCAGTTAATAGTTTGCGCAACGTTGTTGCCATTGCTACAGG
CATCGTGGTGTCACGCTCGTCGTTTGGTATGGCTTCATTCAGCTCCGGTTCCCAACGATCAAGGCGAG
TTACATGATCCCCCATGTTGTGCAAAAAAGCGGTTAGCTCCTTCGGTCCTCCGATCGTTGTCAGAAGT
AAGTTGGCCGCAGTGTTATCACTCATGGTTATGGCAGCACTGCATAATTCTCTTACTGTCATGCCATC
CGTAAGATGCTTTTCTGTGACTGGTGAGTACTCAACCAAGTCATTCTGAGAATAGTGTATGCGGCGAC
CGAGTTGCTCTTGCCCGGCGTCAATACGGGATAATACCGCGCCACATAGCAGAACTTTAAAAGTGCTC
ATCATTGGAAAACGTTCTTCGGGGCGAAAACTCTCAAGGATCTTACCGCTGTTGAGATCCAGTTCGAT
GTAACCCACTCGTGCACCCAACTGATCTTCAGCATCTTTTACTTTCACCAGCGTTTCTGGGTGAGCAA
AAACAGGAAGGCAAAATGCCGCAAAAAAGGGAATAAGGGCGACACGGAAATGTTGAATACTCATACTC
TTCCTTTTTCAATATTATTGAAGCATTTATCAGGGTTATTGTCTCATGAGCGGATACATATTTGAATG
TATTTAGAAAAATAAACAAATAGGGGTTCCGCGCACATTTCCCCGAAAAGTGCCACCTGACGTC

Exemplary Sanger sequencing traces

Sanger sequencing trace obtained for the PCR product covering the Y701C site in STAT1 upon transfection of 0.5 pmol BG-Y701C and 2 pm NH-T288A guideRNA (compare figure 2d). Bystander-free editing is observed at nucleotide 112 (Y701 site, asterisk).

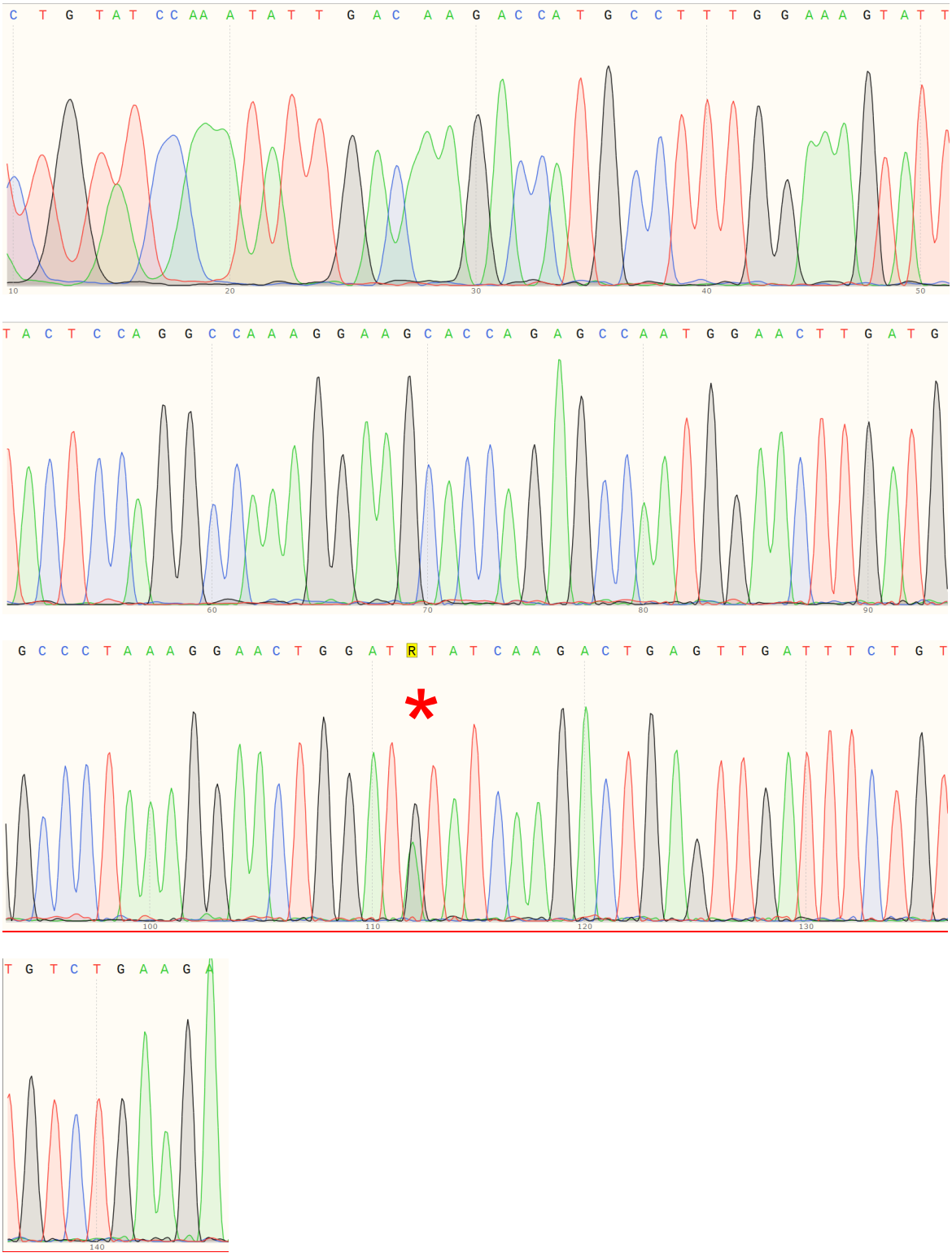

Sanger sequencing trace obtained for the PCR product covering the Y701C site in STAT1 upon transfection of 0.5 pmol NH-Y701C and 2 pm BG-T288A guideRNA (compare figure 2d). No editing is observed at nucleotide 112 (Y701 site, asterisk), as expected.

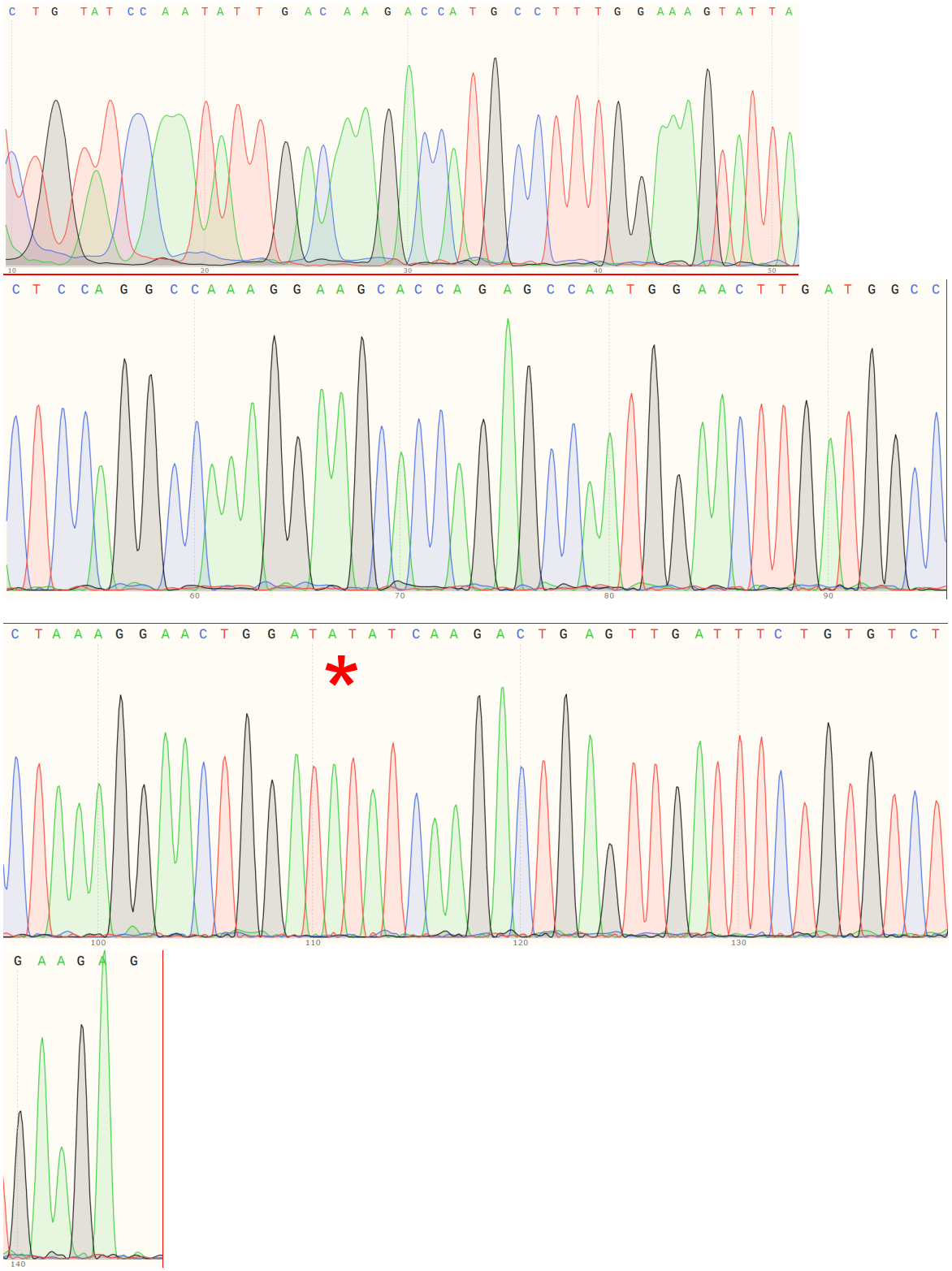

Sanger sequencing trace obtained for the PCR product covering T288A site in STAT1 upon transfection of 0.5 pmol NH-Y701C and 2 pmol BG-T288A guideRNAs (compare figure 2d). Bystander-free editing is observed at nucleotide 171 (T288A site, asterisk).

67


G A A C A T G A C C C T A T C A C A A A A A A C A A A C A A G T G T T A T G G G A C C
180
190
200
210
G C A C C T T C A G T C T T T T C C A G C A G C T C A T T C A G A G C T C G T T T G T
220
230
240
250
260
G G T G G A A A G A C A G C C C T G C A T G C C A A C G C A C C C T C A G A G G C C C
270
280
290
300
G C T G G T C T T G A A G A C A G G G G T C C A G T T C A C T G T G A A G T T G A
N M
310
320
330
340

Sanger sequencing trace obtained for the PCR product covering T288A site in STAT1 upon transfection of 0.5 pmol NH-Y701C and 2 pmol BG-T288A guideRNAs (compare figure 2d). No editing is observed at nucleotide 171 (T288A site, asterisk), as expected.

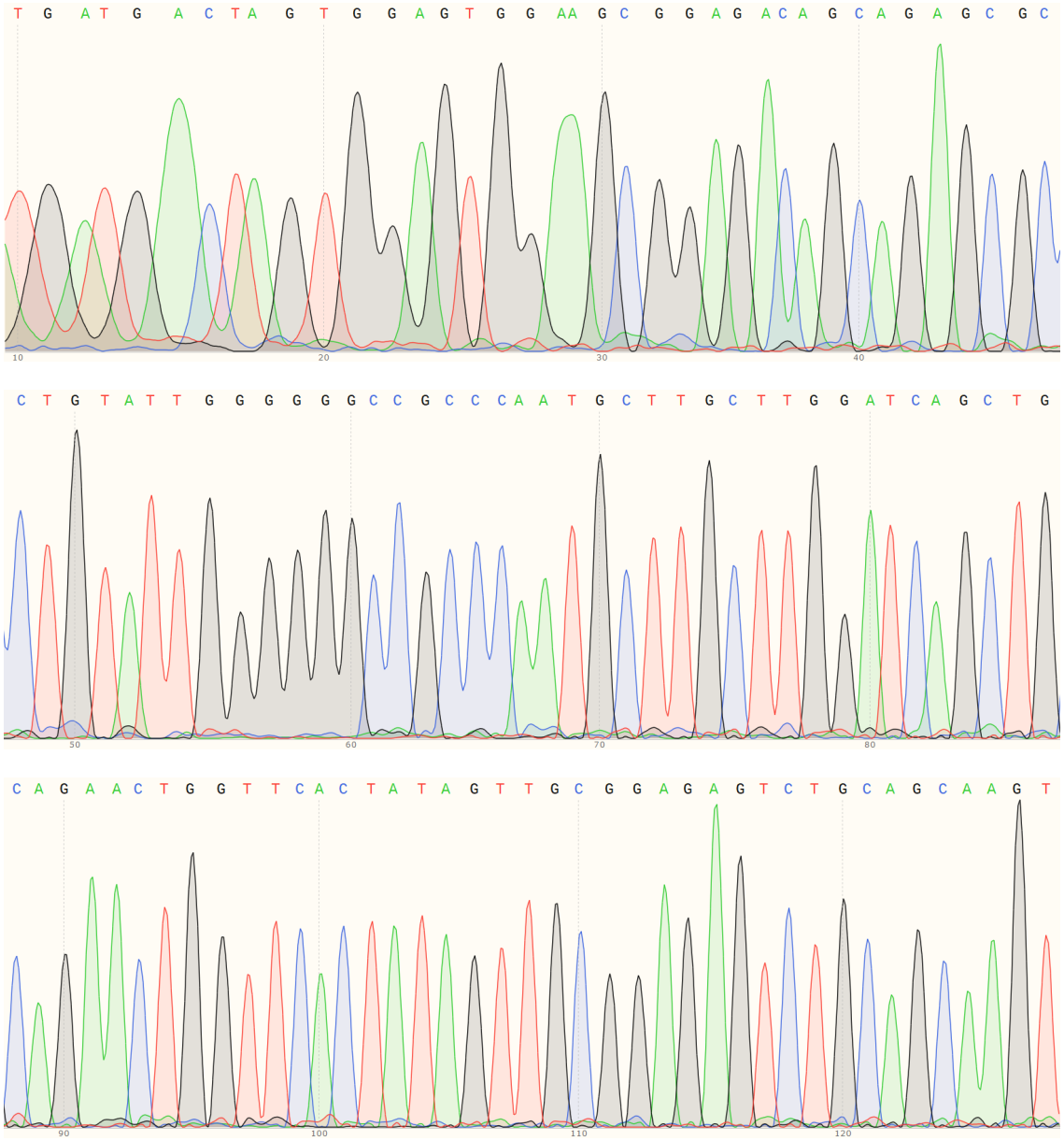

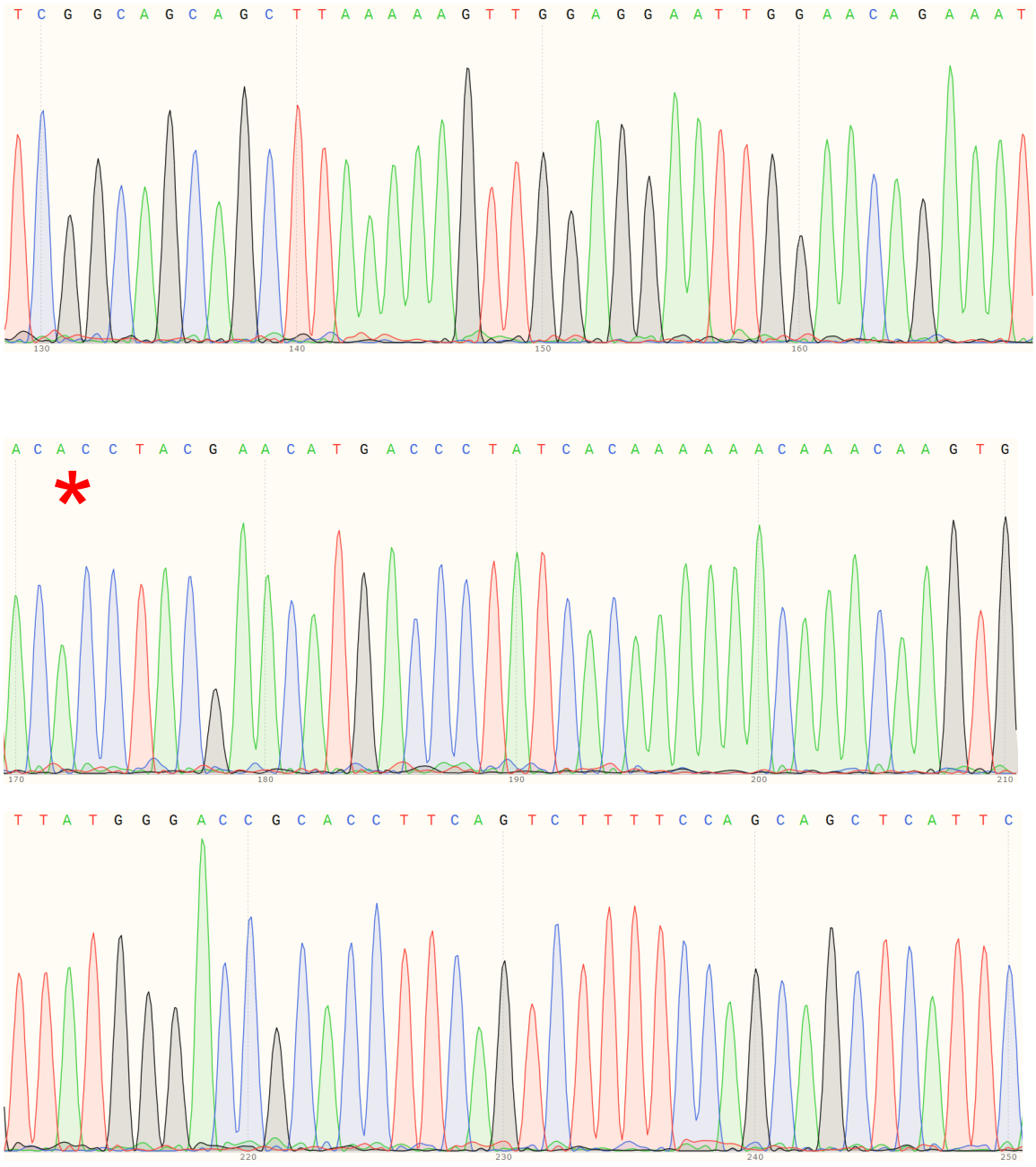
T C G G C A G C A G C T T A A A A A A G T T G G A G G A A T T G G A A C A G A A A T
130
140
150
160
A C A C C T A C G A A C A T G A C C C T A T C A C A A A A A A A C A A A C A A G T G
*
170
180
190
200
210
T T A T G G G A C C G C A C C T T C A G T C T T T T T C C A G C A G C T C A T T C
220
230
240
250

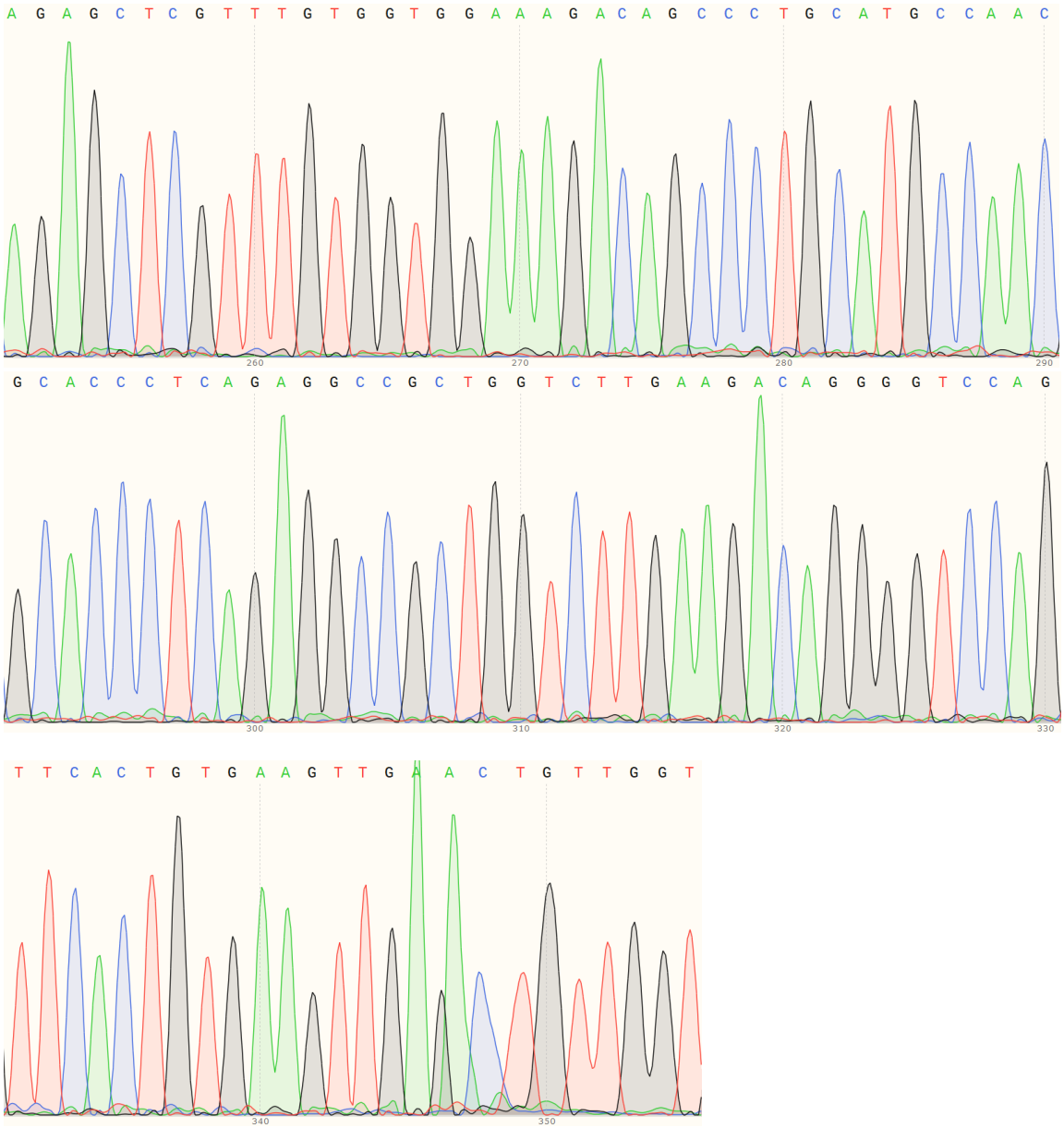
A G A G C T C G T T T G T G G T G G A A A G A C A G C C C T G C A T G C C A A C
260
270
280
290
G C A C C C T C A G A A G G C C G C C T G G T C T T G A A G A C A G G G G T C C A G
300
310
320
330
T T C A C T G T G A A G T T G A A C T G T T G G T
340
350

A.3 Experimental procedures for N-halo

General information regarding chemicals, reaction conditions and analytic methods is given in SI$_{P1}$. For TLC visualization, 0.3 % acidic ethanolic ninhydrin solution and Hanessian's (cerium ammonium molydate) stain were additionally used.

A.3.1 Generation of HALO-His expression plasmid

HALO-His was cloned in a pMG 211 vector via restriction/ligation (NdeI/XhoI, *New England Biolabs*). Prior to restriction, a XhoI site within the HALO-tag was erased by silent mutation of Leu293 by replacing 5'-CTC with the Leu codon most frequently used in *E. coli*, 5'-CTG. A digital version of the plasmid map in Figure 31 containing the full plasmid sequence, including assigned features and restriction sites, can be provided upon request by the Stafforst group.[6]

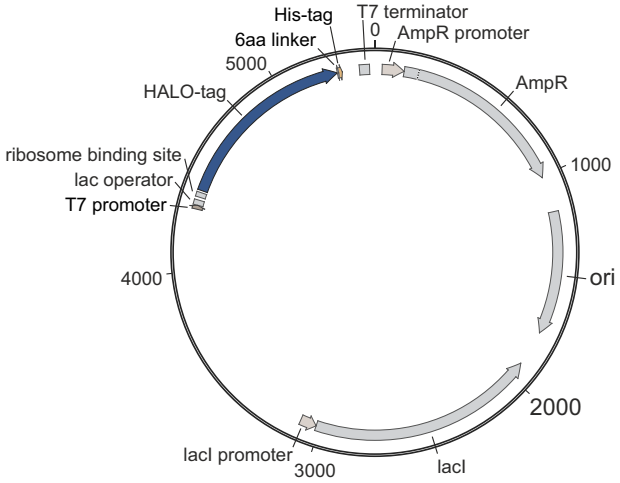

Figure 31. Plamid map of HALO-His in pMG 211.

A.3.2 Synthesis route via reductive amination

Compound 18

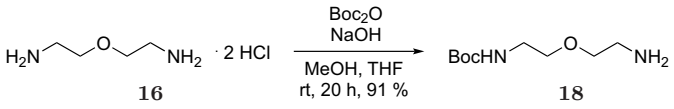

300 mg (7.50 mmol, 3.60 eq) NaOH were dissolved in 45 ml MeOH, 750 mg (4.24 mmol, 2.00 eq) **16** were added and the mixture was stirred at room temperature for 30 min. Subsequently, 450 µl (460 mg, 2.11 mmol, 1.00 eq) Boc_2O in 15 ml THF were added dropwise. After further 20 h at room temperature, the solvents were removed under reduced pressure. The aqueous layer was extracted 3× with DCM and the combined organic layers washed 1× with saturated aqueous NaCl. Removal of solvents under reduced pressure yielded 390 mg (1.91 mmol, 91 %) **18** as a slightly yellow oil, which could be employed without further purification.

[6]Internal plasmid number: pTS 834

R_f (CH:EA, 1:7 + 1 % Et_3N): 0.77.
^{1}H-NMR (300 MHz, MeOD, Figure 32): δ = 1.48 (s, 9 H), 2.82 (t, J = 5.2 Hz, 2 H), 3.27 (t, J = 5.5 Hz, 2 H), 3.49−3.54 (m, 4 H).
^{13}C-NMR (75 MHz, MeOD, Figure 32): δ = 28.9, 41.4, 42.3, 71.1, 73.3, 80.2, 158.7.
LC-MS: t_R = 5.7 min, m/z found for $[C_9H_{20}N_2O_3 + H]^+$: 205.1.

Compound 19

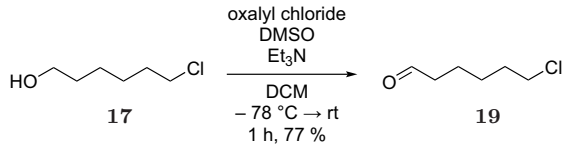

17 **19**

2.29 ml (2.52 g, 32.2 mmol, 2.20 eq) DMSO in 7.5 ml DCM were added to 1.38 ml (2.04 g, 16.1 mmol, 1.10 eq) oxalyl chloride in 35 ml DCM at −78 °C. After 30 min, 1.95 ml **17** in 15 ml DCM were added dropwise. 10.2 ml (7.41 g, 73.2 mmol, 5.00 eq) Et_3N were added after further 15 min and the mixture was allowed to adjust to room temperature and stirred for 1 h. Subsequently, the reaction was quenched with 75 ml H_2O and the aqueous layer was extracted 2× with DCM. The combined organic layers were washed 1× each with saturated aqueous NaCl, 1 % aqueous H_2SO_4, H_2O, 5 % aqueous $NaHCO_3$ and again saturated aqueous NaCl, dried over $MgSO_4$ and the solvent removed under reduced pressure. Purification by flash column chromatography (CH:EA, 9:1 → 5:1) yielded 1.52 g (11.3 mmol, 77 %) **19** as colorless liquid.

R_f (CH:EA, 1:1): 0.77.
^{1}H-NMR (400 MHz, $CDCl_3$): δ = 1.44−1.52 (m, 2 H, H-3), 1.62−1.69 (m, 2 H, H-4), 1.76−1.83 (m, 2 H, H-2), 2.46 (dt, $^3J_{\text{H-5, H-6}}$ = 1.6 Hz, $^3J_{\text{H-5, H-4}}$ = 7.2 Hz, 2 H, H-5), 3.53 (t, $^3J_{\text{H-1, H-2}}$ = 6.6 Hz, 2 H, H-1), 9.77 (t, $^3J_{\text{H-6, H-5}}$ = 1.6 Hz, 1 H, H-6).
Spectroscopic data are in agreement with literature.[323]

Compound 20

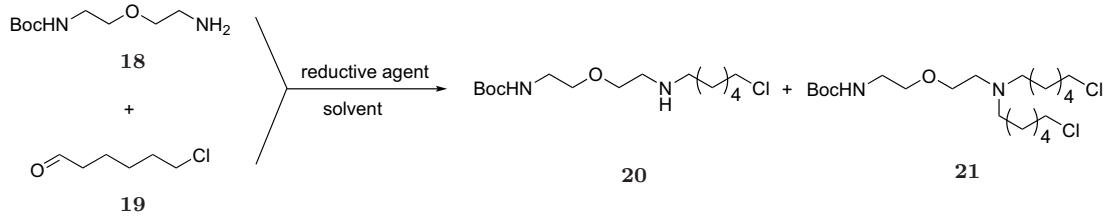

18 + **19** **20** **21**

Procedure 1 A solution of 20 mg (98 µmol, 1.00 eq) **18** and 13 mg (98 µmol, 1.00 eq) **19** in 2 ml toluene with molecular sieve 3 Å was mixed for 2 h at room temperature and further 16 h at reflux. Then, the mixture was filtered, solvent was removed from the filtrate under reduced pressure and the resulting solid redissolved in 1.5 ml THF:EtOH, 9:1. 7 mg (108 µmol, 1.10 eq) $NaBH_3CN$ were added and the pH adjusted to 4.5 with 1.25 M HCl in EtOH. After 17 h at room temperature, the reaction was poured onto a mixture of 4 g ice water and 2 ml saturated aqueous Na_2CO_3. The aqueous layer was extracted 2× with DCM, and the combined organic layers were washed 3× with saturated aqueous NaCl, dried over Na_2SO_4 and the solvents removed under reduced pressure. Flash column chromatography

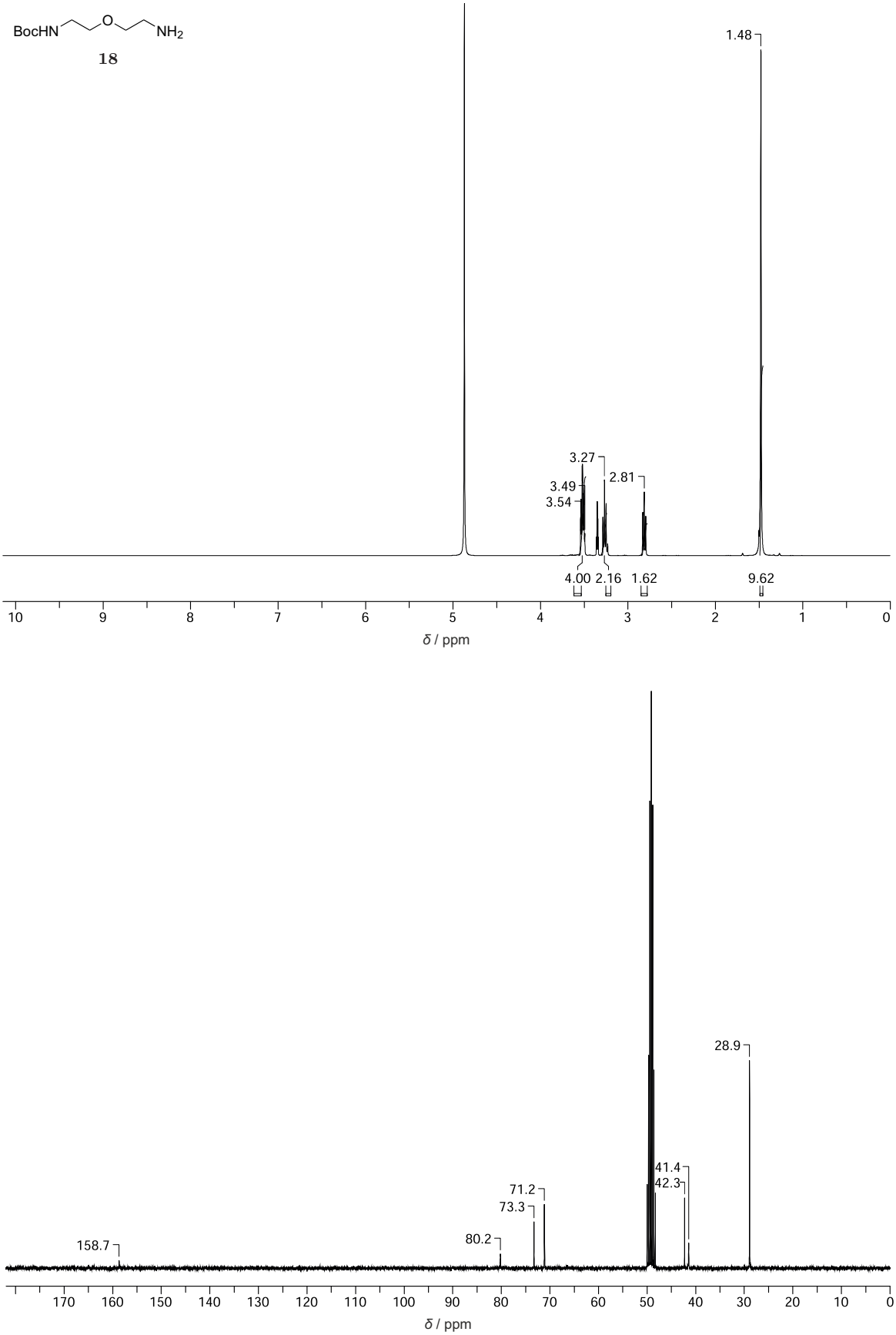

Figure 32. ^{1}H- and ^{13}C-NMR of **18** in MeOD.

(CH:EA, 1:1 → 1:10 → EA → MeOH) yielded small amounts of **20** in the methanolic fraction, which additionally contained substantial amounts of doubly alkylated **21**.

Procedure 2 40 mg (187 µmol, 1.40 eq) $NaBH(OAc)_3$ were added to a solution of 30 mg (147 µmol, 1.10 eq) **18** and 18 mg (134 µmol, 1.00 eq) **19** in 1 ml DCE. After 2.5 h at room temperature, the reaction mixture was quenched with saturated aqueous $NaHCO_3$ and the aqueous layer was extracted 3× with EA. The combined organic layers were washed 1× with saturated aqueous NaCl and dried over $MgSO_4$. Removal of the solvent under reduced pressure yielded a colorless oil consisting of a mixture of **20** with unreacted **18** and substantial amounts of doubly alkylated **21**.

Procedure 3 A solution of 192 mg (0.94 mmol, 1.10 eq) **18** and 115 mg (0.85 mmol, 1.00 eq) **19** in 3.5 ml MeOH with molecular sieve 3 Å was stirred for 22.5 h at room temperature. Subsequently, 51 mg (1.36 mmol, 1.60 eq) $NaBH_4$ were gradually added and mixed for 10 min at room temperature. The reaction mixture was quenched by addition of 1 M aqueous NaOH, Et_2O was added, the mixture filtered and the filtrate reduced under reduced pressure. The aqueous layer was extracted 3× with Et_2O and the combined organic layers washed 2× with saturated aqueous NaCl, dried over $MgSO_4$ and the solvent removed under reduced pressure. Purification by flash column chromatography (CH:EA + 0.1 % Et_3N, 3:1 → 1:1 → 1:7 → EA + 0.1 % Et_3N → MeOH) yielded 73 mg (0.23 mmol, 27 %) **20** with some impurities from the methanolic fraction and 37 mg (84 µmol, 10 %) doubly alkylated **21** as byproduct.

Analytical data **20**:
R_f (CH:EA, 1:4 + 1 % Et_3N): 0.25.
^{1}H-NMR (300 MHz, MeOD, Figure 33): δ = 1.29−1.34 (m, 2 H), 1.45 (s, 9 H), 1.75−1.85 (m, 2 H), 1.94−1.96 (m, 2 H), 3.00−3.06 (m, 2 H), 3.19−3.27 (m, 4 H), 3.47−3.62 (m, 6 H), 3.71−3.74 (m, 2 H).
LC-MS (Figure 34): t_R = 9.1 min, m/z found for $[C_{15}H_{31}ClN_2O_3 + H]^+$: 323.1, 325.1.

Analytical data **21**:
R_f (CH:EA, 1:4 + 1 % Et_3N): 0.59.
LC-MS (Figure 35): t_R = 11.7 min, m/z found for $[C_{21}H_{42}Cl_2N_2O_3 + H]^+$: 439.2, 441.0.

Compound 22

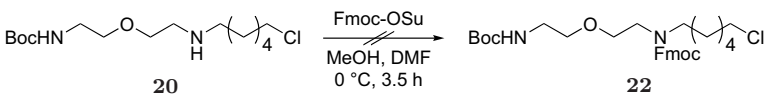

20 **22**

77 µl (56 µg, 550 µmol, 1.00 eq) Et_3N were added to 177 mg crude **20**, synthesized via procedure 3, in 2 ml MeOH. The reaction mixture was cooled to 0 °C and 216 mg (640 µmol, 1.16 eq) Fmoc-OSu in 1 ml DMF were added dropwise. After 3.5 h, the solvents were removed under reduced pressure and the aqueous layer extracted 3× with EA. The combined organic layers were washed 2× with saturated aqueous NaCl, dried over $MgSO_2$ and the solvent removed under reduced pressure. The resulting mixture of several products was separated by flash column chromatography (CH → CH:EA, 9.5:0.5 → 7:1 → 4:1 → 1:1), which yielded multiple products, none of which could be determined to be Fmoc-protected **22** by LC-MS and NMR measurements.

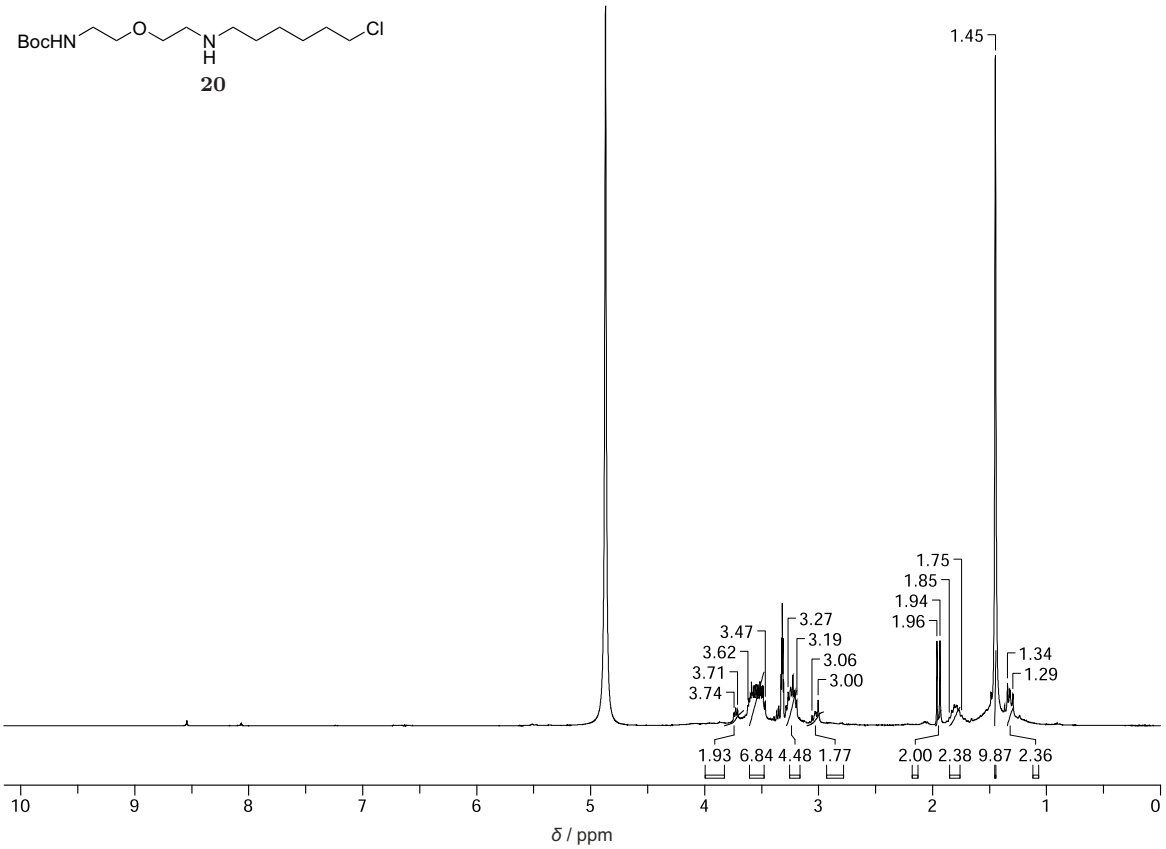

Figure 33. ^{1}H-NMR of **20**, synthesized via reductive amination procedure 3, in MeOD.

A.3.3 Synthesis route via amide

Compound 25

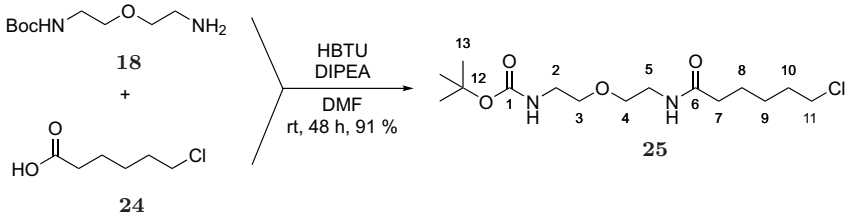

850 mg (4.16 mmol, 1.00 eq) **18**, 626 mg (4.16 mmol, 1.00 eq) **24** and 3.16 g (8.32 mmol, 2.00 eq) HBTU were dissolved in 40 ml DMF. Subsequently, 3.50 ml (2.69 g, 20.8 mmol, 5.00 eq) DIPEA and 24 h later, further 125 mg (0.83 mmol, 0.20 eq) **24** were added. After 48 h, the reaction mixture was concentrated to 10 ml under reduced pressure and poured onto H_2O. The aqueous layer was extracted 3× with DCM and the combined organic layers were washed 3× with saturated aqueous NaCl, dried over Na_2SO_4 and solvents removed under reduced pressure. Purification by flash column chromatography (CH:EA + 0.1 % Et_3N, 1:4 → 1:7) yielded 1.28 g (3.80 mmol, 91 %) **25** as slightly reddish oil.

R_f (CH:EA, 1:7 + 1 % Et_3N): 0.56.
^{1}H-NMR (300 MHz, DMSO-d6, Figure 36): $\delta = 1.31-1.34$ (m, 2 H, 9-H), 1.37 (s, 9 H, 13-H), 1.45−1.55 (m, 2 H, 8-H), 1.65−1.74 (m, 2 H, 10-H), 2.07 (t, $J = 7.2$ Hz, 2 H, 7-H), 3.03−3.09 (m, 2 H, 2-H or 5-H), 3.14−3.20 (m, 2 H, 2-H or 5-H), 3.34−3.36 (m, 4 H, 3-H, 4-H), 3.61 (t,

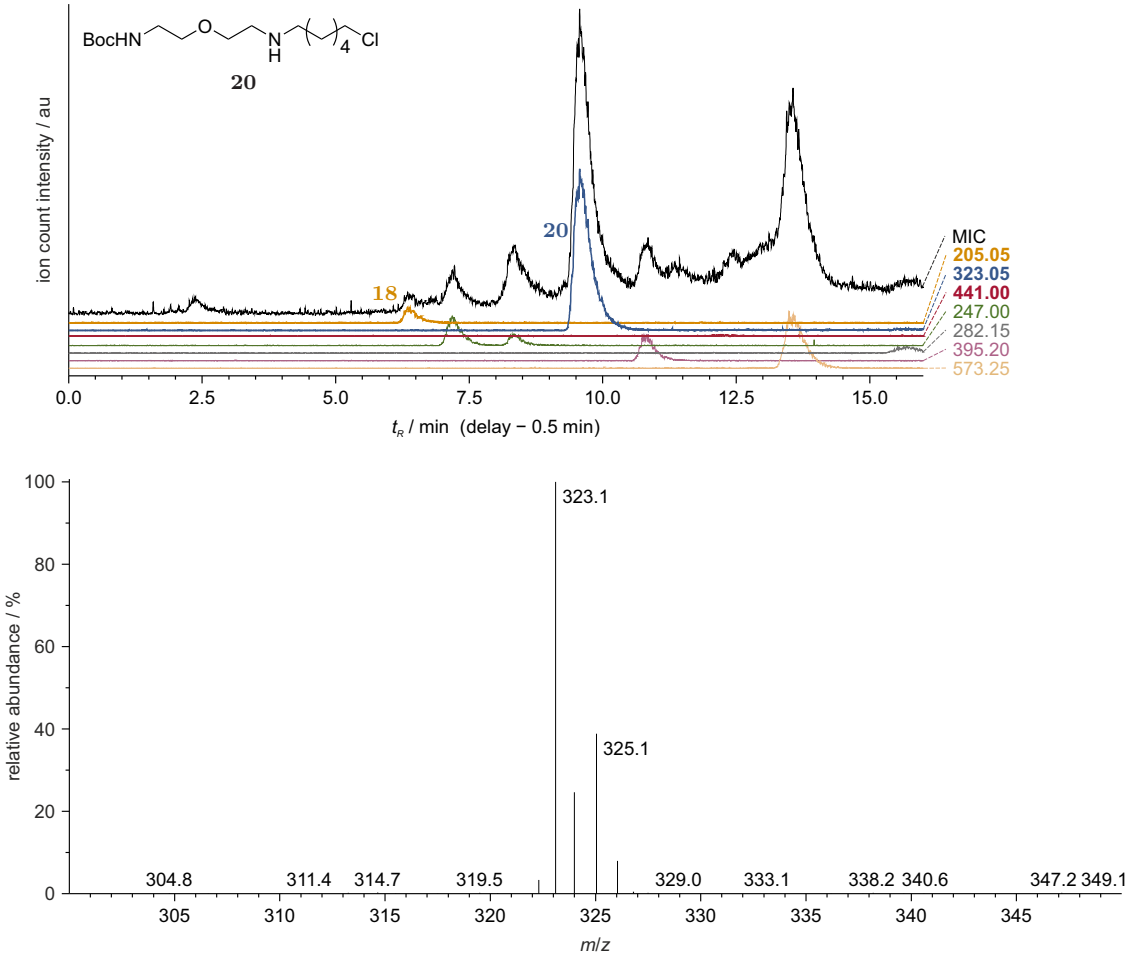

Figure 34. LC-MS and mass spectrum at $t_R = 9.1$ min of **20**, synthesized via reductive amination procedure 3, after flash column chromatography. Mass spectra were detected in positive mode.

$J = 6.6$ Hz, 2 H, 11-H), 6.75 (t, $J = 5.0$ Hz, 1 H, NH), 7.83 (t, $J = 5.3$ Hz, 1 H, NH).
^{13}C-NMR (75 MHz, DMSO-d6, Figure 36): δ = 24.5 (C-8), 25.9 (C-9), 28.2 (C-13), 31.8 (C-10), 35.1 (C-7), 38.5 (C-2 or C-5), 39.7 (C-2 or C-5), 45.3 (C-11), 68.9 (C-3 or C-4), 69.0 (C-3 or C-4), 77.7 (C-12), 155.7 (C-1 or C-6), 172.1 (C-1 or C-6).
NMR signals of **25** were assigned by ^{1}H,^{1}H COSY, ^{13}C,^{1}H HSQC and DEPT-135 measurements.
LC-MS (Figure 37): t_R = 12.2 min, m/z found for $[C_{15}H_{29}ClN_2O_4 + Na]^+$: 359.0, 361.0, found for $[C_{15}H_{29}ClN_2O_4 + H]^+$: 337.0, 338.8.
HRMS (ESI-TOF): m/z calculated for $[C_{15}H_{29}ClN_2O_4 + Na]^+$: 359.17081, found: 359.17120; calculated for $[2(C_{15}H_{29}ClN_2O_4) + Na]^+$: 695.35239, found: 695.35286.

Coumpound 20

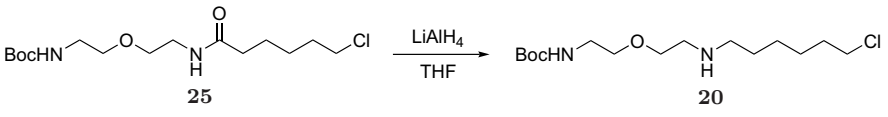

Procedure 1 20 mg (59 µmol, 1.00 eq) **25** in 1 ml THF were cooled to 0 °C and 25 µl (59 µmol, 1.00 eq) 2.4 M $LiAlH_4$ in THF were added. Significant amounts of unreacted **25** were present after 23 h at room temperature and additional 25 µl (59 µmol, 1.00 eq)

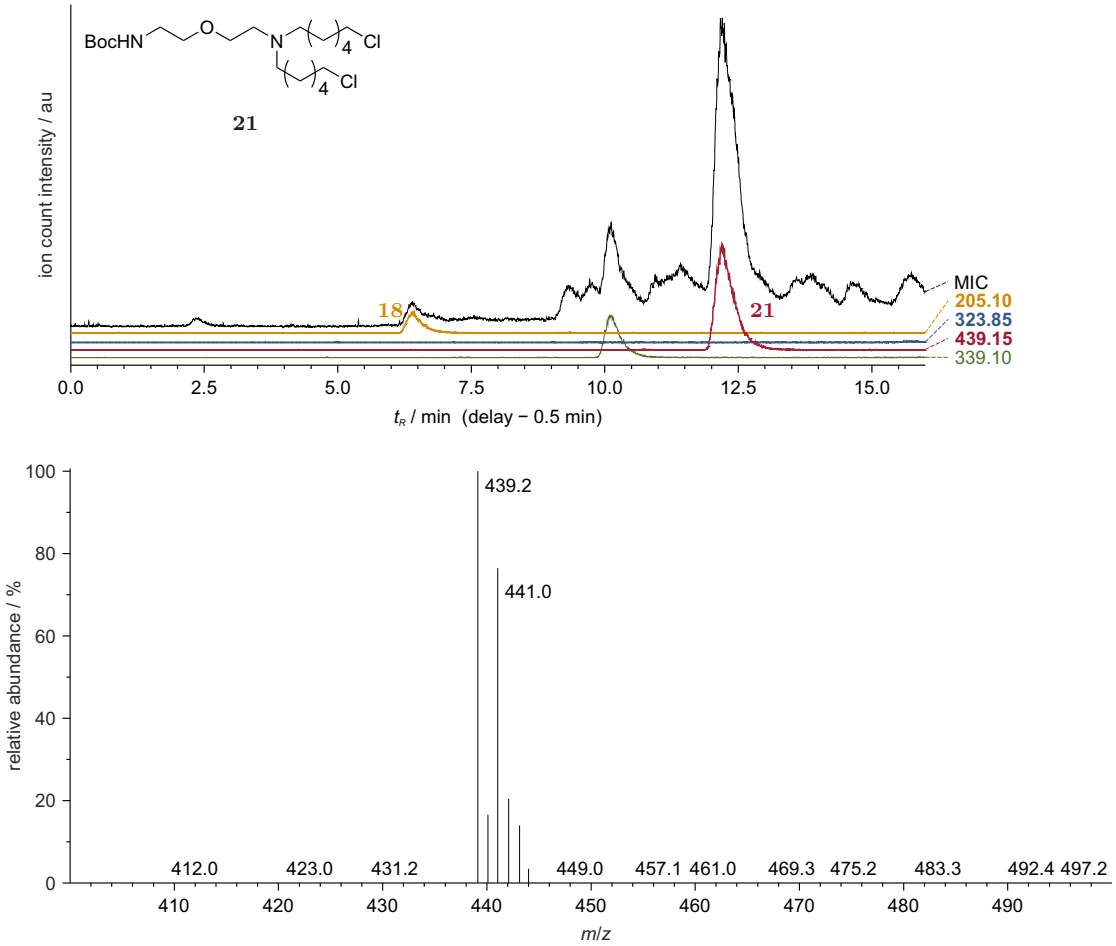

Figure 35. LC-MS and mass spectrum at $t_R = 11.7$ min of byproduct **21**, obtained via reductive amination procedure 3, after flash column chromatography. Mass spectra were detected in positive mode.

2.4 M $LiAlH_4$ in THF were added after 23 h, 43 h and 50 h each. After 67 h, the reaction was quenched with H_2O at 0 °C, 400 µl 10 % aqueous NaOH was added, filtered and the solvents removed under reduced pressure. Purification by flash column chromatography (DCM:MeOH + 0.1 % Et_3N, 9.5:0.5 → 9:5 → MeOH) yielded 4 mg (12 µmol, 21 %) **20** with some impurities as colorless oil.

Procedure 2 500 µl (1.20 mmol, 2.00 eq) 2.4 M $LiAlH_4$ in THF were added dropwise to a solution of 200 mg (0.59 mmol, 1.00 eq) **25** in 3 ml THF at 0 °C. After 24 h at room temperature, the reaction was quenched with H_2O at 0 °C, 2× 37.5 µl 10 % aqueous NaOH were added, filtered and the solvents removed under reduced pressure. Flash column chromatograpphy (DCM:MeOH + 0.1 % Et_3N, 9.8:0.2 → 9.5:0.5 → 9:1 → 8:2 → MeOH) yielded 7 mg (22 µmol, 4 %) **20** as colorless oil and additional 27 mg (84 µmol, 14 %) in mixed fractions. Furthermore, 41 mg (122 µmol, 21 %) unreacted **25** were reisolated.

Procedure 3 To a solution of 20 mg (59 µmol, 1.00 eq) **25** in 1.5 ml THF at 0 °C, 75 µl (178 µmol, 3.00 eq) 2.4 M $LiAlH_4$ in THF were added dropwise and stirred at 0 °C for 30 min. Subsequently, the reaction mixture was heated to 50 °C for 1 h, followed by cooling to 0 °C, quenching with H_2O and addition of 4× 15 µl 10 % aqueous NaOH. The mixture was stirred for further 1 h at 0 °C and 1 h at room temperature, each, filtered and the solvents re-

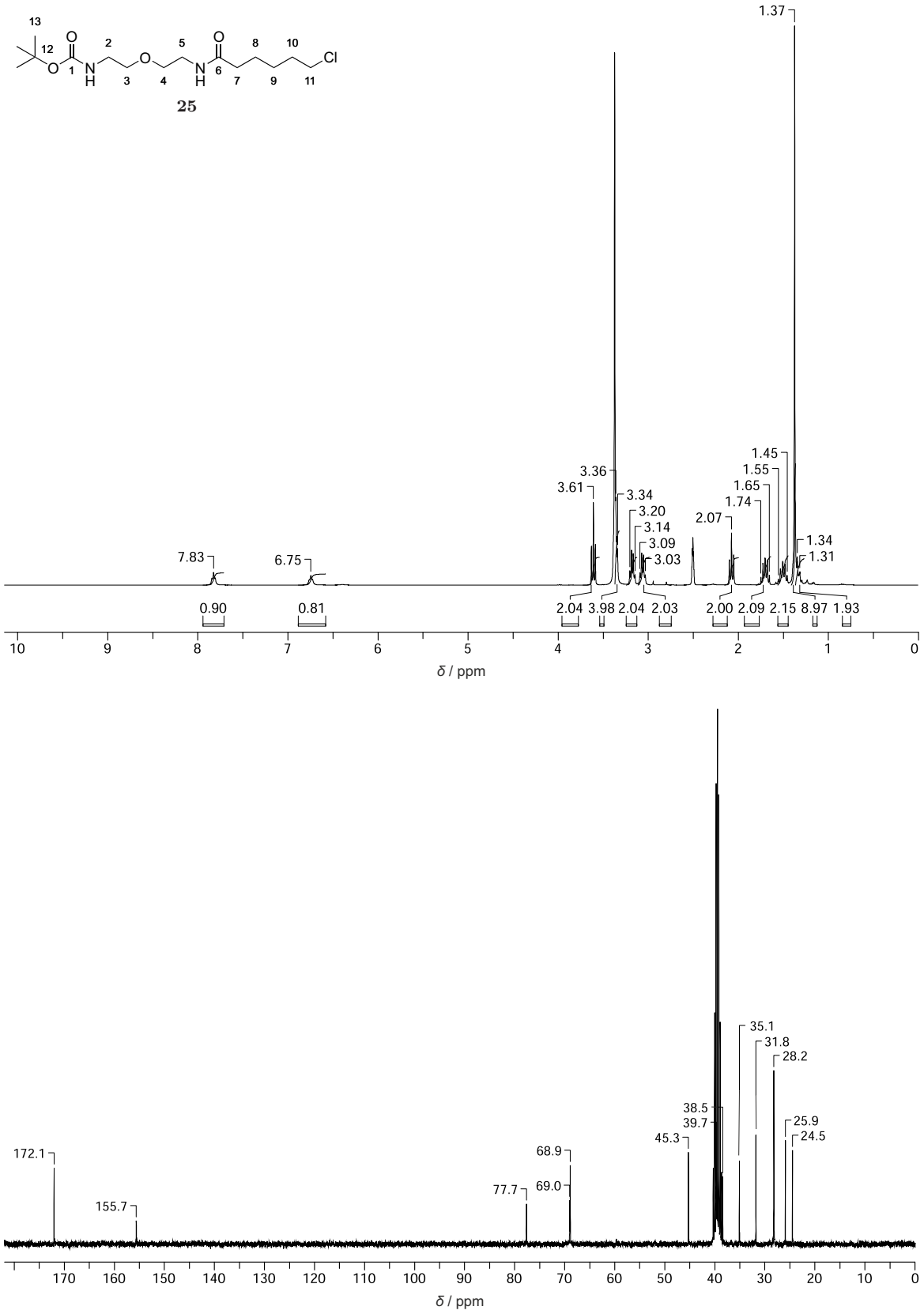

Figure 36. ^{1}H- and ^{13}C-NMR of **25** in DMSO-d6.

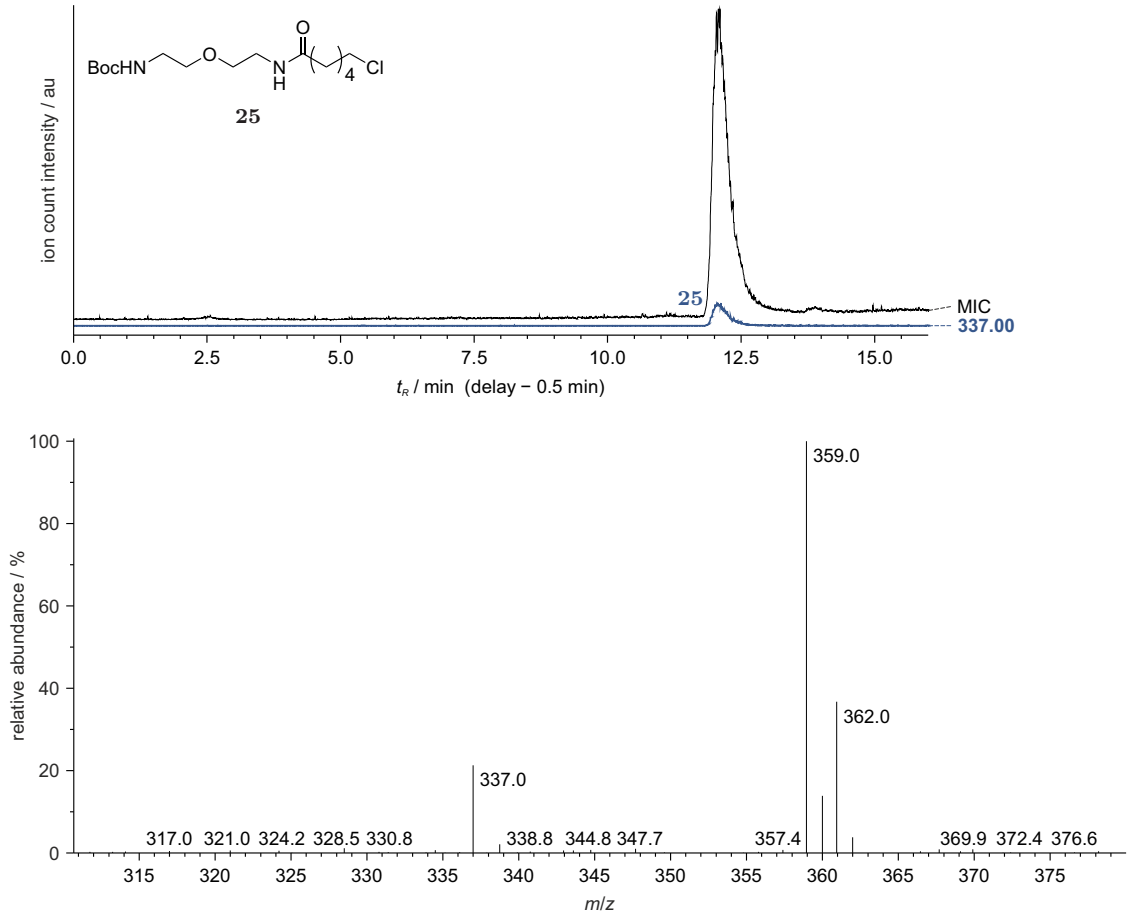

Figure 37. LC-MS and mass spectrum at t_R = 12.2 min of **25**. Mass spectra were detected in positive mode.

moved under reduced pressure. Purification by flash column chromatography (DCM:MeOH, 9.8:0.2 → 9.5:0.5 → 9.25:0.75 → 9:1 → 8:2) yielded 4 mg (12 µmol, 21 %) **20** as colorless oil.

Procedure 4 THF applied for procedure 4 was freshly dried over sodium by heating under reflux and subsequent destillation. 100 µl (59 µmol, 1.00 eq) 0.6 M $LiAlH_4$ in THF were added to a solution of 20 mg (59 µmol, 1.00 eq) **25** in 0.5 ml THF at 0 °C. After 15 min at 0 °C, the mixture was stirred at room temperature for 1 h, then further 50 µl (30 µmol, 0.50 eq) 0.6 M $LiAlH_4$ in THF were added. Since the freshly dried THF did not result in significant improvements, i.e. amide **25** still did not react completely and multiple side products emerged, the reaction was discarded after 19 h.

R_f (DCM:MeOH, 9:1): 0.34.
^{1}H-NMR (400 MHz, DMSO-d6, Figure 38): δ = 0.86−0.89 (m, 2 H), 1.28−1.34 (m, 4 H), 1.38 (s, 9 H), 1.54−1.61 (m, 2 H), 3.06−3.15 (m, 8 H), 3.42−3.45 (m, 2 H), 3.60−3.62 (m, 2 H), 8.33 (bs, 1 H), 8.98 (bs, 1 H).
^{13}C-NMR (75 MHz, DMSO-d6, Figure 38): δ = 25.2, 25.7, 25.8, 28.2, 30.7, 31.8, 45.3, 46.0, 46.7, 65.1, 69.3, 77.7, 155.6.
LC-MS (Figure 40): t_R = 10.4 min, m/z found for $[C_{15}H_{31}ClN_2O_3 + H]^+$: 323.3, 325.3, found for $[C_{15}H_{31}ClN_2O_3 - Cl + 2H]^+$: 289.4.

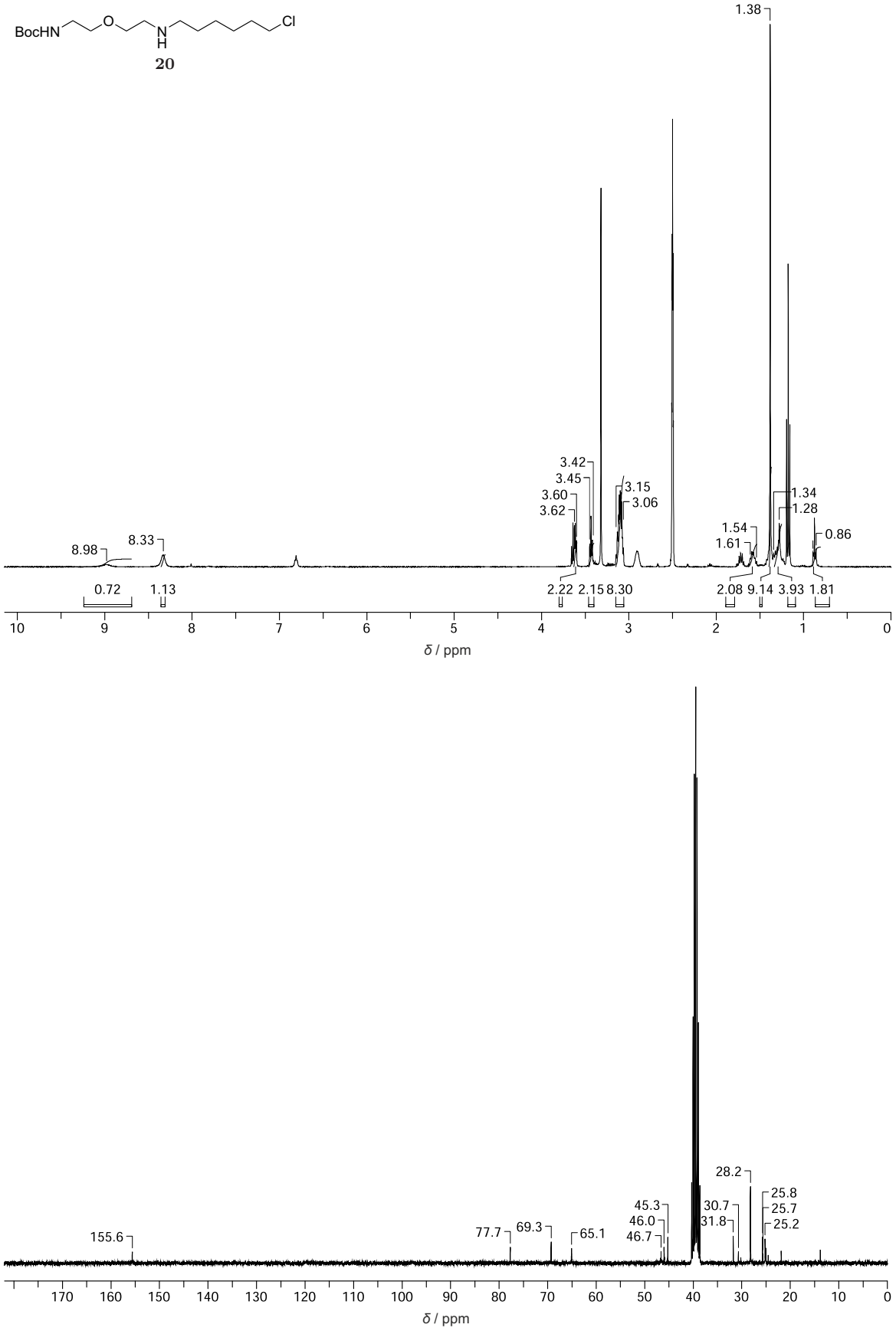

Figure 38. ^{1}H- and ^{13}C-NMR of **20**, synthesized from amide **25** via procedure 2, in DMSO-d6.

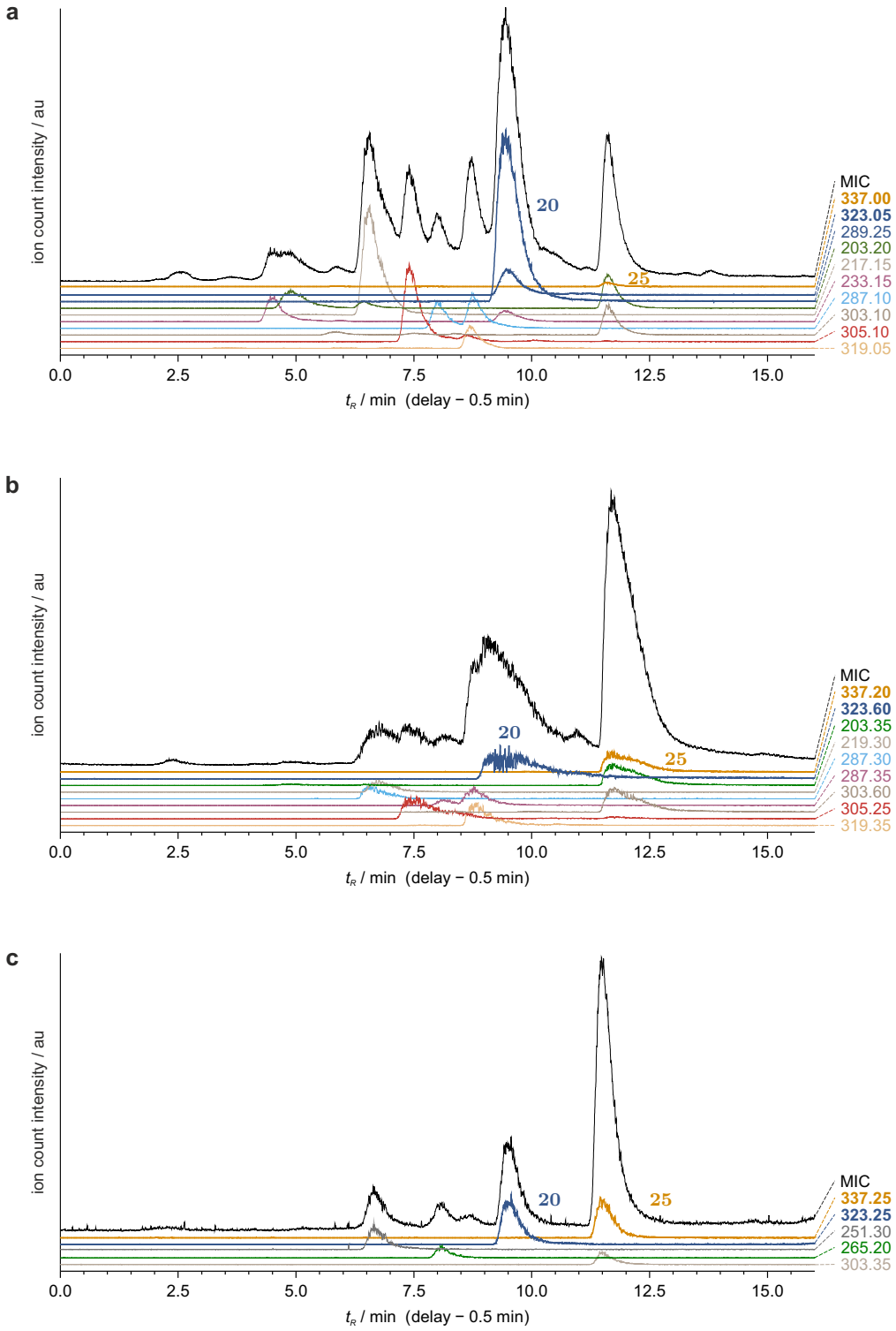

Figure 39. LC-MS spectra of crude product synthesized from amide **25** via **a** procedure 1, **b** procedure 2 and **c** procedure 3, respectively. Product **20** appears at $t_R = 9.1$ min and unreacted reactant **25** at $t_R = 12.2$. Mass spectra were detected in positive mode.

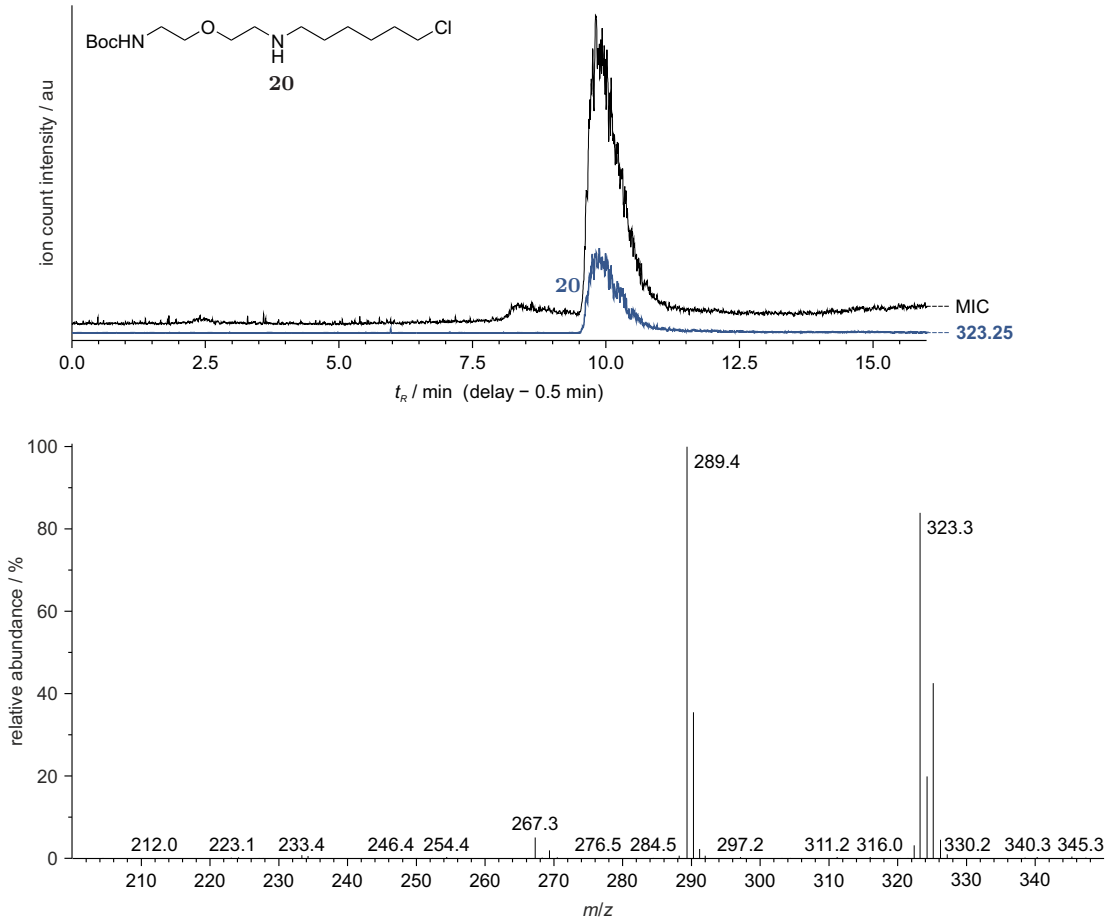

Figure 40. LC-MS and mass spectrum at $t_R = 9.1$ min of purified **20** synthesized from amide **25** via procedure 2. Mass spectra were detected in positive mode.

List of Abbreviations

Ψ	pseudouridine
2'-F	2'-fluoro
2'-MOE	2'-*O*-methoxyethyl
2'-*O*Me	2'-*O*-methyl
2PE	two-photon excitation
5-HT$_{2C}$R	*2C subtype of serotonin receptor*
7-MCM	(7-methoxycoumarin-4-yl)-methyl
A	adenosine
Aβ	β-Amyloid
A1AT	α_1-antitrypsin
A1CF	APOBEC1 complementation factor
A1HD	APOBEC1 C-terminal hydrophobic domain
aa	amino acid
AAV	adeno-associated virus
ABA	abscisic acid
ABI1	abscisic acid insensitive 1
Ac	acetyl
ACE	angiotensin-converting enzyme
ACM	(7-aminocoumarin-4-yl)-methyl
ACTB	*β-actin*
ADAR	adenosine deaminase acting on RNA
AGS	Aicardi-Goutières syndrome
AID	activation-induced cytidine deaminase
AID*	auxin-inducible degron
AlkBh5	AlkB homolog 5
ALS	amyotrophic lateral sclerosis
ANBP	2-(4'-(dimethyl)amino)-4-nitro-[1,1'-biphenyl]-3-yl)propan-1-ol
ApoB	*apolipoprotein B*
APOBEC	apolipoprotein B mRNA editing enzyme, catalytic polypeptide-like
ApoE	apolipoprotein E
ARDS	acute respiratory distress syndrome
Arg	arginine
arRNA	ADAR recruiting RNA
ASGPR	asialoglycoprotein receptor
ASO	antisense oligonucleotide
au	arbitrary units
B	nucleobase
BC	O^6-benzylcytosine
BCP	benzyl-2-chloro-6-aminopyrimidine
BER	base excision repair
BFP	*blue fluorescent protein*
BG	O^6-benzylguanine
BHCM	(6-bromo-7-hydroxycoumarin-4-yl)methyl
BH_4	tetrahydrobiopterin
bipy	2,2'-bipyridine
Boc	*tert*-butyloxycarbonyl
BODIPY	boron-dipyrromethene
bp	base pair
C	cytidine
calcineurin	calcium-dependent serine-threonine phosphatase
cAMP	3'-5'-cyclic adenosine monophosphate
Cas	CRISPR-associated protein
CDS	coding sequence
CFP	cyan fluorescent protein
cGK	cGMP-dependent protein kinase
cGMP	3'-5'-cyclic guanosine monophosphate
CH	cyclohexane

CHD	coronary heart disease
cIAP1	cellular inhibitor of apoptosis protein 1
CID	chemically induced dimerization
CIRTS	CRISPR-Cas-Inspired RNA Targeting System
Cit	citrulline
CM	coumarin-4-yl-methyl
CMV	cytomegalovirus
CNG	cyclic nucleotide-gated
cNMP	3'-5'-cyclic nucleotide
CNS	central nervous system
COSY	homonuclear correlation spectroscopy
CPP	cell-penetrating peptide
CRBN	cereblon
CRS	cytoplasmic retention signal
CRY	cryptochrome
CsA	cyclosporine A
CTEPH	chronic thromboembolic pulmonary hypertension
CTNNB1	*β-catenin*
cupferron	ammonium salt of *N*-nitroso-*N*-phenylhydroxylamine
CURE	C-to-U RNA Editor
CyP	cyclosporine binding cyclophilins
Cys	cysteine
DASA	donor–acceptor Stenhouse adduct
DCE	1,2-dichloroethane
DCM	dichloromethane
DD	deaminase domain
DEA/NO	diethylamino-NONOate
DEACM	[7-(diethylamino)coumarin-4-yl]methyl
DEPT	distortionless enhancement by polarization transfer spectroscopy
DETA/NO	diethylenetriamine-N^2-NONOate
DhaA	*Rhodococcus* haloalkane dehalogenase
DHFR	dihydrofolate reductase
DIPEA	*N*,*N*-diisopropylethylamine
DMA/NO	dimethylamino-NONOate
DMACM	[7-(dimethylamino)coumarin-4-yl]methyl
DMF	dimethylformamide
DMNPP	2-(4,5-dimethoxy-2-nitrophenyl)-propyl
DMSO	dimethyl sulfoxide
DNA	deoxyribonucleic acid
DNA-PAINT	DNA points accumulation in nanoscale topography
dNP	2,4-(dinitrophenyl)
DR	direct repeat
DSH	dyschromatosis symmetrica hereditaria
dsRBD	double stranded RNA binding domain
dsRNA	double stranded RNA
E. coli	*Escherichia coli*
EA	ethyl acetate
EANBP	2-(4'-(bis((2-methoxyethoxy)ethyl)amino)-4-nitro-[1,1'-biphenyl]-3-yl)propan-1-ol
EDRF	endothelium-derived relaxing factor
EF1α	elongation factor 1α
eGFP	*enhanced green fluorescent protein*
eNOS	endothelial NOS
ESI	electrospray ionization
FAD	flavin adenine dinucleotide
FDA	U. S. Food and Drug Administration
FKBP	FK506 binding protein
Flp-In T-REx	Flp-In T-REx system by *Life Technologies*
FMN	flavin mononucleotide
Fmoc	fluorenylmethoxycarbonyl
FRB	FKBP-rapamycin binding domain
FRET	Förster resonance energy transfer
FTO	fatt mass and obesity-associated protein
FU	5-fluorouracil
G	guanosine

GABA γ-aminobutyric acid
GAI gibberellic acid insensitive
Gal galactose
GalNAc *N*-acetylgalactosamine
GAPDH *glyceraldehyde 3-phosphate dehydrogenase*
GA_3 gibberellic acid
GA_3-AM gibberellic acid acetoxymethyl ester
GFP green fluorescent protein
GID1A gibberellin insensitive dwarf 1A
GluR-B *glutamate receptor B*
GlyR *glycine receptor*
GMP guanosine monophosphate
gRNA guideRNA
GSNO *S*-nitroso-glutathione
GST-π glutathione *S*-transferase π
GTP guanosine-5'-triphosphate
GVHD graft-versus-host disease

hADAR human adenosine deaminase acting on RNA
hAGT human O^6-alkylguanine-DNA alkyltransferase
HBTU hexafluorophosphate benzotriazole tetramethyl uronium
HC3M 7-hydroxy-3-hydroxymethyl coumarin
HCM (7-hydroxycoumarin-4-yl)methyl
HEK 293 human embryonic kidney 293 cells
HF heart failure
HFpEF heart failure with preserved ejection fraction
HFrEF heart failure with reduced ejection fraction
HIV human immunodeficiency virus
HOB halo-based oligonucleotide binder
HPLC high performance liquid chromatography
HRMS high resolution mass spectrometry
HSQC heteronuclear single-quantum correlation spectroscopy
HTH helix-turn-helix motif

I inosine
IAA indole-3-acetic acid
IAA17 auxin-responsive protein IAA17
IDUA *α-L-iduronidase*
IFN interferon
IMiD immunomodulatory imide drug
INDQ indole-1,4-quinone
iNOS inducible NOS
IRP iron regulatory protein
ISDN isosorbide dinitrate
ISMN isosorbide mononitrate

KRAS *Kirsten rat sarcoma virus*

LC-MS liquid chromatography-mass spectrometry
LEAPER Leveraging endogenous ADAR for programmable editing of RNA
Leu leucine
LNA locked nucleic acid
lncRNA long non-coding RNA
LNP lipid nanoparticle
LOV light-, oxygen-, or voltage-sensitive protein
Lys lysine

MCP MS2 bacteriophage coat protein
MECP2 *methyl CpG binding protein 2*
MeNPOC 3,4-(methylenedioxy)-6-nitrophenylethoxycarbonyl
MeNPOM α-methyl-(6-nitropiperonyloxymethyl)
METTL methyltransferase-like
MIC multiple ion count
miRNA microRNA
MLC myosin light chain
MPS I Mucopolysaccharidosis type I
mRNA messenger RNA

mTOR mechanistic target of rapamycin
m^{1}A N^1-methyladenosine
m^{5}C 5-methylcytosine
m^{6}A N^6-methyladenosine

NADP nicotinamide adenine dinucleotide phosphate
NANA *N*-acetylneuraminic acid
NCBI National Center for Biotechnology Information
ncRNA non-coding RNA
NES nuclear export signal
NG nitroglycerin
NHA N$^{\omega}$-hydroxy-arginine
NIR near-infrared
NLS nuclear localization signal
NMR nuclear magnetic resonance spectroscopy
nNOS neuronal NOS
NONOate diazen-1-ium-1,2-diolate
NOS nitric oxide synthase
NP natriuretic peptide
NPE 1-(2-nitrophenyl)ethyl
NPOM 6-nitropiperonyloxymethyl
NSAID nonsteroidal anti-inflammatory drug
nt nucleotide
NV 6-nitroveratryl
NVOC 6-nitroveratryloxycarbonyl

OBM 9-methoxy-1-methylene-3-oxo-3*H*-benzo[*f*]benzopyran
***o*NB** *ortho*-nitrobenzyl
ORF open reading frame
OSu *N*-hydroxysuccinimidyl
OTC *ornithine transcarbamylase*

P. dumerilii *Platynereis dumerilii*
PAH pulmonary arterial hypertension
PaPy$_3$H *N,N'*-bis(2-pyridylmethyl)-amine-*N*-ethyl-2-pyridine-2-carboxamide
PDE cyclic nucleotide phosphodiesterase
PEG polyethylene glycol
pGC particulate guanylate cyclase
PINK1 *PTEN-induced kinase 1*
PIP/NO piperazino-NONOate
PKA cAMP-dependent protein kinase
PNA peptide nucleic acid
PNS peripheral nervous system
POI protein of interest
PP2C protein phosphatase 2C
PPG photocleavable protecting group
PPIX protoporphyrin IX
pre-crRNA pre-CRISPR RNA
PROTAC proteolysis targeting chimera
PTC premature stop codon
PTO phosphorothioate
PUS pseudouridine synthase
PWS Prader-Willi syndrome
PYL pyrabactin resistance-like regulatory component of ABA receptors
PYRRO/NO pyrrolidin-1-yl-NONOate

QR1 quinone reductase 1

R arginine-rich domain
Rap rapamycin
RBM47 RNA-binding protein 47
REPAIR RNA Editing for Programmable A to I Replacement
RESCUE RNA Editing for Specific C-to-U-Exchange
RESTORE Recruiting endogenous ADAR to specific transcripts for oligonucleotide-mediated RNA editing
RISC RNA-induced silencing complex
RNA ribonucleic acid
RNAi RNA interference
RNS reactive nitrogen species
rRNA ribosomal RNA
RS recruitment sequence
RSE Roussin's red ester

rt room temperature

salenH$_2$ *N*,*N*'-bis(salicylidene)-ethylenediamine

SDRE site-directed RNA editing

Ser serine

SERPINA1 *serpin family A member 1*

sGC soluble guanylate cyclase

siRNA small interfering RNA

SLE systemic lupus erythematosus

SNO *S*-nitrosothiol

snoRNA small nucleolar RNA

snoRNP small nucleolar ribonucleoprotein particle

SNP sodium nitroprusside

SPER/NO spermine-N^2-NONOate

ssDNA single stranded DNA

ssRNA single stranded RNA

STAT1 *signal transducer and activator of transcription 1*

TAR trans-activation response element

TBP TAR-binding protein

TBS *tert*-butyldimethylsilyl

TCR T cell receptor

THF tetrahydrofuran

TIR1 transport inhibitor response 1

TIVA transcriptome *in vivo* analysis

TMP trimethoprim

TMR tetramethylrhodamine

TOF time of flight

TPH2 *tryptophane hydroxylase 2*

tRNA transfer RNA

Tyr tyrosine

U uridine

UAA unnatural amino acid

UTR untranslated region

VASP vasodilator stimulated phosphoprotein

VHL von Hippel-Lindau

VSMC vascular smooth muscle cell

wt wild-type

YFP yellow fluorescent protein

YTHDF2 YTH N^6-methyladenosine RNA binding protein 2

ZDD zinc-dependent deaminase domain